

A PETROLOGICAL STUDY OF THE APPENITE SUITE
ASSOCIATED WITH THE ARDARA PLUTON, CO.
DONEGAL, IRELAND

Timothy Roderick Yarr

A Thesis Submitted for the Degree of PhD
at the
University of St Andrews



1992

Full metadata for this item is available in
St Andrews Research Repository
at:
<http://research-repository.st-andrews.ac.uk/>

Please use this identifier to cite or link to this item:
<http://hdl.handle.net/10023/15565>

This item is protected by original copyright

A PETROLOGICAL STUDY OF THE
APPINITE SUITE ASSOCIATED WITH THE
ARDARA PLUTON, CO. DONEGAL, IRELAND

Timothy Roderick Yarr

Thesis presented in partial fulfilment of the
Degree of Doctor of Philosophy,
August 1991



ProQuest Number: 10171177

All rights reserved

INFORMATION TO ALL USERS

The quality of this reproduction is dependent upon the quality of the copy submitted.

In the unlikely event that the author did not send a complete manuscript and there are missing pages, these will be noted. Also, if material had to be removed, a note will indicate the deletion.



ProQuest 10171177

Published by ProQuest LLC (2017). Copyright of the Dissertation is held by the Author.

All rights reserved.

This work is protected against unauthorized copying under Title 17, United States Code
Microform Edition © ProQuest LLC.

ProQuest LLC.
789 East Eisenhower Parkway
P.O. Box 1346
Ann Arbor, MI 48106 – 1346

Tu B 93

DECLARATION

I, Timothy Roderick Yarr, hereby certify that this thesis has been composed by myself, that it is a record of my own work, and that it has not been accepted in partial or complete fulfilment of any other degree or professional qualification.

Signed

Date 22 August 1991.

I was admitted to the Faculty of Science of the University of St. Andrews under Ordinance General No. 12 on 1st October 1987 and as a candidate for the Degree of Ph.D. on the 1st October 1988.

Signed

Date 22 August 1991.

I hereby certify that the candidate has fulfilled the conditions of the Resolution and Regulations appropriate to the Degree of Ph.D.

Signed
/

Date 19 August 1991

COPYRIGHT.

In submitting this thesis to the University of St. Andrews I understand that I am giving permission for it to be made available for use in accordance with the regulations of the University Library for the time being in force, subject to any copyright vested in the work not affected thereby. I also understand that the title and abstract will be published, and a copy of the work will be made available to any *bona fide* library or research worker.

ACKNOWLEDGEMENTS

Many people have played a part in this research study. Ed Stephens, my supervisor deserves great praise for his enthusiastic and patient supervision both in the field and at St. Andrews. Thanks also go to Colin Donaldson for many pieces of advice along the way, Antonio Castro for assistance with geobarometry and Bruce Chappell and Allan White for advice on petrography. The technical staff at St. Andrews, namely Jim Allen, Richard Batchelor, Angus Calder, Colin Cameron, Donald Herd and Andrew Mackie provided excellent technical support, without it this thesis may never have been possible. At East Kilbride (S.U.R.R.C) I must give thanks to all technical staff, in particular Terry Donnelly and Alison MacDonald, not forgetting Tony Fallick and Gawen Jenkin who thankfully know rather a lot about stable isotopes.

In Donegal I greatly acknowledge the wise insight and knowledge of Wally Pitcher who provided valuable input and passed on to me much of his expertise on the field relationships of granites. Thanks go to the Herron family at Letterilly who sheltered me during the early days of fieldwork in Donegal. Salutations to Mickey and Etta Gallagher, two people who provided accomodation, freshly baked scones, golf and an abundance of warm hospitality during my stays in Narin-Portnoo. Their never faltering kindness made fieldwork a pleasure, thanks also to the Narin Inn for refreshments!

My peers at St. Andrews made research here an enjoyable pastime, they include Martin Gillespie, Bruce Paterson, Andrew Marshall, Charles Morrison, Mark Errington, Richard Curry, John Reavy and Richard Moore (who got me into this mess and nearly got me out of it again!), Dave Lowry, Stuart Allison, Justin Dix and many other colleagues too numerous to mention. Thanks also to Ian Drew without whom long hours in front of a Mac could all have ended in tears. My heart is warmed by the memory of the carefree hours spent in the company of messers John Seedhouse and Michael MacDonald (especially as it was on long walks with bags of sticks) who helped me appreciate the beauty of the links at St. Andrews and a golf hole called Bobby Jones. I must thank Drs Hancox, Pacey and Dunlop three chaps who have all seemed to lose their hair since they met me and who all wear rose coloured spectacles!

The everlasting patience and support my parents and family have shown during my university career has been priceless, I couldn't have coped without them. Special thanks to Fiona Hempel who has supported me through thick and thin. Finally I must acknowledge all the other great friends I have met while in St. Andrews, in particular the late Jo Copley, a very special person who is greatly missed. This research was funded by the Dept. of Education for N. Ireland and Kates Bar, St. Andrews.

ABSTRACT

Appinites are enigmatic rocks commonly associated with major I-type plutons in the Caledonian orogen, a number of different models have been proposed for the origin of their parental magmas and unusual textural characteristics. The appinite cluster associated with the Ardara pluton has been studied using petrological techniques with the aim of understanding these features as well as their relationships to the main pluton. The approach of this study has been to select a few appinite bodies considered to be representative of the whole Ardara appinite suite, and to study each in detail in parallel with a limited study of the main pluton. The techniques adopted include field mapping, petrography, mineral chemistry, whole rock major and trace element geochemistry. The detailed aims were to constrain the origin of the magma, its emplacement history and differentiation, for each selected body. In one case (Portnoo) the role of fluids was investigated in detail using stable isotope geochemistry.

The Ardara appinite suite comprises a wide variety of generally amphibole-rich rocks typically including hornblendite, meladiorite, diorite, granodiorite and granite. There is one case of cortlandtite. Most have evidence of a significant volatile phase at crystallisation. The intrusions display a wide range in form and emplacement mechanism and most were emplaced prior to, or coeval with, the diapiric granite pluton of Ardara. They have a history of tectonic control on emplacement and are associated with major shear zones acting as potential magma pathways. Mineral geobarometry and geothermometry indicate that the appinites crystallised at 5-8 kb, and selected mineral pairs equilibrated between 800 and 976°C. G1 and G2 of the Ardara pluton crystallised at 5 kb and amphibole-plagioclase equilibrated at around 800°C. These pressures are high if the appinites are high-level diatremes, and this apparent inconsistency is discussed. Variations in bulk geochemistry are considerable and attempts are made to model these as the products of crystal-liquid processes using mass balance major oxide and Rayleigh trace element techniques. The results tend to be dominated by solutions involving amphibole, other mafic minerals and plagioclase, although in many cases no satisfactory result was obtained which suggests that crystal fractionation is not always the sole cause of differentiation. Stable isotope studies of $\delta^{18}\text{O}$, $\delta^{13}\text{C}$ and δD from the appinites and country rocks at Portnoo indicate that the dominant fluid in this appinite was magmatic in origin, although crustal contamination had occurred, while δD data also indicate a role for meteoric fluids. The data show that fluids from the appinite penetrated the limestone aureole to about 40m.

The compositional characteristics of the Ardara appinite suite support a model of derivation of a hydrous basic magma from a mantle source. These magmas undergo differentiation by multiple processes, including crystal-liquid fractionation, as well as contamination by crustal assimilation and possibly by other magmas. The source of G1 & G2 of the main pluton is relatively primitive and could be immature lower crust. It is possible to derive G1 from G2 by crystal fractionation, but probably not *in situ*. The central G3 granite was almost certainly derived from a distinct, rather more mature crustal source.

CONTENTS

List of Contents	Page No.
DECLARATION	i
ACKNOWLEDGEMENTS	ii
ABSTRACT	iii
CONTENTS	iv
CHAPTER ONE	
INTRODUCTION	1
1.1	1
1.2	3
1.3	4
1.4	4
1.5	5
CHAPTER TWO	
PREVIOUS RESEARCH ON APPINITES AND RELATED ROCKS	6
2.1	6
2.1.1	6
2.1.2	6
2.2	8
2.2.1	9
2.2.2	10
2.2.3	12
2.3	13
2.3.1	13
2.3.2	21
2.3.3	28
2.4	28
2.4.1	28
2.4.2	28
2.4.3	30
2.4.4	31
2.5	32
2.5.1	32
2.5.2	33
2.5.3	33
2.6	35
2.6.1	35
2.6.2	37
2.7	38
CHAPTER THREE	
GEOLOGICAL SETTING	39
3.1	39
3.2	41
3.3	41
3.3.1	43
3.3.2	44
3.3.3	44
3.3.4	44
3.3.5	44
3.3.6	45
3.4	45
3.4.1	45
3.4.2	46
3.4.3	48

3.4.4	Thermal metamorphic effects of the intrusion of the Main Donegal granite	49
3.5	THE DONEGAL GRANITES	49
3.5.1	The Ardara pluton	49
3.5.2	Enclaves in the Ardara pluton	54
3.5.3	Emplacement of the Ardara pluton and its implication for appinite emplacement	55
3.5.4	Effects of emplacement of the Main Donegal granite	58
3.6	THE MEENALARGAN DIORITIC COMPLEX	58
3.6.1	Contact relationships	61
3.6.2	Lithological variation	62
3.6.3	Contamination	64
3.6.4	Deformation	65
3.6.5	Minor intrusions	67
3.6.6	Emplacement mechanism	68
3.7	THE SUMMY LOUGH DIORITE	68
3.7.1	Contact relationships	69
3.7.2	Lithological variation	70
3.7.3	Structure	71
3.7.4	Coarse grained appinite	72
3.7.5	Emplacement mechanism	72
3.8	THE MULNAMIN INTRUSION	73
3.8.1	Form of the intrusion and contact relationships	73
3.8.2	Lithological variation	73
3.8.3	Emplacement mechanism	79
3.9	THE NARIN-PORTNOO COMPLEX	80
3.9.1	Narin-Portnoo shore section	80
3.9.2	Portnoo to east Burnfoot intrusions	86
3.9.3	Emplacement of the Portnoo diorites and granites	91
3.10	LAMPROPHYRIC INTRUSIONS OF THE NARIN-PORTNOO AREA	92
3.11	THE KILREAN APPINITIC INTRUSION	93
3.11.1	Contact relationships and lithological variation	93
3.12	MINOR INTRUSIONS AND BRECCIA PIPES	94
3.12.1	The Glenard intrusion	95
3.12.2	The Crockard granite	98
3.12.3	The Kilkenny School intrusion breccia pipe	98
3.12.4	The Biroge breccia pipe	99
3.12.5	The Dunmore Hill intrusion breccia	101
3.13	SUMMARY	102
3.13.1	Form of intrusions	103
3.13.2	Petrology of the intrusions	104
3.13.3	Emplacement mechanisms of the appinitic intrusions	104
CHAPTER FOUR	PETROGRAPHY AND MINERAL CHEMISTRY	106
4.1	PETROGRAPHY OF THE MAIN ARDARA PLUTON	106
4.1.1	Outer quartz monzodiorite (G1)	106
4.1.2	Inner quartz monzodiorite/granodiorite (G2)	108
4.1.3	Central granodiorite (G3)	109
4.1.4	Minor intrusions: microgranite sheets, pegmatites and aplites	109
4.1.5	Enclaves	110
4.2	PETROGRAPHY OF THE APPINITES	111
4.2.1	Appinites of the Ardara suite	111
4.3	THE PETROGRAPHY OF THE SUMMY LOUGH DIORITE COMPLEX	117
4.3.1	Crystallisation of the hornblendite and coarse appinite	118
4.3.2	The pelitic aureole	118
4.4	THE PETROGRAPHY OF THE CROCKARD GRANITE	119

4.5	THE PETROGRAPHY OF THE GLENARD INTRUSION	119
4.6	THE PETROGRAPHY OF THE MULNAMIN INTRUSION	121
4.7	THE PETROGRAPHY OF THE KILREAN INTRUSION	125
4.8	THE PETROGRAPHY OF THE MEENALARGAN COMPLEX	126
4.9	THE PETROGRAPHY OF THE NARIN-PORTNOO SHORE SECTION	130
4.9.1	Foragy Rock	130
4.9.2	Tidy Rock	132
4.9.3	Cathleen's Hole	134
4.9.4	Fairy Coves	136
4.9.5	Eastern, Central and Western granites of the Portnoo area	137
4.10	PETROGRAPHY OF THE BRECCIA PIPES AND INTRUSION BRECCIAS	140
4.11	MINERAL CHEMISTRY	142
4.11.1	Analytical methods	142
4.11.2	Amphibole compositions	143
4.11.3	Hornblende geobarometry	154
4.11.4	Hornblende geothermometry	158
4.11.5	Discussion of results	161
4.12	PYROXENE	163
4.12.1	Pyroxene geothermometry	163
4.13	BIOTITE	166
4.14	PLAGIOCLASE FELDSPAR	171
4.15	EPIDOTE	172
4.16	EXSOLUTION TEXTURES	173
4.16.1	Petrography	173
4.16.2	Microprobe analysis: mineral chemistry and microtextures	174
4.16.3	Origin of exsolution	178
4.17	CONCLUSIONS	180
CHAPTER FIVE	MAJOR AND TRACE ELEMENT GEOCHEMISTRY	182
5.1	INTRODUCTION	182
5.2	COMPOSITIONAL CHARACTERISTICS OF THE ARDARA IGNEOUS COMPLEX	182
5.3	COMPOSITIONAL VARIATIONS BETWEEN APPINITIC BODIES	202
5.4	COMPOSITIONAL VARIATIONS WITHIN INDIVIDUAL APPINITIC INTRUSIONS	207
5.5	COMPARISON OF TRENDS WITHIN APPINITIC BODIES	207
5.6	FRACTIONAL CRYSTALLISATION AND DIFFERENTIATION OF THE ARDARA APPINITES AND GRANITOIDS	212
5.6.1	The Ardara pluton	214
5.6.2	Narin-Portnoo	218
5.5.3	Meenalargan	220
5.5.4	Summy Lough	229
5.5.5	Mulnamin	229
5.7	APPINITE COMPOSITIONS AT A LIMESTONE-APPINITE CONTACT	229
5.8	CONCLUSIONS	235
CHAPTER SIX	A STABLE ISOTOPE STUDY OF THE PORTNOO APPINITE AND ITS AUREOLE	241
6.1	INTRODUCTION	241
6.1.1	Aims and objectives of isotope study	243
6.1.2	Sampling	243
6.1.3	Importance of volatiles in magmas	243
6.1.4	Stable isotope analysis	244

6.1.5	Fluid movement associated with magmatic intrusions	245
6.1.6	Source of magmatic and meteoric fluids	246
6.1.7	Application of stable isotopes to studies of fluid interaction	247
6.1.8	Context of this research	247
6.2	MODELS OF APPINITE-COUNTRY ROCK-FLUID INTERACTION	248
6.2.1	Isotopic composition of model end-members	248
6.2.2	Model variants	250
6.2.3	The limestone-appinite contact at Portnoo	254
6.3	GEOCHEMISTRY	257
6.3.1	Sampling	257
6.3.2	Stable isotope analysis	257
6.3.3	Description of results	257
6.4	INTERPRETATION OF RESULTS	266
6.5	SYNTHESIS OF RESULTS AND INTERPRETATION	272
6.6	THE SHAPE OF GEOCHEMICAL FRONTS	275
6.7	DYNAMIC MODEL OF FLUID-ROCK INTERACTION AT A LIMESTONE/APPINITE CONTACT	275
CHAPTER SEVEN	PETROGENESIS AND EMPLACEMENT OF THE ARDARA COMPLEX: DISCUSSION AND CONCLUSIONS	278
7.1	INTRODUCTION	278
7.2	PETROGENESIS OF THE ARDARA APPINITES	278
7.2.1	Parental magmas	278
7.2.2	Source of volatiles	281
7.2.3	Magma mingling and mixing	282
7.2.4	Crustal contamination	282
7.2.5	<i>In-situ</i> differentiation	283
7.2.6	Petrogenetic model	285
7.3	TECTONIC CONTROLS ON EMPLACEMENT	287
7.3.1	Structural controls	287
7.3.2	Emplacement mechanisms	289
7.3.3	Regional tectonic controls	289
7.4	ARDARA APPINITES: SOME IMPLICATIONS	292
7.4.1	Appinite nomenclature	292
7.4.2	Fluid circulation systems	294
7.4.3	Composition-emplacment mechanism relationships	294
7.5	PETROGENESIS OF THE MAIN PLUTON	294
7.5.1	Parental magmas of G1 and G2	294
7.5.2	Parental magma of G3	295
7.5.3	Characterisation of the granite of the main Ardara pluton	295
7.5.4	Differentiation of the complex	296
7.5.5	Model for the development of the plutonic complex	296
7.6	THE ARDARA PLUTONIC-APPINITIC COMPLEX AND THE CALEDONIAN OROGENY	297
7.6.1	Tectonic setting	297
7.6.2	Emplacement level	298
7.6.3	Regional correlations	300
7.7	SUGGESTIONS FOR FURTHER STUDY	301
7.8	CONCLUSIONS	301
	BIBLIOGRAPHY	304
	APPENDICES	316
APPENDIX 1	Sample location	316
APPENDIX 2	Sample preparation and analytical techniques	319
A 2.1	Stable isotopic analysis-preparation	319
A 2.1.1	Preparation	319

A 2.1.2	Isotopic ratio determination	319
A 2.2	X-ray fluorescence analysis	320
A 2.3	X-ray diffraction analysis	320
APPENDIX 3	Whole rock analysis by X-ray fluorescence	321
APPENDIX 4	Stable isotope analyses	326
A 4.1	Oxygen	327
A 4.2	Carbon	328
A 4.3	Hydrogen	329
APPENDIX 5	Mineral chemistry	330
i.	Pyroxene analyses	330
ii	Hornblende analyses	332
iii.	Biotite analyses	345
iv	Plagioclase analyses	348
v	Epidote analyses	351
APPENDIX 6	GEOLOGICAL MAPS OF THE ARDARA IGNEOUS COMPLEX	352
MAP 1	GENERAL LOCATION MAP OF THE ARDARA AREA	352
MAP 2	THE GEOLOGY OF THE NORTHERN PART OF THE ARDARA PLUTON	352
MAP 3	THE GEOLOGY OF THE MEENALARGAN INTRUSION	352
MAP 3'	THE GEOLOGY OF THE AREA S.E. OF LOUGH LARAGH, MEENALARGAN	352
MAP 4	THE GEOLOGY OF THE SUMMY LOUGH DIORITE	352
MAP 5	THE GEOLOGY OF THE MULNAMIN INTRUSION	352
MAP 6	THE GEOLOGY OF THE NARIN-PORTNOO INTRUSION	352

Frontispiece. Double rainbow over Gweebara Bay, Co. Donegal photographed from the
Kilkenny intrusion breccia pipe.



CHAPTER ONE

INTRODUCTION

1.1 GEOLOGICAL SETTING

A cluster of over 30 appinitic intrusions is centred around the diapiric granitoid pluton of Ardara, Co. Donegal, Eire, (Fig. 1.1 a). The appinites comprise a suite of coarse grained, leucocratic to melanocratic rocks, rich in hornblende and plagioclase. "Appinite" is a broad term used by petrologists to describe rock types with a coarse grain size consisting of varying proportions of acicular hornblende, olivine, augite and/or biotite phenocrysts set in a felsic groundmass dominantly of plagioclase with lesser amounts of alkali feldspar and quartz. Accessories include titanite, magnetite, ilmenite, pyrites, zircon, apatite, epidote, calcite and prehnite. Appinitic intrusions show a wide range of emplacement mechanisms from large stock-like complexes to dome, sheet, sill and dyke intrusions but also diatreme-like breccia pipes with an apparent gas-driven emplacement mechanism.

The appinite suite shows strong chemical affinities with 'wet' basalts and gabbros. They are principally found associated with Caledonian granitic plutons of Scotland and Ireland but examples have been described from other granitic plutons and from different orogens throughout the world. As such they form part of a distinct suite of intrusions, with variable emplacement mechanisms which appear to be genetically associated with the early phases of granitoid plutonism in the later stages of orogenesis. In nearly all cases the appinites were emplaced earlier than, or synchronous with the granitic magmatism, and are taken to be petrogenetically related to these granites. The precise nature of inter-relationship in terms of mantle/crust interaction has not been established. It is also apparent from appinite emplacement mechanisms and petrography that there is an important volatile phase, rich in CO₂ and H₂O. The nature of the fluids associated with the appinitic magmas, their emplacement and crystallisation, and interaction with their country-rock envelope has never been critically evaluated using modern techniques. It is thus pertinent to tackle some of these appinite problems using such techniques applied to an area which shows most of the features and problems associated with appinites, namely textural variation, differing emplacement mechanisms, close temporal and spatial association with a granitic pluton, fluid/crust interaction as well as chemical and petrographic variation in a well exposed area. Such an area is found in the satellite intrusions around the late Caledonian pluton of Ardara, Co. Donegal (Fig. 1.1 b). The intrusions concentrated on are, Crockard, Kilrean, Meenalargan, Mulnamin, Narin-Portnoo and Summy Lough and the breccia pipes of Biroge, Dunmore and Kilkenny.

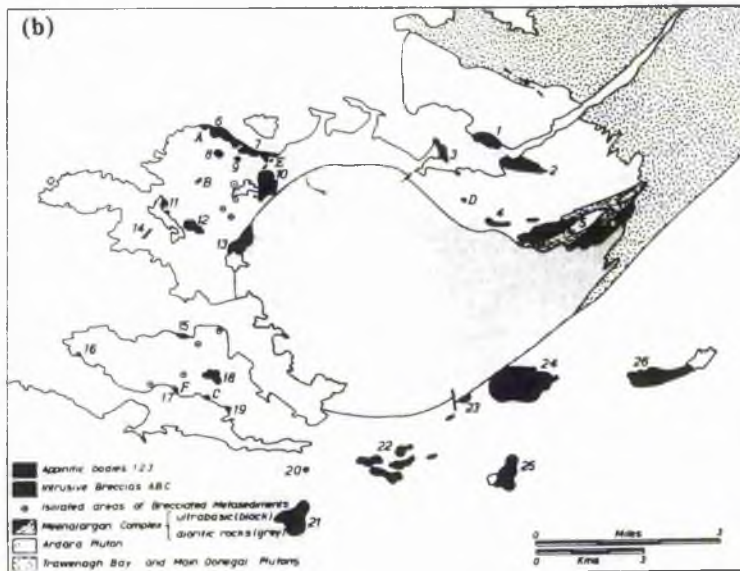
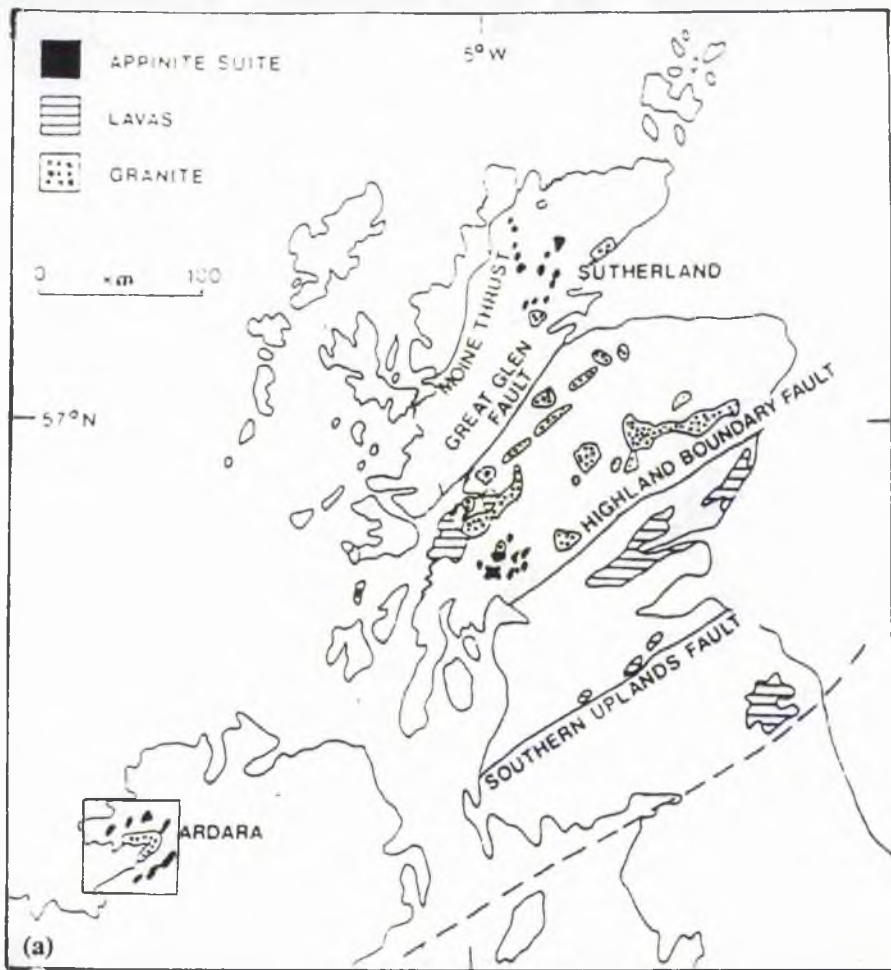


Fig. 1.1 (a) General location map of the appinite suite and associated granites of the Scottish and NW Irish Caledonides after Hammidullah & Bowes (1987). (b) The Ardara cluster of appinitic intrusions, from Pitcher & Berger (1972).

1.2 CONTEXT OF RESEARCH

The origin of the appinite suite in Caledonian geology is important for the following reasons:

(a) Appinites are enigmatic features of orogenic granitoids

(i) They are very common in the Caledonian orogeny but perhaps because of problems in nomenclature they are apparently less common elsewhere.

(ii) Appinites are often referred to in the literature but are poorly defined and described, there have been very few modern studies, Hammidullah (1986) and Hammidullah and Bowes (1987) being recent exceptions.

(b) Magma composition

(i) Appinites form the most basic members of many granitic plutons, a point which is often not appreciated in discussions of pluton petrogenesis.

(ii) They have been compared to "wet basalts" (Hall 1967) but is there a distinct 'appinitic' magma and if so, how is it related to the granitic magma of the main pluton?

(c) Volatile content

(i) Appinites are thought to be volatile-rich with a high percentage of H₂O and CO₂. Their sub-volcanic equivalents, lamprophyres, are currently thought to be mineralised (Rock et al. 1985) sometimes with Au-bearing assemblages.

(ii) The origin of the fluids, their transport mechanisms and the relationships between high level emplacement and fluids in the country rocks, are all currently poorly constrained.

(d) Emplacement

(i) Appinites were emplaced early in the plutonic sequence.

(ii) They show a wide range of emplacement mechanisms.

(iii) The relationships between composition and structure of the appinite and its country rock envelope, and the emplacement history of the appinite to its associated granite are not well understood.

(e) Petrogenesis

(i) Appinites are apparently mantle-derived in what is largely a setting of crustal magmatism. Hall (1967) compared them to wet basalts, Pitcher and Berger, (1972) compared them to cumulates from a pyroxene and amphibole, water-rich facies of a basaltic magma.

(ii) Are they one end-member in a hybrid sequence as suggested by Pitcher and Berger (1972) and Deer (1950, 1953).

(iii) Appinites are apparently most commonly found in the Caledonian orogen. Does the Caledonian orogeny have a special significance in terms of appinite genesis as a function of its space-time composition characteristics?

(iv) Are appinites in any way parental to the granitoid sequence and if so what processes control the generation of granitic rocks?

(v) The relationship of appinite to lamprophyres are interesting. Rock (1984) noted the spatial and temporal relationship of calc-alkaline spessartitic lamprophyres to the post-orogenic granites and more especially to appinite-breccia-pipe complexes. Henney et al. (1989) also noted this granitic association in the British Caledonides and suggested, using AFC modelling that primitive hornblende lamprophyres became contaminated with local crust to form diorites and granodiorites. They thus suggest that lamprophyres are the parental source of less evolved granitic magmas.

(vi) Are appinites a source of enclaves? Akaad (1956) first noted the presence of appinitic xenoliths in the Ardara granitic pluton. If appinites are related to granitic magma, this may be as cognate xenoliths caught up in the granitic magma.

1.3 AIMS AND OBJECTIVES

The Ardara area is probably the best example in the British Isles (and probably therefore in the world) in which to study the varied emplacement mechanisms of appinites. The number of appinitic bodies, the wide variation in petrographic type, form and texture and the quality of exposure all make this area ideal for the study of the structure and composition of appinitic rocks. It is the general aim of this study to relate all the characteristics of these different appinitic bodies and the main Ardara pluton in an attempt to understand the dynamic history of a mesozonal granitic pluton with abundant associated appinites. More generally it is a study of an example of the interaction of mantle-derived and crustal-derived magmatism.

Specifically the aims are:

(a) To understand the petrogenesis of the appinite suite, using several different yet related appinite bodies from the Ardara area.

(b) To understand the emplacement of the appinite suite, using several different appinite bodies from the Ardara area.

(c) To understand the origin, evolution, emplacement and crystallisation history of the magmas constituting the Ardara area.

(d) To compare the appinites of Ardara with those elsewhere in the Caledonides and in other orogens with a view to understanding better, crust-mantle relationships in orogenic granitoid belts.

(e) To classify 'appinite' according to internationally accepted parameters and to standardise the definition of the appinite suite.

1.4 METHODOLOGY

(a) Field mapping: Detailed maps were made of four main areas of appinite as well as parts of the main Ardara pluton and various breccia pipes. Accurate sketch and

base maps of the structure and nature of the intrusions and their contact relationships with the Dalradian country have been drawn up at various scales, (Appendix 6).

(b) Sampling: representative rock specimens were collected for petrographic and geochemical studies, (see appendix one for breakdown of their types and localities).

(c) Petrography: light optic and scanning electron optical (secondary and backscattered electrons) techniques were used to establish textural relationships and crystallisation sequences.

(d) Mineral chemistry: the compositions of minerals were determined by electron microprobe analysis and are used to establish mineral equilibrium features as well as processes such as sub-solidus re-equilibration.

(e) Whole rock major and trace element geochemistry: data on the geochemistry of 'type' rocks of the appinitic intrusions studied are used in modelling the origin of appinitic and granitic magmas and their crystallisation histories.

(f) Isotope geochemistry: both whole rock and mineral separates were used in a single well defined problem concerning fluid migration in the Portnoo appinitic intrusion. This appinite body was investigated by stable isotopes with a particular aim of establishing volatile exchange between magma and host rock.

(g) Integrated approach: many parameters, (field relationships, structure, mineral texture, mineral chemistry, major and trace element geochemistry) were integrated to relate the appinites to their host rocks and associated main pluton.

1.5 THESIS ORGANISATION

Chapter 2 is a review of appinites ranging from the type area of the Appin district to other appinites in the Caledonian orogen as well as similar rock types elsewhere in the world, leading to a discussion of the terms "appinite" and "appinite suite". Chapter 3 describes the geological setting of the appinite suite in the Caledonian orogen and more specifically describes the field relationships of the individual intrusions around the Ardara pluton and the main Ardara pluton. The field relationships are discussed and interpreted. Chapter 4 is a presentation of petrographic features and mineral chemistry of the Ardara appinite suite and the various facies of the main Ardara pluton. Chapter 5 presents the whole rock major and trace element geochemistry of the appinite suite and the main Ardara pluton. Chapter 6 deals with a specific problem involving the role of fluids in the genesis of appinites and contamination/exchange with calcareous country rock, using the stable isotopes of O, H, and C. Chapter 7 discusses the constraints on the petrogenesis of appinites, drawing together all the evidence of the previous chapters in the form of a model for the formation of appinitic magmas, their role in granite magmatism and their bearing on the Caledonian and other orogens, along with presentation of conclusions together with suggestions for further research.

CHAPTER TWO

PREVIOUS RESEARCH ON APPINITES AND RELATED ROCKS

2.1 INTRODUCTION

It is important in the context of this research to consider the environment of appinite genesis, its geological setting and the temporal and spatial occurrence of the appinite suite. In this chapter a brief outline of the orogenic setting of the Caledonian orogen and discussion of the models on Caledonian magmatism are given. A section then follows on known appinite occurrences in the Caledonian of the British Isles and within other orogens around the world. The final part of the chapter is a discussion of the terms "appinite" and "appinite suite" and outlines the current models for appinite petrogenesis.

2.1.1 Regional distribution

Studies of the Caledonian igneous geology of the British Isles have paid scant attention to the importance of the "appinites" and the "appinite suite", so-called after the distinctive rocks of the Appin district of Argyll, Scotland by Bailey & Maufe (1916). As well as occurring in the SW Highlands of Scotland, this suite of rocks is widespread throughout the Caledonides, and as pointed out by Read (1961) they are almost uniquely associated with the Newer Granites in Scotland and Ireland (Fig. 1.1 a).

The Newer Granites are concentrated in a belt striking NE-SW from the Grampian region of NE Scotland to the west coast of Galway. Most of the Scottish granite-appinite occurrences are situated in a belt around the Grampian Highlands between the Highland Boundary Fault (HBF) and the Great Glen Fault (GGF), with only a few located to the north of this latter fault, whilst several major complexes are located to the south of this fault (Fig. 2.1).

2.1.2 Appinites in orogens

The appinite suite is an integral part of the magmatism associated with the Caledonian orogeny. Models of plate subduction for the formation of the orogen are common as are models of associated basic and acid magmatism related to ocean-continent collision involving crustal and mantle input.

Although the basic magmatism of the Newer Gabbros seen in NE Scotland is considerably older (510-480 Ma according to Wadsworth 1982) than the appinitic intrusions and thought to be syn-orogenic with the Caledonian (the appinites are post-orogenic), it is never-the-less an important part of Caledonian magmatism and compares with that seen in the Scandinavian sector of the orogen and also that of the Appalachians of North America (Whalen et al. 1987, Chandler et al. 1987). However, most of the

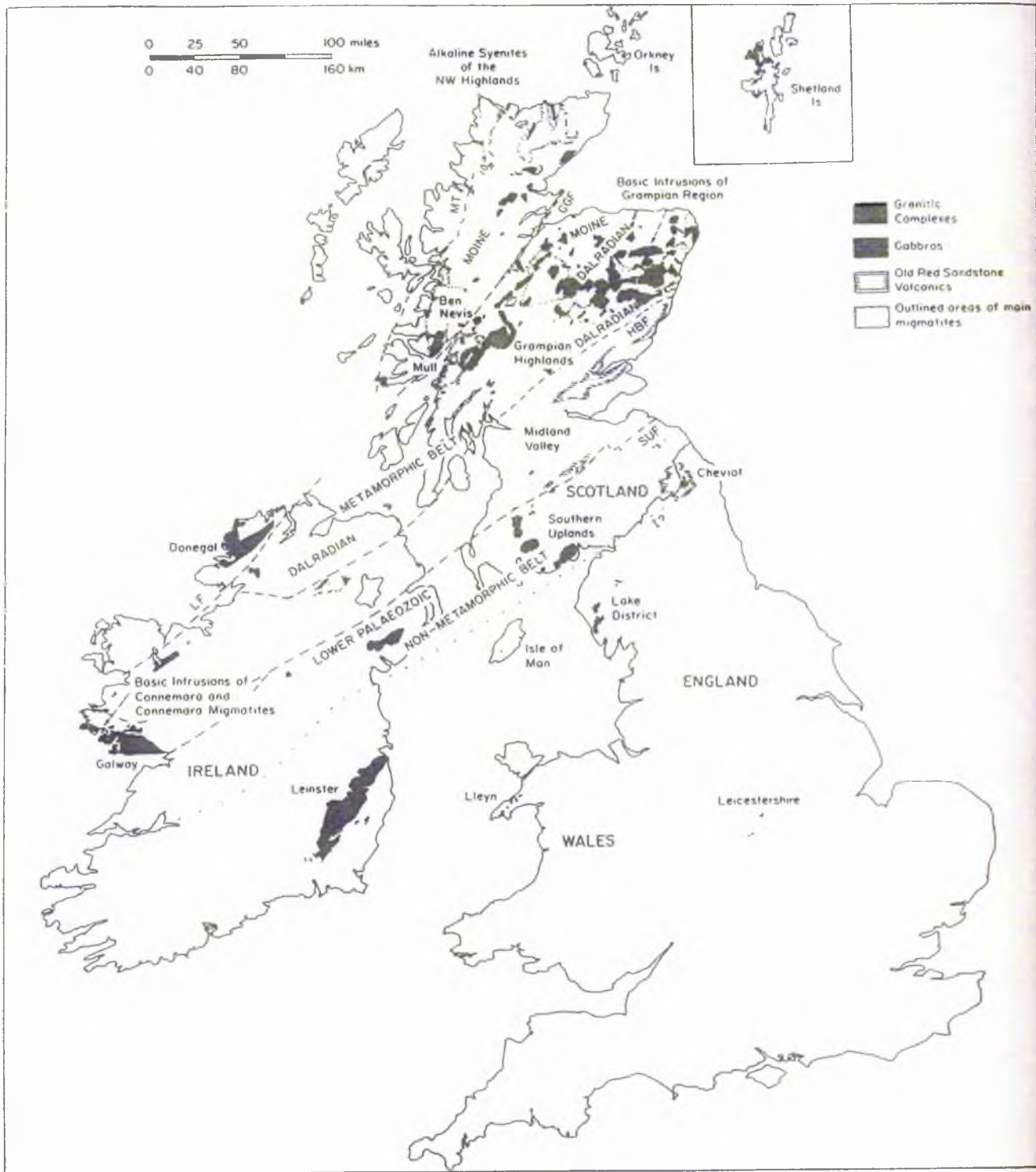


Fig. 2.1 Caledonian intrusions of the British Isles, showing the main zones of the fold-belt, and major faults. MT=Moine Thrust; GGF=Great Glen Fault; HBF=Highland Boundary Fault; SUF=Southern Uplands Fault; LF=Leannan Fault; I, possible course of the Iapetus suture (after King 1983).

appinite magmas are intruded in a post-tectonic setting associated with the Newer Granites in the period around 425 Ma (Rogers & Dunning 1990).

It seems that most major magmatic provinces related to ocean-continent collision settings have associated acid-basic magmas, the basic magma often having an appinitic affinity (Pitcher et al. 1985, Mullen & Bussell 1977) but in continent-continent collision zones this association is always missing. For instance there have been no reports of appinitic rocks from the Himalayas, a region of intense crustal melting and 'S' type granites (LeFort, 1986). The question arises as to whether this granodioritic-appinite association is unique to the Caledonian orogeny, the magmatism of which will now be briefly described.

2.2 MAGMATISM IN THE CALEDONIAN OROGEN

The Caledonian orogenic belt of Scotland and Ireland comprises over 100 granitic and dioritic intrusion complexes ranging in form from small sheets and stocks to large batholithic masses. The majority of the intrusions occur in the Orthotectonic Caledonides, north of the Highland Boundary Fault (HBF). This fault seems to place an important structural control on granite generation and emplacement. Pidgeon and Aftalion (1978) in a U/Pb study of the Newer Granites discovered that zircons separated from some of the granitoids to the north of the HBF yielded upper concordia intercept (inheritance) ages some 800-1000 Ma older than the emplacement ages of the granites. No zircon separates from south of the HBF have yet yielded older age intercepts. As inherited zircon is generated from the assimilation of older crust into the magmas they concluded that the HBF was the southerly limit of old Archaean (Lewisian) basement beneath the Caledonian cover. Stephens & Halliday (1984) defined a Mid-Grampian line as the cut-off between two intrinsically different crustal terranes. Thus there may be a fundamental difference in basement lithologies beneath the Orthotectonic Caledonides (north of the HBF) and the Paratectonic Caledonides (south of the HBF). Kennan et al. (1979) noted fundamental differences in the magmatic signature of the deep crust at the margin of the Iapetus suture indicated by the differences in U/Pb contents. Two of the largest granitic batholiths in Britain and Ireland, with associated appinites, are to be found either side of the Iapetus suture in Leinster and Donegal, (Fig. 2.1)

The first overview of Caledonian granites and their associated rocks was published by H.H. Read in 1961. He divided the granites into 'Older Granites' and 'Newer Granites' and further subdivided the latter into Forceful Granites and Last Granites. Read used the term 'Older Granites' for those intrusions formed during the 'active' deformation of country rocks, often with the formation of 'contact migmatites'; Read took these granites to be relatively early, from the inclusion of boulders of 'Older Granite' in the basal Lower Old Red Sandstone. In fact most of these intrusions were

emplaced shortly after the climax of metamorphism during the early to mid Ordovician (Pankhurst & Sutherland, 1982).

The 'Forceful Newer Granites' were emplaced during the late Ordovician and early Silurian, post-dating the peak of metamorphism by several millions of years and in a post-tectonic setting. The 'Last Granites' of Read's classification he also associated with the Lower Old Red Sandstone, mostly in the form of passive intrusions, emplaced by large-scale ring faulting and cauldron subsidence within the Lower Old Red Sandstone volcanics and sediments, for instance at Ben Nevis and Glencoe. Subsequent classifications have been based on age and geophysical signature (Brown 1979), suites (Stephens and Halliday 1984), associated metalliferous deposits (Plant 1986), and other parameters. In all classifications the appinites are associated with the late, medium to high level I-type plutons. The small basic, and dioritic intrusions found in Argyll, Leinster and Donegal and considered in this thesis, are associated with both varieties of these "Newer Granites".

2.2.1 Tectonic setting

Several models for the development of the Caledonides have been proposed, two contrasting examples are briefly considered here:

(a) Watson (1984) considered that Scotland and NW Ireland were derived from the marginal parts of the N Atlantic continent; the Highland region of Scotland being separated from the continental margin by a more stable block of continental crust represented by the Midland Valley which in turn lay to the north of a prism-block of slope and trench deposits that were stacked up in the Southern Uplands (Legget et al., 1979). Compressive deformation of the Dalradian basin in the Highlands began in the late Cambrian (the Grampian orogeny) which resulted from the collision of a microcontinent which Watson (1984) believed may now underlie the Midland Valley. Ensuing subduction during the Ordovician and Silurian resulted in a narrowing of the Iapetus Ocean as the plates subducted north-westwards of the Dalradian basin. The European and N Atlantic continents became locked together by late Silurian times and were elevated to form the Old Red Sandstone (ORS) continental landmass. At the same time deformation by ductile processes gave way to brittle deformation, the intensity of which decreased as the crust stabilised and became uplifted (Watson, 1984). The final climax came with the emplacement of the Newer Granites, minor intrusions and volcanics (Read, 1961). There is dispute over the actual timing of the collision process (cf. Yardley et al. 1982, Dewey 1982) but most authors agree to a NW dipping subduction zone coupled with lateral, often sinistral (Hutton, 1987) displacement of crustal blocks with the development of arc magmatism at the margin of the N Atlantic continent.

(b) Hutton (1987) proposed a terrane-based model which questioned the existence of a single Iapetus suture line. Instead he recognised a series of terranes which were

broken up and displaced by sinistral strike-slip motion between the Grampian terrane miogeocline and the Midland Valley platform (i.e. between Gondwanaland and Laurasia). He envisaged a three plate model of collision for the Caledonides with collision between three plates, Laurentia, Baltica and Gondwanaland (Fig. 2.2 a). Collision of Laurentia and Gondwanaland coincided with the end of NW subduction on the Laurentian margin, halting at 435-410Ma (mid-Silurian), the time at which most of the Newer Granites were emplaced (Fig. 2.2 b). Sinistral strike-slip occurred between the closing Laurasian (Laurentia and Baltica) plate and Gondwanaland at 410-380Ma. Hutton (1987) believed this sequence of events implies that Gondwanaland carried Laurentia into collision with Baltica which then broke free disrupting the Ordovician and Silurian palaeogeography of the British-North American Iapetus sector, before finally and climactically locking with the plates of this zone in the early Devonian. He envisaged that from mid-Ordovician times onwards, a converging and clockwise rotation of Gondwanaland acted as the main driving force behind the Caledonian orogeny (Fig 2.2 c). The sinistral shear motion advocated by Hutton (1987) may be related to the peak of Caledonian magmatism (435-400Ma). This is supported by evidence from individual plutons, for example the biotite granite of Strontian which is emplaced in a shear zone termination of the sinistral Great Glen Fault (Hutton 1987). This fault, like the HBF, may have acted as a deep-rooted structure with important implications for the emplacement of magma, especially in the light of seismic evidence of Brewer et al. (1983), which indicates that the GGF may reach mantle depths.

The magmatic development of this province is thus related to continental convergence. The early magmatism was largely S-type (Chappell & White 1974) and occurred prior to 430Ma, however the magmatism that is the subject of this thesis occurred during the end stages of the orogeny, in a largely post-tectonic setting. Chappell & Stephens (1988) noted that the Caledonian event did not produce large amounts of new crust, it was primarily a vertical redistribution of older crust. Some of this was of metasedimentary origin but most was of igneous composition formed as an underplate before the main post-tectonic event. It was into this crust that the basic and acid magmas were emplaced, at 430-400Ma, after the cessation of subduction upon closure of the Iapetus Ocean (Watson 1984).

2.2.2 Earlier magmatism

The magmatic events which accompanied the development of the Caledonian fold belt have been summarised by Read (1961) into pre-, syn- and post-tectonic episodes. Within this scheme he recognised early stages of basic and acid plutonism.

(a) Early basic magmatism.

Early basic magmatism was synchronous with the climax of the main regional metamorphism and is represented by the basic peridotites and gabbros of NE Scotland

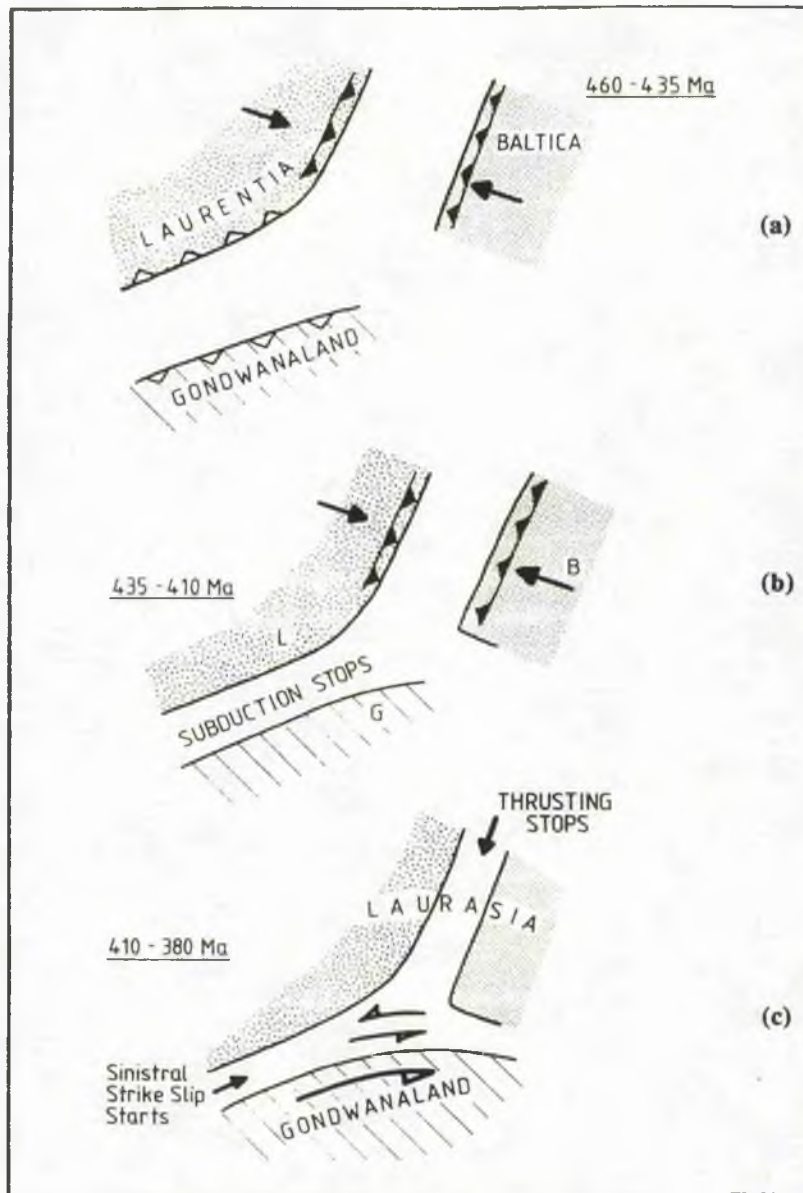


Fig. 2.2 Three-plate model for the closure of the Iapetus suture (after Hutton, 1987). See text for details.

and Connemara (Pankhurst, 1970). In Donegal the earliest signs of basic magmatism took a different form, as the intrusion of tholeiitic quartz dolerite magma as sills into the Dalradian country rock. They were subsequently metamorphosed during the Caledonian but are known to be autochthonous because of the development of static hornfels aureoles around them. The best known of these is the Maam sill which is ~10 to 80m wide and ~24km long, striking parallel to the country rock trend (NE-SW) through Donegal.

(b) Acid magmatism

The first manifestation of granitic magmatism takes the form of largely pre-deformational well-defined masses e.g. Carn Chuineag and Inchbae granites of the N.

Highlands (Pankhurst & Sutherland 1982). The age of these masses is relatively well constrained compared to the widespread so-called 'injection complexes', 'migmatites', 'gneisses' and Older Granites of the Grampian Highlands and the Buchan region of NE Scotland. These rarely form distinct masses, instead taking the form of pegmatitic, syn-tectonic bodies ranging in composition from granodiorite to alkali granite, with abundant apparent potassium metasomatism, a feature common to migmatites.

2.2.3 Later magmatism

The 'Newer Granites' of Read's classification are calc-alkaline plutons of predominantly granodioritic to granitic composition. Many have basic to intermediate facies associated with them, including the appinite suite. Newer granites form distinct plutons with sharp contacts with their envelopes, occasionally with deformed margins, depending on their emplacement mechanism. Thermal aureoles may be developed around them, although this may be a function of emplacement mechanism as well as the size and morphology of the intrusion. Early, outer facies are commonly more basic (diorite to granodiorite) than the inner facies which is usually more felsic (normally granitic).

Modern opinion varies as to the importance of crustal or mantle sources for the post tectonic granites. The Caledonian orogenic belt as a whole developed during a period of increased crustal activity when compared with the Archaean and early Proterozoic and it is clear that the 'Older Granites' are more closely related to anatectic crustal source than the 'Newer Granites'. However modern techniques of isotope geochemistry have highlighted the importance of both the crust and the mantle as important primary sources, as a result a number of 'schools' of thought on their petrogenesis have emerged.

Stephens and Halliday (1984) divided the 'Newer Granites' of Scotland into suites depending on their trace element features and found that there is a geographical difference between those of the Cairngorm, Argyll and the south of Scotland regions, related to differences in magma source and melting conditions. They believe the mantle of the north of Scotland is 'old mantle', attached to the base of the old crust and has been enriched in K, Ba, Sr in the past by metasomatic processes. Various authors have classified the Caledonian granites on the basis of their origin as I- or S-type (Chappell & White 1974). Stephens (1988) applied the I- and S-type classification to the Caledonian granites and demonstrated that broad variations from mostly I-type granite with occasional S-type characteristics occur in the plutons of both the Donegal and Leinster batholiths. Both of these are composite batholiths and are made up of zoned plutons with associated appinitic intrusions.

Simpson et al., (1979), Plant et al. (1980, 1983) and Thirlwall (1981,1982) argued that most of the post-orogenic granites north and south of the Iapetus suture are I-type, derived from trace element enriched, compositionally zoned subcontinental lithosphere by a process that is used to account for changes in the composition of contemporaneous

LORS volcanics across Scotland (Thirlwall, 1981) although they recognised a lower crustal component in these. Plant et al. (1983) and Watson (1984) related changes in magma composition to deep faulting of previously metasomatised mantle/lower crust rather than to magmatism over an active subduction zone. They attributed the S-type characteristics of their I-type magmas to reaction of I-types with hydrous crustal rocks by way of a fluid phase. Thirlwall (1982) suggested that differences in the volcanics of the SW Highlands and the Midland Valley are due to mantle heterogeneity. He proposed a metasomatised LREE-depleted upper mantle and attributed variations in the mantle to mantle layering of both LREE depleted and deeper enriched mantle. The volcanics he studied are predominantly basaltic.

The models summarised above are concerned with the wider problem of the origin of the calc alkaline magmas. The next section however briefly summarises the previous research into the origin of the appinites and their relationships to the granites with which they are associated.

2.3 CALEDONIAN APPINITES

The ultramafic to intermediate rocks with characteristic texture and calc-alkaline to mildly alkaline chemistry which are grouped into the appinite suite commonly form numerous small pipes and larger plutonic complexes across the Caledonian of Scotland and Ireland (Fig. 2.3). Their major and trace element characteristics suggest they have a major mantle input (French 1966, Hall 1967, Pitcher & Berger 1972, Wright & Bowes (1979). Their close temporal and spatial association with the Newer Granites (Read, 1961) has been confirmed radiometrically by Rogers & Dunning (1990). Appinites occur widely throughout the Caledonides but perhaps they are best known from the type area of Appin in the SW Highlands of Scotland, (Bowes & Wright 1967). Some of the general features are tabulated at the end of this section (Table 2.1.).

2.3.1 Scotland

(i) The Appin District

The type area of Appin in the SW Highlands (Fig. 2.4) is a region with >20 appinitic intrusions of widely variable composition, mainly in the form of explosion breccia pipes (Bowes & Wright 1961). Bowes & Wright related the emplacement of these pipes closely to the regional structure of dome-shaped structural traps, with a major control exerted by the regional cleavage and parasitic folds on the axis of the Cuil Bay synform. These authors envisaged the following sequence of events for the genesis of the explosion breccia pipes:

(a) Explosive activity with shattering and brecciation of country rocks.

(b) Emplacement of variable but generally hornblende rich igneous rock types representing crystallisation at high to moderate volatile pressure.

Alkaline Syenites of the
NW Highlands

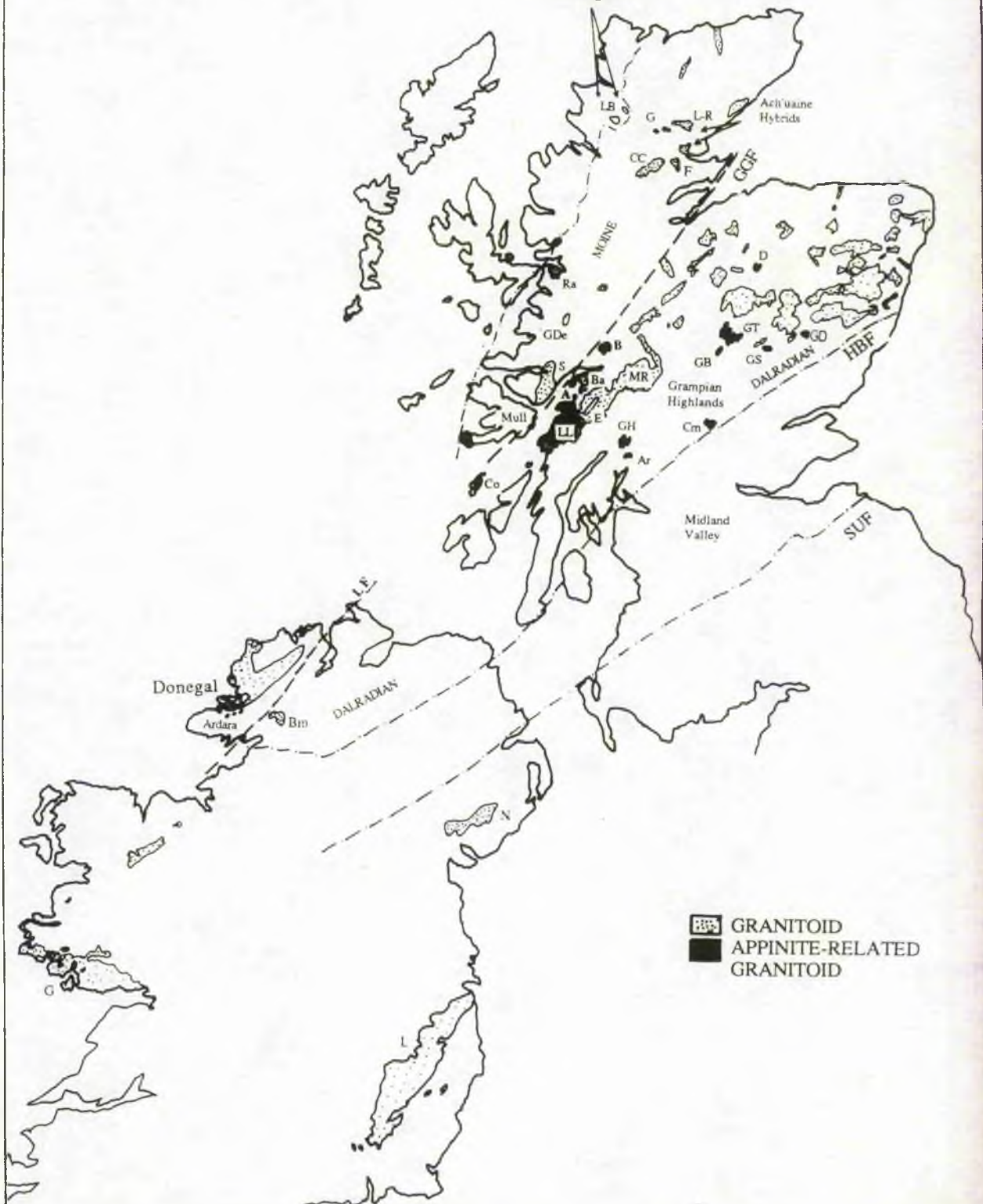


Fig. 2.3. Intrusive granitoid and appinite/diorite complexes in N. Britain and Ireland. Only those granitoids with associated basic (appinitic) intrusions are labelled. Beginning in the north: LB, Loch Borolan; G, Grudie; L-R, Lairg-Rogart; CC, Carn Chuinneag; F, Fearn; D, Dorbach; Ra, Ratagain; GDe, Glen Dessary; GT, Glen Tilt; GD, Glen Doll; B, Ben Nevis; GB, Glen Banvie; GS, Glen Shee; S, Strontian; Ba, Ballachulish; MR, Moor of Rannoch; A, Appin; E, Etive; GH, Garabal Hill; Cm, Comrie; Co, Colonsay; Ar, Arrochar; Ardara, Ardara pluton and associated appinites; Bm, Barnesmore; N, Newry; G, Galway; L, Leinster. The Lorne Lavas (LL) are shown as are major faults: GGF, Great Glen fault; HBF, Highland Boundary Fault; SUF, Southern Uplands Fault; LF, Leannan Fault.

(c) The emplacement of augite diorites or kentallenites representing crystallisation at low volatile pressure.

(d) The emplacement of generally small bodies of leucodiorite to granodiorite, possibly representing secondary hybrid liquids.

They compared this sequence with that which occurs in a volcanic setting, associated with the build up and release of pressure on the breaching of structural traps, formed by a resistant quartzite horizon.



Fig. 2.4 Outline geological map of the Appin district, near Ballachulish, western Scotland, showing the distribution of the appinite suite based on Sheet 53 (Ben Nevis and Glen Coe) of the Geological Survey of Great Britain and Bowes & Wright (1967) after Hamidullah & Bowes (1987).

Bowes & McArthur (1976) used major and trace element geochemistry to illustrate the close relationship between appinite and basaltic magma and postulated phlogopite-hornblende peridotite as a possible parental magma. They also outlined the

general characteristics of the suite. Their study was extended by the work of Hamidullah (1983) and Hamidullah & Bowes (1987) who used extensive major and trace element geochemistry as well as mineral chemistry to model the origin of appinites. On the basis of mineral chemistry Hamidullah modelled magma processes including, crystallisation under variable P_{H_2O} , crystallisation from residual magma, crystal accumulation, fractionation and explosive mixing of cumulates and residual liquid. Hamidullah then related these to the field relationships.

Hamidullah (1983), and Hamidullah & Bowes (1987) has extended the interpretation and database of Scottish appinites and added a new dimension by constraining the depth and temperature of appinitic magma genesis. Hamidullah (1983) used the composition of olivine, plotted as the molar %MgO v %FeO for various rocks of the Kentallen and Ardsheal Hill pipes, to determine whether equilibrium conditions existed between the magma and the minerals. He argued that the ultramafic rocks of Kentallen had a cumulate origin and that olivine was in equilibrium with the melt from which it crystallized. The lamprophyric marginal facies of the Ardsheal pipe was found to show a high degree of olivine fractionation and clinopyroxene accumulation. Hamidullah believed that this does not represent an original melt composition and proposed that complex fractionation processes were important in the genesis of these appinites.

From the pyroxene composition of the appinites Hamidullah & Bowes (1987) observed a transition from alkaline to calc-alkaline type, moreover they believed that P_{H_2O} increased in the pipes because, as crystallisation proceeded Al_z ($Al_z = Al^{iv} \times 100/2$) in pyroxenes shows a decrease with increasing Ti. Using hornblende compositions Hamidullah & Bowes estimated pressure and temperature of formation of the appinite with the equations of Raase (1974) and tentatively proposed ~3kb for overgrowths of actinolite and actinolitic hornblende on the primary pargasite, which they observed to be of greater pressure than the other hornblende in the appinite.

Using whole rock geochemistry Hamidullah & Bowes modelled a fractional crystallisation process to account for the trends seen in the ultramafics (kentallenite, cortlandtite) to appinite and through granodiorite, accounting for observed variations by the peculiarities of the crystallisation conditions in the individual pipes. Using CMAS tetrahedron projection techniques developed by O'Hara (1968) Hamidullah & Bowes plotted and modelled mineral fractionation trends by tracing the paths along which the principal minerals plot, along the different planes of the CMAS tetrahedron.

Application of these methods to the various pipes in the Ardsheal peninsula allowed Hamidullah to recognise how the rock types in the local appinite suite rocks relate to different intrusive parameters. Variations within the suite are explained using the evidence of mineralogy and phase relations. For instance, Hamidullah suggested that a cumulate magma was often emplaced in a mush-like state using the evidence of kinked phlogopite in the groundmass of the cumulates. Typically the hornblende in the appinites of the area

were envisaged to have been emplaced at a high level (<5kb and at 1000°C) into cool country rocks with subsequent amphibolitic overgrowths due to an increase in P_{H_2O} and decrease in temperature. Hamidullah & Bowes proposed that hornblende crystallised at 960-770°C and 2-4kb, while phlogopite formed at 1000°C and 1kb in the kentallenite. The feldspar matrix is thought to be associated with low pressure (1kb) and low temperature (<750°C) conditions and is thought to be related to the development of explosion breccias. Acidic rocks attributed to differentiation products of the feldspathic fraction with late hybrid liquid were produced by solution of silica from quartzite blocks at high pressure and temperature.

On a broader scale Hamidullah & Bowes attempted to relate the chemistry of the Scottish appinites to a subduction-type setting. They support this idea with chemical evidence of increased K_2O , Ba, Sr and Ce as the subduction zone is approached, corresponding to the spatial variation seen in other calc-alkaline rock series associated with destructive plate margins. The appinite suite of Appin may be genetically related to the local Ballachulish pluton. This is a zoned quartz monzodiorite to granodiorite body which post-dates the main phase of appinite emplacement and which shows some hybridisation with appinitic quartz diorites near the SE margin of the Ballachulish pluton (Weiss & Troll 1989).

(ii) Elsewhere in Argyll/Loch Lomond district

(a) Arrochar and Garabal Hill - Glen Fyne complexes

This complex lies just west of the head of Loch Lomond and stretches west to Loch Fyne. It occupies an area of ~25km² where the igneous rocks were emplaced in a largely post-tectonic setting. The Arrochar complex is a stock-like body of porphyritic granodiorite-quartz diorite which is similar to but separate from the Garabal Hill / Glen Fyne complex. A number of small intrusions are seen to cut the associated outer quartz diorite facies and several intrusions of appinite, kentallenite and peridotite occur outside the Arrochar pluton (Anderson 1935, Franchi 1983). These bodies are 10-20m wide and have pipe-like forms. An outcrop of kentallenite 450m wide occurs in the country rock with two small pipes of appinite within it. Thus there are many similarities with the pipes of Appin to the north, particularly in the large variation in composition from ultramafic to granitic. Titanites from a coarse grained appinite in the complex yielded a U/Pb date of 426 ± 3 Ma (Rogers & Dunning 1990)

Like so many of the appinite intrusions a wide variety of rock types occurs ranging from augite peridotite, pyroxene gabbro, olivine-bearing pyroxene mica diorite to xenolithic diorite, quartz diorite and granodiorite. Nockolds (1941) noted interesting reaction relationships between the acid granodiorite magma and more basic dioritic rocks. Both show modification by assimilation of more basic xenoliths, notably the granodiorite which is later than the other rocks of the complex and shows a high degree of

assimilation indicated by large numbers of xenoliths and an increase in ferromagnesian minerals, (biotite and hornblende-rich clots). Nockolds proposed that the pyroxene-mica diorite is the parental magma with progressive crystallisation differentiation accounting for the petrological variations.

(b) Ben Nevis

The Ben Nevis granite complex is located 5 km east of Fort William. The whole complex covers ~51 km² and has been dated between 382-399 Ma, using K/Ar ages from biotite (Hamilton et al. 1980). The granite is a ring-dyke complex emplaced in a tensional regime and is one of the later Newer granites of Read (1961). The complex is concentrically zoned from outer quartz diorite and granite to an inner granite. Haslam (1970) described appinite xenoliths from the north-western, dioritic part of the complex. He proposed that the xenoliths are the result of metasomatic hybridisation of calc-silicate rocks (the Ballachulish Limestone) by calc-alkali magma. He noted that the hornblende, which is rich in Ti, Al and Fe, and pyroxene are chemically different to the hornblende and pyroxene of the Ben Nevis granite and concluded that neither have formed in chemical equilibrium with a magma of the Ben Nevis suite but rather indicate crystallisation in a calcareous environment. He compares this reaction relationship to the findings of Deer (1953) from the Glen Tilt area of Perthshire.

(c) Glen Orchy

On the west side of Glen Orchy an elongate mass (1.3km x 0.15km) and two smaller masses occur. The bodies are dominantly kentalenitic but are locally variable to picrite. The early authors (Hill & Kynaston 1900) described these bodies as being closely related to the Ben Cruachan granite intrusion of Glen Etive, which has been dated at 396 ±12Ma by Clayburn et al. (1983). Other small intrusions in the area, mostly of augite diorite with abundant hornblende, include, Glen Strae, Meall Copagach and Ben Lurachan.

(d) Colonsay

On the island of Colonsay off the west coast of Scotland, Reynolds has described several appinitic intrusions (Reynolds 1936).

(iii) Grampian region (East Scotland):

(a) Glen Tilt

Deer (1953) described appinites from Glen Tilt and believed them to have formed by metasomatic reaction between Dalradian epidiorites in the country rock and the pluton.

(b) Glen Doll

Little has been published on this intrusion (Geological Survey Memoir 1912, Ferrier 1986). There is a wide variety of rock types, and Ferrier (1986) thought that variation diagrams showed a smooth transition from pyroxenite through gabbro, to augite diorite, to appinitic dioritic to diorite and tonalite. He envisaged a fractional crystallisation

process to account for this trend. The appinitic diorite has the characteristic textural and mineralogical features of large hornblendes set in a plagioclase matrix. Appinites in this complex are not apparently in the form of pipes.

(c) Dorback

This is a small complex consisting of five intrusive units - pink granite, quartz diorite, diorite, appinite and lamprophyre (Zaleski 1982) The appinite is typically coarse grained, porphyritic with amphibole up to 3cm in length and pyroxene set in a matrix of plagioclase (An₂₄₋₂₇). The relationship of the appinite to the diorite is apparently gradational with a coarsening of grain size and increase in mafic mineral content.

Zaleski grouped the Dorback complex into two distinct suites, namely the appinite suite, which ranges from quartzdiorite to appinite with appinitic lamprophyre and pink granite, and the granodiorite suite.

(d) Glen Banvie

This is a very small intrusion complex situated ~5km NW of Blair Atholl in Perthshire. It covers an area of 5km² and consists of a tonalite cupola with associated appinitic diorites, transgressed by a granodiorite dome on the SSW side (Holgate, 1950). Contacts between the members are poorly exposed but it is known that the appinitic diorite is the earliest member of the complex and extends along the N and NE margin of the complex. The appinitic diorite consists of a mass of medium to coarse grained rocks with hornblende in a matrix of plagioclase.

(v) North-West Highlands

(a) Strontian

This large intrusion covers 90km² and is a zoned granitoid body with an outer tonalite, inner granodiorite and central biotite granite. The granodiorite has been dated using U-Pb zircon at 425 ±3Ma by Rogers and Dunning (1990). It is situated immediately north of the GGF and was intruded sub-parallel to the Moine country rocks. It has a steep inward dipping, sharp contact with its country rocks. The pluton as a whole is a member of the high-K calc-alkaline suite typical of the Caledonian of Scotland. A restricted number of isotopes are available and range from Sr isotope ratios of 0.7052 - 0.7059 for the outer tonalite and granodiorite to 0.7065 for the inner biotite granite. ε_{ND} values range from +0.6 to -2.1 for the outer tonalite and granodiorite and -3.2 to -6.3 for the inner biotite granite (Holden 1987). This seems to reflect a transition to more crustal signatures in the inner granite. Appinites associated with the Strontian granite take the form of various small appinitic intrusions situated within the outer tonalite and the inner granodiorite (Holden, 1987). Sabine (1963) noted that the size of the appinitic intrusions vary from 200-750m in diameter. The appinites all occur within the pluton, they have steep, irregular and lobate contacts and generally form lenticular outcrops of biotite-hornblende in the core grading outwards to a finer grained, more leucocratic appinitic

margin, thus they are reversely zoned (Holden, 1987). Often the appinites were seen to be chilled at their margins and Holden (1987) took this to be evidence that the appinites were liquid magmas when emplaced and, together with the observed lobate contacts, he concluded that these appinites were intruded into a semi-unconsolidated granitoid magma thus co-existing in space and time with their hosts.

(b) Ratagain

The Glenelg-Ratagain complex is the most northerly of the Newer Granites, it lies on the south side of Loch Duich in the NW Highlands. It covers approximately 20km² and is believed to have been intruded during a period of sinistral shear on the adjacent Strathconan fault (Hutton, 1987, Hutton & McErlean 1991). Baddeleyite crystals from a pyroxene-mica diorite have been used to obtain ²⁰⁷Pb/²⁰⁶Pb ages of 425 ± 3Ma. It is a zoned pluton with diorite, adamellite, syenite and monzonite, and minor syenitic and appinitic bodies. Nicholls, (1951) interpreted these appinites as large xenoliths within the later diorites. He also noted the appearance of appinites with the syenite, he used this evidence of hybridisation, and on a larger scale he uses hybridisation as a process for the formation of the various rocks of the whole pluton. However Halliday et al. (1984) noted that the earliest facies is a pyroxene-mica-diorite which has been subsequently cut by appinitic and dioritic bodies. Whatever the origin of the acid-basic magma it is apparent that the Ratagain complex has extreme compositional characteristics with high abundances of Sr, Ba, Ce and Na (Halliday et al. 1984) compared with the other Newer Granites.

(c) Ach'uaine Hybrids

The rocks of the Ach'uaine complex have long been problematical because of their hybridised nature and age relationships. The Bonar Bridge intrusion is a granite related to the complex and has been dated at ~400Ma by Pidgeon and Aftalion (1978) using U/Pb on zircons. Typically the Ach'uaine hybrids consist of a wide range of co-genetic compositions ranging from mantle-derived shoshonitic types to syenites, through to granites typical of the the local Newer Granites (Fowler, 1988). Also present are mildly alkalic rocks such as kentallenite, monzonite and hornblende-bearing gabbro and intermediate syenite. They take the form of small composite intrusions with blebs, flecks and pillows of basic and intermediate syenite, enclosed in and invaded by, a relatively silicic syenite host which itself is later cut by sheets of granite and quartz syenite and exhibit textures suggestive of hybridisation of two or more different magma types.

Sutherland (1982) described the range in rock types and suggested that it is due to hybridisation of ultrabasic magma by granitic magma. Fowler (1988) agreed with this model and proposed that the distinctive trace element abundances of the Newer Granites of the N Highlands indicates that they may have subduction-related shoshonites. Fowler (1988) proposed a model of derivation from a compositionally zoned magma chamber and proposed hybridisation resulting from the incorporation of crustal material,

particularly in silicic end-members. Fowler supported this model with Harker plots of major and trace elements as the basis of a model involving strong crystal/liquid control. He noted a kink at 62% SiO₂ which he thought may be due to admixture of silicic crustal melt. Petrographically and geochemically the Ach'uaine hybrids are not strictly appinites, for instance biotite is dominant over amphibole, however they may be linked to an overall petrogenetic model as a variant of the appinite suite.

2.3.2 Ireland

(i) Donegal

The early work of the Geological Survey of Ireland, was built on by the school of Pitcher in publications by Gindy (1951), Iyengar et al. (1954), Pitcher & Read (1954), and Akaad (1956). Akaad noted the presence of appinite masses (Fig 1.1 b) as part of his study of the Ardara pluton while Pitcher and Read (1954) described a breccia pipe from Kilkenny which consists of quartzite and calc-silicate fragments set in a granophyric matrix with a hornblendic coating around many of the fragments. The fragments of quartzite were thought on structural grounds to be derived from a depth of 330m below the present level of breccia exposure, and have formed by fluidized brecciation with rounding of the blocks by hot fluids and abrasion during emplacement.

Iyengar et al. (1954) studied the Mulnamin and Meenalargan complexes. He used field relationships to study their emplacement mechanisms. The early work on both these intrusions concentrated on the relationship between the igneous rocks and calcareous horizons within the intrusions. These various workers noted the strong association between the appinites and the Dalradian amphibolites and calcareous horizons, and suspected an origin by contamination. In common with petrologic views of the era Iyengar et al.'s early interpretation of the formation of the Meenalargan complex was by a process of differential migmatization, connected with the very early stages of the formation of the Ardara pluton. The rocks were heated up and soaked by acid magma, leading to migmatization and mobilisation with local intense reaction of calc-silicate, transformed to appinitic amphibolite and incorporation of appinitic magma into migmatitic horizons, while other less reactive horizons of quartzite and semi-pelite showed little reaction. Iyengar et al. also noted the existence of what he called 'appinite of Crocknadreavah type' a coarse mafic-rich rock with interpenetrating layers of brown and green amphibole in a plagioclase matrix. He suggested that the Meenalargan intrusion may be the early manifestation of the magmatism associated with the Ardara main pluton.

Extensive fieldwork was carried out by French (1966,1976) who worked on the appinites of the Ardara area and classified them into two 'series' which he called the 'Appinitic series' and the 'Dioritic series' (French 1966). This classification is based on textural criteria and the colour index. French noted the similarity between the Scottish and Donegal appinites, in particular the common association with breccia pipes. He suggested

that the pipes may represent activity occurring in the roof of the larger appinitic intrusions. French also proposed that the appinite suite is of mixed parentage with appinites and appinitic diorites being derived from cordieritic and pyroxene-mica-dioritic to granitic and acid pegmatite end-members, with minor addition of hornblende rocks due to contamination by calc-silicate horizons. A map of the distribution of appinites around Ardara is presented in Appendix six, Map 1.

French (1976) also supported Bowes & Wrights hypothesis (1967) of addition of quartzo-feldspathic material to basic rocks in the form of net veins which gives the rocks a patchy, almost hybrid-type appearance. He noted the importance of a volatile phase, not only as a component of pegmatic acid veins but as important in the formation of breccia pipes. He suggested that one of the parental magmas of appinite may be pegmatitic and felsic, he drew comparison with the pegmatitic veins of Mulnamin to highlight his point. French (1976) suggested that appinitic leucodiorites formed from differentiation of gabbroic melts, derived by partial melting of eclogite at ~15kb with high concentration of H₂O. He suggested that ophitic texture may have been caused by late precipitation of large amounts of plagioclase, so bringing the melt closer to the low pressure cotectic, probably at the level of emplacement.

Hall (1967) studied the chemistry of several of the appinitic intrusions around the Ardara pluton and ascribed their formation to "crystal accumulation in a basaltic magma enriched in water". He also noted that the appinites had high Al₂O₃ and low MgO, both of which are common features of basalts. He noted that the ultramafic appinites did not correspond to the composition of any volcanic rock, bearing only minor resemblance to picrite by way of MgO content, thus demonstrating the appinites to be a distinctive suite of rocks. Hall also tested the hypothesis that appinites occurred in association with diapiric plutons but discounted this causal link on the basis of the outcrop of appinites in association with the permissively emplaced granite of Ben Nevis. He noted however that the granites associated with appinites had high P_{H₂O} as opposed to granites without associated appinites which had low P_{H₂O} on the basis of their proximity to the various ternary minima and eutectics at different P_{H₂O} values in the Q-Ab-Or system. This may explain the unique aspect of the appinite suite and Hall envisaged appinitic magma as being generated in the mantle at >10kb and >1000°C with acquisition of H₂O in the lower part of the crust.

Hall, like Bowes & Wright used the experimental studies of Yoder and Tilley (1962) to compare the crystallisation trends of appinite minerals to the experimental results on hawaiian basalts but with the addition of H₂O. The crystallisation sequence obtained by Yoder and Tilley (1962) at 5kb was olivine, at 1,120°C, followed by clinopyroxene at 965°C, then amphibole crystallising at the expense of olivine and crystallisation of plagioclase at 825°C until crystallisation is complete at 780°C. Hall noted that this sequence would be consistent with the paragenesis in appinites and proposed that

crystallisation of a basaltic magma enriched in either amphiboles or pyroxenes in the presence of H₂O could be expected to give rise to rocks with compositions similar to those of ultramafic appinites. Certainly the addition of H₂O and any fluid phase is important and is necessary to explain the explosion breccia pipes seen around the appinite bodies (Bailey & Maufe 1960, Pitcher & Read 1952, French & Pitcher 1959, Bowes & Wright 1961, Bowes et al. 1964, Bowes & McArthur 1976 and Hamidullah & Bowes 1987).

A very small appinite body crops out in the Fanad area of NW Donegal within the septum of the Melmore migmatite. It is a biotite-rich body with hornblende and plagioclase and may be related to the Fanad granodiorite, which it pre-dates.

(ii) Leinster

The Leinster batholith consists of a cluster of separate, dome-like diapiric units arranged along a NNE line (Fig. 2.5). The domes were forcefully intruded and have shouldered aside and distended the highly mobile country rocks. Geochemically the granites constitute a calc-alkaline series of early formed diorites to late adamellites, muscovite granites and aplites (Brück & O'Connor, 1977). The plutons have been dated at 404 ± 24 Ma on a whole rock Rb/Sr isochron, with a Rb/Sr initial ratio of 0.708 (O'Connor & Bruck 1976, 1978). All the appinites lie within the aureole of the Leinster granite and were emplaced synchronously with the granite (McArdle & O'Connor 1987). Most appinites are situated on the edge of the Tullow Lowlands pluton and extend into the schist septum between this pluton and the Blackstairs pluton. These appinites have been described by Brindley (1957, 1970) who has shown them to be very similar to those of other Caledonian granite areas. Brindley noted the existence of the two series of French, both appinitic and dioritic, as well as the presence of the typical pegmatite member and associated granite sheets. He has described 18 intrusions similar in form to those around the Ardara pluton in so much as they have similar mechanisms of emplacement and were emplaced slightly earlier than, or synchronous with, the associated granite. He also noted the presence of a high temperature phase of appinite intrusion bearing olivine, a feature also seen in the Scottish and Ardara appinites (Table 2.1)

McArdle & O'Connor (1987) noted that there are over 44 bodies of appinitic and lamprophyric affinity within the Mt. Leinster swarm between the Tullow Lowlands pluton and Blackstairs pluton of the Leinster batholith (Fig 2.5). They noted that the intrusions are spatially related to a major dip-slip ductile shear zone, the E Carlow deformation zone, extending along the SE margin of the Tullow Lowlands pluton. They also noted a close association between the lamprophyric dykes developed in this area and the appinites in the SW grading into lamprophyres in the NE. There is also a lateral variation from microdioritic lamprophyres close to the SE margin contact to

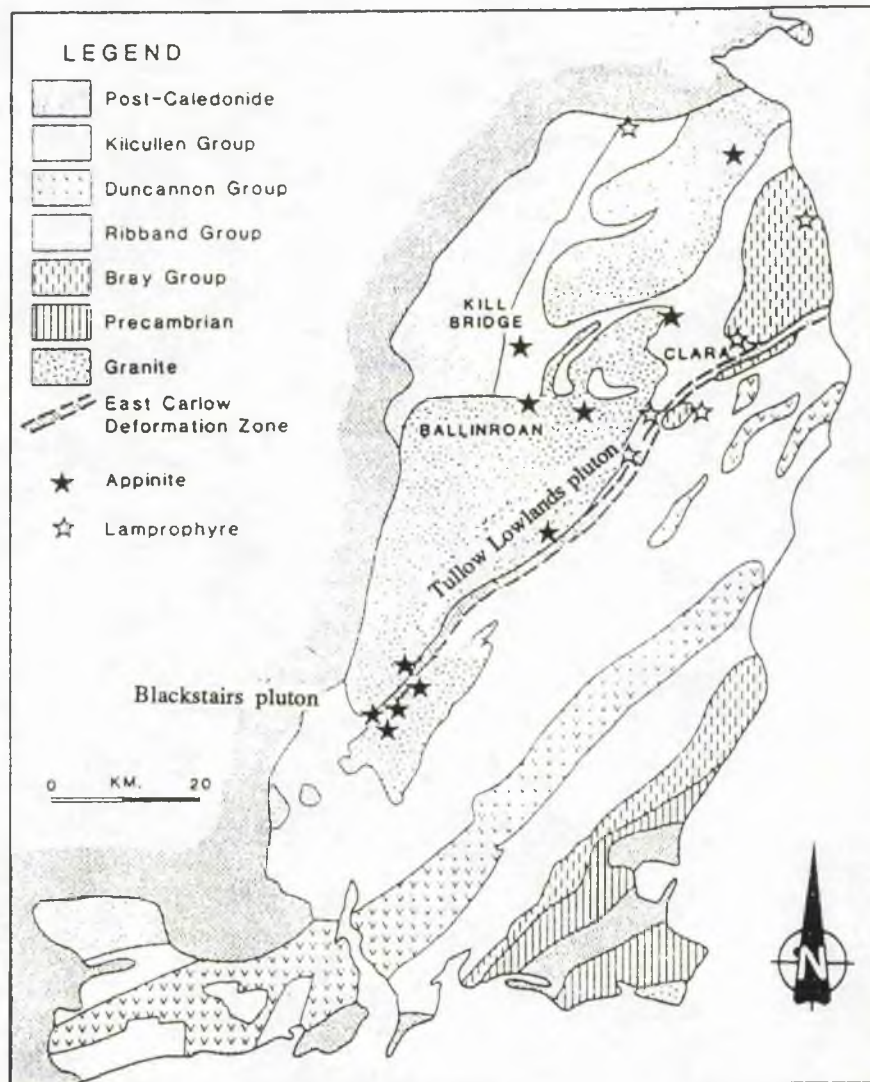


Fig. 2.5 Geology of the Leinster Pluton and associated appinites, after McArdle & O'Connor (1987)

spessartitic lamprophyres further away, which these authors attribute to differences in the thermal regime, microdiorite forming in the hottest parts, spessartite further away.

Petrographically the appinites in the Leinster batholith are compositionally relatively homogeneous. Apart from the ultrabasic cortlandtite of Camaderry the suite is made up of hornblendites. This is in marked contrast to the appinites of Scotland and Ireland and may

be due to fundamental differences in the mantle sources, level of emplacement, and/or petrogenetic history (see Chapter 7 for further discussion).

Chemically the appinites of Leinster are richer in FeO, CaO, P₂O₅ and poorer in Na₂O and K₂O than those of Donegal and the Scottish Highlands. Their trace element signature also differs, being depleted in Ba and Rb, but enriched in Li, V and Pb compared to other appinites in Donegal and the Scottish Highlands. This may reflect the geochemical signature of the associated granitoids with those of Leinster having low Ba, with elevated Li, V and Pb signatures. M^cArdle & O'Connor (1987) believe this to be a signature imparted by the lithospheric mantle source rather than by contamination of basalt magmas by crustal rocks.

(iii) Newry

The Newry complex is a Newer Caledonian granite situated in the SE corner of Co. Down, N.Ireland. It consists of 3 contiguous granodioritic intrusions which originated by fractionation at depth (Meighan & Neeson 1979). Meladiorites and biotite pyroxenites are associated with the pluton and are situated at the NE end of the complex. They are considered to be cumulates from intermediate parental magmas (Neeson & Meighan 1977) and are not strictly appinites.

(iv) Pollakeeran, Barnesmore, Co. Donegal

Six breccia pipes cut the passively emplaced (cauldron subsidence) Barnesmore granite. The pipes are between 10 and 100m wide and contain xenoliths of semipelite and metadolerite which show evidence of abrasion due to transport within the conduit from a considerable depth below the present level of exposure (Pitcher & Berger 1972).

(v) Clara, Co. Wicklow

Connor (1974) described an explosion breccia pipe which contains a heterogeneous mixture of country rock fragments (up to 10cm long) in an irregular igneous matrix which is texturally variable and highly deformed. He noted its association with two lamprophyres but contacts are poorly exposed and relationships unclear. He concluded that the intrusion probably represents a small pipe which filled with highly vesiculated material and may have reached the surface as an explosion vent.

(vi) Corvock, S. Mayo

Appinite dykes are associated with this cross-cutting pluton of Caledonian age.

INTRUSION	SIZE (km)	ROCK TYPES	EMPLACEMENT MECHANISM	XENOLITHS
ARDARA PLUTON	8.4 x 12.35 km	Quartz monzodiorite Monzodiorite Granodiorite	Distensional diapir. Steeply dipping contact	Basic, metasedimentary (calcic, pelitic)
PORTNOO	2.0 x 0.07 km	Hornblende Meladiorite Diorite/biotite diorite Granodiorite Granite dykes Pegmatites/aplites Lamprophyres	Domes, sheets, dykes, plugs, sills, veins.	Basic, metasedimentary (calcic, pelitic)
MULNAMIN	1.0 x 0.4 km	Hornblende Meladiorite Diorite Granodiorite Granite dykes Pegmatites/aplites	Distensional stock, elongate along NW-SE strike. Steeply dipping contacts with country rock.	Basic, cognate, metasedimentary (calcic, pelitic)
MEENALARGAN	4.8 x 1.6 km	Hornblende Coarse diorite Diorite Granodiorite Felsite Pegmatites/aplites	Stoped stock	Basic, metasedimentary (calcic, pelitic)
SUMMY LOUGH	1.0 x 1.5 km	Hornblende Diorite Biotite diorite Pegmatites	Passively emplaced dome	Pelitic
KILREAN	2.0 km x 1.0 km	Cortlandtite Hornblende Appinite	Diapiric distension	Metadolerite, pelite

INTRUSION	AGE	ISOTOPES
ARDARA PLUTON	405 Ma ±5	Sm/Nd = 0.1709 εNd = -1.2 (⁸⁷ Sr/ ⁸⁶ Sr) _i = 0.7062 (Meighan & Dempsey 1989) (⁸⁷ Sr/ ⁸⁶ Sr) _i = 0.7065 (Halliday et al. 1980)
PORTNOO	No field age-relationship	WR δ ¹⁸ O = +6.5 to +9‰ WR δ ¹³ C = -5‰ δD = -70‰ (Hornblende)
MULNAMIN	No field age-relationship	-----
MEENALARGAN	Pre-granite to co-eval	δ ¹⁸ O = +7‰ (Hornblende) δD = -59‰ (Hornblende)
SUMMY LOUGH	Coeval	-----
KILREAN	Late pre-granite	δD = -65‰ (Hornblende)

LOCATION: Strontian
 SIZE: 90 km³
 SETTING: Emplaced in a syntectonic setting associated with movement on the Great Glen fault
 STRUCTURE: Associated with the Great Glen fault, intruded parallel to the Moine country rocks with a steep inward-dipping sharp contact. Pluton is zoned from outer tonalite, inner granodiorite and central biotite granite
 AGE: 425 Ma (Rogers & Dunning, 1990)
 GEOCHEMISTRY: High-K Calc alkaline suite
 ISOTOPES: (⁸⁷Sr/⁸⁶Sr)_i Outer tonalite and granodiorite = 0.7052 to 0.7059,
 Central biotite granite = 0.70649 to 0.70731
 ε Nd Tonalite and granodiorite = +0.6 to -2.1

LOCATION:	Ballachulish
SIZE:	28 km ²
AGE:	412 ± 28 Ma (Brown et al. 1968)
GEOCHEMISTRY:	ε Nd = - 2.7 (Holden 1987)
LOCATION:	Arrochar / Garabal Hill / Glen Fyne
SIZE:	25 km ² in total area of disjointed intrusions
SETTING:	Post-tectonic
STRUCTURE:	Stock-like intrusions of diorite, porphyritic granodiorite, quartz diorite
AGE:	(⁸⁷ Sr/ ⁸⁶ Sr) _i Arrochar: 408 Ma (Titanite sample), (Rogers & Dunning 1990) Garabal Hill / Glen Fyne: 429 ± 2 Ma (Zircons), (Rogers & Dunning 1990) 422 Ma (Titanite), (Rogers & Dunning 1990)
LOCATION:	Ben Nevis
SIZE:	51 km ²
SETTING:	Ring-dyke complex emplaced in a tensional stress regime in a late post-tectonic setting
ZONING:	Crudely concentrically zoned from outer quartz diorite and granite to an inner granite
AGE:	Lower Devonian 410 ± 6 Ma (Brown et al. 1968)
LOCATION:	Glen Banvie
SIZE:	0.5 km ²
SETTING:	Post-tectonic
ZONING:	Granodiorite to tonalite with appinitic diorites. Appinitic diorite is the earliest member of the complex and extends along the north and north east margin of the complex as a NNE-dipping sheet.
LOCATION:	Leinster
SIZE:	~ 200 km ²
FORM:	Largest batholith in the British Isles. Cluster of separate dome-like diapiric units arranged along a NNE lineament. Domes were forcefully intruded, effects of which have been the shouldering aside and distension of the highly mobile rocks. Appinites lie within the aureole of the Leinster granite and are emplaced synchronously with the granite (McArdle & O'Connor 1987). Most appinites are situated on the SE edge of the Tullow lowlands pluton. Emplaced as bosses and sheets related to elongated schistosity in the schist septum between the Blackstairs pluton (McArdle & O'Connor 1987).
GEOCHEMISTRY:	Granites constitute a calc-alkaline fractionation series of early-formed diorites, adamellites and aplites (Brück & O'Connor 1977)
AGE:	404 ± Ma (⁸⁷ Sr/ ⁸⁶ Sr) _i = 0.708 (O'Connor & Brück 1978)
LOCATION:	Newry
SIZE:	440 km ²
FORM:	Intruded in a diapiric fashion, en-echelon slightly oblique to the regional Caledonian strike
ZONING:	Three contiguous granodiorites originated by fractionation at depth in a differentiation series with possible minor crustal contamination (Meighan & Neeson 1979). Appinitic, dioritic and monzonitic rocks may have originated by fractionation in-situ.
AGE:	399 ± 21 Ma (O'Connor 1975)

Table 2.1 Outline of the main features of the appinitic intrusions and their associated major plutons in the Scottish and Irish Caledonides

2.3.3 Summary

Although it is apparent from the above review that the appinite suite is a highly complex and variable assemblage, several general features are apparent:

(a) Appinites are most commonly associated with Newer Granites of Scotland and Ireland. They were emplaced before, or in some cases coeval with, these Newer Granites in a post-tectonic setting.

(b) They are a highly heterogeneous assemblage of rock types which often show signs of hybridisation.

(c) They have mantle-derived affinities, and their compositions are akin to wet basalts (Wright & Bowes, 1979).

(d) There is a fluid and gas component in some members of the appinite suite which may be important in their textural development and emplacement histories.

(e) Some appinitic intrusions show close association with pre-existing amphibolites and/or calc-silicate horizons.

(f) The appinites also have a close association with deep ductile shear zones, notably the Highland Boundary Fault and Great Glen Fault, and the suite is most commonly associated with plutons located north of the Iapetus suture line in the block between the Highland Boundary Fault and the Great Glen Fault.

2.4 APPINITES OUTWITH THE CALEDONIAN

Many appinitic intrusions have been described outwith the Caledonides, however due to differences in classification and terminology use of the term appinite is less common and thus correlation with the type appinites is difficult. One factor that is apparent is the strong association between mafic magmas and large granitic plutons. The following is a brief summary of some of the occurrences of "appinites" in other parts of the world.

2.4.1 The Cadomian orogeny

The Cadomian orogeny has associated appinitic bodies in Jersey in the U.K. Channel Isles. Magmatism with appinitic affinities has been active since the late Proterozoic onwards. Wells & Bishop (1955) and Lees (1990) characterised appinitic rocks from the UK Channel Isles emplaced during the Cadomian orogeny (Thorpe 1982) at ~650Ma (Adams 1976) in association with gabbroic to granitic rocks.

2.4.2 The Hercynian orogeny

(i) N Italy

The intrusion of calc-alkaline granitic plutons associated with small intrusive bodies of basic to intermediate type is found in the Hercynian of the northern Italian Alps. As in so many appinitic associations there is a strong dependence on structural

lineaments. In the Serie dei Laghi, a set of faults known collectively as the Cossato-Mergozzo-Brissago Line (CMB) of late-Proterozoic age have recently been activated. The appinites are emplaced into a belt of high grade metasediments and are apparently older than the anatexis of the country rock which is dated at ~295Ma, determined from U/Pb age of a monazite from a migmatite (Koeppel & Gruenfelder 1979) and also older than the granites which have also been dated at 275Ma by U/Pb methods by Koeppel and Gruenfelder (1979). The appinites take the form of vertical sheets and stocks elongate in a NE-SW direction, parallel to a fault zone which is orthogonal to the CMB. These faults may have acted as margins to pull-apart zones or as transform faults, (Borioni et al. 1988). The appinite suite varies in composition from gabbro to diorite and granodiorite (even in the same dyke). There are also the later more leucocratic parts of aplite and pegmatite (cf the Caledonides). Many of the dykes and sheets are breccias with fragments of foliated gabbro-diorite cemented by a more leucocratic, non-foliated matrix (cf. Kilkenny, Co. Donegal).

In summary, the appinites of the Serie dei Laghi in N Italy show similar features to those of the Caledonian, particularly in terms of composition, temporal relationships to their granitic counterparts, and relationships to deep-seated tectonic lineaments for their emplacement.

(ii) Spain

Cortlanditic enclaves (mineralogically comparable to the cortlandtite found in the Kilraean intrusion at Ardara, Co. Donegal and Camaderry, Leinster) are associated with calc-alkaline granites have been reported from the Tapis-Asturias belt of NW Spain by Galan & Suarez (1989). The enclaves occur within basic rocks related to post-tectonic epizonal granites. Other authors (Figuerola et al. 1980, Galan 1984) noted that the cortlandtite may occur as small stocks around the granitoids. The authors suggest that a basic magma with high Al content was involved in the genesis of the subsequent calc-alkali granite. The cortlandtite may represent an early stage of the fractionation of basaltic magma but subsequent contamination with crustal material may have been an important factor in the genesis of the calc-alkali granites. Other ultrabasic rocks have also been described by de la Rosa & Castro (1990) from the Castillo de las Guerdas massif near Seville. Among the mafic rocks are gabbros with pegmatitic facies as pods or sub-horizontal layers, and while not strictly appinitic they are associated with a felsic component, analagous to the basic-acid association of the Caledonides.

(iii) France

Letterier (1972) described Variscan cortlandites in the Querigut area of the French Pyrenees.

2.4.3 The Cordillera of North and South America

The magmatism of the Cordillera of North and South America is of subduction-margin type, well demonstrated by the western Cordillera of the Central Andes. This plutonism differs from that of the Caledonides in several ways:

- (i) Plutonism is associated with great volumes of andesite and dacite eruption.
- (ii) There are great linear arrays of batholiths, often composite.
- (iii) Plutonism is episodic and of long duration.
- (iv) Plutonism is related to vertical movements with lateral shortening.

The style of plutonism is thus very different from that seen in the Caledonides, with the dominance of tonalite over granodiorite, strictly dioritic xenoliths as opposed to the mixed populations of Caledonian magmas, and greater abundance of hornblende.

Cordilleran magmatism is largely related to crustal thickening where a typical sequence of events might begin with oceanic subduction leading to crustal extension with trough production and subsequent infill by sedimentation and volcanicity. This is followed by magmatic underplating with deformation, batholith emplacement, uplift and erosion, firstly in the eugeocline and then in the miogeocline, followed by later establishment of a new volcanic arc and deposition of subarc volcanics (Cobbing 1985). This subduction model is exemplified to varying degrees by the plutonic and volcanic rocks of the Cretaceous of the west coast of North and South America. The plutonic rocks of this setting comprise voluminous early gabbro to diorite, tonalite and felsic granite, with tonalite being dominant. The magmatism is entirely I-type (Chappell & White 1974). The occurrence of any appinitic textures and emplacement features are minor and a very localised phenomenon.

(a) Western Cordillera of Mexico

Basic rock types have been described from the western Cordillera of the American continent by Mullan & Bussel (1977) and Pitcher et al. (1985). Mullan & Bussel (1977) described cumulate zones in the plutons of the western cordillera of Mexico. They distinguished an ultramafic zone and a gabbroic zone both of which show cumulate textures suggesting that they crystallised in large static magma chambers. The mineralogy of the layered gabbros shows them to contain pargasitic hornblende with diopside, intercumulus plagioclase (An 60) and minor ilmenite; the great abundance of hornblende suggests that this crystallised from a hydrous-rich magma. These layered bodies are genetically linked with extrusive andesite volcanics and later granitic rocks.

(b) The Peruvian Batholith

Pitcher et al. (1985) studied a series of gabbro plutons in Peru, concentrating on the axial zone of the Peruvian batholith. These plutons are earlier than the granitoids and range widely in scale, from sills and plugs to large-scale plutons several hundreds of square kilometres. There is considerable variation in composition and texture.

Regan (1985) noted three overall stages in the intrusion history of the basic plutons:

- (i) Cumulate-type crystallisation from a magma at depth.
- (ii) Recrystallisation while still hot and undergoing deformation.
- (iii) Amphibolitisation associated with late-stage explosive brecciation and penetration by water-rich volatiles.

Although no "appinite" (*sensu stricto*) has been described in the Peruvian batholith, point (iii) of Regan (1985) is an important stage that seems to have strong similarities with appinite genesis. Regan (1985) found that processes of amphibolitisation and hybridisation may cause wholesale conversion of the pre-existing lithologies due to in-situ reconstitution associated with deformation. The results of these processes have been compared to the heterogeneous, net-veined hybrid dioritic and appinitic plutons of the Caledonides (Regan, 1985). This reconstitution is thought to take the form of either the penetration of pre-existing rocks by quartz dioritic material - often by net-veining along dilated or brecciated fissures, related to hydraulic fracturing or the hybridisation without development of net-veins by metasomatic transformation. As a result most of the growth of amphibole is at the expense of other minerals. Regan also noted that some of the amphibole is magmatic, developing in comb-layered net-veins and as hollow shells in pegmatitic pockets. Both of these features are also characteristics of "appinite" from Donegal (Table 2.1).

The only field evidence that Regan (1985) quoted for a genetic relationship between these basic and acid bodies is the occurrence of hybrid rocks along the contact with, and locally gradational into, the Santa Rosa tonalite. Regan noted that elsewhere contacts between the two are sharp.

Pitcher et al. (1985) proposed that the hornblende-bearing early gabbros represent early tholeiite magmas derived by partial melting of a mantle wedge, possibly as a result of the release of heat and volatiles above a postulated Cretaceous subduction zone. In their opinion the melt for the later (I-type) tonalites was derived from the mantle wedge in the sub-continental mantle with a volatile input from the underlying subduction zone; this basic magma then solidified to be remelted episodically.

2.4.4 Other regions

(i) Japan

Agata (1981) described a hornblende-rich gabbro diorite sequence in the Oura igneous complex near Maizuru city, Japan. He described the sequence as a lenticular outcrop of hornblende-rich rocks with a small amount of albite leucotonalite. The hornblende-rich rocks occur by resorption of a plagioclase-clinopyroxene assemblage in cumulate rocks that had formed on the floor of a magma chamber. He ascribed the hornblende to hydrothermal activity (Agata 1981) and attributed its formation to mineralisation and alteration by fluids which escaped from the magma forming the appinite sequence.

(ii) Australia

In the Hartley and Ben Bullen complexes of Australia, relationships exist similar to those seen in Scotland and Ireland, between early gabbro and dioritic intrusions and later cross-cutting granitic bodies (Joplin 1959).

(iii) NE America

Calc-alkaline acid and basic magmas of a similar compositional range to the late Caledonian of Scotland and Ireland are seen in Newfoundland. Here numerous terranes form a complex network in a similar subduction setting, as a continuation of the Caledonian belt into N America and although not strictly appinites these rocks have important appinitic affinities.

(a) Topsails Complex, Newfoundland

The Topsails complex on the west coast of Newfoundland (Whalen et al. 1987) has an acid-basic association of early gabbroic magma, rich in hornblende and in many cases with appinitic textures. These are later intruded by diorite, tonalite and granodiorite in a post-subduction setting.

(b) The Cortlandt Complex, New York State

This intrusion gives its name to the most ultrabasic rock types of the appinite suite - cortlandtite. The Cortlandt complex consists of six successively intruded, more-or-less contemporaneous plutons (Bender et al. 1982). These are from oldest to youngest: hornblendite to hornblende gabbro, diorite, clinopyroxenite, cortlandtite to amphibole pyroxenite, norite, and clinopyroxenite. The norite of the central part of the complex has been dated to 411 ± 51 Ma (whole rock Rb/Sr isochron). Bender et al. believed that the diverse lithologies of the complex formed by magmatic fractionation of an alkali basaltic melt which underwent fractionation to a diorite and subsequent liquid immiscibility and various degrees of crustal assimilation.

2.5 THE TERMS "APPINITE" AND "APPINITE SUITE"

2.5.1 Appinite

The original definition of "appinite" was given by Bailey & Maufe (1916) who described appinite as "the plutonic equivalent of vogesite and spessartite". Since then other authors have based their definitions on those of Bailey & Maufe but have tended to concentrate on the textural appearance of the rock:

(a) Hall (1967) described "appinite" as, "a medium to coarse grained melanocratic rock composed mainly of green or brown idiomorphic hornblende in a matrix of feldspars and quartz".

(b) Pitcher & Berger (1972) describe it as "a dark, medium to coarse diorite which is largely composed of idiomorphic hornblende set in a groundmass of plagioclase and quartz, sometimes with a little potash feldspar".

(c) Hamidullah & Bowes (1987) designated the term "appinite" as "a rock in which large idiomorphic amphibole dominates in a mafic rock of gabbroic to dioritic affinities".

(d) French (1966) described the type "appinite" as consisting of "long prismatic amphiboles in a groundmass of plagioclase with or without essential quartz". French, like many authors noted the existence of a number of texturally variable rock types associated with the type "appinite"; he thus distinguished two 'series', appinitic and dioritic, based largely on colour index and by the dominant mineralogy of the rock.

(e) The Tomkieff Dictionary of Petrology (1983) defines "appinite" as "mesocratic to melanocratic rocks of medium to coarse grain, composed of conspicuous hornblende in a base of plagioclase (oligoclase or andesine) and/or orthoclase \pm quartz (commonly as micropegmatite)"

(f) The term "Vaugnerite" is used by the French to describe "a coarse, dark rock occurring as a dyke, with abundant biotite, inconspicuous green hornblende, white plagioclase feldspar, quartz, accessory orthoclase, apatite, pyrite and titanite" (Johannsen, 1938).

In this study the term "appinite" will be used for a medium to coarse grained, basic to intermediate melanocratic rock type with an igneous texture of interlocking, acicular to stumpy amphiboles, within a matrix of plagioclase (oligoclase-andesine), with alkali feldspar, quartz and minor calcite.

2.5.2 Appinite suite

The original definition of appinite (Bailey & Maufe 1916) encompassed a wide range of mineralogically different rock types from ultramafic to felsic. These were a spectrum of rock types seen in association with the type "appinite" and included olivine gabbro, hornblendite, pyroxene-mica diorite, diorite, biotite diorite through to granodiorite, and were referred to by Bailey & Maufe (1916) as the "appinite suite". In cases where mafic minerals, other than hornblende, become important (notably olivine and augite) the correct petrological name should be given to the rock but if it is spatially, temporally, and in other ways associated with appinites then such bodies may be included in the "appinite suite".

2.5.3 Discussion

If rigid rules of nomenclature are applied such as Streckeisen (1976), many appinitic rocks would plot in the fields of quartz monzodiorite, quartz diorite, monzodiorite, diorite monzogabbro and gabbro. In most cases the prefix mela- would be appropriate. When describing the mineralogical characteristics of these appinitic rocks the rules of Streckeisen (1976) will be used to avoid ambiguity. However where texture, emplacement mechanism and volatile content fit the definition the term appinite will also

be used. Only where the texture and form of appinite are consistent with the definition will the term "appinite" be employed.

To avoid confusion over definitions of rock types it may be practical to use the term "appinite suite" to encompass the wide range of rock types associated with "appinite" and the term "appinite" only used when referring to the texturally characteristic rock type corresponding to the above definition. It is one of the aims of this study to clarify the nomenclature used in reference to appinites, as such the following definition of terms will be employed in this thesis:

(i) "appinite" (always in inverted commas) will be used for the type rock of the 'appinite suite', namely, "a medium to coarse grained, basic to intermediate melanocratic rock type with an igneous texture of interlocking, acicular to stumpy amphiboles, within a matrix of plagioclase (oligoclase-andesine), with alkali feldspar, quartz and minor calcite" (see above). This term includes textural and mineralogical factors and implies an association of high volatile content. When describing the mineralogical proportions the definitions of Streckeisen (1976) will be used (see below).

(ii) "appinite suite" (always in inverted commas) refers to any rock type with "appinite" associations, this includes hornblendite, cortlandtite, meladiorite, diorite, granodiorite and lamprophyre.

(iii) appinitic is used as a term to describe a basic to intermediate rock type which has abundant idiomorphic, stumpy or acicular hornblende.

(iv) appinite: (no inverted commas) is used in the text to denote a rock type which has all of the following features:

- occurs within the 'appinite suite',
- has appinitic affinities in terms of mineralogy and texture,
- is related to a granitic intrusion, temporally and spatially,
- has a high volatile content as indicated by carbonate and hydrous mineralogy.

(v) appinitisation refers to the process of transformation of a pre-existing basic or metamorphic rock, often calc-silicate, by reaction with an appinitic fluid and/or magma. This has been said to result in the development of new textures and minerals in the rock through the process of recrystallisation and new crystal growth.

(vi) intrusion breccia (Harker 1908) is used where the matrix is of igneous material and the fragments are locally derived.

(vii) explosion breccia (Tyrell 1928) is a rock where an igneous matrix is lacking but still with little transport of the fragments.

(viii) intrusive breccia (Reynolds 1954) is a rock with or without an igneous matrix, but where entrained material can be shown to have travelled a considerable distance.

2.6 CURRENT VIEWS ON THE PETROGENESIS OF THE APPINITE SUITE

In preparation for the detailed study of the Ardara appinites in later chapters and the discussion of their petrogenesis it is pertinent here to review existing models proposed to account for the origin of appinites.

2.6.1 Models

(i) Model of Deer (1953) and Haslam (1970)

Deer (1953) envisaged a process of hybridisation and mixing to explain the textural characteristics of the various rock types. He explained the origin of a group of appinites at Glen Tilt by metasomatic interchange between xenoliths of epidiorite schist and an enclosing magma, rich in hornblende as well as contamination of acid magma with a pre-existing hornblendite to form a quartz-orthoclase appinite. Haslam (1970) described a process of contamination of calc-alkali magma by calc-silicate country rocks along the contact zone of the Ben Nevis granite, where cooling was slow and where volatiles were concentrated. Both these processes are seen by the authors as local processes and it seems unlikely that they can be used to explain the large volumes of appinitic magma seen elsewhere and the presence of appinite in contact with calc-silicate is not always observed.

(ii) Model of Hall (1967)

Hall highlighted the association of granites with appinites and the fact that the granites associated with appinites are richer in Na and poorer in K and Si than those not associated with appinites, and also that the granites plot in a region corresponding to the liquidus minimum at high water pressures. From this he concluded that the granites associated with appinitic rocks had crystallised from magmas existing under conditions of high water pressures. He compared the chemistry of the appinitic rocks with that of typical basalt, notably in terms of aluminium and magnesium content and noted that the pyroxene and hornblende-rich appinite may have been derived from early and later cumulates of an amphibole-rich magma which, based on the work of Yoder & Tilley (1962), would initially crystallise olivine then pyroxene before eventually forming hornblende over a prolonged period. This may lead to the fractionation of increasingly intermediate rock types. He ascribed the minor chemical differences between appinite and basalt to their water contents and attributed the special nature of appinitic magma to an origin under conditions of high water pressure. He proposed that appinite was derived from the mantle and not from the melting of basic rocks in the crust, and that the water in the appinite magma was derived from the lower crust where granite (whose composition shows them to have originated under conditions of high water pressure) is indicative of the high water pressures obtaining in regions of the crust through which appinites must have penetrated. If basaltic magma incorporated water from this area its ensuing differentiation path would be very different from that of anhydrous magma, it would

favour hornblende fractionation as well as lowering the viscosity (due to the presence of water) whilst providing a medium to allow the emplacement of the magmas by explosive brecciation.

(iii) Model of French (1976)

French (1976) built on the work of Nockolds (1934), Reynolds, (1936) and Joplin (1959) all of whom proposed a mixed parentage for the rocks of the 'appinite suite'. French did not wholly support this idea but instead proposed a model which viewed the appinitic rocks in general as being accompanied by a set of more basic pyroxene-bearing rocks, including peridotite, cortlandtite, mica-peridotite and pyroxene-mica diorite (Wells & Bishop 1955, Pitcher & Berger 1972, Hamidullah & Bowes 1987). He also observed that these ultrabasic rocks are formed early in the history of the intrusive complexes and while not as volumetrically abundant as the appinites they have chemical affinities with each other and their intermediate and acid associates. French suggested these rocks are genetically linked and he proposes a two-stage model of appinite petrogenesis. Firstly a suite of basic and ultrabasic rocks were formed analagous with a gravity differentiation series, initially derived by partial melting of eclogite at 25-30 kb, with the precipitation of large amounts of plagioclase bringing the melt closer to the low pressure cotectic. Secondly the appinitisation of the pyroxene-rich rock series and metamorphic rocks of appropriate composition occurred with the production of new textures and mineral assemblages by recrystallisation and the action of a more tenuous fluid (French 1976).

(iv) Model of Pitcher & Berger (1972)

Pitcher & Berger considered the presence of two types of ultrabasic rock hornblende rich and pyroxene rich, indicated an origin as cumulates from amphibole- and pyroxene-facies basaltic magmas respectively. In their view, because these magmas have such contrasting compositions, they cannot be regarded as direct equivalents of one another. Pitcher & Berger did not explain the differentiation process which led to the range of rock types but suggested that mechanisms of wall and roof zone differentiation may be important in the Mulnamin and Meenalargan intrusions respectively. They accounted for the formation of the acid and leucocratic types by hybridisation, where acid material may have come from the associated granites or from the partial melting of wall rock already softened and mobilised, coupled with crystal fractionation, as advocated by Hall (1967).

Pitcher & Berger's overall model is one of crystal differentiation along two paths with the direction (hornblende or pyroxene) depending on volatile content, modified by the introduction of a second magma originating from the associated granites or from the partial melting of mobilised wall rock or by processes of crystal differentiation as advocated by Hall (1967). They argued, however, against the appinites and granites

forming a continuous co-magmatic series but believed that the associated granites may have supplied an acid fraction together with much of the water.

(v) Model of Hamidullah & Bowes (1987)

These authors accounted for the considerable petrogenetic variation in the appinite suite on the basis of crystal differentiation from an original magma of high K calc-alkaline type under variable gas pressure. They proposed successive fractionation of the major mineral phases leading to the progressive development of the rocks of the appinite suite (kentallenite to granodiorite), some as cumulates, some as crystallised from residual liquids, some due to mixtures associated with explosive emplacement. They envisage that the magmas from which the appinite suite of the Appin district crystallised were mantle-derived at depths of 200km and associated with subduction on a NW dipping plate in Caledonian times, and that a process of differential scouring of elements from the lower crust may be an important factor in accounting for the anomalous geochemical features of this suite and those of the associated granites. The authors believed the emplacement of basic diapirs of hot magma into the lower crust whilst it was in an anatectic state could have been a major factor in the development of late Caledonian granites.

2.6.2 Summary

The models described above represent a wide range from crystal differentiation, to hybridisation, to volatile control, to metasomatism. Most authors believe the appinites were the products of mantle-derived magmas and envisage some process of internal differentiation to be responsible for the mineralogical variation. However differences of view are reflected in the origin of the more felsic magmas, from the crystal fractionation model of Hall (1967) and Hamidullah & Bowes (1987) to the incorporation of crustal material by Pitcher & Berger (1972). Hybridisation is strongly supported by Pitcher & Berger (1972), while French envisaged 'appinitisation' as an important process. These authors noted the importance of a second magma of a more acid composition but Pitcher & Berger (1972) believed that these two magmas were not co-magmatic. On a local scale contamination by metasomatism is seen to be an important factor in the production of appinite textures, (Deer 1953, Haslam 1970), especially in the contact zones of calcareous country rock. It is also clear that appinites are more commonly associated with I-type rather than S-type granites or with the early syn-tectonic older granites and gabbros of the Caledonian. They are not catazonal rock types nor are they associated with the post-tectonic alkali granites, (A-types) found in stable cratonic settings. It thus seems that the "appinite suite" is peculiarly associated with subduction or post-subduction collision setting of the Caledonian orogeny.

2.7 CONTEXT OF THESIS

In this chapter an attempt has been made to rationalise the nomenclature, setting and petrogenesis of appinites described in the literature. The review has highlighted some problems of particular interest which will be pursued in the remainder of this thesis. These include:

- (i) The nature of the parental magma(s) involved, their source(s) and depth(s) of generation.
- (ii) The role of differentiation processes such as crystal fractionation, hybridisation, and contamination by wall or country rocks.
- (iii) The relationship, if any to the Caledonian granitoid plutons with which they are associated temporally and spatially.
- (iv) The structural relationships important in the emplacement of appinites.
- (v) The role of fluids and the origin of the hydrous fraction of appinitic magmas.

The Ardara area offers an excellent opportunity to investigate these problems. It has the unique benefits of possessing the greatest number and widest variety of appinitic intrusions associated with a single granitoid pluton, ranging from large complexes to small metre-sized breccia pipes. It also has extensive intimate contact relationships with calcareous country rocks, and overall, excellent exposure.

A new approach to these problems using modern techniques including electron beam imagery, major, trace and isotope geochemistry coupled with the more conventional techniques of field geology and optical petrography may provide additional constraints to those available to the authors of the models described under 2.6 in the hope that a choice between these models becomes possible. If none of these models proves entirely satisfactory then new models must be erected that satisfy these new constraints.

The next chapter is concerned with the field relationships seen amongst a number of appinitic complexes in the Ardara area and their relationships to the main Ardara granitoid pluton. Each section includes descriptions of the different bodies and their emplacement mechanisms. Later chapters will deal with compositional aspects including whole rock chemistry, mineral chemistry and stable isotope geochemistry before returning to discuss these aspects in the context of this chapter in the final chapter.

CHAPTER THREE

GEOLOGICAL SETTING

3.1 INTRODUCTION

This chapter outlines the basic geological setting of the Ardara pluton and its associated appinite suite as well as the country rocks into which they were emplaced. A brief resume of the stratigraphy is given followed by the detailed field relationships of each individual intrusion. The region is covered by the 6" to 1 mile sheets, numbers 64,65,73 and 74 of the Ordnance Survey of Ireland. Grid references quoted are those corresponding to the Ordnance Survey of Ireland sheets (1" to 1 mile) for Donegal.

The appinitic intrusions of Donegal were emplaced into a succession of Dalradian metasediments consisting of quartzite, marble, semi-pelite and pelite. The sediments were deposited in a shallow shelf environment that shows a general facies change from quartzites to the north and north-west of the Main Donegal Granite to finer grained calcareous facies in the south and south-east. The metasediments are broadly equivalent to the metasediments of the Appin group of the Ballachulish succession (after Pitcher & Shackleton 1966).

During the Caledonian regional deformation, which reached intermediate greenschist facies, the pelitic rocks were altered to chlorite-garnet-muscovite schists, whilst the quartzites and limestones were recrystallised. These rocks of NW Donegal are intruded by various granodioritic plutons which make up the Donegal batholith. The largest mass is the main Donegal granite, an elongate intrusion striking NE-SW from Carrickart in NE Donegal to Glenties and Trawenagh Bay in the SW. The south-western contact of this granite cuts the stalk-like projection of the Ardara pluton (Fig 3.1).

The Ardara pluton has become recognised as a classic distensional diapir following the work of Akaad (1956) and Holder (1979). It has a circular outcrop pattern with an eastern contact that shows deformation fabrics due to the intrusion of the Main Donegal Granite (MDG). The pluton is zoned from outer quartz diorite inwards across a gradational contact to quartz monzodiorite, granodiorite into a central granite. Hall (1966) accounted for this variation by crystal differentiation but he believed it was possible that there may also have been a degree of basic contamination judging from the evidence of mafic schlieren and discoid xenoliths of basic origin. These may be related to coeval, synchronous appinitic intrusions associated with the pluton.

The appinitic intrusions and breccia pipes describe are all spatially associated with the Ardara pluton. There are over 30 of these in the area, many of which form a series of satellite intrusions but only three of these are in mutual contact with the pluton. The intrusions selected for detailed study are those which apparently best illustrate the variations in emplacement, mechanisms, petrological facies, internal relationships, relationships to the host pluton and overall exposure, namely:

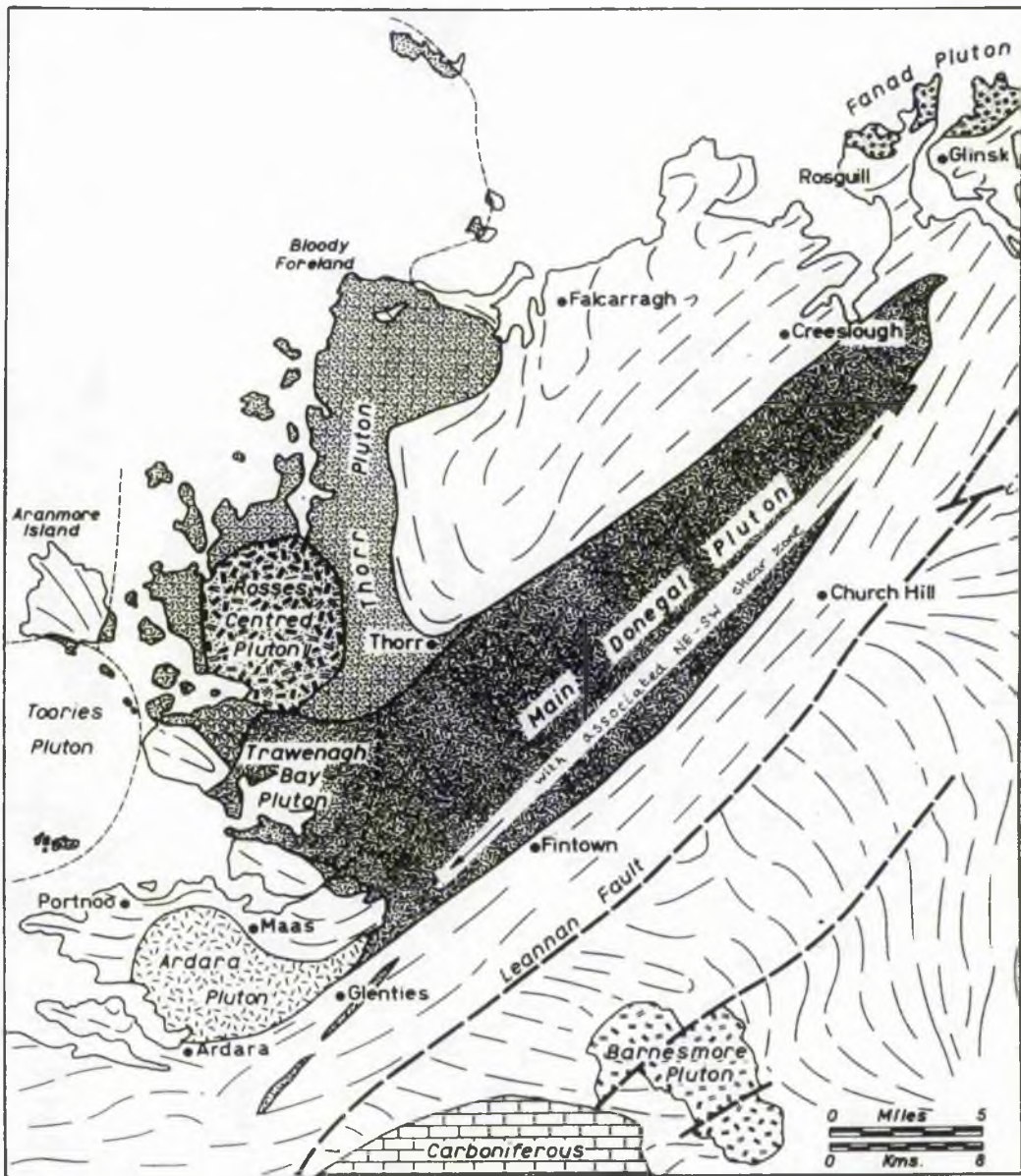


Fig 3.1 Sketch map showing the location of the Donegal Granites. The study area of the Ardara pluton and its associated appinitic intrusions is located in the SW of Donegal between the villages of Portnoo, Maas, Glenties and Portnoo. After Pitcher & Berger (1972).

1. Meenalargan: the largest intrusion complex which has contact relationships with both the main Ardara pluton and the MDG.

2. Narin-Portnoo: excellent coastal exposures of complex contact relationships between various dioritic rock types as well as calcareous country rocks.

3. Summy Lough: like Meenalargan shows contact relationships with the Ardara pluton.

4. Mulnamin: coastal intrusion with dioritic, calcareous and deformational contact relationships.

Other intrusions are included in wider discussions of field relationships and petrology.

3.2. GEOMORPHOLOGY

The topography of the Ardara area is one of rugged hills with low lying moorland giving way to an indented coastline of cliffs, wave-cut platforms and sandy beaches. The dominant feature is a roughly circular area running northwards from the villages of Ardara and Glenties in the south to those of Portnoo and Maas in the north (Fig 3.1). This circular region roughly defines a lowland area of peaty moorland dotted with numerous loughs and rocky knolls, coinciding with the outcrop of the Ardara granite. Marginal to this moorland is a swathe of higher ground corresponding to the contact rocks of the inner thermal aureole of the Ardara pluton. To the east lie the hills of the Meenalargan appinitic complex and further south east the main Donegal granite cuts the neck of the pluton. To the west lie the low hills of the Summy Lough intrusion and its largely pelitic envelope, while along the northern contact lie the hills of pelite and marble defining a distinct grassy swathe which runs from Maas westwards to Narin and Portnoo (Fig. 3.2 a). The southern margin is largely a low lying area within the Owenea river valley which flows into Loughros More Bay. It is in the boggy ground of the Owenea river that the most primitive of the Ardara appinites is found at Kilrean (Fig 3.2 b). The coastline of the region is typically highly indented consisting of rocky headlands and inlets with cliffs and wave-cut platforms leading to long stretches of beach. The coastline is particularly important in providing almost total exposure, especially in the appinitic foreshore of Narin-Portnoo.

3.3 COUNTRY ROCK SUCCESSION

The field relationships of the Ardara appinite suite require a knowledge of the lithologies into which they were emplaced. The succession consists of Dalradian metasediments comprising quartzites, limestones, semi-pelites and pelites. The stratigraphy used is that defined by Iyengar et. al. (1954), see Fig 3.3. Pitcher and Shackleton (1966) correlated the succession with that of the Creeslough succession of NW Donegal and with

the Ballachulish succession (Appin group) in Argyllshire on the basis of similarities of facies and lateral stratigraphic continuity.

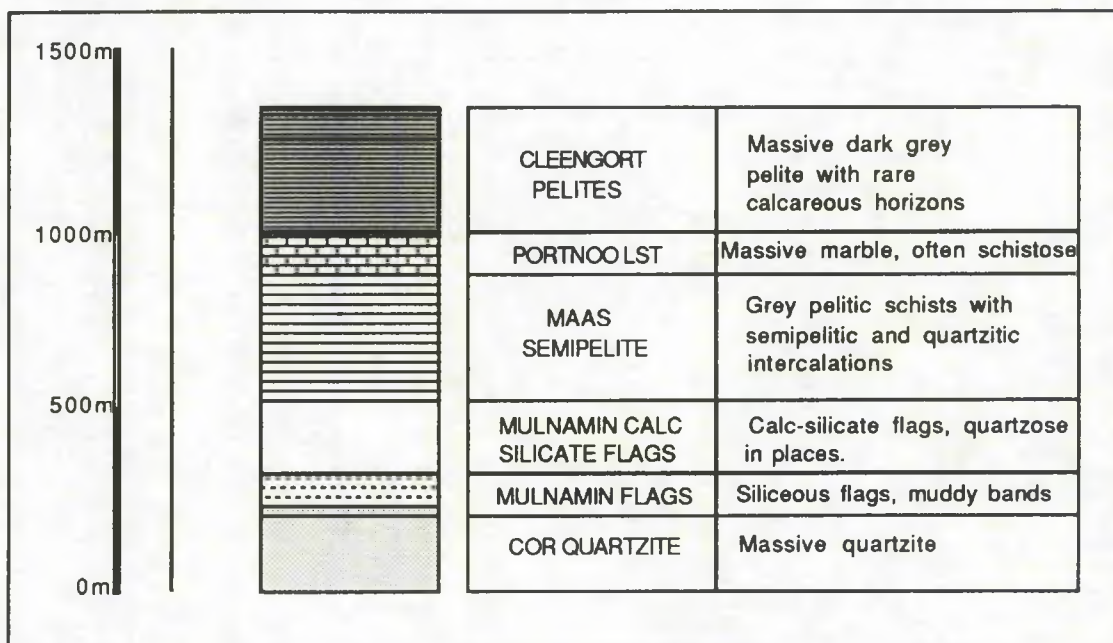


Fig 3.3. Stratigraphic column of the metasediments present in the study area (after Iyengar et al. 1954), with thicknesses as seen in the type area of Maas shown in metres.

3.3.1 The Cor Quartzite

This is the lowermost member of the succession and outcrops in the east of the area, with a maximum thickness of 70m. The best outcrops are seen in two places:

a) Crockard Hill (G7920 9720)

Here the quartzite is relatively undeformed, it dips steeply to the north and is white to dull grey in colour with pink feldspar grains within a highly siliceous matrix which often weather out to give a pock-marked appearance. No muddy bands are found. Bedding ranges from 1cm-1m, with occasional fine laminae of muscovite mica.

b) South Meenalargan Hill (G8087 9690)

Although this is a mega-enclave caught up in the Meenalargan complex diorites it has similar textures to the type area of Crockard Hill stretching from (G8200 9775 to G8000 9650), a distance of >800m. It is creamy white but it has more micaceous bands as well as cross bedding in the larger beds, indicating that it is the correct way up. Deformation associated with the emplacement of the Ardara pluton and MDG takes the form of intense stretching, with formation of rod-like mullions parallel to the extension direction. A pervasive stretching lineation is developed along 060°, plunging 20° south-

west. The two outcrops seem to be linked structurally to a faulted anticline and although their stratigraphic relations are unclear as the outcrop on Meenalargan Hill is a large roof enclave, both quartzites have very similar mineralogical characteristics.

3.3.2 Mulnamin Siliceous Flags

Immediately overlying the Cor quartzite to the north of Crockard hill are the horizons of the Mulnamin siliceous flags. They form boggy ground around L. Nagarnaman (G7930 9770), striking west towards the Maas river (7740 9790) and east to L. Nacroaghy (G8258 9840). Outcrops of the flags are poor but where visible they comprise thinly bedded muddy quartzite, yellowy brown in colour up to 83m in thickness. No cross bedding was seen. Around L. Nagarnaman the flags form a broad anticlinal structure disrupted by a late dextral wrench fault.

3.3.3 Mulnamin Calc Silicate Flags

This group is probably best seen along part of the southern margin of the Mulnamin intrusion, (G7890 9885) where it reaches up to 250m in thickness. It is also an important horizon found at the western end of the Meenalargan intrusion (G7880 9690), especially around Lough Laragh. In this area it forms thinly bedded brown pelitic horizons with abundant patches of pale green actinolitic and epidote rich bands in siliceous and calc siliceous bands, possibly caused by a metasomatic reaction with the appinitic magma. Iyengar et al. (1954) noted several distinct tracer horizons of pure limestone and quartzite around Ranny Point (G9720 9930). Most notable of these is a basal creamy yellow, blocky calcite limestone up to 10m thick. This was not seen in the Meenalargan area, the succession being disclosed by the pelitic and calc silicate nature of the majority of the succession.

3.3.4 Maas Semi-Pelite

This rather homogeneous group is only found close to the Ardara pluton, near Maas, where it forms grey semi-pelitic, finely laminated beds. It also outcrops along the northern margin of the Mulnamin intrusion and is isolated on Carrickfad (B7250 0050) and Inishkeel Island (B7050 0030). In total it forms over 300m of exposed semi-pelite.

3.3.5 Portnoo Limestone

This group is thought to be transitional from the underlying Maas semi-pelite, as a thin limestone band is found at the top of the semi-pelite. No contact is seen in the Maas area due to a dislocation (Iyengar et al. 1954). As the name suggests the Portnoo Limestone is best seen around the type area of Portnoo. Here it takes the form of a variable muddy limestone up to 160m thick. It varies in colour from pale cream to yellow and grey. It may show a high mica content, giving it a schistose appearance e.g. east of Dunmore Hill

(G6910 0005). Local development of garnet along the Narin-Portnoo foreshore is due to the thermal effects of the Ardara granite. The limestone forms a hilly swathe of grassy ground striking east from the coast west of Dunmore (6900 9991) to the low grassy hills of Drumshantony and the saltmarsh at Clashagh (G7620 9870).

3.3.6 Cleengort Pelites

The passage from the underlying Portnoo Limestone appears relatively rapid with no obvious transition. The majority of the pelite is a dark grey to brown micaceous pelite often hornfelsed with occasional semi-pelite and calcareous bands within it. This group is found mainly in the west of the area and is thought to form up to 260m of metasediment (Iyengar et al 1954). It also forms the hills immediately north of the Ardara pluton, and is in contact with the granite where it records the thermal metamorphism of the intrusion. The mineralogy of the pelite shows increasing grade from chlorite-biotite-andalusite-sillimanite-cordierite as the contact is approached.

3.4 STRUCTURAL HISTORY AND METAMORPHISM

The structural history of Donegal has been described by Pitcher & Berger (1972) which along with the work of other authors, including that of McCall (1953) and Rickard (1962) provides a comprehensive coverage of the regional structure. The sequence of events was placed in chronological order and up to six different deformation events were attributed to the Caledonian.

The structural relationships of the region under study are best seen in the area north of the Ardara pluton, particularly around Gweebarra bay (G7950 9900) and are based on the work of Meneilly (1982,1983). Structural characteristics of cleavage and folding were noted in the field and although these did not form the main thrust of the thesis they were used in the structural interpretation of the country rocks and igneous emplacement.

3.4.1 Regional deformation

Major fold structures in Donegal postdate the D1 deformation. The best developed phase is the D2-D3 set of recumbent folding. Perhaps the best developed of these are the Errigal syncline and Aghla anticline. These are gently inclined, facing up to the north west and are responsible for large-scale repetitions of stratigraphy in north west Donegal. No major recumbent folds of this type are seen in W. Donegal, instead, tight D2 and upright, open folds of a later (D4) age are dominant.

Before describing the structure in more detail it is important to note the importance of granitic plutons to the deformation history of Donegal. The two most influential plutons in this respect are the Main Donegal and the Ardara intrusions. Both exert strong deformational effects on their country rock envelopes. Meneilly (1983) described the structure from the two best exposed areas, both north of the Ardara pluton,

namely the Portnoo-Rosbeg and Gweebarra areas, and the following is a brief summary of the main features:

(a) Portnoo - Rosbeg

The regional deformation is best seen in the Cleengort Pelite (Upper Falcarragh Pelite). The main cleavage is a penetrative S2 fabric dipping to the south. F2 folds are developed on a relatively large scale west of Portnoo and at Rosbeg, these face upwards to the north. In places S2 cleavage is cut by a gently dipping crenulation cleavage (S3) which verges and faces south on the long limbs of F2 folds. In the Portnoo area the S2 and S3 cleavages become composite and cross-cut folds at a low angle, sub-parallel to bedding, generally dipping to the south.

As previously mentioned the intrusion of the Ardara pluton has had an important effect on the structure of the area. The deformational effects of the diapir on its envelope has developed an upright cleavage - S4 which strongly folds S2 and S3 and tightens pre-existing folds causing tangential flattening and also faulting out bedding (Fig 3.4 a & b).

Bedding and S2, S3 cleavage are greatly steepened close to the contact changing from 20°-40° up to 80°. Very close to the contact these beds are highly disrupted and boudinaged. In the case of east Clooney (G7450 9900) a strike-slip fault, the Maas-Ardlougher dislocation, is related to intrusion of the central component-G3 (Pitcher & Berger, 1972). This fault may have important implications for the emplacement mechanism of both appinite and granite as it is one of many strike-slip faults of the area which may be relatively deep-reaching fractures that have been frequently reactivated and may provide a pathway for emplacement of magma.

(b) Gweebarra Bay

Like the Portnoo-Rosbeg area the structure of this area is dominated by a composite S2 S3 cleavage schistosity, deformed by the regional S4 crenulation cleavage. The major folds of the area, the Mulnamin anticline and Maas syncline strike NW-SE at Gweebarra Bay and swing to a ENE strike at Mulnamin Hill, and are upright, open folds. Meneilly (1983) interpreted the Mulnamin anticline as a north-facing asymmetric fold with a moderate to gentle south-dipping axial plane coeval with the F4 Maas syncline. The D4 deformation is the dominant phase of deformation here and it is seen to become more intense as the Ardara granite is approached. The most striking deformation occurs 250m from the contact where there is no separate S4 schistosity, instead bedding and cleavage are parallel, planar and steep. No F4 folds are present as the distension involved in the diapirism has flattened out all structures into a steeply dipping planar fabric as on the west side of the pluton.

3.4.2 Regional metamorphism

The regional metamorphism of the study area reached its peak during the second phase of deformation (D2) according to Pitcher and Berger (1972). This metamorphism

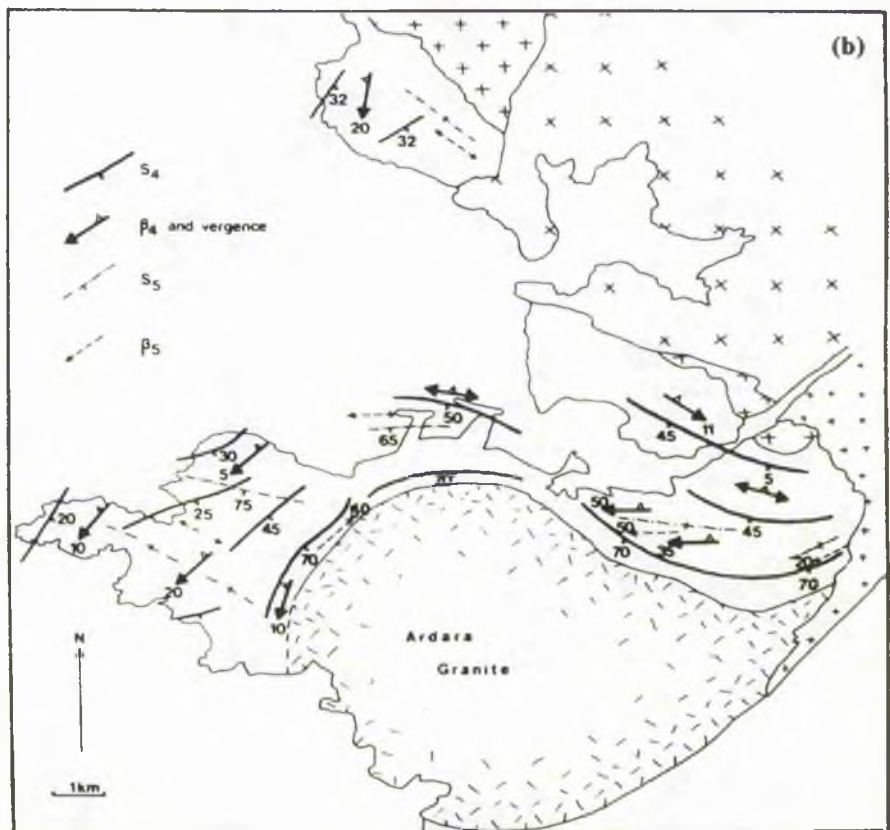
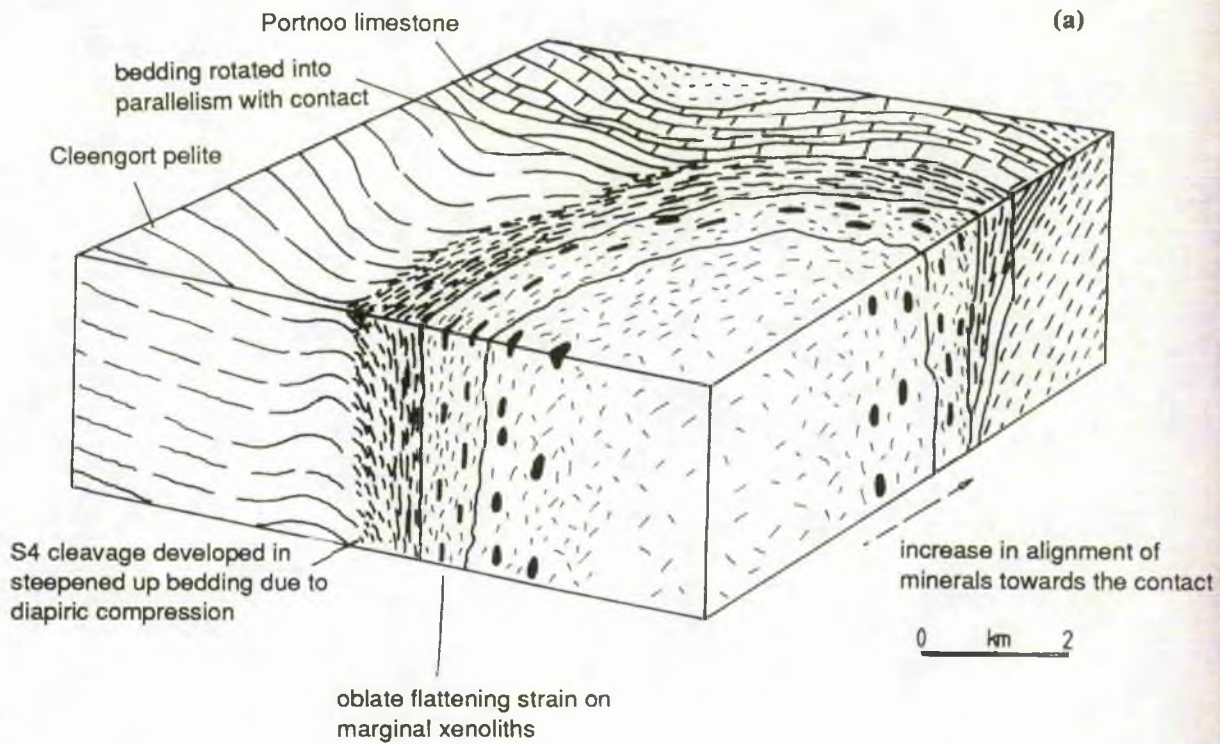


Fig 3.4 (a) Diagrammatic section through the north western part of the Ardara pluton showing the flattening strain on the xenoliths and the country rocks (based on Pitcher & Berger 1972). (b) Map of the occurrence of S₄ and S₅ including intersection lineations (β_4 and β_5) in the Ardara area (Meneilly 1982)

reached upper greenschist facies in this area and coincided with the development of a major F2 recumbent fold phase and an associated crenulation cleavage. The effects of the regional metamorphism are best seen in the pelitic country rocks, namely the Clooney pelite and Mulnamin calc silicate flags situated to the north of the Ardara pluton.

The first stage of deformation resulted in the formation of S1, the bedding schistosity, which is poorly defined in the area. The dominant schistosity is that of S2 which is a penetrative crenulation schistosity with associated garnet and ilmenite growth, now largely replaced by chlorite and plagioclase which grew later during D3 and D4. The growth of the garnet is thought to have occurred just after D2 deformation had ceased but before D3, as they were rotated by a D3 flattening event which formed inclusion trails within the garnet.

The next major growth of minerals occurred during D4 where random porphyroblasts of biotite overgrow the S2 and S3 cleavages, locally replacing garnet. A retrogression of garnet and biotite to chlorite is thought to have occurred during D4 but in some places D2 garnet is locally replaced by a late retrogressive D2 chlorite, although the D2 garnet is preserved within the Maas semi pelites which acted as a more competent horizon (Meneilly 1983).

This sequence of events is a broad generalisation and it is complicated by the effects of thermal metamorphism in particular the contact effects associated with the diapiric Ardara pluton.

3.4.3 Thermal metamorphic effects of the Ardara diapiric intrusion

The structural effects of the Ardara pluton were to superimpose a steep cleavage, S4, on the contact schists of the envelope. These contact schists have been shown by Akaad (1956) to have an almost contemporaneous recrystallisation extending in an aureole up to 1.5km from the intrusion. In the outer margins of the aureole, biotite may be seen to replace chlorite of the regionally metamorphosed schists, including the chlorite which replaces garnet that now forms tiny aggregates of biotite. As the contact is approached a belt of andalusite-rich rock up to 500m wide is found which may be accompanied by staurolite and sometimes even kyanite, often enclosed within andalusite. The next zone closest to the intrusion is dominated by a sillimanite-rich area which also contains new garnet. The sillimanite zone consists of felted needle masses associated with ragged elongate biotite parallel to the schistosity, or as inclusions within quartz. The thermal garnet in this zone, like that seen at Portnoo, is highly corroded and forms irregular masses with irregular crystal shape.

Finally, closest to the contact, yellow pinitised cordierite is present in bands up to 15cm thick with biotite and quartz inclusions in a hornfels best seen at Clooney (G9895 7250). This zone is adjacent to the main pluton which also contains sporadic tourmaline pegmatite veins and veinlets along the plane of contact.

3.4.4 Thermal metamorphic effects of the intrusion of the Main Donegal Granite

The mineralogical effects of the intrusion of the Main Donegal Granite (MDG) are not well seen in the study area but according to Pitcher and Berger (1972) as the growth of kyanite, staurolite and garnet developed in 'sweat-outs' aligned parallel to the main schistosity in the rocks east and NE of the area. Another mineralogical feature described by Hall (1966) is the loss of triclinicity in microcline in the Ardara pluton which he attributed to reheating of microcline by the main granite. The deformational effects of the intrusion are seen in the form of development of a steep S5 cleavage which crenulates hornfelsed aureole rocks, folds pegmatite sheets and deforms thermal muscovite (Meneilly 1983). Most notable of the deformational effects is the rotation of all structures towards 056° at the SW tail of the MDG and the development of a steeply plunging lineation within all rock types in the aureole of the MDG. In the Mulnamin calc silicates upright F5 folds of S4 trend are found parallel to the shear zone associated with the emplacement of the MDG.

3.5. THE DONEGAL GRANITES

The dominant form of magmatism in Donegal is granitic in the form of the eight Caledonian granitic plutons of Thorr, Ardara, Rosses, Trawenagh Bay, Fanad, Main Donegal, Barnesmore and Toories. Several methods of intrusion are involved (Pitcher & Berger 1972) ranging from the different forms of stoping exhibited by Thorr, Fanad and Trawenagh Bay to the emplacement by magmatic wedging in a sinistral shear zone of the Main Donegal granite, while the Rosses and Barnesmore plutons were emplaced by a process of cauldron subsidence. The Toories and Ardara plutons however were emplaced by a process of diapiric distension of the wall rocks. The various plutons are all related to one another temporally and spatially and are emplaced within the so-called Donegal batholith. Evidence from field observation and radiogenic methods of Rb-Sr dating by Halliday et al. (1980) indicates that much of the granite magmatism occurred around 400 Ma and developed in the following sequence: MDG, Rosses, Ardara, Trawenagh Bay, Fanad and Barnesmore.

Appinitic intrusions have been documented from both the Fanad and Barnesmore intrusions (Walker & Leedal 1954, Pitcher & Berger 1972) but the pluton with the most numerous appinite intrusions by far is Ardara.

3.5.1 The Ardara Pluton

Various aspects of the diapiric pluton of Ardara have been described in detail by Akaad (1956), French (1966), Hall (1966), Pitcher & Berger (1972) and Holder (1979). Thus the description here is based on their observations coupled with new field and petrographic observations made during this present work. The Ardara pluton (Fig 3.4 b) has a broadly rounded outline which narrows in the east to form a 'tail' region where it comes into direct contact with the deformation associated with the MDG. It measures

8.5km from the northern margin to the southern and 12.35km from the western margin to the end of the 'tail'. The pluton is estimated to have a total area of 240km² (Holder 1979).

(i) Pluton zoning

The pluton is zoned from margin to core, with a quartz monzodioritic outer facies passing inwards to a quartz dioritic zone which grades into a central granodiorite (Plate 3.1 a-c).

The margin (G1) consists a coarse grained megacrystic quartz monzodioritic facies (G1). The mineralogy of G1 comprises megacrystic plagioclase with biotite and hornblende as the ferromagnesian phases, biotite is dominant over hornblende and together with the enclaves define the foliation which is concentric with the marginal contacts. Quartz and orthoclase are minor phases in comparison to plagioclase. Accessories include titanite, zircon and epidote. This zone is largely continuous around the margin of the whole body but is broken in the NE by the intrusion of an inner facies of quartz monzodiorite granodiorite (G2). The contact between the two is sharp in the area of L. Nagurragh but north of L. Fad this contact is gradational and interdigitating.

The G2 facies is finer grained than G1 with a more equigranular texture and coarse plagioclase laths decreasing in grain size towards the core and whilst biotite is dominant over hornblende it becomes texturally less distinctive. The percentage of quartz increases slightly while that of orthoclase stays the same. The foliation is defined by biotite and enclaves which, like that of G1 lie parallel to the margin at a relatively steep angle. North of L. Derryduff G2 passes gradationally over a distance of 10m into the central granodiorite (G3).

G3 forms a circular outcrop which takes in the low-lying terrain in the core of the intrusion. It has distinctive field characteristics of decreased biotite with increased quartz content and a more equigranular isotropic nature, these quartz crystals are often as big as the plagioclase and orthoclase and thus when they weather they give the granodiorite a rubbly, pellet-like texture.

(ii) Contact Relationships

(a) Pelite-G1 Contact:

The contact between the Falcarragh pelite and G1 is a relatively sharp, planar and steep junction. The pelite is steepened up in the contact zone and has developed a strong flattening cleavage (S4) (see section 3.4.3). In the region of Narin crossroads (G7205 9865) and Clooney (G7330 9907) sinistral shear bands can be discerned both in the pelite and the quartz monzodiorite of G1 and the pelite/G1 contact is defined by a 10cm thick tourmaline pegmatite that lies in the plane of the contact and strikes into the pelite west of Clooney (G 7277 9900). It is apparent that sinistral shearing has opened up gaps for pegmatites and caused simple shear within the pelite, as well as deforming S4 folds within the shear zones (Fig 3.5). The intense strains described by Holder (1979) within the pluton

Plate 3.1 (a). Quartz monzodiorite (861) from the outer unit (G1) of the Ardara pluton showing clot-like form of biotite and hornblende defining a crude foliation. Plagioclase phenocrysts form subhedral laths with smeared biotite grains. K feldspar and quartz occupy the mesostasis.

Plate 3.1 (b). Quartz monzodiorite/granodiorite (Y32) from the inner unit (G2) of the Ardara pluton with fewer plagioclase megacrysts than G1. Texture appears almost equigranular with interlocking plagioclase, K feldspar and quartz. Biotite occurs as small euhedral flakes.

Plate 3.1 (c). Central granodiorite (Y37) from the central unit (G3) of the Ardara pluton. Texture is typically equigranular with distinctive rounded quartz crystals along with plagioclase and K feldspar and ragged, squat biotite crystals.



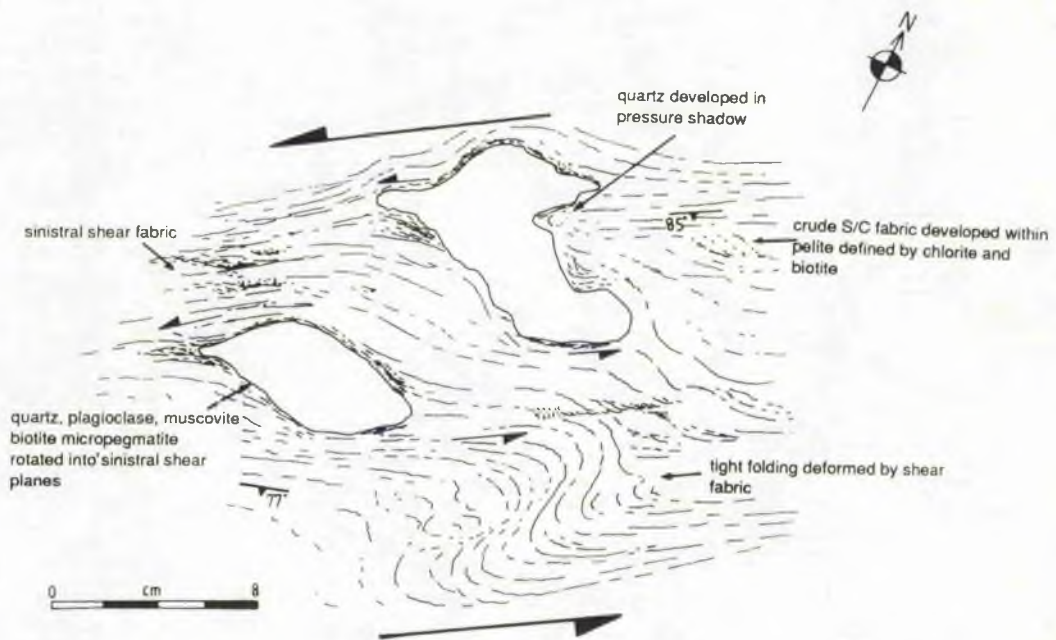


Fig. 3.5 The shear fabric associated with the intrusion of the Ardara pluton. From the northern contact aureole, Clooney.

are most apparent at the margins of the outer unit (G1) with a relatively rapid decrease in strain fabrics within G1. The presence of strain fabric within G2 in the form of deformed enclaves may correlate with discontinuities in the strain regime at a local level.

Within the quartz monzodiorite there is evidence of sinistral shear shown by the smearing of biotite around the megacrystic plagioclase in an S/C style fabric (Plate 3.2) and it also apparent from the average X/Z ratio of the basic enclaves at the contact (about 6:1) that there has been intense flattening deformation. Above Maas (G7650 9762) the pelite is steeply folded and contorted parallel to the contact and in places it appears to be almost partially mobilised by the intrusion, whilst at Summy Lough the outer G1 facies is deformed by crude dextral shear bands striking along 020° . The relationship between the sinistral and dextral shear bands may relate to the emplacement mechanism of the Ardara pluton, the shear bands are localised and affect the grain size of G1 over a distance of 2m

where the plagioclase is granulated and broken down and the biotite defines a strong shear foliation (Fig 3.5). At that time G1 must have been in a highly ductile state as the foliation is rotated away from 020° by miniature dextral shears in small zones (30 x 5cm). This deformation may be related to the large shear zone which passes north of the G1- Summy Lough diorite contact but which shears the Summy Lough diorite.

(b) G1-G2 Contact:

The contact relationships between the coarse grained and equigranular G2 are difficult to find in the field. A sharp boundary between G1 and G2 has been observed only in a few places. At SE L. Namanlough (G7615 9745) it is a steep sharp but sinuous contact, while at Letterilly House G1 also has a sharp, steep contact with G2 and in places G2 can be seen to intrude G1 in the form of metre-wide dykes. Elsewhere in the north of the pluton no such contact was seen, instead a traverse across the two facies reveals a possible intermixing contact up to 10m wide with subtle changes over a few metres then a reversion to the G1 until G2 proper becomes dominant (Fig 3.6).

(c) G2-G3 Contact:

This contact is wholly gradational over a distance of ~30m. The main difference is the increased quartz content of G3 compared with G2, the relative lack of enclaves and the smaller degree of strain. This is not always the case as the composition of G3 and the numbers of enclaves are variable. Plagioclase is no longer megacrystic but more equigranular and it has mutually interfering crystals with igneous contacts.

(d) G2-G1 and Main Donegal Granite contact

The Main Donegal granite comes into contact in the area of west Tievebrack Hill (G825 965) along a SW strike to Woodtown (G8220 9535). West of Tievebrack Hill the G2 Main Donegal granite contact is poorly exposed but from the evidence of a few rock knolls it appears to be relatively sharp and maps out as interdigitating with fingers of Main Donegal Granite up to 30m long and 10m wide veining G2. These fingers generally strike parallel to the main foliation of the Main Donegal granite. Numerous Main Donegal pegmatites vein G2 and some of these are folded by later shear movements within the Main Donegal granite.

Contact of the Main Donegal granite with G1 occurs in the area of Woodtown (G8220 9535). Again parallel to the Main Donegal granite foliation of 056° , G1 is rotated and has a steep, sharp contact, marked by a break in slope in a stream valley. G1, like G2 has a strong foliation, imposed by the Main Donegal granite and is highly veined by aplo-pegmatite veins related to the Main Donegal granite.

Plate 3.2. Sinistral shear zone within outer unit (G1) of the main Ardara pluton. Note the heterogeneous texture of G1 within the S plane. Mafic banding of amphibole and biotite is developed along the C plane. Quarry in G1, Clooney. Lens cap is 50 mm in diameter.



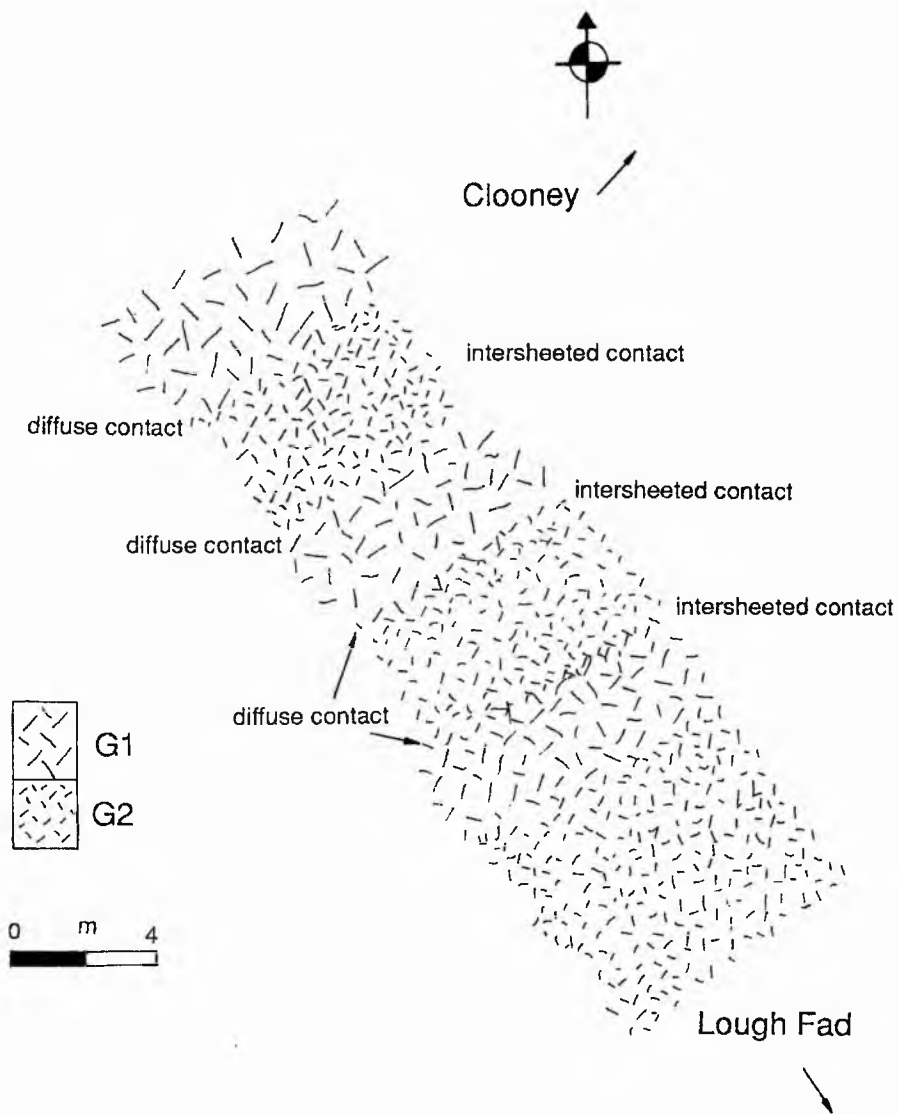


Fig. 3.6 Nature of the contacts between the outer unit (G1) and the inner unit (G2) of the Ardara pluton in the northern part of the pluton.

(iii) Lithological Variation

Facies G1

The outer facies is a coarse grained quartz monzodiorite forming an almost continuous ring 250 - 1000m wide around almost the whole intrusion except for the stalk where the inner G2 intrusion is in direct contact with the MDG. G1 is strongly foliated and coarsely porphyroblastic with numerous enclaves (see section 3.5.2). In the field G1 appears as a grey white speckled rock with abundant porphyroblastic plagioclase which is

sporadic in occurrence and non-uniform in terms of texture and grain size. At its margins biotite is abundant and can define a strong foliation fabric which, when associated with plagioclase, defines a weak sinistral S/C fabric along the northern margin and dextral shear along the western margin.

Facies G2

This rock type varies from a quartz monzodiorite to a granodiorite depending on the amount of plagioclase and quartz which are highly variable. In the field it appears to be more equigranular than G1 with a pink grey colour and dominant plagioclase with lesser amounts of quartz, orthoclase and abundant biotite. As the intrusion is traced inwards towards the south it passes transitionally into a more quartz rich-facies with equigranular texture.

Facies G3

The central member of the Ardara pluton forms a rounded body 3-4km wide in the low-lying boggy ground around L. Nagurragh (G7310 9710), L. Derryduff (G7450 9700) and L. Machugh (G7650 9550). It is compositionally and texturally variable and spatially has a variable number of enclaves. In the area around L. Nagurragh it appears as a quartz rich rock, pale pink in colour with pebbly texture due to the erosion of quartz fragments. The rock contains more quartz than G2 and less biotite.

3.5.2. Enclaves in the Ardara pluton

Enclaves within the different facies of the Ardara pluton are variable in terms of composition, number, occurrence, size and strain:

(a) Enclave composition

The following types are abundant within the pluton:

(i) Pelite and calc pelite: these probably represent fragments of Falcarragh pelite, and are most commonly found in the outer facies of the pluton, G1. These are true xenoliths accidentally included in the magma. They tend to have straight edged contacts with the enclosing medium and show little or no reaction. However in some cases the pelites are resorbed into the granitoid as schlieren broken up along bedding laminae with increased growth of biotite.

(ii) Basic clots: these include basaltic, hornblenditic and dioritic xenoliths all of which show similar textures but vary according to grain size, composition and texture. The basic clots are mostly biotite-rich as opposed to hornblende-rich and only a very few have a textural similarity to "appinite". Commonly the basaltic and metadoleritic xenoliths show the least alteration and may have sharp uncomplicated contacts with the granitoid. In some cases, as with the dioritic and hornblendite xenoliths, reaction occurs in the form of varying degrees of assimilation where edge crystals grow across the contacts which are often diffuse and sinuous. Porphyroblasts of plagioclase and orthoclase often grow within the xenoliths and in extreme cases the xenoliths become schlieric and are wholly or

incompletely resorbed. Some of these enclaves may be xenoliths of host basic rocks (e.g. metadolerite), but many (possibly the majority) are enclaves of igneous material possibly included at depth derived from a pre-existing basic magma.

(b) Occurrence

In general the number of metasedimentary xenoliths is greatest at the margin of the contact between G1 and the pelite. Basic enclaves are present within G1 as part of the overall suite but this number increases near the contact with G2 whilst the number of metasedimentary xenoliths falls. As G3 is approached the number of enclaves decreases in the north of the area but in the south G3 contains more enclaves.

(c) Size of the enclaves

The enclaves range in size from a few centimetres to several tens of metres, as in the area NE of Summy Lough (G7080 9740). Most commonly they average ~9cm in length and 4.5 cm in width but dimensions depend on location within the pluton. Marginal enclaves are more elongate and narrower than those within the centre of the pluton, which has been attributed to complex strain histories within the pluton.

3.5.3 Emplacement of the Ardara pluton and its implication for appinite emplacement

The Ardara pluton has long been considered to be a diapir, and Akaad (1956), Pitcher & Berger (1972) and Holder (1979) have all described its form. Its markedly rounded shape and intensely deformed aureole support the diapir model. Pitcher & Berger (1972) interpret the intrusion as being initially diapiric but later becoming distensional as the diapir "ballooned". The age of the pluton in relation to the regional structure of the envelope is relatively determined by its thermal metamorphism. This metamorphism is synchronous with D4; andalusite and staurolite porphyroblasts overprint the S4 cleavage and are later tightened around them. The S4 cleavage is also later overprinted by biotite formed during the thermal reaction, which strongly suggests that the intrusion was synchronous with D4.

Holder (1979) showed, using enclave shapes that the strain increases along with the foliation away from the core (which shows negligible strain values) to an X/Z ratio of ≈ 5 at the margin. This strain is oblate with the X/Y plane lying parallel to the contact (see Fig 3.7).

Sanderson & Meneilly (1981) analysed the 3D strain of andalusite fabrics from the northern aureole of the pluton. They found that rotation of andalusite porphyroblasts was due to deformation of the envelope by the expanding pluton. They calculated that the strain was a flattening strain ($K < 1$) of the order of $X/Z \approx 11$. They reconcile this large strain ratio by arguing that the initial diapiric strain may not be recorded by enclaves in the early magma. The higher strains found on the aureole side of the contact may thus be a record of the combined strains during the development of the initial diapir and its later expansion. Meneilly (1982) noted various things may occur because of the intrusion of a diapir:

(i) A change in rheology: rocks which deform by dislocation creep or diffusion creep have apparent viscosities which are strongly dependent on temperature (White 1976) and thus the hotter rocks around the granite will have lower viscosities.

(ii) Stress redistribution: pressure exerted from within the expanding pluton will produce a radial distribution of maximum principal stress, σ_1 . This could be superimposed on a regional stress system but close to the granite σ_1 will be at a high angle to the contact.

(iii) Low angle stress: if expansion is not always perpendicular to the contact but is oblique then depending on the competence of the contact rocks, the influence of the shear systems at this time may be variable and may also depend on any inhomogeneities in the magma. Oblique expansion may develop tension gashes on a large scale along pre-existing weaknesses such as bedding planes, and this may aid the emplacement of magma outside the main pluton area.

(iv) Enclave strain: Holder (1979) measured the dimensions of a number of enclaves from within the Ardara pluton and using the balloon model of Ramsay (1980) determined changes in the shape of enclaves within the pluton and related these to changes in the volume of the pluton as due to influxes of magma in different pulses. He noted that the position of magma influxes gained from freezing surfaces (ratio of xenolith radius and total radius) coincided with the position of internal contacts between G1, G2, and G3. From the evidence of the enclaves he concluded that 72% of the volume of the pluton was achieved by magma intruding and deforming country rocks in three distinct plutonic and thermal events as three pulses of magma. He also concluded that a degree of current activity was the cause of distribution of basic enclaves from the Meenalargan appinitic intrusion.

The emplacement of appinites requires a mechanism that takes into account the deep structure of the crust, probably related to a wrench fault shear zone mechanism. The observation of sinistral S/C fabric on the northern side of the pluton (Plate 3.2) during this study may have important implications for the emplacement mechanism of the Ardara pluton and the satellitic appinitic intrusions. Sinistral shear at Clooney is apparent from the evidence of biotite and pelitic schlieren. This shear is most obvious at the margin close to

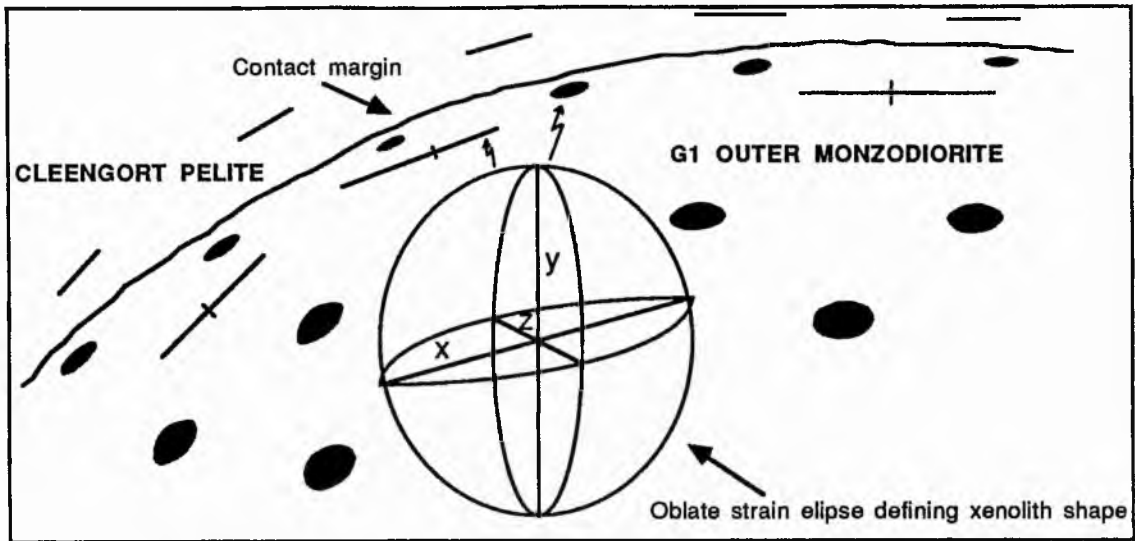


Fig 3.7 Cartoon showing the principal strain orientations at the margin of the Ardara pluton. The deformed enclaves exhibit most intense strain at the contact of the pluton with the country rocks. The foliation planes marked on the diagram define the orientation of the X-axis corresponding to the X-axis shown on the strain ellipse.

the contact and is less obvious further within G1. Shear bands can initiate very early during granite emplacement as soon as the material has a bulk solid behaviour, i.e. during the last stages of crystallisation (Gapais & Bale 1990, Gapais & Barbarin 1986) and this seems to be the case for the outer unit of the Ardara pluton (G1). Plagioclase is not obviously deformed but biotite has been plastically deformed as it is deformed around plagioclase.

Sinistral shear may be important in appinite emplacement. If a shear stress was active during and after emplacement of the Ardara pluton in an environment comprising extension and compression then this may have provided the space for their emplacement.

If the Meenalargan intrusion was intruded prior to the Ardara intrusion and if the stresses of diapiric compression were active then the oblique angle which the intrusion has to the Meenalargan intrusion and the calc silicate country rocks may have facilitated the opening of a gap for the intrusion to be emplaced (Fig 3.8 a). If the compressional regime active in the diapir was one of diapiric compression then there would be a component of extension perpendicular to that of compression acting on the marginal rocks of the contact zone and in bedding that is oblique to these forces the boudins that form in the country rock will be slightly oblique to the pluton contact and gaps related to shear zones may form (Fig 3.8 b). Hence the coeval Summy Lough diorite may have been intruded into this regime which could explain its boudined elongate shape. Thus the two models described may have some application for all the intrusions seen in the area.

3.5.4 Effects of the emplacement of the Main Donegal Granite

The Main Donegal Granite was emplaced as a syn-deformational intrusion after the emplacement of the appinite suite and the Ardara diapir and had important structural effects on both of these. This deformation and structure is most pronounced in the east of the area, in the neck of the Ardara pluton. The eastern margin of the pluton and the eastern margin of the Meenalargan intrusion are drawn out, stretched and foliated into parallelism with the NE-SW strike of the simple shear zone associated with the MDG (Fig.3.1).

Interestingly Holder (1979) noted a finite neutral point where no intrusion has a dominant foliation between the concentric strains in the Ardara pluton and the sinistral shear zones of the Main Donegal Granite. This is exhibited by foliation patterns and enclave strain which plunge at 20° to the south-west at L. Nacroaghy (G8258 9840) until at Shruhangerve Bridge (G8030 9500) there is little or no obvious strain or foliation and further west the foliation of the Ardara pluton is dominant (Fig 3.9 a). Pegmatite dykes are common near the contact of the Main Donegal Granite with a NNE-SSW strike which suggests this phase may imply that they are tension gashes within the shear zone representing incompletely consolidated magma during the shearing. These pegmatites are in turn occasionally deformed by MDG stretching parallel to 056° and in places folded in the same plane (Fig 3.9 b). In the hills of the Meenalargan intrusion D5 deformation is seen either as a steeply dipping crenulation cleavage or as a gently plunging β_5 fold axis with WNW-ESE trend. D5 also crenulates pegmatites in the zone immediately adjacent to the pluton. These D5 structures are thought to be due to NE-SW sinistral shear (the WNW trending folds in the west of the area may be the first formed folds at $\sim 45^\circ$ to the shear zone) with intense shearing rotating S5 into parallelism with the shear zone Fig 3.4 (b).

3.6 THE MEENALARGAN DIORITIC COMPLEX

The Meenalargan igneous complex forms an elongate, arcuate intrusion extending for 4.8km x 1.6km (Map 3, appendix 6). The northern contact, just west of Lough Laragh (G7840 9685) intrudes along 090° and continues to strike W-E until at Crocknadreeavargh (G7957 9690) it rotates towards 056° and extends in this direction until it is transected by the Main Donegal Granite on the north eastern side of Lough Nacroaghy (G8310 9850). Its southern contact swings even more sharply from 120° in the west to 090° south of Crocknadreeavargh and eventually parallel to 056° in the east.

The northern contact is bounded by the Mulnamin Calc Silicate Flags along its western margin with a faulted contact with Crockard quartzite further east and for most of its northern boundary it again lies in contact with the Mulnamin Calc Silicate Flags. In the SW the intrusion is intruded by G1 of Ardara which passes into G2 further east along most of its southerly contact until it is intruded by the Main Donegal Granite with its strong contact deformation aureole at the NE margin. The complex is crossed by numerous fault zones, the most dominant of which is that associated with the Main Donegal Granite.

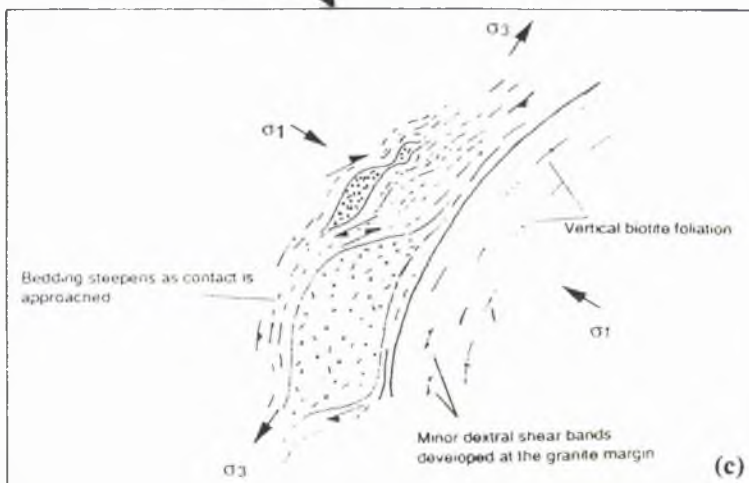
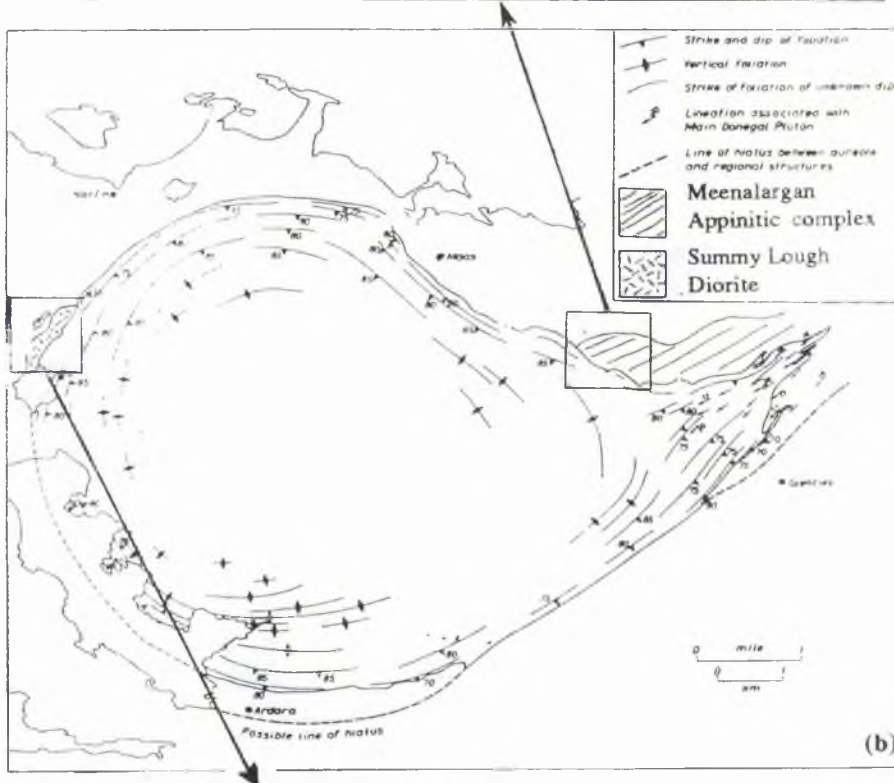
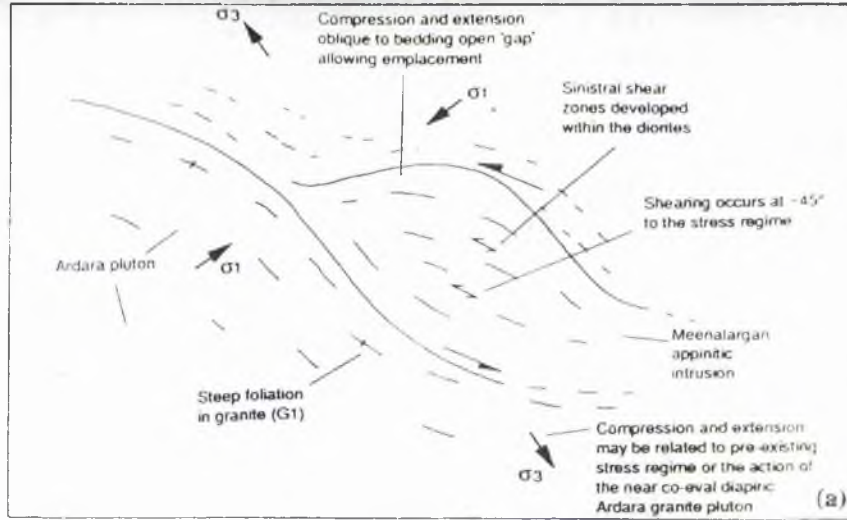


Fig.3.8 (a) Model of emplacement of the Meenalargan intrusion in relation to the stress regime of the eastern margin of the Ardara pluton. (b) Map of the Ardara pluton illustrating the foliation patterns and the locations of the Summy Lough diorite and Meenalargan Appinitic complex (c) Model of emplacement for the Summy Lough diorite intrusion based on the stress regime of the western part of the Ardara pluton

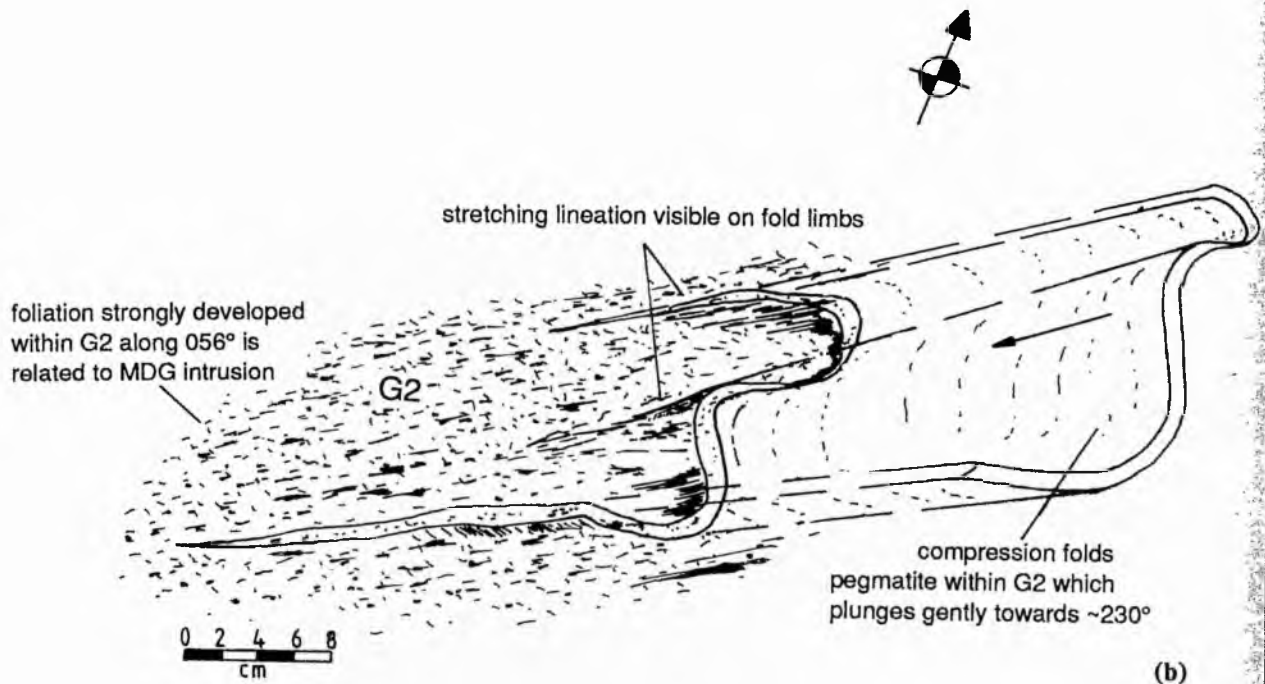
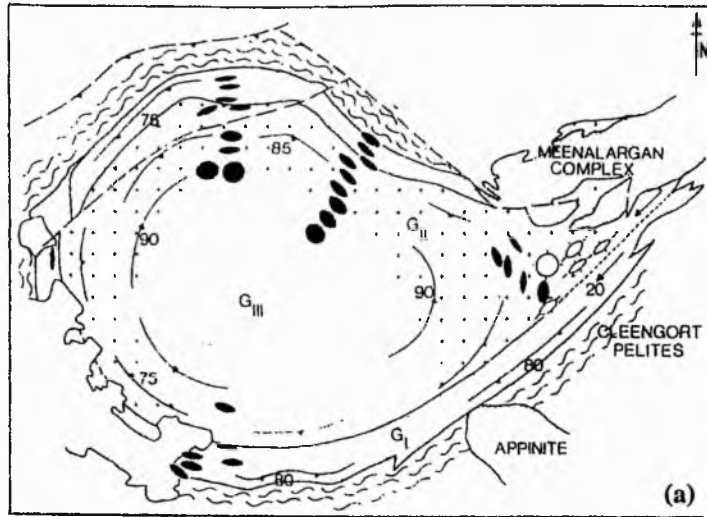


Fig. 3.9.(a) The Ardara pluton and its associated strain ellipse and foliation patterns (after Holder 1979). Open circle defines area of isotropic fabric within the inner unit (G2) of the Ardara pluton.(b) Sketch of deformed Main Donegal pegmatite within the inner unit (G2) of the Ardara pluton, from the contact zone of the MDG and the Ardara pluton. Note the intense stretching lineation and foliation caused by stresses associated with the emplacement of the Main Donegal granite.

3.6.1 Contact relationships

The intrusion is composed of several different rock types, the most dominant of which is a diorite. This forms a crude encasing envelope to a coarse grained variant of this diorite, found in the core of the intrusion, both striking parallel to the intrusion. Both facies are locally variable to meladiorite, biotite diorite, "appinite" and granodiorite types, often with contamination by country rocks, and are thus highly heterogeneous. The intrusion is in contact with the G1 and G2 facies of the Ardara pluton and it is transected by the pegmatitic facies and shear zone of the Main Donegal Granite.

(i) G1-Meenalargan

The outer facies of the Ardara pluton forms a thin strip ~500m wide along the southern margin of the complex. The contact trends in a sinuous fashion WNW to ESE until it terminates in a tongue-like intrusion of the diorite east of Boleyard (G792 965). The actual contact is steep and sharp, forming a sinuous line without any evidence of exchange or contamination of either component.

(ii) G2-Meenalargan

G2 is in contact with rocks of the Meenalargan complex from the area of Boleyard (G7875 9628), eastwards to west of Tievebrack Hill (G8215 9660) as can be seen from the map (Map 3 Appendix 6). The contact maps out as being highly sinuous and although only exposed in a few places it is sharp and often crenulate suggesting that the Meenalargan rocks may still have behaved in a plastic manner during the intrusion of G2. The line of contact trends west to east in the area just south of Loughcrillan but further east follows a NE to SW trend presumably rotated by the intrusion of the Main Donegal Granite. Both the diorite, coarse diorite and G2 are highly deformed which complicates the contact relationships of the two facies. As the contact is followed NE it locally encloses coarse diorite south east of Loughcrillan (G8138 9630) and interdigitates locally on a metre-scale with marginal diorite.

The diorite on the Meenalargan side is strongly foliated and in places shows growth of porphyroblasts of plagioclase in felsic schlieren and clots. This gives the rock a migmatitic aspect which is an effect both of the intrusion of G2 and deformation associated with the Main Donegal Granite. South of Loughcrillan is a narrow 5-10cm wide zone of exchange on either side of the contact. This appears to be a reaction zone where the diorite becomes more felsic with growth of plagioclase, orthoclase and quartz while G2 becomes more mafic with growth of hornblende and especially biotite. Each rock type appears to have exchanged material with the other over this narrow zone. This suggests that the diorite of Meenalargan was still hot during the intrusion of G2. This same outcrop also contains a 1m thick granite vein which strikes along the contact of G2 and the diorite; the vein is felsic; microgranite, probably a late-stage dyke utilising this line of weakness.

In general G2 is later than the diorite, from the evidence of cross-cutting, sharp, interdigitating contacts but evidence such as sinuous and crenulate margins as well as

partial convergence of mineralogy suggests that G2 may have been intruded before complete consolidation of Meenalargan, certainly before it was fully cooled.

(iii) Main Donegal Granite-Meenalargan

The most striking evidence of the strain imposed by the intrusion of the Main Donegal Granite occurs at the NE end of the Meenalargan intrusion, where it comes into contact with the Main Donegal Granite, in the area of Lough Nacroaghy (G8258 9840). These are:

(a) Rotation of the fabric and rocks of the Meenalargan intrusion from 090° in the west and central part to 056° in the extreme NE. This brings the rocks of the Meenalargan intrusion into direct parallelism with the Main Donegal Granite.

(b) Intense development of a stretching lineation plunging 20° towards 056° . This is often concentrated in shear bands within discrete zones concentrated in the contact area (Fig 3.9 a).

(c) Superimposed deformation on the already plastic and mobile rocks of the Meenalargan Hill and Lough Nacroaghy area forms an almost migmatite-like texture in the rock with schlieren and partial segregation into leucosome and development of agmatite amongst diorite, coarse diorite and metadolerite sills.

(d) At Straboy Hill intense interfingering of Main Donegal Granite pegmatites and coarse granite with the rocks of the Meenalargan intrusion leads to the "podding" and eventual break up, into raft trains along 056° within a Main Donegal Granite matrix with plastic flow and development of sinistral shear fabrics within the xenoliths caught up in the Main Donegal Granite.

(e) The effects of the Main Donegal Granite apparently become less intense towards SW to Shruhangerve Bridge where the foliation reaches a finite neutral point (Holder 1979) in the G2 facies of the main Ardara pluton and west to Lough Laragh where the foliation and fabric are less intense (Fig. 3.9 a).

3.6.2 Lithological variation

(i) Diorite

The typical diorite consists of subhedral to euhedral hornblende crystals either forming large single phenocrysts or aggrational clots of highly intermingling crystals in a finer grained plagioclase matrix (Plate 3.3 a). The rock has a grey spotted appearance and may be texturally highly variable. The colour index is ~60-70% and as grain size and mafic content increase the diorite passes into coarse grained diorite and meladiorite. Pyroxene, if present, is a relatively minor phase remaining after its replacement by hornblende or as an altered core to hornblende.

East of L. Laragh the diorite shows evidence of intense reaction with the Mulnamin Calc Silicate Flags (MCSF). At the western end of the intrusion the MCSF strikes into

Plate 3.3 (a). Diorite (1856) from the Meenalargan dioritic complex. Rounded hornblende with typical clot-like form set in a groundmass of actinolitic hornblende and plagioclase. Clots of hornblende have a sinuous contact with the plagioclase matrix. Clots are composed of single hornblende phenocrysts and aggregates of finer grained hornblende. Coarse diorite of the same intrusion is similar to this diorite but has more hornblende and is coarser in texture.

Plate 3.3 (b). Diorite (S5) from the Summy Lough diorite intrusion. Subhedral dark green to brown hornblende forms a highly interlocking texture with plagioclase mesostasis. Many of the hornblende crystals are euhedral in form and are apparently enclosed within plagioclase.



contact with the diorite. As a result the diorite becomes highly xenolithic and the calcareous country rock itself shows evidence of alteration. This may take two forms:

- (a) calcareous country rock skarn-type formations,
- (b) pelitic country rock contamination.

The calcareous contamination is particularly apparent to the south east of L. Laragh where beds of MCSF are metamorphosed to hornblende and clinozoisite-rich skarns (Map 3', Appendix 6).

Between Croaghkinny (G8000 9650) and Meenalargan Hill (G8200 9775) a large quartzite raft is in contact with diorite and coarse diorite. This raft dips moderately to the north west and strikes NE-SW. The quartzite appears to belong to the Cor quartzite member and has at its margins relicts of pelite and metadolerite of the overlying Mulnamin Silicate Flags (MSF) and MCSF. This quartzite appears to be a large roof pendant capping the diorite and coarse diorite of the intrusion.

(ii) Coarse Diorite

The coarse diorite forms a crude core to the intrusion and is best seen in the area of Crocknadreeavargh where it is in its least-deformed state and is largely enclave-free. Generally the coarse diorite has fewer enclaves than the diorite and these are of a pelitic nature. It consists of variable amounts of coarse subhedral hornblende crystals which often have altered augite cores. These hornblende crystals may form crudely interfering aggregates and are enclosed by a finer grained plagioclase, orthoclase and a minor quartz-rich mesostasis. Biotite is only important as a replacement mineral to the hornblende crystals. As in the diorite, clinozoisite, calcite and pyrites are important accessories. In the field the coarse diorite is distinguished from the diorite by its colour index (80%) and its coarser grain size but also by its pock-marked texture formed by the apparent weathering out of plagioclase and hornblende.

The relationship between the diorite and coarse diorite is mostly gradational, typically over 1m. For example at south Crocknadreeavargh the gradation is associated with a change in grain size, an increase in biotite and plagioclase content and different hornblende textures. Occasional isolated outcrops of coarse diorite within the diorite may be due to local magma differences or controls on amphibole growth rates.

(iii) Meladiorite

The outcrop of the meladiorite is limited to small isolated patches, often within the coarse diorite, and it may even be a more mafic fraction of the coarse diorite. It has the overall texture of a mafic equivalent of the coarse diorite with up to 60% hornblende crystals forming a highly interwoven lattice of very small grains in typical aggregate form. The felsic matrix is limited to highly sericitised plagioclase and orthoclase. The contact between the felsic and ferromagnesian phases is highly interdigitated. Augite is conspicuous by its absence. In general the felsic mesostasis is a minor part of the rock, the relationship of the meladiorite to the diorite and coarse diorite is gradational (Map 3',

Appendix 6). Few good contacts are seen but gradations in the amount of hornblende close to the contacts are seen, suggesting that the meladiorite is a mafic-rich pocket within these dioritic types.

(iv) Appinite

True "appinite" is located sporadically throughout the rocks of the complex where it is typically a lensoid, pocket veining the diorite or coarse diorite and has typical texture of acicular subhedral to euhedral hornblende crystals of medium to coarse grain size set within a now highly albitised plagioclase mesostasis. Sphene, calcite and pyrites are important accessories.

3.6.3 Contamination

The contamination seen in the Meenalargan complex takes two main forms, namely, that due to the reaction of calc silicate with diorite, and that due to the reaction of pelite with diorite.

(a) Calc silicate contamination: at the west end of the Meenalargan complex the Mulnamin Calc Silicate Flags strike into contact with the diorite of the complex. Throughout the western part of the intrusion these calc silicate beds are variously disjoined within the diorite forming small xenoliths to large blocks of calc silicate either enclosed within diorite or interdigitated within it. The effect of the diorite on the calc silicate is often spectacular, particularly in the area around L. Laragh (see Map 3', Appendix 6). Just to the SW of L. Laragh the calc silicate is altered by the intrusion of dioritic material. It shows development of hornblende and tremolite and clinozoisite along bedding laminae by metasomatism, which is irregular and in places the more pelitic bands within the Mulnamin Calc Silicate Flags are flow folded and boudinaged parallel to 274°.

Perhaps the most spectacular example of alteration of calc silicate is found SW of Crocknadreeavarh (G7901 9650). Here a calc silicate raft 20m long and 5m wide has a highly diffuse and sinuous contact with diorite and coarse diorite. The pelitic bands within it are not altered but the calc silicate shows abundant growth of hornblende and actinolite needles as well as clinozoisite. The abundance of hornblende varies between 5% and 30% and forms subhedral crystals full of inclusions of clinozoisite and quartz which overprint the original matrix. The edges of the hornblende are highly corroded and appear to be texturally secondary. At the west end of the raft the diorite brecciates the calc silicate and within this breccia small 5cm-sized xenoliths are broken off from the calc silicate raft and are enveloped within a dioritic matrix which shows similar alteration to the large raft.

To the north of Crocknadreeavarh (G7957 9698) on a steep cliff, relict bedding dipping south may be found within the coarse diorite. This bedding appears to be a ghost raft of Mulnamin Calc Silicate Flags caught up within the coarse diorite which has retained its bedding. It shows development of secondary actinolite and hornblende within the original plagioclase and clinozoisite and calcite matrix of the calc silicate. The coarse diorite

appears to have intruded the calc silicate in a sill-like fashion which has largely preserved the original bedding of the calc silicate (Fig 3.10).

Other examples of alteration of the calc silicate may be found in accidental xenoliths throughout the intrusion, although the most spectacular alteration phenomena are found at the western end of the intrusion.

(b) Pelitic contamination: in direct contrast with the alteration of calc silicate, pelitic beds within the Mulnamin Calc Silicate Flags show a different type of alteration when in contact with diorite. For example, at the western margin of the intrusion (G7857 9670) on the path west of L. Laragh, apparently in-situ pelite is mobilised and veined by non-porphyrific granodiorite. Pelite is deformed into a strong dextral S/C fabric. The diorite which veins the pelite is mineralogically and texturally highly heterogeneous. It can become more or less mafic, equigranular or porphyritic over a few centimetres. Often the diorite shows signs of granitic segregation with growth of porphyroblastic plagioclase and K feldspar as well as biotite. The pelitic xenoliths occasionally show evidence of partial assimilation. The diorite may become more felsic and granitic veins may be developed by segregation.

Whilst felsic segregation may be the result of pelitic assimilation there is a more mafic residue left. This is seen in the high cliffs east of L. Laragh (G7895 9680), where the diorite becomes highly xenolithic with pelite and calc silicate and has a meladiorite composition (CI=90%) enriched in hornblende and biotite with abundant disseminated pyrites. The composition varies depending on the number of incorporated xenoliths. In this area deformation of pelite is intense and the pelite becomes highly mobilised and partially incorporated into the diorite with development of flow folds and quartz-rich pygmatic veins within more resistant pelite.

3.6.4 Deformation

Throughout the whole length of the intrusion the effects of deformation are apparent. On a large scale the strike of the intrusion rotates in a sinistral direction from W-E in the west to NE-SW in the north eastern part of the intrusion. This is due to the effects of the intrusion mechanism by sinistral shear of the MDG which obliterates the preceding structural characteristics of the Meenalargan and Ardara bodies.

(i) Foliations and lineations:

In accordance with the swing in strike of the rocks of the intrusion, the mineral foliation of biotite, hornblende or plagioclase within the intrusion are also rotated. South of L. Laragh the dominant foliation direction within the diorite is parallel to that of the main Ardara pluton, (along 100°) and this pattern continues on the south side of the intrusion eastwards to Boleyard and Gobnagrow until east of Croaghkinny the foliation begins to rotate towards 080° at Gobnagrow and 056° east of Croaghkinny (see Map 3, Appendix 6).

However on the north side of the intrusion, to the immediate east of L. Laragh and

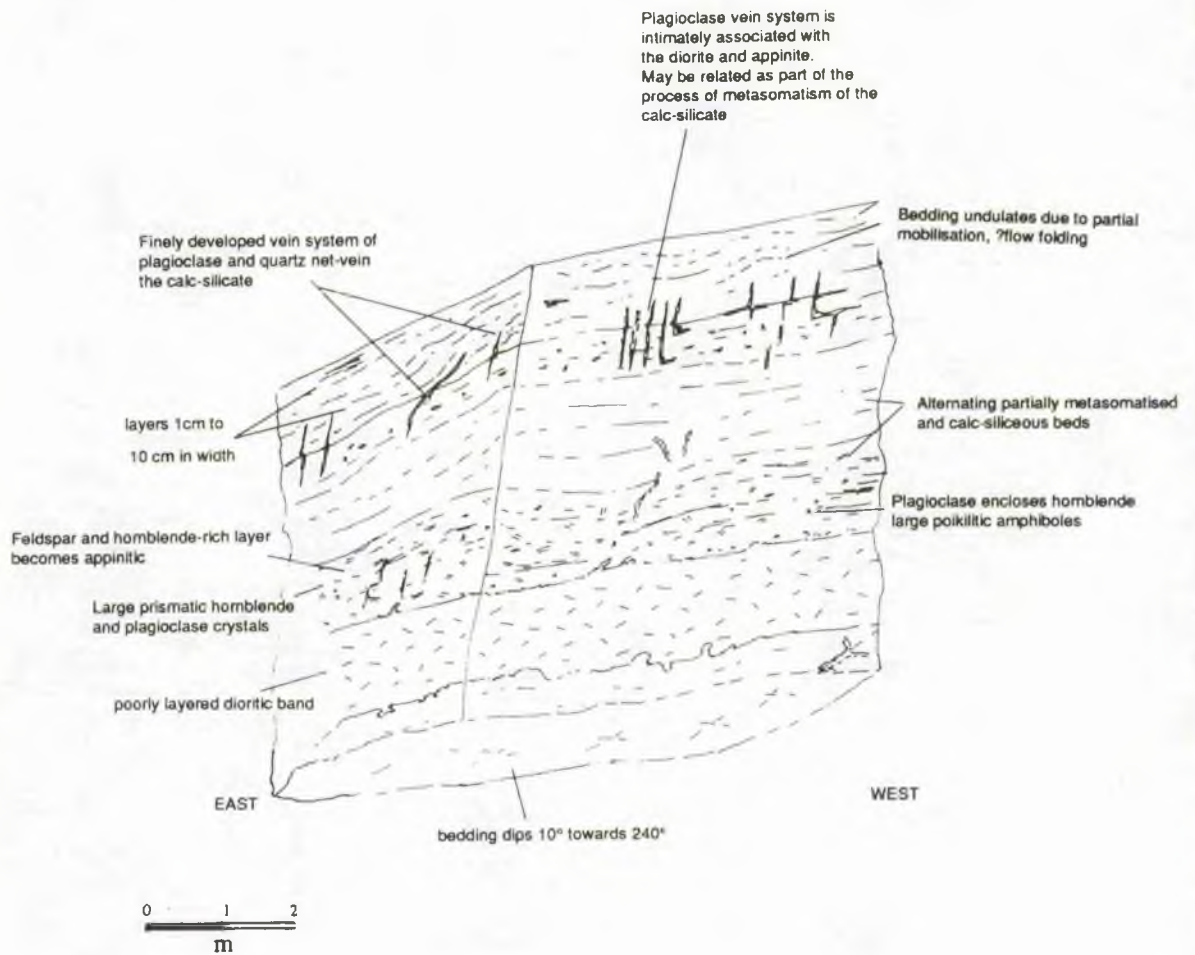


Fig. 3.10 Sketch drawing of the textures of diorite, appinite and the Mulnamin Calc Silicate Flags seen on the northern slope of Crocknadreeavarrh. Bedding in calc silicate is partially metasomatised by the infiltration of magmatic fluid from the nearby diorite.

running in a line NE of this point the foliation is consistently parallel to 056° . This suggests that there may be a strong overprinting of MDG associated fabric. This close association with the MDG is best seen in the large Cor Quartzite raft on the south side of Meenalargan Hill. This quartzite is strongly rodded and has a marked lineation parallel to 056° plunging

10-20° SW. This foliation and lineation can be traced NE to the MDG which itself shows sinistral shear bands and lineations parallel to 056°.

(ii) Shear bands:

The main orientation of shear banding is parallel to 056° and is most intense in the area of L. Nacroaghy and Meenalargan Hill. Here the various effects on the different rock types are basically similar. Within the coarse diorite and diorite, both are extended along 056-064° due to the deformation associated with the MDG but they also show a degree of intermingling related to their emplacement. At west Meenalargan Hill metadolerite sills within the Mulnamin calc silicates are deformed into boudins and net veined by felsic material and as this cliff is traced to the NE towards the Main Donegal granite contact the metadolerite is highly foliated, the foliation being defined by plagioclase with closely spaced shear bands developed.

The coarse diorite contains islands of shear within it. South west of L.Nacroaghy the shear bands within the metadolerite and pelite are sinistral S/C fabrics and have a very narrow angle between the S and C fabric of 15° or less. The diorite in this region becomes finer grained and develops these closely spaced shear bands due to recrystallisation in the stress field. The hornblende is broken down and plagioclase and quartz become highly granulated with undulose extinction.

(iii) Late stage faulting:

The Meenalargan intrusion is cut by NE-SW to N-S faults of a wrench type. These may be related to a late stage brittle episode.

3.6.5 Minor intrusions

(i) Agmatitic breccia at Croaghkinny:

A unusual outcrop at G804 79635 measuring 20m x40m is composed of diorite highly net veined by plagioclase and quartz-rich veins. The basic 'block' consist of biotite and hornblende, the biotite appears to have formed due to the retrogression of hornblende. The fragments appear angular and in places may be shown to have a jigsaw fit but on a millimetre scale the contact between the felsic fraction and basic fraction is highly interdigitating and sinuous. The cause of the breccia is unclear but may be related to entrapment of volatile-rich felsic material below the quartzite raft to the north and their escape in this area or simply due to local occurrence of volatiles.

(ii) Dykes:

The type of dykes found in the Meenalargan complex range in composition from felsite to basalt. The felsite dykes are most commonly found in the east of the area, around Meenalargan Hill (G8127 9755) and Meenalargan Townland (G8220 9720). They are 0.5 to 1.0m thick and have sharp, steep contacts with both the country rock and rocks of the Meenalargan intrusion. Texturally they appear as fine grained granular rocks with dominant plagioclase laths which are corroded by the granular quartz and orthoclase mesostasis.

Biotite forms a minor ferromagnesian phase as irregular ragged deformed grains. The felsite dykes have an approximately N-S trend and occur as a late stage of the igneous activity but before the deformation associated with the Main Donegal granite, as they are folded by F5 and are cut by the strong 056° lineation.

Basaltic dykes are found sporadically throughout the intrusion, they are undeformed and were probably intruded during the Tertiary period of igneous activity.

3.6.6 Emplacement mechanisms

In order to account for the emplacement mechanism of the Meenalargan intrusion it is necessary to consider the evidence of the field relationships. Perhaps the most striking aspect of the Meenalargan intrusion is its concordancy with the metasediments. If the deformational effects of the MDG could be unravelled and removed the intrusion may be found to be totally concordant suggesting a sill-like or sheet-like intrusion mechanism. The nature of the contacts is variable, relatively sharp against quartzite but intimate against pelite and especially calc silicate. These facts together with the evidence of abundant xenoliths showing different degrees of assimilation suggest a prolonged period of reaction with the metasediments, perhaps at depth. They are also suggestive of emplacement by stoping of a sheet-like, elongate body approximately parallel to bedding.

The main problem concerns the nature of the relationship between the coarse diorite and the diorite. Both have intimate contacts with metasediments and there is no indication in the field that one is any earlier than another, indeed the contact between the two is gradational and the coarse diorite is only locally mafic, although generally coarser grained. In most instances the diorite has a hybrid texture compared to the coarse diorite. To account for this apparent reverse zoning with basic core and more felsic margin requires that there has been side-wall crystallisation or that the diorite is slightly later than the coarse diorite and has suffered intense reaction with metasediments to give it a more felsic aspect (schlieren and veining support this). The diorite may even have been disrupted by the rise of the diorite during a phase of volatile entrapment in the roof zone of the body. The emplacement mechanism is complicated by the intrusion of the Ardara pluton and its deformational aureole, and later by the deformation associated with the MDG.

3.7 THE SUMMY LOUGH DIORITE

The Summy Lough diorite (See Map 4, Appendix 6) is located on the western flank of the main Ardara pluton (G7030 9650). It is situated between the Falcarragh Pelite to the west and the outer (G1) quartz monzodiorite to the east. The intrusion is largely made up of a relatively homogeneous green grey spotted diorite rock with hornblende crystals enclosed in a plagioclase, orthoclase and quartz matrix. Biotite is a relatively minor phase but is important in biotite-rich patches. Xenoliths of surrounding pelite are minor in occurrence,

more importantly the intrusion is transected by a dextral shear zone whose sense of movement is uncertain.

3.7.1 Contact relationships

The Summy Lough diorite is in contact with two different lithologies, on its western flank with Cleengort Pelite and with the outer part (G1) of the Ardara pluton on its eastern border. In the north the diorite pinches out against the pelite and G1 and to the south the diorite contact passes below Sheskinmore Lough.

(i) The G1-Summy Lough diorite contact

The contact with the outer unit of the main Ardara pluton is poorly exposed. At the centre of its eastern margin (G7050 9645) the contact is sinuous and steep (vertical to 65°E). In this area the contact may be highly interdigitating, with diorite net-veined by granitic veinlets from G1. In places the contact is diffuse over 1m and G1 appears to be contaminated by medium grained microdiorite patches and becomes more basic with growth of biotite and the presence of schlieren of diorite. This changes the texture of the granite (which is coarse grained) with the development of porphyroblasts of plagioclase. Against the hornblendite the contact appears diffuse with rounded contact margins suggesting that the hornblendite was still relatively warm when G1 was intruded.

The granite shows evidence of shear parallel to the margin of the intrusion defined by biotite flakes which have been smeared around plagioclase porphyroblasts, however the sense of movement is difficult to determine as the granite is plagioclase porphyroblastic. These shear bands are localised into 'islands' ~2m apart, in these shear bands the plagioclase is highly granulated and rotated. This shear is not well developed in the diorite although it does have a strong foliation which appears to swing into parallelism with the contact. Xenoliths within G1 consist of pelite and calc-pelite as well as basic enclaves and schlieren similar in composition to the diorite. These basic xenoliths can occur in swarms adjacent to the contact but are not visibly derived from the diorite.

(ii) Summy Lough diorite -Cleengort pelite contact

In general contacts with the Cleengort Pelite along the western margin of the diorite are steep and sharp without any evidence of exchange. As the pelite is traversed, dip, bedding and cleavage are greatly steepened towards the contact. There is no obvious chill facies of the diorite against the pelite. A lens of diorite is isolated within the pelite, the contacts of which can be seen to within 1m. These contacts describe a swing parallel to the contact of the pelite on both the western and eastern sides which traces a large pinch and swell structure. The pelite itself is locally intensely boudined on a smaller scale along a line parallel to the strike of the granite contact. This contact has important implications for the age of the intrusion of the diorite as it must be of similar age to the deformation associated with the boudinage and steepening of dip of the pelite adjacent to the granite. This steepening of bedding and cleavage is the cleavage S4 defined by Pitcher & Berger (1972)

and can be shown to be related to the intrusion of the granite. If the diorite was still plastic when G1 was intruded then it too would have been deformed along with the pelite. Crystal deformation of the diorite is weakly developed however hornblende and plagioclase define a strong foliation parallel to the length of the intrusion. Two major joint sets which strike along 030° and 350° respectively may be related to an extension (along 010°) and compression (along 100°) regime active during the emplacement of G1.

(iii) Metadolerite-Summy Lough diorite contact

A metadolerite sill outcrops at the NW end of the diorite intrusion. This is a relatively coarse grained rock which can be confused with the diorite but is distinguishable from the diorite by the fact that the metadolerite weathers with a grey tinge and has a distinctive lichen growth, closely spaced cubic jointing pattern, and is generally of a more homogeneous nature lacking the coarse grain size of the diorite or appinite. The metadolerite occurs within metasediments (pelite in this case), and is folded along with the metasediments. In this case the metadolerite deforms to a biotite-hornblende-rich rock which becomes highly foliated within the shear zone.

3.7.2 Lithological variation

Variations on the normal diorite include a coarse grained diorite, biotite diorite, hornblendite and "appinite". The term biotite diorite is used to describe the occurrence of highly localised biotite-rich patches within the main diorite.

(i) Diorite:

In the field the typical diorite appears as a dark green grey rock with a mottled texture of interlocking hornblende and plagioclase (Plate 3.3 b). In its least deformed state, the hornblende crystals are equant to acicular and these, together with augite phenocrysts are intergrown with a felsic matrix of plagioclase, orthoclase, biotite and quartz. Calcite is present as a late stage mesostatial mineral as well as within brittle veins and veinlets.

In its deformed state both the hornblende and plagioclase become aligned in the plane of foliation with sporadic plagioclase segregations.

(ii) Coarse Diorite:

Occasional outcrops up to 1-2m in diameter occur within the diorite. These outcrops show an increase in the size of hornblende and plagioclase and the fact that they show diffuse, almost gradational contacts with the diorite suggests that they are local areas of volatile entrapment that have provided an environment conducive to crystal growth.

(iii) Biotite Diorite:

This rock type is rare and like the coarse diorite is a localised facies of the main diorite where biotite dominates over the other mafic minerals.

(iv) Hornblendite:

An isolated outcrop of hornblendite occurs enclosed within the outer quartz monzodiorite (G1). The outcrop is 8m in width and 10m in length and consists of large, stumpy crystals of green brown hornblende within a matrix of smaller hornblende crystals with minor interstitial plagioclase and quartz. The intrusion is sporadically veined by "appinite" veinlets with acicular hornblende crystals up to 1cm long suggesting the presence of volatiles. In its southernmost part the hornblendite has a diffuse contact with a meladiorite of slightly finer grain size. This meladiorite is limited in its outcrop and appears to be a more mafic facies of the hornblendite.

(v) "Appinite"

This occurs as a vein-like, late-stage facies within the diorite and hornblendite. It occurs in the form of small veins and pockets and has a diffuse, often gradational contact with its host.

3.7.3 Structure

The Summy Lough diorite is bisected by a late shear zone of uncertain sense of movement. It strikes NNE-SSW from the SW end of Summy Lough to N. Sheskinmore Lough. The shear zone is ~100m wide and has within it distinct "islands" of intense shear 1-3m wide (Plate 3.4 a), spaced 5-10m apart. In these areas the texture of the diorite is defined by a parallelism of plagioclase and granulation of all the mineral phases, and it does not seem to be related to the dextral shear seen in the outer margin of G1. The diorite is also transected by two late faults striking ENE across the eastern margin, firstly a sinistral wrench of ~100m in the vicinity of Mooney's Lough (G7080 9687) and a dextral wrench also of ~100m just south of the Duvoge River (G7040 9620), both these faults are later than the intrusion of G1 and G2.

The Summy Lough diorite appears to have been intruded parallel to the strike of already steeply dipping Falcarragh Pelite. In view of the lack of xenoliths of pelite within the diorite and the fact that there is no marginal alteration of the diorite or the pelite in terms of chilling, metamorphism or veining it is possible that the diorite was intruded slightly before the G1 intrusion as a bulbous sill-like plug into already warm, dilated country rock (Fig 3.11).

From the evidence already discussed, the Ardara granite and Summy Lough diorite magmas were probably coeval and so the initial plasticity of the pelite may have been generated at depth by the rising diorite followed closely by the diapiric granite magma.. If the dextral shear seen in the outer margin of G1 is associated with the emplacement of the outer facies of the Ardara diapiric pluton, and if the diorite were intruded into a tectonic regime of oblique distension shortly before the Ardara granite then this oblique distension may have provided the space for its emplacement.

Plate 3.4 (a). Closely spaced shear bands within diorite at Summy Lough. These shear bands occur in discrete 'islands' which in this case are 1.2 m in width. The shear bands are defined by felsic bands seen below the pen and to the left of the photo. Pen is 15 cm in length.

Plate 3.4 (b). Breccia on small island, Mulnamin showing varying degrees of assimilation of calc silicate enclaves (red/brown fragments in centre of photo) and pre-existing igneous rocks (dark hornblendite) in a dioritic matrix. Lens cap is 50 mm in diameter.



3.7.4 Coarse grained appinite

An elongate intrusion of coarse hornblendite occurs ~200m north of the Summy Lough diorite within the outer margin of G1. Only one contact is seen between the hornblendite and G1, this is relatively sharp and steep. The actual form of the body is thus difficult to determine, it is 20-25m in width and 80-90m in length and has the characteristics of a xenolith or a later dyke. It is composed of squat subhedral to euhedral hornblende phenocrysts with minor biotite within a sparse plagioclase matrix, quartz and orthoclase are rare, accessories include calcite and pyrites both of which are late stage minerals typical of appinite. Texturally it is similar to the hornblendite seen at the eastern margin of Summy Lough diorite further south. The hornblendite is frequently veined by "appinite" in the form of late-stage pockets and veins which have a diffuse contact with the hornblendite. The pockets are up to 1m in length and 0.4m in width with typical acicular amphiboles in a plagioclase matrix.

Its origin is thus difficult to determine, it appears to be related to rocks of the "appinite suite" by its composition and texture. If it is a dyke intruding G1 then this has important implications for appinite genesis and requires that there is a late stage presence of appinitic magma after the emplacement of the outer unit (G1) of the Ardara pluton. Evidence against this being a dyke is the difficulty in finding other outcrops of this type along strike or anywhere in the area. Alternatively it may be a large enclave of hornblendite although the strike of the body is oblique to the foliation of G1. Another possibility is that this body may have a relationship similar to the hornblendite seen isolated at the eastern margin of the Summy Lough diorite in that it may be related to the diorite but has become surrounded by G1 which has given it an isolated appearance. Texturally this hornblendite is similar to that seen further south and its oblique strike and lack of outcrop elsewhere in the area all support this latter idea.

3.7.5 Emplacement mechanism

The Summy Lough diorite shows important evidence of the close temporal and spatial relationships between basic rocks of an appinitic nature and associated granite. Evidence of the timing of the intrusion of diorite and granite confirms the relationships seen elsewhere of early appinite and slightly later granite. The spatial relationship is less clear, dextral shear in the margin of G1 is not as well developed within the diorite. Poorly developed shear foliations are present along with (?dextral) shear joints in the isolated lens on the western side of the intrusion. This intrusion may prove the coeval relationship between the diorite and G1 in the way that it is boudined in association with the steepening-up of the bedding and cleavage (S4) in the pelite. Judging from the near coeval nature of the intrusion of diorite and granite, the diorite may have been intruded into already plastic pelitic country rock as a semi-concordant dome-like mass which was under an oblique extensional and compressional regime associated with the distensional diapirism of the

granite. The Summy Lough diorite is remarkably homogeneous in composition for a rock type associated with the appinite suite, this may be related to its intrusion mechanism and crystallisation path. It was emplaced into pelite but reacted little with it and slow cooling of the mass may have imparted a relatively homogeneous texture on the diorite. A model for the intrusion of the Summy Lough diorite is presented below (Fig 3.11).

3.8 THE MULNAMIN INTRUSION

The Mulnamin appinitic intrusion (Map 5, Appendix 6) is located in the north of the study area, to the north of the Meenalargan intrusion, on the south bank of the Gweebarra River where it enters the bay (G7855 9900). The intrusion was studied by French (1966), and much of the present study is based on his observations and maps.

3.8.1 Form of the intrusion and contact relationships

Contact relationships with the country rock are poorly exposed but at the north west end of the intrusion a sharp, apparently steep contact exists with a 10m thick metadolerite sill. This contact with metadolerite is parallel to bedding, however the contact relationships elsewhere are cross-cutting and French (1966) noted that the contact at the junction of the Maas Semi Pelites and Mulnamin Calc Silicate Flags was cross-cutting and dilational.

On the northern side of the intrusion, along the coastal contact with a siliceous marble with pelitic partings, a member of the Mulnamin Calc Silicate Flags appears to be concordant and in intimate contact. On the northern flank the marble has a concordant strike and steep dip to the NE but as this member is traced to the east the contact becomes cross cutting and the dip becomes very steep. However, within the intrusion the marble is highly folded and the diorite mimics this folding. In the south east, although contacts with the Mulnamin Calc Silicate Flags are cross cutting they swing into parallelism with the contact and are seen to steepen up next to the contact. The intrusion appears to have caused a local increase in the dip of the metasediments along its margin.

3.8.2 Lithological variation

French (1966) divided the main lithologies of the intrusion into 3 groups elongate parallel to the long axis of the intrusion (Fig 3.11). In the south he noted a zone of dioritic hornblendites and coarse spotted diorites. This is bounded to the north, in the core of the complex by a diorite zone, and along the northern margin of the intrusion, a zone of appinitic hornblendite and appinite. Mapping along the coast where exposure is best confirms this general pattern although it is locally more complex (Map 5, Appendix 6). Along this coastal section intimate contact relationships exist between diorites and hornblendite and the calc silicate of the country rocks.

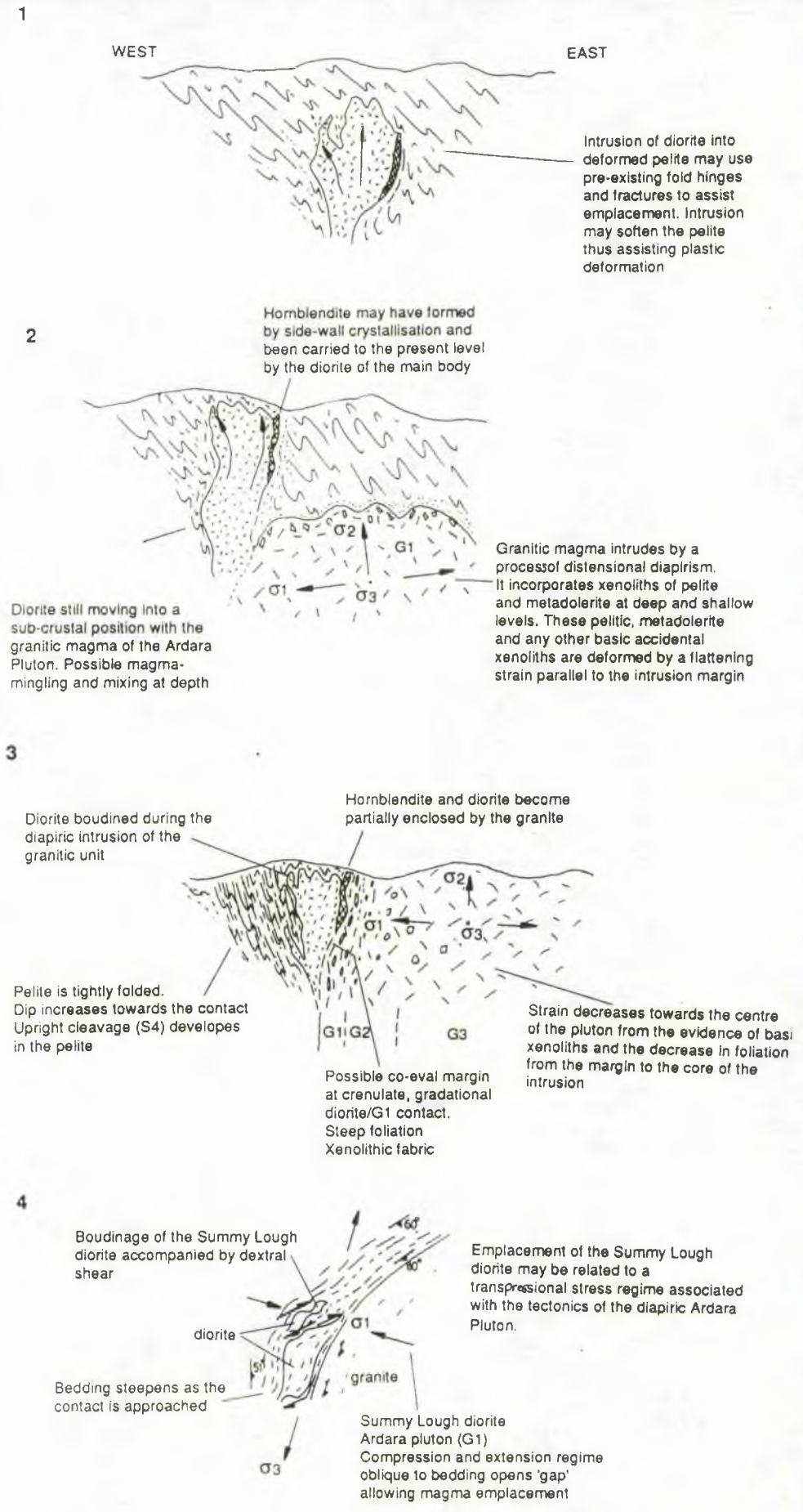


Fig 3.11 Model of emplacement for the Summy Lough diorite intrusion. Cartoons (1-3) show the development of the Summy Lough diorite and the western margin of the main Ardara pluton in cross section. Cartoon (4) is a plan view highlighting the possible stresses which may have effected the emplacement of the Summy Lough diorite in relation to the distension associated with the main Ardara pluton.

(a) Diorite - dioritic hornblendite

The southern part of the intrusion is dominated by a rock composed of mafic clots within an intermediate groundmass. The mafic clots are usually 0.5cm in diameter and are crudely circular to elongate, and consist of various amounts of hornblende, augite, diopside, biotite and actinolite. The texture of these clots is almost wholly replacive and commonly clots consist of glomeroporphyritic hornblende and augite, replaced by actinolite and biotite. Contact with the mesostasis is diffuse and this consists of a recrystallised intergrowth of plagioclase and euhedral to subhedral hornblende with minor biotite, equigranular quartz and orthoclase in the groundmass, accessories include clinozoisite, sphene, chlorite and calcite. Shear stress is apparent from the development of preferred orientation and intense recrystallisation of all phases. The diorite is highly heterogeneous in terms of a coarsening and change in the ratio of the mineral phases which can occur over a

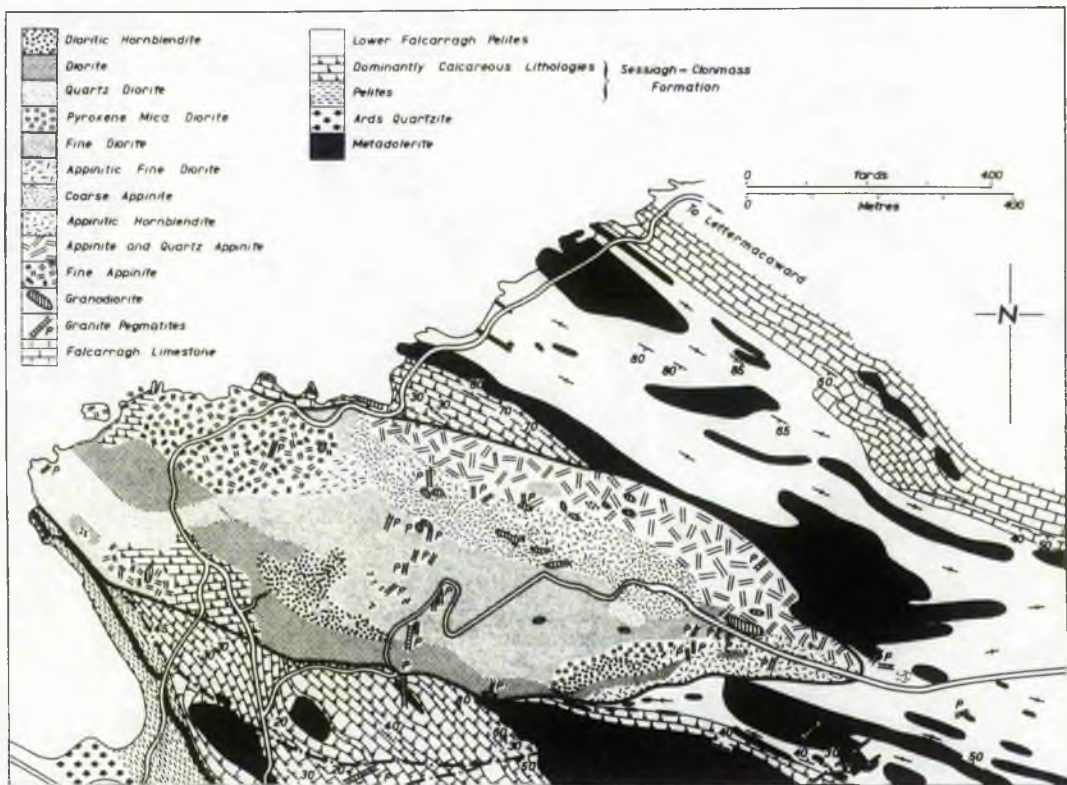


Fig 3.12 Geological map of the appinitic intrusion of Mulnamin More (after French 1966).

few centimetres, variations in hornblende content giving rise locally to meladiorite. One such common textural change in the amount and size of the hornblende leads to the formation of coarse meladiorite best seen on the coast which consists of 0.5 -1.0 cm sized crystals of stumpy hornblende and augite set within a plagioclase, orthoclase and quartz mesostasis. The mesostasis is less common in this as the hornblende in particular is euhedral and stumpy. The augite crystals are also squat and euhedral, commonly possessing an overgrowth of rounded granular hornblende. The hornblende crystals are considerably recrystallised into a patchwork of subhedral crystals with a highly interlocking texture. The mesostasis consists of plagioclase which is highly sericitised and includes abundant apatite needles, clinozoisite and calcite which has grown late as primary magmatic plates.

(b) Appinite

French (1966) described appinite in the south east corner of the intrusion but this also takes the form of hornblende diorites with appinitic texture along the coast to the north west. These rocks consist of euhedral to subhedral hornblende crystals up to 1cm long which are mutually interfering. The hornblende commonly has a dusty iron oxide core. Diopside and or augite forms the main pyroxene phase which is replaced to different degrees by hornblende, usually as a corrosion rim but occasionally as granular crystals growing across the crystals.

Hornblende and augite form the main mafic phases with biotite usually as a secondary replacement mineral. The mesostasis is formed consistently of plagioclase which occurs as rounded to lath shaped plates in the mesostasis occasionally enclosing hornblende and pyroxene.

Contacts with the diorite are often diffuse and sinuous suggesting a close relationship between the two. In some places the appinite becomes very coarse grained in pockets and veins. This appinite is similar to that seen at Rubha Mor, Argyllshire. It consists of coarse hornblende up to 1cm in length, often with plagioclase and calcite for cores enclosed within a plagioclase and hornblende matrix with abundant pyrites. This rock type is "appinite" and appears to be a late stage volatile-rich facies.

The appinite facies vary in composition between "appinite", dioritic appinite and appinitic hornblendite. Those with greater amounts of hornblende and less plagioclase outcrop along the northern side of the intrusion. Appinite on the north coast is hornblendite and consists of coarse hornblende in a sparse medium grained mesostasis. Within this zone the hornblendite has sharp contacts with diorite sheets and lenses which strike parallel to bedding in the calc silicate. Also within the hornblendite there are slightly more felsic areas of dioritic appinite with diffuse contacts. This dioritic appinite is intimately associated with the Mulnamin Calc Silicate Flags. One hundred metres east of the quay (G7870 9910), parallel to the strike of tightly folded calc silicate the dioritic appinite takes up the bedding within the metasediment so that it appears to be folded along with it. It is apparent that the

calc silicate forms relict bedding within the diorite. It seems that a fluid of magmatic origin has been responsible for the metasomatism of the calc silicate with growth of hornblende, plagioclase and clinozoisite.

The main rock type in this area varies between hornblendite and hornblende meladiorite. It is a medium grained hornblende-rich rock with minor feldspathic mesostasis. In an outcrop of the most mafic composition seen on Mulnamin Hill an apparently late feature is seen within a hornblendite, similar to that seen on the coast at the highest point on Mulnamin More (G7935 9877). This is a ramifying network of feldspathic veins which form intimate relationships with the mafic host. The sparse plagioclase in the mafic fraction may be seen to grow into the felsic vein as if it were draining the mafic fraction of its felsic melt. This may be a late stage felsic vein formed at a stage when the magma was still in a mush-like state before final crystallisation of the plagioclase.

The rocks in this area are poorly exposed, they exhibit gradational compositional variation in the amount of hornblende and its grain size. However these variations are neither sharp nor consistent. This Mulnamin Hill area is however poorly exposed though the hornblende seen here is much coarser than that seen on the coastal section.

(c) Relations between diorite and hornblendite

The contact between the diorite to the south and hornblendite to the north appears to be relatively sharp and strikes NW-SE parallel to the long axis of the intrusion. Xenoliths of hornblendite are found on the island 30m west of the quay (G7840 9908). These have square, sharp contacts with the host diorite and resemble the hornblendite with the diffuse contact found within the hornblendite. It may represent an early magma, parental to the other rock types. Thus the diorite may be slightly later than the hornblendite seen on Mulnamin Hill.

(d) Intrusion breccia on Mulnamin Island

A small 1m x 3m intrusion breccia pipe as defined in section 2.4.3 (vi) (Plate 3.4 b) is found on the island 35m west of the quay (G7840 9908) (Fig 3.13). The breccia pipe has gradational contacts with the diorite around which it becomes contaminated by rounded, altered blocks of calc silicate arranged in a chaotic manner. These calc silicate xenoliths are complicated by occasional hornblendite xenoliths whose margins are slightly corroded due to reaction with the dioritic host. The calc silicate xenoliths show all stages of reaction and metasomatism from development of hornblende and actinolite parallel to bedding to a ghost xenolith formed of finer grained hornblende with little or no plagioclase; clinozoisite and quartz are minor phases. The host diorite is similar in composition to the diorite around the intrusion and no sharp contact can be found with the diorite of the breccia and the diorite of the main mass. As the breccia is approached the number and size of xenoliths increases, the basic xenoliths resemble the hornblendite xenoliths found in the hornblendite diorite to the north and the hornblendite found on Mulnamin Hill. The square

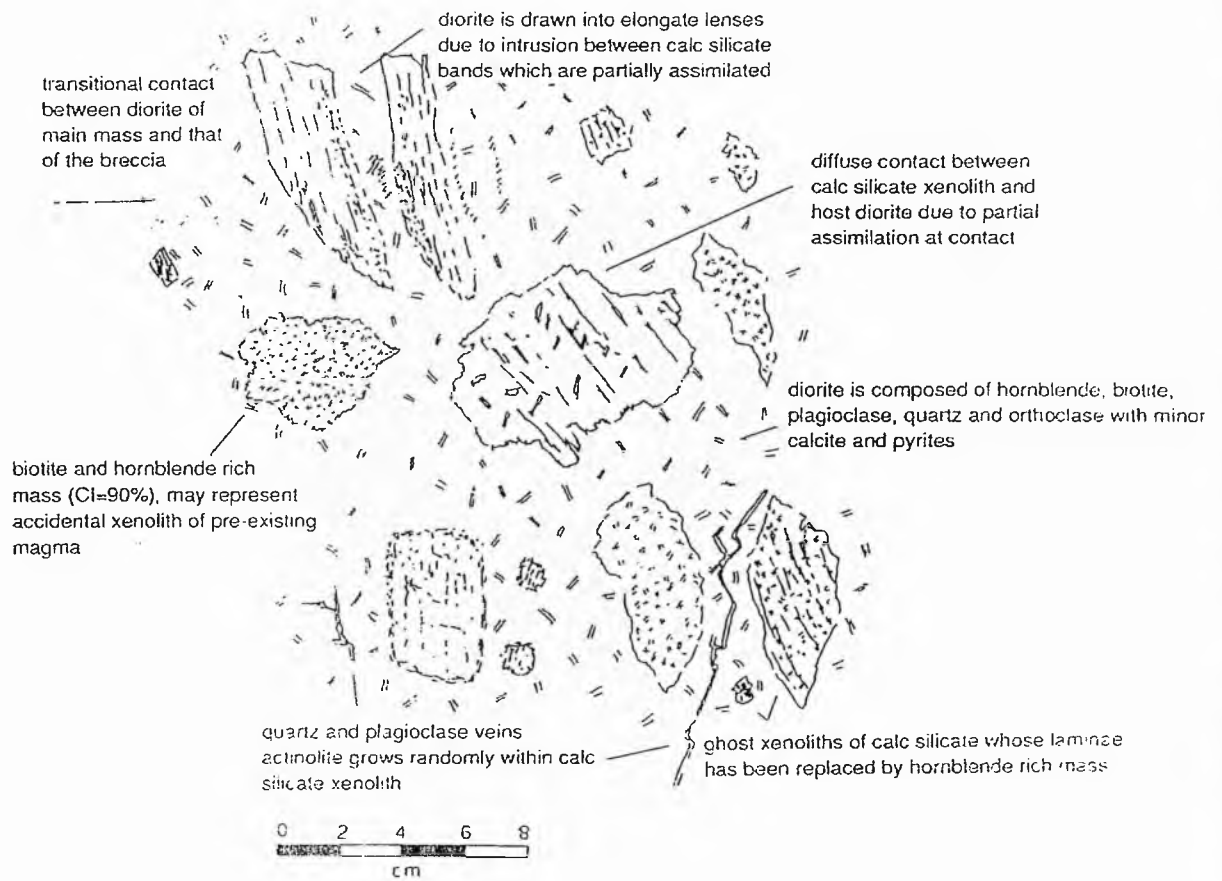


Fig 3.13 Sketch of the breccia pipe on the island at Mulnamin More for comparison with the textures shown in Plate 3.4 (b).

margins and slight corrosion at the margin of the basic xenoliths suggest they were already solidified before incorporation within the magma and may have been an earlier genetically-related rock type.

(e) Country rock rafts

A large xenolithic raft 100m x 40m of Mulnamin Calc Silicate is found within the diorite just to the west of the quay (G7850 9910). Bedding in this xenolith strikes NW-SE,

again parallel to the strike of the long axis of the intrusion. However there is an intimate relationship between the diorite and calc silicate, which develops hornblende at the margins in contact with the diorite. The diorite mingles with the calc silicate which shows evidence of flow-folding notably in the pelitic portion, which is not as compositionally altered as the calc silicate. Contacts with the diorite are interdigitated and there is always a retention of bedding within the calc silicate though it is obviously altered at the margins.

(f) Granodiorite/quartz diorite sheets

This rock type forms several cross cutting sheets and dyke-like intrusions. One of the best exposed of these occurs on the coast and takes the form of a concordant sheet striking NW-SE. It forms sharp contacts with its calc silicate host rocks and forms cross-cutting contacts against the diorite in the area. Compositionally it consists of corroded, sericitised plagioclase laths, often corroded by quartz. Orthoclase occurs as a minor interstitial phase with a rounded habit. Biotite is the main ferromagnesian mineral and forms fleck-like crystals aligned in the direction of the foliation, flowing around plagioclase which alters to chlorite. The texture is indicative of shear, notably by granulated crystals and a strong foliation defined by biotite. This appears to be a late stage event and not associated with the emplacement of the granodiorite/quartz diorite.

(g) Pegmatites

Sporadically intruded across the intrusion are a number of thin pegmatite sheets. These trend along $\sim 030^\circ$ and dip steeply NW or SE and may extend for several metres. They consist of coarse grained orthoclase, quartz and albite intergrowths with muscovite and minor garnet and tourmaline. These pegmatites are related to the Main Donegal Granite intrusion to the NE of the Mulnamin intrusion.

(h) Plagioclase veinlets

These occur throughout the appinitic rocks and form cross-cutting contacts with the host rocks, but in some places may form ramifying networks. In places this extends to a net-veining complex but appears to be localised. The contacts between the veinlets and host rock are relatively sharp though are gradational on the centimetre scale. These veinlets may be related to pegmatite bodies seen in the area. French (1966) described the veinlets within the appinite as occurring as offshoots of larger pegmatites associated with the Main Donegal Granite. The veinlets may represent a stage before the final solidification of the host magma as none of the contacts with the appinite can be proven to be brittle. No constraints for their age relationship with the Main Donegal Granite have been found.

3.8.3 Emplacement mechanism

The Mulnamin intrusion shows evidence of emplacement by dilation and expansion of its country rocks associated with intrusion by stoping of, and reaction with, calc silicate country rocks. The NW-SE trend of the lithological facies within the intrusion may be related to the structure of the surrounding country rocks and the structural regime active at

the time. Several different rock types are present, ranging from hornblendite (both as distinct facies and as xenoliths within other facies), to hornblende appinite (hornblende meladiorite), to diorite (in which grain size is highly variable). Also present is "appinite" in its typical form of pockets and veins, and late stage granodiorite dykes and veins. The close but localised association between the hornblendic magma and calcareous country rock is clear, and it is apparent that the prolonged reaction of calc silicate with appinitic magma has led to some of the mineralogical changes seen in the field. This contamination is shown to be a two way process in the fragmentary breccia pipe at Mulnamin where the calc silicate xenoliths form ghost xenoliths incorporated into the magma. The end process of this incorporation is the breaking up of these fragments leading to complete assimilation.

3.9 THE NARIN-PORTNOO COMPLEX

The strip of coastline between Portnoo and Dunmore was studied in detail by French (1966), however little is known about the Narin-Portnoo section and the contact relationships between calcareous country rocks and appinitic facies. This area of coastline between Sheehan rock (G7105 9920) near Narin to a point east of Dunmore Breccia Pipe (B6927 0020) west of Portnoo was mapped in detail (Map 6 in Appendix 6). The coastline affords fine exposure of the contact relations between many highly heterogeneous appinitic intrusions intruded within the calcareous lithologies of the Portnoo Limestone. The area was selected for study in order to understand better the following:

- (a) importance of calcareous lithologies in appinite genesis,
- (b) small scale relationships between different appinitic facies,
- (c) relationships of acid bodies to early basic bodies,
- (d) form and shape of the appinitic bodies and their emplacement mechanisms.

3.9.1 Narin-Portnoo shore section

The Narin-Portnoo coastal section contains three areas of interest:

- (a) Foragy Rock to Tidy Rock
- (b) Cathleen's Hole
- (c) Fairy Coves

Each of these areas contains a varied assemblage of appinitic lithologies intruded into limestone and metadolerite lithologies. The rock types associated with these intrusions and the area west of Portnoo include a spectrum of acid and basic rocks with associated lamprophyric types.

(a) Foragy Rock (Map 6)

The Portnoo Limestone into which the diorites are intruded outcrops to the east of the intrusion at Sheehan rock. Here a phyllitic limestone strikes west-east dipping moderately to the south and is highly sheared and folded in what appears to be an inclined F3 syncline plunging 40° towards 128°. Also folded within the Limestone is an 8m thick

metadolerite sill which, although it does not take up the folding because it is more competent than the limestone, is still strongly deformed. Both lithologies are cross-cut by thin lamprophyric dykes which themselves are highly folded and sheared. There appear to be three ages of dykes, an early NE-SW set which is cut by a later NW-SE set and a later minor W-E-trending set. The dykes and limestone and metadolerite are all sheared by a number of fine sinistral and dextral shears up to 10cm wide that are concentrated in this coastal section.

Two hundred metres west of Sheehan rock the appinitic intrusion of Foragy rock is found. The intrusion is ~50m in length and more than 20m wide but its full extent is uncertain as it is covered by the sea to the north. It is dominated by meladiorite to hornblendite which appear as medium to coarse grained dark grey rocks with occasional foliation and layering (Plate 3.5 a). The meladiorite (Plate 3.5 b) and hornblendite lithologies have numerous limestone xenoliths within them in different stages of modification and pass gradationally into contaminated appinite. The appinite appears grey green in outcrop with squat hornblende phenocrysts up to 1cm in diameter. The actinolitic hornblendes are set within a finer grained granular groundmass of plagioclase, clinozoisite, quartz and disseminated pyrites. The contaminated appinite is often a marginal facies and is associated with brecciation of metasediments (Map 6, Appendix 6). The texture may be the result of late stage alteration by circulating groundwaters using the contact as a channel. Also present within the hornblendite are typical pockets and veins of "appinite" with the usual diffuse and sinuous contacts with the enclosing meladiorite.

(i) Contact Relationships:

The marginal relationships of the Foragy Rock intrusion with the country rock are variable, on the east side the contact is sharply cross-cutting with a 0.5m wide intrusion breccia formed due to the force of the intrusion. This appears as a mass of clast-supported disjointed limestone fragments with little obvious igneous matrix (Plate 3.6 a) although in places there is a scarce dioritic groundmass which appears to have caused the crystallisation of hornblende and clinozoisite within the outer margins on the limestone blocks. At the eastern margin of the Foragy Rock intrusion the hornblende appinite is veined by calcite and there is considerable mobilisation within the limestone. As the southern contact with the limestone is approached the plane of contact becomes relatively concordant with the west-east strike of the Portnoo Limestone and the zone of brecciation dies out along this contact. Thus where contacts with country rocks are parallel the intrusion contact is less disrupted than where the intrusion is cross-cutting. In support of this it can be seen that the number of xenoliths is greater along the eastern side where the contact is cross-cutting. Along the southern margin the contact with the limestone is relatively concordant dipping 50° to the south parallel to the dip and strike of the Portnoo Limestone. There is an apparent change in composition in some places from meladiorite with granodioritic veining (Plate 3.6 b) to contaminated appinite (Fig. 3.14). This change is gradational over 10cm and the

Plate 3.5 (a). Hornblendite (Hb) from the Foragy rock, Narin-Portnoo intrusion. The rock is composed of elongate hornblende crystals which in this case define an upright foliation. Plagioclase is almost totally absent.

Plate 3.5 (b). Meladiorite (27520) from the Foragy rock, Narin-Portnoo intrusion. Large rounded hornblende phenocrysts are set within a finer grained matrix of hornblende and plagioclase. The sample is cut by a late felsic vein and contains minor pyrite crystals (top right)



meladiorite passes into a more felsic facies, with a large number of secondary minerals including actinolite and clinozoisite. This band of contaminated appinite stretches parallel to the strike of the Portnoo Limestone for almost all of the length of the intrusion. The contaminated appinite often has a foliation parallel to this and numerous xenoliths of the Portnoo Limestone within it; its width varies from 0.5m to 3m. One area in the central part of the exposed outcrop has a diffuse contact with hornblendite and contains abundant limestone xenoliths possibly representing calc silicate beds disrupted by appinitic magma which have reacted with this medium to form secondary actinolite and clinozoisite (Plate 3.7 a). To the west of Foragy Rock, the intrusion is continuous into the hornblendite and meladiorite of Tidy Rock (G7067 9940). Within the hornblendite a highly diffuse zone of quartz dioritic material is found between two screens of Portnoo Limestone which has a highly sinuous contact with the hornblendite. The quartz diorite consists of variable amounts of hornblende in a feldspathic matrix which in places is porphyroblastic. The feldspar is plagioclase largely replaced by crystals of clinozoisite and sericite. In some places the quartz diorite loses the porphyroblasts of plagioclase and a more medium grained equigranular texture of similar mineralogy is dominant. This variability of grain size gives the quartz diorite a layered appearance with alternating layers of porphyroblastic and medium grained diorite up to 3cm thick dipping NW at 30° towards 350°. This diorite is veined in some places by steeply-dipping hornblende-rich veins that are related to the hornblendite. The relationship is that the diorite is a local variant of the hornblendite though with more felsic constituents.

The meladiorite is composed of a chaotic array of calc-silicate xenoliths and the whole area shows intense variation. At its western end the meladiorite shows evidence of forceful intrusion against meladiorite, the contact dipping steeply 60° to the west. There is no brecciation of the meladiorite but it is highly crystalline due to recrystallisation upon intrusion of the appinite. At the extreme NW end of the intrusion the meladiorite is again in contact with Portnoo Limestone. Here it is typically xenolithic and the xenoliths of Portnoo Limestone are altered to hornblende and clinozoisite-rich rock. The contact between the Portnoo Limestone and hornblendite is steeply dipping 80° to the south.

(ii) Emplacement:

Field evidence suggests that intrusion occurred at a high level into variable lithologies which reacted differently depending on their angle of strike and dip to the intruding magma and the composition of the Portnoo Limestone. If the Portnoo Limestone lies at a high angle and parallel to the magma it tends to have a passive and in places reactive contact, whereas if it lies at a low angle of dip and oblique to the intruding magma an explosion breccia may form, or the contact may be heavily disrupted by the magma intrusion. The hornblendite has many altered xenoliths within it at its margins and these are mostly of a calc-siliceous nature, those of pure limestone tend not to react as readily but

Plate 3.6 (a). Breccia of Portnoo Limestone blocks within the intrusion of Foragy Rock, Narin-Portnoo shore section. Brecciated blocks of Portnoo Limestone show chaotic array without obvious igneous matrix. A lens of hornblendite veins the limestone in the bottom left corner of the photo. Lens cap for scale.

Plate 3.6 (b). Meladiorite veined by granodiorite material at Foragy Rock. Angular contacts exist between the meladiorite and the granodiorite. Granodiorite veins meladiorite in a net-vein fashion. Area to immediate left of lens cap shows granodiorite with diffuse contact with meladiorite.



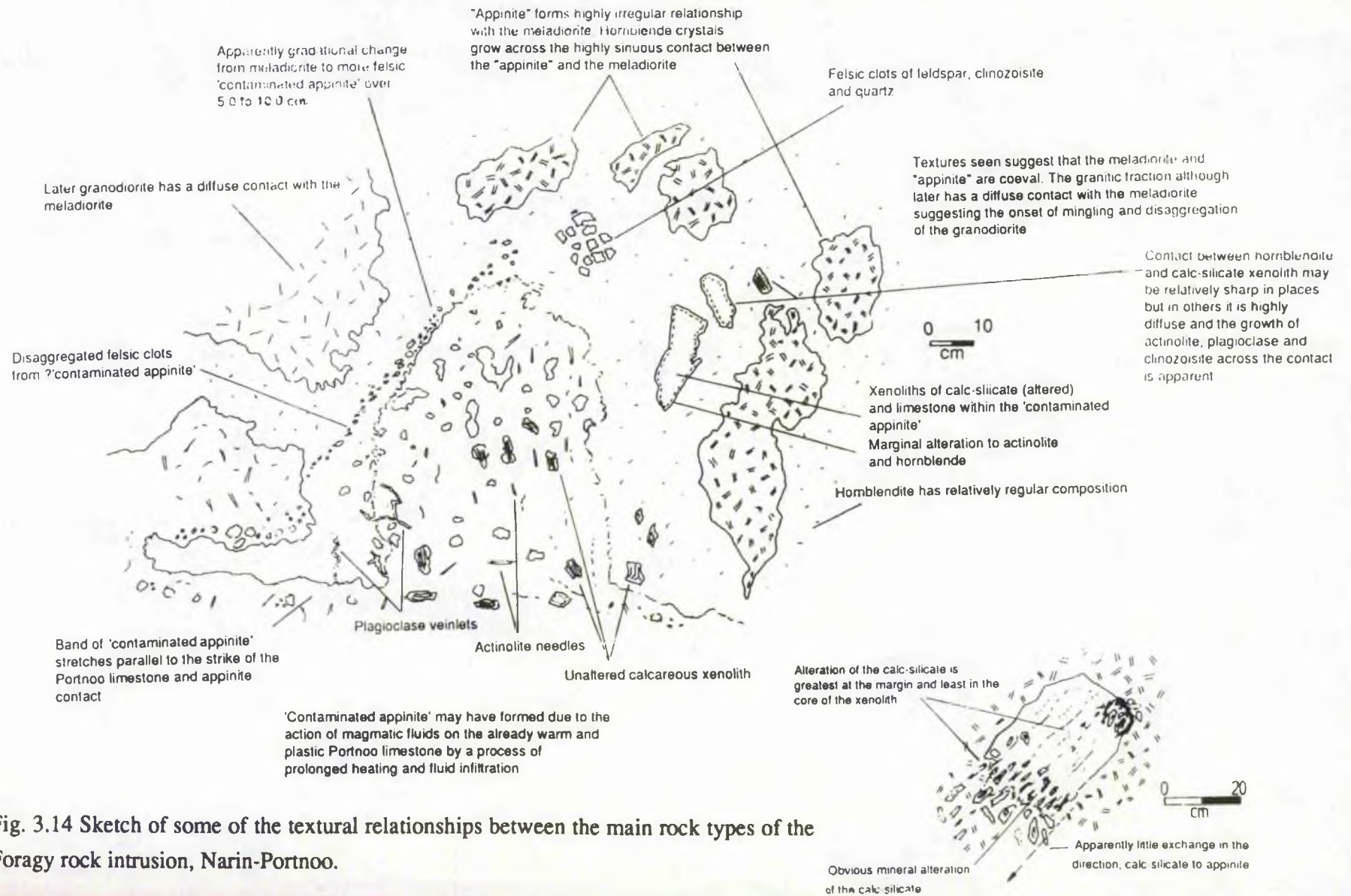


Fig. 3.14 Sketch of some of the textural relationships between the main rock types of the Foragy rock intrusion, Narin-Portnoo.

instead have recrystallised into marbles. Where hornblende is intruded parallel to the strike of the limestone in some places a zone of alteration exists within the appinite, this is suggested to have been caused by the circulation of late-stage groundwaters through the appinite along its contact with the limestone. Against metadolerite the contacts are steep without any brecciation. The steep outward-dipping contacts suggest intrusion by a mechanism of doming and utilisation of bedding planes where possible, thus explaining the screens of Portnoo Limestone within the hornblende.

(c) Cathleen's Hole

Twenty metres west of the Foragy Rock intrusion are located the appinitic rocks of Cathleen's Hole. The dominant rock type of this intrusion is a medium to coarse grained rock, dioritic to meladioritic in composition, described here as meladiorite.

(i) Contact relationships:

The eastern part of the intrusion consists of a hybrid diorite which shows a cross-cutting contact with Portnoo Limestone of 50° in the north to 80° in the south of the exposed area. The hybrid diorite is highly heterogeneous in terms of composition, it has a medium grained mesostasis of hornblende, plagioclase and replacive clinozoisite which enclose irregular clots of microcline and graphic quartz. These clots are up to 1cm in diameter and appear to have a gradational contact with the mesostasis. Occasionally the hybrid diorite contact becomes more hornblende-rich due to the presence of localised 'pools' of hornblende accumulation or due to the intense growth of hornblende adjacent to, and within, calc-siliceous xenoliths.

Ten to twenty metres further west the hybrid diorite changes gradually to hornblende diorite on the northern side and to meladiorite on the south side. The contact between these different lithologies is often difficult to define. For instance, the hybrid diorite and hornblende diorite contact is obviously diffuse and relatively sinuous, whilst the contact with the meladiorite is subtly diffuse over 10-20cm and changes are very subtle, mostly related to the amount and form of the hornblende. The hornblende diorite is composed of augite and hornblende phenocrysts with interstitial plagioclase and minor quartz, while clinozoisite is rare. In some places the hornblende diorite becomes ultra-coarse grained with development of hornblende crystals up to 1.5cm long and a high colour index (CI=80-90%). It is possible that this represents a cumulate rock.

The contact between the hornblende diorite and meladiorite is crenulate and diffuse and as the meladiorite veins the hornblende diorite on a small scale it is probably slightly later than the hornblende diorite. The composition of the meladiorite is variable depending on the abundance of plagioclase, orthoclase and biotite. In general terms however it is a medium grained rock consisting of hornblende and augite phenocrysts within a mesostasis of plagioclase, orthoclase and minor quartz. Clinozoisite alteration gives the rock a green, altered appearance as it overgrows the hornblende and plagioclase. Along its length the

meladiorite has a strong mineral lineation, usually of hornblende and plagioclase dipping at 5° towards 260° . This may have been intruded as a sheet from a westerly direction.

Like the hybrid diorite the meladiorite also contains "appinite" in typical pocket and vein form with diffuse and sinuous contacts. The majority of the intrusion is composed of meladiorite as a sheet gently dipping 5° to 20° towards 258° which incorporates a large number of xenoliths. Some of these xenoliths are metasomatised and partially incorporated within the meladiorite. Typically the hornblende and plagioclase grows parallel to bedding, and clinozoisite is a common phase usually overprinting the former. Metadolerite is strongly veined in contact with the "appinite" but there is no evidence of strong agmatization or alteration apart from recrystallisation. Lamprophyre dykes are sporadically distributed through the intrusion, these are often sheared by numerous sinistral and dextral shear bands which utilise the dykes as planes of weakness.

The meladiorite passes from a gently dipping sheet dyke 60° SW into limestone pavement at its western end. The limestone is a garnet-rich (grossular), highly-recrystallised limestone due to thermal metamorphism by the appinite intrusion. The contact with the limestone is sharp and the meladiorite is veined by late granitoid veins which have diffuse contacts. Isolated pods within the Portnoo Limestone have a moderate dip of 50° to the SW and exist as offshoots of the main meladioritic mass.

(ii) Emplacement mechanism

The contact in the eastern part of the intrusion is steep, sharp and cross cutting. To the north where it is parallel to bedding it is more concordant and sill-like, which is also the case in the west. It thus seems to have been intruded as a mass parallel to bedding, except where fractures in the limestone influence the emplacement it is intruded as a cross cutting boss. Reaction characteristics with the envelope rocks are rare in this case.

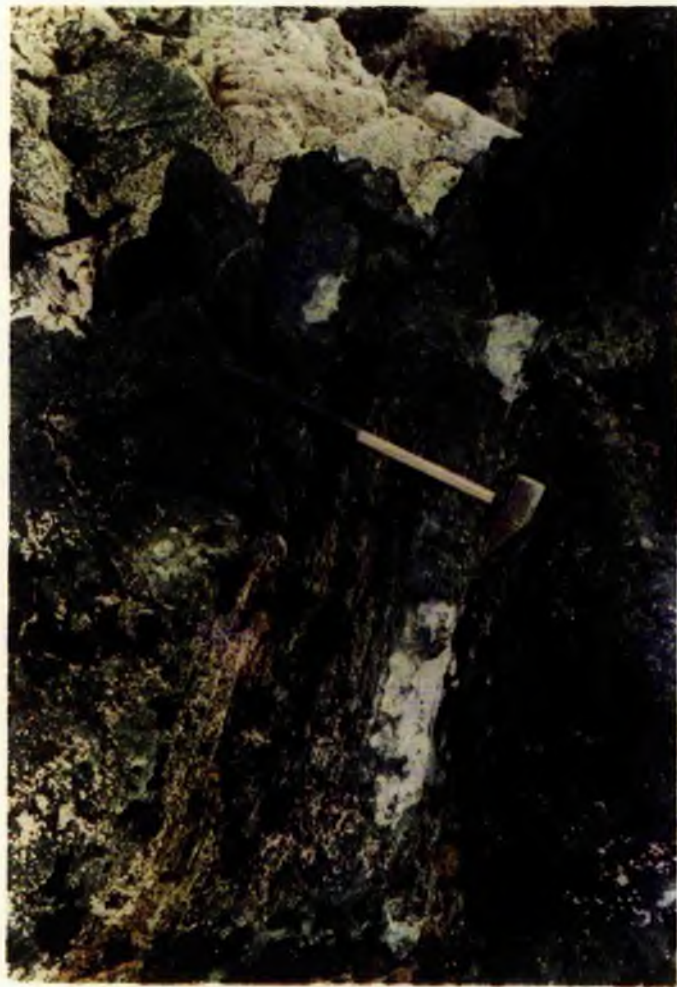
(d) Fairy Coves Intrusion (Map 6)

This intrusion is separated from the Cathleen's Hole intrusion to the east by over 20m of Portnoo Limestone. The first indications of the presence of another intrusion is the intrusion of a moderately-to-steeply dipping 1m wide dyke of biotite diorite which is intruded into the hinge of an antiform in the Portnoo Limestone. The biotite diorite passes laterally into a coarser grained xenolithic biotite diorite which in turn is in contact with hornblende diorite. Xenoliths consist of intensely altered and deformed calc-silicate. In places this biotite diorite entirely encloses Portnoo Limestone and may be seen to be concordantly intrusive (Plate 3.7 b). The biotite diorite is medium to coarse grained and consists of hornblende in rounded aggregates within a plagioclase and quartz matrix with biotite phenocrysts.

The biotite diorite has a sharp, steep contact with the hornblende diorite, the dominant rock type of this intrusion, which is locally variable to diorite in the west. It has a relatively coarse grained texture occasionally becoming ultra-coarse grained in places.

Plate 3.7 (a). Xenolith of Portnoo Limestone enclosed and veined by hornblendite at Forgay Rock. Limestone xenolith retains bedding but shows growth of actinolite and clinozoisite due to reaction with the hornblendite. Contacts are diffuse in places. Hammer is 80 cm in length.

Plate 3.7 (b). Biotite diorite concordantly intruded in sill-like fashion within Portnoo Limestone at the Fairy Coves area of the Narin-Portnoo intrusion. Biotite diorite occupies upper part of photo with limestone below. Portnoo Limestone and biotite diorite are both folded in the upper part of the photo.



Throughout the complex the diorite is highly veined by granitoid material both in sinuous and clot and pod forms. These veins have an often diffuse contact with the diorite suggesting that there is a degree of synchronicity between the emplacement of these two rock types, indeed further west of Fairy Coves evidence of mingling in early stages is apparent. Here a granodioritic intrusion has vertical diffuse and crenulate contacts with the hornblende diorite (Fig. 3.15) which is apparently intermingled with the granodiorite. A granite dyke is later than the lamprophyres and net veins the granodiorite.

The mingling of the granodiorite and hornblende diorite suggests that both were in a plastic state at similar times but the granodiorite was probably intruded slightly later than the hornblende diorite.

(ii) Emplacement Mechanism:

The biotite diorite found to the east of Fairy Coves passes into a moderately-dipping mass of biotite diorite which in turn has a steep contact with hornblende diorite, this intrusion is a steep-sided boss using bedding planes where possible. This is best seen in the small cove east of Portnoo Quay where it is concordantly intrusive (Plate 3.6).

3.9.2 Portnoo to east Burnfoot intrusions (Map 6)

The coast from Portnoo (G7000 9945) to Burnfoot (B6927 0020) contains several disjointed intrusions which are all apparently part of the same intrusive phase. The strip of coast studied is over ~500m long and the wave cut platform exposure is ~90m in width. The area west of Burnfoot has not been studied in the same detail but consists of a steep-sided plug-like intrusion of hornblende diorite and meladioritic rocks. This plug is linked spatially to a more dioritic sheet and dyke-like intrusive mass which constitutes the rocks of the study area of Burnfoot to Portnoo. The three main components of this intrusion are the Eastern granite, the Central granite and the Western diorite. Lamprophyres are few in this area.

(a) The Eastern granite:

Working from east to west, the first igneous intrusive activity is a granitic dyke which cuts across the Portnoo Limestone 30m west of the quay at Portnoo Harbour. It is sharply cross-cutting, has steep contacts with little alteration of the limestone, and is probably linked to the larger granite basic mass seen further west near Dirty Rock. This body is an example of the complex relationships between acid and basic rock types. It is possible to see acid material veining basic with crenulate mutual contacts. The acid portion is much more abundant than the basic diorite.

The granite consists of orthoclase, quartz and biotite with minor plagioclase. It is little affected by the basic material except when xenoliths (a few mm to several metres in diameter) become so disaggregated that individual minerals become incorporated into the granite. The basic component is dioritic in composition with biotite and hornblende phenocrysts enclosed within a plagioclase and quartz mesostasis. Biotite is dominant over

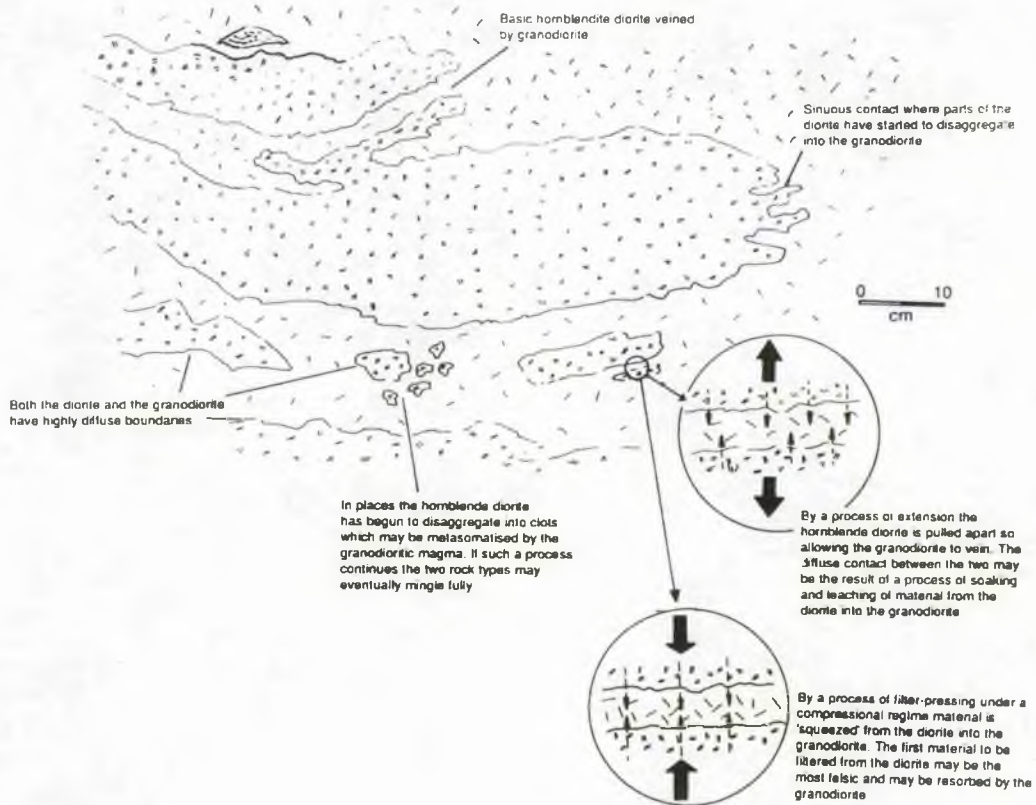


Fig. 3.15. Textural characteristics of hornblende diorite veined by granodiorite, Fairy Coves, Narin-Portnoo.

hornblende and plagioclase is highly altered. The dioritic inclusions may have been incorporated upon intrusion or brought up from slightly deeper levels of exposure as suggested by their rounded form.

The form of the granite here is of a steep-to-moderately-dipping dyke within the Portnoo Limestone. Its contacts are sharp and non-reactive with the limestone. This outcrop of granite is part of a large area of granite which encloses and pinches off blocks of limestone and invades and veins metadolerite in both a brittle and crenulation fashion at Dirty Rock. (Plate 3.8 a and b). The basic rock type has a coarse grained texture and is maybe diorite rather than metadolerite. This may be a zone of mingling but further west these are apparently sharp unreactive contacts between granitoid and metadolerite which show no evidence of mingling.

(b) Central granite

The granite present on Dirty Rock is a steeply dipping sheet with numerous xenoliths and is heterogeneous in composition. The purest form of granite is similar to that seen elsewhere with orthoclase, quartz and irregular plagioclase phenocrysts with minor biotite. Within the intrusion however the composition varies with contamination by xenoliths and mingling with dioritic rock types. The xenoliths of limestone and metadolerite remain unaffected. The abundant xenoliths give the granite and diorite a variable composition and texture giving the rock a hybrid-type appearance, (hybrid diorite of Map 6, Appendix 6). Some of these inclusions are only 1-2cm in diameter while others are up to 1m wide. The diorite is commonly medium grained with less hornblende than in other diorites; biotite is more common and the diorite also tends to have a more equigranular texture becoming fine grained, almost felsitic in places. There is an outcrop of felsite 20m east of Burnfoot forming a gently-inclined, cone-shaped lens within the granite with fine grained felsitic components.

Locally the partial assimilation of diorite gives the granite an increased biotite percentage and schlieren of partially assimilated diorite exist within the granite. The contact between granite and medium grained diorite is diffuse over 1cm and this diorite appears to be part of another intrusion, most of which is underwater. This diorite has the same composition as many of the diorite inclusions and may be the source of the xenoliths. Most of the rest of the granite intrusion is relatively homogeneous in composition with inclusions of metadolerite and Portnoo Limestone. This granite passes north west and westwards into diorite and remains highly xenolithic with occasional more felsic bands up to 2m in width.

Evidence for the emplacement mechanism is apparent at the contact of this part of the central granite and the Portnoo Limestone (Fig 3.16). The deformation and steepening up of Portnoo Limestone and metadolerite together with the pinching off of calc-silicate and metadolerite by the granite indicate an upward, forceful emplacement mechanism, which also explains the large number of xenoliths within the granite (Plate 3.9).

At the south western margin of the central granite, the granite appears to pass gradationally into another biotite diorite facies, the western diorite. The two intrusions are linked by a thin dyke with biotite diorite forming the western side and granite with biotite diorite inclusions on the eastern side. This dyke cross-cuts the Portnoo Limestone at an angle of 60-70° and the contact with the marginal granite is diffuse over 1-2cm. Laterally however the contact with the main granite intrusion is gradational over 1m. As this connecting dyke with the granite margin is traced southwards the angle of contact and strike become parallel to that of the Portnoo Limestone and the intrusion forms a 6m thick sill-like body.

This marginal granitic skin is present on the south side of the intrusion for much of its length and in places may be seen to have an intimate relationship with the biotite diorite. The composition of the diorite is variable although generally it is of a relatively medium

Plate 3.8 (a). Mingled character of basic and granitic rock types at Dirty Rock. Outcrop is dominated by granitic material veining basic rock of dioritic to metadoleritic composition. Note the rounded shape of many of the basic enclaves suggesting a coeval relationship between the two magmas. A thin granite vein transects the intrusion just below the hammer. Dirty Rock, West of Portnoo Quay.

Plate 3.8 (b). Granitic pods and lenses veining basic material of dioritic to metadoleritic composition. Note the rounded form of the contact between the basic and acid components. Knife is 8 cm in length. Dirty Rock, West of Portnoo Quay.



grained, equigranular nature with hornblende and biotite in a plagioclase and orthoclase matrix. There is a strong foliation of biotite and to a lesser extent hornblende, parallel to the strike of the sill, along a NW-SE direction. This sill passes northwestwards into the Burnfoot area where it shows intimate relationships with the granitic margin. Twenty metres SE of Burnfoot the eastern diorite is cross cut by a later granite dyke which passes NE towards the eastern granite on the northeastwards side of a Portnoo Limestone and metadolerite screen (Map 6, Appendix 6).

The contact between this granite dyke and the larger granite of the central mass is difficult to see as the dyke thins at the contact suggesting that it may have used the contact as a plane of intrusion. It was apparently emplaced later than the eastern diorite as it has sharp, steep contacts with it.

(c) The Western diorite

The geology of Burnfoot is highly complex in terms of rock relationships, essentially it is a continuation of the eastern diorite into the western diorite, consisting essentially of biotite diorite and granite (Plate 3.10). West of Burnfoot its outcrop continues to a point east of Dunmore Hill (B6927 0020). Where the appinite is more dominantly hornblende rich. However at Burnfoot the composition of the appinite is generally more xenolithic compared with the rocks further east, but it is intimately mingled with granitoid in the form of layers, veins and pockets of mingled material.

The two main areas of interest are those to the west and those towards the east. The intervening area is a more uniform biotite diorite with biotite and hornblende phenocrysts set in a plagioclase, orthoclase and quartz matrix with medium grained texture. Occasionally the feldspar forms in pools.

(i) Western Burnfoot

In this area biotite diorite forms a contact with granite to the west. The diorite has many basic clots, and ranges in composition from biotite diorite to meladiorite to "appinite" over several centimetres. The contact with the granite is highly diffuse and crenulate and both members appear to be contemporaneous. These basic clots and xenoliths are not related to the metadolerite but rather appear to be disrupted fragments of an earlier magma of appinitic affinity. Contacts between these and the biotite diorite are highly rounded and diffuse over 1cm. Many have a felsic rim on the outer rim of the xenolith as evidence for a degree of chemical interaction.

Many of the xenoliths have smaller compositional and textural enclaves within them. These take the form of hornblende and plagioclase-rich clots and veins with euhedral hornblende and plagioclase with calcic cores. These hornblende-rich areas form obvious dioritic patches within these basic enclaves and their presence in vein form suggests the movement of volatiles along channelled pathways. In some places the hornblende can be shown to grow from the biotite diorite (which becomes more xenolith-rich) into the vein

Plate 3.9. Forceful intrusion of Central Granite into Portnoo Limestone. Note steepening-up of Portnoo Limestone against granite and the steep angular contact. Margin of granite is defined by quartz veins in the plane of contact which feed veins perpendicular to the contact in upper and central part of photo. Hammer is 80 cm in length. Portnoo shore section.

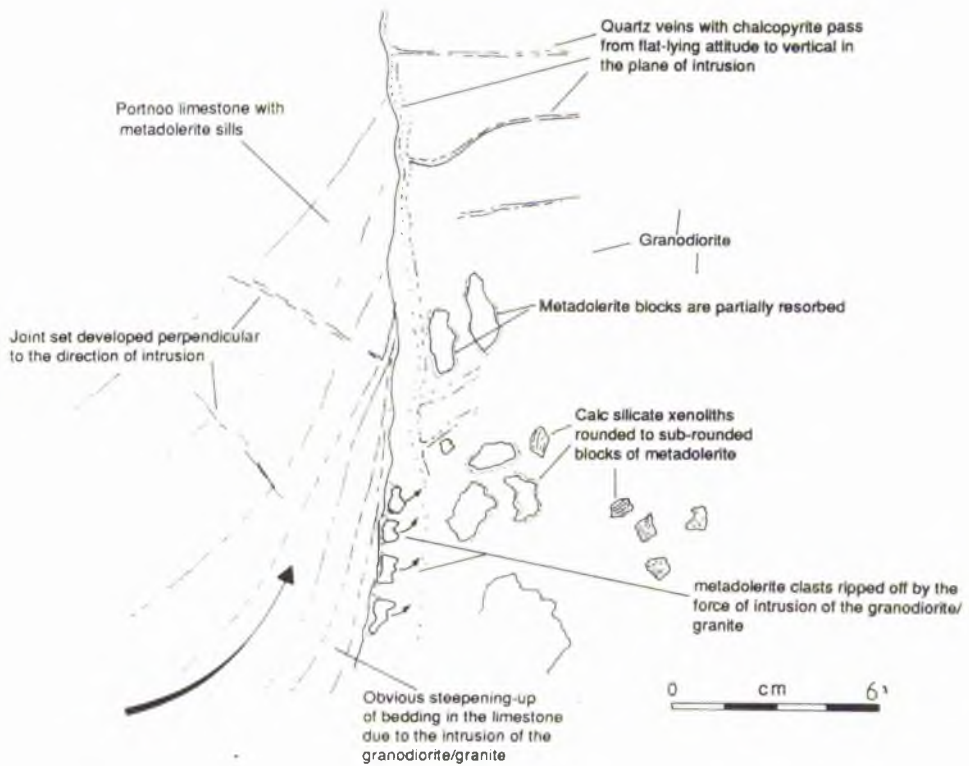


Fig. 3.16 Sketch of the view looking onto the plane of contact between part of the central granite and the Portnoo Limestone, west of Dirty Rock.

suggesting that a process similar to that seen at Mulnamin (see section 3.8.2) involving the 'leaching' of felsic melt into biotite diorite has occurred. This enclosing granite leads from a cross-cutting dyke in the Portnoo Limestone. Other xenoliths of biotite diorite also occur in the granite but reaction is limited. Relationships are better seen on the eastern side of Burnfoot where granite and biotite diorite are intimately mingled.

(ii) Eastern Burnfoot (Fig. 3.17)

Four main rock types exist in eastern Burnfoot, namely meladiorite (1), biotite diorite (2), granodiorite (3) and biotite granite (4). Only the biotite granite can be proven to be a late stage phase as it occurs as sharply cross cutting dykes and veins. The biotite diorite which constitutes most of the outcrop of the Burnfoot area is variable in composition and is often intimately intermingled with a more felsic variant of granodioritic composition. The biotite diorite contains numerous xenoliths of both metadolerite and calc silicate types, as well as coarse grained, basic hornblende and biotite-rich elongate zones and rounded enclaves which are often stretched and plastically deformed including the meladiorite. The granodiorite also contains schlieric xenoliths mostly of an apparently pelitic nature. In the field the dominant rock type is biotite diorite while the felsic granodiorite (termed 'mingle 2') occurs with later granitic sheets, metadolerite and calc silicate xenoliths labelled as such on the following figures. The basic xenoliths within the meladioritic facies of the biotite diorite may represent pre-existing rock as cognate xenoliths derived from a deeper level.

The relation of the biotite diorite to granodiorite is highly diffuse and intimate suggesting contemporaneous intrusion. The granodiorite may have formed in much the same way as the felsic rim of porphyroblastic feldspar and quartz formed along the margin of metadolerite and the basic xenoliths within the biotite diorite. These xenoliths appear similar in composition to the meladiorite and are commonly rounded to sub angular and show diffuse reaction margins with the biotite diorite and often have a felsic rim similar in composition to the granodiorite. These xenoliths also have within them mafic enclaves which may be accidental xenoliths caught up within the magma, which now forms a xenolithic phase of the biotite diorite. The contact between the biotite diorite and granodiorite is commonly marked by a more mafic margin like the meladiorite however the composition of both members is so highly heterogeneous that it is difficult to link this to a rim reaction. In general the contact between the the biotite diorite and the granodiorite is parallel to the foliation and elongate in that direction. Contact with the Portnoo Limestone varies from sharp and cross cutting to parallel contacts and sill-like apophyses. No strong mineralogical effects were seen apart from some minor hornblende and clinozoisite development in the contact limestone members which are also strongly recrystallised and locally deformed.

Plate 3.10 (a). Biotite diorite (761) from the Western diorite area of the Narin-Portnoo intrusion. Plagioclase, orthoclase and quartz-rich matrix with biotite as the main ferromagnesian defining a horizontal foliation with minor clot-like hornblende.

Plate 3.10 (b). Granite (Y1952) from the Western diorite area of the Narin-Portnoo intrusion. Shows typical texture of dominant plagioclase, quartz and K feldspar along with biotite which defines a foliation indicating a degree of strain during the emplacement of the granite.



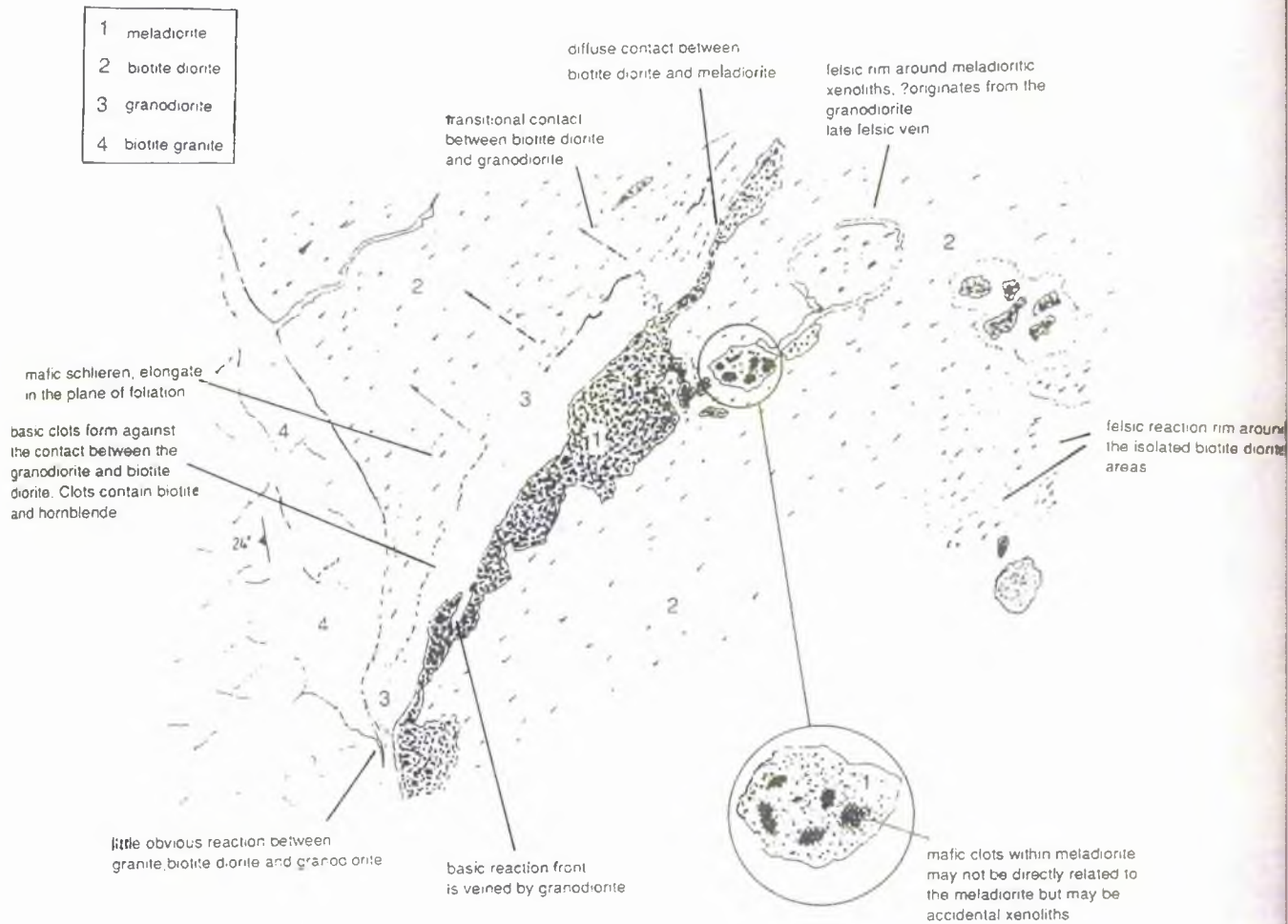


Fig. 3.17 Contact relationships between meladiorite, biotite diorite, granodiorite and biotite granite of the eastern Burnfoot intrusion, Portnoo.

3.9.3 Emplacement of the Portnoo diorites and granites

The diorites and granites of the Portnoo coast all appear to have been emplaced as steeply dipping stocks and plugs, they are highly xenolithic as seen in the central granite which forcibly intruded its envelope rocks steepening them up at their contacts by over 20°. The granodiorite and diorite appear to be relatively synchronous and both rock types also share similar emplacement mechanisms. The large number of relatively unaltered xenoliths

in the rocks suggests that they are relatively high level intrusions, emplaced in a brittle-ductile regime.

3.10 LAMPROPHYRIC INTRUSIONS OF THE NARIN-PORTNOO AREA

The term lamprophyre is used in this section to describe any dyke-rock of basic composition with hornblende and or biotite as the main ferromagnesian and having orthoclase or plagioclase with minor quartz. Other components may include augite, chlorite and clinozoisite or epidote. The lamprophyric dykes seen along this stretch of coastline are highly variable in composition as a group and within the dykes, both laterally and vertically. Close spatial relationships observed between lamprophyres and appinitic intrusions in the Narin-Portnoo area are significant.

(i) Composition

The lamprophyres vary from spessartites with dominant hornblende and plagioclase to vogesites with abundant hornblende and orthoclase. More rarely kersantites with biotite, chlorite and plagioclase occur. The hornblendic lamprophyres appear as dark grey, fine to medium grained rocks with stumpy to elongate hornblende phenocrysts up to 1cm in length set within a finer grained felsic matrix. They are predominantly basic in composition but some pass within the same intrusion into more felsic fractions where either plagioclase or orthoclase becomes more dominant. In general chloritic lamprophyres are less common than the hornblendic lamprophyres and where present tend to be the result of alteration of biotite, and have a finer grained more massive texture than the hornblendic lamprophyres.

(ii) Orientation

In the field it is difficult to define a distinct strike or direction due to the sinuous nature of the dykes, however at the eastern end there appear to be three sets of dykes, a NE-SW, a NW-SE set and a minor W-E set. Two dykes of the former set intersect and it is the NW-SE dyke which cuts the NE-SW trending dyke. No other such contacts have been seen in the area thus this age relationship is viewed with caution. To attempt to define the relative ages in terms of compositional variation is also difficult as the main lamprophyre types, vogesite, spessartite and kersantite are present in equally variable numbers in both main sets of dyke trends. French (1977) suggested that the hornblende lamprophyres were emplaced later than the chlorite rich lamprophyres which contained a greenschist facies assemblage of minerals, and so may have been related to a higher ambient temperature, forming at an earlier higher temperature period than the hornblende lamprophyres which he thus thought of as a later phase. The lamprophyre dykes associated with the Foragy Rock intrusion do not appear to be related to any such NW-SE trend but instead seem to have been intruded perpendicular to the main intrusion, and although none can be seen to adjoin the main intrusion it is possible that they may be linked at depth. In the Cathleen's Hole

intrusion one such dyke does actually pass gradationally into the coarse facies fraction of the appinitic body, over a zone of ~2-3m.

(iii) Lithological relationships

Some of the most interesting lamprophyric intrusions are found in the eastern shore section between Portnoo and Narin, particularly in the area of Sheehan Rock (G7100 9940). Here an outcrop of deformed limestone and metadolerite has several thin lamprophyre dykes intruded into it. One of these is laterally variable in composition from kersantite to a felsitic-granophyric composition. It has numerous offshoots into the metasediments and is apparently not affected by the deformation which affects the limestone and metadolerite. In some places the more felsic facies of the appinite contains numerous limestone fragments and forms small areas of breccia within the walls of the dyke. One such small dyke is felsitic in character and cuts across the main dyke with a NW-SE strike, and is also highly xenolithic.

(iv) Structure

The dykes are commonly transected by small shear zones which cut across the dykes but more often run parallel to the dyke trend.

(v) Occurrence

Most of the lamprophyres are concentrated in the east of the Narin-Portnoo shore section. Few are present west of Portnoo where granitic dykes are dominant.

3.11 THE KILREAN APPINITIC INTRUSION

The appinitic intrusion of Kilrean lies along the southern contact of the Ardara pluton, 5km west of Glenties (Fig. 3.2b). The intrusion itself is poorly exposed in boggy ground, which makes field relationships difficult to ascertain. However the intrusion maps out as a rounded form, over 1.5km in length and 1km in width. The intrusion was studied by French (1966) and Pitcher & Berger (1972) and was also studied during this research as it was a potential end-member of the mafic-rich magmatic appinite suite.

3.11.1 Contact relationships and lithological variation

The Kilrean intrusion (Fig 3.2 b) was emplaced into the Cleengort pelites whose contact is best seen at the break of slope east of Drumnacross school (G7970 9145). Along this margin the pelite strikes parallel to the contact with a steep southerly dip. It is strongly hornfelsed and can be seen to be compressed and boudined similar to the contact rocks of the Ardara pluton. Further south of the contact the pelite dips less steeply while the strike remains parallel to the contact. In the western part of the intrusion there is a large enclave of metadolerite and tightly folded pelite to semi-pelite up to 500m in length and 140m in width. The enclave seems unaffected by entrapment within the intrusion. At the northern end of the intrusion appinite is truncated by the intrusion of the Ardara pluton on the north

side of the road, but no contact was found, however French (1966) described a margin of no obvious reaction. No foliation or lineation is visible in the rocks of the intrusion although at the margin some of the hornblende shows a foliation parallel to the contact. The appinite at the contact with the pelite is in fact a highly variable diorite and meladiorite which form the main part of the intrusion. Other petrological variations exist within the main body of the intrusion.

(i) Appinite-meladiorite

This facies has a composition varying from "appinite" with acicular hornblende and plagioclase mesostasis to meladiorite with abundant hornblende and minor plagioclase.

(ii) Hornblendite:

This rock type is mainly found adjacent to the cortlanditic core and basically consists of two populations of hornblende, the first is ~1cm in length and forms a highly interlocking meshwork, and the second comprises millimetre-sized hornblende crystals within a scant mesostasis of alkali and plagioclase feldspar. No contact was seen with the cortlandite or meladiorite.

(iii) Hornblende pyroxene olivine gabbro (cortlandite)

This is the best known rock type of this intrusion and it is the most primitive of all the igneous rocks in Donegal. It comprises of green hornblende, augite and hypersthene with minor amounts of olivine. The hornblende has a poikilitic relationship with the other mafic minerals in the rock. In almost all cases the olivine is altered to a red mineral thought to be bowlingite in composition but which may also be serpentinitic. Biotite is present as a secondary mineral after hornblende and, to a lesser degree, olivine. The gabbro forms a central core crudely defined with no observable contacts with the hornblendite. These have similar microscopic hornblende textures and the content may be gradational.

(iv) Emplacement mechanism

Judging from the similar deformational relationships to those of the Ardara pluton and steep dip of the country rocks, the Kilrean intrusion may have been forcefully emplaced as an upright magma stock without explosive activity, although the high frequency of accidental xenoliths is difficult to explain by this mechanism. The textures and compositions of the rocks of the Kilrean intrusion provide good evidence of magmatic crystallisation without significant contamination. The relationships between the mineralogy of the various members of the intrusion will be discussed in the next chapter.

3.12 MINOR INTRUSIONS AND BRECCIA PIPES

This section describes the intrusions in the Ardara area where field relationships cannot be used to link them with the Ardara pluton or other main centres. This includes the Glenard and Crockard granitoid intrusions found at the west end of the Meenalargan intrusion, NE of the Ardara pluton. Some of the numerous intrusion breccias will also be

described in order to underline their general form and importance in the overall genesis of appinitic magmas. The nomenclature used in the description of these breccia pipes is based on that of Pitcher & Berger (1972), as described in section 2.5.3.

3.12.1 The Glenard intrusion

The Glenard intrusion is located to the immediate west of the Meenalargan intrusion (G7700 9730) (Map 3, Appendix 6). It is an elongate intrusion (750m x 75m) striking parallel to the Mulnamin calc silicate flags and associated metadolerite sills trending 280°. The intrusion consists of two main facies, a dominant granodiorite and a minor hornblende granodiorite facies, concentrated on the northern side of the intrusion. Associated with these are two meladiorite and hornblendite bodies. The intrusion is transected by numerous aplite, pegmatite and micro leucogranite sheets and veins.

(i) Glenard granodiorite

The main part of the intrusion comprises a medium grained xenocrystic granodiorite (CI=30-40%) texturally similar to that of G2/G3 of Ardara with occasional hornblende phenocrysts now largely replaced by biotite. It is dominantly composed of plagioclase, orthoclase and quartz with interstitial biotite and chlorite which defines the foliation and secondary clinozoisite with abundant pyrite. The contact with the Calc Silicate Flags is best seen along the southern margin where it is steep and sharp without any veining or dyking of the country rock which dips steeply NNE. Further west, against metadolerite, the contact is similarly sharp and steep with only local net veining of the metadolerite. In the extreme west of the intrusion (G7760 9730) there is evidence of granodioritic offshoots into the country rock which show intense plastic flow on a centimetre scale. These show tight flow folding and ptygmatic structures of leucogranite which are folded around bedding, suggesting that they may have formed as a result of the intrusion of the granite. Numerous xenoliths and rafts of calc silicate within the granite also exhibit this intense flow folding. Such are the number of calc silicate xenoliths in this western margin that an emplacement mechanism by stoping parallel to the strike and dip of the envelope is suggested.

(ii) Hornblende granodiorite

This is found on the northern side of the intrusion (G781 972) as an elongate body, some 250m x 50m. It consists of strongly foliated granodiorite (CI=70%) with a near vertical foliation defined by elongate hornblende crystals as well as biotite which pseudomorphs the hornblende and forms corroded clots in a matrix of biotite, hornblende, plagioclase, orthoclase, quartz and abundant pyrites. There are xenoliths of calc silicate but also of a centimetre-sized fine to medium grained basic rock within the hornblende granodiorite. If these basic clots are derived from the appinite then this indicates that the granite is somewhat later in relative terms. The relationship between the hornblende granodiorite and Glenard granodiorite appears to be gradational and field evidence suggests

this is a local facies, possibly associated with the development of an appinite pipe also located on the north side of the intrusion (G7795 7836).

(iii) Appinitic intrusions associated with the Glenard granodiorite

Two intrusions with appinitic affinity are associated with the Glenard intrusion on its northern side, they range in composition from meladiorite to hornblendite. The most striking of these is located on the northern side of the Glenard body (G7795 7836). It is a broadly elliptical intrusion ~10m in width and is neatly transected by a steep cliff which provides a partial section of the pipe from top to bottom. Like other appinitic intrusions, there is little uniformity of texture or composition. The main rock type is a coarse grained meladiorite (CI=80%) which is gradational to hornblendite (CI=95%). Hornblende forms squat crystals with a plagioclase and orthoclase mesostasis and concentrations of pyrites, commonly in association with hornblende. Variations in the amount of plagioclase and the texture of the hornblende occur sporadically in the form of patches and veins, often the plagioclase occurs as cores to the hornblende. The base of the intrusion shows the development of true appinite which exhibits spectacular development of hornblende as euhedral crystals up to 10cm long, again often with plagioclase cores within a plagioclase and pyrite-rich matrix. Meladiorite can be seen to be partially disrupted by a plagioclase and hornblende melt and elongate hornblende crystals grow into the plagioclase clot in one locality (Fig 3.18, Plate 3.11 a). In other places hornblende crystals grow into the plagioclase clot perpendicular to the meladiorite contact, suggestive of side-wall crystallisation (Fig 3.18). On the whole it is not possible to see any marked vertical structure in the pipe. The relationship between the hornblende granodiorite and this appinite pipe is difficult to determine as no good contact relationships exist, although there is an impression of a diffuse contact. The other appinitic intrusion is also located on the northern side of the intrusion. It is also broadly elliptical and although poorly exposed appears to be ~8m x 5m. Its texture is consistently hornblenditic with closely interlocking squat hornblende crystals, with minor interstitial plagioclase and secondary biotite and clinozoisite, again with abundant pyrites. Augite and calcite are rare accessories. Neither pipe shows any evidence of brecciated margins or inclusions of country rocks. They have obvious volatile affinities as shown by their textural and mineralogical characteristics, notably the abundance of pyrite. The lack of country rock fragments may be due to the depth of emplacement or emplacement into already steeply dipping calc silicates. The granodiorite may have intruded later than the appinite but contacts are poorly developed rendering any relative age determinations speculative.

(iv) Minor intrusions

The whole intrusion is transected by granite, pegmatite and aplite veins, and sheets. The pegmatite and aplite veins are most common in the west of the intrusion and on the margin where they cut the hornblende granite. There is no dominant trend and they do not appear related to the Main Donegal Granite; they may be a late-stage facies of the

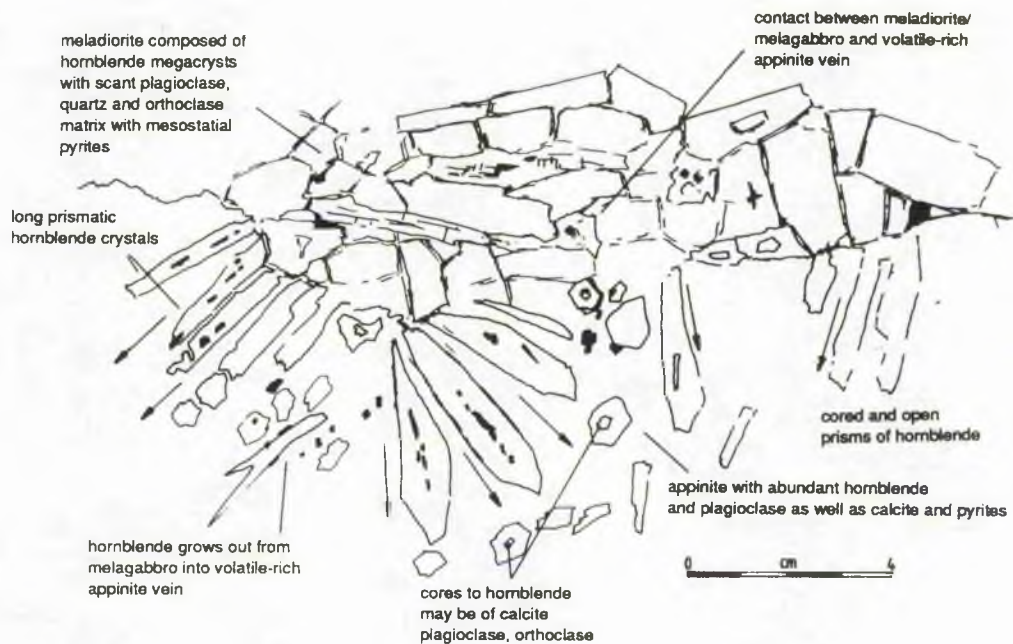


Fig 3.18. Ultra-coarse texture within "appinite" vein and meladiorite from the appinitic intrusion at Glenard.

Glenard granite. Various microgranite sheets cut across the intrusion, they are medium grained with a NW or NE strike and bear close affinities to those which cut G2 of the main Ardara granite (?G3).

(v) Origin of the Glenard intrusion

From the field relationships it is difficult to determine whether the Glenard granodiorite and hornblende granodiorite are derived from a magma related to the main Ardara pluton. The texture of the granodiorite is similar to that of G2 and if the granite sheets that transect the intrusion can be demonstrated to be of G3 type then this puts a relative timing constraint on the intrusion and by implication a genetic affinity to the Ardara

magmas. However the granodiorite may be related to the Menalargan intrusion as a more felsic magma situated solely at the west of the area.

(vi) Emplacement mechanism

The evidence for emplacement is best seen along the western margin of the intrusion. The steep, sharp contact of the xenolithic granodiorite with steeply dipping calc silicate and its deformation characteristics suggests a mechanism of passive stoping over a prolonged period.

3.12.2 The Crockard granite

The Crockard granite is located on the NW side of the Meenalargan intrusion (G7930 9720). It is a small elliptical body intruded into Cor quartzite. Its form is plug-like and it has steep, sharp contacts with the quartzite which is recrystallised to a crystalline mass. Veins of granite intrude the quartzite and they appear to be fairly homogeneous. Two xenoliths of quartzite ~1m across were found in the granite. The granite (CI=55%) is medium to coarse grained with an equigranular xenocrystic texture and is texturally similar to the G2 facies of Ardara. It appears to have been intruded as a steeply dipping sheet into brittle quartzite beds where the contact is marked by an 8-10m vertical break in slope.

The nature of the Crockard granite, like the Glenard granite makes estimation of age difficult. Texturally the granite is very similar to G2 of Ardara and could be a local stock of this magma. The major difference between G2 and Crockard granites is the lack of basic and metasedimentary xenoliths and foliation within the Crockard granite which could reflect the competency of the quartzite country rock and the style of intrusion of the granite.

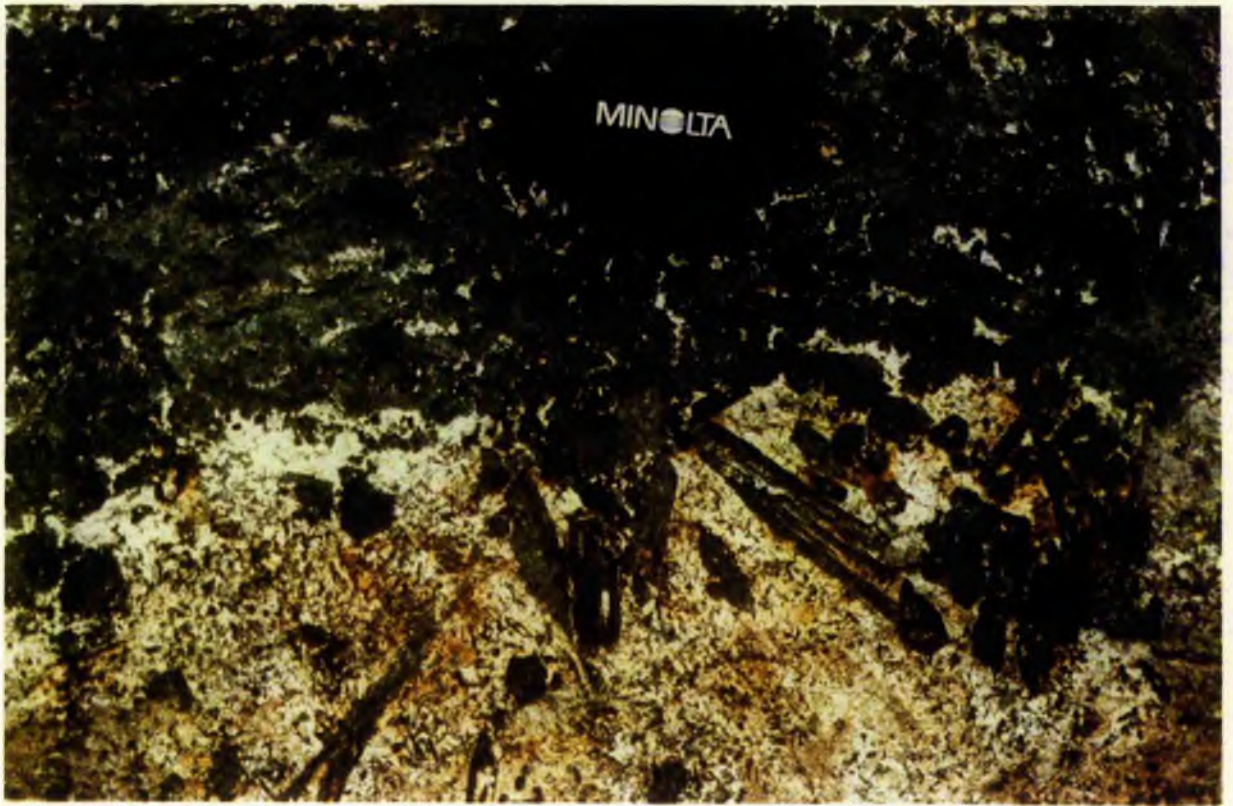
3.12.3 The Kilkenny School intrusion breccia pipe

The intrusion breccia pipe of Kilkenny outcrops on a knoll near the top of the hill 500m south of Kilkenny school (G7770 9885). The intrusion is elliptical in form and measures ~10m x 28m. It consists of two main parts, the first is a breccia of quartzite fragments set in a fine grained acid matrix. This forms the central part of the intrusion breccia with poorly exposed contacts with the other main part of the intrusion, the calc silicate breccia.

The quartzitic part of the intrusion breccia consists of creamy white rounded, ovoid shaped fragments of quartzite. These breccia fragments are clast-supported with a preferred orientation of long axes dipping gently to the west (Plate 3.11 b). The clasts vary in size from 2-12 cm in length and are up to 4cm in length. They have a coating of green grey micaceous material which consists of hornblende, biotite and chlorite with interstitial quartz and plagioclase. The sparse matrix consists of coarse grained quartz and plagioclase with minor biotite which has an almost metamorphic texture of closely interlocking grains with common sub-crystal domains developed.

Plate 3.11 (a). Growth of acicular hornblende at contact between meladiorite and appinite vein. Hornblende is aligned roughly perpendicular to the contact and commonly has plagioclase and calcite in the core. Appinite pipe at Glenard. Lens cap is 50 mm in diameter.

Plate 3.11 (b). Quartzite pebbles (white) enclosed by granophyric matrix (grey). Pebbles have obvious elongate sub-rounded form and are inclined to the west at 30°. Kilkenny school intrusion breccia. Marker pen is 12 cm in length.



The calc silicate part of the intrusion breccia consists of a hornblende diorite with calc silicate fragments, which like those of Biroge are well rounded and heavily altered. Less altered calc silicate fragments appear to be similar to the surrounding Mulnamin Calc Silicate Flags. As a general rule the calc silicate xenoliths can be distinguished from their hornblende host by their finer grain size and grey colour. The host matrix consists of hornblende which is dominant over a plagioclase and quartzitic mesostasis. Biotite is present as a replacement mineral of hornblende, pyrites is the main opaque phase.

In considering the source of the breccia fragments, the similarity of the calc silicate xenoliths to the Mulnamin Calc Silicate Flags, suggests that they were probably derived from this horizon. Pitcher and Read (1952) considered the calc silicate xenoliths to be derived from this horizon which is ~300m thick and is exposed in this area, so vertical transport of these xenoliths from their source may not have been great. The quartzite xenoliths may have originated from the Cor Quartzite which is ~400m below the top of the Mulnamin Calc Silicate Flags (Pitcher & Read 1952). The fragments may have travelled at least 400m and probably a great deal further if the beds were dipping. This great vertical distance may be supported by the fact that the quartzite fragments are well rounded and striated with a glassy texture. This fact together with the alteration seen in the rounded calc silicate xenoliths suggests extreme reaction of quartzite with the transport medium. There may have been so much reaction that silica from the quartzite may have been removed in the process of transport and suspension in the magma that they may now be represented by the granophyric matrix around the quartzite fragments. On the other hand the calc silicate fragments may have reacted with their suspension medium to form the hornblende diorite matrix. Pitcher and Read (1952) considered that a fluid of sodic composition which was gas-charged caused the alteration in the respective rock types which was apparently greater in the calc silicate fragments than in the quartzite. Pitcher and Read (1952) also explain the mafic coating of the quartzite fragments as occurring in-situ after the magma had begun to consolidate.

3.12.4 The Biroge breccia pipe

The Biroge Breccia pipe is situated 1km SW of Portnoo where it intrudes Upper Falcarragh Pelite (Fig 3.19). It is approximately oval in shape, 150m long and 45 m wide, with poorly exposed contacts with the pelite which seem to be shouldered aside by the intrusion. The intrusion appears to dip moderately to steeply southward and slightly cross-cuts bedding in the pelite which dips gently southwards.

This intrusion has been studied by French (1977) who noted that the contact pelites show evidence of thermal metamorphism with reduction of schistosity, chloritisation of muscovite and biotite, replacement of plagioclase and some quartz by calcite. He also noted the alteration of the igneous rock at the contact with similar chloritisation and growth of

calcite after amphibole and even the occurrence of drusy cavities of calcite along the contact.

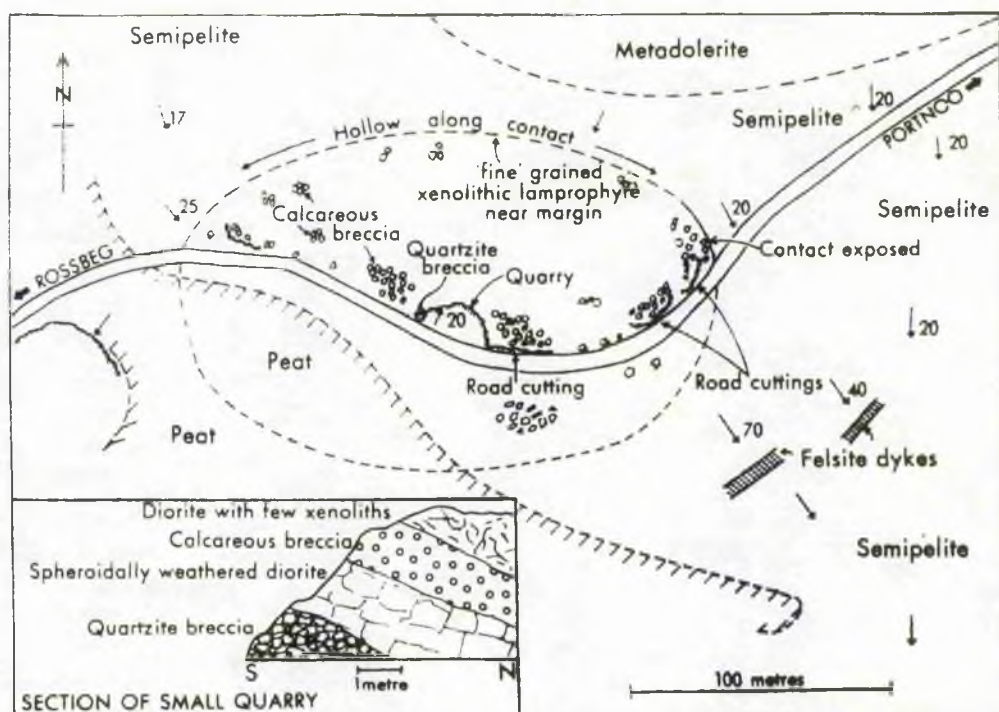


Fig. 3.19. Sketch map of the Biroge Breccia Pipe (after French 1977)

The intrusion consists of rounded fragments of calc silicate and quartzite, matrix-supported by heterogeneous diorite. The calc silicate and quartzite xenoliths occasionally show a bedding structure as if only slightly disrupted by the diorite. Within these beds the calc silicate pebbles dominate and are clast-supported, although few laminae may be seen in the pebbles which are highly altered. The quartzite brecciates in a brittle manner with recrystallisation into a glassy form and forms the obvious breccia within a small quarry (G6890 9880) at the core of the intrusion. It consists of broken sub-angular fragments, cubic to rhombic shaped measuring ~5 x 10 x 4cm, arranged in a haphazard, structureless manner.

The breccia of calcareous fragments, like that seen at the margin of the breccia pipe consists of clast-supported rounded pebble-sized fragments ranging in size from a few centimetres to several centimetres in diameter. Bedding and lamination are only occasionally preserved and they take the form of grey to green pebbles with green hornblende phenocrysts. Reaction relationships with the diorite are visible in the form of millimetre-scale growth of hornblende, pseudomorphed by biotite either perpendicular or parallel to the contact (Plate 3.12).

The dioritic matrix is coarser than the matrix of the pebbles and consists of subhedral but often acicular brown hornblende commonly replaced by secondary pale hornblende and biotite with titanite. The hornblende is often enclosed in a highly altered albite matrix, where calcite is present as an interstitial, late-stage mineral. Calcite also forms in cracks parallel to the hornblende cleavage. Needles of acicular apatite are well developed as inclusions within quartz and plagioclase, and prehnite is a late-stage interstitial mineral suggesting the presence of a hydrothermal phase. Granular clinozoisite and pyrites are important accessory minerals. In general the mineral texture of the diorite is highly deformed with pseudomorphic replacement of hornblende by actinolite, with a matrix of sericitised plagioclase and strained quartz. The texture is not metamorphic but more suggestive of strain due to the emplacement of the breccia.

On a larger scale, contacts between the calcareous breccia and the quartzitic breccia are diffuse. Pitcher and Read (1952) concluded that the calc silicate xenoliths entrained in the Birroge breccia pipe were derived from a depth of 700m below the present level of exposure using the knowledge of the surrounding stratigraphy and structure.

3.12.5 The Dunmore Hill intrusion breccia.

This intrusion breccia is located ~1km north west of Portnoo (G6900 0010) on an exposed cliff outcrop (Fig 3.20). The intrusion is elliptical in shape and sharply cuts across the Portnoo Limestone (Falcarragh Limestone) at a steep angle. The breccia pipe measures 160m x 58m and consists of a central core region of limestone breccia with a matrix of hornblende felsite. The breccia consists of limestone fragments which either randomly arranged or are a closely interlocking network of metre-sized blocks with a matrix of smaller centimetre-sized chips. Around this core of calcic breccia is a marginal area of much less contaminated felsite. This is also a hornblende felsite but tends to be slightly coarser than the matrix felsite. It consists of crudely foliated acicular actinolitic hornblende, often replaced by opaques, clinozoisite and biotite. This hornblende is set within a matrix of highly interlocking plagioclase, quartz and orthoclase with minor biotite, chlorite and muscovite.

Plate 3.12. The Biroge breccia pipe showing calc-silicate pebbles with rare relict bedding and hornblende margin up to few millimetres in width enclosed within dioritic matrix, with elongate hornblende, plagioclase, K-feldspar and quartz in the mesostasis.



2 cm

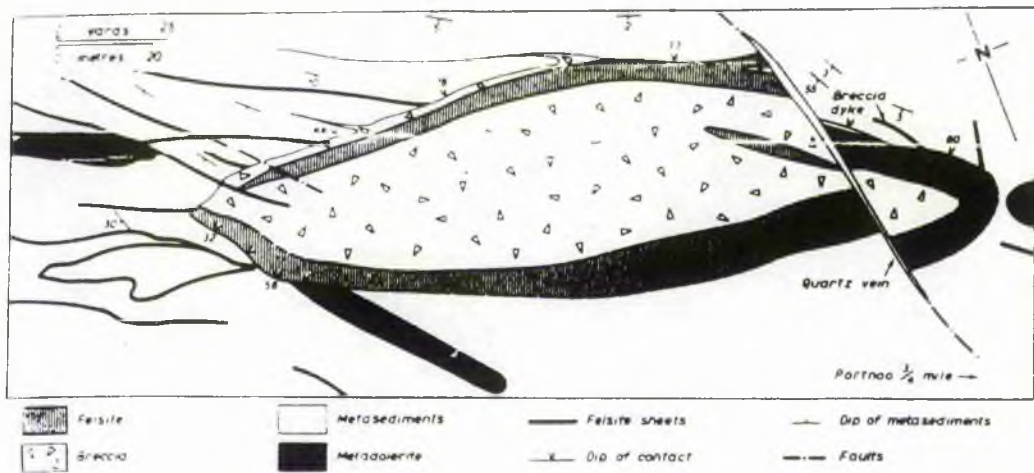


Fig 3.20. The geology of the breccia pipe of Dunmore (after French & Pitcher 1959).

This felsitic margin surrounds the breccia along the south side of the intrusion but on the north side the limestone breccia is in direct contact with the limestone country rock from which it was derived. The contact is relatively sharp but it is apparent that the breccia is derived from the Portnoo Limestone at the present level. The felsite in this northern area sends off several veins into the brittle Portnoo Limestone.

The felsite of the matrix is finer grained than the outer ring and consists of a mineralogy similar to the marginal felsite, except for the fact that the hornblende is more equant and less altered. French and Pitcher (1959) believed from the evidence of metasomatism and the igneous matrix that the breccia was permeated by hot gases, probably rich in H_2O and CO_2 , in the form of a gas charged magma. This may be supported by the great abundance of a pyrite and or magnetite as well as minor calcite in the felsite. French and Pitcher (1959) believed that, unlike the breccia pipes of Birroge and Kilkenny, the limestone fragments were not far removed from their source. This seems to be confirmed by the gradational contact between limestone and limestone breccia along the northern contact.

3.13 SUMMARY

This section provides a brief overview of the important field relationships outlined in the previous sections, including the form of intrusions, petrology and the mode of emplacement of the individual intrusions. The form, petrology and emplacement of the

various intrusions in the Ardara area is uniquely widely variable over a relatively small area and provide an important insight into the nature of the petrogenetic history of appinitic intrusions. The following summary will outline the most important aspects of each of these in turn.

3.13.1 Form of intrusions

The Ardara granitic diapir is the focus for the associated appinitic intrusions clustered around it. As a relatively later granitic pluton it has a direct contemporaneous link with only one of the appinitic intrusions, the Summy Lough diorite, (it also has intimate contacts with the Meenalargan and Kilrean intrusions). The emplacement mechanism of the Ardara pluton may have had important implications for the co-eval emplacement of the Summy Lough diorite by way of distension and extensional shear parallel to the contacts of the Ardara pluton. The steep-sided distensional margins of the pluton adjacent to the Summy Lough diorite, coupled with the component of extensional shear also active may have provided part of the space for the emplacement of dioritic intrusion. Sinistral shear is apparent in the northern side of the Ardara pluton, near Clooney (G7372 9920), and it is also important in the emplacement of the Main Donegal Granite to the east.

The Main Donegal Granite is a later-stage granitic intrusion, emplaced along an active sinistral shear zone which passes through the south-eastern part of the Ardara pluton and to the immediate east of the Meenalargan intrusion, although it does have splays of the main shear zone which pass through the core of the Meenalargan intrusion.

The Meenalargan intrusion has an elongate, dome-like form with relatively steep-sided contacts with its enclosing rocks. It is in contact with the Ardara pluton and although it can be proved to be slightly earlier than the Ardara pluton, the nature of these contacts, like those of the Summy Lough diorite is evidence of the near coeval timing of the two intrusions. Of all the intrusions, Meenalargan has perhaps the best preserved core zonation, with a central coarse basic core, crudely enclosed within an outer, finer grained slightly less mafic marginal facies. Within parts of both these zones "appinite" is present in the typical form of veins and pockets. The same feature is found in parts of all the other intrusions but never seems to have a well defined mode of occurrence which tends to form randomly in late stage veins and clots. In general terms the Meenalargan intrusion is the most stock-like, plutonic intrusion of all the intrusions in the area by virtue of its size, contact and internal relationships.

The Summy Lough diorite has an elongate outcrop with intimate contacts with the outer (G1) facies of the Ardara pluton and was emplaced parallel to the strike of the country rocks. Similarly, the intrusion of Mulnamin also has an elongate outcrop pattern, intruded parallel to the NW-SE strike of the country rocks in a distensional manner. The various disjointed intrusions concentrated along the coast from Narin to Portnoo take the form of numerous sheet-like, dyke, and domed intrusions with sinuous margins and shallow to

steep-sided contacts, and often intimate contact relationships with the local Portnoo Limestone. These intrusions, like those of Mulnamin and Summy Lough, have utilised large scale fractures and bedding planes as intrusion paths. The form of the various intrusion breccias and pipes found in the area underline the volatile nature of the appinitic magmas of the region with their explosive and reactive field characteristics.

3.13.2 Petrology of the intrusions

The appinitic intrusions have petrological similarities throughout the area. Each intrusion has a generally dioritic composition and variations through granodiorite, meladiorite and hornblendite exist. The Kilrean intrusion contains the most basic rock types and is the only intrusion to contain olivine as a major phenocryst phase and with its abundant hornblendite and pyroxene gabbroic rocks it has the most primitive petrology of all the intrusions. Meenalargan, Mulnamin and Narin-Portnoo have compositions which range from hornblendite and meladiorite to diorite and appinite, with late stage granodiorite sheets and dykes. In all the intrusions appinite is a sporadically developed rock type and these intrusions are dominated by a dioritic-meladioritic composition which show local variation to both hornblendite and leucodiorite. The association of granitic and dioritic rock types is most intimate at Portnoo and appears to reflect a late stage mingling between two magma types.

The effects of contamination and assimilation of country rock are seen within many of the intrusions, particularly against calc silicate rocks. Meenalargan and Mulnamin both show features associated with reaction against such rock types, but the most extreme reaction characteristics are found on the Narin-Portnoo coast, where the effects of magmatic and meteoric fluids can be demonstrated (see Fig. 3.14, page 83).

3.13.3 Emplacement mechanisms of the appinitic intrusions

The mechanisms of emplacement of the appinites are variable but similarities can be found between the different intrusions. Kilrean, the most primitive intrusion, appears to have been intruded as an upright magmatic stock-like body and like that of Meenalargan it has xenoliths of country rock suggesting a degree of stoping involved in the intrusion process.

Both Mulnamin and Summy Lough may have been emplaced during a process of dilation and compression of the country rocks as elongate bodies intruded parallel to the strike of the country rocks. Certainly Summy Lough has suffered a degree of boudinage during coeval emplacement with the Ardara pluton. It seems likely that such a process of emplacement along weaknesses in association with a degree of extension and shear may have been responsible for the emplacement of the disjointed intrusions found along the Narin-Portnoo coast. These form a number of dome-like, sheeted, and dyke intrusions that locally can be shown to have been forcefully emplaced into the Portnoo Limestone, causing

a steepening-up of surrounding metasediments. There is also evidence of brecciation associated with emplacement into calcareous country rocks at Narin-Portnoo and Mulnamin, which suggests a release of CO₂ from the limestone country rocks.

Such explosive potential is supported by the pattern of emplacement of the minor intrusions in the area. The numerous breccia pipes and intrusion breccias of Biroge, Kilkenny, Mulnamin and Dunmore, whose dominant rock type and character is a volatile-rich assemblage including appinite, coarse diorite, granophyre with hydrous volatile minerals such as actinolite, calcite and pyrites, and a close association with calc-silicate country rocks (which may have provided a source of CO₂ for the explosive emplacement process to occur).

Such field relationships are characteristic of the appinite suite in Ardara and have similarities with other parts of the Caledonides, however no comparable data has the diverse range of form, petrology and emplacement mechanism as those associated with the Ardara pluton. The petrological characteristics of the Ardara appinite suite are outlined in the following chapter.

CHAPTER FOUR

PETROGRAPHY AND MINERAL CHEMISTRY

4.1 PETROGRAPHY OF THE MAIN ARDARA PLUTON

The pluton consists of three main granitoid members, namely an outer unit (G1), an inner unit (G2), and a central unit (G3). The degree of deformation and the mean grain size of the pluton as a whole both increase towards the margin. Distinction between the three members is possible as each has a characteristic facies in the field as described in chapter three. The contact between G1 and G2 is found to be steep and sharp in only one place (Maas) and elsewhere appears gradational and intersheeted. The contact between G2 and G3 is gradational over several metres. Petrographically the different facies are easily distinguished using textural and mineralogical criteria and classify within the IUGS scheme of Streckeisen (1976) as shown in Fig. 4.1. Modal abundances were estimated for each rock type and the results are tabulated in Table 4.1. The petrography is illustrated by representative samples using both conventional photomicrographs and Z-contact images (ZCI) generated by backscattered electron imagery techniques (see Appendix 2).

4.1.1 Outer quartz monzodiorite (G1)

G1 forms an annular ring to the pluton, only breached south of Meenalargan (in the eastern 'neck') by G2 (Map 1). The most striking feature of G1 is its megacrystic and strongly foliated texture which is due to the presence of large aligned plagioclase laths around which biotite is deformed. Plagioclase is present in the form of elongate laths with a weak zoning of An₂₀₋₂₅ in the core to An₁₇₋₂₀ in the rim. There are two sizes of plagioclase, one set is similar in size to the other mineral constituents of the rock, up to 0.1cm in diameter, the second forms a distinct set of phenocrysts up to 1.0cm across. Both sets are subhedral to euhedral in shape and may contain inclusions of muscovite, biotite and zircon, especially in the core. The phenocrysts also contain domains of deformation particularly at their margins with embayments and rounding of the crystals. Myrmekitic texture is occasionally found associated where the plagioclase is in contact with microcline. Contact with quartz is always anhedral but with biotite it is intimate and the biotite is often aligned against plagioclase forming a distinct foliation, which locally (e.g. Clooney) defines a weak sinistral S/C fabric.

Microcline is the dominant alkali feldspar and forms turbid grains. It usually shows euhedral crystallographic contacts with the plagioclase, whilst contacts with quartz are rounded and intimate suggesting contemporaneous crystallisation of microcline and quartz. Quartz takes the form of small rounded interstitial crystals whilst biotite defines a strong mineral foliation arranged around plagioclase which is occasionally fractured along its

length. Biotite typically forms clots of ragged brown flakes along with small rounded quartz crystals, titanite, clinozoisite and hornblende.

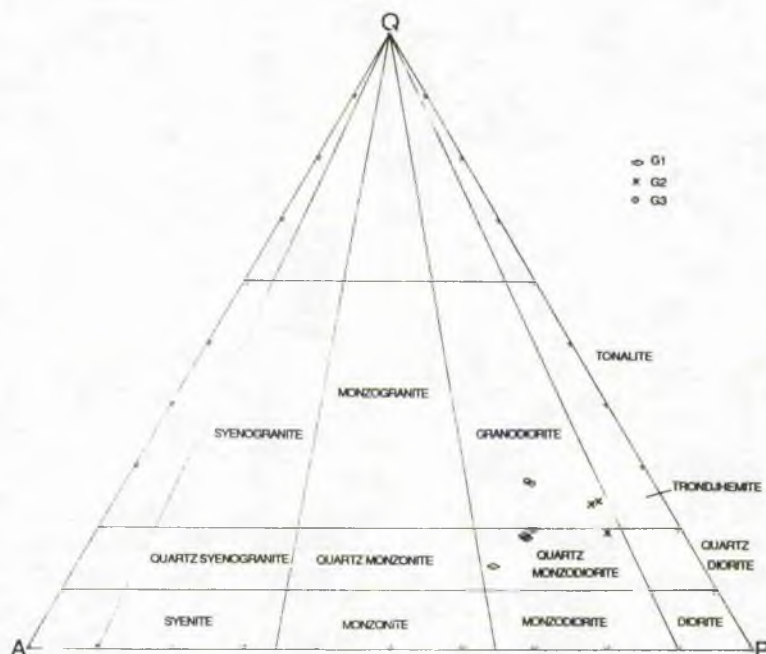


Fig. 4.1 Q-A-P plot of Main Ardara granitoid members (G1, G2 and G3)

ROCK TYPE	SAMPLE	QUARTZ	A-F'SPAR	PLAG	BIOTITE	HBLENDE	AUGITE	ILM/MAG	CLINOZ/EPID	ZIRCON	APATITE	TITA	MUSCO	TOTAL %
G1	861	14.80	18.00	50.00	13.60	0.40	0.00	0.00	0.60	0.60	0.00	1.00	1.00	100.00
	863	16.00	16.20	48.20	13.20	1.80	0.50	0.20	1.20	0.10	0.00	2.00	0.60	100.00
	865	11.00	23.30	46.30	12.60	4.40	0.50	0.00	0.60	0.00	0.00	0.30	1.00	100.00
	866	13.00	20.10	46.00	10.00	6.50	1.50	0.40	0.90	0.00	0.00	1.20	0.40	100.00
	1261	15.20	18.50	47.00	15.00	2.00	0.00	0.20	1.50	0.00	0.00	0.60	0.00	100.00
G2	868	19.75	7.25	54.00	17.30	0.70	0.00	0.30	0.20	0.20	0.00	0.20	0.00	100.00
	8611	15.20	6.80	42.80	18.80	9.10	1.50	0.00	3.00	0.20	0.20	0.00	2.40	100.00
	1264	16.60	8.60	60.00	10.10	2.90	0.00	0.00	1.10	0.00	0.10	0.60	0.00	100.00
G3	34	25.60	13.00	42.00	13.80	0.60	0.00	0.00	2.60	0.00	0.20	0.60	1.60	100.00
	37	25.40	15.04	49.19	8.80	0.00	0.00	0.00	1.00	0.20	0.00	0.00	0.40	100.00
	962	24.05	15.04	49.19	9.50	0.00	0.00	0.00	2.00	0.00	0.00	0.20	0.00	100.00
Minor	90	30.00	10.00	40.00	10.00	0.00	0.00	0.50	2.70	0.20	0.40	0.20	3.00	100.00
	94	20.00	10.00	25.00	40.00	0.00	0.00	0.10	3.40	0.20	1.00	0.10	0.20	100.00
Intrusions	SH1	15.00	5.00	20.00	20.00	30.00	0.00	0.10	8.10	0.10	1.50	0.10	0.10	100.00
	967	10.10	4.50	19.80	20.00	38.00	0.00	0.20	5.75	0.20	1.40	0.05	0.00	100.00
Crockard	Granite (Gr)	27.00	5.00	49.00	11.00	6.10	0.00	0.00	1.30	0.10	0.40	0.10	0.00	100.00
Glenard	Hb Granod (Hb Gd)	20.00	4.90	24.50	16.00	28.80	0.00	0.20	4.70	0.05	0.81	0.04	0.00	100.00
	Granod (Gd)	20.00	10.30	40.70	20.00	5.50	0.00	0.10	2.00	0.15	0.80	0.00	0.45	100.00
	Appinite (11)	4.60	3.80	10.00	20.00	57.70	0.00	0.80	2.00	0.50	0.20	0.40	0.00	100.00
Dunmore	Felsite	15.00	5.00	40.50	17.50	16.50	0.00	1.00	1.60	0.40	0.30	0.20	2.00	100.00

Table 4.1 Modal analyses of Main Ardara granite facies (G1, G2, G3) for representative samples. Samples were counted for 1000 points per sample .

Hornblende is variable in abundance but rarely accounts for >5% by modal volume. It commonly forms subhedral squat to elongate crystals associated with biotite with which it may be intimately intergrown. It varies in pleochroism from yellow green (α) to dark green (β) and green (γ), and may have a dark green core full of quartz inclusions.

Accessories include epidote and clinozoisite which are usually associated with biotite as a breakdown product forming elongate granular grains that may be broken up along the length of biotite. Also present are apatite, zircon, rare allanite, titanite and occasional opaque, commonly associated with hornblende. A typical view of the outer unit (G1) is shown in Plate 4.1 (a).

4.1.2 Inner granodiorite/quartz monzodiorite (G2)

The G2 member separates the outer G1 member from the central G3 facies. The differences between G1 and G2 are mainly related to the abundances of quartz, K-feldspar and plagioclase. Texturally plagioclase is less megacrystic in G2 than G1. The plagioclase in G2 is finer grained than that of G1 and is euhedral with occasional rounded outlines and embayments. Zoning is weak within plagioclase whose composition varies from An_{20-25} in the margin to An_{20} in the core. Contacts with plagioclase and microcline may be relatively sharp but may also be deeply embayed by microcline, whilst against quartz they are typically rounded.

K-feldspar occurs dominantly as microcline forming the main part of the mesostasis between plagioclase crystals, occasionally showing micropertitic textures. Quartz typically forms rounded and strained grains larger than those in G1 commonly cracked due to late stage deformation.

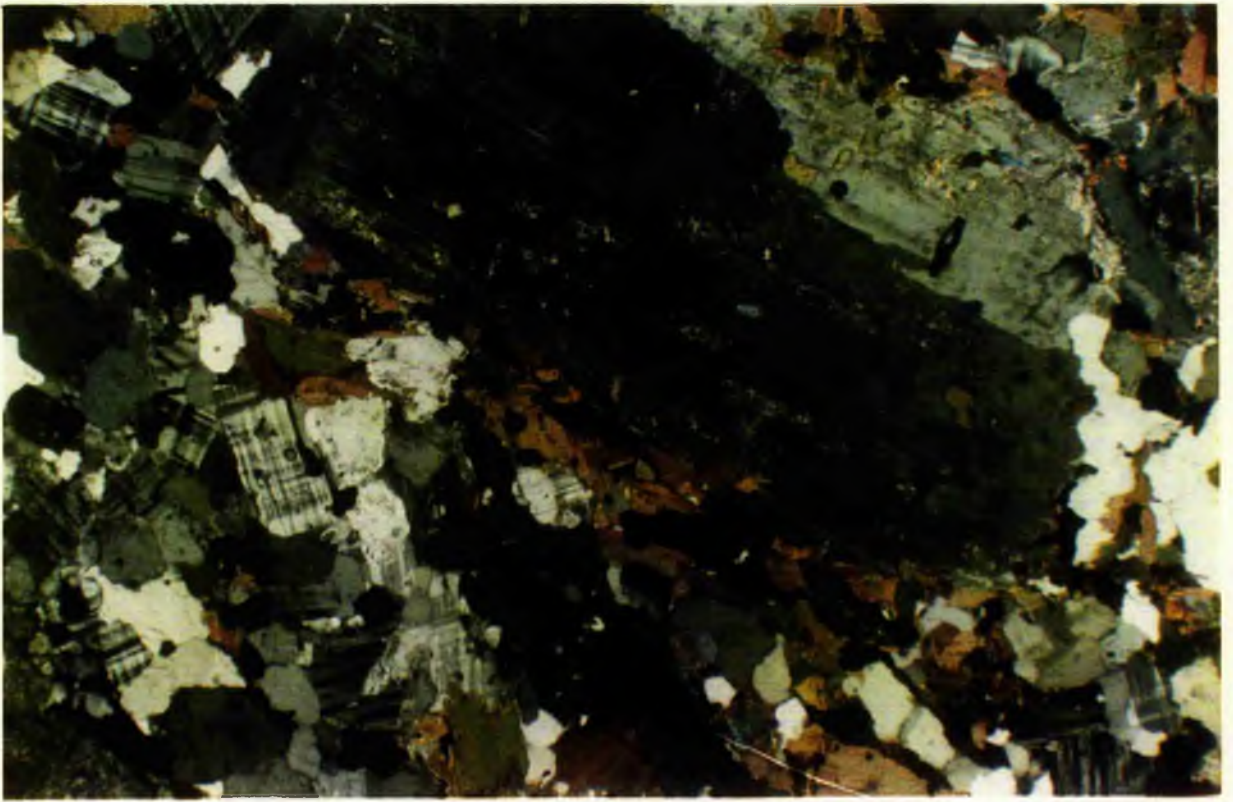
Biotite forms rather euhedral flakes, often in clots up to 3-4 mm across associated with hornblende, titanite and clinozoisite. Pleochroism varies from yellow-green (α) to brownish-green ($\gamma=\beta$). Biotite is sometimes kinked and aligned in the foliation and is subhedral in form. Deformation textures are seen within the stalk region of Meenalargan where G2 is present, these deformation textures are related to the later Main Donegal Granite which imparts a cataclastic fabric on G2. Biotite is deformed against plagioclase, quartz and microcline, all of which are highly recrystallised and develop as domains in the most intense areas of deformation.

Hornblende is similar in texture and occurrence to that of G1, although the amount of hornblende decreases as G3 is approached (in the northern part of the pluton) and is absent in the margins of G3.

Accessories include clinozoisite, typically associated with biotite in the form of anhedral rounded grains with granular texture, as in G1. Epidote is occasionally present as yellow subhedral to anhedral crystals, probably formed in the late stages of crystallisation. Titanite, apatite and zircon are also present. A representative view of G2 is shown in Plate 4.1 (b)

Plate 4.1 (a) Transmitted light XPL photomicrograph of a thin section of rock from the outer unit (G1) quartz monzodiorite of the Ardara pluton (Y861). Plagioclase forms the main phenocryst phase with weak zoning, surrounded by biotite and minor hornblende. Microcline forms squat grains in the groundmass along with rounded quartz. Strain domains are apparent in the megacrystic plagioclase phenocryst and quartz grains in the top right and centre right of the photomicrograph respectively. Width of field of view 12.5 mm, Mag. x1.2.

Plate 4.1 (b) Transmitted light XPL photomicrograph of a thin section of rock from the inner unit (G2) quartz monzodiorite/granodiorite of the Ardara pluton (Y8613). Plagioclase forms a crude layering that is slightly bent due to deformation associated with emplacement. Note also the rounded outline of the plagioclase and rounded embayments in contact with quartz. Hornblende is present in the bottom right of the photomicrograph with sieve-textured biotite in the bottom centre. Width of field of view 7.5 mm, Mag. x2.



4.1.3 Central granodiorite (G3)

G2 passes gradationally into G3 in the northern part of the pluton. G3 is texturally and compositionally very different from the other two facies described above. It has an almost equigranular, xenomorphic texture with an increase in the amount of quartz and decrease in the plagioclase content relative to G1 and G2. The plagioclase has weak reverse zoning from An₂₀ in the core to An₂₃ at the margin. Plagioclase commonly forms mutually interfering crystals which are oscillatory zoned, defined petrographically by areas of sericitisation. Occasionally albitic rims are located where plagioclase adjoins other plagioclase crystals and vermicular intergrowths of quartz and albite form against microcline.

K-feldspar is present primarily in the form of microcline which occurs most commonly as phenocrysts but also as small crystals in the mesostasis. It may be microperthitic and often has inclusions of quartz and occasional plagioclase within it. Contact with plagioclase is commonly anhedral and rounded.

Quartz is second only to plagioclase in modal proportion and forms highly deformed rounded to square crystals up to 4mm in diameter. This gives G3 its characteristic pebbly texture observed in the field. The crystals are often square in form with abundant internal crystal domains.

Biotite is the dominant ferromagnesian mineral, forming ragged, squat crystals, often highly chloritised which concentrate at the corners and intersections of plagioclase and microcline crystals. It is commonly associated with elongate clinozoisite and zircon crystals.

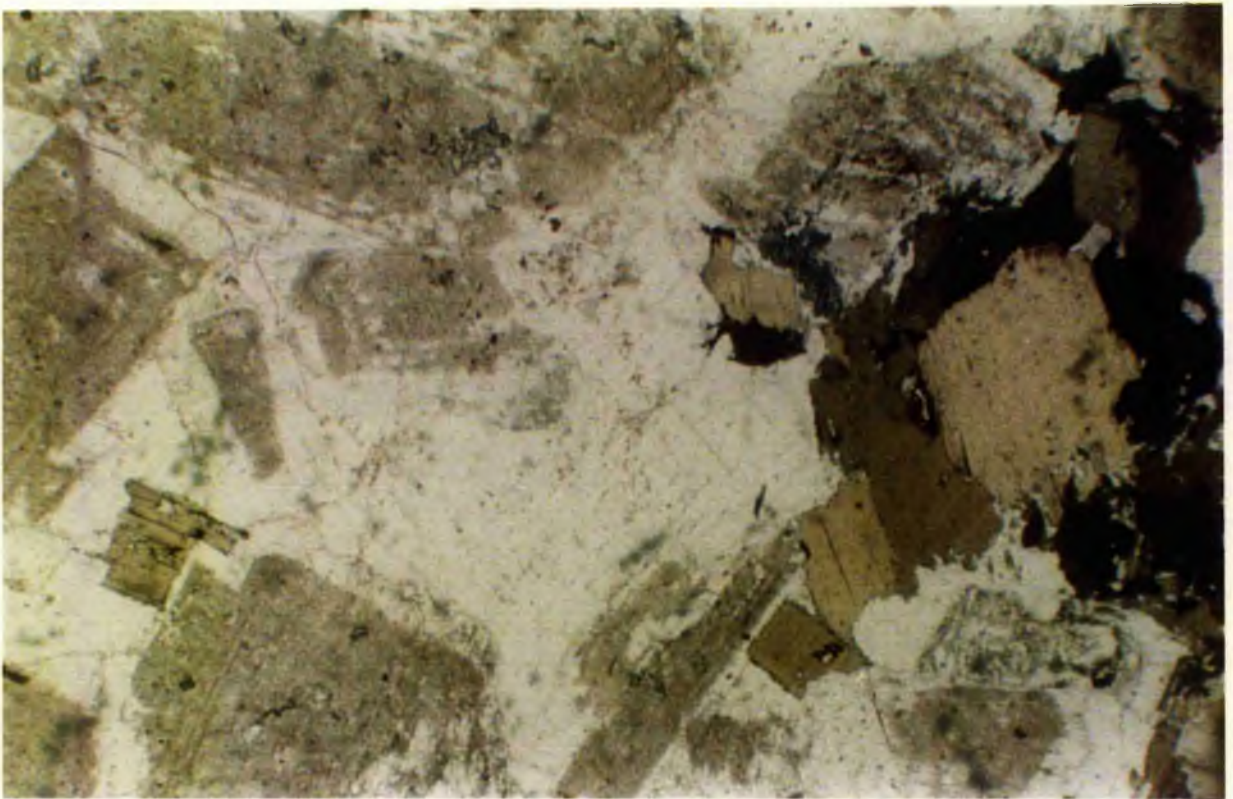
Hornblende is a relatively minor mineral forming small squat, often euhedral crystals. Other minor phases include epidote and clinozoisite, sporadically found in the mesostasis as anhedral to subhedral granular crystals with yellow to colourless pleochroism often associated with biotite. Accessories typically include apatite, zircon and rare allanite, while titanite is normally absent opaques are very rare. A representative view of G3 is shown in Plate 4.2.

4.1.4 Minor intrusions: microgranite sheets, pegmatites and aplites

(i) Microgranite Sheet (East Sheskinmore)

The mineralogy of the microgranite sheets formed within the pluton is similar to that of G3. They are essentially granodioritic in composition (Table 4.1) and have a fine to medium grained texture. Plagioclase is present as poorly zoned squat subhedral to anhedral crystals with numerous inclusions of clinozoisite and squat hornblende microcrysts. K-feldspar is present in the form of microcline as typical square to rounded mesostatial patches, often highly deformed, whilst quartz is abundant as highly domained crystals up to 2mm in diameter, also highly deformed. The main ferromagnesian mineral is biotite which forms single crystals with ragged outlines or as smaller crystals forming trail-like

Plate 4.2 (a) and (b). Transmitted light XPL (top) and PPL (bottom) photomicrographs of a thin section of a rock from the central granodiorite of the Ardara pluton (Y963). Plagioclase occurs as mutually interfering crystals with weak zoning defined by sericitised core and marginal rim. Perthitic microcline is present (centre of photomicrograph) and biotite forms the main ferromagnesian phase (right of photo) as ragged squat crystals. Width of field of view 7.5 mm, Mag. x2.



formations arranged against angular quartz and plagioclase. Hornblende is occasionally found as rare individual crystals sometimes pseudomorphed by biotite with a green (α) to dark green (γ) pleochroism. Clinozoisite is apparent as granular crystals in association with biotite. Accessories include zircon, apatite and minor allanite.

(ii) Pegmatites/Aplites

These comprise of plagioclase, quartz, microcline and perthitic feldspar along with minor biotite, muscovite. The textural variations are not described in detail here as they have not been included in this study. However it is notable that tourmaline is sometimes present and that the pegmatites associated with the MDG have abundant muscovite and garnet, which are absent from Ardara pegmatites, allowing the two types to be distinguished.

4.1.5 Enclaves

Two main types of enclave occur within the Ardara pluton, namely pelitic and calc pelitic metasedimentary xenoliths and medium grained microdioritic enclaves, and the general petrographic features are described below.

(i) Calc pelitic and pelitic xenoliths differ significantly from the dioritic enclaves in both mineralogy and texture. The xenoliths are generally of finer grain size and have more biotite and quartz. Plagioclase forms fine grained anhedral crystals which are full of apatite inclusions and are highly sericitised and aligned in the direction of relict bedding. K-feldspar occurs as rare orthoclase which forms small rounded turbid grains. Quartz occurs as typical anhedral interstitial grains with abundant crystal domains. Biotite forms green to brown elongate crystals which define strong foliations and are apparently recrystallised, typically in interlocking forms with hornblende. Hornblende may occur as small granular crystals with a brown to olive green colour most commonly intergrown with biotite. Epidote and clinozoisite are present as granular minerals associated with hornblende and biotite.

Pelitic xenoliths may be distinguished from calc pelitic xenoliths by the presence only of biotite as the main ferromagnesian phase (Plate 4.3 a), no garnet was present, however andalusite is pseudomorphed by biotite, chlorite, plagioclase and quartz. Both these types of metasedimentary xenolith have strongly defined bedding laminations which are retained in most xenoliths. Where intense reaction within the granite has occurred both types of metasedimentary xenolith lose their pre-existing metasedimentary structure and begin to be partially resorbed into the granite.

(ii) Basic enclaves are generally dioritic in composition with medium grain size. Plagioclase forms stumpy to elongate laths with straight and angular contacts with quartz. The crystals are deeply embayed by biotite and hornblende. The plagioclase is distinctively rich in inclusions of apatite, with muscovite and clinozoisite as alteration products. In some cases plagioclase may be seen to replace hornblende. Orthoclase forms the main K-feldspar

Plate 4.3 (a) Transmitted light PPL photomicrograph of a thin section of a pelitic xenolith (SH1) from the outer unit (G1) of the Ardara pluton. Field of view shows S_3 represented by biotite, chlorite, plagioclase and quartz. Upper centre part of photomicrograph is occupied by andalusite pseudomorphed by biotite, chlorite and plagioclase. There is also evidence of sinistral shear rotation of the porphyroblast. Width of field of view is 7.5 mm, Mag. x2.

Plate 4.3 (b) Transmitted light PPL photomicrograph of a thin section of a dioritic xenolith (S2) from the outer unit (G2) of the Ardara pluton. Hornblende has two forms, the first is as euhedral phenocrysts with an actinolitic rim. The second forms small ragged grains that often form aggregates (top centre) replacing hornblende or augite along with biotite. Plagioclase forms the groundmass as small laths with minor epidote and clinozoisite forming squat speckled grains (bottom left). Width of field of view 3.75 mm, Mag. x4.



phase as turbid, non-perthitic mesostatial crystals. Quartz occurs as fine grained rounded crystals also full of inclusions of apatite in acicular form. Biotite occurs as greeny/brown euhedral to anhedral flakes associated with clinozoisite and hornblende. There appear to be two generations of hornblende phenocrysts, the first is euhedral, formed slightly earlier than the more ragged second form (Plate 4.3 b). Hornblende is present as grass-green (α) to dark green (γ) prismatic crystals largely replaced by biotite found in mafic clots along with biotite and clinozoisite. Clinozoisite and epidote form irregular, granular overgrowths of the felsic minerals, and as replacements of biotite and hornblende. Accessories are dominated by apatite which is concentrated within plagioclase. Minor ilmenite and magnetite is associated with hornblende.

Most dioritic enclaves have similar mineralogical assemblages to that described above but there are significant variations in the ratio of biotite to hornblende. In other enclaves the main K-feldspar is microcline.

4.2 PETROGRAPHY OF THE APPINITES

The petrography of the appinitic rocks of the type Appin, Ardara and other areas has been described by various authors (Bailey & Mauffe 1916, Bowes & Wright 1967, French 1966, Pitcher & Berger 1972), all of whom drew attention to the uniquely complex textures within individual intrusions. These textures have been related to differentiation in situ (i.e. gradation from granite to hornblendite within the individual intrusion, including an amphibole and/or pyroxene bearing basaltic parental magma (Pitcher & Berger 1972), hybridisation of magmas (Deer 1953), crystal fractionation at high water vapour pressure (Hall 1967), and crystallisation from a volatile rich basaltic magma, with accumulation of mafic phases as cumulates and the disruption by residual fluids and explosive activity (Hammidullah & Bowes 1987).

The petrography, textures and chemical relationships of the major rock types of each intrusion will be described in turn, based on petrographic summaries of representative examples, together with average modal compositions (Table 4.2). The approach is to describe the representative rock types and their settings in general terms followed by any significant variations from these type rocks.

4.2.1 Appinites of the Ardara suite

Eight major varieties have been selected from the considerable variation observable within and between the many individual appinite intrusions of the Ardara area, and these are described in summary below. Additional detailed information is available in Pitcher & Berger (1972), Hall, (1967) and French (1966).

(i) Hornblendite

The typical hornblendite of the area is medium to coarse grained, comprising dominantly of hornblende (0.05cm to 0.8cm in diameter) and augite, both of which may

Rock Type	Sample	Olivine	Hornblende	Cpx	Opx	Biotite	Plag	Quartz	A-F'spar	Clinoz/Epld	Opaque	Titanite	Calcite
Cortlandite	K11r	25-35	27-32	20	9-18	0	0	0	0	0	0.5-2	0	0
Hornblende	76c	0	80	0-10	0	2	10	2-5	3	2	0.5	0	1
Meladiorite	AP2	0	50-60	0-5	0	0-2	20-30	5	2	1	1	0-1	0-1
Diorite	Y1856	0	30-40	2-10	0	5-10	30	5-10	2	2	1	1	1
Appinite	Y26510	0	30	10-20	5	20-30	5	5	1-5	2	1	1	2-5
Biotite Diorite	Y6614	0	5-10	0	0	10-20	30	30	30	0	1	1	2-5
Granite	Y169, Y261	0	0	0		10	25-40	10-25	30	0	0	0	2

Table 4.2 Average Modal analyses of the major basic rock types of the Ardara appinite suite using representative samples. Samples were counted for 500 points per sample .

form a crude interlocking, and in places, a layered fabric. The interstices of this fabric are filled by plagioclase which may often be poikilitic. K-feldspar and minor quartz may also be present. Augite forms elongate crystals up to 3mm in length but more commonly occurs as stumpy anhedral crystals with corroded edges. The augite has a complex intergrowth with skeletal ilmenite either in the form of a fine dusting or discrete lamellae cross cutting the cleavage. The augite typically has a light brown to grey-green pleochroism. Both the augite and hornblende are replaced by biotite and actinolitic hornblende. Biotite forms elongate to stumpy flakes and is often associated with ilmenite. Biotite crystals grow along the cleavage and margins of the augite in association with granular titanite and larger crystals of opaque (?ilmenite). The hornblende often takes the form of a marginal pseudomorph. In this form it has brown to green pleochroism but it also forms needle-like pale green actinolitic crystals within and at the margins of the augite.

Primary hornblende is present as brown, mutually interfering stumpy anhedral crystals, often replaced by biotite and chlorite flakes which are arranged across the grains parallel to a weak foliation which often cross-cuts hornblende. The crystals are often heavily corroded by mesostatial plagioclase, biotite and chlorite. The hornblende may have a crudely defined margin of actinolitic amphibole.

The groundmass contains oligoclase (An_{35}) as rounded, recrystallised crystals which often form irregular contacts with hornblende and augite grains. Twinning is poorly defined in the plagioclase due to deformation, recrystallisation and sericitisation which give the plagioclase a turbid, speckled appearance. Quartz is trapped in late stage interstitial areas between plagioclase and hornblende and as inclusions within hornblende, while orthoclase may occur as a minor interstitial form (Plate 4.4 a). Accessories include calcite which together with pyrite, clinozoisite and titanite occur as late stage minerals in the interstices or as inclusions within the felsic or mafic minerals. Hornblende in particular is cut by calcite and clinozoisite veins, some of which are probably brittle veins formed in the late stages of crystallisation.

(ii) Meladiorite

The main difference between the meladiorite and the hornblendite is the higher plagioclase/hornblende ratio in the meladiorite. Biotite may also be more common in meladioritic rocks. The meladiorite commonly has two dominant hornblende types; the first occurs as large prismatic to squat crystals with honey-brown to bottle-green pleochroism which are mutually interfering and with highly interlocking textures. Occasional hornblende crystals are euhedral and are enclosed within plagioclase, this hornblende type may also form crystals up to 3mm in diameter in clots which are often over 10mm in width. The second type of amphibole is colourless actinolite and occurs as ragged, rounded grains which are associated with the euhedral hornblende in clots. Biotite occurs as anhedral plates that are often found in the cores and margins of large hornblende crystals. These may also be present as small crystals replacing hornblende, parallel to cleavage, where it is commonly associated with clinozoisite and epidote.

Plagioclase typically varies in composition from An_{25-60} . The plagioclase in contact with primary hornblende forms angular embayments and is overgrown by smaller crystals of later hornblende (Plate 4.4 b). Plagioclase is poorly twinned and lacks good crystal structure when trapped between interlocking hornblende crystals, occasional crystals may reach 0.5 - 1.0 mm in length and have euhedral shape. Sericitisation is widespread.

K-feldspar is occasionally present as rounded grains which are interstitial and have a turbid internal structure which, like the plagioclase, has common grain boundary recrystallisation. Quartz occurs as a rare late stage interstitial mineral and as inclusions within plagioclase and hornblende. Accessories include opaques and apatite inclusions within plagioclase, hornblende and biotite.

Plate 4.4 (a) Transmitted light PPL photomicrograph of hornblendite from the Narin-Portnoo intrusion (Y2657). Hornblende dominates as highly interlocking euhedral to subhedral crystals commonly embayed in contact with plagioclase. Augite is also present (top centre). Plagioclase dominates the mesostasis along with clinzoisite (centre left) and titanite. Calcite occurs as inclusions within plagioclase and hornblende. Width of field of view 3.75 mm, Mag. x4.

Plate 4.4 (b) Transmitted PPL photomicrograph of meladiorite from the Narin-Portnoo intrusion (Y2658). Hornblende forms large elongate to small stumpy crystals, mutually interfering with ragged outline, often in clot-like aggregates (top right). Actinolite forms occurs as needles (centre left). Plagioclase forms the main interstitial crystals along with calcite. Width of field of view 12.5 mm, Mag. x1.2.



(iii) Diorite

Diorite forms the commonest rock type within the Ardara appinite suite. Numerous compositional and textural variations occur amongst the diorite group ranging from coarse grained diorite with crystals >10 mm in diameter to fine grained diorites with an average grain size of 0.5 mm. Diorite is distinguished from "appinite" by the absence of acicular hornblende crystals.

The most common type of diorite is a medium grained, closely knit, highly interlocking and weakly to strongly foliated rock type, with a texture dominated by brown to green hornblende with minor augite set within a groundmass of plagioclase, quartz and minor K-feldspar. The augite is often partially or wholly replaced by amphibole and has light grey to pale green pleochroism, commonly forming an intergrowth of hornblende and augite. Amphibole may form squat to prismatic grains but may also occur in the form of actinolite which is typically a secondary replacement mineral of early hornblende forming needle-like crystals with colourless to grey pleochroism (Plate 4.5 a).

Biotite may form ragged, elongate crystals in the mesostasis or occur as a replacement mineral associated with late stage replacement of amphibole along with chlorite.

Plagioclase is the dominant felsic phenocryst mineral and occurs as lath and stumpy crystals, up to 0.8cm in diameter. They may be zoned from An₅₀ in the core to An₂₂ at the margin. This calcic core is typically altered to a sericitic assemblage of white mica and clinozoisite (Plate 4.5 b). Deformation has the effect of granulating plagioclase and hornblende crystals, essentially at the margins but also within crystals along cross-cutting shear zones, which may be defined by the growth of chlorite along the shear plane (Plate 4.6 a).

Orthoclase occurs in the form of small anhedral interstitial crystals with quartz-like habit and is of minor abundance compared with plagioclase. Crystals typically appear to be dusty, turbid grains with minor sericitisation. Quartz forms small globular and bleb-like crystals with intense recrystallisation fabric. Clinozoisite is a secondary product after hornblende and plagioclase, along with biotite.

Accessories include calcite, formed as a late stage breakdown product of augite along with secondary amphibole with which it forms irregular interstitial plates along with quartz. Chlorite is found as a late stage replacement mineral associated with biotite. Titanite may be associated with the replacement reaction of hornblende and augite. Clinozoisite is associated with ilmenite/rutile/magnetite in reaction between the opaques and hornblende (Plate 4.6 b). Magnetite and ilmenite are the dominant opaques, commonly found intergrown with hornblende.

(iv) Coarse diorite

Coarse diorite is recognised as a separate rock type because of its striking field appearance and common occurrence amongst the appinite suite. It has mineralogy similar to

Plate 4.5 (a) Transmitted PPL photomicrograph of diorite (Y25512) from the Meenalargan dioritic intrusion. Hornblende forms rounded crystals with interlocking texture. Actinolite is present as grey needle-like grains (bottom left) at margin of prismatic hornblende. Plagioclase dominates the mesostasis with dusty sericitic cores. Titanite is present as alate stage overgrowth in hornblende (centre). Width of field of view 3.75 mm, Mag. x4.

Plate 4.5 (b) Transmitted XPL photomicrograph of diorite (M5) from the Meenalargan dioritic intrusion showing elongate plagioclase with dusty core and margin overgrown by clinzoisite and muscovite. Hornblende forms elongate to prismatic crystals with actinolitic rims at right and bottom left. Width of field of view 12.5 mm, Mag. x1.2.

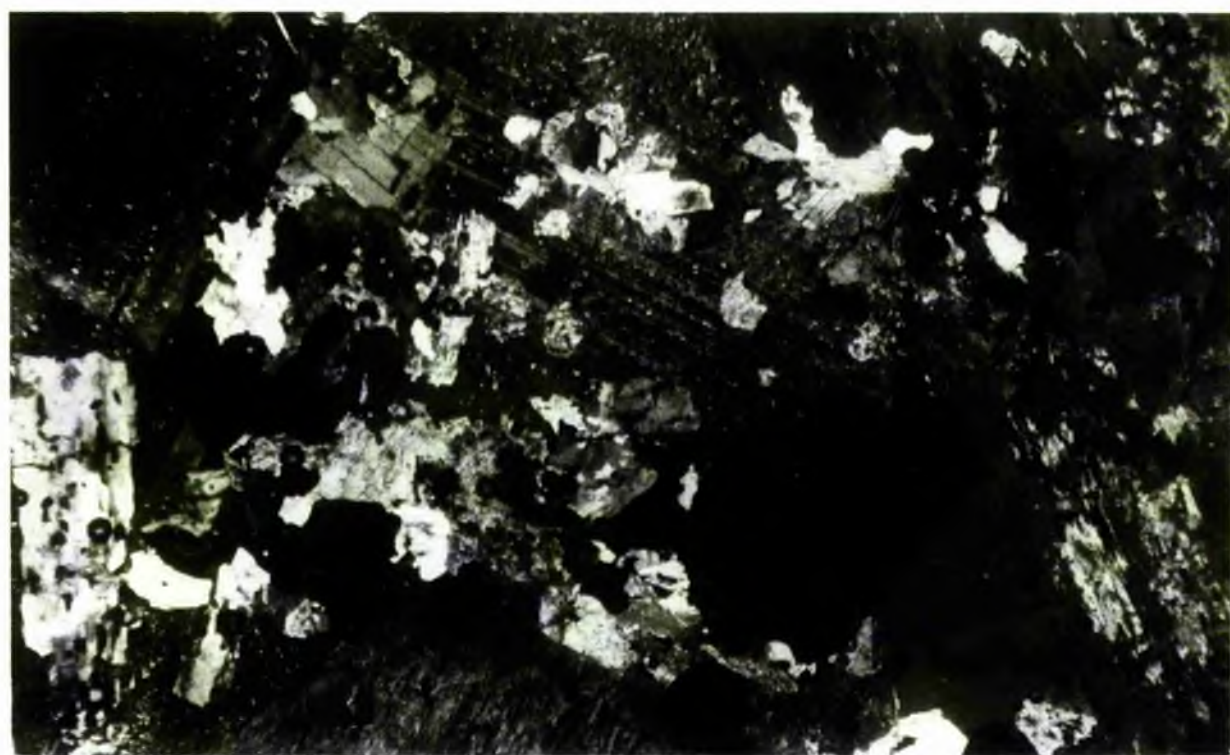
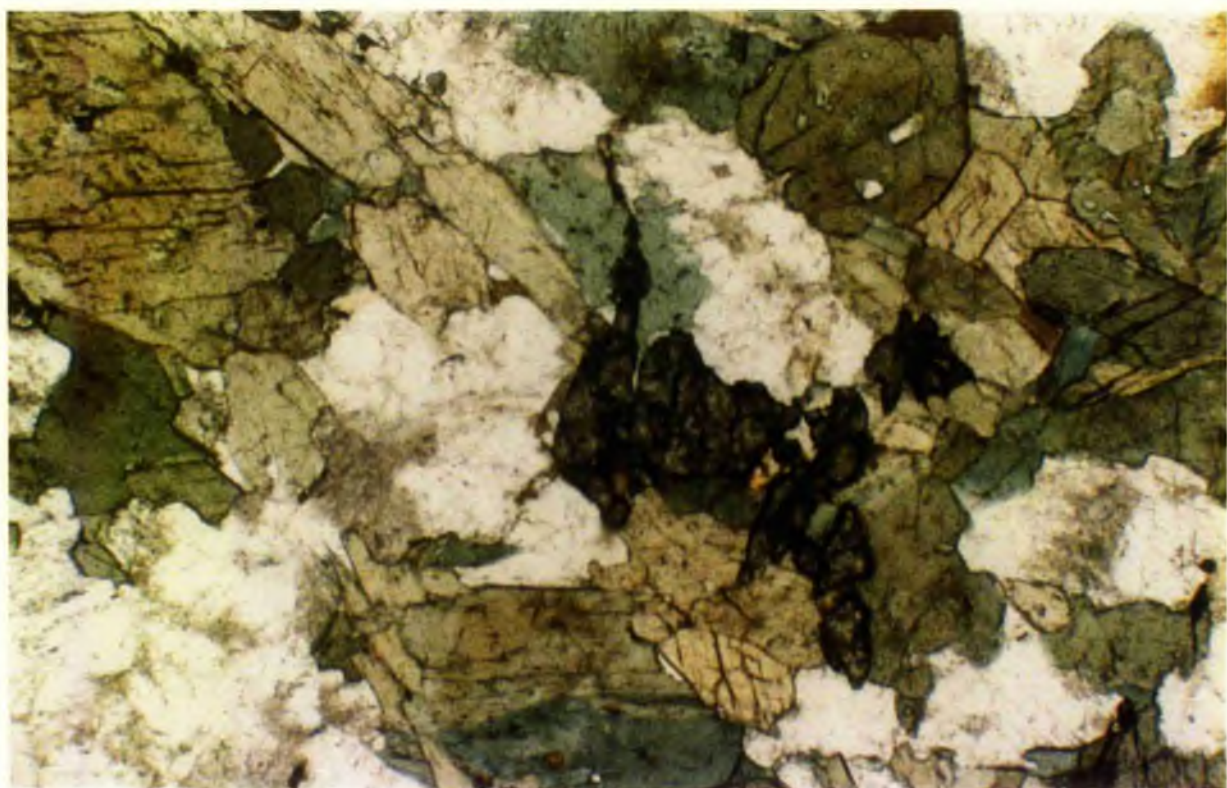
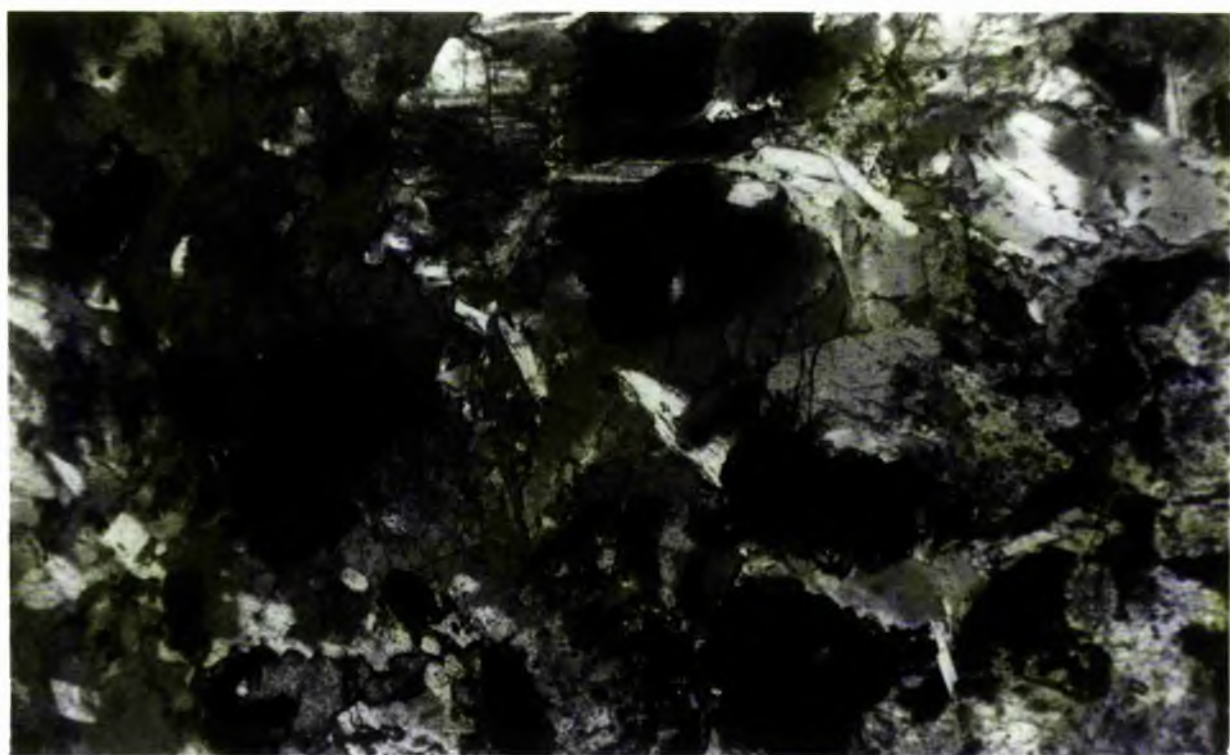
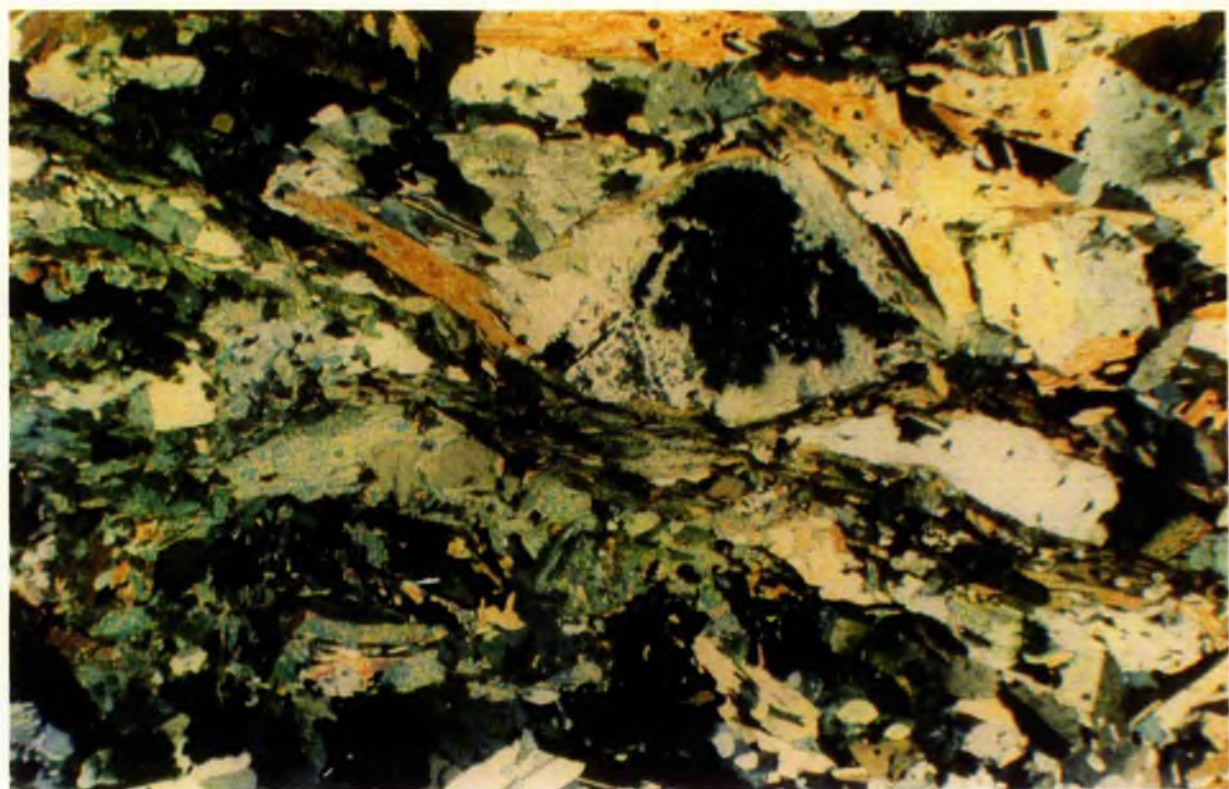


Plate 4.6 (a) Transmitted XPL photomicrograph of diorite from sheared diorite (Y1853) from the Meenalargan intrusion. Field of view shows dextral shear planes defined by biotite, muscovite and chlorite. Shear plane (bottom right to top left) rotates hornblende crystal with highly altered core. Shear gives rock a granular texture. Width of field of view 12.5 mm, Mag. x1.2.

Plate 4.6 (b) Transmitted light photomicrograph of diorite from the Meenalargan dioritic intrusion (Y25515) showing amorphous hornblende mass overprinted by ilmenite-rutile crystals. Ilmenite may have formed as part of a replacement reaction of augite by hornblende. Width of field of view 7.5 mm, Mag. x2.



that of the diorite but differs in the larger size of the hornblende crystals (up to 1.5cm in diameter) which are commonly equant in shape, and the plagioclase which may often form large lath-shaped crystals which dominate the mesostasis along with small crystals of hornblende. The remainder of the mineralogy resembles that of the diorite described above.

(v) Cortlandtite

This rock type is rare in the Caledonian and is the most primitive rock type of the appinite suite of the area. It is essentially a pyroxene hornblende olivine gabbro with a coarse grained texture with common poikilitic relationships, particularly between olivine, augite and hornblende. Orthopyroxene is also present as squat grains enclosed by hornblende. The textures allow the determination of an order of crystallisation, summarised at the end of this section.

Hornblende occurs as two types in the cortlandtite, the first and principal form is that of large poikilitic crystals enclosing all the other main mineral phases in the rock, whilst the second is a smaller set of small euhedral to subhedral grains in the mesostasis. Both types have green pleochroism but this is often masked by the degree of serpentine alteration. Occasional colourless rounded crystals seen included within the amphiboles are thought to be hornblende, these may contain traces of ilmenite dust and relicts of tiny augite crystals which may suggest that the hornblende in this case is pseudomorphing the augite. French (1966) considered that the hornblende may have grown from the breakdown of the augite and olivine on the basis of the optical continuity of cleavage across augite and olivine boundaries and the way in which serpentinisation passes from the olivine into the hornblende.

Augite is the second major mafic phase and occurs as prismatic plates up to 3mm in diameter usually surrounded by hornblende with which it has a ragged and embayed contact (Plate 4.7 a and b).

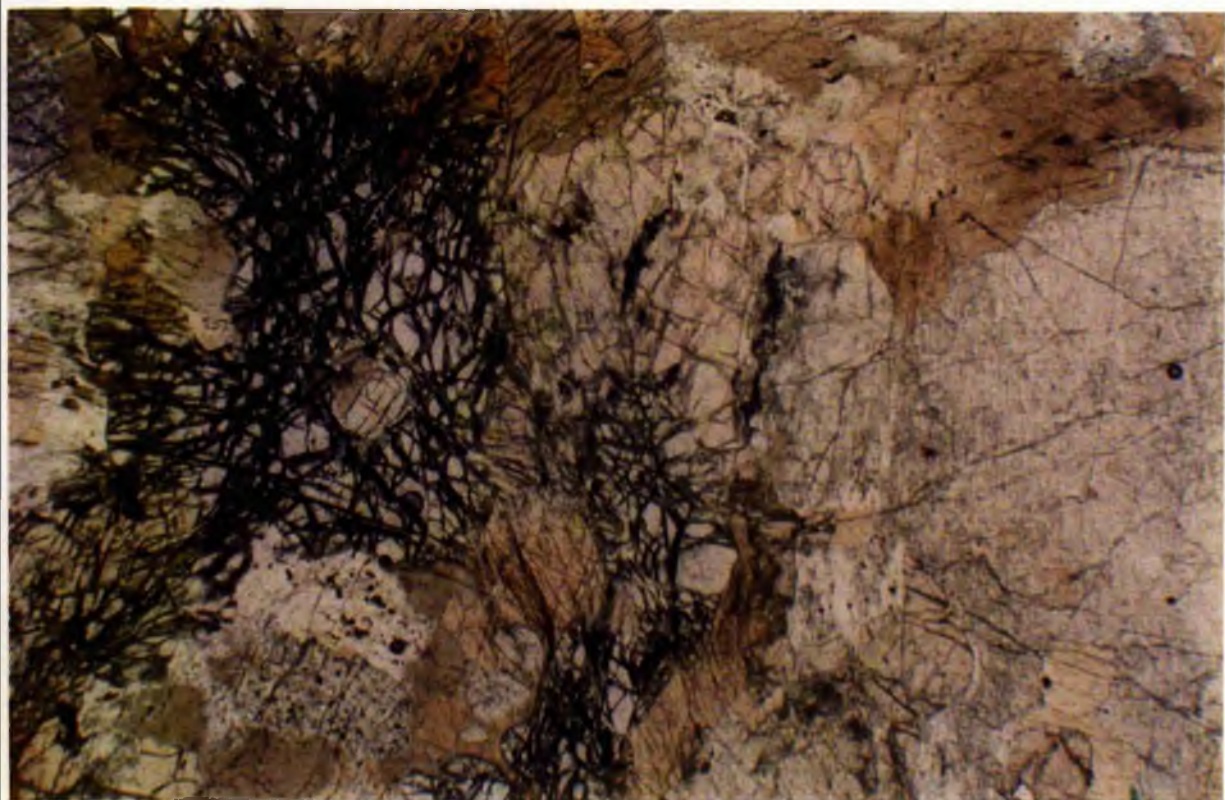
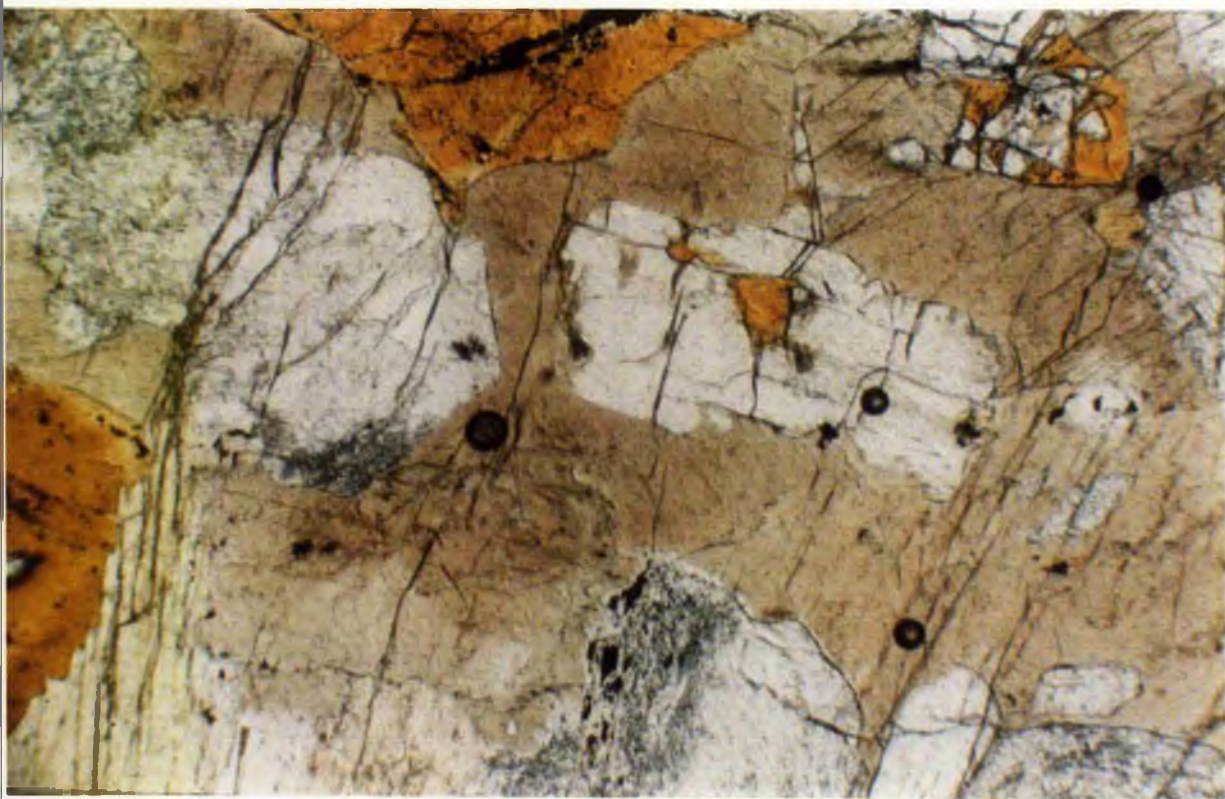
Hypersthene forms distinctive 2-3mm sized grains. In its typical form it may enclose olivine and augite as large poikilitic grains which in turn are enclosed by hornblende (Plate 4.7 b). The most noticeable feature of the olivine is its intensely cracked nature. These cracks are filled by black opaque dust, and the grains are also strongly serpentinised with the production of a fibrous yellow/brown alteration mineral thought to be bowlingitic in composition (French 1966). Alteration of the olivine by this mineral may locally be total or may be patchy and takes the form of a colourless serpentinitic mineral. Both minerals may infill the fissures seen in the olivine, however despite their alteration these olivine crystals have a typical rounded form with only occasional embayments, and are usually enclosed by augite, hypersthene and hornblende. Accessories are relatively rare in this rock but include zircon which most commonly occurs as inclusions in hornblende.

(vi) "Appinite"

The typical texture of "appinite" consists of squat to acicular hornblende crystals set within abundant euhedral plagioclase which have grown together and form a largely bi-

Plate 4.7 (a) Transmitted PPl photomicrograph of Kilrean cortlandtite (Kilr) showing coarse grained interlocking texture of hornblende (bottom left), orthopyroxene (middle), olivine (right) and augite (bottom). Olivine is strongly altered to red ?bowlingite-serpentine assemblage and magnetite-haematite along cracks. Augite encloses this in bottom left, orthopyroxene and olivine are enclosed by hornblende. Hornblende has an embayed contact with augite (bottom left). Width of field of view 12.5 mm, Mag. x1.2.

Plate 4.7 (b) Transmitted PPL photomicrograph of Kilrean cortlandtite (Kilr) showing rounded prismatic orthopyroxene crystals enclosed by brown hornblende. Red-brown crystals are altered olivine crystals. Note rounded nature of contacts. Width of field of view 12.5 mm, Mag. x1.2.



mineralic suite with only minor quartz, K-feldspar, calcite and opaques within the mesostasis, although individual samples can show variation in the proportion of these latter minerals (Plate 4.8 a).

Augite is typically replaced by hornblende and calcite which commonly replaces the cores of augite (Plate 4.8 b). Hornblende forms large crystals up to 5cm in length, but more typically around 1.0 cm in length which are often patchily zoned and replaced parallel to cleavage by biotite and chlorite. The margins of the hornblende are embayed against plagioclase and minor quartz but this is a later secondary feature associated with sericite and clinozoisite alteration. Elsewhere the plagioclase has an apparently straight-edged margin and individual crystals may interlock or include the hornblende crystals.

Plagioclase most commonly forms highly albitised and sericitised grains within the appinite suite which are altered to both clinozoisite and sericitic mica. Orthoclase may occasionally be intergrown with plagioclase in the mesostasis, and quartz may be found in the interstices.

This rock is compositionally very similar to some of the hornblende diorites mentioned above. The presence of a late-stage volatile-rich fluid is indicated by calcite and prehnite which infill interstitial gaps but which can also be infill minerals of late-stage brittle veins. Pyrite is common and other important accessories include apatite, zircon and titanite. Biotite is often present in some appinite samples as a distinct primary mineral which may have a red/brown pleochroic scheme indicating a relatively high fO_2

The biotite diorite differs from diorite in its higher content of biotite. It typically has an inequigranular texture of interlocking plagioclase with a mesostasis of K-feldspar, quartz, biotite and hornblende Plate 4.9 (a).

Biotite forms large ragged flakes up to 1.5mm in length and also smaller more obviously replacive grains, on average 0.08mm in length, which replace hornblende. The larger biotite crystals form elongate, sometimes euhedral crystals, which formed later than plagioclase but before quartz. These large biotite crystals sometimes form in clots along with epidote and clinozoisite and minor quartz crystals which may replace hornblende.

Hornblende takes the form of prismatic to stumpy crystals with green/brown to grey pleochroism. The prismatic crystals tend to have a green/brown pleochroism while the stumpy green crystals form an overgrowth texture suggesting a late stage of hornblende growth.

Plagioclase is the main phenocryst of the rock and is poorly zoned with typically embayed margins of biotite, hornblende and clinozoisite and altered cores of sericite and clinozoisite. K-feldspar takes the form of minor orthoclase which forms turbid grains. Strained quartz, fills the interstices.

Accessories include clinozoisite and epidote associated with the alteration of hornblende, plagioclase and biotite. Opaques form occasional square to corroded grains

Plate 4.8 (a) Transmitted PPL photomicrograph of "appinite" (Y66a) from the Narin-Portnoo intrusion showing acicular needles of hornblende set within a plagioclase matrix. Crude zonation of hornblende is apparent (bottom left and top right). Width of field of view 12.5 mm, Mag. x1.2.

Plate 4.8 (b) Transmitted PPL photomicrograph of "appinite" (Y26510) from the Narin-Portnoo intrusion showing the replacement of augite by brown hornblende and feldspar and calcite in the core. The matrix consists of altered plagioclase, late titanite and chlorite (top left centre). Width of field of view 12.5 mm, Mag. x1.2.

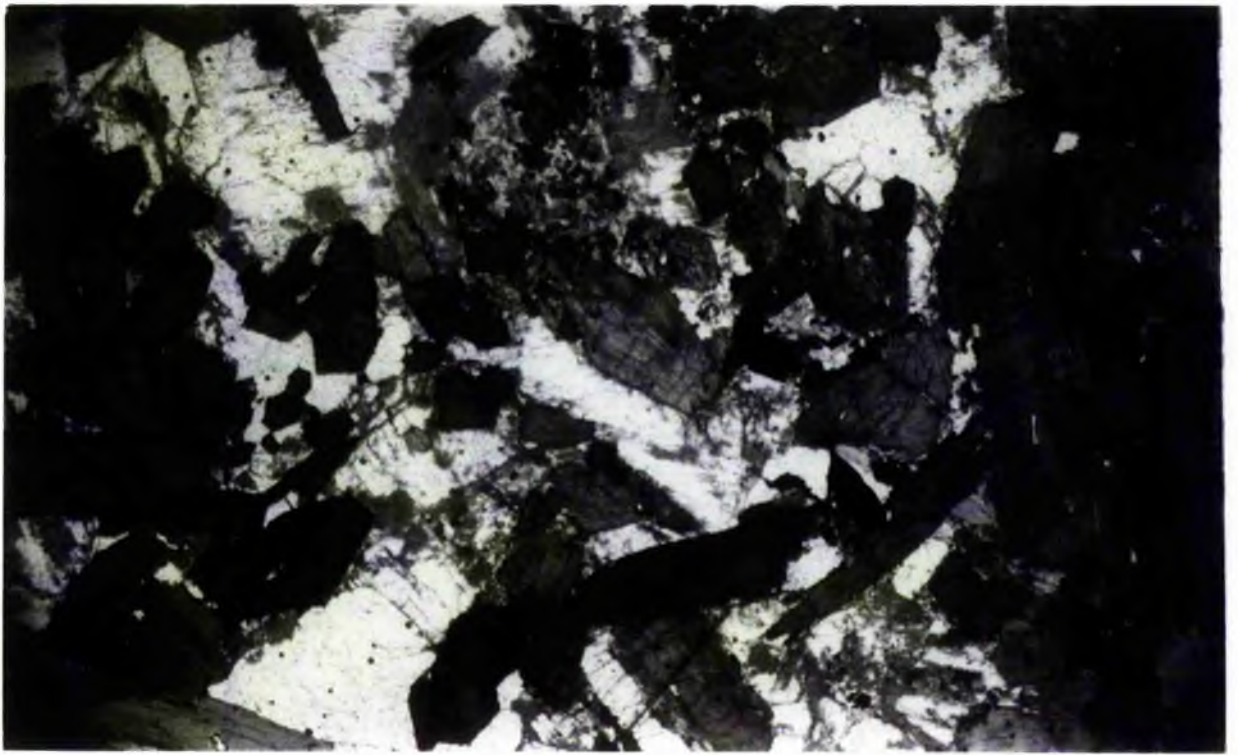
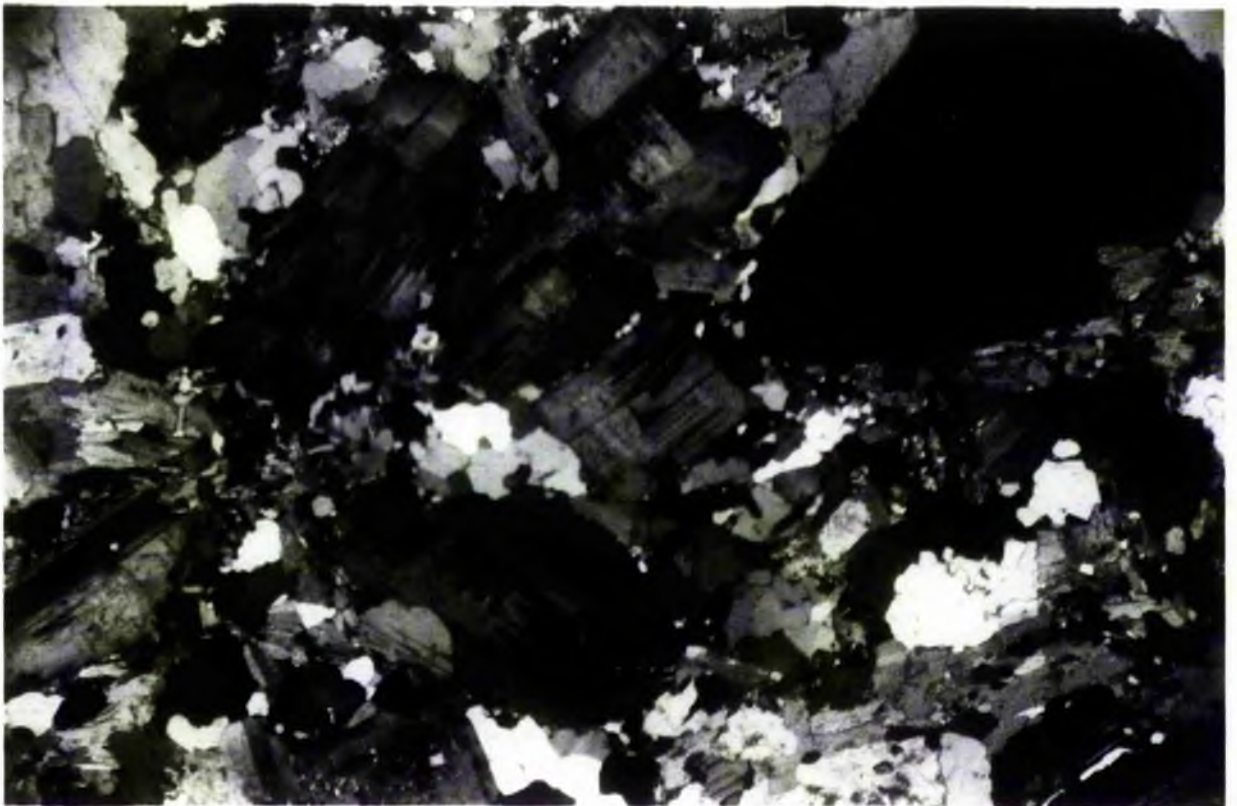
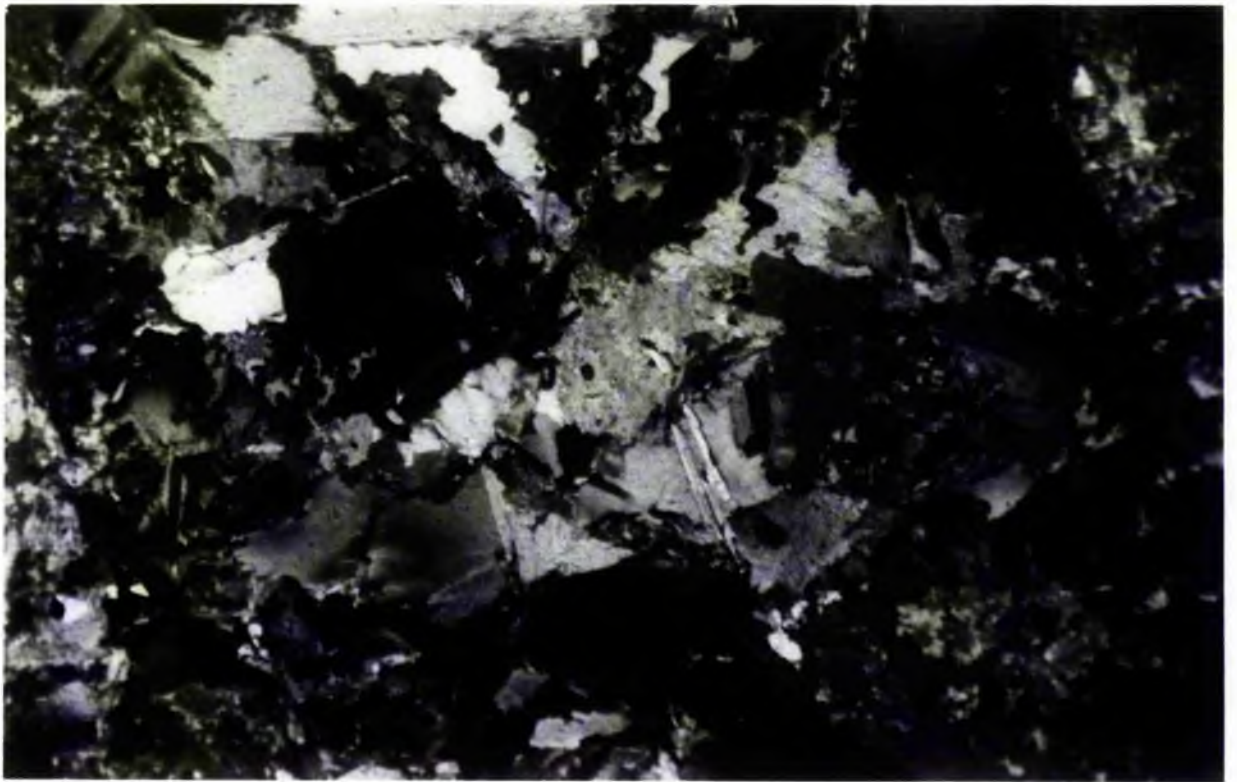


Plate 4.9 (a) Transmitted XPL photomicrograph of biotite diorite (Y6614) from the Narin-Portnoo intrusion. Inequigranular texture of interlocking zoned plagioclase, K-feldspar and biotite. Ragged contacts between crystals reflect the effects of metamorphism on the rock. Width of field of view 7.5 mm, Mag. x2.

Plate 4.9 (b) Transmitted XPL photomicrograph of granitic sheet (Y23) from the Mulnamin intrusion showing a metamorphic-type texture of triple point contacts between squat plagioclase laths with crude zoning and quartz. Biotite has a ragged contact with plagioclase (bottom right). Width of field of view 7.5 mm , Mag. x2.



possibly of ilmenite and pyrite. Apatite forms stumpy and elongate needle-like inclusions in association with biotite.

(viii) Granite/granodiorite

Numerous granitic dykes, sheets and small plugs are found associated with the appinitic intrusions of the area. Their composition ranges from granodiorite to granite.

Plagioclase is the earliest formed mineral and forms square to lath-shaped crystals with highly corroded contacts with quartz and perthitic microcline. The cores of the plagioclase crystals are highly sericitised, overgrown and altered by white sericitic mica and rare calcite plates. Plagioclase, like the quartz, has developed sub-grain boundaries and has suffered recrystallisation (Plate 4.9 b). K-feldspar is present in the form of perthitic microcline which, like the plagioclase and quartz, have embayed margins. The K-feldspar often encloses small plagioclase crystals and may partially enclose others, it has angular contacts with the plagioclase and later quartz.

Quartz is a major constituent of these rocks and forms anhedral crystals up to 1.5mm in diameter which usually contain many internal domains and sub-grain boundaries particularly at the contacts.

Biotite is the main ferromagnesian mineral of the rock and forms elongate thin crystals that have been sheared between quartz and plagioclase/K-feldspar grains. They have a deep red/brown pleochroism which may be a reflection of low fO_2 . Although the biotite has a deformed habit it does not define a foliation within the rock.

Other minerals include secondary calcite which replaces plagioclase, and accessory apatite which is associated with the biotite. Muscovite is occasionally associated with biotite but more commonly forms large flakes within the sericitic alteration of the plagioclase.

4.3 PETROGRAPHY OF THE SUMMY LOUGH DIORITE COMPLEX

The Summy Lough Diorite complex is dominated by a diorite which varies little in composition from the type diorite described in section 4.2 (iii). In hand specimen the typical diorite has a coarse grained mottled texture of green hornblende and minor augite in a grey feldspathic matrix. The hornblende and augite form acicular to equant crystals set in a mesostatial to ophitic matrix of plagioclase, quartz and orthoclase with late brittle calcite veins.

The small hornblendite intrusion (see map 4 in Appendix 6) consists of abundant augite and hornblende up to 1.5cm in length (Plate 4.10). The hornblende is commonly dusted in the core with ilmenite and occasionally may enclose the augite. Plagioclase ranges in composition from An_{40} in the core to An_{31} in the margin and has a poikilitic habit enclosing augite, hornblende and titanite. Other minerals include quartz and clinozoisite in the mesostasis and accessories such as titanite, zircon and apatite. K-feldspar is absent.

The coarse appinitic dyke found to the north of the main diorite intrusion also has mineralogy and textures similar to the hornblendite but differences include the coarseness

of grain size and the presence of biotite as a breakdown product of hornblende and the minor presence of K-feldspar and pyrite.

4.3.1 Crystallisation of hornblende and coarse appinite

It is apparent that both these rocks have similar origins, as both show the development of large hornblende crystals with augite inclusions and a groundmass which contains smaller augite and hornblende set in a plagioclase-rich matrix. The large hornblendes must have grown when the magma reached a point in the hornblende stability field that promoted growth of a few large hornblende nuclei. This may have been due to the influx into the magma of a hydrous-rich fluid leading to the extensive growth of hornblende rather than augite (Fig. 4.2). This coarse hornblende was then supplemented by many new hornblende nuclei and these and many augite crystals grew again in the mesostasis along with poikilitic plagioclase. Fig. 4.2 outlines the crystallisation sequence:

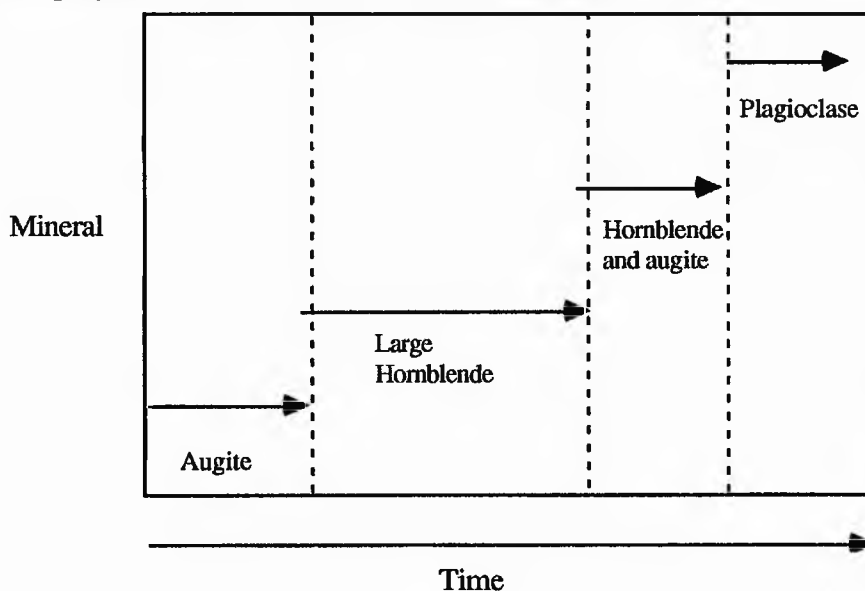


Fig. 4.2 Paragenetic crystallisation sequence of the hornblendite and coarse appinite at Summy Lough.

4.3.2 The pelitic aureole

The pelitic aureole shows the development of a new cleavage (S4) due to the intrusion of the Ardara granite, at the same time as it suffered thermal metamorphism. Whether this was due to the main granite or to the local diorite intrusion is unclear. This metamorphism takes the form of the growth of sillimanite which seems to have grown at the expense of regional muscovite.

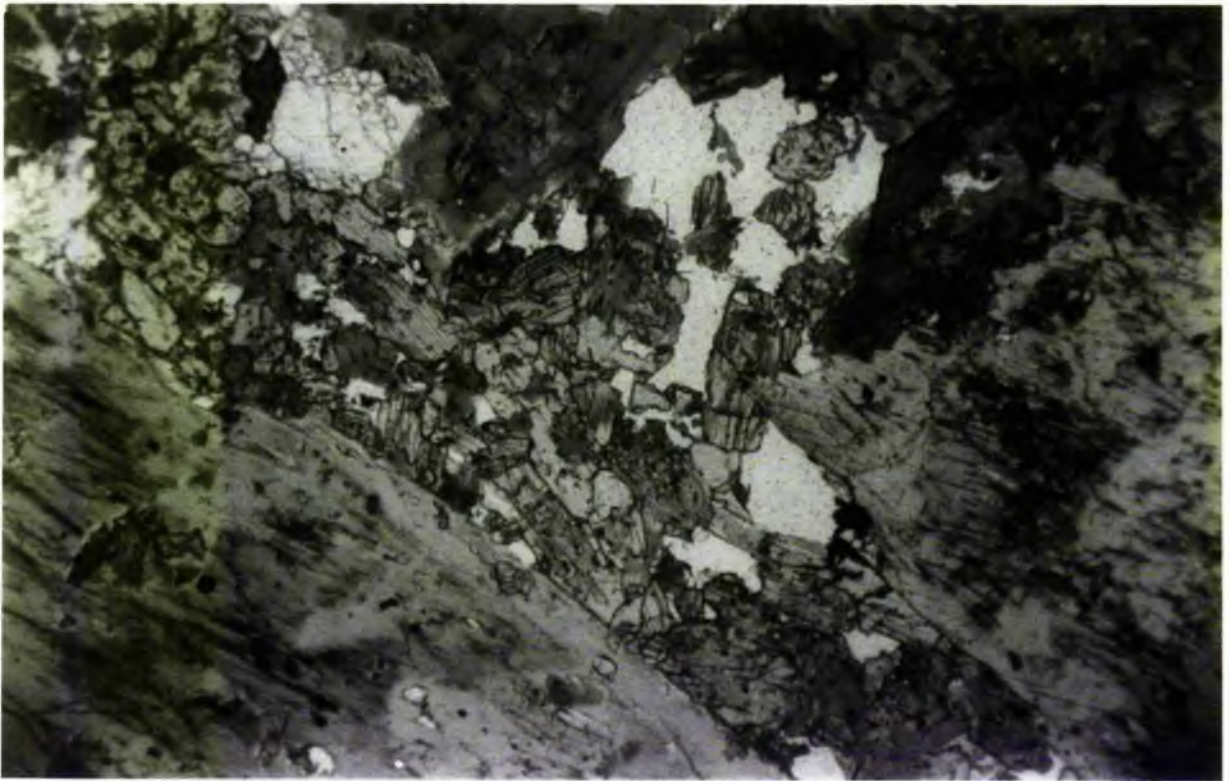


Plate 4.10 Transmitted PPL of hornblendite (Y21) from the Summy Lough diorite. large hornblende crystals surround a smaller set of tabular augite and hornblende crystals in a plagioclase mesostasis. Titanite is present as an overgrowth of hornblende (top right) along with minor clinozoisite. Width of field of view 12.5 mm , Mag. x1.2.

4.4 THE PETROGRAPHY OF THE CROCKARD GRANITE

The Crockard granite is a relatively homogeneous, medium to coarse grained granite with a texture dominated by a closely welded equigranular texture of plagioclase and quartz within a matrix of biotite and rare green hornblende, with epidote and chlorite as accessories. There is evidence of recrystallisation in the presence of embayed angular margins to crystals and an abundance of granoblastic triple junctions. Plagioclase is present in the form of oscillatory zoned, subhedral laths and squat crystals which often have corroded margins in contact with rounded quartz and minor K-feldspar. Biotite is the main ferromagnesian mineral and it preferentially rims or encloses green hornblende, or occurs interstitially to plagioclase and may enclose quartz as squat poikilitic crystals. It is commonly replaced by chlorite along the 001 cleavage plane. Hornblende is minor and tends to occur as rounded to squat crystals of a characteristic bottle-green (γ) to pale green (α) pleochroism. Texturally the hornblende is interstitial to plagioclase and is commonly replaced by biotite. Accessories include epidote occurring as bright yellow subhedral crystals often in association with biotite, but in a few places apparently forming primary magmatic contacts with plagioclase and quartz. Apatite and zircon also form inclusions within biotite and plagioclase.

4.5 THE PETROGRAPHY OF THE GLENARD INTRUSION

The Glenard intrusion consists of several members, principally a hornblende granodiorite, the main granodiorite and some associated appinitic intrusions which occur on the northern side of the mass.

(a) Hornblende granodiorite

This is a medium grained granodiorite with dominant hornblende phenocrysts now partially pseudomorphed by biotite and plagioclase. Recrystallisation has given the granodiorite a metamorphic fabric. It has a typical granitic to granodioritic mineralogy but has an abundance of hornblende and minor augite. Hornblende forms squat, subhedral grains with honey brown (γ) to green (α) pleochroism which commonly contains inclusions of quartz, clinozoisite, biotite and opaques (Fig. 4.3). Augite is only present as relict cores of hornblende crystals and often has associated dusty magnetite and biotite. Clinozoisite occurs as discrete grains or clots.

(b) The main granodiorite

This is a medium to coarse grained foliated granodiorite with occasional phenocrysts of hornblende which are partially pseudomorphed by biotite in a matrix of plagioclase, quartz, K-feldspar, biotite and clinozoisite (Fig. 4.3). Biotite defines the foliation and although it is a relatively late stage mineral, it has inclusions of quartz, it is pleochroic from grassy green to yellow and forms typically ragged flakes or smaller mantling crystals at the edges of plagioclase. It commonly forms clots of interlocking grains along with ilmenite, clinozoisite and quartz, and these may be pseudomorphs after

hornblende. Accessories include clinzoisite which is present in the form of anhedral grains formed due to the breakdown of plagioclase and sericite, biotite and hornblende

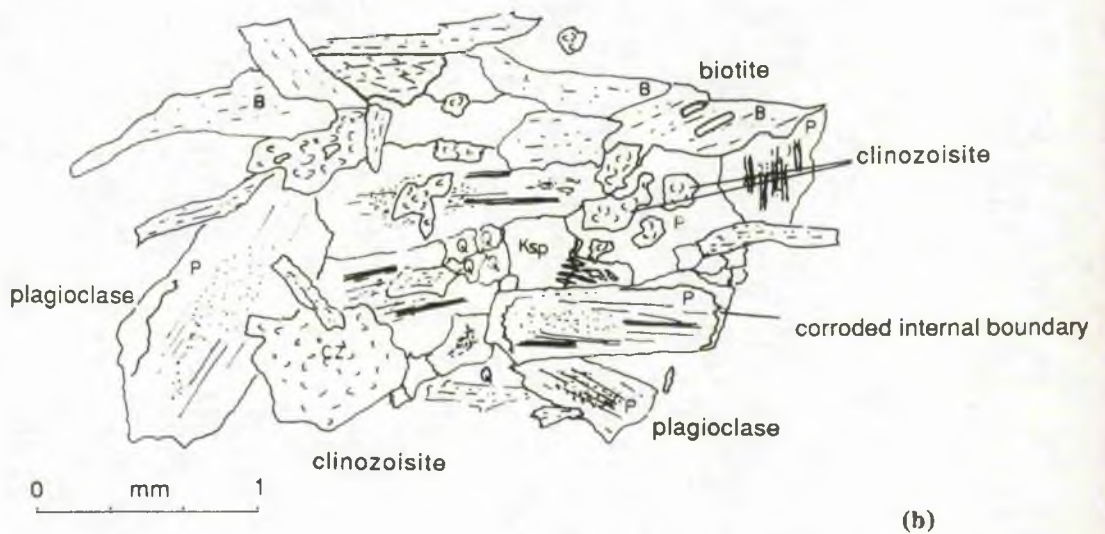
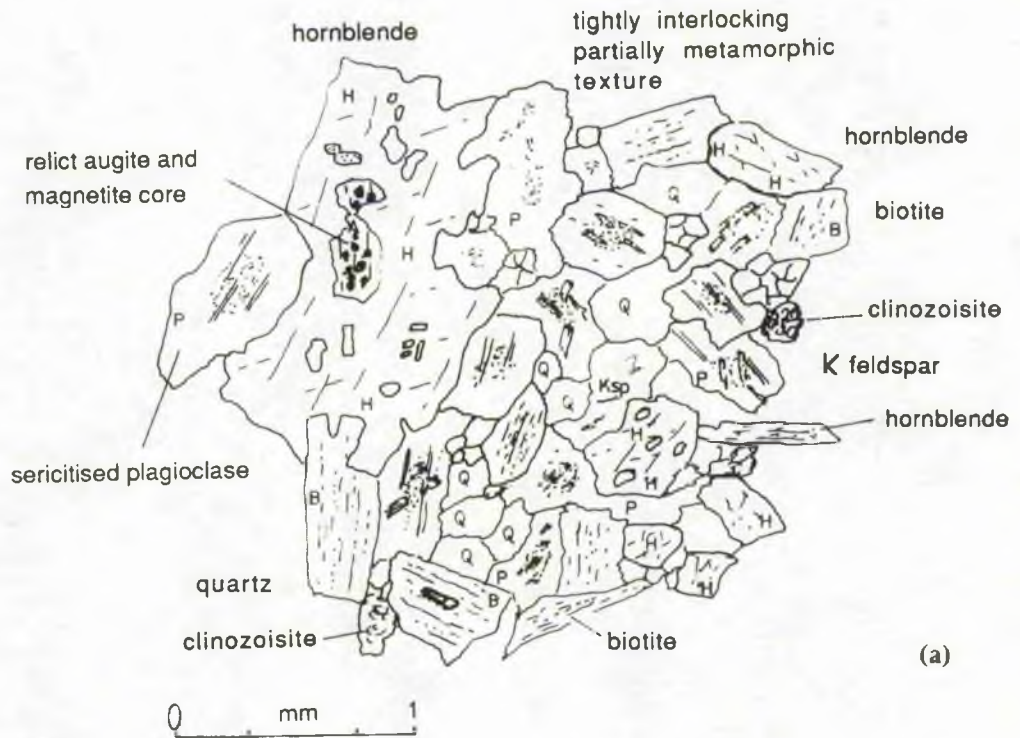
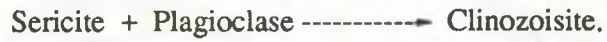


Fig. 4.3 A representative view of the type facies of the Glenard intrusion, (a) Glenard hornblende granodiorite (GLGR1), (b) Glenard granodiorite (GL1).

(c) Glenard appinite

This rock is strictly a hornblendite in composition and consists of subhedral hornblende phenocrysts within a matrix of plagioclase, alkali feldspar and quartz (Fig. 4.4). Hornblende is the dominant mineral forming a highly interlocking network of elongate phenocrysts already stated above. These hornblende phenocrysts are commonly dusted by ilmenite with some pyrite. In some "appinite" outcrops at Glenard and elsewhere the grain size of the appinite can become ultra-coarse (crystals in excess of 6cm in length) and the amount of plagioclase in the mesostasis increases so that the rock becomes apparently biminerale. Diopside occurs as dusty grains in the interstices. Biotite is present as ragged flakes and as secondary crystals replacing hornblende. Calcite and pyrite are important accessories.

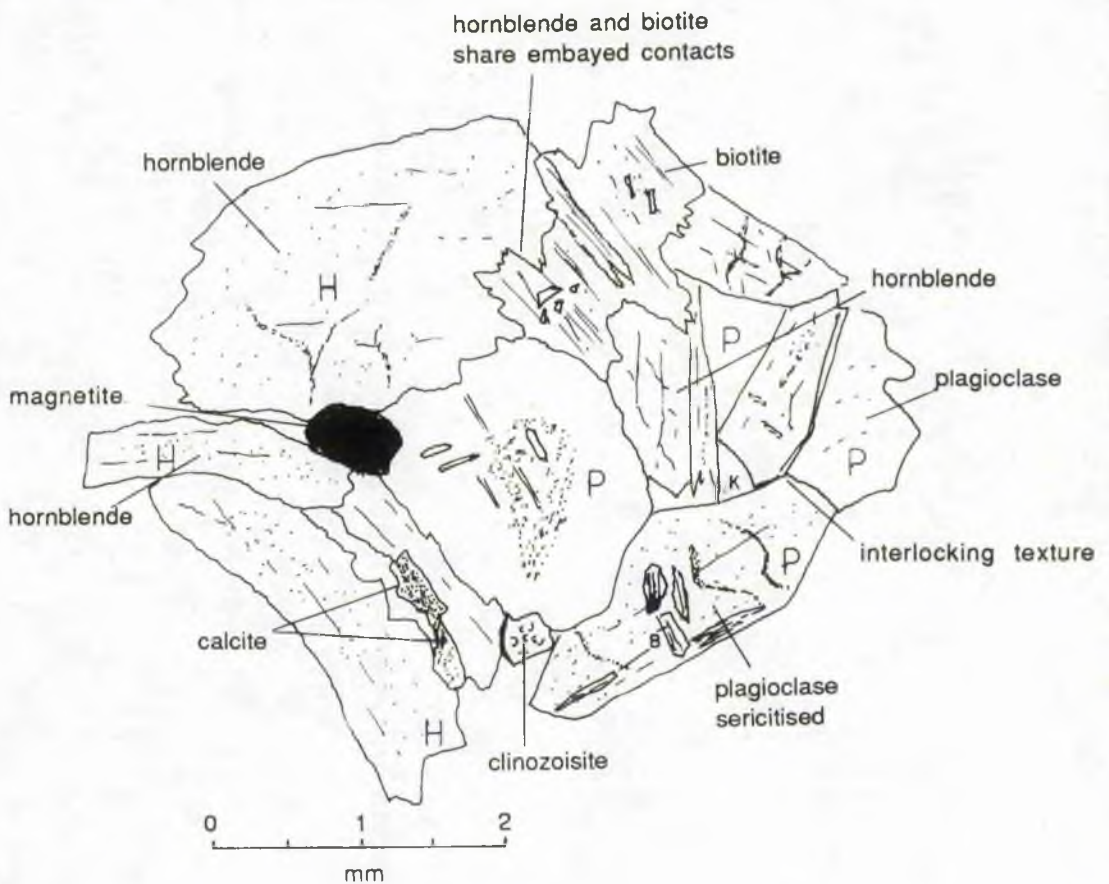


Fig. 4.4 Representative view of appinite at Glenard (GLAP).

4.6 PETROGRAPHY OF THE MULNAMIN INTRUSION

The Mulnamin intrusion is composed of a range of rock compositions described earlier in section 4.2.1. Only variations from the type compositions will be outlined below.

(a) Hornblendite

The dominant mafic minerals of the hornblendite are hornblende and augite. The mineralogy and texture correspond to those outlined in section 4.2.1(i). Hornblende forms elongate, tabular crystals with corroded margins altered to actinolite and overgrown by occasional clinozoisite. The augite forms elongate crystals up to 3mm in length but more commonly occurs as stumpy anhedral crystals with corroded edges. Augite is replaced by biotite and hornblende. Biotite forms elongate to stumpy flakes and seems to be associated with ilmenite and hornblende and occurs as stumpy mutually interfering crystals. The groundmass contains oligoclase as rounded, recrystallised crystals which often form irregular contacts with hornblende and augite grains. Twinning is poorly defined in the plagioclase due to deformation, recrystallisation and sericitisation which give the plagioclase a turbid, speckled appearance. Quartz is a minor phase trapped in late stage interstitial areas between plagioclase and hornblende and as inclusions within hornblende. Orthoclase is lacking in the hornblendite.

Accessories include calcite which together with pyrites, clinozoisite and titanite occur as late stage minerals in the interstices or as inclusions in the felsic or mafic minerals. Hornblende in particular is transected by calcite and clinozoisite veins, some of which are probably brittle veins formed in the late stages of crystallisation.

(b) Coarse meladiorite

This rock type is coarse grained with an average grain size of 0.4cm and consists primarily of hornblende and plagioclase. The hornblende takes two forms, the first of which is brown to pale brown, stumpy subhedral and embayed, up to 1cm in width. These brown hornblende crystals are in turn altered to pale actinolite and biotite in the form of felted needle-like masses and irregular platy biotite grains respectively. The actinolitic hornblende has a pale grey to yellow pleochroism and forms ragged interfering crystals with irregular contacts with the felsic groundmass and the brown hornblende. Augite occurs as rare primary phenocrysts 0.5 - 1.0cm in length. This augite is largely replaced by granular brown hornblende as well as having highly interdigitating actinolite and a dusty ilmenite rim.

The felsic mesostasis is formed by plagioclase of composition An_{35} which, like the hornblendite, is highly sericitised. Twinning is apparently deformed but the grains do not seem to be as highly recrystallised as those in the hornblendite. They form irregular embayed contacts with the hornblende and it is apparent that the plagioclase has penetrated the hornblende along its cleavage planes, probably by volume expansion related to the crystallisation of sericite and white mica. Quartz occurs as a late stage, interstitial mineral which appears to have crystallised along with primary late stage calcite and titanite (Fig. 4.5). Calcite and titanite are more common in the diorites than in the appinite and occur in association with actinolite and plagioclase as replacement products. Other accessories

include clinozoisite which replaces hornblende along with actinolite, and pyrite, zircon and apatite as inclusions.

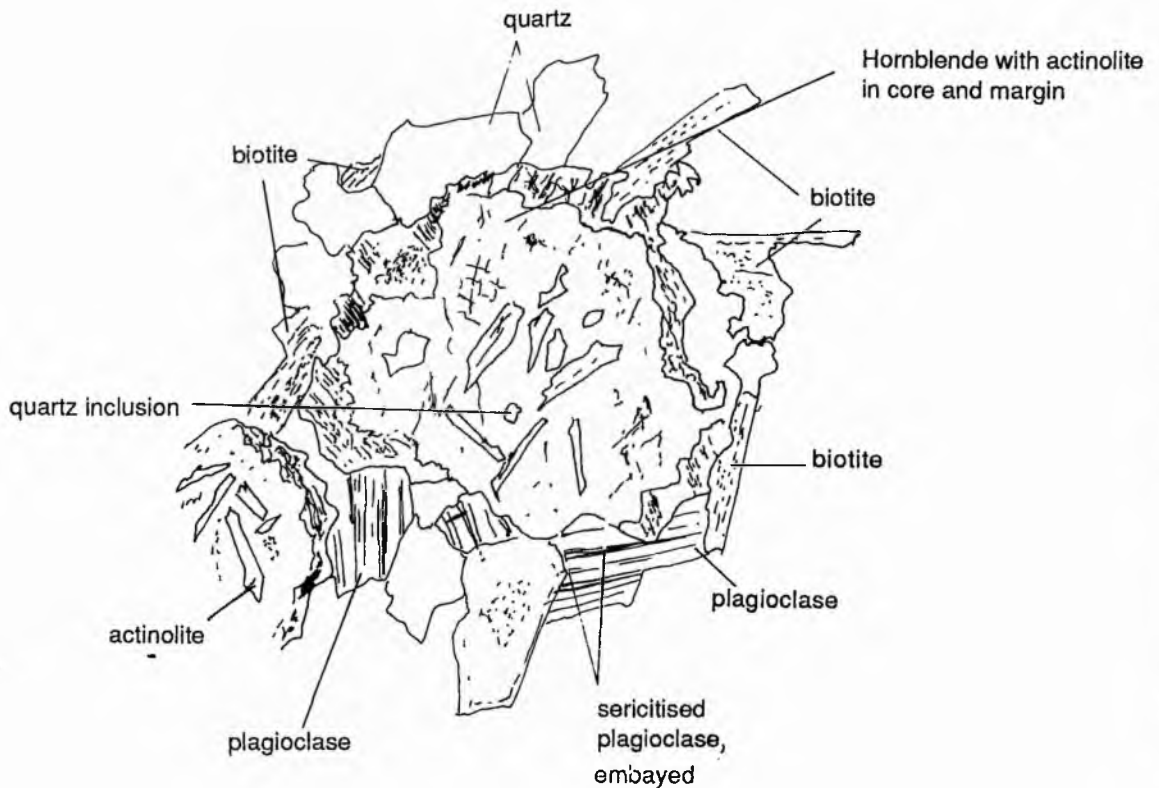


Fig. 4.5 Representative view of typical meladiorite from the Mulnamin appinitic intrusion (Y18).

(c) Appinite

The appinitic rocks are highly heterogeneous and grain size in particular is variable from medium to ultra coarse grained megacrystic. The mineralogy is similar to that of the diorite.

Hornblende is green to pale green and forms elongate crystals that are replaced by secondary actinolitic hornblende. The primary hornblende has a highly embayed contact relationship with the enclosing plagioclase and K-feldspar, and has abundant quartz inclusions and veinlets of plagioclase. Actinolite replaces the hornblende as needle-like grains.

The mesostasis plagioclase is highly altered to sericite along with abundant equant clinozoisite. The plagioclase is rounded and its crystal boundaries interdigitate with the

adjacent minerals, hornblende and quartz. K-feldspar becomes highly turbid occurring as rounded crystals.

Accessories other than clinozoisite include pyrite, abundant titanite, rutile, chlorite, and calcite, the latter being deposited as a late stage infill within the interstices.

(d) Diorite varieties

The distinctive spotted texture seen in some diorite outcrops is due to clots of hornblende which may reach up to 7mm in diameter. The clots are dark grey to brown with a dusty light brown core. The margin between the core and rim is sinuous and jagged due to the growth of secondary actinolitic crystals which are found in the core and which impinge on the margin. These crystals are acicular, mutually interfering and occur in most of the large hornblende phenocrysts. The original phenocryst has a pyroxene form and may have been replaced by hornblende, inclusions of quartz and ilmenite are also common.

A smaller set of granular hornblende crystals is present in the matrix consisting of hornblende and squat augite crystals replaced by secondary actinolite, and may also contain quartz and plagioclase inclusions. The felsic groundmass consists of squat subhedral to anhedral plagioclase laths of An_{35-40} and rounded interstitial quartz with undulose extinction. The granular hornblende aggregates may be flattened in the plane of foliation and the foliation is well developed where biotite is present in the groundmass. This foliation is also defined by small elongate hornblende crystals with abundant quartz inclusions and appears to be magmatic in origin as crystals are not broken or show evidence of strain. Such a fabric is similar to that described as "pre-full-crystallisation" textures by Hutton (1989).

Accessories include sericite within plagioclase, minor clinozoisite and titanite, associated with hornblende breakdown. Zircon is occasionally found within the plagioclase.

The spotted diorite is coarser than the meladiorite and contains essentially the same mineralogy but with a slightly higher content of plagioclase. The spotted diorite may simply be compositionally equivalent to the meladiorite but crystallised under different conditions controlling nucleation and growth rate leading to a different texture.

(e) Granite/granodiorite

The granitic and granodioritic sheets consist of embayed plagioclase laths with slight sericitisation (Plate 4.9 b). Zoning in the plagioclase takes the form of a core An_{55} and a rim of An_{45} with oscillatory zones of alternating calcic and sodic composition. K-feldspar accounts for 15-30% of these rocks and forms rounded, often deeply embayed grains that began crystallisation after plagioclase crystallisation ceased. The K-feldspar is embayed by quartz and has a turbid appearance, the quartz which embays the K-feldspar and embays the plagioclase forms rounded, highly recrystallised crystals with triple junctions and crystal domains. Occasional myrmekitic intergrowths of quartz, plagioclase within K-feldspar are found at the margins of large plagioclase crystals. Quartz is

granulated and strongly recrystallised in discrete shear bands. These shears are best defined by biotite which occurs as flaky crystals (often with quartz inclusions) interstitial to quartz and feldspar and flowing around them in the plane of foliation. Hornblende is also present associated with small clots of biotite and chlorite. Accessories include sericite, minor clinozoisite associated with biotite, apatite and zircon. Chlorite replaces biotite.

4.7 PETROGRAPHY OF THE KILREAN INTRUSION

(a) Cortlandite

The sequence of crystallisation of this rock (see section 4.2.1 v) begins with olivine followed by augite, both of which continued to grow together until hypersthene began to crystallise, which encloses both the former phases. Crystallisation of hornblende followed and this seems to have occurred by the partial breakdown of augite, olivine and hypersthene. French (1966) attributed the crystallisation of these three last minerals to normal crystallisation from a basic magma but that the hornblende had crystallised from a residual magma rich in volatiles. The order of crystallisation is summarised in Fig. 4.6.

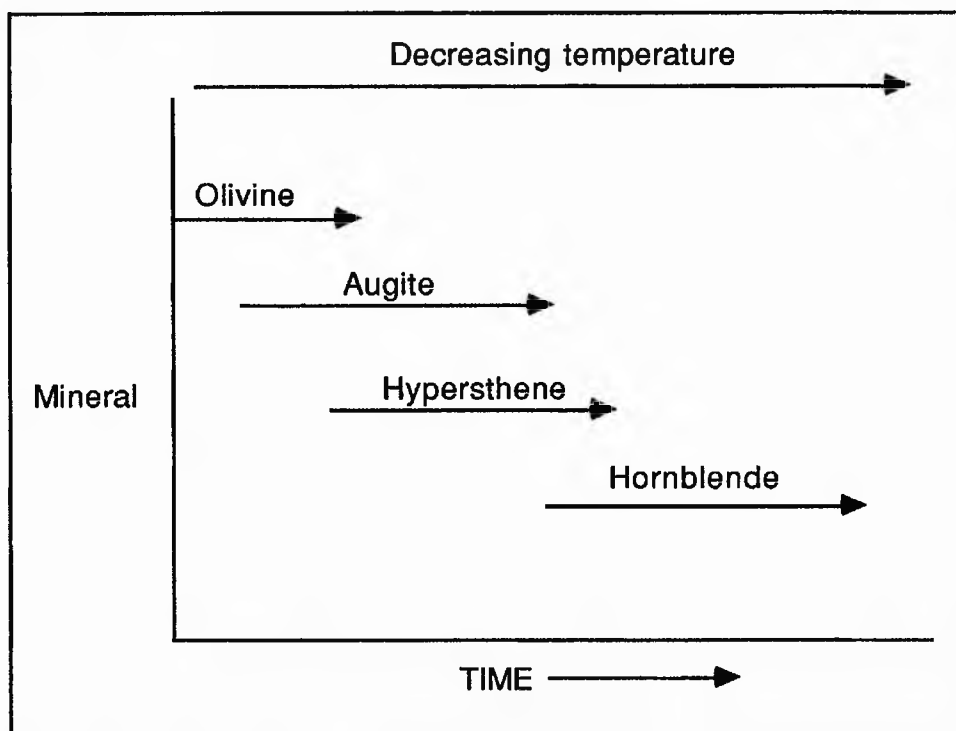


Fig. 4.6. Proposed crystallisation sequence of cortlandite ferromagnesian minerals.

(b) Hornblendite

The hornblendite of Kilrean is a foliated rock with interlocking crystals of hornblende, minor biotite and rare felsic minerals (Plate 4.11). The dominant mineral is hornblende while pyroxene is absent. The hornblendite is similar to the type hornblendite

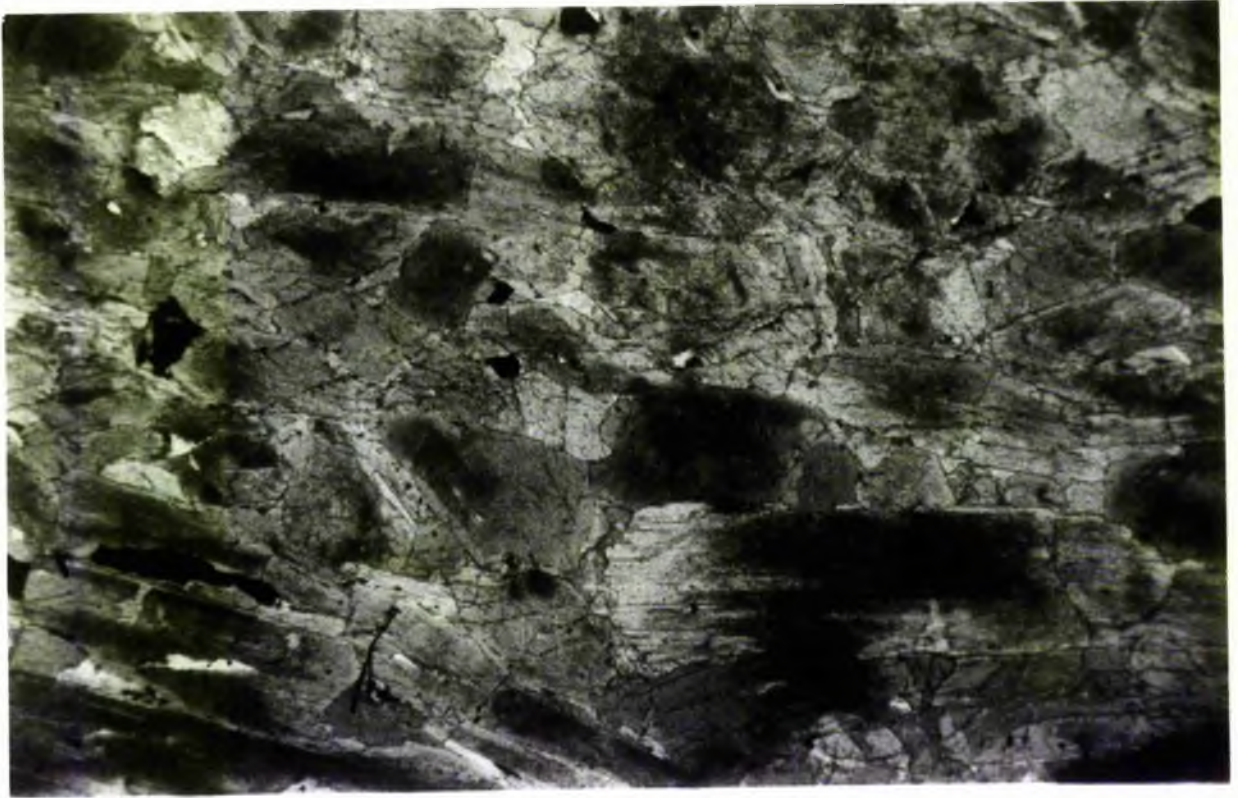


Plate 4.11 Transmitted PPL photomicrograph of hornblendite from Kilrean (Kilr HB rim). Prismatic hornblende forms highly interlocking layers with brown oxide-dusted cores. Ilmenite fills interstitial gaps. Width of field of view 7.5 mm, Mag. x2.

(section 4.2.1 (i)) but hornblende is more equigranular. Hornblende forms mutually interfering subhedral to euhedral prismatic crystals with angular interstices and ilmenite dusting. Some of the hornblende crystals have noticeably brown cores and green margins, although pleochroism is greatly masked by the oxide dusting. Biotite is present in the form of ragged flakes (up to 3mm) which commonly occur in association with hornblende replacing it along cleavage planes. Apatite and zircon are abundant in the biotite. Plagioclase forms rare single albite crystals which are highly altered to sericite. Quartz is rare but occurs as interstitial crystals.

4.8 PETROGRAPHY OF THE MEENALARGAN COMPLEX

The main rock types within the Meenalargan complex are diorite, coarse diorite and meladiorite as described in section 4.2.1 (ii-iv). Petrographic features are described below where they depart from the representative types described above

(a) Diorite

The average diorite of Meenalargan is a medium grained, closely knit, highly interlocking and weakly to strongly foliated rock type, dominated by brown to green hornblende with minor augite set within a groundmass of plagioclase. Some augite grains are largely unaffected by amphibole replacement and are found to have light grey to pale green pleochroism, but more typically they are patchily replaced by hornblende to form an intergrowth of hornblende and augite (Fig. 4.7). Hornblende is present as a replacement mineral of augite, principally around its margins with a remnant augite core which is colourless and has an abundance of ilmenite dust as well as inclusions of biotite and clinozoisite as alteration products. This hornblende forms prismatic to squat shaped crystals. Mantling this is a green hornblende with a fine dusting of highly birefringent clinozoisite. Smaller hornblende phenocrysts forming squat to prismatic grains with euhedral shape up to 0.5mm in diameter and may be present in the form of aggregates of mutually interfering crystals. Occasionally these aggregates are concentrated in the cores of augite crystals and may have formed as a result of augite replacement, but more commonly they are a mesostasis mineral which is occasionally partially zoned at its margins to colourless actinolitic hornblende in the form of colourless, needle-like crystals .

Biotite forms relatively ragged plates of reddy-brown colour, suggesting crystallisation under relatively reducing conditions. Plagioclase is zoned from An₄₄ in the core to An₂₈ in the margin. Deformation has the effect of granulating plagioclase grains, essentially at the margins but also within the crystal along cross-cutting shear zones, resulting in granulated plagioclase crystals and also the growth of biotite, chlorite and clinozoisite along the shear plane (Plate 4.6 a). Hornblende and biotite phenocrysts are rotated and recrystallised into tightly interlocking glomeroporphy.

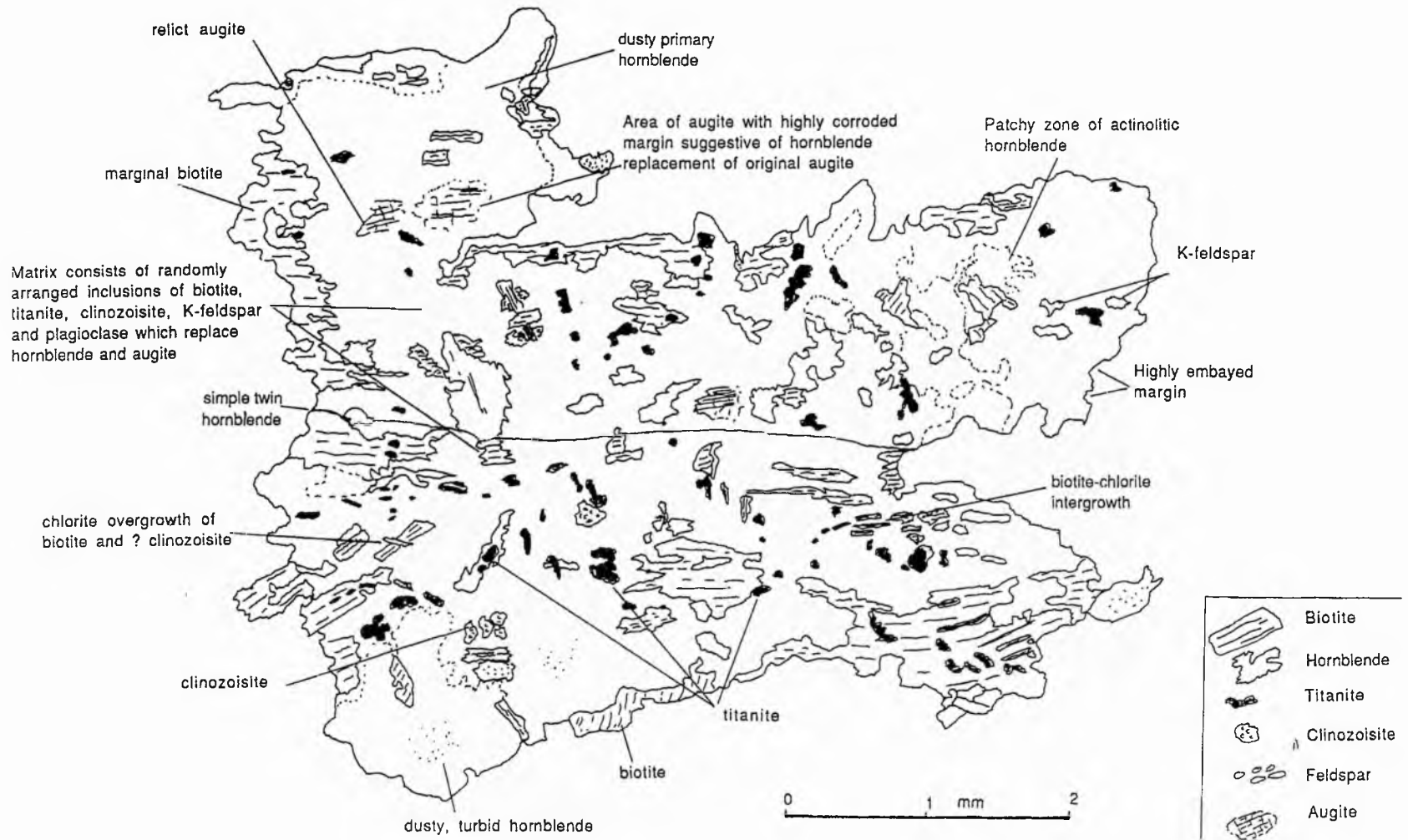


Fig. 4.7 Representative view of the relationship between hornblende and augite in diorite (M14) from Meenalargan.

Accessories include calcite, formed as a late stage breakdown product of augite along with secondary amphibole with which it forms irregular interstitial plates along with quartz. Chlorite is found as a late stage subsolidus alteration product. Titanite may be found as an alteration product of the replacement reaction of hornblende and augite. Magnetite is the dominant opaque and is commonly found intergrown with hornblende.

(b) Coarse diorite

In hand specimen the typical coarse grained diorite is grey when weathered and speckled black and white when fresh, with an irregular clot-like aggregate of hornblende set within a plagioclase, quartz and alkali feldspar matrix. Biotite is present but the modal proportions are highly variable (Table 4.2).

The main difference between the coarse diorite and the diorite is the occurrence of hornblende in large clot-like form in the former with distinctive pock-marked weathering style in the field. Texturally the coarse diorite has intimate intergrowths of hornblende and plagioclase where single plagioclase crystals may be overgrown and embayed by polycrystalline aggregates of hornblende. Pyroxene was a phenocryst now largely replaced by hornblende and biotite. Shear deformation is defined by the foliation of biotite which wraps around the major phenocryst phases.

(c) Meladiorite

The meladiorite is dominated by hornblende and there is some evidence of the replacement of augite by amphibole. Hornblende forms large prismatic to squat crystals, mutually interfering with highly interlocking texture and honey brown to bottle green pleochroism. Occasional hornblende crystals are euhedral and are enclosed within plagioclase, however most form crystals up to 3mm in diameter in clots which are often more than 10mm in diameter. This form is overprinted by a replacive form which is colourless and occurs as ragged, rounded grains forming replacive clots. This secondary hornblende is actinolitic as confirmed by electron microprobe analysis (section 4.11.2).

Biotite occurs as large anhedral plates in the cores, and margins of large hornblende crystals. These may also be present as small crystals growing over hornblende. The typical breakdown assemblage is biotite, actinolite and clinozoisite. Plagioclase typically shows the same embayed and corroded characteristics as seen in the diorite and coarse diorite. The composition of the plagioclase is relatively constant at An_{32-34} . The most corroded areas occur in contact with hornblende and it forms angular embayed contacts with the primary mineral and is overgrown by smaller crystals of hornblende, it does however overlap with the crystallisation span of the hornblende. The form of the plagioclase is therefore corroded to form rounded crystals with common grain boundary recrystallisation. Sericitisation is widespread.

K-feldspar is occasionally present as rounded grains which are interstitial and have abundant cross-cracking and turbid internal structures which like the plagioclase, have common grain boundary recrystallisation. Quartz occurs as a rare late stage interstitial

mineral and as inclusions within plagioclase and hornblende. Rutile is found as an alteration product of titanite which forms clot-like aggregates and single crystals (Plate 4.12). Accessories include opaques and apatite inclusions within plagioclase, hornblende and biotite.

(d) Appinite

The appinite has textural characteristics similar to those described in the type appinite (section 4.2.1 vi).

(e) Felsite

This is a plagiophyric rock with abundant plagioclase phenocrysts forming crystals up to 2.5mm in length. These crystals have oscillatory zoning, with irregular cores passing into a more calcic internal area, which in turn pass into less calcic margins (Plate 4.13). This plagioclase is set in a fine grained matrix of granulated plagioclase and quartz with minor amounts of biotite. Plagioclase commonly forms hexagonal to lath-shaped euhedral to subhedral plagioclase phenocrysts with striking oscillatory zoning which ranges from An₂₅₋₃₂ in the core to An₅₂ in the internal calcic zone to An₂₈₋₃₆ at the rim (Plate 4.13). Contacts between the plagioclase phenocrysts and the groundmass are highly embayed by groundmass minerals whilst sericitisation is irregular.

Quartz is the main component of the groundmass taking the form of anhedral rounded grains with abundant strain domains and as myrmekitic quartz intergrowths with large plagioclase phenocrysts. K-feldspar occurs as small, rounded globular crystals

Biotite is the main ferromagnesian mineral forming small red to brown, ragged, anhedral flakes within the groundmass which locally wrap around the plagioclase and define the foliation. Epidote and clinozoisite occasionally occur as squat crystals associated with biotite and plagioclase alteration.

The felsite is obviously later than the other rocks of the Meenalargan complex and may be related to an offshoot of the G3 intrusion of Ardara given their similar bulk compositions and patterns of plagioclase zoning. Both are also deformed by MDG-age deformation fabrics.

(f) Country rocks of the aureole

Altered calc-silicate lithologies are generally found to the east of L. Laragh (Map 3', Appendix 6) and have been hydrothermally altered. The metasediment is fine to medium grained with abundant clinozoisite, phlogopite, actinolite, plagioclase, perthitic feldspar and quartz. The original assemblage and texture have been recrystallised and overprinted by the growth of actinolite, clinozoisite and phlogopite, however relict bedding is still present.

Actinolite takes the form of euhedral to subhedral prismatic crystals, often full of inclusions and form colourless to yellow crystals; the edges of the crystals show corrosion and reaction with the plagioclase, quartz and clinozoisite. These crystals also contain inclusions of plagioclase, quartz and clinozoisite and are occasionally overprinted by actinolite in needle-like form. Diopside is a minor prismatic which forms euhedral

Plate 4.12 Z-contrast image (ZCI) of titanite in the form of single crystals and crystal clots (grey minerals) showing evidence of alteration to rutile (bright mineral). Conditions 15 kV, 20 nA, scale bar 100 μm (Y25515, diorite with mafic patch).

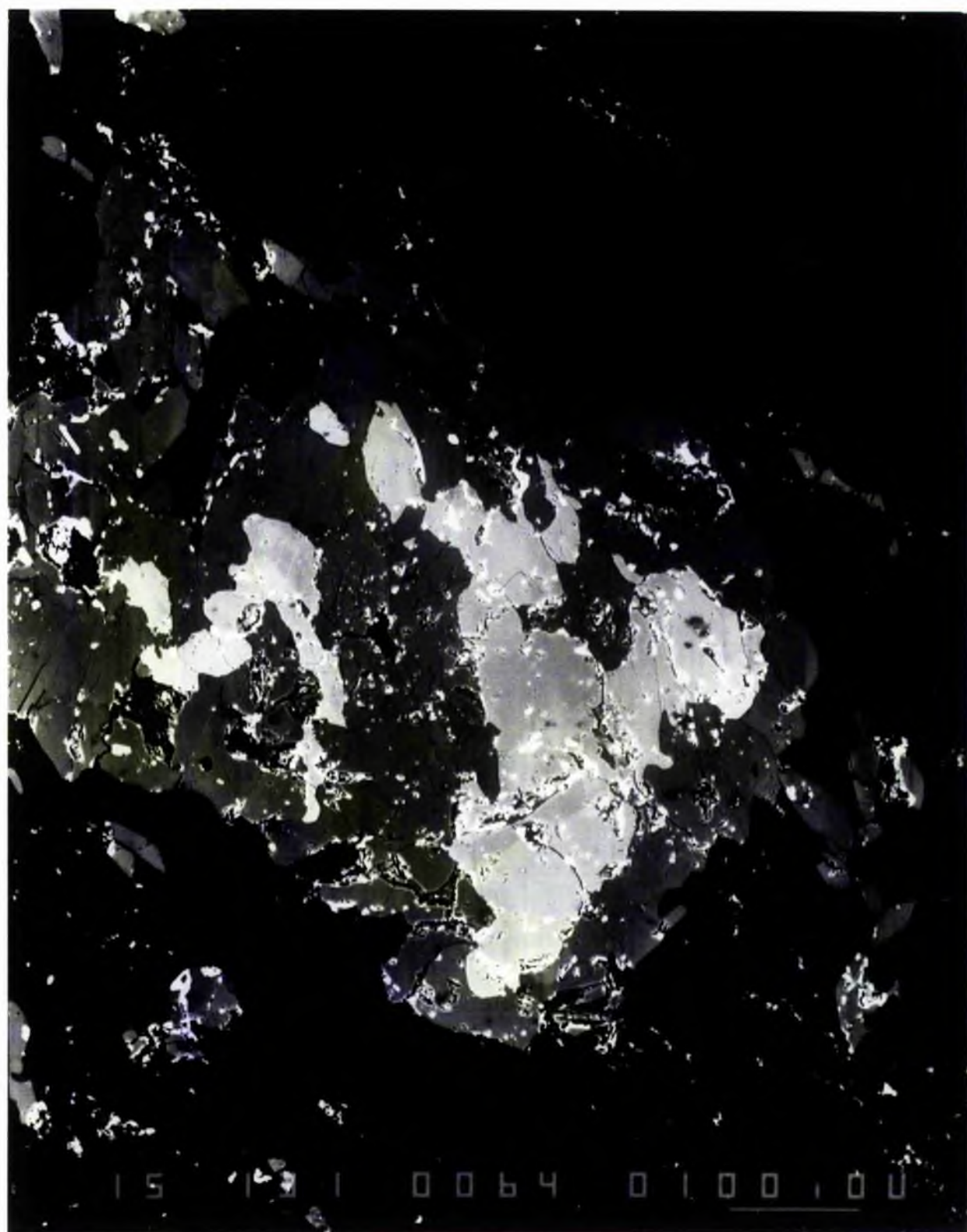
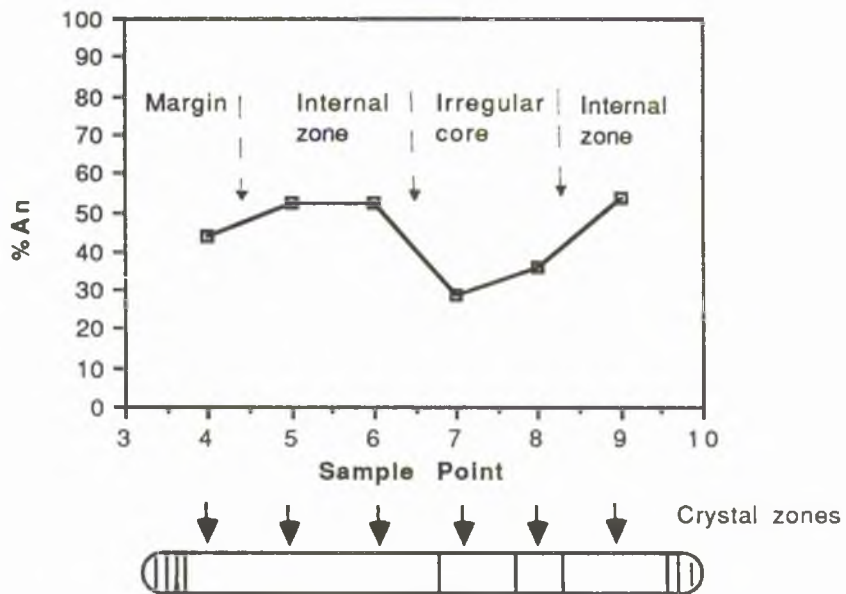
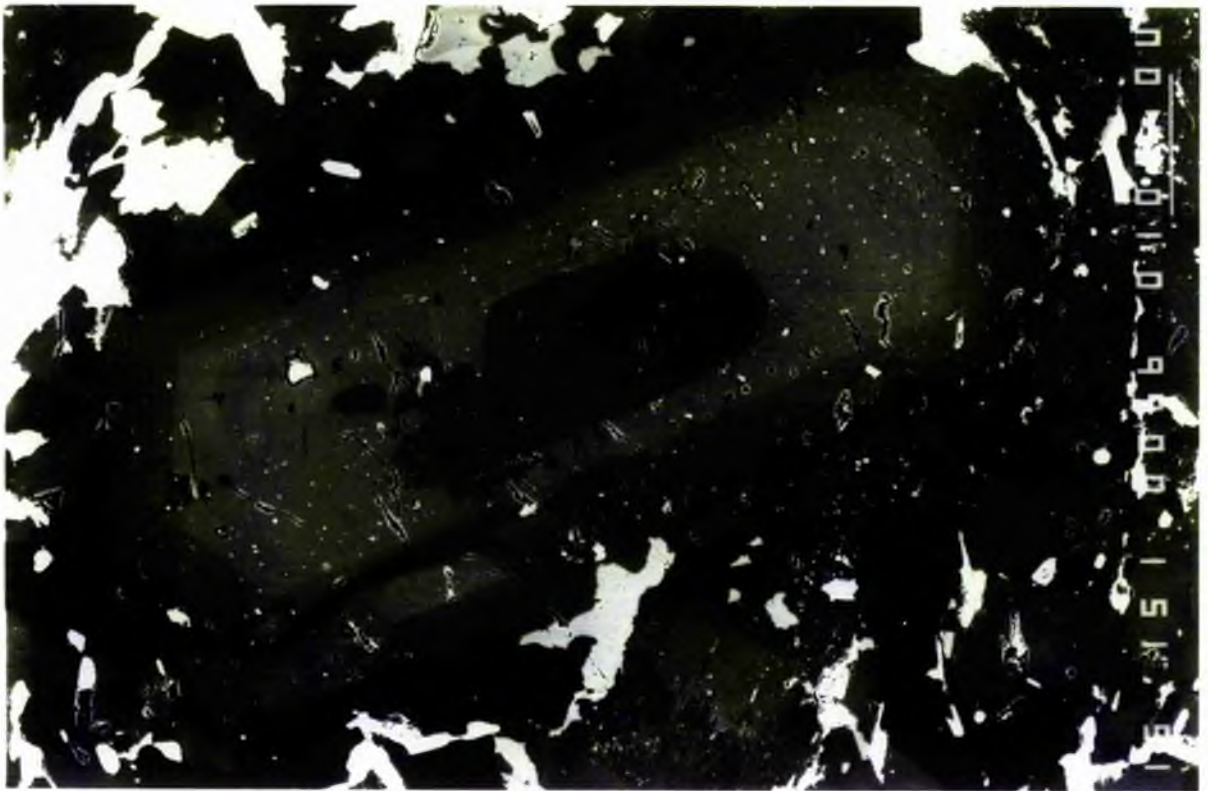


Plate 4.13 ZCI of zoned plagioclase from a granitic/felsitic dyke (Y25514) from the Meenalargan dioritic intrusion. Plagioclase has a more sodic core than the central area which in turn is more calcic than the margin. See diagram below for explanation of the zoning. Conditions 15 kV, 20 nA, scale bar 100 μm .



phenocrysts up to 0.25mm in diameter. Clinzoisite is an almost equigranular matrix mineral and often forms abundant inclusions within actinolite suggesting that it is an earlier mineral. It occurs as elongate to tabular crystals with granular texture. Sometimes epidote granules are associated with clinzoisite as yellow squat subhedral crystals. Phlogopite occurs as ragged yellow crystals which appear to be intimately intergrown with plagioclase and quartz of the matrix. It is deeply embayed by the clinzoisite and is overprinted by actinolitic needles.

Plagioclase, K-feldspar and quartz are all present as groundmass minerals with squat to rounded habit and show evidence of deformation in the form of sub-crystal domains.

The original mineralogy of quartz, plagioclase, clinzoisite, phlogopite and calcite has been recrystallised and altered to an assemblage of actinolite and clinzoisite with the loss of calcite. Less altered areas tend to show a finer grained texture but may bear late calcite brittle veins and calcite plates within an assemblage of clinzoisite, epidote and plagioclase. Pyrite is present in small amounts with minor hornblende and actinolite.

On the north side of Crocknadreavargh Hill a steep cliff shows relict bedding of calc-pelitic lithologies with intrusion of diorite. The diorite has been largely affected by the assimilation of the calc pelite. The resultant effects on the mineralogy are similar to those seen to the east of L. Laragh in that there is abundant recrystallisation of pre-existing minerals and the formulation of new minerals. Augite has grown and appears as non-pleochroic grains with closely spaced cleavage and corroded margins which are occasionally replaced by hornblende. Plagioclase is sericitised and hydrothermally altered by clinzoisite but some unaltered grains remain. Large cavities with druses filled with prehnite and single calcite plates, and often clinzoisite are found in this cliff section.

4.9 PETROGRAPHY OF THE NARIN-PORTNOO SHORE SECTION

The Narin-Portnoo section is divided into a number of sub-sections each of which will be dealt with in turn.

4.9.1 Foragy Rock

Four rock types of this subsection include hornblendite, meladiorite, altered appinite and quartz diorite.

(a) Hornblendite

In this rock type hornblende forms phenocrysts which define a foliated, layered texture. The mesostasis is filled by plagioclase, biotite and late calcite and the texture and mineralogy are similar to that described in section 4.2.1(i).

Large hornblende crystals up to 4mm in length form phenocrysts and there are also small anhedral crystals filling gaps in the mesostasis. The phenocrysts are euhedral to subhedral prismatic crystals often with patchy pleochroism ranging from honey brown (α) to dark brown (γ). This form lacks the dustiness of ilmenite seen in hornblendic rocks from

Meenalargan and Mulnamin. The margin of these hornblende prisms, both in the case of the large phenocrysts and the smaller hornblende form, is a bottle green hornblende. The margins may also be corroded and embayed, particularly in contact with mutually-interfering hornblende crystals. Inclusions within the hornblende include K-feldspar and biotite.

Plagioclase is found only as a mesostatial mineral which is highly altered. It normally forms single grains which fill the mesostasis but these are now replaced by sericite and clinozoisite. Plagioclase is sometimes replaced by late-stage calcite as well as rare phlogopitic mica. Quartz forms interstitial late-stage grains of the mesostasis.

Biotite tends to form along the cleavage planes of hornblende, while the chlorite is an alteration form of both hornblende and more commonly biotite, occurring parallel to the cleavage. Clinozoisite is an important alteration product of both hornblende and plagioclase, and forms granular grains with anhedral sinuous margins.

(b) Meladiorite

This rock type has a similar texture to the hornblendite and has slightly higher more plagioclase giving it a more felsic aspect. It has textures which are similar to those in the hornblendite and is similarly altered.

(c) Altered appinite

This is found at the margin of the Foragy Rock intrusion and has suffered intense hydrothermal alteration with the resultant formation of a largely actinolitic and clinozoisite assemblage. The original mineralogy of the rock appears to have been an intimate intergrowth of medium grained brown/green hornblende with a mesostasis of plagioclase, K-feldspar and quartz, but the rock is now mainly clinozoisite.

Hornblende forms squat to prismatic, highly embayed and altered grains with brown to green pleochroism. which occur as phenocrysts and form straight contacts with the plagioclase of the mesostasis.

Plagioclase occurs as tightly interlocking phenocrysts in the mesostasis. These occur as perthitic to antiperthitic crystals, heavily replaced by clinozoisite and white sericitic mica. Actinolite forms colourless to pale-yellow grains with both prismatic and acicular habit. Some grains pseudomorph original hornblende phenocrysts with patchy zoning, but others may also occur as clot-like grains replacing pre-existing hornblende crystals. Clinozoisite occurs as dark grey to orange-brown crystals which have an amorphous, granular crystal form that occurs dominantly as an alteration product of plagioclase but which also affects hornblende. Biotite is almost absent from the rock, only occurring as a minor replacement mineral associated with actinolite. Accessories in the rock include titanite, pyrite and calcite, which all occur as late-stage interstitial minerals along with minor interstitial amounts of quartz. The 'altered' label is derived from the abundance of clinozoisite, calcite and actinolite which overprint primary hornblende and plagioclase and may have been derived from the interaction of magmatic fluids pervading the country rocks and the appinite.

(d) Quartz diorite

The quartz diorite of Foragy Rock is similar in composition to 'type' diorite (4.2.1 iii) however it has more quartz which commonly forms small millimetre-sized pools.

4.9.2 Tidy Rock

The intrusion of Foragy Rock passes east into the Tidy Rock area which shows the same range of rock types but with a few variations.

(a) Quartz diorite

This comprises primarily of clots of plagioclase which give the rock a spotted texture in the field. These felsic clots are altered to clinozoisite and are surrounded by a matrix of medium grained hornblende and opaques. Hornblende is the main mafic phase and typically forms deeply embayed light brown to greeny brown crystals (against plagioclase and quartz) in the form of squat to prismatic subhedral crystals. In most cases the hornblende forms grains up to 1.5mm in diameter but typically 0.5mm in diameter, largely replaced by clinozoisite. Biotite is associated with hornblende which is itself replaced by chlorite. Augite also forms ragged, embayed crystals, associated with the hornblende and largely replaced by it.

Plagioclase forms highly altered grains up to 1.0 cm in diameter, with highly sinuous margins which are heavily overprinted by a clinozoisite and sericite assemblage, making determination of the original plagioclase composition impossible.

Clinozoisite typically replaces plagioclase, and opaques and quartz are late-stage interstitial minerals. The texture suggests that many of the opaques may be developed by the breakdown of hornblende and the release of Fe, and these opaques give the rock a speckled dusty texture. Calcite and apatite are both late-stage minerals which occur as inclusions (apatite) and infill minerals and gaps in the mesostasis.

(b) Banded hornblende diorite

The banding in this diorite is caused by alignment in the horizontal plane of honey brown hornblende between megacrysts of highly sericitised plagioclase. Fig. 4.8 illustrates the layering and alteration features of this rock.

Hornblende is more abundant than in the other diorites of Fairy Cove, it is deeply embayed and full of inclusions and crystals are up to 5mm in length. The mesostasis is composed of plagioclase, now largely altered to sericite and clinozoisite. These crystals originally formed a closely interlocking matrix of laths which, like the hornblende, are now highly embayed. Biotite and chlorite are similar to quartz diorite while the accessory minerals include opaques, and minor apatite inclusions within the plagioclase and hornblende.

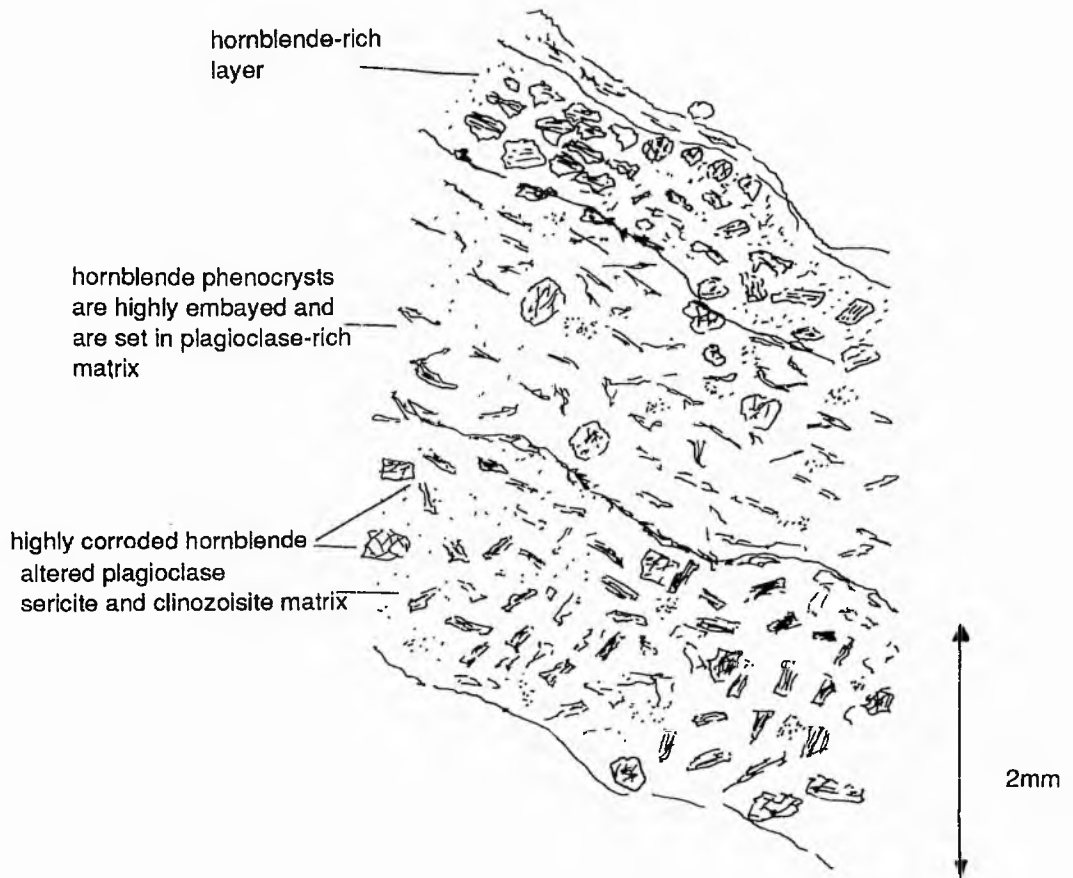


Fig. 4.8 Representative view of the layering in hornblende diorite from Tidy Rock, Narin-Portnoo intrusion (Y27518).

(c) Meladiorite

This is similar to that seen on Foragy Rock with large green/brown hornblende phenocrysts which are highly embayed and occasionally cross-cut by fractures with biotite and late chlorite replacement. Hornblende crystals form prismatic to squat phenocrysts which are intergrown with plagioclase and opaques, up to 1mm in diameter. Biotite is present as large plates. Plagioclase typically is altered to sericite and clinozoisite but some grains may be found which are less altered, and are zoned from An₃₅ at the margin to An₄₃ in the core. K-feldspar in the form of orthoclase is present as occasional mesostatial grains with sericitic cores. Quartz forms late-stage interstitial grains with common sub-domains. Accessories include apatite inclusions within biotite. Variations on this typical texture include intense recrystallisation of ferromagnesian within hornblende clots, and sericitisation. Hornblende forms small clots which may, along with single yellow-green actinolite crystals, replace the larger hornblende crystals and overgrow plagioclase.

In one occurrence the meladiorite has a banded appearance, which resembles relict bedding, in which hornblende and clinozoisite are the main minerals with a medium to fine grained texture. The hornblende is present in two forms. The first is in the form of

phenocrysts, 0.7 to 1.0mm in diameter of green to brown hornblende which are replaced and overgrown by clinozoisite and prehnite. The second form of hornblende has a yellow to green pleochroism and forms an almost equigranular mesostasis with plagioclase and clinozoisite (which alters the plagioclase). Plagioclase makes up most of the felsic matrix and alters to sericite and clinozoisite. It forms crystals of uniform grain size throughout this layered rock whilst the hornblende defines the layering of the rock. These layers are alternately dark and light coloured, the dark bands contain coarse clots of hornblende set in an altered hornblende and plagioclase matrix. The light bands contain equigranular plagioclase and small hornblende crystals which lie in the plane of the bedding.

4.9.3 Cathleen's Hole

Four different rock types exist in the area of Cathleen's Hole, most of which show mineralogical and textural features similar to those already described. The rock types include hybrid diorite, hornblende diorite, meladiorite and "appinite".

(a) The hybrid diorite

The texture is similar to that of the altered appinite of Tidy Rock. It contains abundant hornblende, augite and plagioclase that once formed highly interlocking prisms and laths but which are now overgrown by clinozoisite. The main difference between these two rock types relates to the greater abundance of augitic pyroxene. Augite is a principal mineral of the rock and takes the form of euhedral and subhedral prismatic crystals set within a now largely albitised plagioclase mesostasis (Fig. 4.9). K-feldspar is present in the form of sometimes-perthitic microcline in brittle veins associated with late stage recrystallisation of augite and with apatite and quartz needles up to 1mm in length. Amphibole is a minor mafic mineral of the rock and forms actinolitic needles in interlocking glomeroporphyritic textures which sometimes replace the augite. Calcite is present in the form of small irregular plates in the interstices of the diorite. Epidote is scattered sporadically within the mesostasis.

(b) Hornblende diorite

This has large acicular to squat amphiboles and minor augite set within an altered plagioclase, quartz and K-feldspar matrix. The grain size is generally coarse and ranges from 0.5 to 1.0cm. Hornblende is the dominant ferromagnesian with typical prismatic form and yellow to pale green-brown pleochroism, altering to actinolite. The hornblende has relatively sharp contacts with plagioclase and the felsic groundmass, whilst against quartz the hornblende has an embayed margin. Pyroxene forms small, prismatic crystals. Plagioclase may contain inclusions of this augite as well as clinozoisite. Plagioclase forms square to lath shaped phenocrysts which have primary igneous contacts with the other plagioclase crystals and embayed contacts with quartz. Plagioclase sometimes encloses euhedral hornblende crystals and both minerals overlap in their crystallisation history. The plagioclase is heavily sericitised and altered to clinozoisite.

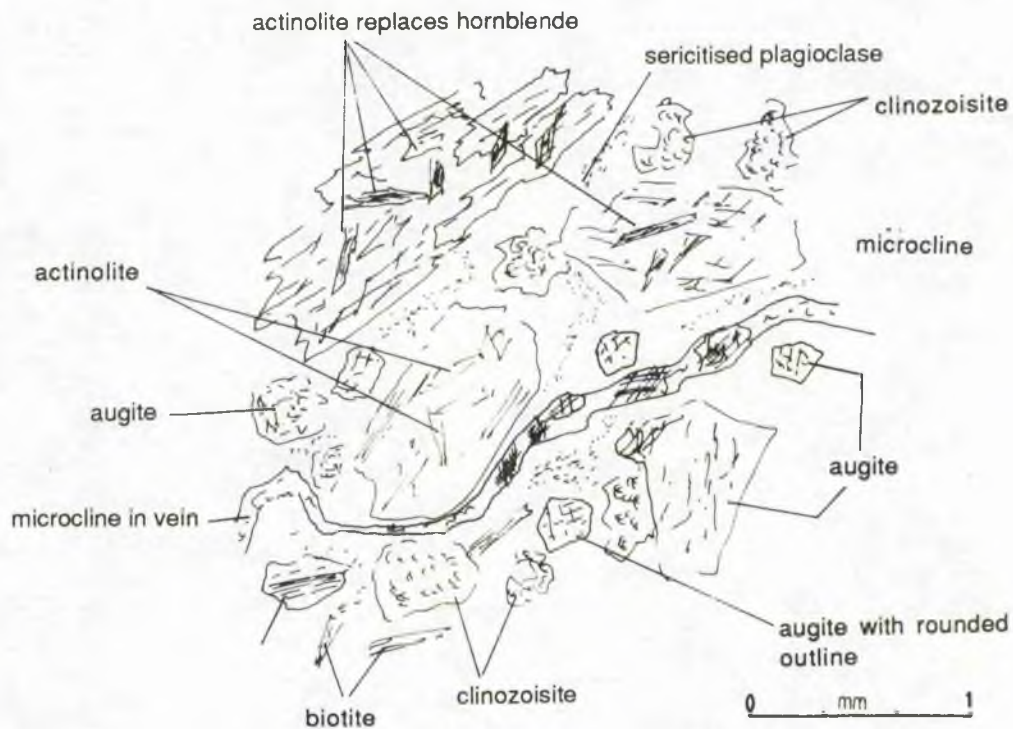


Fig. 4.9 Representative view of the textures found in hybrid diorite from Cathleen's Hole, Narin-Portnoo appinitic intrusion. (Sample Y2656)

(c) Meladiorite

This differs from the hornblende diorite in having a more equigranular texture with stumpy subhedral hornblende set within a plagioclase mesostasis. The plagioclase tends to fill gaps between the interlocking hornblende crystals. Hornblende forms brown crystals which are replaced by actinolitic crystals as well as biotite and it dominates the mode while plagioclase is less important and there is a marked decrease in the amount of quartz and K-feldspar present in the rock.

(d) "Appinite"

This has the typical texture of this rock type with squat to acicular hornblende crystals set within abundant euhedral plagioclase which have grown together and form a largely bi-mineralic suite with only minor quartz, K-feldspar, calcite and opaques within

the mesostasis. The presence of a late volatile-rich assemblage is indicated by calcite and prehnite which fill interstitial gaps but which can also fill the late-stage brittle veins. Pyrite is common and other important accessories include apatite, zircon and titanite. Biotite is often present as a distinct primary mineral in some appinite samples which sometimes has a red/brown pleochroic scheme.

4.9.4 Fairy Coves

Three main rock types are distinguished at Fairy Coves, namely biotite diorite, augite diorite and granodiorite.

(a) Biotite diorite

This shows large differences in grain size throughout the outcrop and also varies in modal mineralogy, particularly in the amounts of plagioclase, biotite and quartz. The rock is similar to other biotite diorites with subhedral plagioclase laths, up to 1.5mm in diameter, intergrown with red-green biotite, which forms ragged flakes with minor hornblende.

(b) Augite diorite

This has similar textural characteristics to that seen at Foragy Rock and Cathleen's Hole, however this diorite contains abundant augite and microcline as opposed to hornblende and plagioclase. Augite dominates over hornblende but tends to occur in the mesostasis whereas hornblende is a major phenocryst. The augite forms elongate prisms which form an interlocking framework between and overprinting plagioclase and microcline. Occasionally the augite has an altered core of hornblende and never overgrows the large hornblende crystals. Hornblende forms large subhedral to euhedral crystals with brown to green pleochroism and alters to an actinolite-biotite assemblage but also has inclusions of microcline, opaques and quartz. It generally has straight, though in places rounded and embayed, contacts with the groundmass minerals and also has a green margin. Plagioclase forms subhedral to euhedral grains within the mesostasis, these grains are overgrown by augite crystals and late-stage actinolic hornblende. The composition of the plagioclase ranges from An₅₀ in the core to An₂₂ at the margin and is the most important felsic mesostatial mineral. Quartz and K-feldspar form the late stage interstitial component with crystals up to 1.5mm in diameter. The K-feldspar is microcline, and epidote is found rarely along with quartz as a final crystallisation product within the interstices, with straight-edged contacts with plagioclase.

(c) Granodiorite

The granodiorite of Fairy Coves occurs as sporadic sheets, sills and veins. These typically have sharp contacts with the limestone and the other igneous rocks in the area. Occasionally however diffuse contacts between diorite and granodiorite are apparent in net-vein complexes of a few metres width, indicating a near coeval relationship between diorite and granodiorite.

4.9.5 Eastern, Central and Western granites of the Portnoo area

(i) Eastern Granite: two main rock types are present in the area, namely granite and diorite.

(a) Granite

Granite takes the form of dykes and steep-sided intrusions further to the west. In both forms it consists of abundant quartz with obvious sub-grain boundaries, perthitic microcline and laths of plagioclase, with minor biotite and associated muscovite. The texture is typically xenomorphic with squat to rounded crystals of plagioclase and microcline with a mesostasis of quartz and biotite. The textures developed in the granite indicates some stress-induced recrystallisation.

Quartz is the dominant mineral of the rock and forms crystals up to 1.5mm in diameter which usually contain many internal domains and sub-grain boundaries, particularly at the contacts with plagioclase. Plagioclase is the earliest formed mineral and forms square to lath-shaped crystals with highly embayed contacts with quartz and perthitic microcline. The cores of plagioclase crystals are altered to white sericitic mica and rare calcite plates. Plagioclase, like the quartz, has developed sub-grain boundaries and has deformed twin planes as a result of post-crystallisation stress. K-feldspar is present in the form of perthitic microcline which, like the plagioclase and quartz, have embayed margins. The K-feldspar often encloses small plagioclase crystals and may partially enclose others, it has angular contacts with the plagioclase and later quartz.

Biotite is the main ferromagnesian mineral of the rock and forms elongate thin crystals that have been sheared between quartz and plagioclase/K-feldspar grains. They have deep red/brown pleochroism. Although the biotite is deformed it does not define a foliation within the rock.

Accessory minerals include secondary calcite which replaces plagioclase and accessory apatite which is associated with the biotite. Muscovite is occasionally associated with biotite but more commonly forms large flakes within the sericitic alteration of the plagioclase.

(b) Diorite from the acid/basic contact zone.

This comprises principally of hornblende and plagioclase with late actinolite in a highly interlocking coarse grained framework. The more basic facies may be derived from appinitic magma disrupted by the granitic magma, as described from field relations in section 3.9.2 (a).

Amphibole has two forms, the first is as a brown primary mineral with prismatic shape, thought to be primary, up to 3mm across but more commonly 0.7-1.0mm. This form is loosely interconnected to a plagioclase framework that closely overlaps the hornblende crystallisation. The second amphibole form is an actinolite which overprints the primary hornblende as single needles and glomeroporphyritic clots with a highly interlocking nature.

Plagioclase is the next most important phase in the rock, forming elongate laths between interconnecting hornblende prisms. Elsewhere the plagioclase may form anhedral mesostatial gaps along with quartz and minor K-feldspar, both of which are minor minerals. Other minor minerals include biotite and clinozoisite which account for ~2% of the rock by volume. Clinozoisite is present in the form of a highly birefringent fine dusting of hornblende which gives the rock a dirty-brown appearance in plane polarised light.

(c) Granitic facies of the acid/basic contact zone

The acid facies of the area is similar in composition to that of the granite dyke (Y 165) just to the west of Portnoo Quay, with similar proportions of K-feldspar (perthitic microcline) plagioclase and quartz. Exchange between the two sides of the acid/basic contact is shown by fragments of basic material being severed from the xenoliths and hornblende and biotite of the diorite becoming incorporated into the granite.

(ii) The central granite

This includes granite, diorite and biotite diorite. Both the granite and diorite have broad similarities to those in the eastern granite area, with minor local differences.

(a) Granite

In the central granite area the granite is very similar to that of the eastern granite with an overall texture of square and squat oscillatory zoned plagioclase crystals with interstitial microcline and quartz, with minor biotite. Plagioclase is commonly sericitised and has embayed contacts with the other minerals. It forms the primary phenocryst of the rock, along with microcline. Microcline is the dominant form of K-feldspar and forms anhedral crystals up to 1.5mm across, but more typically 0.5mm and have embayed contacts with plagioclase. Quartz typically forms large crystals which have strain domains, and also occurs as minor small quartz grains which are typically interstitial to plagioclase and microcline. Biotite, like that of the granitic dyke, is green/brown which is typically deformed against the felsic minerals of the rock, and concentrated in linear patches.

Deformation in the granite may take the form of linear concentrations of biotite and granulations of the felsic minerals. The squat plagioclase and microcline are surrounded by highly granular quartz which is broken into small rounded crystals along with any small grain-sized mesostatial microcline crystals, forming a mortar texture. The larger grains are rounded and deeply embayed by quartz. Biotite is highly elongate and forms banded segments across the rock which may indicate the sense of shear of the area.

Local variations on the granite texture described above include a hybrid granite which differs in having more of the biotite in the form of clots and which may also have a finer grain size than the enclosing granite host. The clots of clinozoisite and biotite along with opaques give the rock a dusty, brown, turbid appearance, but compositionally the granite is similar to granites elsewhere in the area.

(b) Diorite and biotite diorite

These are much coarser grained than the granite and have more and coarser biotite. Plagioclase is highly altered by sericite and clinozoisite as well as biotite which occurs in fractures within the plagioclase. Calcite commonly replaces plagioclase in the form of aggregates of single plates. Quartz forms highly fractured crystals whilst K-feldspar is a minor interstitial mineral, not obviously altered, with occasional perthitic textures. Biotite is the dominant ferromagnesian and forms a foliation where large plates are intergrown with smaller flakes that often split crystals parallel to shear planes. Titanite is often intergrown with the biotite, along with calcite.

(iii) Western Granite (Western Burnfoot)

The main rock types in this area are biotite diorite and granite.

(a) Granite

The granite is similar in texture and composition to that of the central granite and will not be described again in this section.

(b) Biotite diorite

This has an inequigranular texture of interlocking plagioclase with K-feldspar and quartz in the mesostasis. Biotite and hornblende form the ferromagnesian phases and these are mesostatial to the plagioclase. Plagioclase (An₃₀) is the main phenocryst of the rock and is poorly zoned with typically embayed margins and altered cores. The alteration takes the form of sericite and clinozoisite whilst the margins are embayed by biotite, hornblende and clinozoisite, arranged parallel to the margin. K-feldspar takes the form of minor microcline which forms turbid grains, and deformed quartz commonly fills the interstices.

Biotite forms large ragged flakes up to 1.5mm in length and also smaller (0.08mm) grains which replace hornblende. The larger biotite crystals form elongate, sometimes euhedral, crystals which formed later than plagioclase but before quartz. These large biotite crystals sometimes form in clots along with epidote and clinozoisite and minor quartz crystals and may replace hornblende. Hornblende forms elongate to prismatic to stumpy crystals with green/brown pleochroism. The prismatic elongate crystals tend to have a green/brown pleochroism while the stumpy crystals form an overgrowth texture suggesting a later stage of hornblende growth.

Accessories include clinozoisite and epidote associated with the alteration of hornblende, plagioclase and biotite. Opaques form occasional euhedral to corroded grains of oxide and pyrite. Apatite is common in association with biotite.

A local variation in the western Burnfoot area is the development of a zone of hornblende crystal-rich clots up to 1m in width within the biotite diorite. These hornblende crystals are set within a matrix of medium grained diorite consisting of plagioclase, microcline and a matrix of finer grained hornblende and biotite. Contacts of the plagioclase

with its matrix are largely embayed. Microcline and quartz both form interstitial minerals to the plagioclase, hornblende and biotite. The amount of microcline is greater than that of the diorite and is locally perthitic.

Hornblende in the host diorite takes the form of small ragged brown prisms which may have crystallised along with plagioclase. Biotite, however forms ragged grains within the matrix along with hornblende. Occasional clots and aggregates of brown subhedral to euhedral hornblende occur within this medium grained dioritic host. These crystals may be acicular to strongly prismatic in form and are crudely embayed by the host matrix. They are up to 1.0cm in length and are replaced by biotite with a fine dusting of clinozoisite. Where these clots are best developed the hornblende crystals are set in a more quartz-rich matrix with differing amounts of biotite, clinozoisite and small subhedral hornblende crystals. The hornblende clots appear to be associated with a vein-like channel which has allowed growth of hornblende within a quartz, plagioclase and orthoclase matrix.

(iv) Western granite (Eastern Burnfoot)

Four main rock types comprise the lithologies of the eastern area of Burnfoot, namely biotite diorite, granodiorite, biotite granite and meladiorite. Both the biotite diorite and the meladiorite are similar to the type descriptions and so only the granodiorite and biotite granite are described here.

(a) Granodiorite

This has a coarse grained texture with plagioclase laths forming an interlocking matrix with abundant interstitial quartz and minor K-feldspar also in the interstices. Biotite is the dominant ferromagnesian and forms ragged, altered crystals deformed against plagioclase, and occasionally forming clots.

(b) Biotite granite

This has biotite and muscovite in the mesostasis. The biotite forms similar ragged flakes that are often elongated in the direction of the foliation, and biotite is abundant in the form of squat clots. The deformation is intense in this rock, with deformed quartz, rounded plagioclase and deformed biotite.

4.10 PETROGRAPHY OF THE BRECCIA PIPES AND INTRUSION BRECCIAS

(i) The Biroge breccia

This comprises calcareous fragments, like those found at the margin of the breccia pipe, and consists of clast-supported rounded pebble-sized fragments ranging in size from a few centimetres to several centimetres in diameter (Fig. 4.10). Bedding and lamination are not preserved and the pebbles take the form of grey to green pebbles with green amphibole porphyroblasts. Plagioclase is oligoclase (An_{16}) in composition and the matrix consists of actinolitic hornblende with fine grained calcite and chlorite. Reaction relationships with the diorite are minimal with only millimetre-scale growth of hornblende,

pseudomorphed by biotite both perpendicular or parallel to the contact. The dioritic matrix is coarser than the matrix of the pebbles and consists of subhedral, but often acicular brown hornblende commonly replaced by secondary pale amphibole, and biotite with titanite. The hornblende is often enclosed in a highly altered albite matrix, where calcite is present as an interstitial, late-stage mineral. Calcite also forms in cracks parallel to the hornblende cleavage. Needles of acicular apatite are well developed as inclusions within quartz and plagioclase, and prehnite is an interstitial mineral suggesting the presence of a late stage volatile-rich fluid. Granular clinzoisite and pyrite are important accessory minerals. In general, the mineral texture of the diorite is highly deformed and with pseudomorphic replacement of hornblende by actinolite, in a matrix of sericitised plagioclase and strained quartz. The rounding and granulation seen in some crystals suggests mechanical corrosion during the emplacement of the breccia.

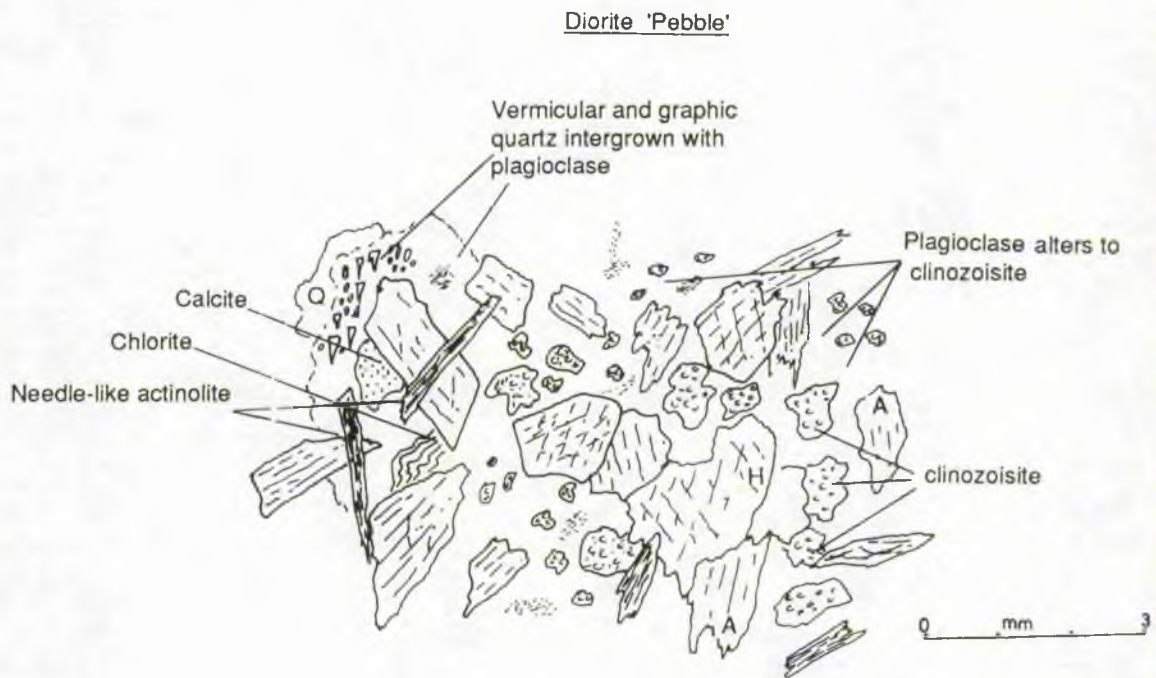


Fig. 4.10 Representative view of the Biroge breccia 'pebble' fragment. (Bir. Di.)

(ii) The Kilkenny intrusion breccia

This consists of two main parts, firstly a detrital part composed of quartzitic fragments in a granophyric matrix, and secondly a minor area of calc silicate fragments in a

hornblende-rich matrix. The quartzitic breccia consists of quartzite fragments forming a highly interlocking network of elongate grains with minor amounts of feldspar, chlorite and calcite with cubes of pyrite. These fragments are mantled by an assemblage composed of irregular amounts of hornblende, biotite, titanite, and granophyric quartz and minor plagioclase with late stage chlorite. This mantle has a diffuse contact with the quartzite fragments and the matrix comprises plagioclase with minor amounts of biotite, all of which form an interlocking texture.

The calc-silicate breccia forms the main part of the intrusion breccia at a lower level of outcrop than the quartzitic fraction. It is essentially a hornblende-rich rock with enclosed calc silicate fragments defining an east-west foliation. The hornblendic matrix consists of coarse grained amphiboles with minor amounts of interstitial plagioclase and quartz. Hornblende phenocrysts vary from colourless to grey-green, replaced locally by minor amounts of biotite. The calc silicate fragments are composed of variable amounts of hornblende and diopside aggregates set in a quartz and albitised plagioclase mesostasis.

(iii) The marginal felsite of the Dunmore intrusion breccia

This consists of phenocrysts of colourless to grey-green hornblende in elongate corroded prisms which are partially pseudomorphed and altered to biotite and titanite with opaques. Biotite and corroded hornblende also form ragged grains within the felsite matrix. This matrix consists of a complex intergrowth of zoned plagioclase, quartz and orthoclase. All of these constituents are highly intergrown and have irregular margins. This marginal felsite may be finer or coarser grained and noticeably in the finer grained sections, the hornblende appears more euhedral and less altered by biotite. Felsite from the core of the breccia pipe is similar in composition to the marginal felsite, but contains numerous limestone xenoliths which do not appear to affect the composition of the felsite.

4.11 MINERAL CHEMISTRY

The compositions of the mineral phases (principally amphibole, pyroxene, plagioclase and biotite) were determined by electron microprobe. These minerals were analysed in order to define the compositional variations within the various magmatic bodies. Back-scattered electron imagery was used to study microtextures, particularly compositional zoning. The aim of the study was to constrain the nature of the mineral compositions and their variability within individual intrusions and amongst the suite of appinitic and granitic bodies in the Ardara area. P,T and compositional parameters controlling crystallisation were also investigated in order to determine the nature of the crystallisation regime, particularly for the amphiboles, and to highlight similarities and differences between the magmatic bodies.

4.11.1 Analytical Methods

Analysis was performed using a JEOL JCSXA733 electron probe microanalyser operating at 15 kV and 20nA, using pure metals, oxides and minerals as reference

standards. Apparent concentrations were corrected using the conventional ZAF correction procedures. Structural formulae were calculated according to the method of Deer, Howie & Zussman (1966).

4.11.2 Amphibole compositions

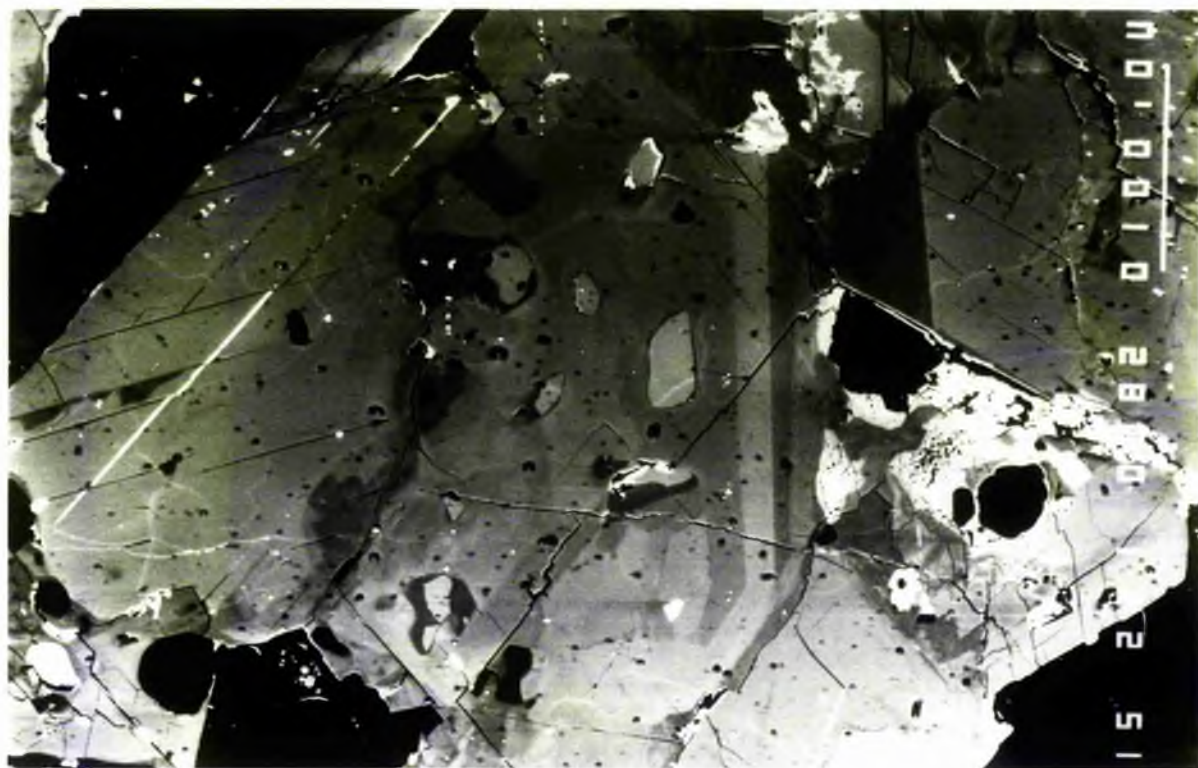
Amphibole is the primary ferromagnesian mineral of almost all of the Ardara igneous rocks and it is amphibole which displays the greatest range in composition and texture of the mafic minerals, hence this mineral group has been studied in greatest detail. Amphibole nomenclature used here follows the system of Leake (1978). The amphiboles in the appinitic rocks range from actinolite to edenite, magnesio-hornblende and ferroan pargasite, it can be regularly and patchily zoned, mostly involving substitution of Si-Al and Fe-Mg (Plate 4.14). One notable compositional exception in the appinites is the hornblende from the Kilrean intrusion which is magnesio-hastingsitic in composition, reflecting significantly its higher Mg/Mg+Fe ratio. The amphibole composition in the granitoids of the main pluton is magnesio-hornblende. The range of amphibole compositions in the various appinite and granitoid samples is plotted in Fig. 4.11. Actinolite is common in all appinitic intrusions and tends to occur along with primary amphibole with which it has both sharp and diffuse contacts, it is commonly marginal but also clotted, replacive in needles and patch-like throughout the samples (Plate 4.12 b). Actinolite has a consistently higher Mg/Mg+Fe and SiO₂ and lower TiO₂, Al₂O₃, Na₂O and K₂O than the hornblende (Table 4.3). In the classification scheme of Leake (1978) these amphiboles plot in the actinolitic hornblende and actinolite fields. Some of the variation in amphibole composition within and between appinitic and granitic intrusions is described below.

(i) Differences in amphibole composition between appinitic bodies.

Most appinites have a similar overall range in amphibole composition. Variations do exist between the more primitive intrusions, e.g. Kilrean which has high Mg-type amphiboles (Fig. 4.12 a), and the appinitic breccias of Biroge and Mulnamin which have more actinolitic amphiboles (Fig. 4.12 d).

Plate 4.14 (a) ZCI of zoned hornblende from diorite (Y3153) of the Narin-Portnoo intrusion. Two main zones exist, dark and light, parallel to the crystal margin. The dark zone is enriched in SiO_2 and MgO compared to the bright area which is enriched in FeO and Al_2O_3 . The rounded inclusion is augite. Conditions 15 kV, 20 nA, scale bar 100 μm .

Plate 4.14 (b) ZCI showing patchy zoning of actinolitic hornblende (dark patch) in hornblende with actinolitic needles parallel to the cleavage of hornblende. Light mineral on the left is clinozoisite. Conditions 15 kV, 20 nA, scale bar 100 μm .



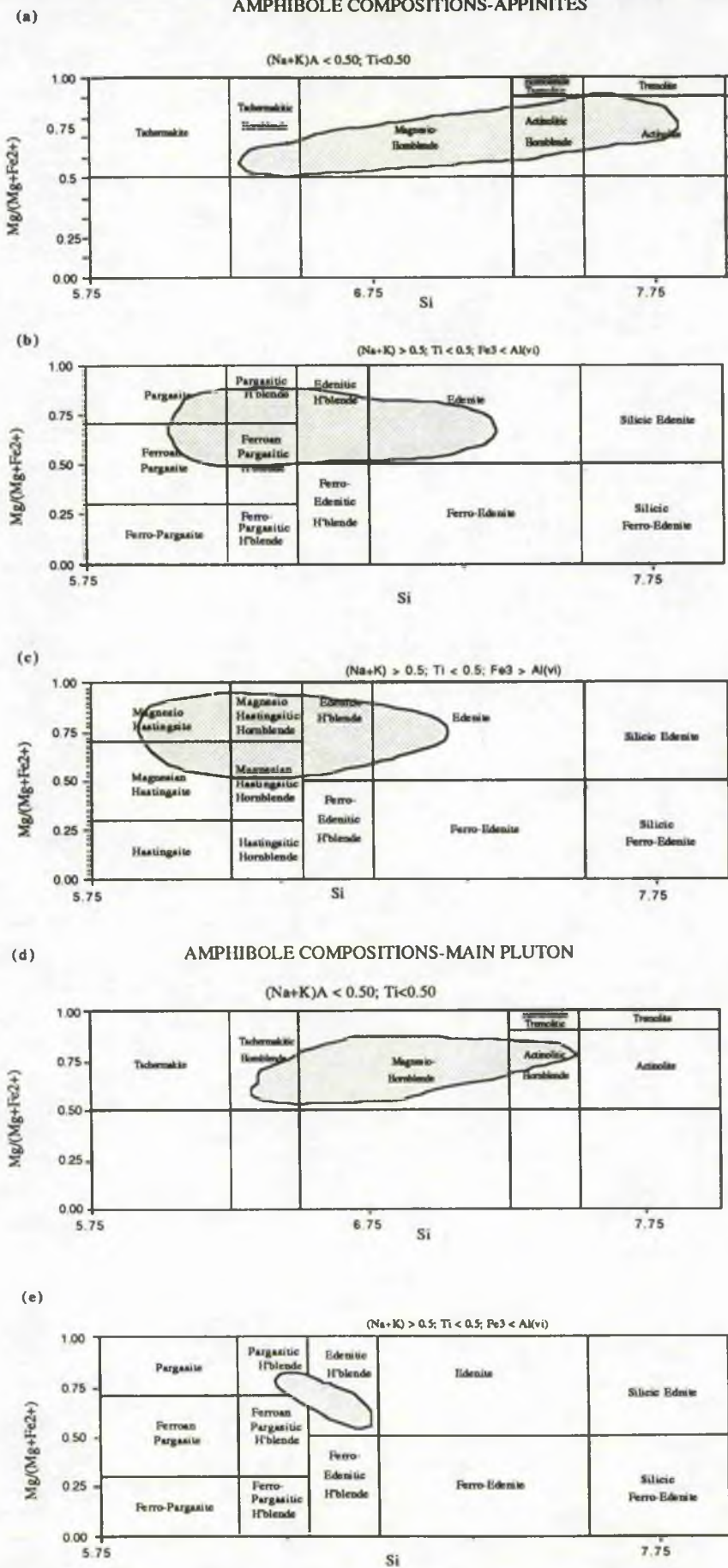


Fig. 4.11. Amphibole compositions in the Ardara igneous rocks within the classification scheme of Leake (1978). Shaded fields represent the range of analyses. (a) - (c) appinite compositions, (d) - (e) main pluton.

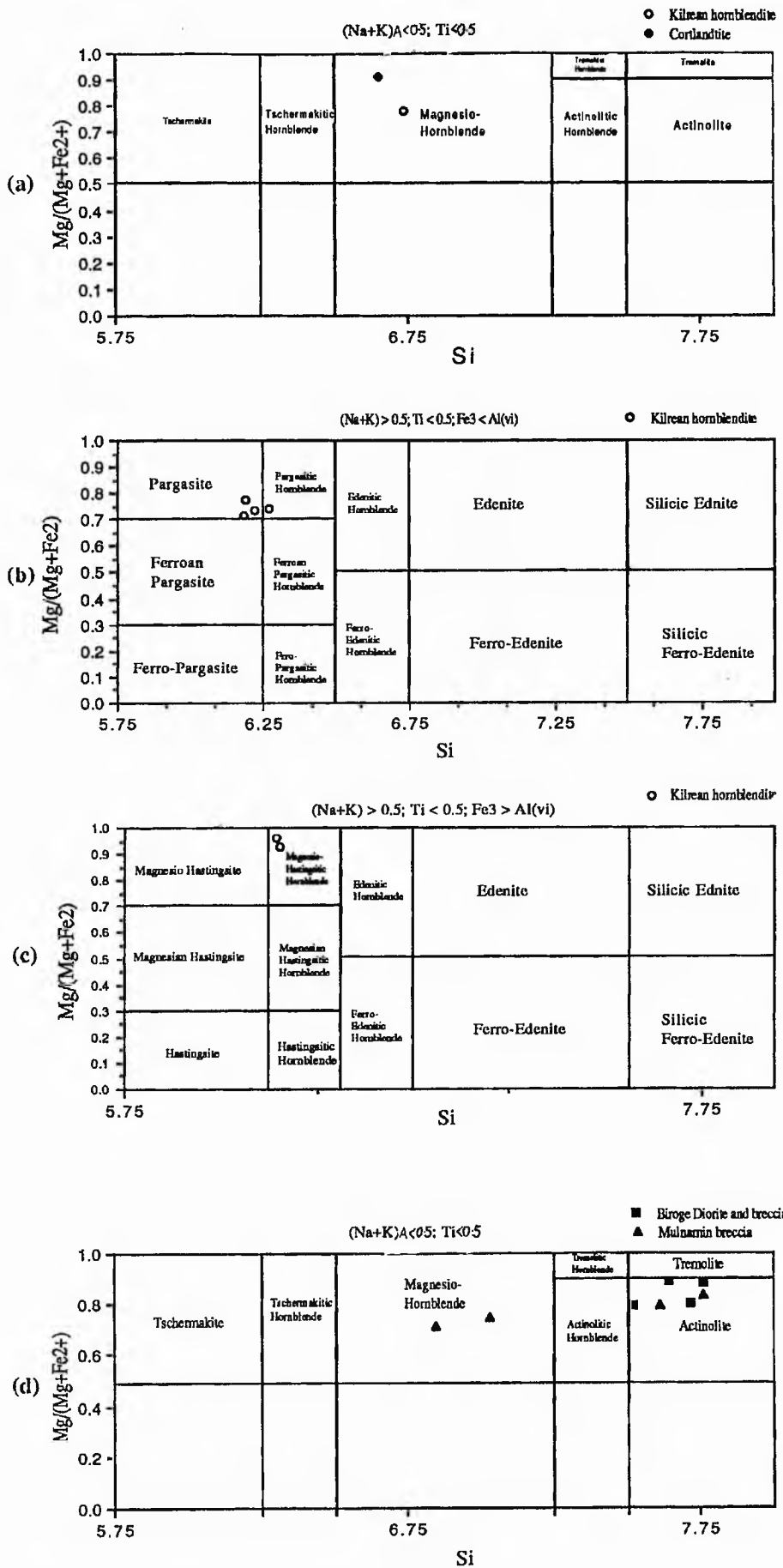


Fig. 4.12 (a-c) Amphibole compositions within the Kilrean cortlandtite, (d) amphibole compositions within the appinitic breccias of Biroge and Mulnamin.

(ii) Amphibole composition of the main Ardara pluton and Glenard granite.

The amphiboles from the outer unit of the main Ardara pluton (G1) have tschermakitic to magnesio-hornblende compositions and a Mg# similar to amphiboles from the diorite of Summy Lough. The inner unit of the Ardara pluton (G2) has higher Mg# than the outer unit (G1), but also ranges in composition from magnesio-hornblende to actinolitic hornblende, a range similar to that of the appinites (Fig.4.13).

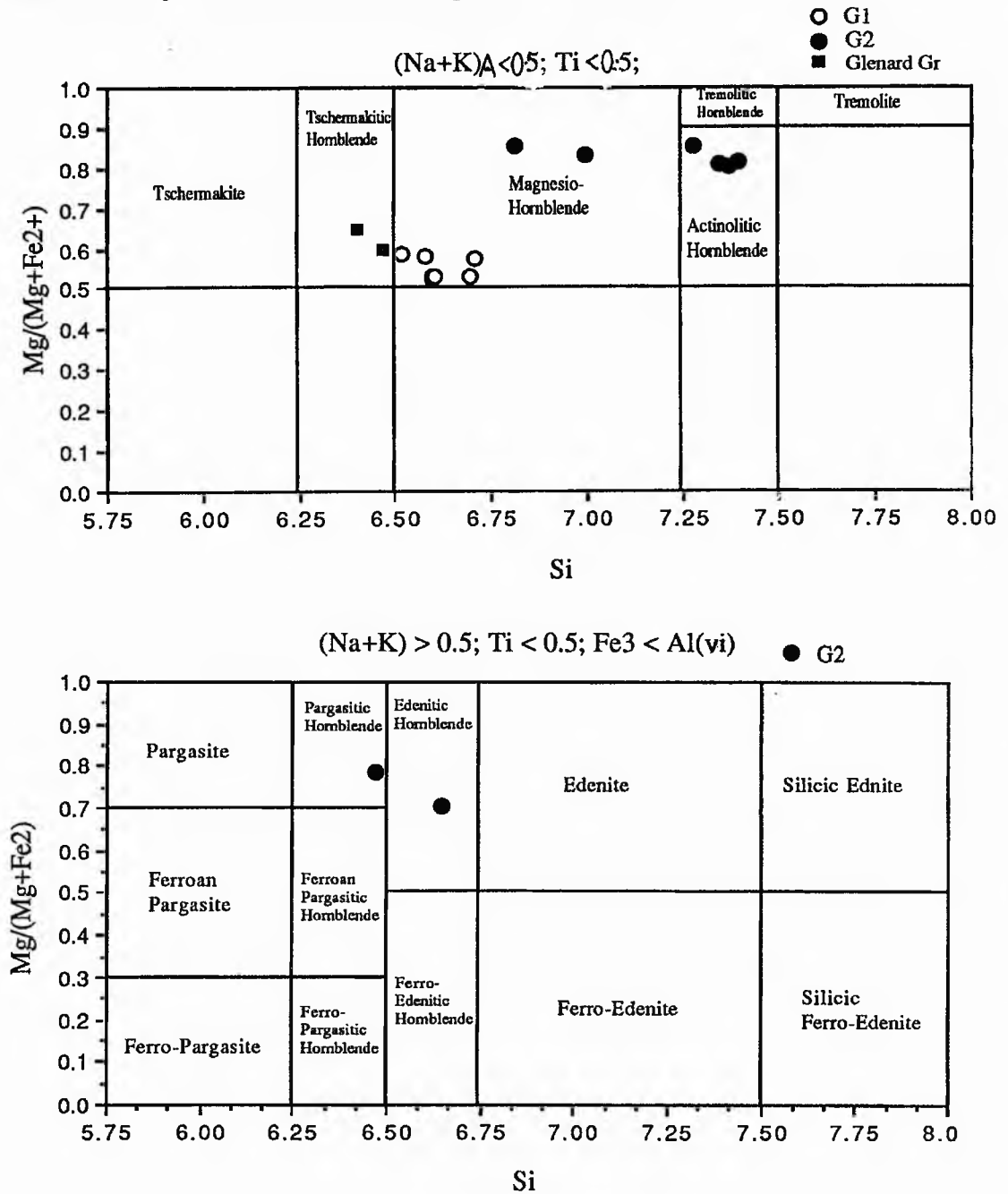


Fig 4.13. Compositional variation within amphiboles for the granitic units (G1, G2) of the main Ardara pluton

(iii) Amphibole variation within individual appinitic bodies.

(a) Meenalargan

The primary amphiboles from the diorite and coarse diorite have a ferroan pargasite composition (Fig. 4.14 a). Amphiboles with replacive textures have a range from magnesio-hornblende to actinolite (Fig. 4.14 b). No obvious difference exists between the diorite and coarse diorite of the Meenalargan intrusion.

(b) Summy Lough diorite

Amphiboles from the Summy Lough dioritic intrusion show a range from edenite to magnesio-hornblende and actinolite in both the diorite and hornblendite (Fig. 4.15)

(c) Mulnamin

The amphiboles of the diorite, hornblende diorite and appinite of Mulnamin have a composition which ranges from tschermakite to magnesio-hornblende and actinolitic hornblende. The amphibole from the Mulnamin breccia pipe has a range similar to the diorites, but is more actinolitic (Fig. 4.16).

(d) Narin-Portnoo

All rock variations show a similar range of replacive amphibole composition from magnesio-hornblende to actinolitic hornblende and actinolite (Fig. 4.17 a), however there is variation between the hornblendite and meladiorites, diorites and 'appinite'. Hornblendite and meladiorite have a range in composition from edenitic hornblende and ferroan pargasite, magnesio hastingsite and magnesio-hastingsitic hornblende, reflecting the more MgO-rich composition of these amphiboles (Fig. 4.17 b & c). The diorites have a ferroan pargasite composition while the appinites have a pargasite to pargasitic hornblende composition (Fig. 4.17 b).

(e) Kilrean

The cortlandtite and hornblendite of the Kilrean intrusion both have (secondary) amphibole compositions which fall in the range of magnesio-hornblende. The typical primary amphibole of the cortlandtite is a magnesio-hastingsite while the typical amphibole of the hornblendite ranges from pargasite to pargasitic hornblende (Fig. 4.12 a-c).

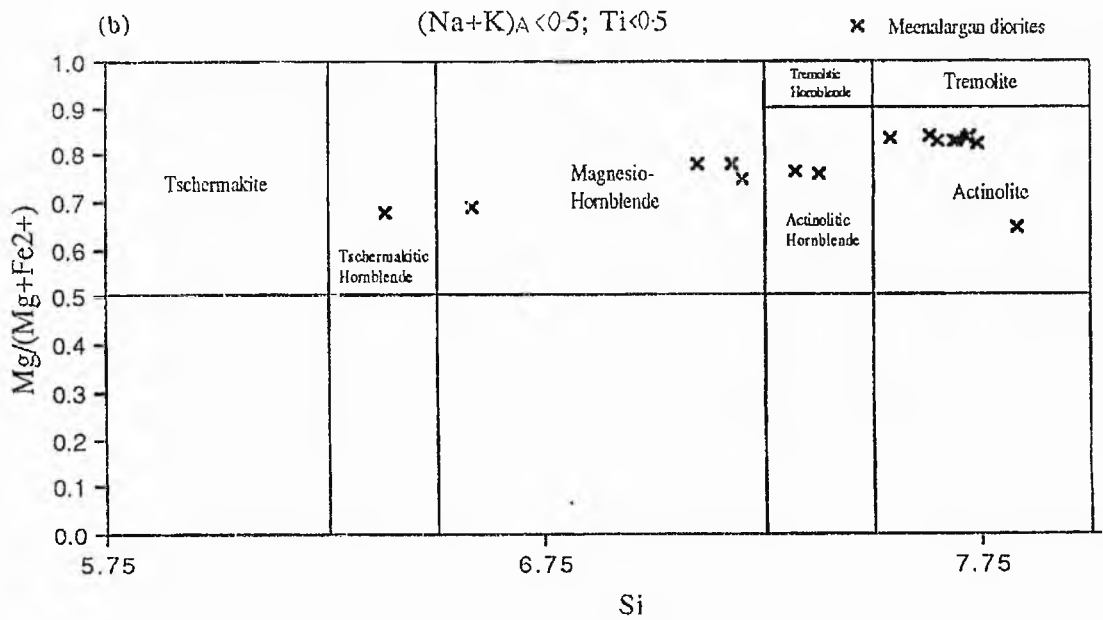
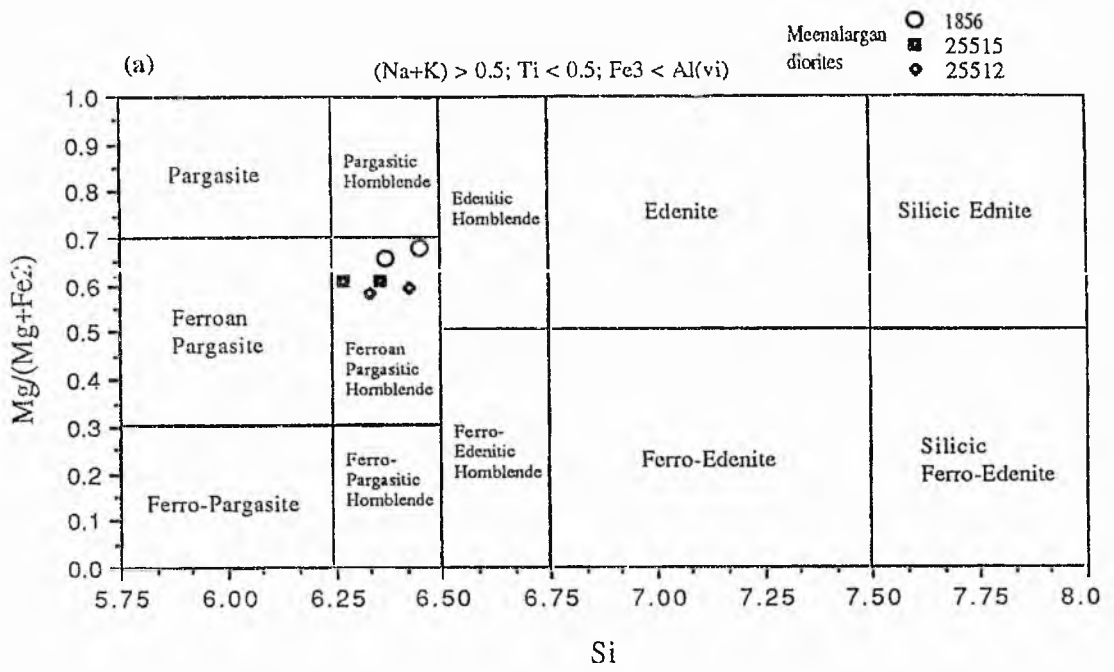


Fig. 4.14 (a & b) Si versus Mg# plot of amphibole compositions in the diorites of the Meenalargan complex, after classification scheme of Leake (1978).

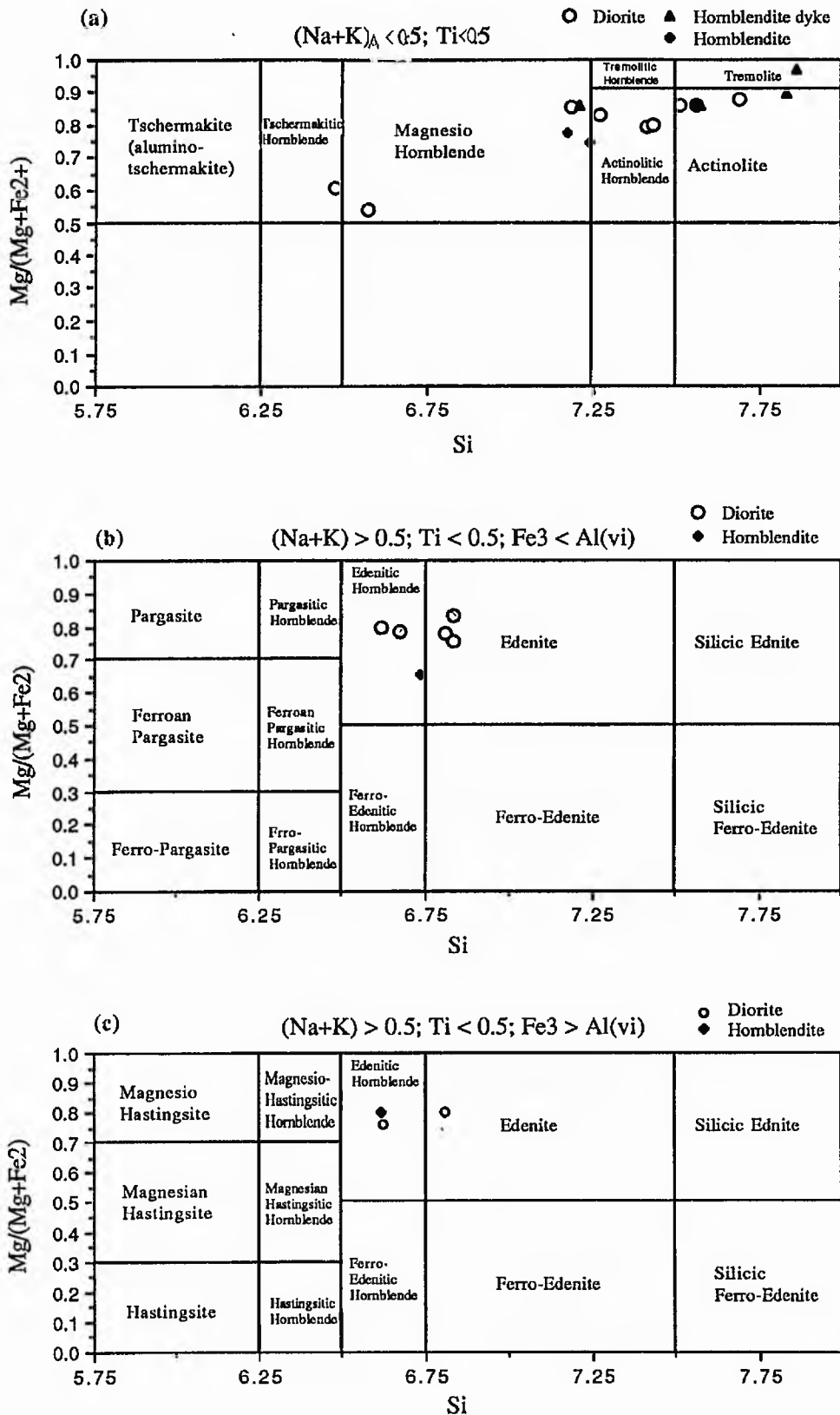


Fig. 4.15 Si versus Mg# plot of amphibole compositions in the hornblendite and diorite from the Summy Lough complex, after Leake (1978).

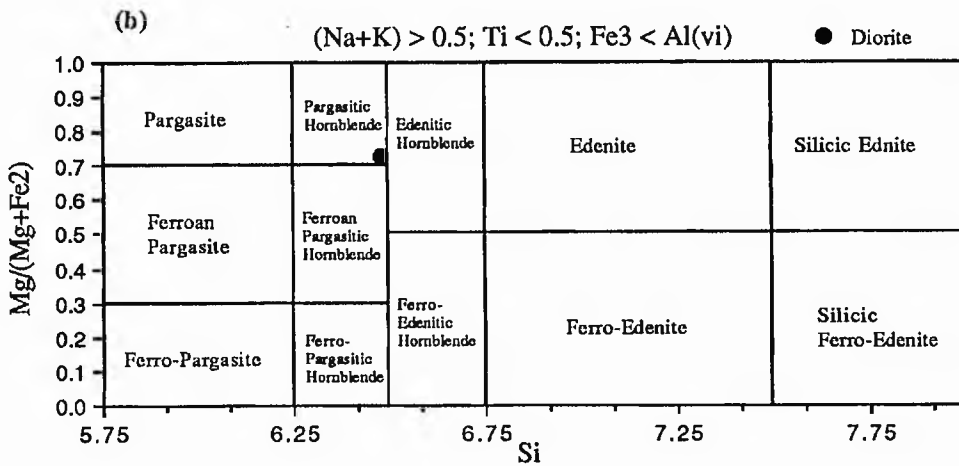
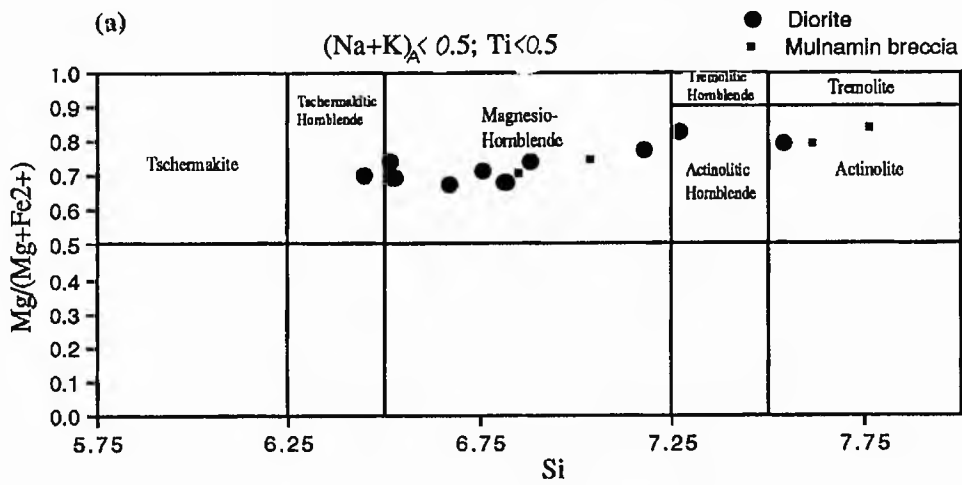


Fig. 4.16 Si versus Mg# plot of amphibole compositions in the Mulnamin complex, after Leake (1978).

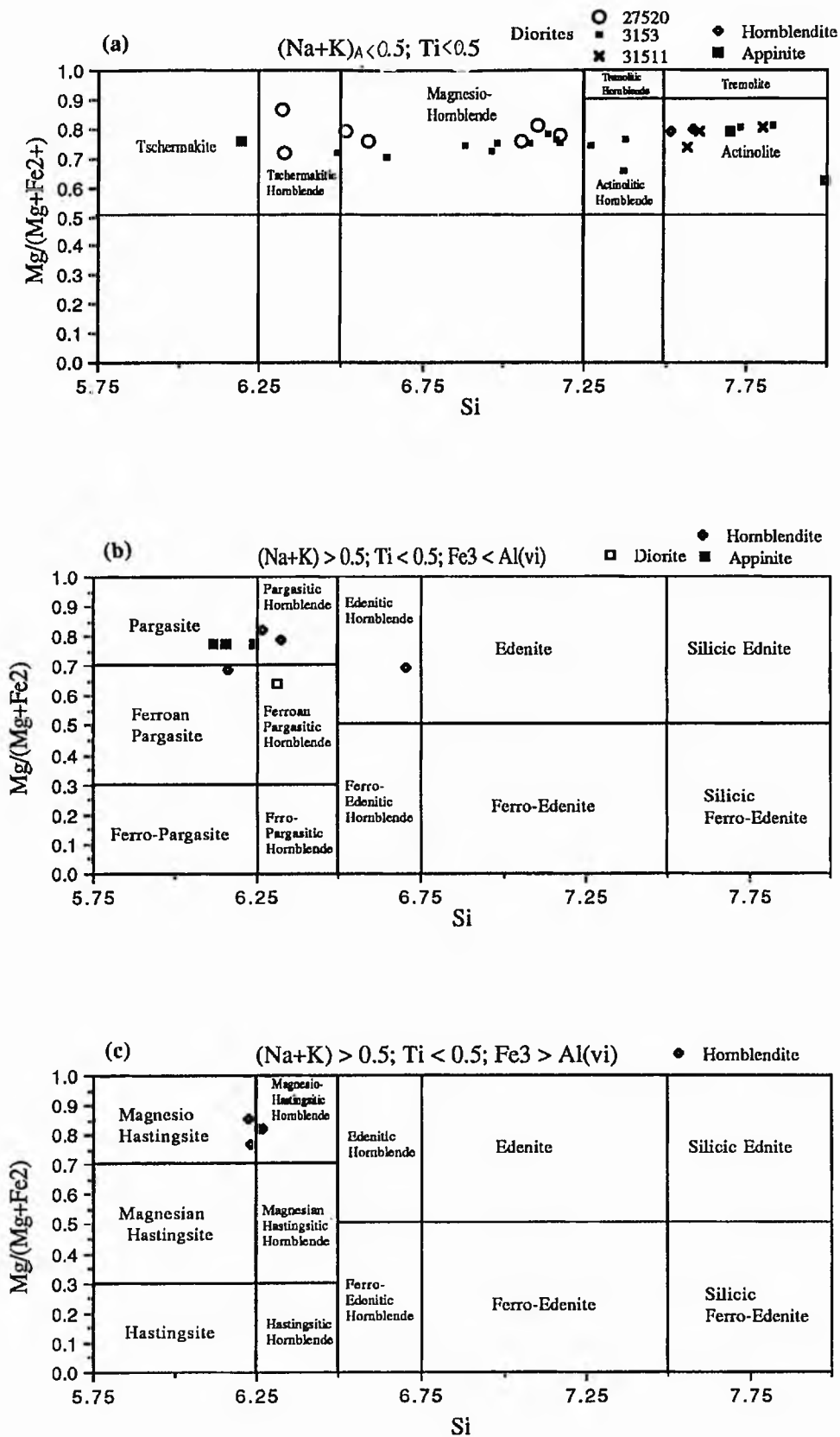


Fig. 4.17 Si versus Mg# plot of amphibole compositions in the Narin-Portnoo intrusions, after Leake (1978).

(iv) Variation in mineral Mg# with whole rock composition

The most primitive rock type (the Kilrean cortlandtite) shows enrichment in Mg, both in whole rock and amphibole. This is also the case for the hornblendite of Summy Lough. The other meladiorites, hornblendites, diorites and appinites have a composition which is intermediate between that of the hornblendite of Summy Lough and the outer granite G1 of the main Ardara pluton (Fig 4.18 a). The composition of the inner unit of the main Ardara pluton (G2) is similar to that of the diorites of the Ardara area although it has a lower whole rock Mg#. Overall there is a trend from primitive cortlandtitic and hornblenditic compositions to meladiorite, diorite and appinitic composition towards Mg depleted granitic compositions. This trend is reflected in plots of Mg# in biotite which have a similar pattern. The Summy Lough diorite has higher Mg# hornblende with slightly lower Fe and Si values compared to those of the Ardara pluton, again probably related to whole rock values (Fig. 4.18 b). The appinites show a concentration of Mg within the hornblende relative to the biotite and in the biotite relative to the whole rock (Fig. 4.18 c).

(v) Variations in hornblende composition in relation to appinite emplacement mechanism

The two extreme mechanisms of appinite emplacement, namely passive and explosive, are reflected in variations in hornblende composition. The Biroge breccia pipe has an actinolite-tremolite composition which is relatively enriched in Mg but relatively depleted in Al^{IV} compared with hornblende from the Biroge diorite, Kilrean (Fig. 4.12 a), and Narin-Portnoo (Fig. 4.17). Hornblende from within the appinitic breccia at Mulnamin reflects the composition of the Biroge breccia however it is also of a similar composition to the hornblende from more passively emplaced intrusions (Fig. 4.19 a). This pattern is reflected by total iron, which is slightly more depleted in the explosively emplaced Biroge breccia compared to the more passively emplaced Kilrean, Narin-Portnoo and Meenalargan intrusions, which as a group have similar compositions (Fig 4.19 b). This variation in composition may reflect pressure effects on Al in amphibole and T-P_{H2O}-fO₂ controls on octahedral Mg/Fe.

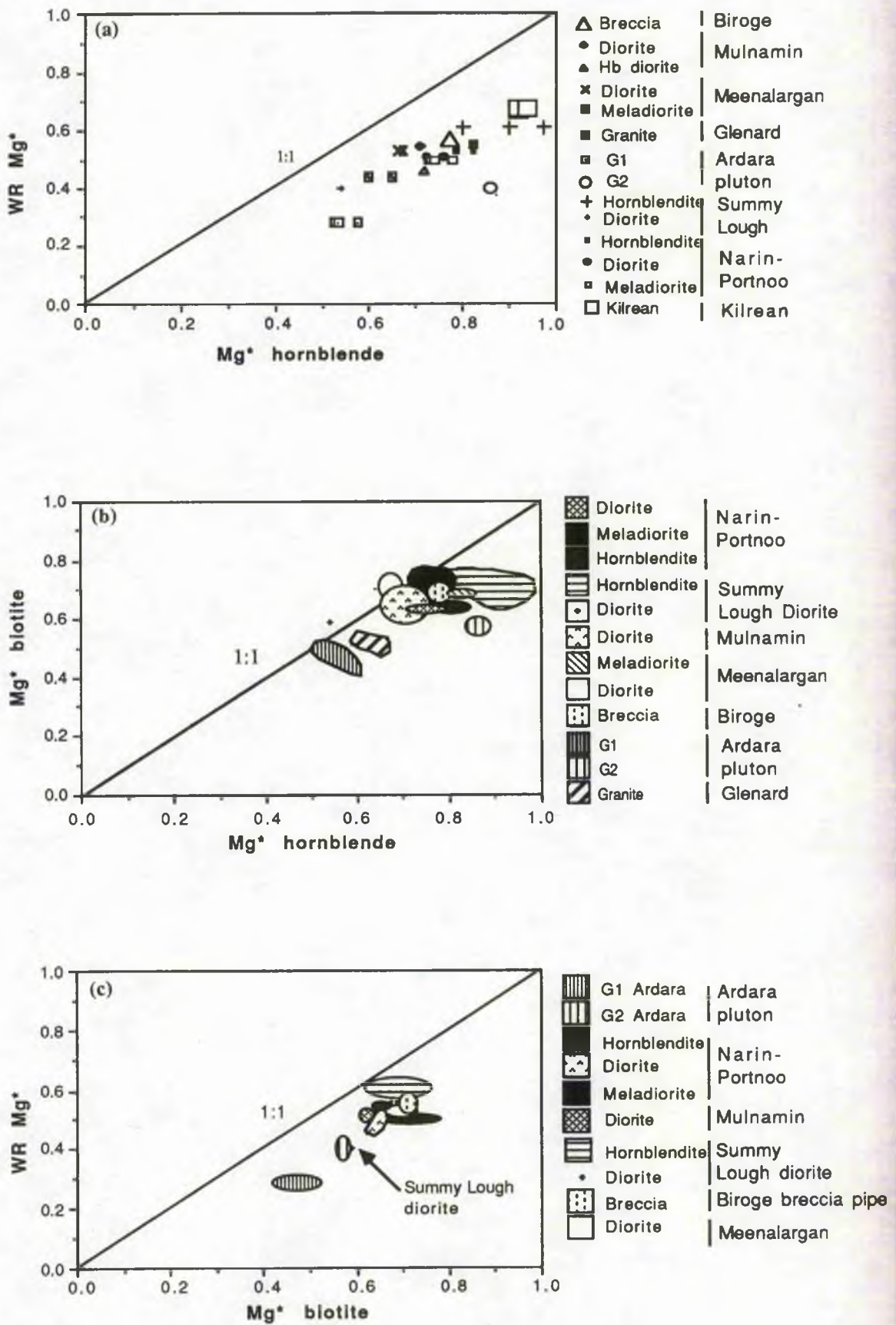


Fig. 4.18 (a-c). Mg# plots illustrating the relationship between hornblende and whole rock (4.18 a), biotite and hornblende (4.18 b), and whole rock (4.18 c).

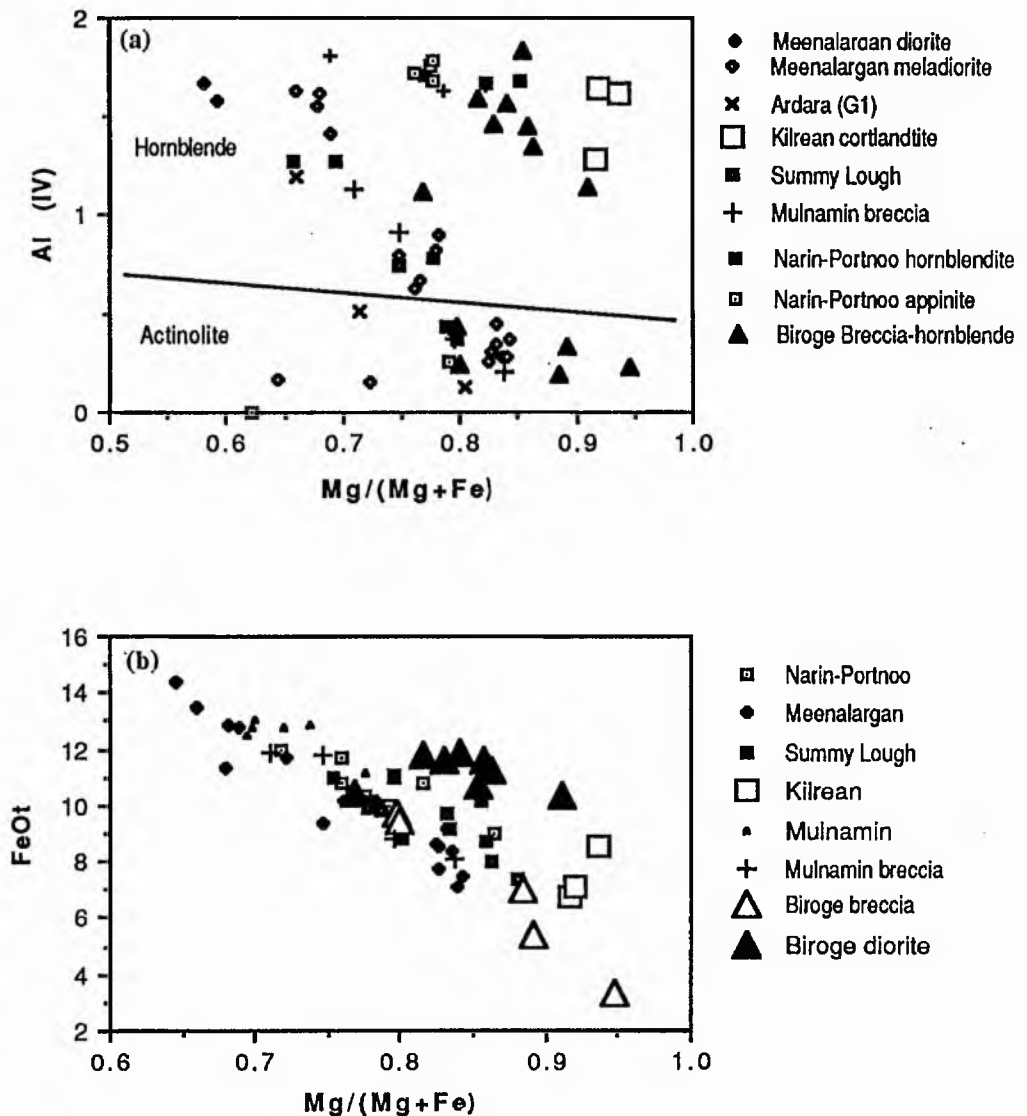


Fig 4.19 a-b. Mg# variations in the amphiboles of the Biroge breccia pipe and some of the more passively emplaced appinitic and dioritic intrusions.

4.11.3 Hornblende geobarometry

In order to estimate the pressure conditions of crystallisation of the appinitic and granitic magmas of the Ardara igneous complex a study of mineral geobarometry within a number of samples was made. The pressure (and temperature) of crystallisation of hornblende was estimated using the $Al^{IV} - P$ calibrations of Hammarstrom & Zen (1983, 1985, and 1986), Hollister et al. (1987), and Johnson & Rutherford (1988). The geobarometer of Hollister et al. (1987) was also used to find if it was possible to determine whether final crystallisation of amphibole occurred at depth or at the actual level of

emplacement of appinite and granite by analysing rim and core compositions of the amphiboles.

(i) Procedure

As hornblende composition is known to vary significantly with rock composition, pressure and temperature, the use of the hornblende geobarometer requires the fulfillment of certain conditions related to the mineral assemblage of the rock. A calc-alkaline rock typically has 10 major components or oxides (SiO_2 , TiO_2 , Fe_2O_3 , FeO , Al_2O_3 , K_2O , MgO , CaO , Na_2O , H_2O), and the mineral phases typically may include plagioclase, quartz, orthoclase, biotite, hornblende, titanite and magnetite. Assuming that melt and an H_2O -bearing vapour phase are present at the end of crystallisation, there will be a total of 9 phases present at the end of crystallisation, which according to the Phase Rule gives the system a variance of 3; namely P, T, and one compositional degree of freedom.

According to the assumptions of Hollister et al. (1987) only one degree of freedom at a specified temperature, fugacity of oxygen and plagioclase composition exists. They concluded that in order to apply an empirical geobarometer based on hornblende composition, the following conditions must be met:

(a) the phases quartz, plagioclase, hornblende, biotite, orthoclase, titanite and magnetite must have crystallised together from the melt;

(b) only the rim compositions of the hornblende should be used because these are the only parts of the hornblende crystals that have crystallised with the last remaining melt of the rock, so that the final temperature of crystallisation may be limited to a small range;

(c) although hornblende can crystallise between 950°C and 650°C in calc-alkaline magmas (Helz 1982), the temperature range is thought to be relatively narrow compared to the total range over which amphibole is stable in the crust and upper mantle (Hollister et al., 1987). Hollister et al (1987) indicated that the pressure should be more than ~ 2 kb as the temperature of crystallisation increases rapidly with a drop in pressure. They base this on the findings of Clemens & Wall (1981) who noted a considerable increase in temperature with a drop in pressure.

(d) the rim plagioclase composition should be within a well defined range, which ideally should be between $\sim\text{An}_{25}$ and An_{35} .

(ii) Results

(a) Ardara granitoids

Hornblende analysed from the outer unit (G1) of the Ardara pluton which fulfills the conditions outlined in section 4. 11.1 (i) gives a crystallisation pressure range of 3.7 - 5.7 kb (Fig. 4.20), whilst that of the inner unit (G2) yields a pressure range of 4.1 - 5.9 kb.

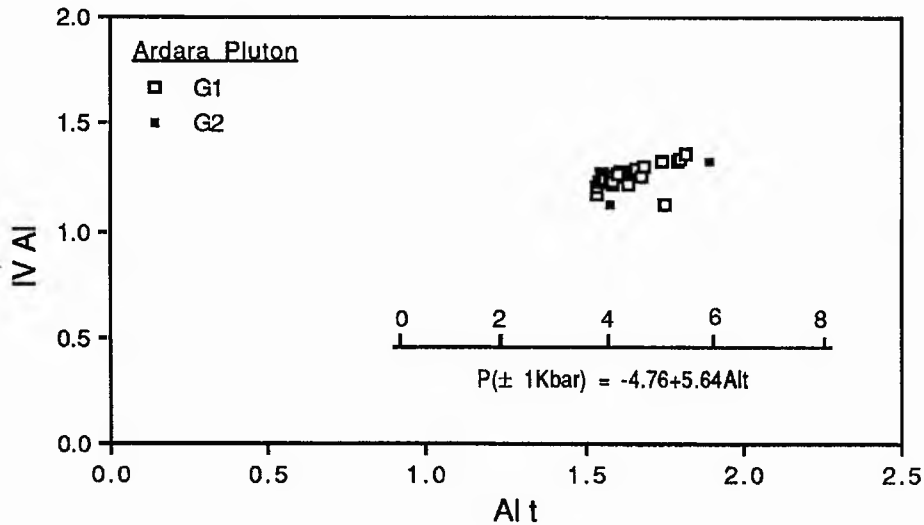


Fig. 4.20. Hornblende geobarometry for G1 and G2 of the Ardara pluton. (Error of calibration according to Hollister et al. (1987) is ± 1 kb).

(b) Appinite

Results obtained for the rocks of the appinite suite in the various intrusions are presented in Fig. 4.21. problems existed in obtaining consistent plagioclase compositions throughout the intrusions and so measurements were made in the range An₃₀₋₅₅. Other problems concern the criteria outlined in section 4.11.1 (i), for instance the use of edge compositions in the hornblende may lead to spurious results considering that much of the primary hornblende has an actinolitic margin, although all measurements quoted below were made at primary hornblende margins. The presence of quartz in the appinites was also a problem, only those appinitic samples which contained quartz in direct contact with plagioclase were used. The restriction on the use of the hornblende geobarometer to pressures greater than 2 kb may also be invalid as the appinites are thought to have been emplaced as high level intrusions (Hall 1967, Hammidullah & Bowes 1987).

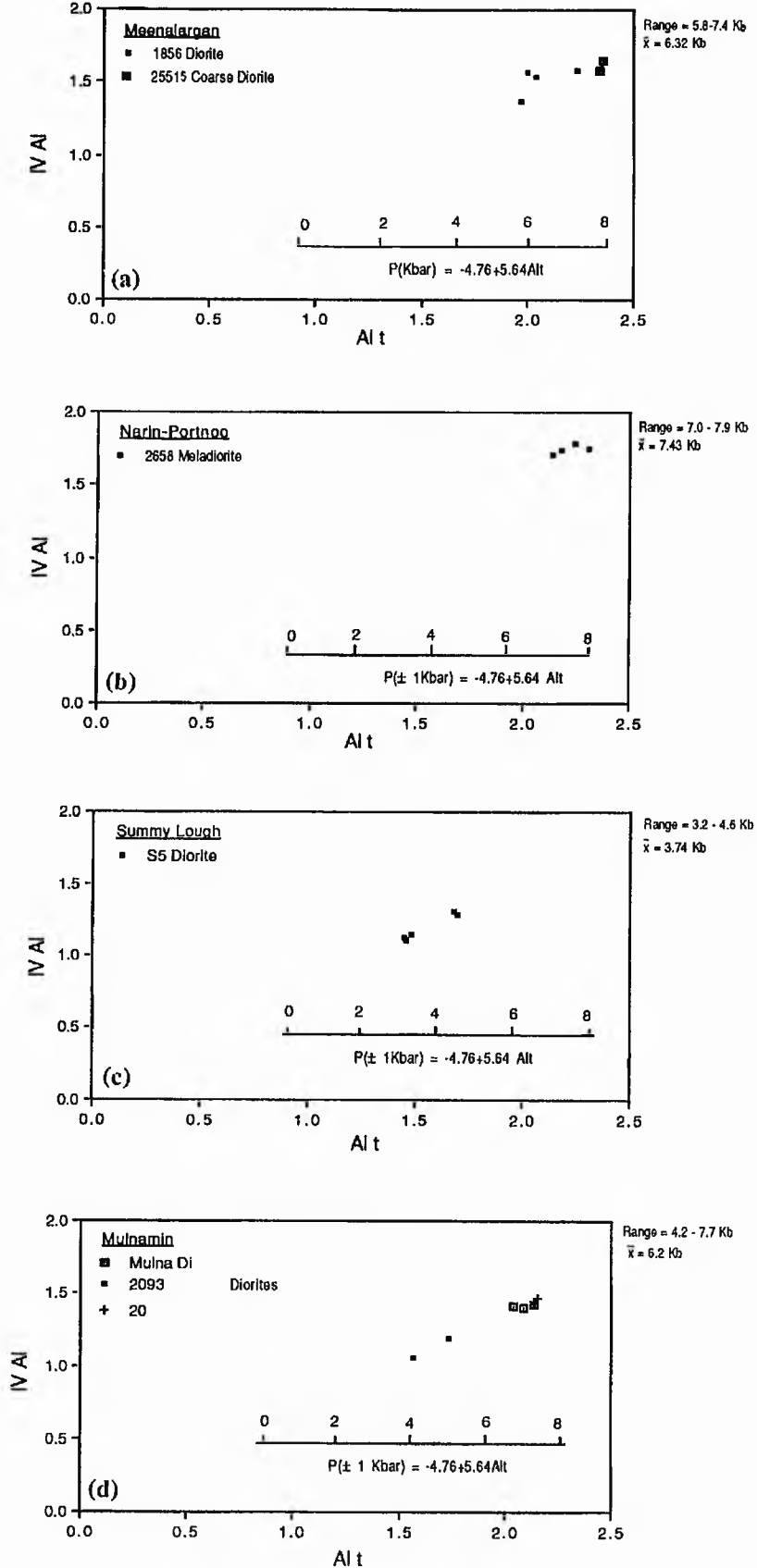


Fig. 4.21. Al_I versus Al_{IV} plots with hornblende geobarometry results for appinites of the Ardara area: (a) Meenalargan (diorite sample, Y1856, coarse diorite sample Y25515), (b) Narin-Portnoo (meladiorite sample Y2658), (c) Summy Lough (diorite sample S5), (d) Mulnamin (diorite samples Mulna di, Y2093 and Y20). (Error of calibration is ± 1 kb).

Meenalargan: geobarometric measurements for the diorite and coarse diorite of Meenalargan give results of 8 kb (coarse diorite) and 5.8 - 7.4 kb for the diorite (Fig. 4.21 a). These results could be suspect because of the problem of sub-solidus re-equilibration of the hornblende and the instability of biotite. Textures described in section 4.8. show that the hornblende may be derived from pyroxene and actinolitic patches within the hornblende, which make analysis difficult and consequently the accuracy could be open to question.

Narin-Portnoo: pressures of 7.0 - 7.9 kb were estimated for the meladiorite at Cathleen's Hole (Fig. 4.21 b).

Summy Lough Diorite: this intrusion is most closely linked to the outer unit (G1) of the Ardara pluton and returns estimated pressures of crystallisation ranging from 3.2 - 4.6 kb (Fig. 4.21 c). This value is within error (± 1 kb) with the estimated pressure of the outer unit (G1) of the Ardara pluton (3.7 - 5.9 kb) (Fig. 4.20). Considering the coeval relations which the Summy Lough diorite shows with the outer unit of the Ardara pluton such pressure estimates for the Summy Lough diorite may be reasonable.

Mulnamin: the estimated pressure for the diorite of Mulnamin ranges from 4.2 - 7.7 kb (Fig. 4.21 d).

4.11.4 Hornblende geothermometry

Tentative estimates were made of the temperatures of formation and crystallisation of co-existing hornblende and plagioclase in the various rock types using the amphibole - plagioclase geothermometer of Blundy & Holland (1990). This geothermometer covers a temperature range of 500-1100°C, with a calculated error range of $\pm 75^\circ\text{C}$. It has pressure as an input variable, and requires an amphibole composition of $\text{Si} < 7.8$ and $X_{\text{An}} < 0.92$, as errors may become too large beyond these limits (Blundy & Holland 1990). Application of the geothermometer yielded the following results:

(a) Ardara Granites

The geothermometer was applied to samples of the outer unit (G1) of the Ardara pluton, where the pressure estimate of 5.0 kb for final crystallisation was apparently consistent. At this pressure the temperature of co-existing plagioclase and hornblende was 670 - 710°C (Fig. 4.22). At a pressure of 4 kb the temperature was also $\sim 700^\circ\text{C}$. Such temperatures are close to the experimentally-determined tonalite solidus at 2 kb and 5 kb of 710°C after Piwinski (1968).

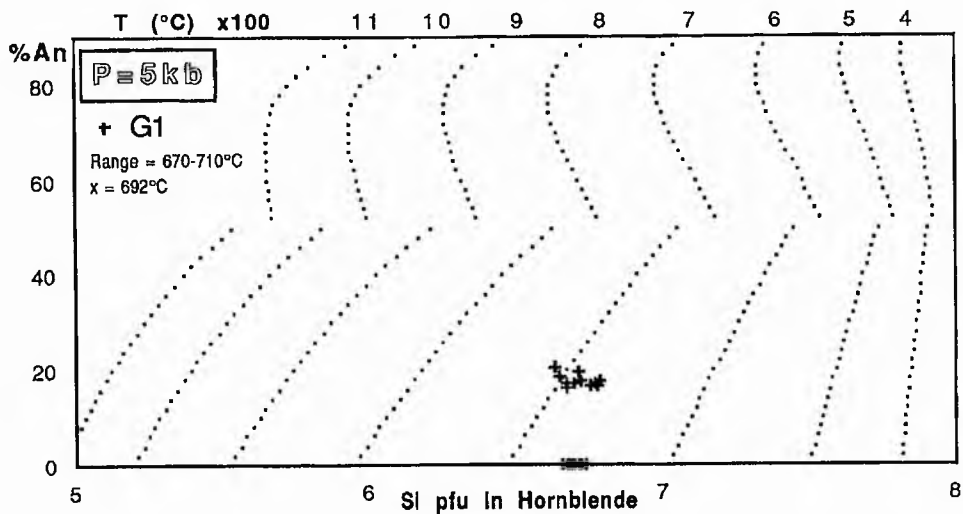


Fig. 4.22 Geothermometry results of the Ardara granite unit (G1). The range of temperatures determined are displayed on the graph. The calculated error is $\pm 75^\circ\text{C}$ (Blundy & Holland, 1990)

(b) Appinites

Geothermometry results for the appinite suite may be unreliable because of doubts over the accuracy of geobarometry results (section 4.11.3 b). The Mulnamin intrusion yields a temperature of $730\text{-}750^\circ\text{C}$ at 5 kb (Fig. 4.23). The Summy Lough diorite yields an approximate crystallisation pressure of 3.2 - 4.6 kb (Fig. 4.21 c). This value is within error ($\pm 1\text{kb}$) with the estimated pressure of the outer unit (G1) of the Ardara pluton (3.7 - 5.9 kb) (Fig. 4.20). Considering the coeval relations which the Summy Lough diorite shows with the outer unit of the Ardara pluton such pressure estimates for the Summy Lough diorite may be reasonable.

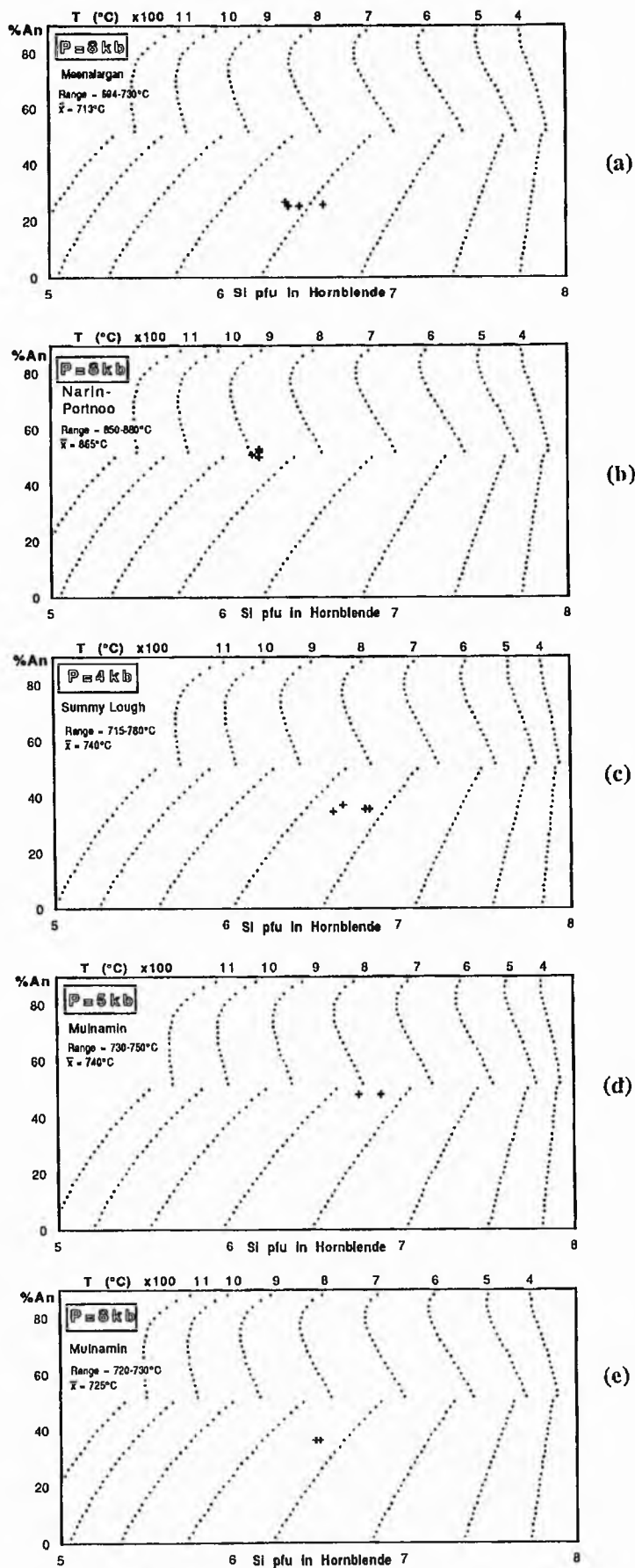


Fig. 4.23 Graphs showing the estimated crystallisation temperatures for some Ar dara appinites, using the method of Blundy & Holland (1990). (a) Meenalargan at 8 kb, (b) Narin-Portnoo at 8 kb, (c) Summy Lough at 4 kb, (d) Mulnamin at 5 kb, (e) Mulnamin at 8 kb. The range of temperatures and the average temperature are displayed on each graph. The calculated error of the geothermometer is $\pm 75^\circ\text{C}$ (Blundy & Holland, 1990).

Estimated temperatures fall within the range of 694-880°C for the crystallisation of co-existing hornblende and plagioclase. Fig. 4.24 shows the temperature variation estimated from the geothermometer of Blundy plotted against Mg# to show the variation in relation to experimentally calculated solidus/liquidus determinations. The decrease in Mg# may reflect a lack of oxidation at near solidus conditions, which is supported by the abundance of late stage pyrite in many appinite samples.

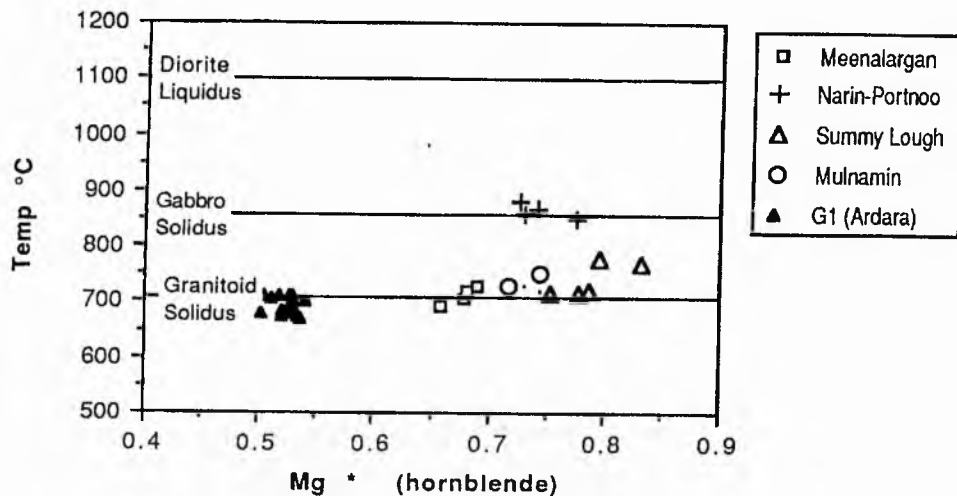


Fig. 4.24 Mg# versus temperature variation in granites and appinites from the Ardara igneous complex. Temperatures are those calculated in Fig. 4.22 & 4.23. Horizontal lines show reference temperatures for water saturated rock compositions. The diorite liquidus is from 1 kb experiments of Blundy (1989); the gabbro solidus at 2 kb is from Holloway & Burnham (1972) and is used in comparison with appinite results from the Ardara igneous complex; the granitoid solidus at 2 kb is from Piwinski (1975) is used to compare to the results for the Ardara pluton. (After Blundy & Holland 1990).

4.11.5 Discussion of results

The results presented above indicate a range of pressures of crystallisation of hornblende and plagioclase from ~3-8 kb. Such pressure are relatively high and suggest a depth of formation of 10-25 km for the appinites analysed. This is clearly an unrealistic result in view of the apparently high level characteristics of the rocks of the appinite suite, namely, associated explosion breccia pipes, emplacement of the appinites as sheets, plugs and domes of pipe-like form and the high content of volatiles of the appinites. Although none of the appinitic intrusions analysed in this barometry study were taken from breccia pipes, the Narin-Portnoo intrusion does exhibit some signs of brecciation but yields

pressures of ~ 8 kb. The Summy Lough intrusion which is one of the most intimately linked intrusions to the main Ardara pluton yields a pressure range of 3.25 - 4.55 kb. This result overlaps with that for the outer unit of the Ardara Pluton, (3.7 - 5.9 kb). Field evidence suggests a coeval relationship between the outer unit (G1) of the Ardara pluton and the Summy Lough diorite and the geobarometry data are consistent with this interpretation. However geobarometry estimates of ~ 3.7 - 5.9 kb for the Ardara pluton itself raise questions as to the accuracy of the geobarometer, as such pressures are difficult to reconcile in view of the proposed emplacement mechanism of the Ardara pluton, as a high level diapiric intrusion (Pitcher & Berger, 1972) although current views on diapirism indicate that they cannot be emplaced at very high levels (Miller et al. 1987). The accuracy of the geobarometer must be viewed critically. Vyhnal et al. (1991) indicate that the factors controlling Al substitutions in natural hornblendes, upon which the theory of the hornblende geobarometer depends have not yet been satisfactorily resolved. These factors include textural and chemical equilibrium.

(i) Textural Equilibrium

For aluminium in hornblende geobarometry to be applicable, quartz+plagioclase+K feldspar+hornblende+biotite+titanite+magnetite or ilmenite must be present as a magmatic, equilibrium assemblage (Hammarstron & Zen, 1986). All of these minerals are present in the thin sections analysed. Textures of the samples analysed correspond to the textures outlined earlier in this chapter (see sections 4.1 and 4.2) for granitoids from the main Ardara pluton (G1 and G2), diorite and coarse diorite from Meenalargan, meladiorite from Narin-Portnoo, diorite from Summy Lough and Mulnamin. Rare augite crystals in the granite of the main Ardara pluton often have concentric rims of hornblende which are interpreted as having formed by incomplete reaction of augite with the melt (Spear 1988). Textural relationships in the granitoids suggests that magnetite, plagioclase and K-feldspar crystallised early followed by hornblende (after augite), biotite, quartz and titanite and show typical magmatic-type mutual contacts. In the appinites it is more difficult to prove the primary nature of the textural relationships as some of the mutual contacts between minerals have angular metamorphic-type contacts as well as magmatic-type mutual contacts. Textural contact relationships suggest that primary hornblende, plagioclase and magnetite formed early followed by biotite, K-feldspar, titanite and quartz.

(ii) Chemical Equilibrium

The attainment of chemical equilibrium between the phases with the most variable composition in the samples studied, plagioclase, hornblende and biotite is difficult to prove, especially for the appinites. The presence of high levels of volatile in the form of H₂O and CO₂ and H₂S and the sub-solidus reactions which are thought to have occurred make the attainment of equilibrium very difficult to demonstrate. Linear trends on Mg# plots

of mineral pairs (section 4.11.2 iv) suggests that mafic minerals approached equilibrium compositions.

(iii) Calculated pressures and temperature of emplacement

Model crystallisation temperatures and pressures for each intrusion (Fig. 4.20-4.24) have been calculated. Blundy & Holland (1990) noted a strong temperature dependence of Al_{tot} in hornblende co-existing with plagioclase and suggested that barometric comparisons would only be valid if all rocks equilibrated at the same temperature. Temperature estimates for the granites vary from 670-710°C while those of the appinites vary from 694-880°C, (Fig. 4.24). For the appinites as a whole this temperature range is relatively large, although within individual intrusions the range is comparatively small. Indeed there seems to be a relationship between the calculated temperature and the pressure calculated for each intrusion (Fig. 4.25 a-e). This correlation is greatest for the outer unit of the Ardara pluton (G1) (Fig. 4.25 e). The temperature data indicates that over a small temperature range there is a relatively large pressure change, this suggests that the temperature effect alone cannot explain the data above.

It is concluded that the results of geobarometry determined for the appinites be viewed with caution because they may not meet all the constraints of the geobarometer as well as a real variation in the pressure through the interval of amphibole growth. The results for the granites must also be viewed with caution, although they have a more consistent trend and may be a more accurate indication of the approximate pressures of crystallisation of the Ardara pluton and are consistent with the estimated pressure of 3.7 - 4.0 kb and temperature of 500 - 700°C for the reaction,



for assemblages found in the Ardara thermal aureole (Naggar & Atherton, 1970).

4.12 PYROXENE

Compositions of the pyroxenes analysed in some of the rocks of the Ardara igneous complex are plotted in Fig. 4.26 (a). The most primitive rock type, cortlandtite from Kilrean, has both endiopside and orthopyroxene. Pyroxene from the outer unit (G1) of the Ardara pluton has an augitic composition and is often replaced by hornblende and/or biotite (Plate 4.15).

4.12.1 Pyroxene geothermometry

Estimates of the temperature of crystallisation of coexisting augite and orthopyroxene were made using the two-pyroxene geothermometer of Lindsley (1983), who proposed a graphical thermometer based on experimental data for Ca-Mg-Fe pyroxenes. Application of Lindsley's thermometer was made on pyroxenes from the

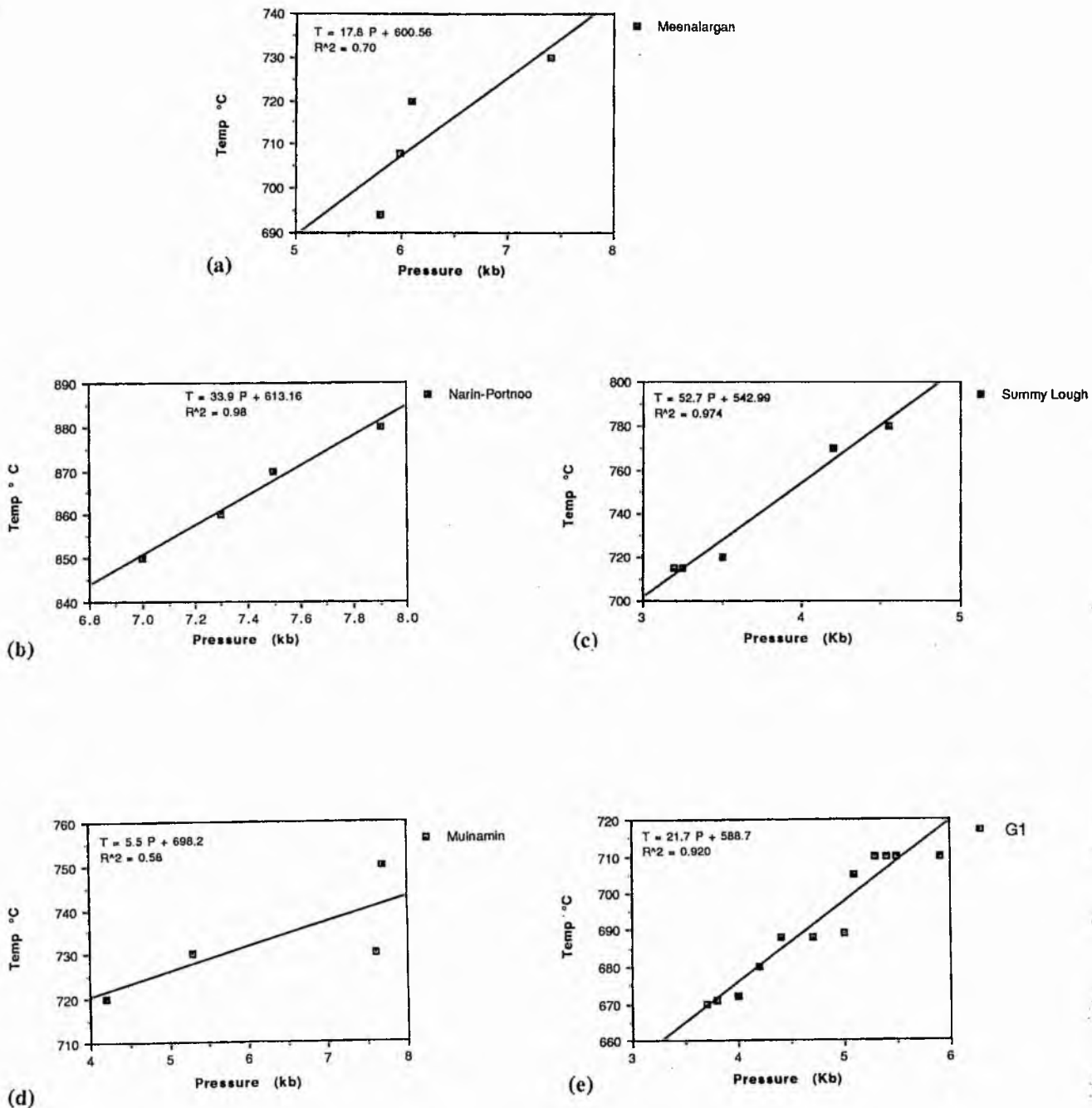
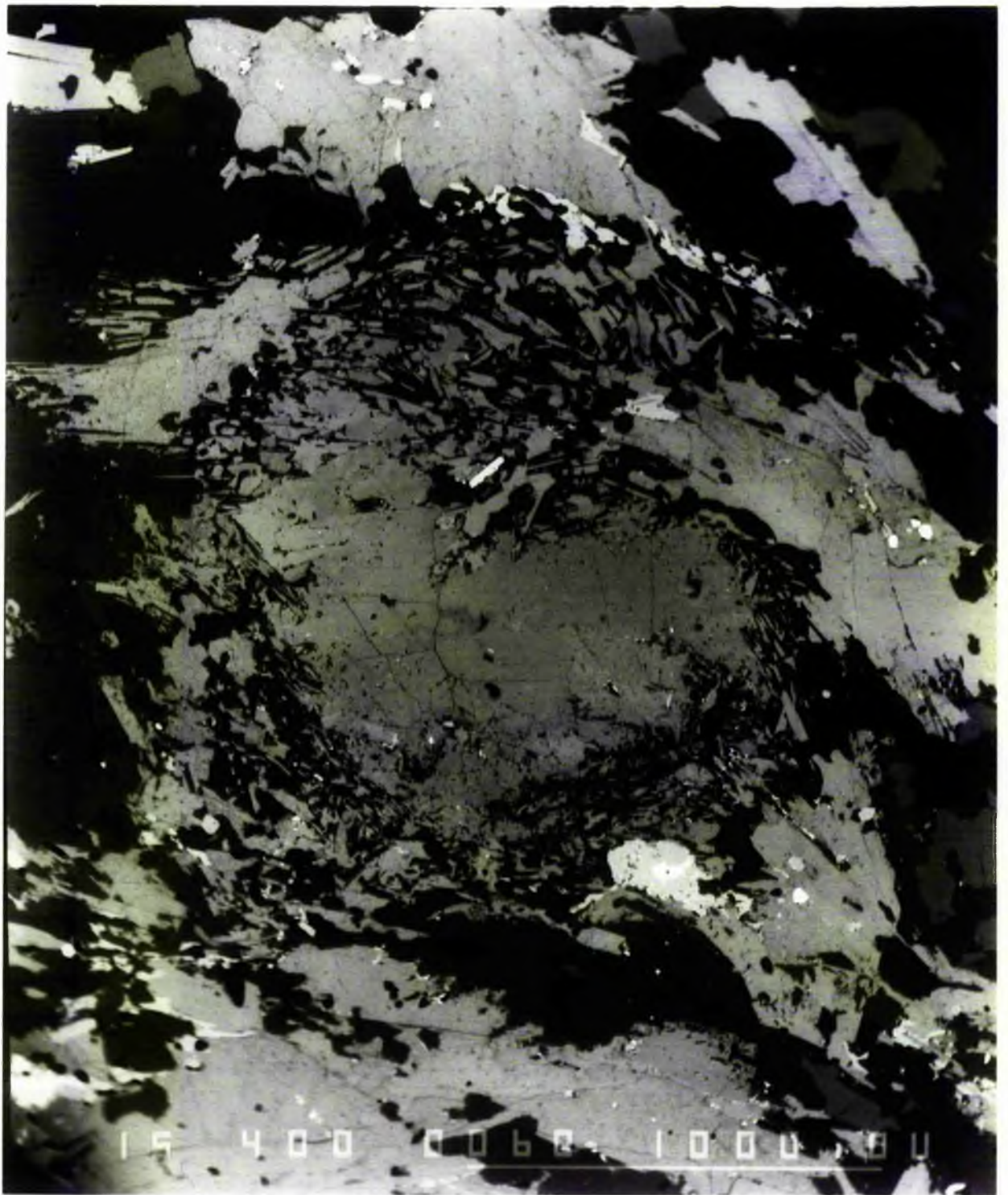


Fig. 4.25. Relationship between equilibration temperature, calculated from the hornblende-plagioclase geothermometer of Blundy & Holland (1990), and emplacement pressure, calculated from Hollister et al. (1987) based on Hammarstrom & Zen (1986). (a) Meenalargan, (b) Narin-Portnoo, (c) Summy Lough, (d) Mulnamin, (e) Outer granitoid unit (G1) Ardara Pluton.

Plate 4.15 ZCI of augite with biotite and quartz corona from the outer unit (G1) of the Ardara pluton (861). Augite forms the central part of the ZCI, it has a ragged margin which is corroded by a combination of intergrown quartz (dark grey) and biotite (light grey) in a graphic-type texture. Elongate (grey) minerals at the margins of the ZCI are hornblende. Conditions 15 kV, 20 nA, scale bar 100 μm .



cortlandtite from the Kilrean intrusion and also melagabbro from the Meenalargan intrusion (see section 4.16) and compared with the temperature estimates determined using the hornblende-plagioclase geothermometer of Blundy et al. (1990). Both the cortlandtite and the melagabbro contain coexisting augite and orthopyroxene, in the latter occurrence the augite and orthopyroxene are intergrown and may exhibit exsolution textures. Results obtained from the augite-orthopyroxene pair from the Kilrean cortlandtite are plotted in Fig. 4.26 (b). At a pressure of 5 kb the estimated temperature of crystallisation of the augite-orthopyroxene pair was 960°C. (b).

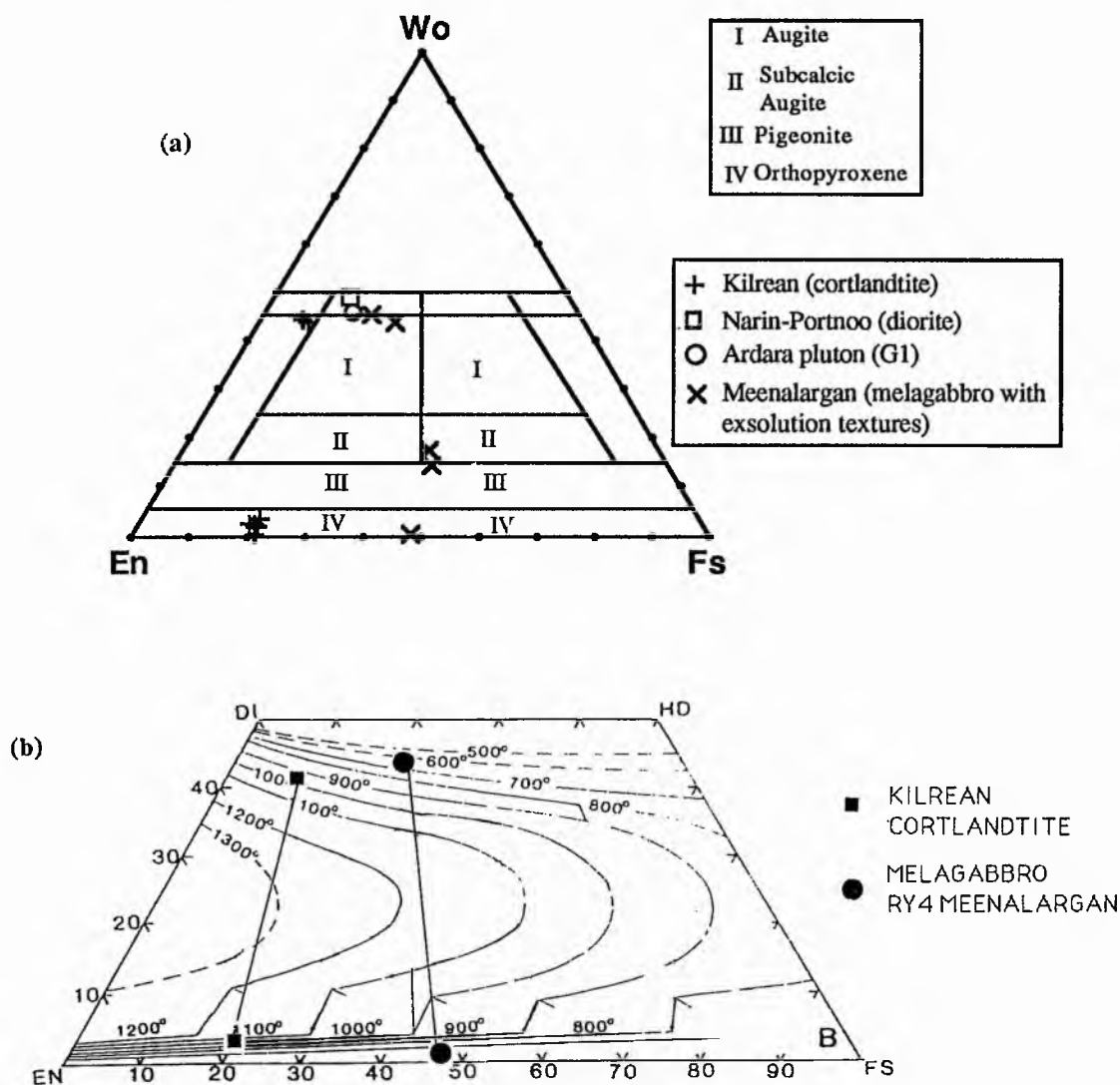


Fig. 4.26 (a) Compositions of pyroxenes analysed from the rocks of the Ardara igneous complex. (b) **Wo-En-Fs** compositions of augite and orthopyroxene of the Kilrean cortlandtite, projected onto the graphical thermometer of Lindsley (1983), using the correction procedure of Lindsley and Anderson (1983).

4.13 BIOTITE

The biotites from the granitic parts of the study area are largely unaltered and form distinct grains whereas those from some appinite intrusions can appear as replacement minerals associated with hornblende; only those biotites with primary characteristics were analysed. Biotites from the appinitic plutons exhibited limited compositional variation although marked differences exist between those of the main pluton and the appinites, (Fig. 4.27 a-d). No internal zoning patterns were discerned.

The most obvious difference between biotites in the granites and the appinites relates to variations in Mg and Fe in the octahedral site. The granitic biotites, including those of minor intrusions have Mg p.f.u. of 2.0 - 2.8 and Fe p.f.u. content of 2.0 - 2.6 compared with appinitic biotites which have Mg p.f.u. of 2.8 - 4.0 and Fe p.f.u. of 1.4 - 2.2 (see Fig. 4.27 a-d). The Mg# variations show a general overlap in composition of the appinites, with a depletion in Mg of the granites relative to the appinites Fig. 4.28.

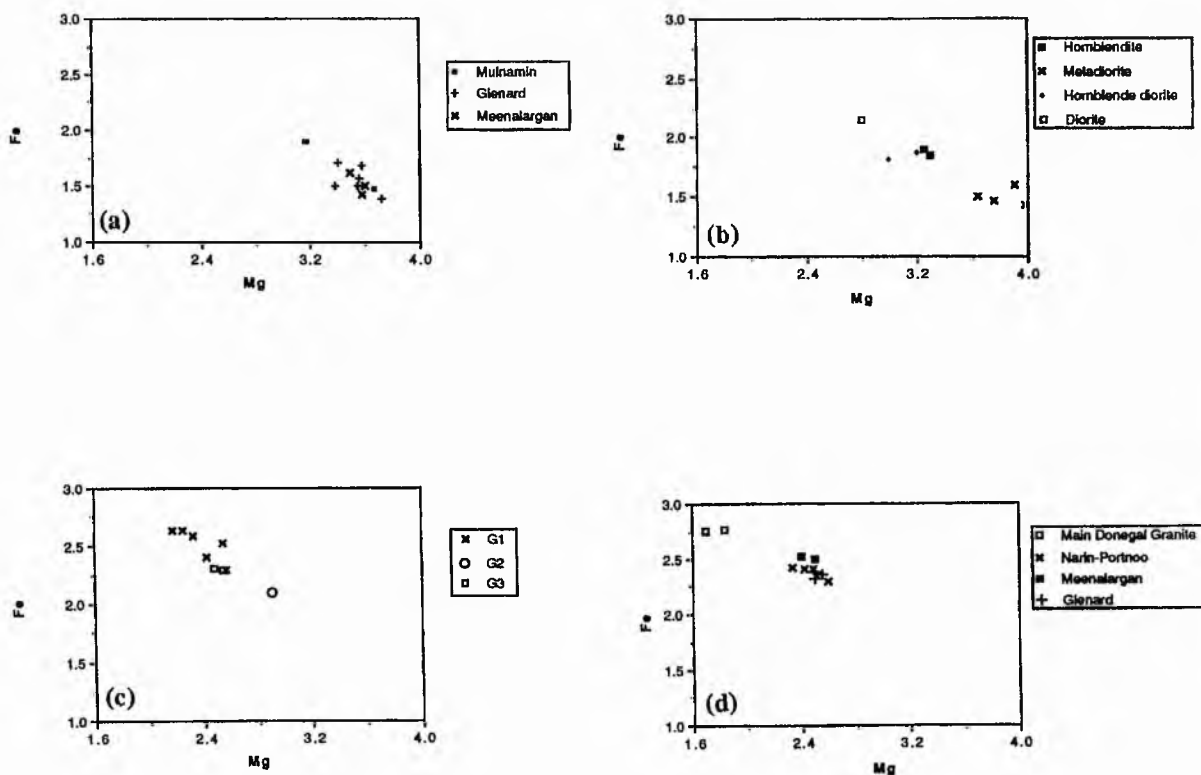


Fig. 4.27 a-d. Plots of Mg vs Fe in biotite highlighting the differences between biotite from granitoids and biotite from the appinites of the Ardara igneous complex.

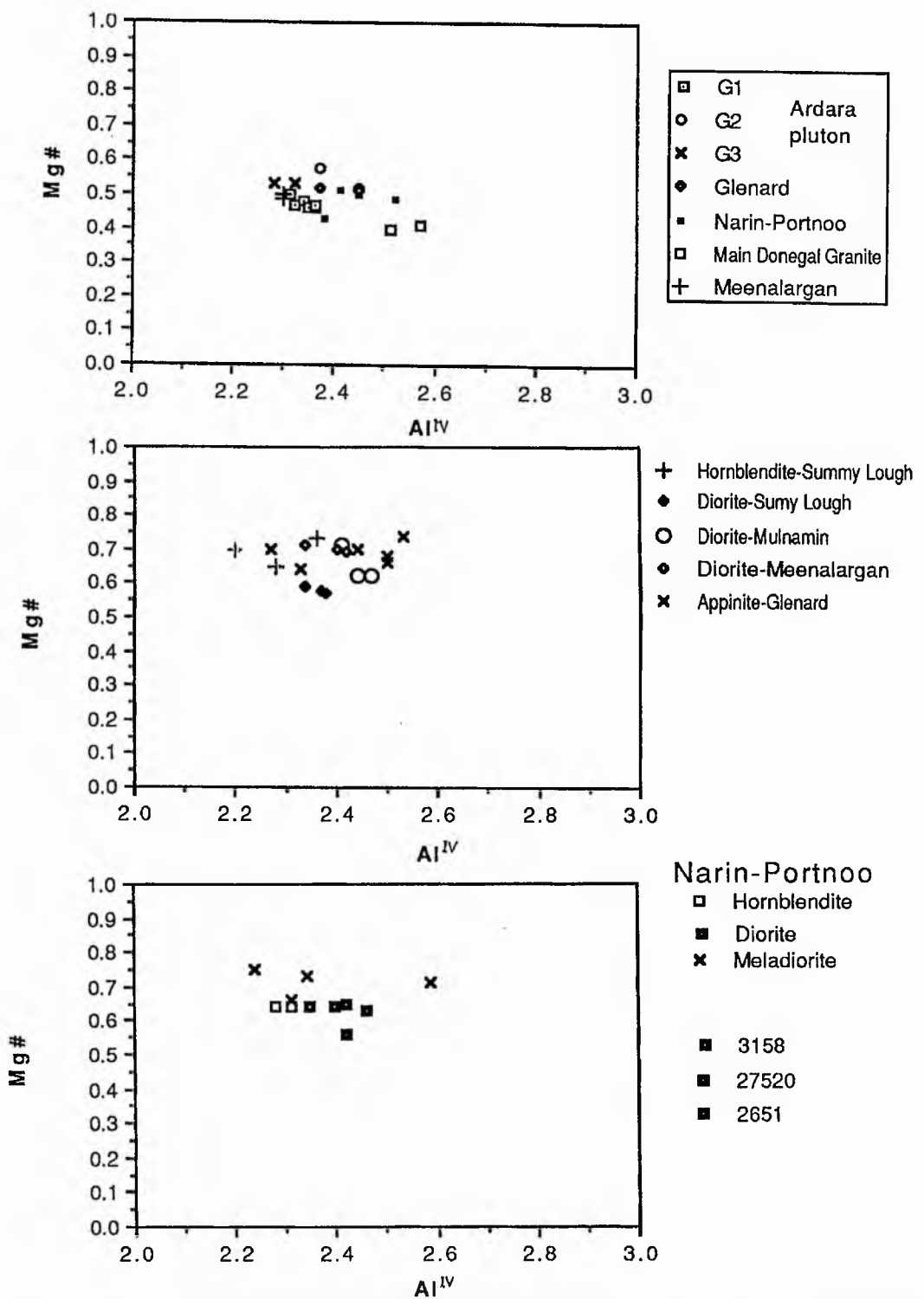


Fig. 4.28 Tetrahedral Al vs Mg# in biotite highlighting the differences between biotite from the granitoids and biotite from the appinites of the Ardara igneous complex.

Variation in biotite composition between the three granite facies of the Ardara pluton is limited to Mg/Fe content, being higher in Mg within the outer unit (G1) than the inner and central units (G2 and G3). The inner unit (G2) has the most Fe-rich biotites of the intrusion but there is no systematic link between the appinite and granite. Ti values for the granites (Fig. 4.29 a) are slightly higher than those of the appinites (Fig. 4.29 b-c). Within the granites and appinites there is a wide range in tetrahedral Al (Fig. 4.29 a). Al in the octahedral site is slightly greater in the appinites than the granites. This may relate to the

amount of Mg and Fe in the octahedral site as both of these are major constituents of the octahedral site (Fig. 4.30).

In terms of Si and K there is a general overlap in the compositions of the biotites from the appinites and granitoids (Fig. 4.31).

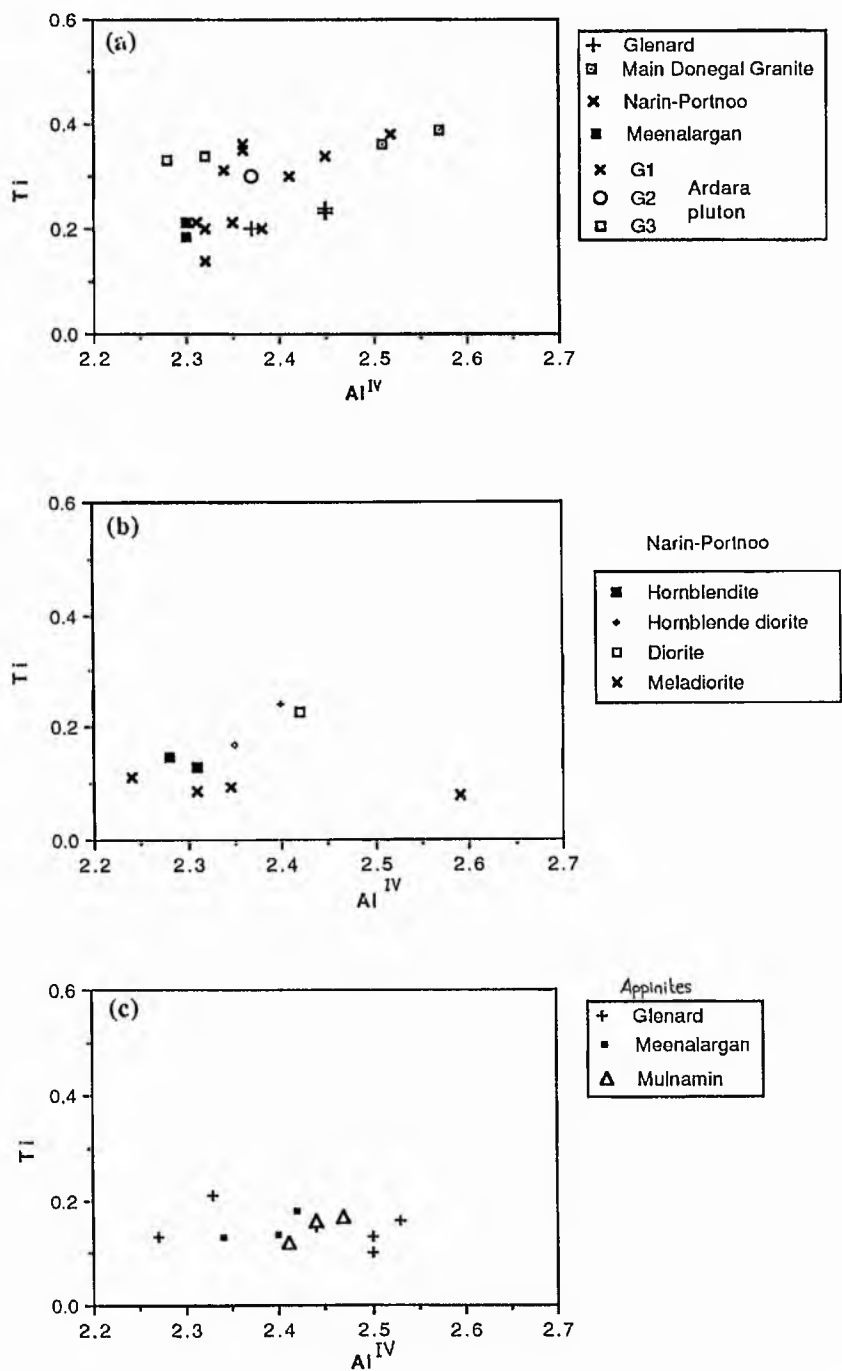


Fig. 4.29 Al^{IV} v Ti variation plot comparing the composition of the (a) granites of the Ardara pluton and igneous complex with (b) the appinites of the Narin-portnoo complex and (c) the Glenard, Meenalargan and Mulnamin complexes

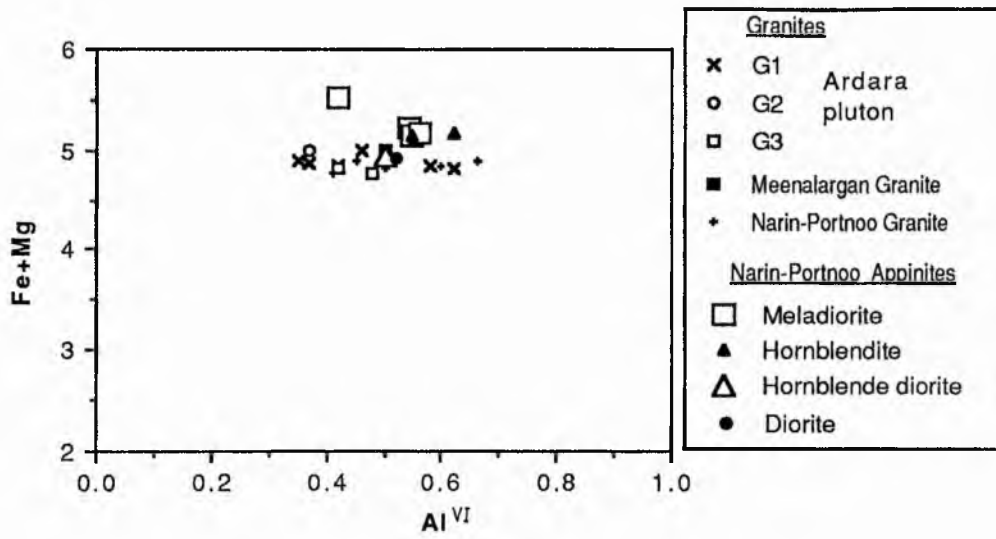


Fig. 4.30 Octahedral Al v Fe+Mg variation plots in biotites from granitoids and appinites of the Ardara igneous complex.

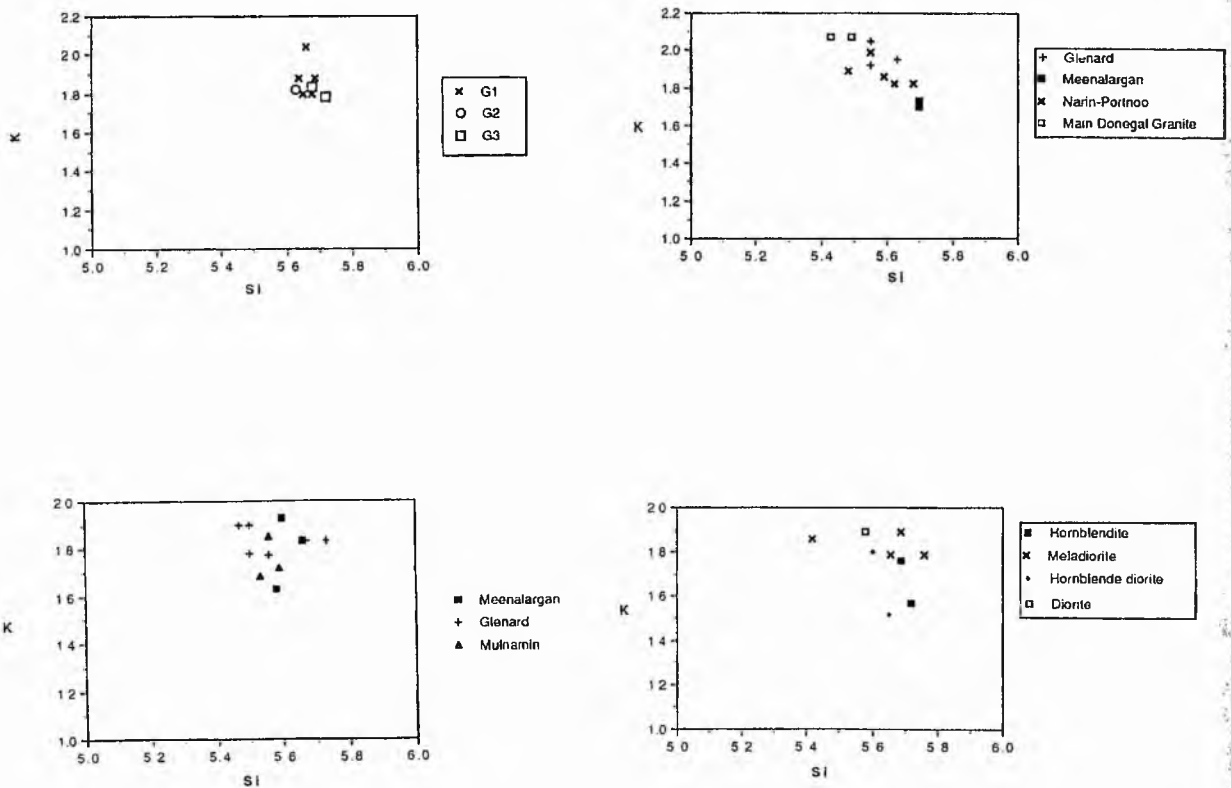


Fig. 4.31 Si v K variation in biotites from the granitoids and appinites of the Ardara igneous complex.

Compositionally the biotites of the appinites and granites are both phlogopites and biotites (Deer et al. 1966) (Fig. 4.32).

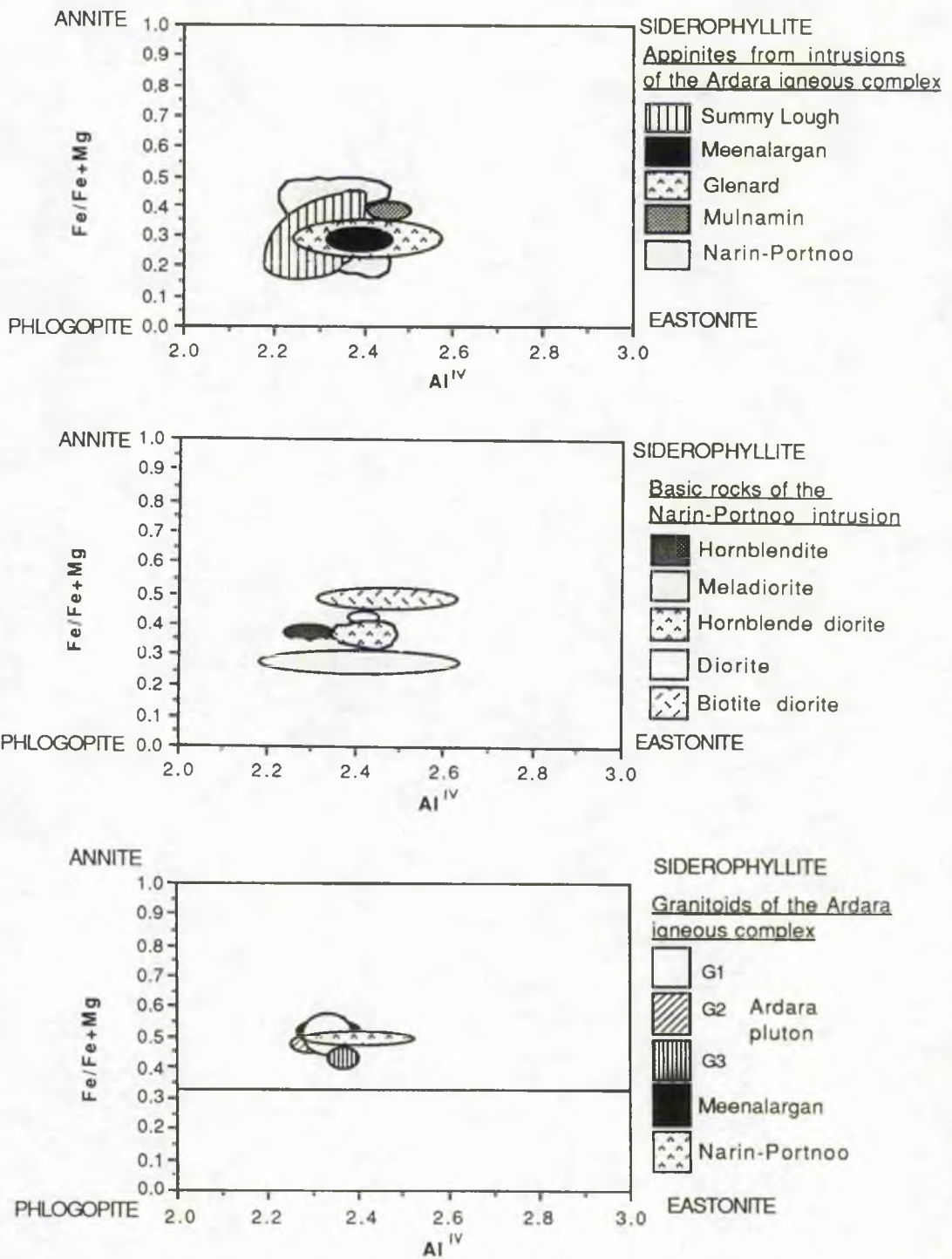


Fig. 4.32 Compositions of biotites from the appinites and granites from the Ardara igneous complex within the classification scheme of Deer et al. (1966).

4.14 PLAGIOCLASE FELDSPAR

Plagioclase is commonly zoned in both appinites and granites. The nature of the zoning has been described in sections 4.1 and 4.2, and the results of microprobe analysis are discussed briefly here.

(i) Appinite

The most calcic compositions are found in meladiorites but zoning is not well defined in the appinites. It is often continuously zoned with a calcic core and more sodic margin, but the calcic core is often sericitised. Fig. 4.33 shows the variations in An of plagioclases from the different intrusions of the Ardara igneous complex.

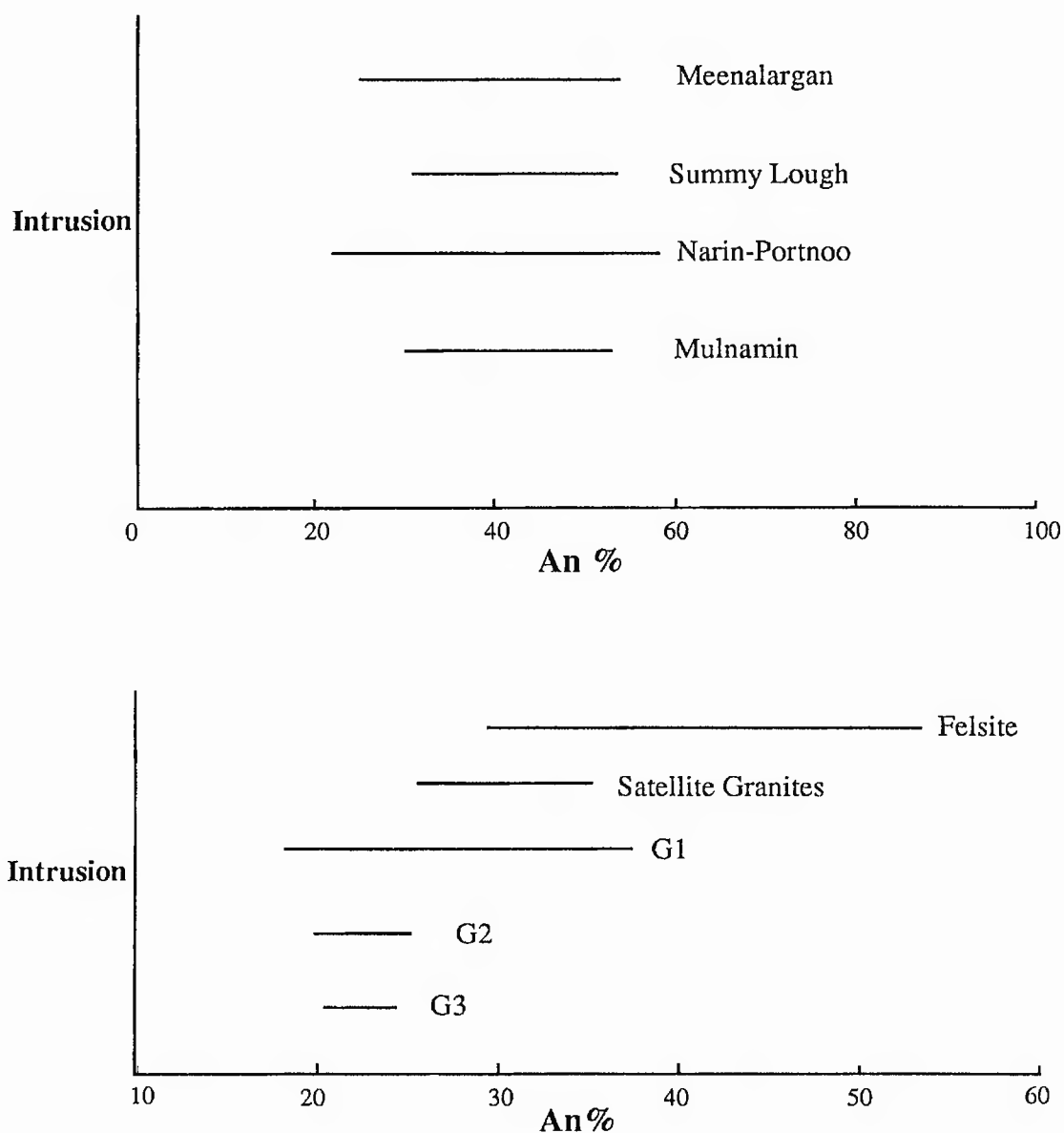


Fig. 4.33. Plagioclase composition plots for members of the Ardara igneous complex.

(ii) Granite

Plagioclase compositions in the main Ardara pluton units (Fig. 4.33) are more sodic than the appinites and vary between An_{13} and An_{27} . Zoning is best seen in the central unit of the Ardara pluton where plagioclase usually has a continuously zoned form. Other satellite granite intrusions show similar zonation patterns as the main Ardara pluton, with fine zones of differing An composition between core and margin (Plate 4.13).

4.15 EPIDOTE

Epidote was found in some appinite and granite samples, mostly in the form of a late stage hydrothermal mineral associated with clinozoisite and muscovite. However in a few samples epidote was found in association with hornblende and biotite (Plate 4.16) with apparent primary igneous contacts. Primary epidote has been described from a tonalite and granodiorite complex in the Feather River region of northern California (Zen & Hammarstrom, 1984), as euhedral grains against biotite and enclosing rounded and highly embayed hornblende crystals, which elsewhere in the Feather River region are enclosed within plagioclase. It is therefore apparent that the epidote crystallised around the hornblende resorbed by the melt and not in sub-solidus reaction. This magmatic origin of epidote is further supported by its occurrence in flow banding within the granitoid of the Feather river region (Zen & Hammarstrom, 1984). Such primary textural criteria are met by the epidote of Plate 4.16 and although the textural criteria to distinguish magmatic epidote from epidote that forms by subsolidus (deuteric) reactions are not well established (Vyhnal et al. 1991), the epidote in this particular meladiorite does not overgrow allanite and does not form wormy intergrowths with plagioclase, which are some of the criteria outlined by Zen & Hammarstrom (1984) to determine the magmatic nature of epidote. One important criterion which might suggest a subsolidus origin of the epidote in the above meladiorite is the occurrence of epidote in rocks which are effected by deuteric alteration.

Naney (1983) in experimental studies of granitic systems, noted the appearance of epidote between 600 and 700°C at 8 kb but not at 2 kb and depending on the H₂O content of the melt the epidote crystallised with biotite and plagioclase. He noted a maximum temperature range of 30°C in which epidote and hornblende co-existed. Naney showed the epidote to have a pistacite (atomic Fe⁺³/(Fe⁺³+ Al)) content of 27-30% and the hornblende to contain 2.2 Al per 23 oxygens. Zen & Hammarstrom, like Naney (1983), also described epidote with 27-30 % pistacite in association with hornblende of Al = 2.2. Significantly epidote from the meladiorite of Plate 4.16 has a composition of 25% pistacite and hornblende has 2.23 Al. The experimental data showed that within the melt interval the assemblage changes from:

Plagioclase+hornblende+biotite+melt ————— plagioclase+epidote+biotite+melt

Plate 4.16 ZCI of hornblende, biotite and epidote from meladiorite (Y2658) from the Narin-Portnoo intrusion. Hornblende is the large dark crystal with a light actinolitic rim in bottom left of photomicrograph. This hornblende has an embayed contact with a small biotite crystal (centre) which in turn has an apparently primary igneous contact with a zoned epidote crystal. Note also the patchy zoning of hornblende. Conditions 15 kV, 20 nA, scale bar 100 μm .

In the Narin-Portnoo intrusion there is evidence for both primary epidote formed by the above reaction (Plate. 4.16) and secondary formed after hornblende and biotite. The epidote illustrated above (Plate 4.16) has an apparently primary contact with biotite adjoining hornblende, although where directly in contact with hornblende it appears distinctly anhedral. The estimated pressure of crystallisation of the meladiorite from which the epidote is analysed using the hornblende geobarometer is 7.0-7.9 kb which may support the primary crystallisation nature of this epidote. However, alternatively given the presence of deuteritic-type alteration in this rock, the epidote may be a product of sub-solidus reaction of hornblende in association with biotite.

4.16 EXSOLUTION TEXTURES IN A MAFIC ROCK FROM MEENALARGAN

A mafic rock sample taken from 10m south of Crocknadreavarh (G7952 9687) was found to contain augite and hornblende crystals with exsolution lamellae, which have not been described before from any metadolerite in the Caledonides of the British Isles. The sample examined comes from an isolated outcrop of melagabbro (CI=90%) with uncertain field characteristics. The outcrop is isolated by moss and peat and contact relationships with the other rocks of the intrusion are uncertain. It appears in the field as a lensoid intrusion surrounded by diorite and may be a continuation of a metadolerite sill seen to the east, although it has a higher colour index (CI=90%) than that of typical metadolerite (CI=70%). The rock is greeny-black in colour when fresh, with a porphyritic texture of 5mm diameter rounded clots of hornblende and pyroxene surrounded by a finer grained mesostasis of both pyroxene and hornblende and minor plagioclase.

4.16.1 Petrography

The melagabbro has a texture of rounded globular glomeroporphyritic clots of augite, orthopyroxene, hornblende and ilmenite enclosed pseudo-ophitically by elongate and stumpy plagioclase laths in the mesostasis.

Glomeroporphyrites occur as rounded clots composed of mutually interfering, highly interlocking crystals of augite (40%), hypersthene (5%) and hornblende (20%). Plagioclase is present in the clots as an interstitial phase trapped between interfering crystals of pyroxene. Augite forms colourless to grey crystals of rounded form with occasional grass-green pleochroism which appear dusty and granular due to the presence of orthopyroxene inclusions and microscopic lamellae. Anhedral hypersthene crystals form an enclosing mesostasis between augite crystals and also occur as bleb-like inclusions within augite. Hornblende occurs in two discrete textural forms. The first occurs within the clots as ragged green crystals which replace, and sometimes enclose, augite (Plate 4.17). The second occurs outside of the clots and is described below. Biotite occurs within the clots forming ragged secondary flakes which replace augite parallel to cleavage (010) at a late stage in the crystallisation sequence.

Plate 4.17 ZCI of the pyroxene exsolution textures from a melagabbro enclave within the Meenalargan dioritic complex. Orthopyroxene forms the bright crystal to the top of the ZCI and bright inclusions within augite which forms the rounded grey crystals occupying most of the photomicrograph. Actinolitic hornblende forms small ragged clots within augite, these often transect the lamellae. Augite has rounded contacts with plagioclase. Conditions 15 kV, 20 nA, scale bar 100 μm .



The groundmass is formed of interlocking plagioclase and some large phenocrysts of hornblende. The hornblende also occurs as large crystals up to 0.5cm across which have good igneous contacts with plagioclase and also enclose it, suggesting an overlap in the period of growth of the two minerals. These large hornblende crystals have a fine dusting of iron oxide giving the hornblende a turbid appearance. Plagioclase occurs as fresh crystals of plagioclase (An₄₀₋₅₅) as interlocking laths which enclose augite clots. The plagioclase laths are occasionally embayed by the augite clots and plagioclase crystallisation appears to have occurred towards the end of augite crystallisation. Quartz forms a minor mesostatial phase commonly associated with plagioclase. The lamellar intergrowth of pyroxene apparently involves subsolidus intergrowth in the mafic phases, particularly pyroxene, and consequently a detailed textural/compositional study of this feature was performed using electron microprobe techniques.

4.16.2 Microprobe analysis: mineral chemistry and microtextures

Electron microprobe analyses were made of all the main phases within the glomeroporphy, as well as the exsolution lamellae within the different phases. The phases present were found to be augite, subcalcic augite, hypersthene and calcic hornblende (Fig. 4.34). Backscattered electron imagery highlights differences in composition according to the mean atomic number (Z number). The difference between minerals is seen as variation in degree of grey-scale minerals with a high mean atomic number such as hornblende, pyroxene, opaques are white or light grey while those with a low mean atomic number have a dark grey colour. Those minerals with intermediate mean atomic numbers have intermediate shades of grey.

The pyroxene host to the exsolution lamellae has a calcic augite composition. The lamellae which are enclosed within this augite have a complex form. They form two sets, which intersect at 70° in this section with an apparent crystallographic control. In some crystals one set of lamellae is dominant over another (Plate 4.17). The dimensions of the lamellae are not consistent, width varying from 1-2µm and length varying up to 50µm but more typically ~20µm. The lamellae have irregular apophyses which often pinch out sharply. Plate 4.17 also shows a later stage of hornblende replacement which takes the form of rounded elongate inclusions of hornblende within pyroxene. These appear to overprint the pyroxene structure and never occur within the hornblende; thus they may be related to a late stage of hornblende growth or alternatively may be a later stage where pyroxene has crystallised after the hornblende and the lamellae formed.

Plate 4.17 shows typical relationships between the individual phases within the crystal aggregates. Within augite the two orientations of lamellae can be seen to intersect at 70°. These have been analysed at their widest parts and are found to be subcalcic augite. Blebs and inclusions of hypersthene are present in the augite. These often lie parallel to the sub calcic augite lamellae and seem to be of a similar size to them, however they do not

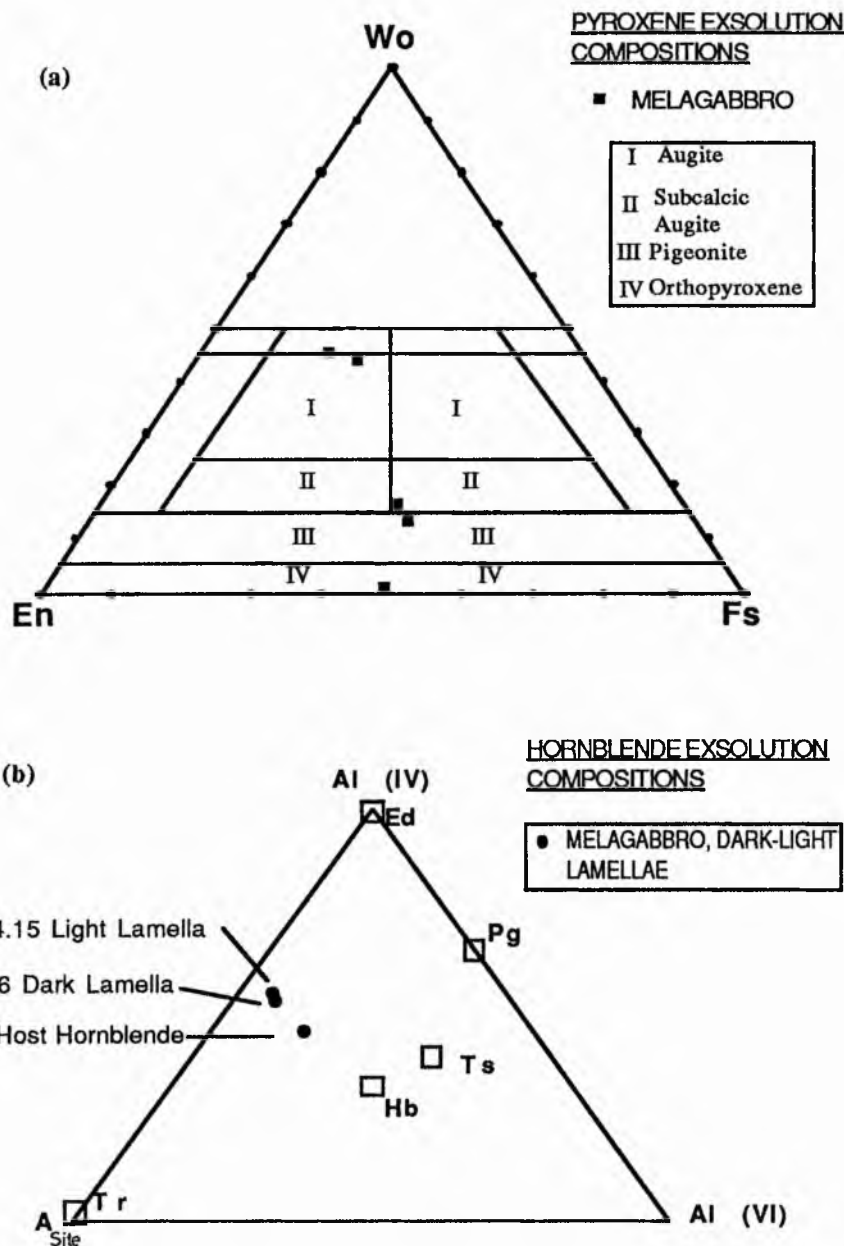


Fig. 4.34 Compositions of the mineral phases involved in exsolution textures in melagabbro: (a) Pyroxene compositions plotted in the pyroxene quadrilateral, (b) Hornblende compositions plotted in relation to Al^{IV} and Al^{VI} and vacancy in the A site (Ed=edenite, Pg=pargasite, Ts=tschermakite, Hb=hornblende, Tr=tremolite/actinolite).

appear to be an exsolution feature as they are irregular in form and also occur as a primary phenocrysts along with augite; thus they are more likely to be inclusions. The sub calcic augite lamellae are depleted in TiO₂, Al₂O₃, CaO and Na₂O and enriched in FeO, and MgO compared with the host augite (Table 4.7).

Element	Sample	Sample	Sample	Sample	Sample
	Orthopyroxene	Augite Host	Subcalcic Augite	Subcalcic Augite	Augite Host
	RY4.1	RY4.2	RY4.4	RY4.5	RY4.10
SiO ₂	50.60	50.22	50.83	50.62	50.90
TiO ₂	0.21	0.35	0.20	0.23	0.50
Al ₂ O ₃	1.35	2.17	1.60	1.83	2.84
Cr ₂ O ₃	0.00	0.00	0.00	0.03	0.03
Fe ₂ O ₃	0.66	2.39	1.47	1.37	1.53
FeO	28.02	9.48	24.49	25.96	10.05
NiO	0.00	0.00	0.00	0.01	0.03
MnO	0.53	0.25	0.54	0.63	0.29
MgO	17.27	11.59	13.90	14.02	11.39
CaO	1.06	21.77	8.31	6.72	22.13
Na ₂ O	0.00	0.44	0.11	0.11	0.49
K ₂ O	0.00	0.02	0.00	0.01	0.01
Total	99.71	98.68	101.45	101.54	100.19

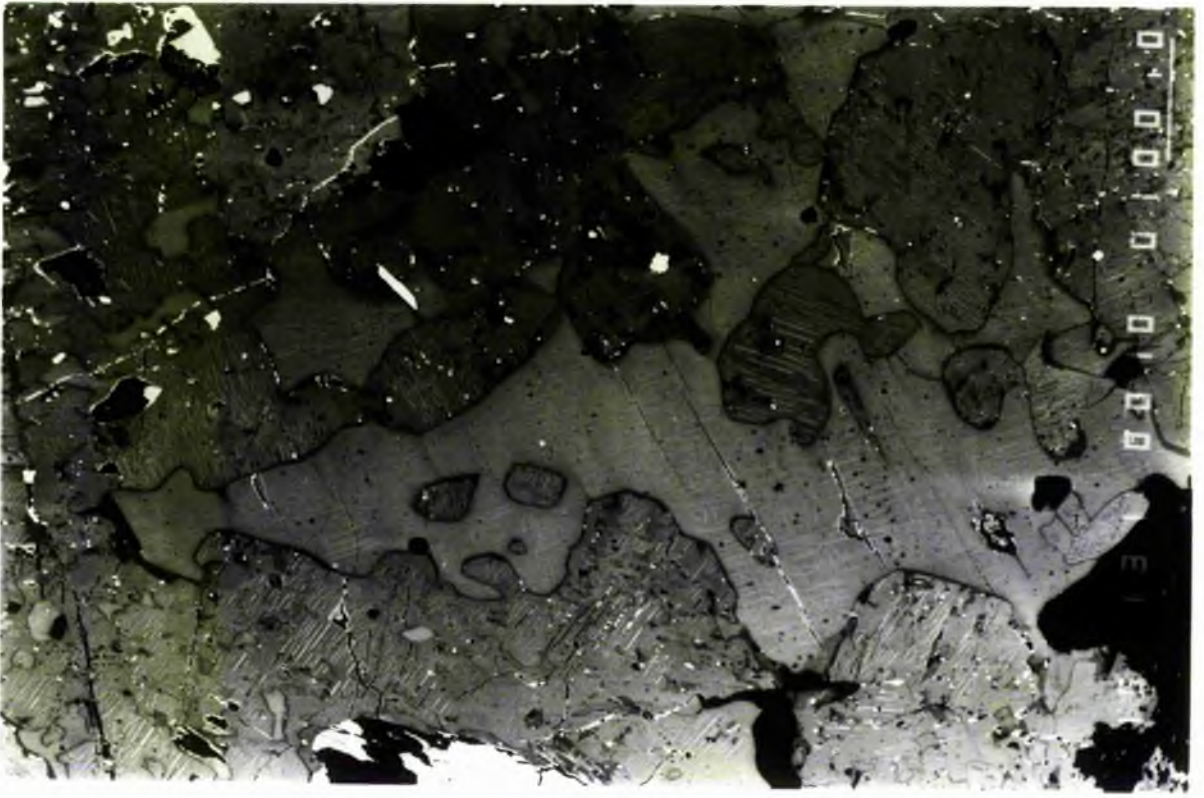
Table 4.7 Pyroxene compositions of the main phases, orthopyroxene, augite host and subcalcic augite lamellae compositions from melagabbro sample RY4. Structural formulae are tabulated in Appendix 5.

Plates 4.18 (a and b) show the relationship between the hornblende and pyroxene lamellae in backscattered electron imagery. The orthopyroxene lamellae within augite in Plate 4.18 (a) have relatively high mean atomic numbers and appear as bright mineral lamellae compared to the augite and hornblende. The hornblende appears as a light grey phase with poorly defined exsolved lamellae. Plate 4.18 (b) shows three crystals of augite and orthopyroxene lamellae enclosed within one single hornblende prism, both crystal types show exsolution but the contact between the two exhibits a zone of reaction of two variable compositions (dark and very dark) of actinolitic composition. This reaction appears to overprint the exsolution as in some places the lamellae may be seen to pass through the reaction zone.

The hornblende crystals within the glomeroporphy also show exsolution features similar in form to those of the pyroxene crystals. Within the hornblende the lamellae are less well defined although, as in the augite, there are two sets of lamellae that appear to be crystallographically controlled intersecting at $> 80^\circ$ (Plate 4.18 b). The hornblende lamellae have similar dimensions and pinch out sharply at their ends. Compositionally the lamellae vary in a more irregular fashion than the augite lamellae (Table 4.8)

Plate 4.18 (a) ZCI of pyroxene and hornblende exsolution textures from a melagabbro enclave within the Meenalargan dioritic complex (RY4). Rounded augite within orthopyroxene and subcalcic augite blebs and lamellae are enclosed within a large hornblende crystal. The hornblende is light grey with poorly defined exsolution lamellae (see text for composition). Rounded hornblende (actinolite) overgrows augite (top left of photomicrograph). Conditions 15 kV, 20 nA, scale bar 100 μm .

Plate 4.18 (b) Higher magnification ZCI of centre of Plate 4.18 (a) showing pyroxene and hornblende exsolution textures from a melagabbro enclave within the Meenalargan dioritic complex (RY4), showing three augite crystals with subcalcic augite lamellae enclosed by a large hornblende crystal. The hornblende crystal exhibits irregular lamellae, two sets of lamellae intersecting at 80° . There is an actinolitic (dark) alteration rim around the augite lamellae. This rim also overgrows the hornblende with lamellae suggesting that it is later than both these phases. Conditions 15 kV, 20 nA, scale bar 100 μm .



ELEMENT	SAMPLE	SAMPLE	SAMPLE	SAMPLE
	Host RY4.1	Light Lamella RY4.15	Dark Lamella RY4.16	Actinolite clot RY4.2'
SiO ₂	45.424	45.981	45.806	54.300
Al ₂ O ₃	9.204	9.152	8.917	1.155
TiO ₂	1.035	0.030	0.045	0.110
FeO	19.281	18.039	20.142	13.897
MnO	0.270	0.162	0.299	0.130
MgO	11.003	10.672	10.823	15.827
CaO	10.312	11.545	9.572	12.118
Na ₂ O	1.180	0.845	0.813	0.000
K ₂ O	0.793	0.501	0.512	0.041
Total	98.502	96.927	96.929	97.690
Number of ions based on 24 oxygens				
Si	6.85	7.21	7.24	7.49
Al IV	1.16	0.79	0.76	0.51
Al VI	0.46	0.87	0.88	0.32
Ti	0.12	0.04	0.01	0.01
Fe	2.45	2.36	2.66	1.63
Mn	0.03	0.02	0.04	0.01
Mg	2.47	2.49	2.57	3.25
Ca	1.67	1.93	1.62	1.79
Na	0.34	0.26	0.25	0.03
K	0.15	0.10	0.10	0.01

Table 4.8 Compositions of hornblende host, light and dark lamellae from melagabbro sample RY4, Meenalargan.

The exsolution lamellae are of generally similar composition to their host (Table 4.8) but vary in SiO₂, Al₂O₃, MgO, FeO and CaO by a maximum of 2 wt% (Fig. 4.35). It may be seen from the graph that there is a 0.24% decrease in Al₂O₃ and a 1.90% decrease in CaO, but an increase of 0.15% for MgO and 2.15% for FeO between host and lamella. There is an overall trend of decreasing Ca and increasing Fe in the hornblende lamellae compared with the host. It should be noted that problems of background interference and the problem of lag in the position of the peaks and troughs not always being precisely coincident with the lamellae (due to the small size of the lamellae and the scan rate not matching the response time of the detectors) make accurate analysis by electron microprobe difficult, although the trace generally supports the findings of the point analyses on the lamellae.

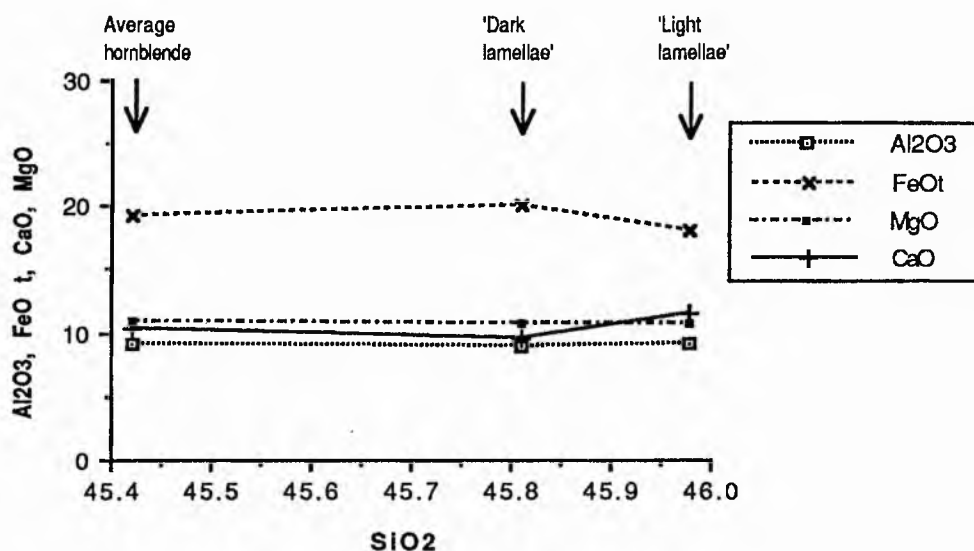


Fig. 4.35 Plot of SiO₂ versus Al₂O₃, FeOt, CaO and MgO showing the compositional differences between host hornblende and lamellae

4.16.3 Origin of exsolution

Within the pyroxenes and amphiboles of this melagabbro there has been exsolution of various phases as described above. Such features have been taken by various authors to imply solid state reaction, (e.g. Tagiri 1977, Robin & Ball 1988, Ollila et al. 1988, Ghose 1981). The process of the exsolution of one mineral within another occurs because the originally homogeneous crystal becomes supersaturated with a dissolved element or oxide, usually as a result of a decrease in temperature (Henderson 1982). The process of exsolution is one of redistribution of elements and may occur by one of two processes.

(a) Nucleation and growth of the phase, where the nucleation is homogeneous or heterogeneous and the exsolved phase is of a fixed stoichiometric composition. The compositional fluctuations are large in magnitude but small in extent (Buseck et al. 1982).

(b) Spinodal decomposition which occurs when the exsolved phase is of a variable composition but not very different from that of the host and there is no separate nucleation event. Spinodal decomposition occurs as compositional waves are set up within the homogeneous phase in the initial stages of exsolution. These compositional modulations subsequently develop as regularly spaced exsolution lamellae (Ghose 1981), and unlike those formed by nucleation, they are large in extent and small in magnitude (Buseck et al. 1982).

Slow cooling rates are thought to favour homogeneous nucleation with the exsolved phase reaching its complete development over a short time. Rapid cooling rates however

are thought to favour spinodal decomposition and if cooling is very rapid the exsolved phase may not attain its full development. Spinodal decomposition is less dependent on element diffusion and can occur at lower temperatures than homogeneous or heterogeneous nucleation (Henderson 1982).

For hornblende exsolution Tagiri (1977) suggested that the lamellar intergrowths of actinolite and hornblende in some metamorphosed igneous rocks represent an equilibrium assemblage which may indicate a miscibility gap. Oba (1980) found that amphibole compositions from skarns and marbles showed the existence of a compositional gap whereas amphiboles from the igneous environment at high temperature and high pressure did not show a compositional gap. Immiscibility is to be expected between two amphiboles where:

(i) The M4 site is filled by large cations such as Ca^{2+} in one amphibole and small cations such as Fe^{2+} and Mg^{2+} in the other (e.g. Hornblende-Cummingtonite).

(ii) The A site is fully or partially occupied in one and empty in the other (e.g. Hornblende-Actinolite, Hornblende-Cummingtonite).

(iii) The M4 site is Ca^{2+} in one and Na^{2+} in the other (e.g. Actinolite-Riebeckite), Ghose (1981).

It is necessary to prove the existence of chemical equilibrium in order to use such mineral pairs as immiscibility gaps. The small variation in composition of the hornblende seen may suggest disequilibrium or that the feature may be an intergrowth of one amphibole in another. To prove this a single crystal X-ray study is required.

Exsolution in pyroxenes is a complex function of bulk composition, maximum temperature and cooling rate (Robinson et al. 1982). Pyroxenes from basalts, dolerites and gabbros tend to show the most complex arrays of exsolution lamellae because, in the case of gabbros, the pyroxenes initially crystallised at high temperatures ($>1000^\circ\text{C}$), and then underwent slow cooling during which exsolution lamellae could form. Growth of lamellae requires solid state diffusion and diffusion rates are sensitive to temperature. Hence high temperature lamellae tend to be large and few in number, while low temperature lamellae which form by slow diffusion will be large in number and small in size. The two different orientations of pyroxene lamellae seen in this study may have formed as a result of the anisotropy with respect to diffusion which pyroxenes exhibit (Robinson et al. 1982). As a result of this anisotropy it is possible that finer lamellae of one composition may form in one direction which differ in composition from those coarser lamellae growing in another orientation. Furthermore, localised ion exchange processes may occur between the host and lamellae that may complicate the pattern of exsolution lamellae.

The temperature of formation of co-existing augite and orthopyroxene from the melagabbro was estimated using the experimental two pyroxene thermometer of Lindsley & Anderson (1983). Estimated results show that at an arbitrary pressure of 4 kb the temperature of crystallisation of co-existing augite and orthopyroxene is $633 \pm 14^\circ\text{C}$ (Fig.

4.26). This temperature is much lower than the experimentally determined temperature of crystallisation of pyroxenes of Lindsley (1981) who found that pigeonite forms at $825 \pm 10^\circ\text{C}$ at greater pressure than those of the melagabbro, (11.5 kb) and that pyroxenes are stable at $800\text{-}1000^\circ\text{C}$. Exsolution of orthopyroxene and augite has been described from anorthosites, mangerites and charnockites from the Adirondacks and elsewhere by Bohlen & Essene (1978) who noted that the exsolution lamellae of coarse pyroxenes and small equant coexisting pyroxenes (with little/no exsolution) similar to those of this study yield estimated temperatures of 750°C , which Bohlene & Essene found to be consistent with equilibration during granulite-facies metamorphism.

4.17 CONCLUSIONS

(i) Amphibole present in appinites ranges in composition from ferroan pargasite, magnesio-hornblende to edenite and actinolite.

(ii) Variation in amphibole composition is present within some individual appinitic intrusions, notably from Narin-Portnoo where the range in rock types is most variable. The more explosively emplaced appinitic intrusions in the Ardara area, Biroge and the Mulnamin breccia are more actinolitic in composition with Mg enrichment and depletion in Al IV.

(iii) Amphiboles from the granites of the main Ardara pluton have a compositional range from tschermakite to magnesio-hornblende and actinolitic hornblende. The amphiboles from the inner unit (G2) have a slightly higher Mg content than those of the outer unit (G1).

(iv) Hornblende geobarometry of the granitic units of the main Ardara pluton yields apparent crystallisation pressures of:

3.7 - 5.7 kb (G1)

4.1 - 5.9 kb (G2)

(v) Appinite geobarometry results are viewed with caution in the light of the parameters outlined by Hollister et al. (1987). Results obtained yield very high estimated pressures of :

- | | |
|----------------------------|----------------------------|
| (i) Meenalargan: | 8.0 kb (coarse diorite) |
| | 5.8 - 7.4 kb (diorite) |
| (ii) Narin-Portnoo: | 7.0 - 7.9 kb (meladiorite) |
| (iii) Summy Lough Diorite: | 3.2 - 4.5 kb (diorite) |
| (iv) Mulnamin: | 4.2 - 7.7 kb. (diorite) |

(vi) Appinite geothermometry, assuming a pressure of 5.0 kb yielded a temperature for co-existing hornblende and plagioclase of 750 - 900°C.

(vii) Granite geothermometry using the amphibole-plagioclase geothermometer of Blundy yielded a temperature of crystallisation of co-existing hornblende and plagioclase of 680 - 710°C at 5.0 kb for the outer unit (G1).

(viii) Results of pyroxene geothermometry using Lindsley's two-pyroxene geothermometer (Lindsley 1983) yielded a crystallisation temperature of 960°C at a pressure of 5 kb in the Kilrean cortlandtite.

(ix) Biotite composition is relatively similar amongst the individual appinitic intrusions. The granites vary markedly in Mg and Fe content in relation to the appinites. Within the granites variation exists between the outer unit (G1) and the inner and central units (G2, G3). Biotites from the granites and appinites fall towards the phlogopitic end of the biotite solid solution series.

(x) Plagioclase zoning in the appinites tends not to be well developed, while it is usually better developed within the granites.

(xi) Epidote is probably a late hydrothermal mineral. One instance of epidote with textural characteristics of primary epidote, in contact with biotite and hornblende, is thought to represent a sub-solidus reaction and not a high pressure primary magmatic assemblage.

(xii) Exsolution textures in hornblende and augite are present in a mafic rock, thought possibly to be a melagabbro (coarse metadolerite). The compositional variation between orthopyroxene, augite, sub-calcic augite and hornblende hosts and exsolution lamellae is minor. The cause of the exsolution is thought to be related to sub-solidus reactions possibly relating to thermal metamorphism of the metadolerite due to entrapment as a xenolith within the magma of the Meenalargan complex. This sub-solidus reaction model is supported by two-pyroxene geothermometry which yielded a temperature of crystallisation of orthopyroxene and augite of 676°C which is well below the experimental crystallisation temperatures determined by Yoder & Tilley (1962).

CHAPTER FIVE

MAJOR AND TRACE ELEMENT GEOCHEMISTRY

5.1 INTRODUCTION

The major and trace element geochemistry of some appinitic intrusions of the Ardara area was studied by Hall (1967) and later work by French (1977) involved the major and trace element geochemistry of some appinitic breccia pipes of the Ardara area. The major and trace element geochemistry of the main Ardara pluton has previously been studied by Hall (1966). Isotope geochemical studies of the main Ardara pluton are limited to the whole rock Rb-Sr dating of the inner unit (G2b) by Halliday et al. (1980) and a single Sm-Nd isotope analysis of the same unit, by Dempsey & Meighan (1989).

Hall (1967) characterised the composition of the appinitic suite around the Ardara pluton, comparing it to the appinite suite in Argyll, Scotland and to basaltic rocks. None of the above studies studied the Ardara appinitic intrusions in relation to their structure, mode of emplacement, and it is the aim of this chapter firstly to characterise the units forming the main Ardara pluton, and the surrounding appinitic and associated granitic bodies in terms of their overall geochemistry, to compare the granitic units of the Ardara pluton with other granites, and to compare the appinites with potential analogues such as basalts and lamprophyres. The second aim is to determine the geochemical relationships between the various appinitic intrusions in terms of their structure and emplacement mechanisms, and a third aim is to examine the intrusions of the Ardara igneous complex by modelling crystallisation processes, making use of trace element partition coefficient and mass balance constraints. Finally the potential effects of contamination are examined.

5.2 COMPOSITIONAL CHARACTERISTICS OF THE ARDARA IGNEOUS COMPLEX

The granitic units of the Ardara pluton and those granites associated with the appinitic intrusions are calc-alkaline to high-K calc-alkaline in composition (Figs. 5.1 and 5.2). The AFM plot (Fig. 5.2) shows how the granites describe an evolutionary trend, typical of orogenic granitoids and destructive margin volcanic suites.

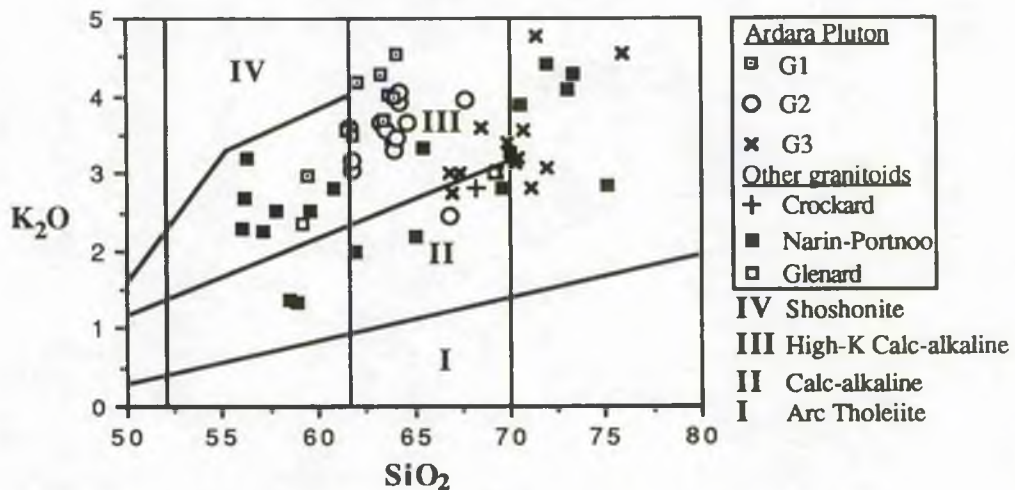


Fig. 5.1 K_2O - SiO_2 plot of granitic samples of the Ardara igneous complex. Field boundaries are the Peccerillo & Taylor (1976) calc-alkaline classification.

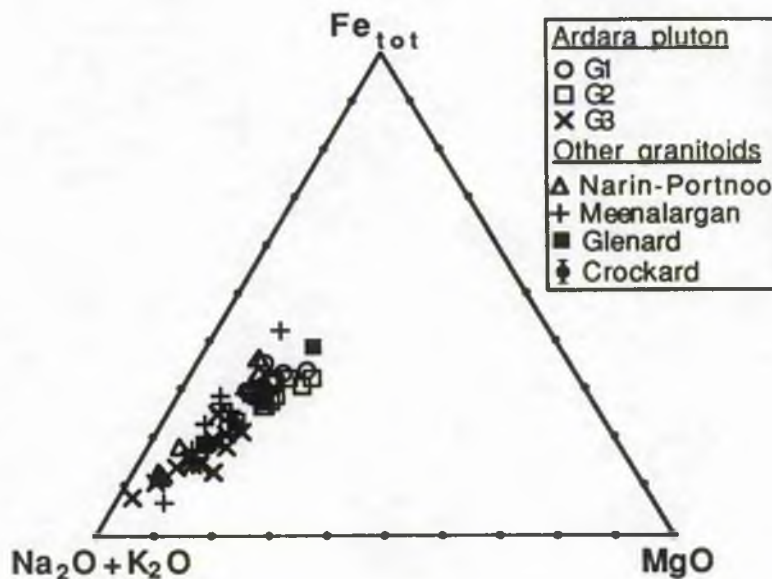


Fig. 5.2 AFM plot of the granitic rocks of the main Ardara pluton (G1, G2, G3) and those granitic rocks associated with appinitic intrusions.

The main Ardara pluton is a metaluminous granitic intrusion forming part of the Donegal batholith (Pitcher & Berger 1972), emplaced at c.405 Ma into greenschist facies metasediments of the Dalradian Supergroup (Halliday et al. 1980). Sm-Nd and Rb-Sr isotopic studies (Table 5.1) indicate a mafic magma source, probably the upper mantle or young basic lower crust (Dempsey & Meighan 1989). However, the presence of inherited

zircons in the Ardara pluton certainly indicates the presence of at least some crustal component (Halliday et al. 1980). The Na₂O-K₂O plot (Fig. 5.3) shows that none of the granite units of the main Ardara pluton, nor any of the granites associated with the surrounding appinitic intrusions, plot within the field of S-type granites from the type area of the Lachlan fold belt of SE Australia (White & Chappell 1983), and all display characteristics similar to those of Lachlan I- and A-types, though often geochemical and mineralogical criteria rule out the A-type classification of these rocks.

Granite Intrusion	(⁸⁷ Sr/ ⁸⁶ Sr) _i	ε Nd _i
Ardara (G2a)	0.7062	-1.2
Rosses (G1)	0.7066	-8.0
Main Donegal	0.7062	-8.2
Thorr	0.7051	-5.1

Table 5.1 (⁸⁷Sr/⁸⁶Sr)_i and ε Nd_i data for some of the granites of the Donegal batholith (data from Dempsey & Meighan, 1989)

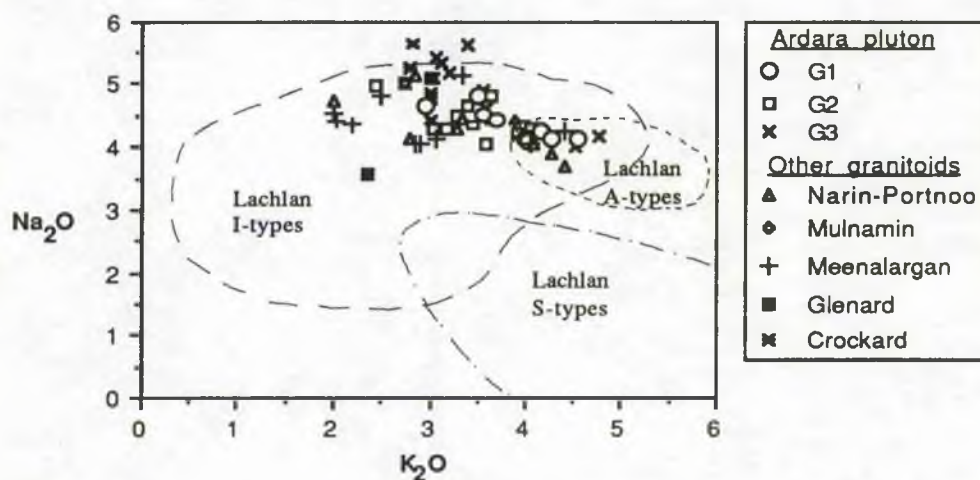


Fig. 5.3 Plot of Na₂O vs K₂O for the Ardara igneous complex with fields for I- and S- and A-type granites of the Lachlan fold belt, Australia shown for comparison (Chappell & White, 1983).

Classification of the Ardara granitoids according to the classification scheme of Pearce et al. (1984) indicates that the granites fall within the field of collision granites, volcanic arc and ocean ridge granites, Fig 5.4(a). The Ardara granites Fig. 5.4 (b) do not show the high Rb contents of syn-collision granites and are more enriched in Ba relative to typical post-collision granite 5.4 (c) using Pearce's criteria. Whether these Pearce plots are

robust indicators of tectonic setting must be doubted for such an orogen as the Caledonian where there are wide variations in trace element abundances in apparently similar magmatic and tectonic settings.

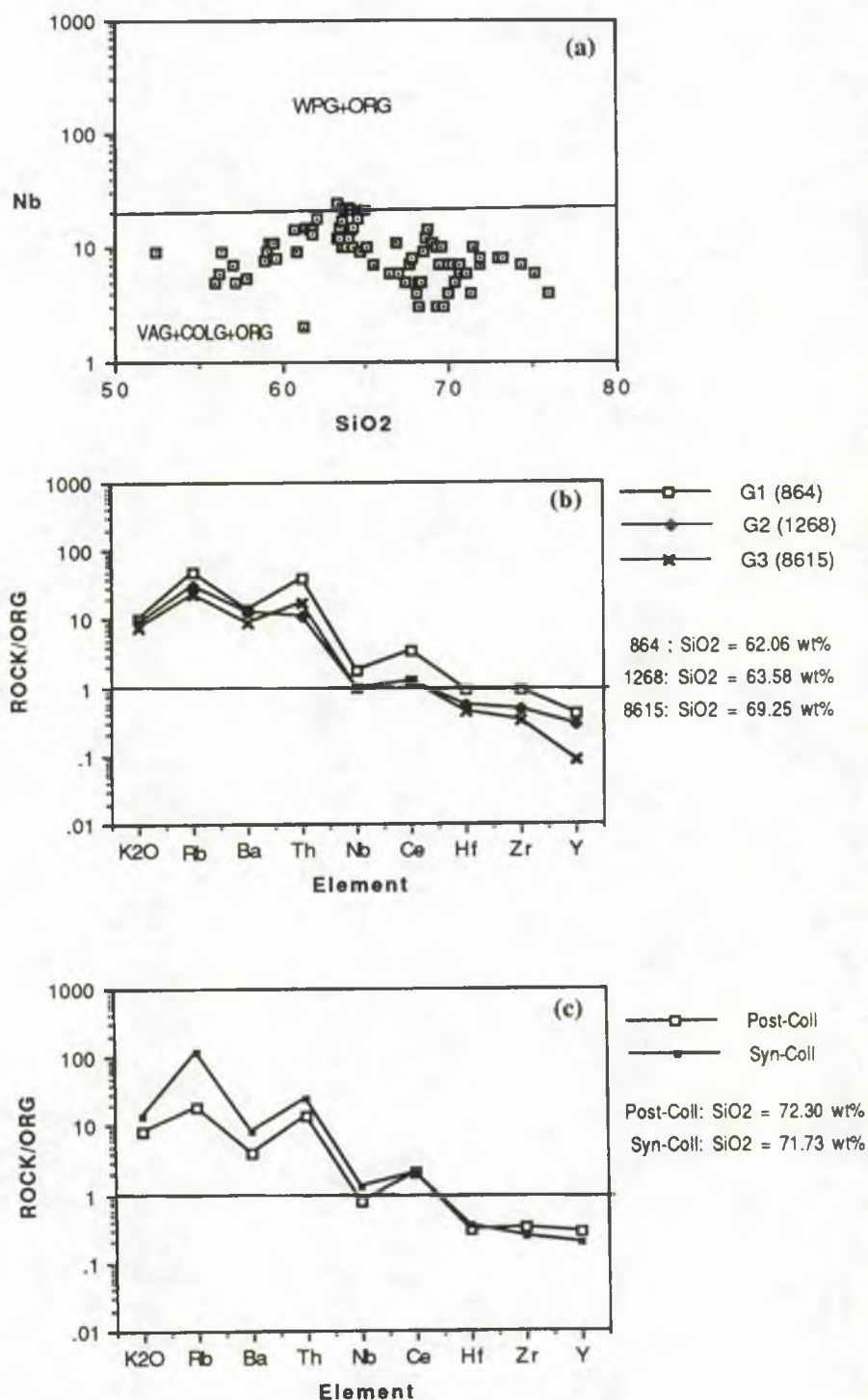


Fig 5.4 Classification scheme of Pearce et al. (1984). (a) SiO_2 v Nb plot, (b) Chondrite normalised plots for granites of the Ardara pluton, (c) Chondrite normalised plots for post-collision granites and syn-collision granites. WPG = within-plate granite, ORG = ocean ridge granite, VAG = volcanic arc granite, COLG = collision granite

(i) The Ardara Pluton

Major element geochemistry of the units of the Ardara pluton indicates the presence of a 'silica gap' at 65-67 wt % SiO₂ (Fig. 5.5 a), between the two outer units (G1 and G2) and the central unit (G3). This central unit has a higher SiO₂ content (70.0 wt %), and contains less TiO₂, Al₂O₃, Fe_{total}, MgO and CaO (Fig 5.5 a-b) than G1 & G2, reflecting an increase in the quartz and alkali feldspar and a decrease in the biotite and plagioclase contents of G3.

Trace element geochemistry of the outer and inner units (G1 and G2) is generally similar, however differences exist in the contents of Rb, Zr, Ti, Y, Hf, Nb, Ce and Th which are somewhat higher in G1 than G2. Sr shows a wide range from G1 to G2 but G1 values are often equal to, or lower than those of G2 (Fig. 5.5 b). G3 has lower abundances of P₂O₅ (Fig. 5.5 b) Ba, Y, Rb, V, Th, Zr, Zn, and Nb (Fig 5.5 c). This suggests that the central granodiorite (G3) may represent a different pulse from that which forms the outer and inner units (G1 and G2) as Rb in particular as an incompatible element would be expected to increase with of magmatic fractional crystallisation, in the assemblages formed.

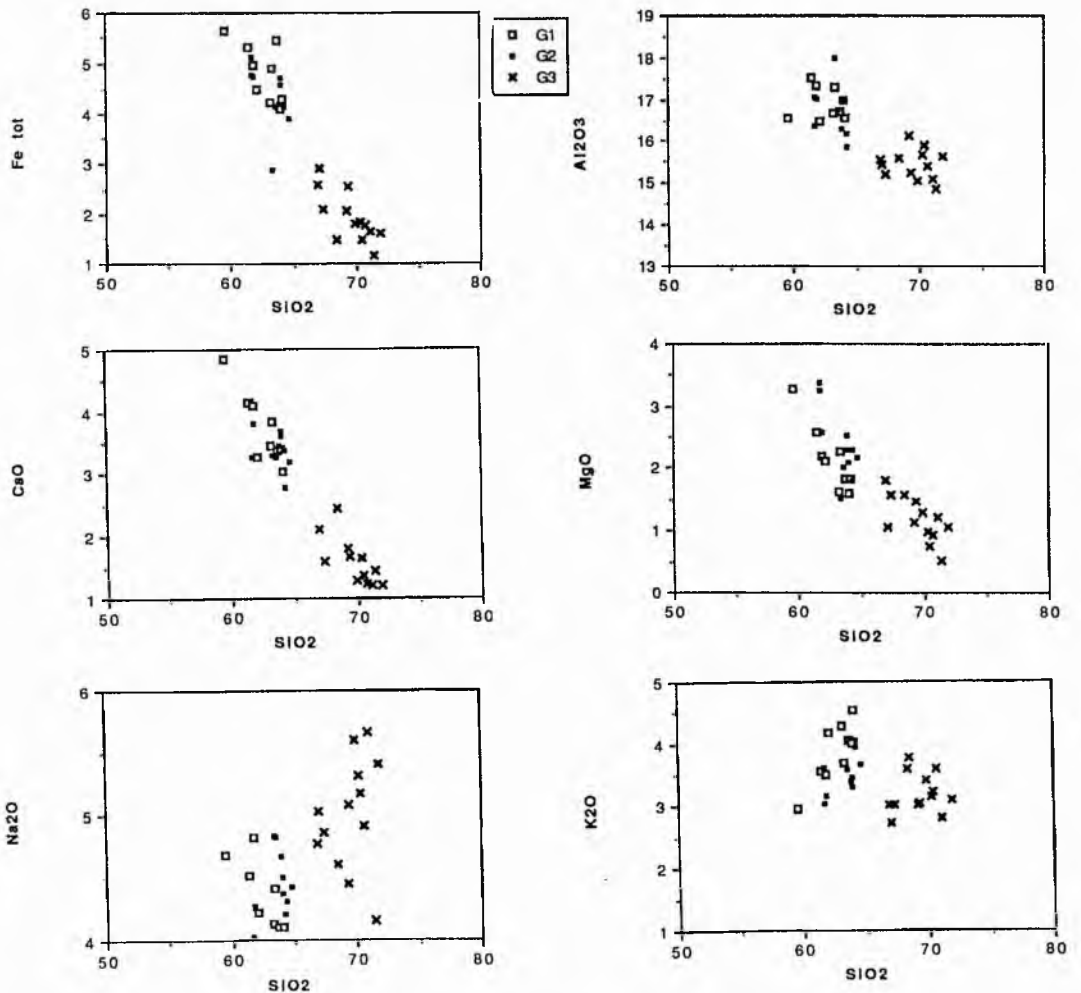


Fig. 5.5 (a) Harker plots for units (G1 and G2) and the central granodiorite (G3) of the Ardara pluton.

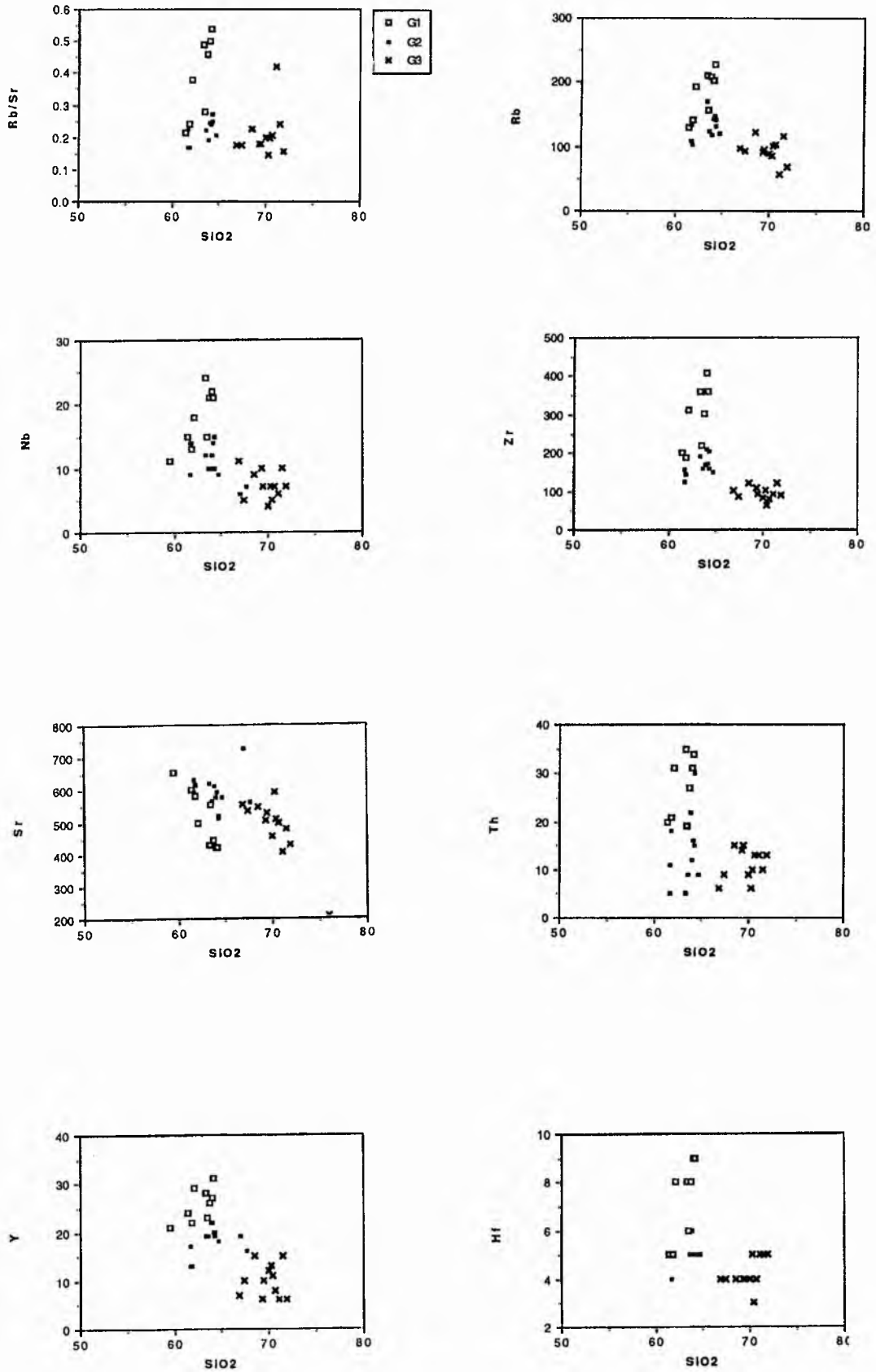


Fig. 5.5 (b) Trace element Harker plots for the main units of the Ardara pluton

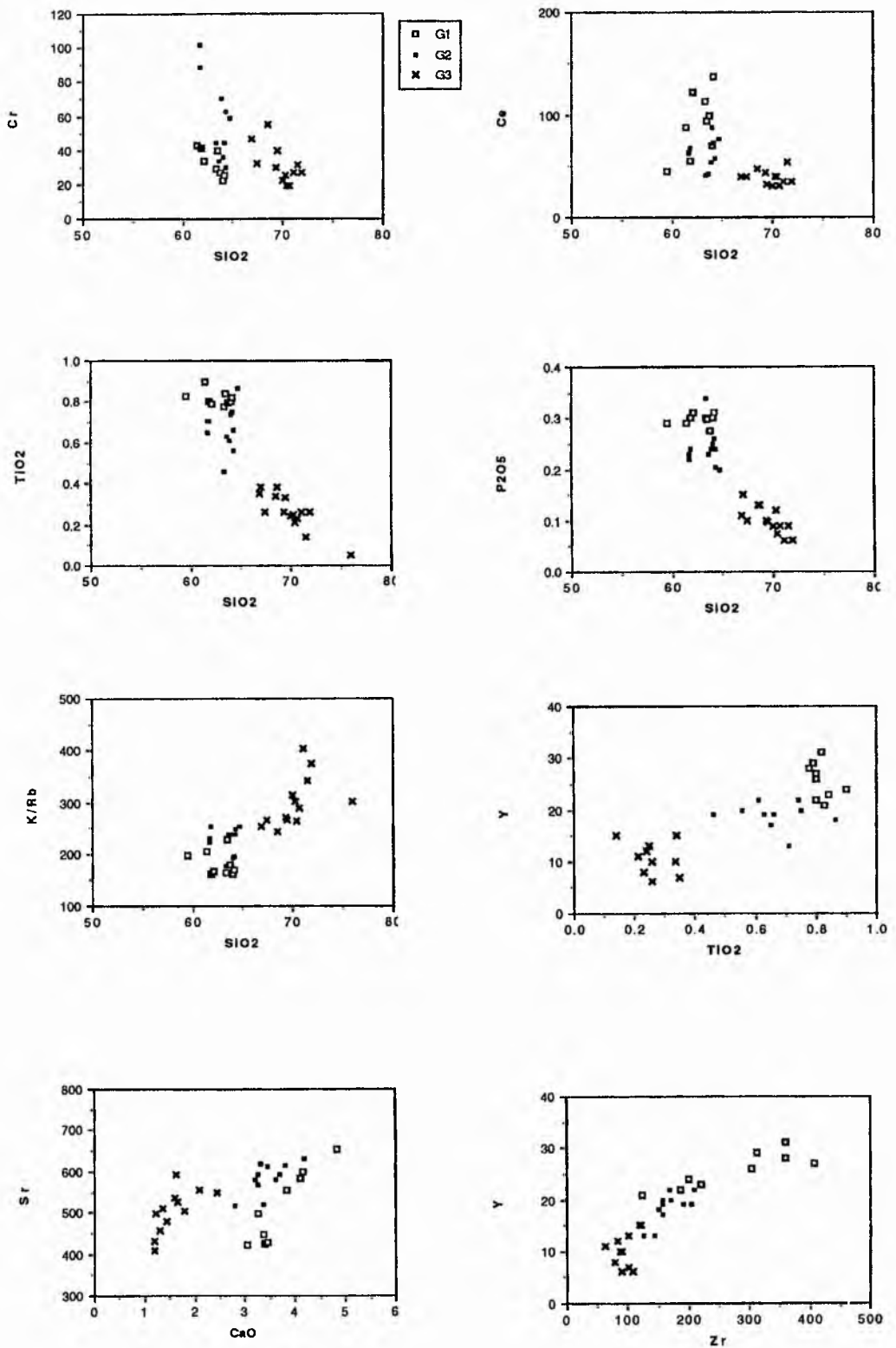


Fig. 5.5 (b) Trace element Harker plots for the main units of the Ardara pluton

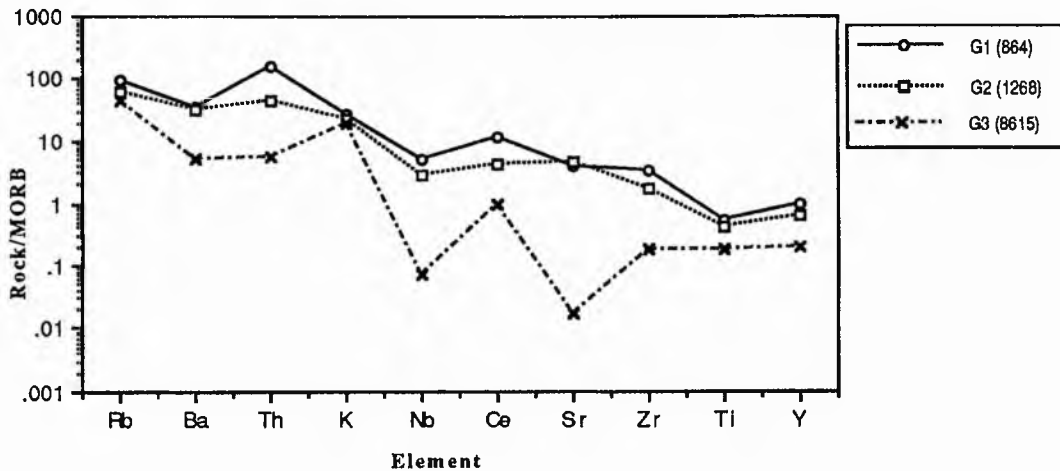


Fig. 5.5 (c) MORB normalised ratio plot of samples representative of the G1, G2 and G3 units of the Ardara pluton. Note the marked difference between the units G3 and G1/G2. Samples plotted are G1 = 864, G2 = 1268, G3 = 8615 (MORB values after Pearce 1983).

The spatial variation in major and trace element geochemistry along a north-south traverse of the northern part of the Ardara pluton has been studied. Sample localities are shown in Fig. 5.6 and the variation diagrams with distance in Fig. 5.7 and 5.8. There is a general decrease in oxides such as TiO_2 , P_2O_5 , Al_2O_3 , K_2O , and total Fe_2O_3 from G1 to G3, (Fig. 5.7), and trace elements Th, Y, Ce, Ba, Rb, Zr (Fig. 5.8). G3 shows marked differences from G1 & G2 in SiO_2 , MgO, CaO, total Fe_2O_3 , MnO and V suggesting that it may not be formed by a simple evolutionary process from G1 and G2. The relationship between G1 and G2 is enigmatic, G2 is enriched in MgO, total Fe_2O_3 , Ni, Cr, V and Sr relative to G1. The relationship between the granitic units of the Ardara pluton will be examined later in this chapter by means of geochemical modelling.

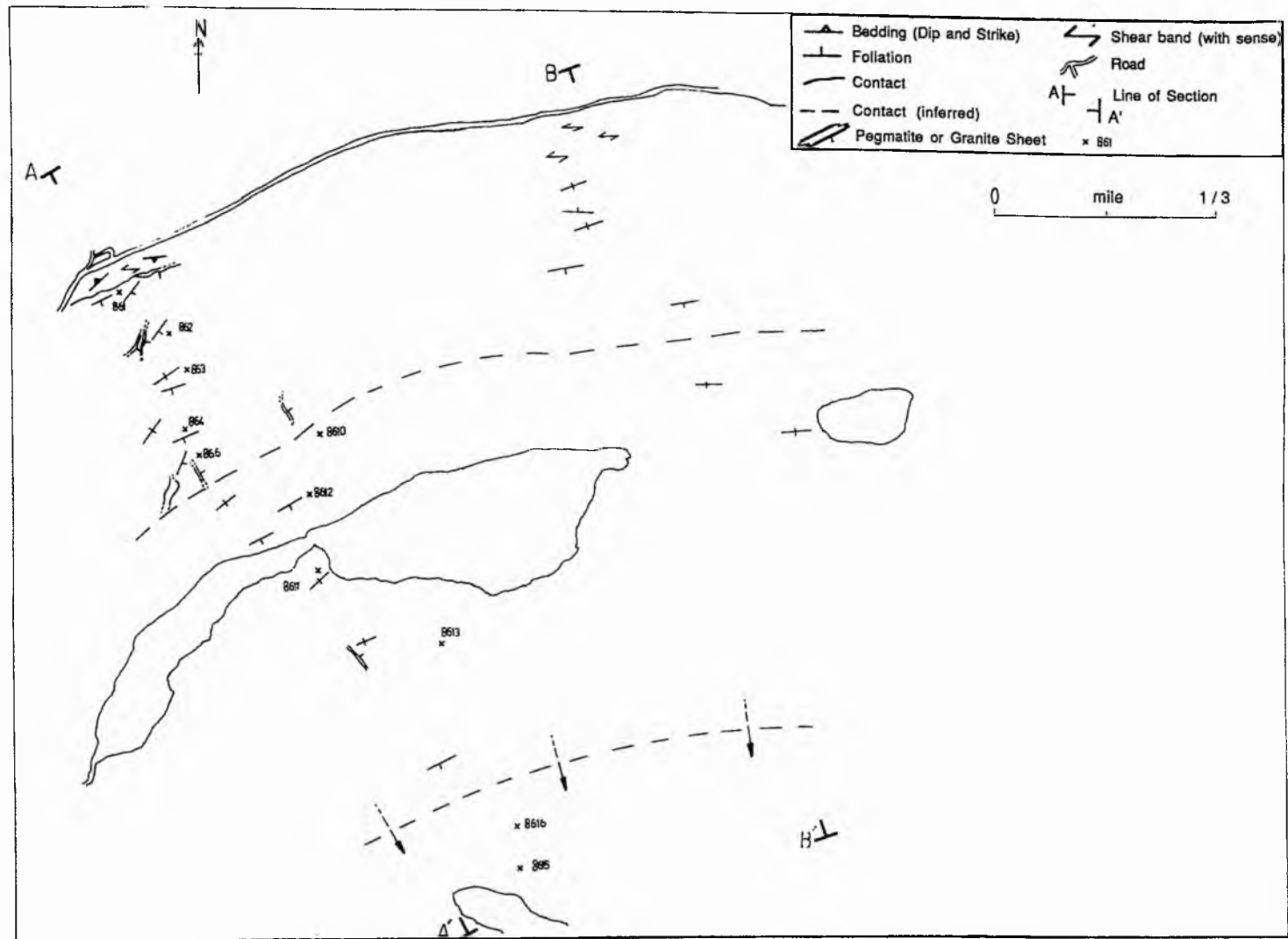


Fig. 5.6 (a). Sample location map of the northern part of the Ardara pluton showing the locations of samples used in the major and trace element geochemical traverse presented in Figs. 5.7 and 5.8.

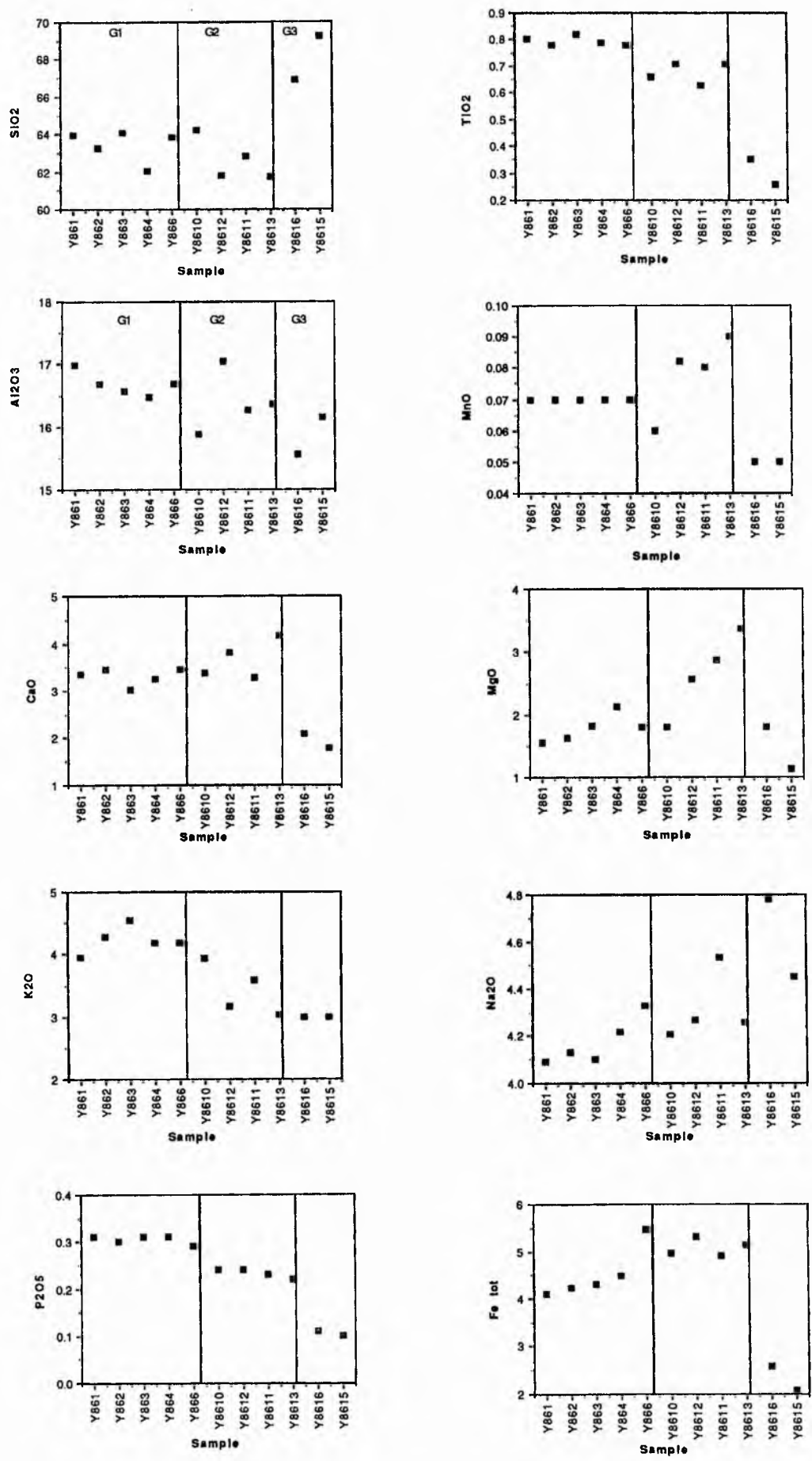


Fig. 5.7 Variations in major elements along the traverse indicated in Fig 5.6.

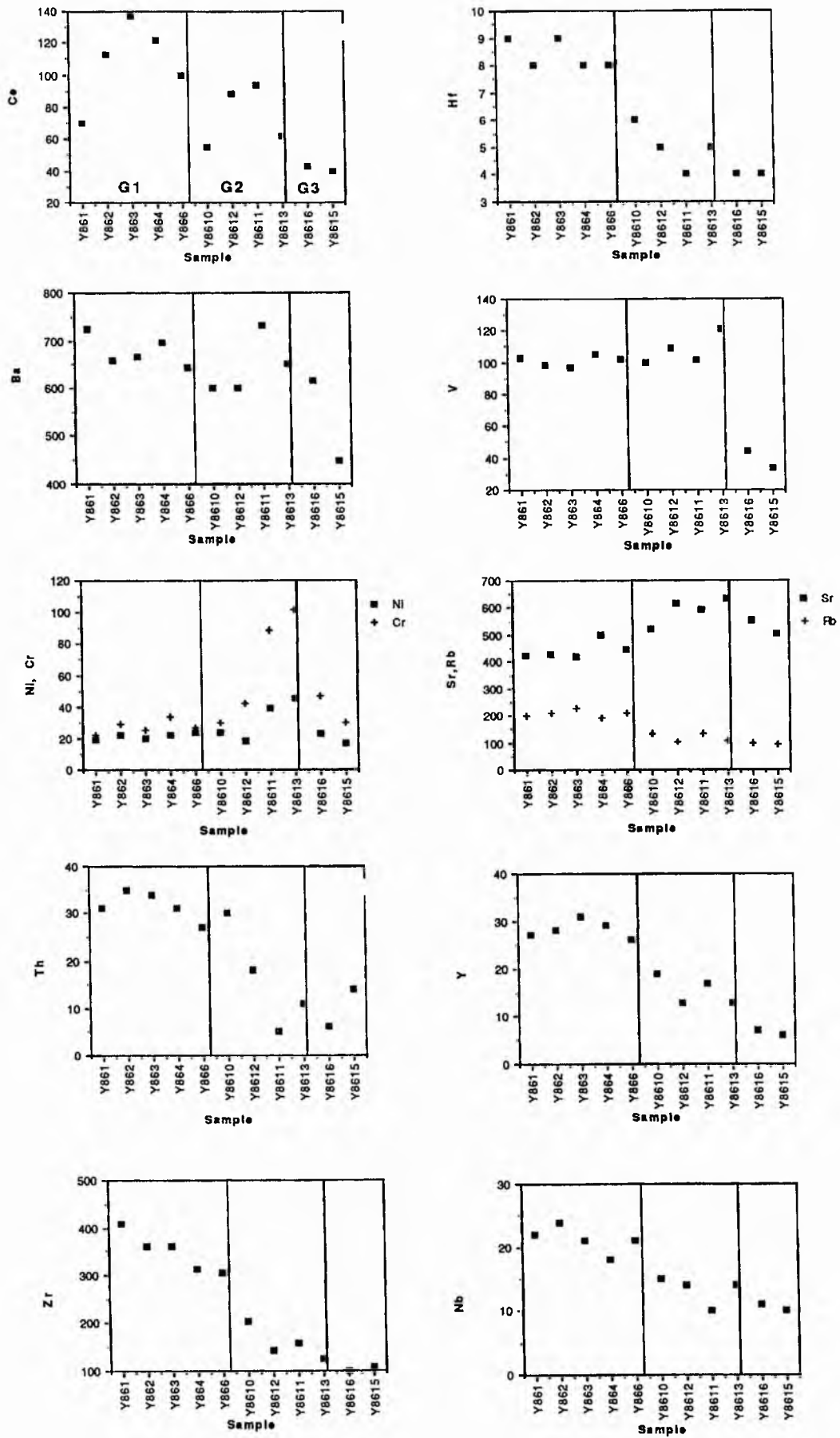


Fig. 5.8 Variations in trace elements along the traverse indicated in Fig 5.6

(ii) Geochemical characteristics of the Ardara appinitic suite

Taken collectively the appinites from the four intrusions studied have several characteristic features. The appinitic suite has a SiO_2 range of 42-61 wt%, and have high abundances of NiO, Cr_2O_3 , and Sr. The AFM plot of the main appinitic intrusions (Fig. 5.9) indicates that the basic rocks of the Ardara igneous complex show a broad span of compositional variation. The most primitive rock type is the Kilrean cortlandtite, while the most evolved are the rocks of the Narin-Portnoo intrusion. The rocks of the Meenalargan complex show a wide spread of composition while those of the Summy Lough diorite have a relatively limited compositional range. Notwithstanding the scatter, the trend from cortlandtite is broadly similar to the primitive portion of the calcalkaline trend shown by many destructive margin igneous complexes.

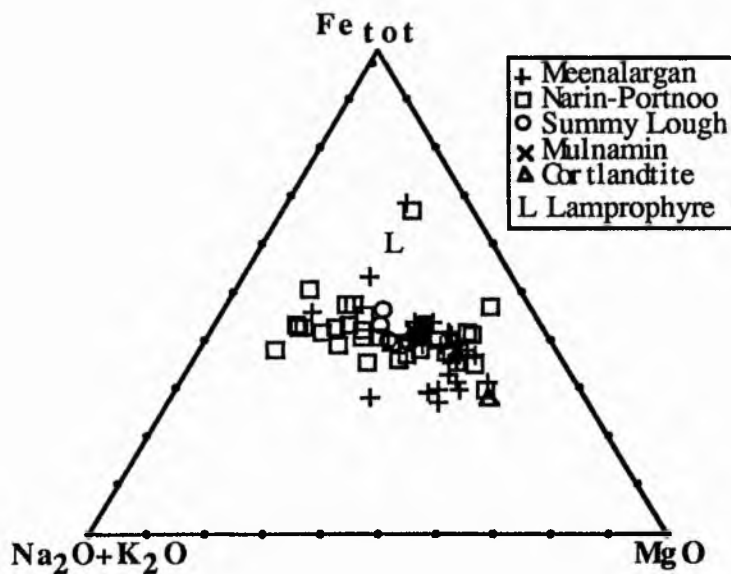


Fig. 5.9. AFM plot of the main appinitic intrusions in the Ardara area. Average calc-alkaline lamprophyre composition from this study.

A K_2O - SiO_2 plot (Fig. 5.10.a) shows that the appinites are mostly calc-alkaline and high-K calc-alkaline within the classification of Peccerillo & Taylor (1976), while a few fall within the shoshonite field, reflecting the enrichment in K_2O (relative to SiO_2) of some of the Narin-Portnoo intrusions. The mildly alkaline composition of some of the appinites is illustrated by Fig. 5.10 (b)

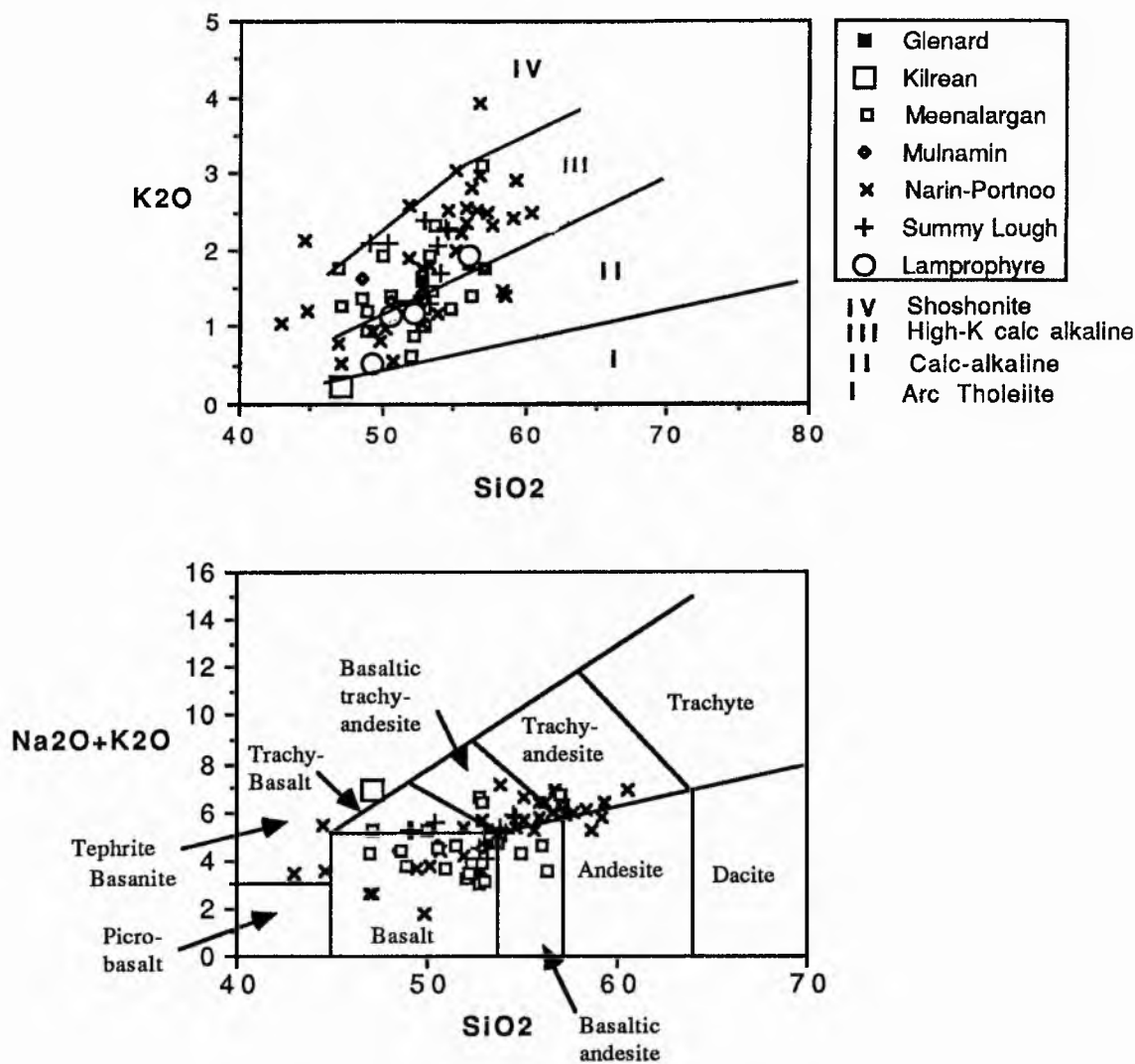


Fig. 5.10 (a) K₂O vs SiO₂ plot for appinitic samples from the main Ardara intrusions. Field boundaries of the Peccerillo & Taylor (1976) calc-alkaline classification are shown for comparison. (b) SiO₂ vs Na₂O+K₂O plot of some of the appinites from the Ardara complex.

(iii) Geochemical comparison of appinites with basalts

Fig. 5.11 (a) is a MORB-normalised trace element plot of some members of the appinite suite and a typical calc-alkaline basalt. Although the appinites show slight enrichment in Sr, Rb, Ba, Th, Nb, and Ce, with depletion in Zr and Y compared with the basalt. The most primitive rock type of the appinite suite, the Kilrean cortlandtite, is depleted in LILE and HFS elements relative to the rest of the appinite suite rocks and basalt. The appinites and the basalt have similar trace element compositions, particularly in terms of Ni and Cr (Fig. 5.11 b). On this Cr v Ni plot the appinites scatter widely but do include values similar to calc alkali basalt. Fig 5.11 (c) shows similar diorites and meladiorites normalised against chondrite with average calc alkali basalt of Whitford (et al.

and Sun (1980) plotted for comparison. The diorites of Ardara show a general similarity to the basalt composition, although they are somewhat enriched in Th, Rb, Ti and Y.

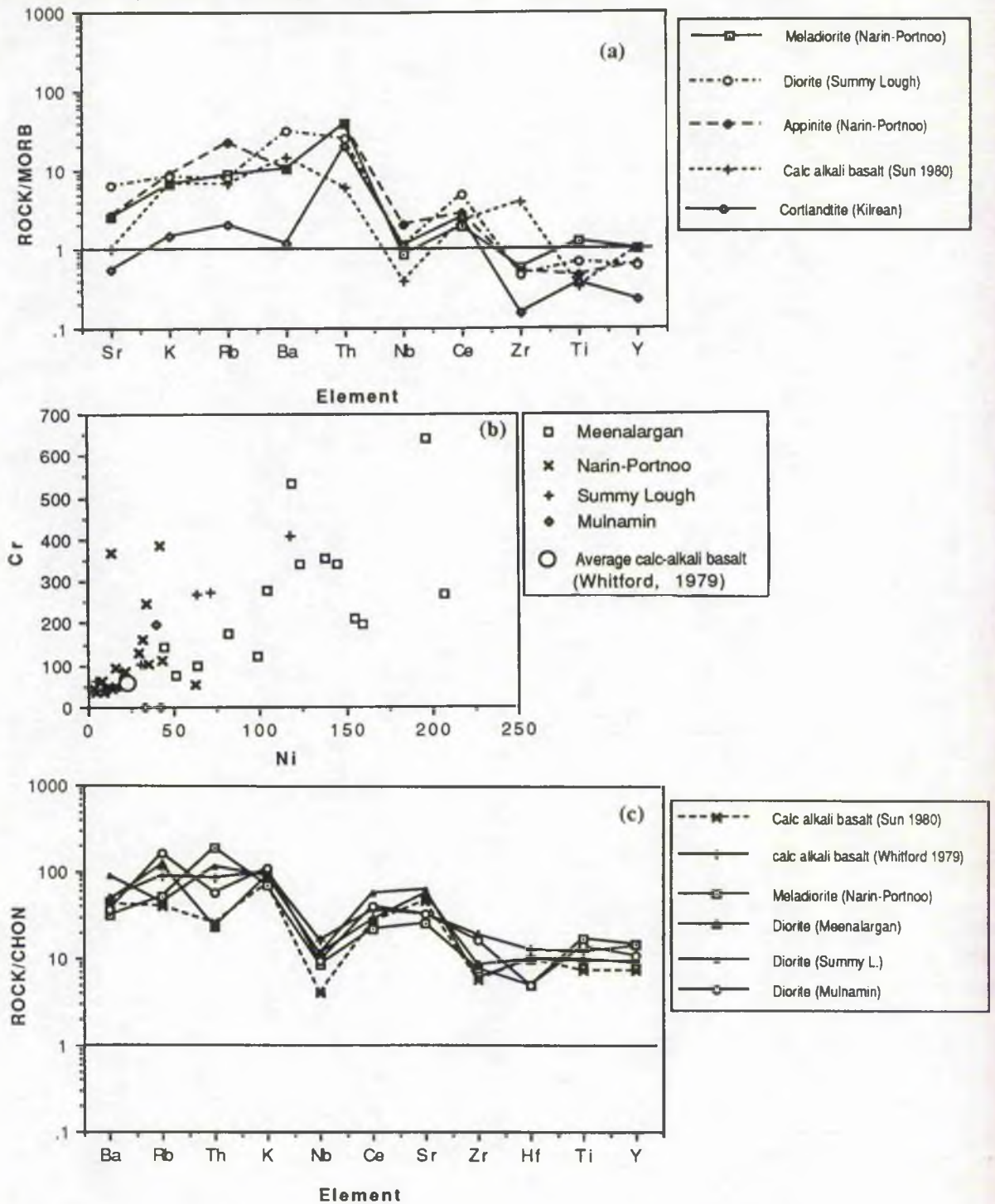


Fig. 5.11 (a) Trace element MORB-normalised ratio plot of members of the appinite suite; average calc-alkaline basalt (after Sun, 1980) is shown for comparison.

(b) Variation plot of Ni versus Cr to show the similarity of average calc-alkali basalt to appinites of the Ardara igneous complex.

(c) Trace element chondrite-normalised plot of diorite and meladiorite. Two average calc alkali basalts are included for comparison.

The cortlandtite, the most primitive rock of the Ardara igneous complex, is depleted in many of the trace elements compared to kentallenite, an analagous rock in the Scottish Caledonides (Fig 5.12 a) while meladiorite from the Ardara igneous complex has a similar composition to other rock types from similar orogenic settings in the Caledonides. For instance, the incompatible elements from various Proterozoic dykes (N1 and 77284699) thought to be subduction-related magmas emplaced deep in the crust beneath tonalite-granite batholiths and Cordilleran volcanoes (Thompson et al. 1984) are very similar to appinites from modern subduction-related environments (Fig 5.12 b). Weaver & Tarney (1981) linked the Scourie dykes with magmas of present day island arcs, while Thompson et al. (1984) concluded that these dykes were originally the deep crustal root of major batholiths.

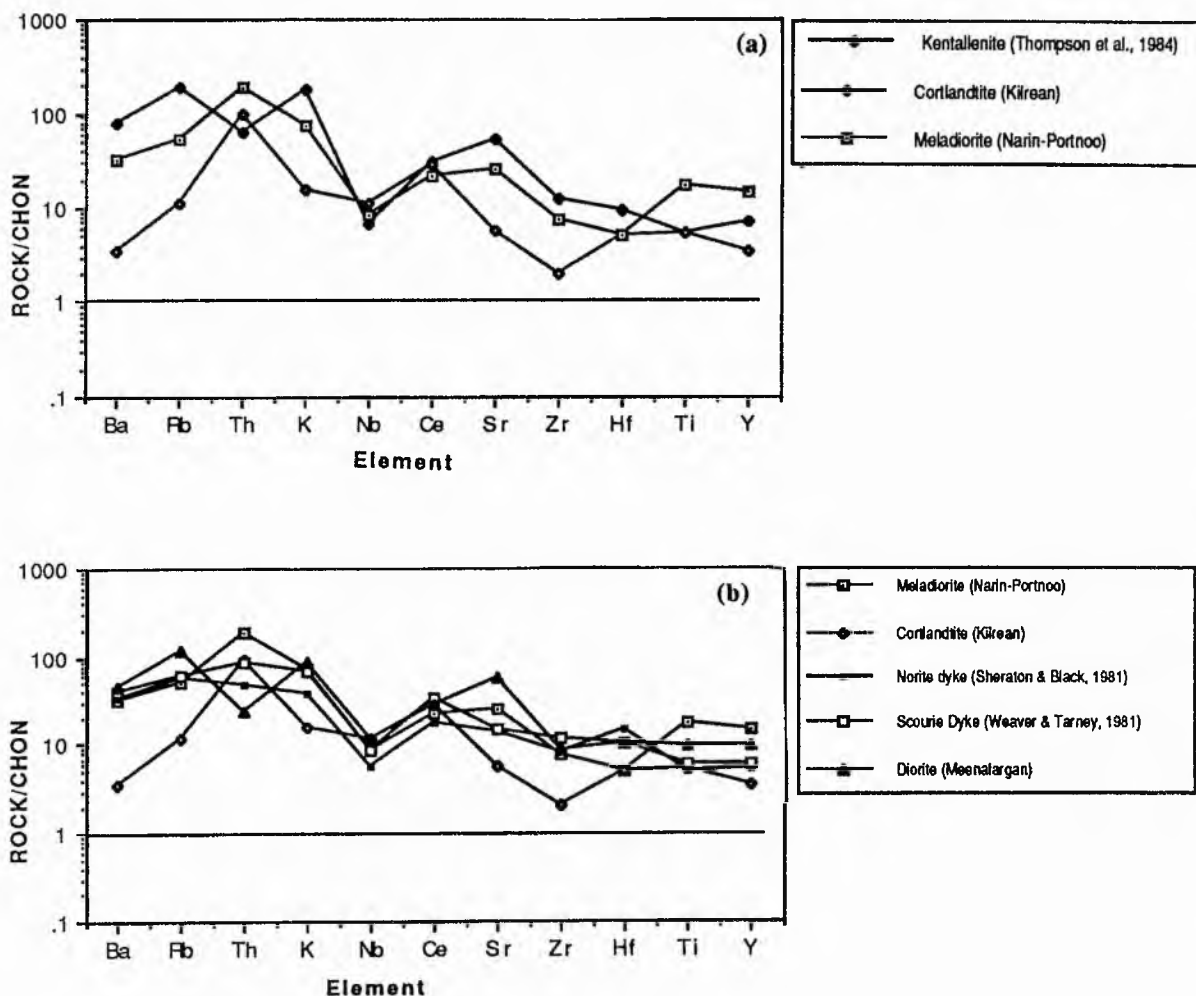


Fig. 5.12 (a) Chondrite-normalised ratio plot of cortlandtite and kentallenite from Argyll, Scotland in comparison with a meladiorite from Narin-Portnoo.

(b) Chondrite normalised ratio plot of some Ardara appinites and similar rocks from subduction-related areas

(iv) Geochemical comparison of appinites and lamprophyres

Lamprophyres are a suite of H₂O- and/or CO₂-rich, alkaline rocks ranging from sodic to potassic and from ultrabasic to intermediate (Rock 1991). Commonly, they exhibit a distinctive inequigranular texture resulting from the presence of macrocrysts (and in some cases megacrysts) set in a fine-grained matrix. The megacryst/macrocryst assemblage may consist of rounded to euhedral crystals of magnesian ilmenite, Cr-poor titanian pyrope, forsteritic olivine, Cr-poor clinopyroxene, phlogopite, enstatite, Ti-poor chromite, kaersutitic amphibole and alkali feldspar. The matrix minerals may include second generation euhedral primary olivine, clinopyroxenes and amphiboles, phlogopite-biotite (commonly rich in Ti and/or Ba), feldspars, feldspathoids, mellilite, Mg-Mn-bearing ilmenite, perovskite, spinel, monticellite, apatite and primary late-stage Ca-Mg-Fe carbonate and chlorite-serpentine. Amphibole and/or phlogopite-biotite are essential primary phases. Irregular to spherical, felsic globular structures, filled with combinations of carbonates, chlorite, feldspars, feldspathoids and zeolites are widespread. The replacement of early-formed minerals by deuteritic chlorite-serpentine, carbonates, epidote and zeolites is common. Lamprophyres typically form en-echelon dykes, sills, pipes and vents which, although individually small, may aggregate into extensive swarms or clusters. Brecciation of country-rocks or of the lamprophyre intrusions themselves is common.

In field occurrence lamprophyres are medium grained, hypabyssal rocks, most commonly occurring in the form of dykes and sheets. In the Ardara area, the most common occurrence of lamprophyre is in the form of spessartite and vogesite, i.e. calc alkaline lamprophyre (CAL of Rock 1991). Spessartites and vogesites were related to the appinite suite by French (1966) who recognised a close field association between appinites and lamprophyres. Lamprophyres are associated with appinite-breccia pipes such as those of Biroge (French, 1977 and section 3.12.4) and the type area of Appin, Scotland. At Kentallen, lamprophyres occur as dyke margins or appinitic bodies (Walker 1927, Bowes & Wright 1961, Wright & Bowes 1968, 1979). Thus there appears to be a temporal, spatial, and possibly genetic link between appinites and calc alkaline lamprophyres (CAL).

Geochemically the Ardara lamprophyres have similar major and trace element geochemical characteristics to the appinites of Ardara (Fig. 5.13). The typical calc-alkali lamprophyre composition (CAL) of Rock (1991) may be used to demonstrate the similarities of appinites to the lamprophyre suite of the Scottish Caledonides (Fig. 5.14 a). The compositions of the appinites, including the average appinite composition of Rock (1991), are all slightly depleted relative to CAL except for the Lomond appinite, and the comparison of dioritic and hornblende compositions with CAL indicate the complex trace element variability of the appinite and lamprophyre magmas (Fig. 5.14 b and c). On a MORB-normalised plot (Fig. 5.14 d) the appinites and lamprophyres have pronounced Th peaks and are depleted in Nb (typical of destructive-margin magmas). The Ardara appinite is depleted in Zr and Ti compared with the Argyll appinite, lamprophyre and Ardara

lamprophyre. The presence of a Th peak combined with low Nb and Sr may indicate the retention of Nb in the source during partial melting.

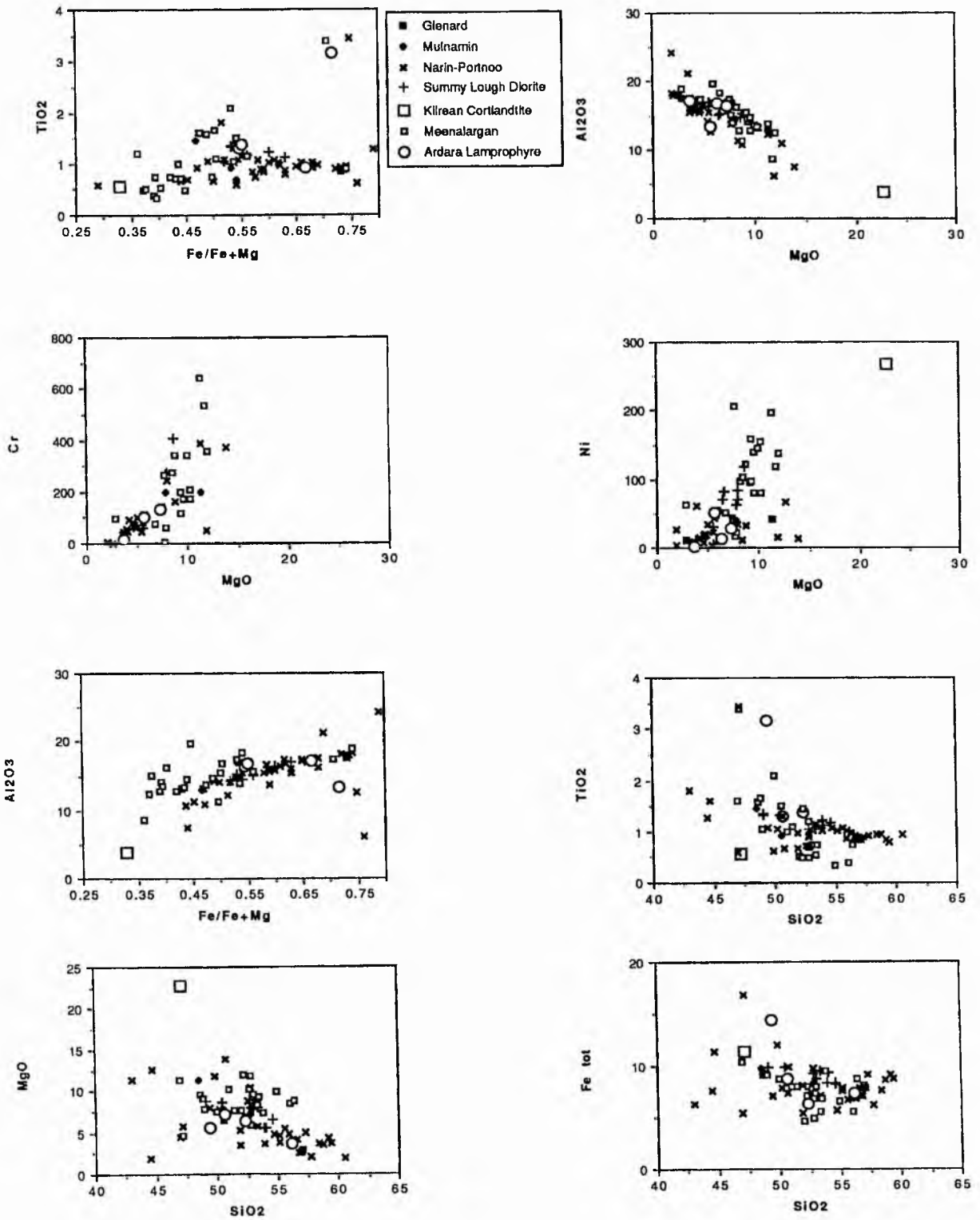


Fig. 5.13 Major oxide characteristics of the Ardara appinite and Ardara lamprophyre compositions.

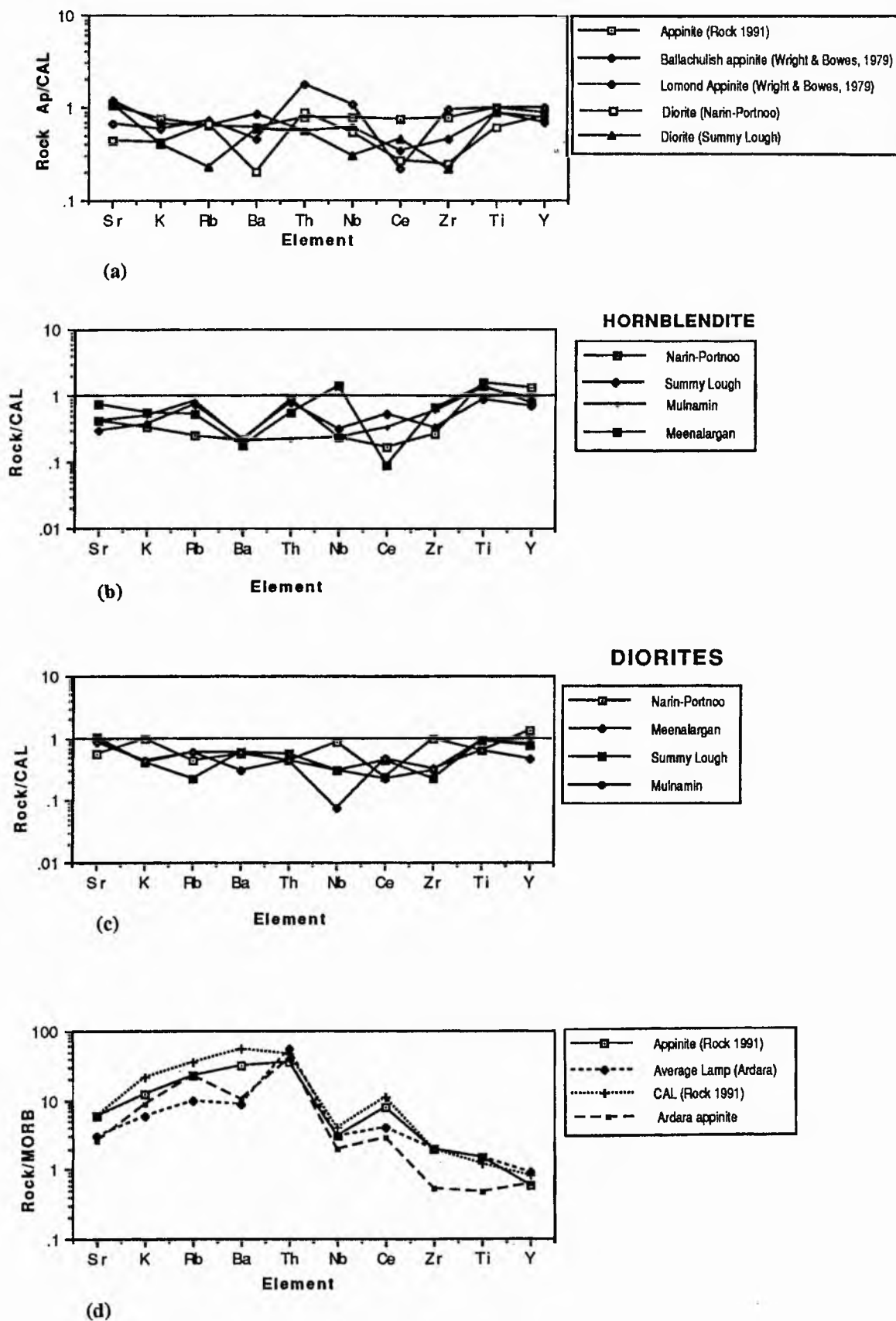


Fig. 5.14 Trace element normalised ratio plots of representative appinite compositions and lamprophyre compositions from the Ardara igneous complex and from the literature (source is quoted in brackets), Figs. (a-c) are normalised against CAL (Rock 1991), (d) is normalised against MORB (Sun 1980).

(v) Geochemistry of the granites associated with the Ardara appinitic intrusions.

The minor granitic intrusions associated with the Meenalargan appinitic complex are more primitive in composition than other granites associated with appinites in the Ardara area. The granites of the Meenalargan complex are enriched in Ca, Ti, Sr, Ba, Ce, Th, Zr, Hf relative to the Narin-Portnoo granites, while the latter are more enriched in Rb (Fig. 5.15 a). Considered as a group, the granites of the appinite suite are broadly similar to one another in terms of trace element geochemistry (Fig. 5.15 b). These granites associated with the satellite appinite intrusions compare with the G1 and G2 units of the Ardara pluton but differ greatly in composition compared to the central unit (G3) of the Ardara pluton (Fig. 5.15 c).

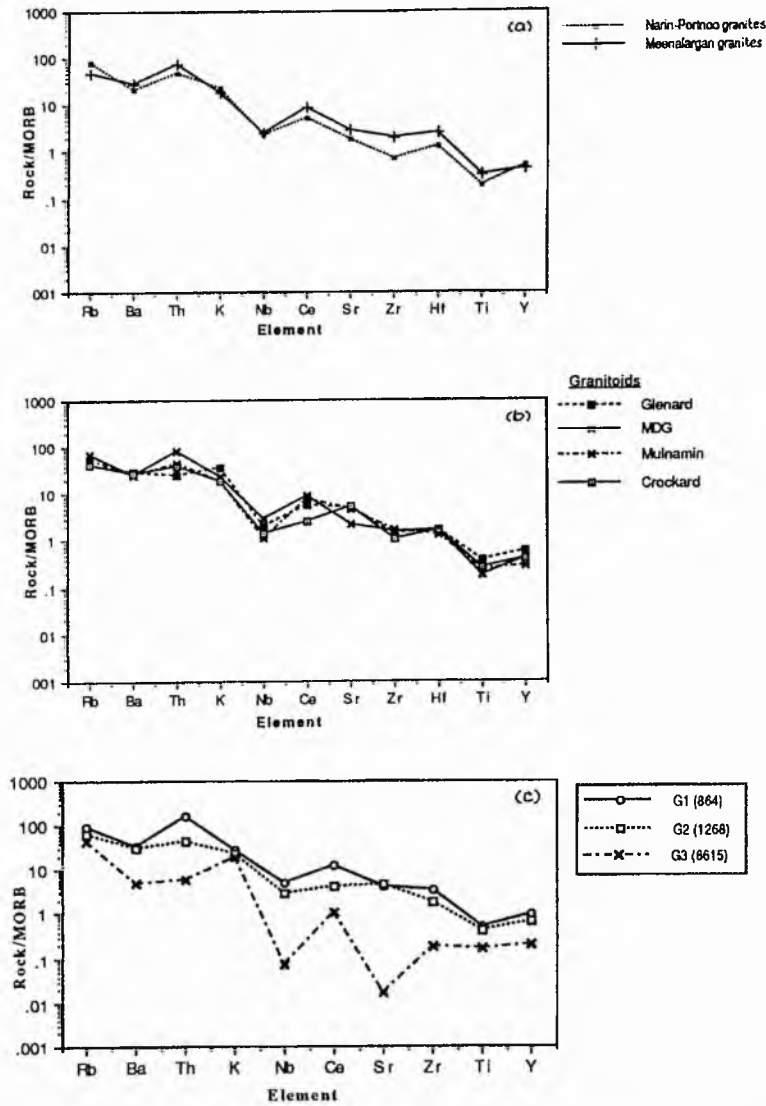


Fig. 5.15. (a) MORB-normalised ratio plot of representative granites associated with the Meenalargan and Narin-Portnoo appinitic intrusions,

(b) MORB-normalised ratio plot of representative granites associated with the appinitic intrusions of the Ardara area. The composition of the Main Donegal granite (MDG) is included for comparison.

(c) MORB-normalised ratio plot of representative samples from the Main Ardara pluton.

(vi) Geochemical links between appinites and the granites of the main Ardara pluton

It is apparent from Fig. 5.16 that many of the more evolved of the appinitic rocks overlap in composition with the granites and this is emphasised by the similarity of the trace element geochemistry of evolved appinite and typical granite compositions. On the evidence of these variation plots there seems to be some continuation of trend between elements such as Ti, Mg, Ca, K, some important trace elements, including Rb, Sr, Ba, Ni and Cr do not relate as clearly. The trace elements in Fig. 5.16 show that the granites continue the trends from the more evolved appinite bodies leading to the possibility that appinitic magmas could be parental to the main granites and related through processes of fractional crystallisation. These trends can be largely explained qualitatively by the removal of pyroxene and/or amphibole. A quantitative test of this hypothesis is presented later.

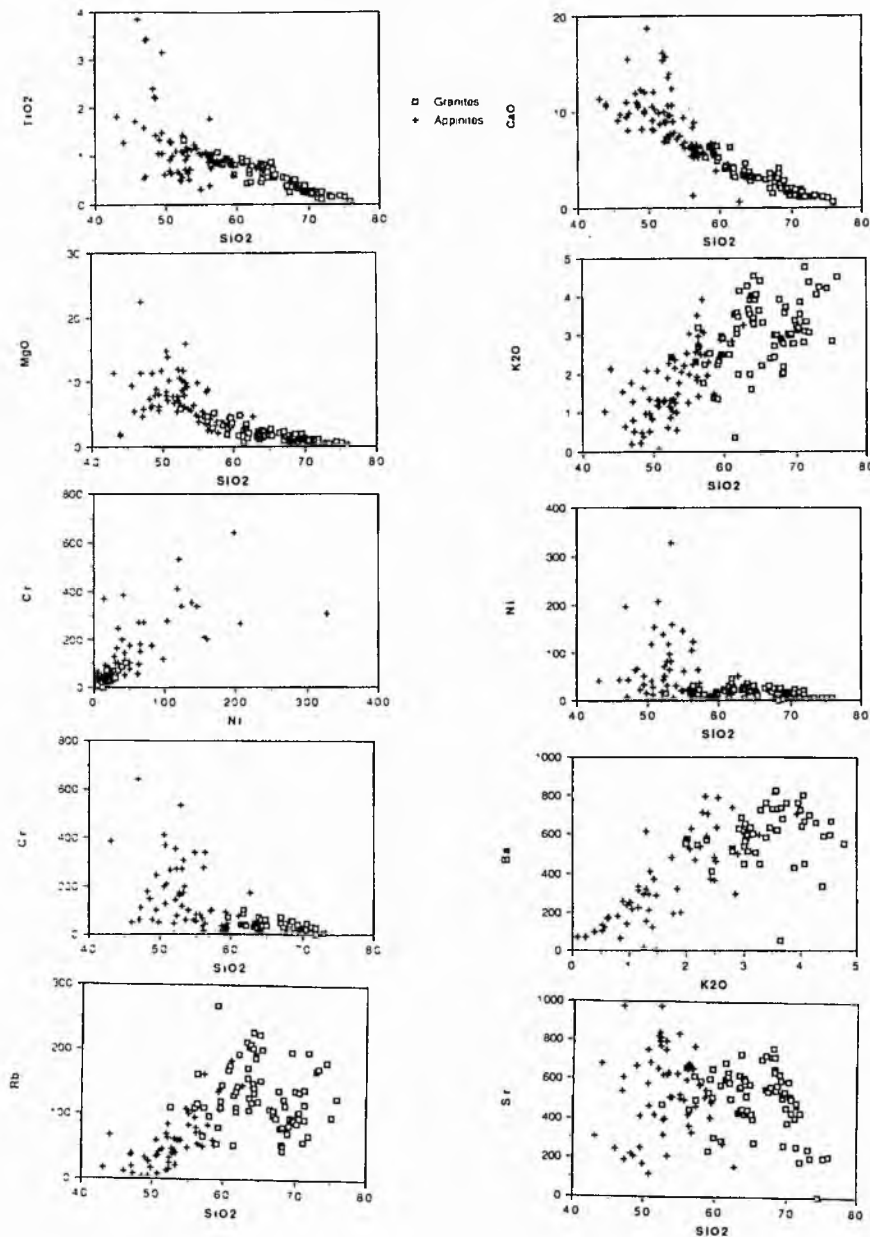


Fig. 5.16 Variation plots for all samples from appinites and main granites of the Ardara igneous complex.

from Narin-Portnoo. The biotite diorite has a similar trace element composition to the less evolved granite compositions (G1, G2, Narin-Portnoo) but contrasts strongly with G3, the most evolved unit of the Ardara pluton.

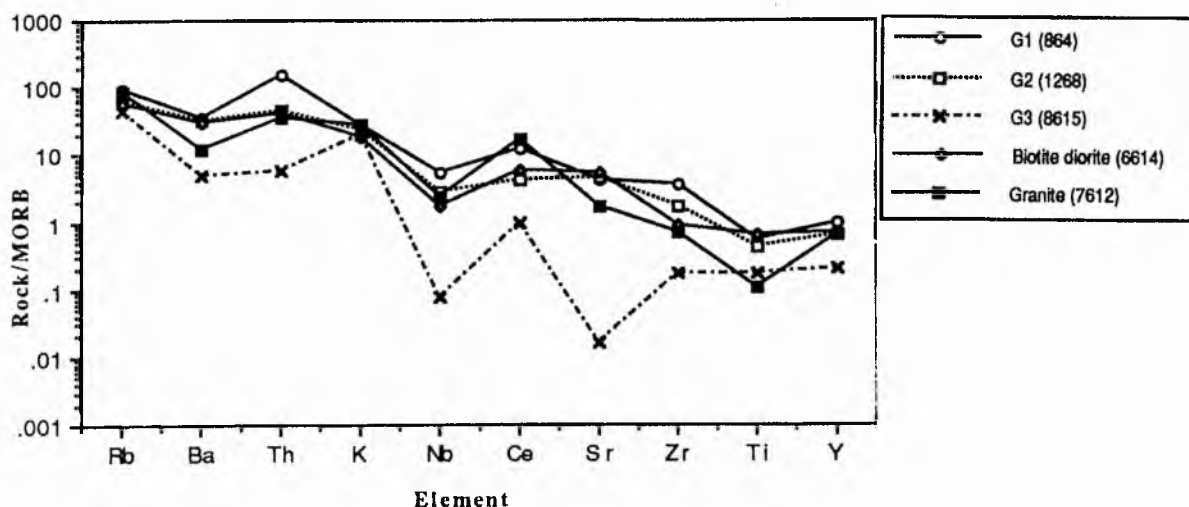


Fig 5.17. MORB-normalised ratio plot of biotite diorite and typical granite compositions from Narin-Portnoo.

5.3 COMPOSITIONAL VARIATIONS BETWEEN APPINITIC BODIES

The composition of the four main appinitic intrusions is examined in terms of the appinitic suite as a whole. Two complexes have relatively contrasting geochemistry, these are the Meenalargan and Narin-Portnoo masses and these intrusions are compared and contrasted below. The Kilrean cortlandtite is briefly geochemically summarised while the other intrusions are compared geochemically.

(i) Meenalargan and Narin-Portnoo Complexes.

The AFM plot (Fig.5.18) highlights the fact that the Meenalargan complex has somewhat greater mean MgO/FeO content than the Narin-Portnoo complex, the latter being richer in total Fe₂O₃. Meenalargan tends to be richer in CaO and depleted in K₂O, Al₂O₃ relative to Narin-Portnoo (Fig 5.19).

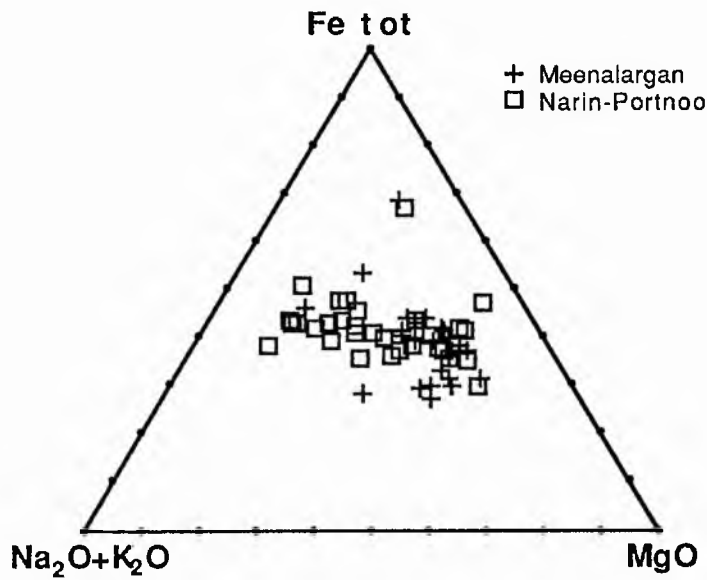


Fig. 5.18. AFM plot for the appinites of the Meenalargan and Narin-Portnoo intrusions.

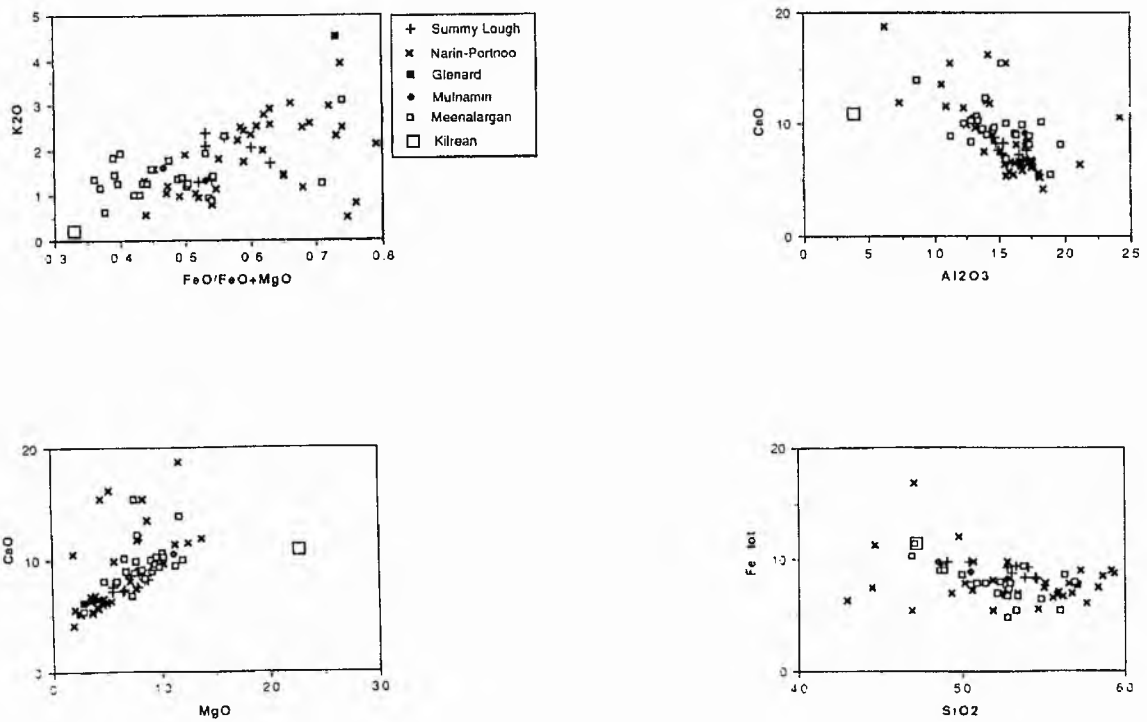


Fig. 5.19. Variation diagrams for the Meenalargan and Narin-Portnoo, Mulnamin, Kilrean, Summy Lough and Glenard appinitic complexes

Trace element differences between the Meenalargan and Narin-Portnoo complexes include enrichment of Cr and Ni in both intrusions, and depletion of Pb, V, Ce and Rb-Sr in Meenalargan relative to Narin-Portnoo (Fig 5.20).

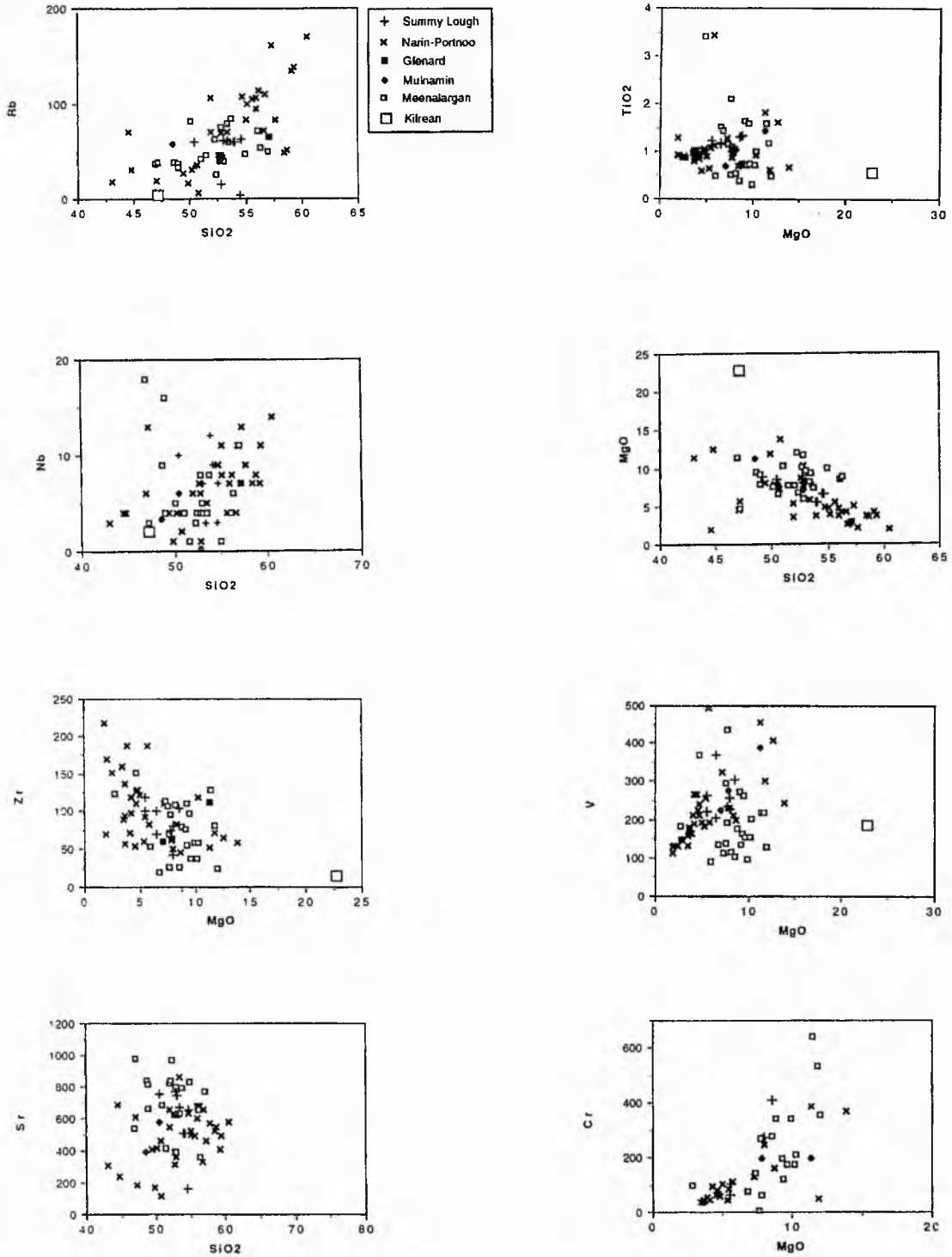


Fig. 5.20 Trace element plots for the Narin-Portnoo, Meenalargan, Kilrean, Summy Lough, Mulnamin and Glenard appinitic complexes.

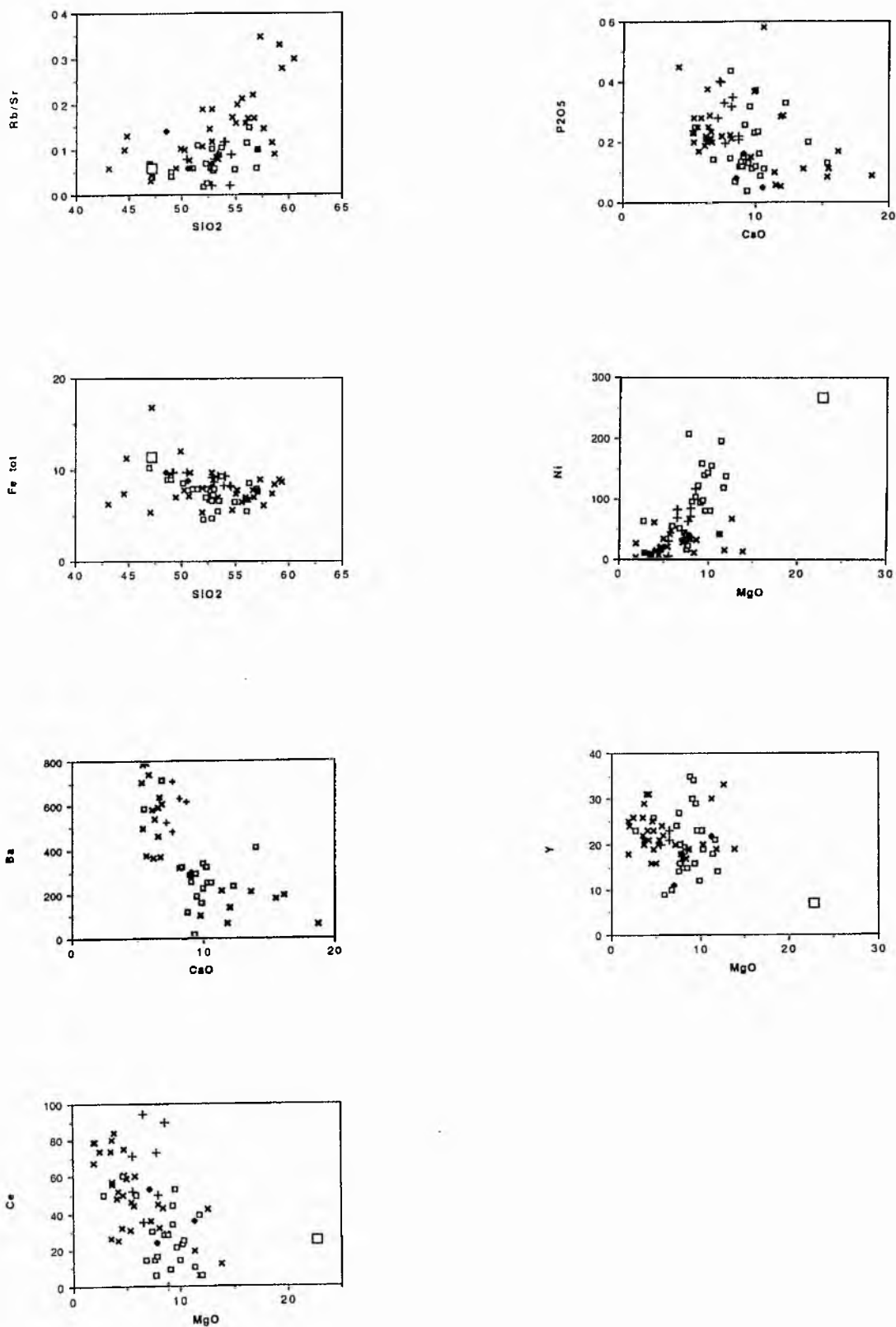


Fig. 5.20 (continued). Trace element variation diagrams for the Narin-Portnoo, Meenalargan, Kilrean, Summy Lough and Glenard appinitic complexes.

(ii) Kilrean

MgO, CaO, Fe₂O₃tot, MnO, Ni, Cr are all enriched in the cortlandtite of this intrusion, while K₂O, Nb, Zr, Rb and Y are depleted.

Trace element variations in cortlandtite, hornblendite and diorite rock types from all the main intrusions are compared as MORB-normalised plots in Fig 5.21.

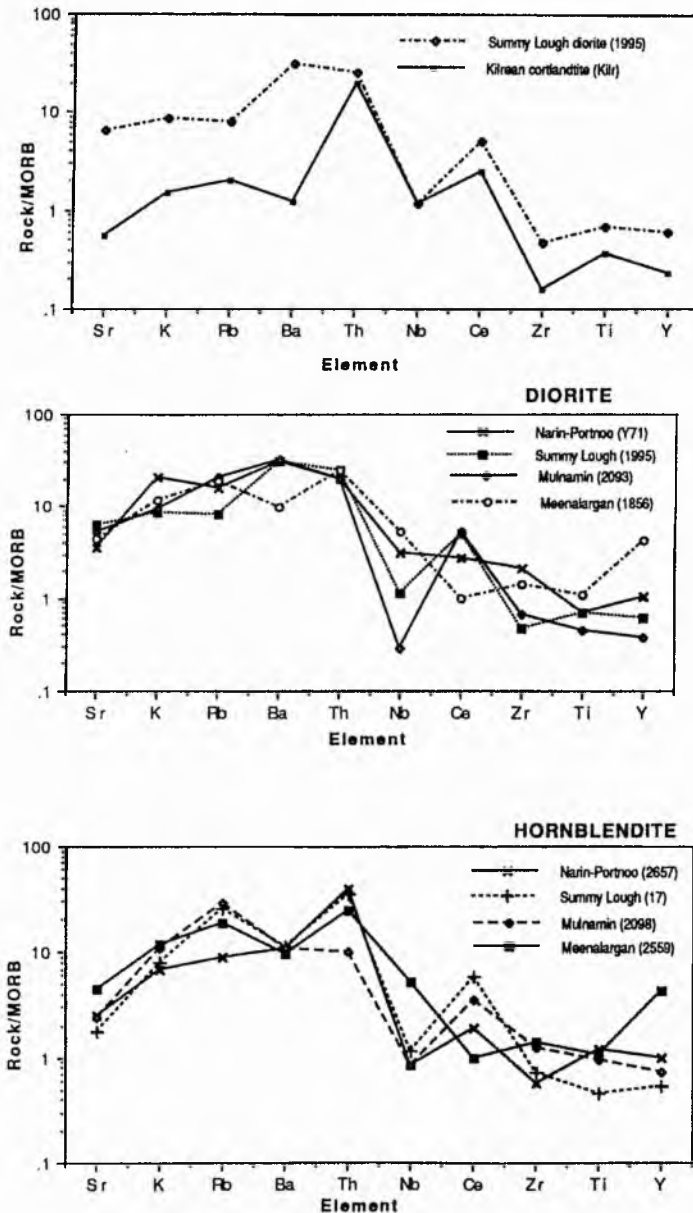


Fig. 5.21. MORB-normalised ratio plots of representative samples of cortlandtite, hornblendite and diorite from the main Ardara appinitic intrusions.

5.4 COMPOSITIONAL VARIATIONS WITHIN INDIVIDUAL APPINITIC INTRUSIONS

(i) Meenalargan

The main rock types of the Meenalargan appinitic complex, namely hornblendite, diorite and 'appinite' display a wide range of composition. As SiO_2 increases with magmatic evolution so Al_2O_3 and K_2O (with two exceptions) increase, Cr decreases and MgO and Fe_2O_3 tot are relatively invariant (Fig. 5.22).

(ii) Narin-Portnoo

The main rock types of the Narin-Portnoo intrusions, including hornblendite, hornblende diorite, hybrid diorite, biotite diorite and 'appinite' have a wide variation in composition. As SiO_2 and Al_2O_3 increase with magmatic evolution then MgO, Fe_{tot} and Ni decrease. K_2O and the Rb/Sr ratio rises sympathetically (Fig. 5.23). It is possible to distinguish between the diorites and the appinite on the basis of their SiO_2 , MgO, Ni and Cr compositions; the appinite is relatively enriched in MgO, Cr and Ni compared with the other diorites (Fig. 5.23).

(iii) Summy Lough diorite

The trends of elements of the rocks of the Summy Lough diorite intrusion are less well defined than those of Meenalargan and Narin-Portnoo. It is clear that with magma evolution Ni and MgO decrease with slight decrease in CaO accompanied by an increase in Al_2O_3 from hornblendite to diorite. Rb/Sr falls with increasing K_2O (Fig. 5.24).

(iv) Mulnamin

The diorites of Mulnamin show limited variation in major and trace elements in the rocks analysed (Fig. 5.25).

5.5 COMPARISON OF TRENDS WITHIN APPINITIC BODIES

(i) There is a general decrease in MgO, Cr and Ni with increasing SiO_2 in all intrusions while Al_2O_3 increases sympathetically indicating that no peraluminous phase (e.g. biotite) is fractionally removed as part of the appinite differentiation process.

(ii) The Narin-Portnoo body evolves to high Rb/Sr with increasing K_2O while the opposite is true in the Summy Lough diorite.

(iii) CaO remains relatively invariant in all intrusions.

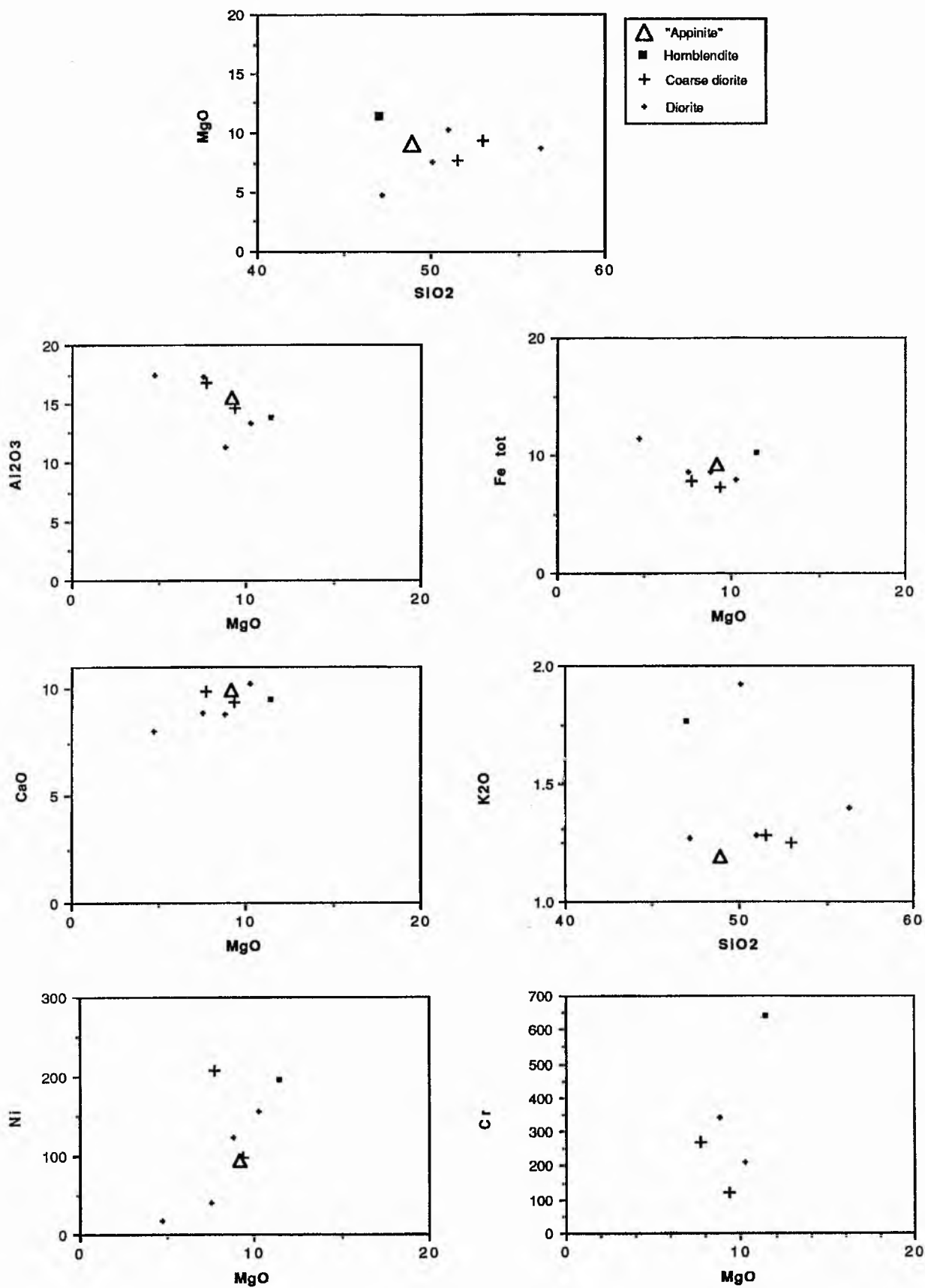


Fig. 5.22 Variation plots for the Meenalargan dioritic complex

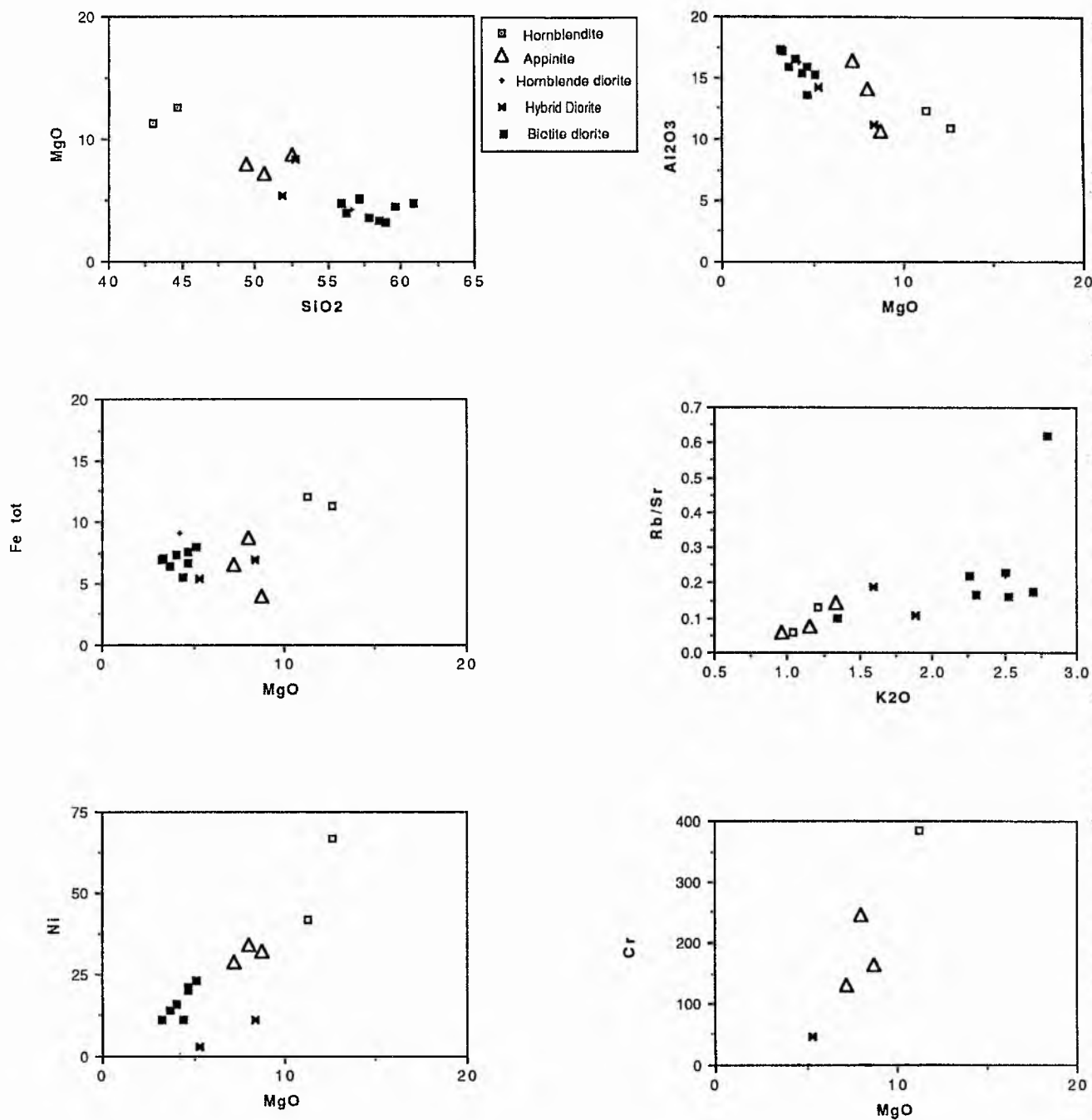


Fig. 5.23 Variation diagrams for the Narin-Portnoo appinite intrusions.

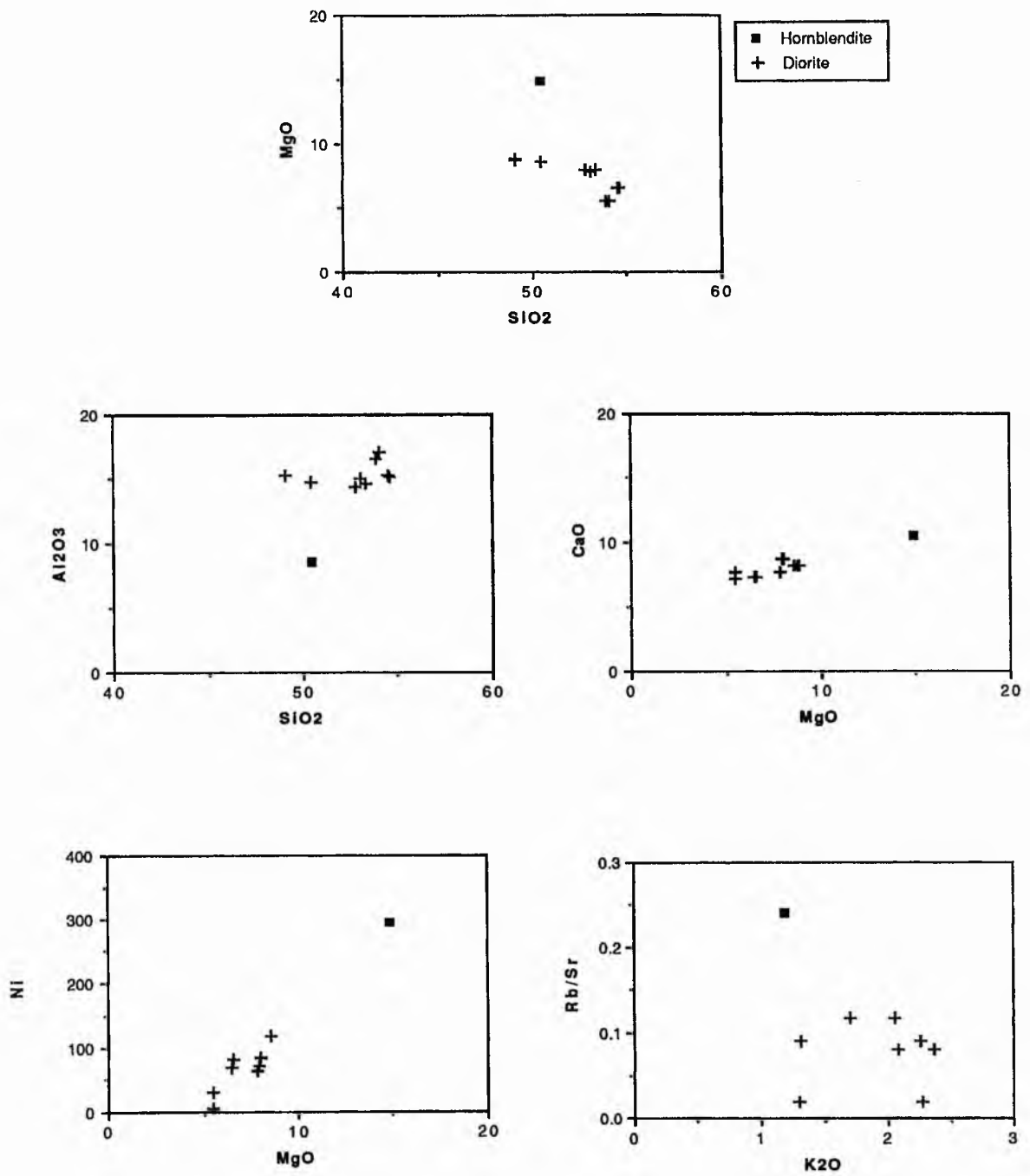
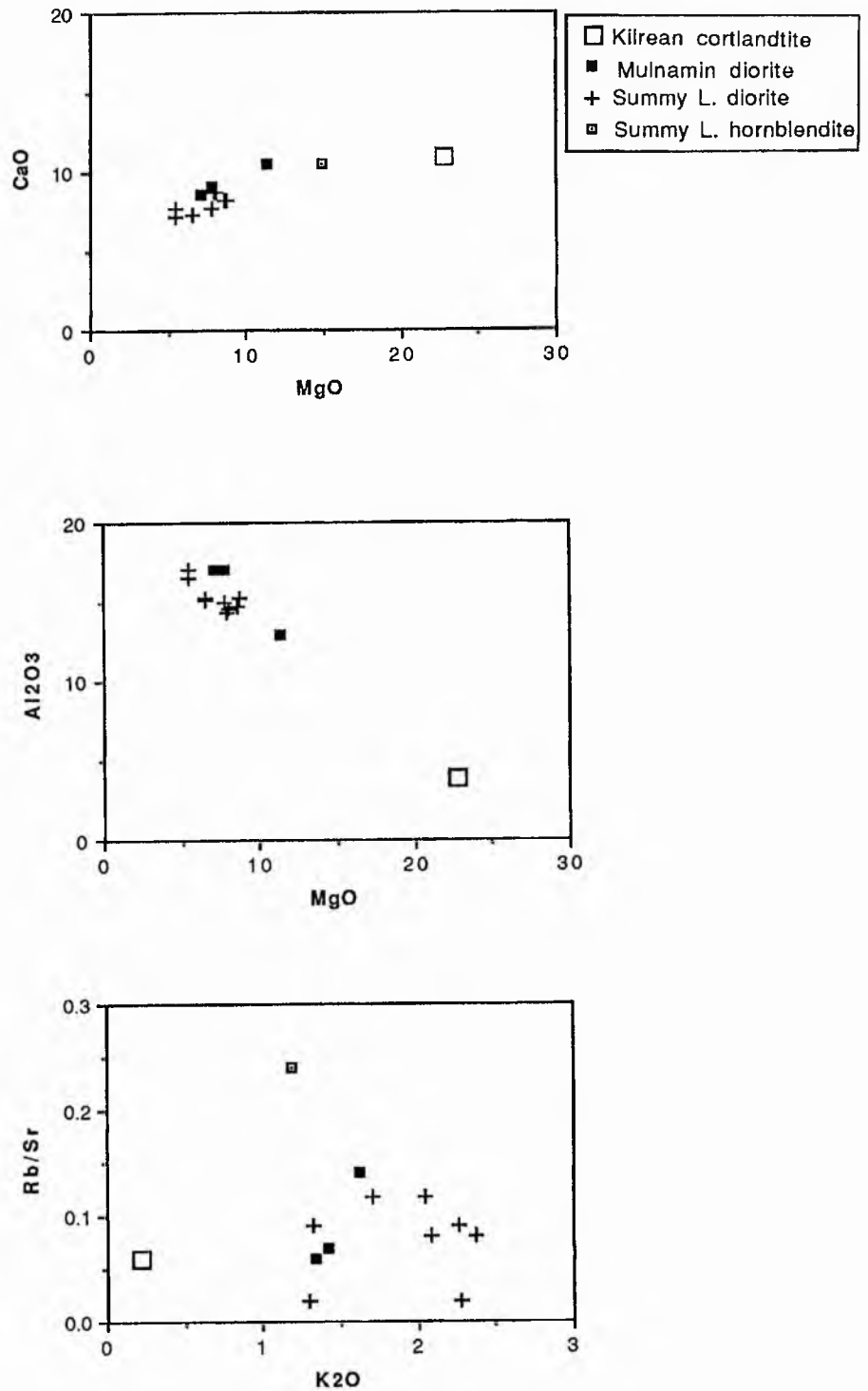


Fig. 5.24 Variation diagrams for the Summy Lough intrusion



5.6. FRACTIONAL CRYSTALLISATION AND DIFFERENTIATION OF THE ARDARA APPINITES AND GRANITOIDS

In this section various models for fractional crystallisation for the generation of the diverse rock types of the Ardara igneous complex are proposed and tested. Two main types of modelling of magmatic suites are employed based on (a) the constraints imposed by crystal-liquid partition coefficients on the trace element distribution patterns, and (b) mass balance constraints on the major element abundances. Samples for starting and target magma compositions were chosen on the basis of a representative analysis which is taken to represent a particular rock type based on field relations, geochemistry and petrographic texture. The presence of an apparently cumulate texture would for example, exclude a sample as would unusually high MgO, Cr or Ni abundances for a given SiO₂ level. The most primitive fresh sample without any such cumulate features can be a good candidate for a parental magma.

(a) Trace element modelling

This modelling is quantitative and is based on plots of trace element variations with superimposed vectors representing the effects of fractional crystallisation (assuming Rayleigh fractionation in all cases) using the partition coefficients of Pearce & Norry (1979), Cox, Bell & Pankhurst (1979) and Arth (1976) using values for basic, intermediate and acid melts where available or appropriate. The effect of mineral extraction is determined by the relationship between the theoretical distribution coefficient value and element content of the rock according to the equation:

$$\frac{\text{Concentration in mineral}}{\text{Concentration in liquid}} = K_D$$

The vector arrows marked on the figures define the fractionation path the magma would take should there be crystallisation of that particular mineral during fractionation of the melt (the origin of the arrow is zero). Values are plotted on log axes. The main relationship tested is the degree of control on fractionation trends exerted by pyroxene, amphibole, biotite, plagioclase, K-feldspar and accessory phases in the main rock types of the Ardara igneous complex. Elements with similar behaviour are grouped together as:

- (a) LIL elements (Rb, Sr, Ba)
- (b) HFS elements (Zr, Nb, Ti)
- (c) RE (or RE-like) elements (La, Ce, Y)
- (d) Compatible elements (Cr, Ni, V).

(b) Mass balance modelling

The members of the Ardara pluton and one appinite body (Narin-Portnoo) are modelled quantitatively with the aim of estimating the amount of mineral extraction required

to derive specified fractionation products from a postulated parental starting composition. The mathematical basis of this model is in effect a numerical expression of the lever rule ("some of it plus the rest of it, equals all of it"). A linear mixing calculation dealing with, in this case crystal fractionation, states that compositions of the extraction assemblage, the parent magma and the daughter magma must be linearly related (Ragland 1989). The basic equation for all types of linear mixing is

$$Z = NX + (1 - N)Y \quad (\text{after Ragland, 1989})$$

where Z = Parent magma

N = Fraction crystallised

X = Extract

Y = Residual liquid

The definitions of X, Y, Z and N depend on what process is being modelled, fractional crystallisation or crystal accumulation and in effect represent vectors or arrays of major element (oxide) compositions. Table 5.2 defines these terms for each process.

Process	Y	Z	X	N
Fractional crystallisation	Residual liquid	Parent crystallised	Extract	Fraction of crystal extracted
Accumulation	Melt	Cumulate crystals	Cumulus	Fraction of crystals accumulated

The technique of mass balance modelling used was that of Geist et al. (1989), based on the principle of mass balance described in Stormer & Nicholls (1978). Using measured mineral and whole rock compositions of the 'parent' samples a 'daughter' composition is calculated from the extraction of major mineral phases (hornblende, augite, plagioclase, and so on) which is represented by the percent cumulate of extracted crystals. The statistical significance of the calculation is obtained by the sum of the weighted residual squared (R^2), the smaller this value the better the calculated fit, ideally the R^2 value should be close to 0.0 but values up to 1.0 are normally regarded as acceptable.

In this instance four main relationships are modelled:

- Relationships between the units of the main Ardara pluton
- Relationships within an appinite intrusion (Narin-Portnoo). This body was selected because of its wide range of rock types and apparently magmatic textures.
- Relationships between evolved appinites and the granites of the main Ardara pluton.

- The relationships between evolved appinites, granites associated with appinites and the granites of the main Ardara pluton.

5.6.1 The Ardara pluton

(i) Trace element vector modelling

The presence of a sharp contact between the outer unit (G1) and inner unit (G2) in the northern part of the complex (south of Maas) and the gradational contact between the inner unit (G2) and the central unit (G3) suggest the presence of two granitic pulses, an outer unit (G1) and an inner and central unit (G3), (Pitcher & Berger 1972). It should be noted that the presence of sharp internal contacts however does not preclude differentiation at somewhat deeper levels with periodic pulses sampling a successive residual magma.

The presence of compositional gaps and considerable scatter in the geochemistry of the granitoids of the Ardara pluton has already been noted (Fig. 5.5 and 5.7). The trends of incompatible element depletion (Rb, Th, Y) and compatible element depletion (Cr, Fe, Mg) from G1 to G3 suggest the early crystallisation of minerals including calcic plagioclase, augite, hornblende, biotite and Fe - Ti oxide.

(a) LIL Elements.

The plots for incompatible elements are consistent with the removal of various combinations of plagioclase, biotite, hornblende and alkali feldspar (Fig. 5.26 a-c)

(b) HFS elements

The HFS trends are shown in Fig. 5.26 (d-f). Both Nb and Zr decrease with fractionation controlled by biotite and hornblende crystallisation while magnetite removal is also required to explain the decrease in TiO₂ abundance. The observed decrease in Zr can be explained by the crystallisation of zircon. The behaviour of Y may be controlled by accessory phases such as zircon and apatite. The HFS trace element geochemistry indicates two apparent trends. Trend 1 from G1 to G2, is dominated by the removal of plagioclase, biotite and hornblende, while trend 2 from G2 to G3 is dominated by the removal of biotite and to a lesser extent hornblende.

(c) REE

Fig. 5.26 g supports the fact that hornblende has a low K_d for LREE including Ce but a high one for HREE like Y. Hornblende and biotite as well as accessory minerals concentrate Ce and it is apparent that crystallisation of hornblende and biotite have an important control on the fractionation paths of G1 and G2, and even within G3 (Fig 5.26 g).

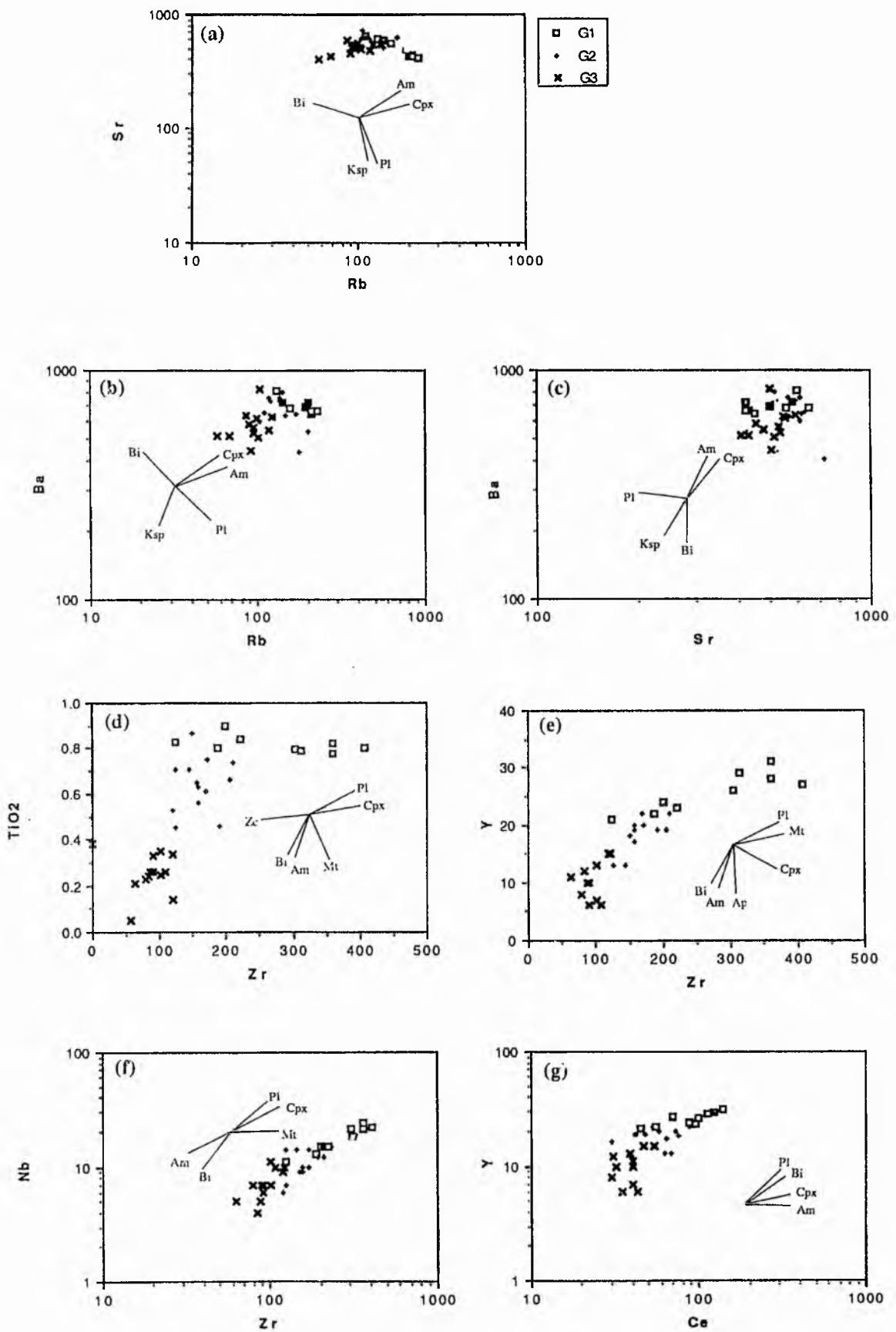


Fig. 5.26 (a-c) Variation plots of LIL elements Rb, Sr and Ba with superimposed mineral vectors from the units of the main Ardara pluton. (d-f) Variation plots of HFS elements Zr, Ti, Y, Nb from the units of the main Ardara pluton. (g) REE plot for the units of the main Ardara pluton. Am = amphibole, Bi = biotite, Cpx = clinopyroxene, Pl = plagioclase, Ksp = K feldspar, Mt = magnetite, Ap = apatite, Zc = zircon.

(d) Compatible elements

Plots for elements which are compatible with mafic mineral assemblages such as hornblende, augite and biotite are shown in (Fig. 5.27)

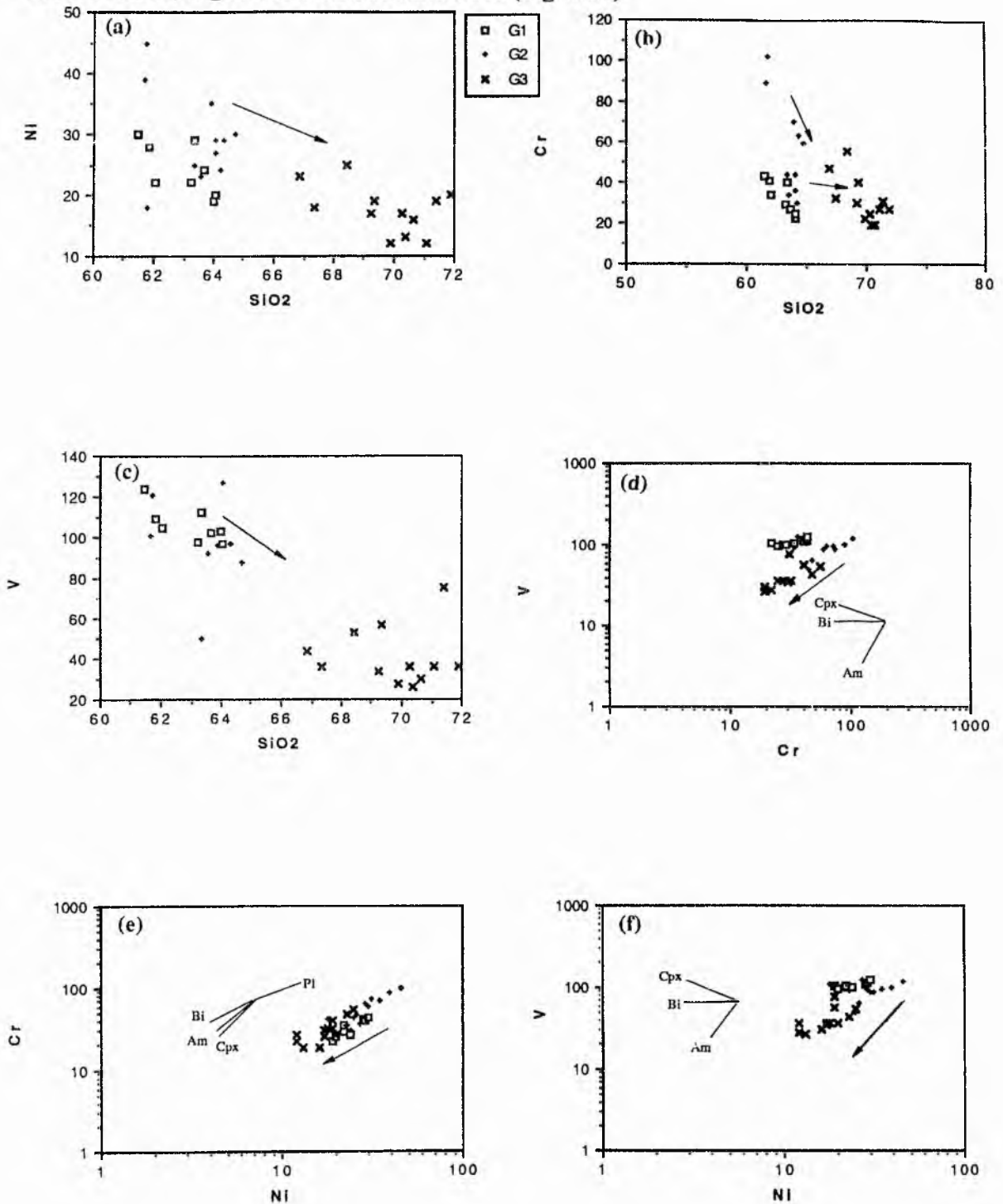


Fig. 5.27. Trace element variation plots of Ni, Cr and V for the units of the main Ardara pluton. Mineral vectors and apparent fractionation directions are superimposed. See Fig. 5.26 for key to mineral symbols.

Fractionation trends in G1 and G2 are strongly controlled by the extraction of biotite and to a lesser degree by amphibole, while evolution of G3 can be related to the same minerals but in different proportions (Fig. 5.27). The level of V in G3 is markedly lower in G1 and G2 suggesting a quite separate magma pulse (see Figs 5.27 d and f). In the cases of Ni and Cr, both of which fractionate into mafic minerals, G2 appears to be more mafic in composition than G1. This is difficult to explain by a simple fractionation from G1 to G2. Both G1 and G2 show overlap in SiO₂, apparent from a geochemical traverse of the northern part of the Ardara pluton (Fig. 5.7 a). This is important when considering the relationship between G1 and G2. It might suggest that G2 represents a more primitive pulse emplaced prior to the full crystallisation of G1.

From trace element evidence it is likely that fractional crystallisation of plagioclase, augite and hornblende exerted a strong control on the compositions of G1 and G2, whilst fractional crystallisation of amphibole and biotite seem to have controlled the composition variation in G3. In order to quantitatively test these fractionation models mass balance modelling was performed on the various units of the main Ardara pluton and the results of these various models are presented in Table 5.2 (a). Among the principal models tested were the generation of a G2 daughter from a G1 parent, the generation of a G3 daughter from a G2 parent, and the generation of a G3 daughter from a G1 parent, all by extraction of observed early phases of hornblende, augite, plagioclase, biotite and oxides.

(a) Generation of G2 from a G1 magma.

Six models are presented in Table 5.2 (a), ranked according to their R² value (a measure of the quality of the fit of the model). The model with the lowest R² (0.44) involves 33% removal of a cumulate comprising of 8% augite, 26% biotite, 64% An₃₀ and 2% titanite to form G2 (Table 5.2 a). This model is petrographically reasonable as augite, biotite and plagioclase are important early minerals. The amount of titanite required for this model is relatively high but is possible based on the evidence of calculated modal percentages (Table 4.1.) Augite is minor compared to hornblende which replaces it and has a significantly higher modal percentage. Consequently a model involving fractionation of hornblende was tested (Table 5.2 a). This model may be the most realistic in view of the petrographic constraints and the modal compositions of G1 and G2. One point which is difficult to reconcile is the fact that G2 contains higher values of Ni and Cr than G1 (Fig. 5.27). This is difficult to explain by simple trace element models of fractional crystallisation of mafic minerals from G1 to G2 however it is consistent with major element constraints using mass balance calculations.

(b) Generation of G3 from a representative G2 magma.

None of the models listed in Table 5.2 (a) satisfactorily derived statistically significant daughter compositions approximating G3 from a G2 parent. The model with the lowest R² (2.78) value is unrealistic as it requires very large amounts of fractionation of

hornblende, magnetite and titanite. These results suggest that G3 is not related to G2 by any simple crystal-liquid process.

(c) Generation of G3 from a representative G1 magma.

Results of fractionation of G1-type magma indicate that it is very difficult to obtain a realistic daughter of G3 composition by fractionational crystallisation of a G1 parent and it is also unlikely for G3 to be directly related to G1 by simple crystal-liquid processes (Table 5.2 a).

(d) Conclusions

Geochemical modelling has enabled the importance of mineral phases in controlling the geochemistry of the granitoid units of the main Ardara pluton to be assessed. It is clear from vector diagrams and mass balance modelling that hornblende, pyroxene, biotite and plagioclase are dominant controls on the compositions of these units. The evidence of geochemistry indicates that G3 is a separate pulse of magma, not simply related to the outer and inner units (G1 and G2). It is possible to derive a magma of G2 composition from a parent with a G1-type composition, however the Ni, Cr and V geochemistry indicates that G2 is more mafic than G1. It is thus possible that G2 may represent a different pulse from G1. Although field evidence indicates a sharp contact between G1 and G2 in only one place (south of Maas) and a gradational, intersheeted contact elsewhere (north of Lough Fad) the two magmas may be related at depth. It is also apparent from geochemical modelling that generation of a G1-type daughter from a G2 parent in situ is not possible as it requires unrealistic masses of cumulate to obtain a daughter composition similar to that of G1.

5.6.2 Narin-Portnoo

(i) Trace element vector modelling

(a) LIL elements

The rocks of the Narin-Portnoo appinitic intrusion display a range of composition from hornblendite to diorite, biotite diorite and evolved granites. Ba and Rb increase with SiO₂ while Sr decreases (Fig. 5.28 a-c). The mineral vectors plotted on the variation diagrams of (Fig. 5.28 d-f) underline the importance of hornblende and plagioclase, and to a lesser degree biotite crystallisation in the early stages of evolution of the magma from hornblendite to diorite as shown by Trend 1 (Fig. 5.28) with plagioclase and K feldspar dominating the crystallisation trend of the later evolved granites, Trend 2 (Fig. 5.28). The difference in trend seen on Fig. 5.28 (d) from hornblendite to diorite and diorite to evolved granite may be due to the crystallisation of hornblende in the early stages of magma evolution, followed later by crystallisation of biotite, plagioclase, and K feldspar leading to the formation of the granites. The granites of the Narin-Portnoo intrusion display trends which lie off the general trend of the basic and intermediate rocks of the intrusion

(Fig. 5.29 a and b) suggesting that the granites may not be related directly by fractional crystallisation to the basic rocks of the intrusion.

(b) HFS elements

Both Zr and Nb increase during fractional crystallisation of basic and intermediate magmas (Pearce & Norry 1979) and this is also the case in the Narin-Portnoo intrusion (Fig. 5.29 b and c). From these plots it is apparent that the Narin-Portnoo granites lie off the fractionation trend of the dioritic rocks, supporting the evidence of LIL elements.

(c) RE elements

Ce increases with SiO_2 (Fig. 5.29 f) suggesting that it is behaving wholly as an incompatible element. On the other hand Y decreases in the early stages, probably due to amphibole removal, but then increases after amphibole removal ceases (Fig. 5.29 d).

(d) Compatible elements

Ni, Cr and V all decrease with increasing SiO_2 (Fig. 5.30 a-c). Mineral vectors indicate early clinopyroxene fractionation followed by later fractionation of biotite and hornblende. Fig. 5.30 (d-f) show the granites again to lie off the general trend which could be more strongly controlled by biotite fractionation.

Overall the trace element patterns are well accounted for by hornblende, biotite (and some clinopyroxene) removal with the removal of plagioclase being important in the late stages. The granites may not be singly related to the more primitive members of the appinite suite.

(ii) Mass Balance modelling

The aim of this modelling was to determine, by taking a representative dioritic parental magma composition and extracting various minerals, whether it is possible to generate magma or cumulate compositions similar in composition to analysed compositions of hornblendite, biotite diorite and evolved granite collected from the Narin-Portnoo appinite intrusion.

(a) Generation of hornblendite from diorite

The model of crystal accumulation of 16% biotite, 83% An60, 1.0% magnetite and 0.3% titanite or by crystal accumulation of 19% biotite and 81% An60 has no statistical significance for the generation of hornblendite from diorite. The results of this modelling are presented in Table 5.2 b.

(b) Generation of biotite diorite from diorite

The model of blending augite, hornblende and/or biotite, epidote and magnetite has no statistical significance for the generation of biotite diorite from the dioritic composition used in the model (Table 5.2 b). The most realistic model involves 54% crystal extraction of augite, hornblende and magnetite and has an R^2 value of 15.00. A

different dioritic parent magma (diorite 2, Table 5.2 b) does not improve the fit. Although the results indicate the limitations of this modelling in dealing with rocks which illustrate broad geochemical variation and diversity they also indicate that the dioritic rocks of Narin-Portnoo may not be behaving as simple fractional crystallisation systems.

(c) Generation of evolved granite from biotite diorite

Cross-cutting the Narin-Portnoo intrusion are several late-stage granitic dykes and sheets which have a geochemical signature that is broadly similar to that of the most evolved member of the Ardara pluton (G3). Magmatic modelling of an evolved granitic composition from an evolved appinitic composition (biotite diorite) does not seem to be possible (Table 5.2 b). This supports the geochemistry and field observations. The granites are highly evolved ($\text{SiO}_2 \geq 67\%$) and with 55% extraction of a mix comprising 37% plagioclase, 36% hornblende, 22% biotite, 2% titanite and 3% magnetite a composition with an R^2 value of 7.25 is obtained.

(d) Generation of evolved granite (Narin-Portnoo) from a G2 or G3 (Ardara) parent

Results of modelling the generation of evolved appinitic granite from a parental main pluton (G2 or G3) composition are presented in Table 5.2 (c). Starting with G2 with 24% fractional crystallisation and extraction of a cumulate of 13% augite, 43% biotite, 37% plagioclase, 1% magnetite and 5% titanite, the residuals are 1.89. A more realistic model, from the point of view of petrography, is 22% fractionation with extraction of a mix of 10% hornblende, 47% biotite, 33% plagioclase 2% magnetite and 8% titanite results in an R^2 value of 2.71. Neither model is a good statistical fit and each requires large degrees of fractionation of, for instance, titanite. The generation of evolved granite of Narin-Portnoo from a G2 Ardara parent composition may not be too unrealistic. Generation of the granite of Narin-Portnoo from a parental G3 composition requires 4% fractionation of 64% hornblende and 36% plagioclase or pure biotite extraction (Table 5.2 c).

5.6.3 Meenalargan

(i) Trace element vector modelling

(a) LIL elements

The rocks of the Meenalargan intrusion display a wide scatter for Rb, Sr and Ba (Figs. 5.31 a-c). There appears to be an increase in Rb and Ba with SiO_2 towards the granites whilst Sr is very scattered (Fig. 5.31 a-c). The mineral vectors plotted on the LIL variation diagrams (Fig. 5.31 d-f) show that hornblende, plagioclase, augite, and to a lesser degree K feldspar, fractionation could account for the minor variation trends. The Sr-Ba plot (5.31 d) indicates that both elements are totally incompatible suggesting that there has been no feldspar removal until the granites which appear to be quite separate.

(b) HFS Elements

A wide scatter in the analyses is apparent from the Harker diagrams (Fig. 5.32 a-c). The best defined trend is that of SiO_2 vs TiO_2 (Fig. 5.32 a) where there is a negative

correlation through hornblende to diorite to granite. While Zr and Y change little with SiO₂, there is a marked decrease in Nb with increasing SiO₂, and this could result from early hornblende fractionation depleting the residual melt in Nb. The importance of amphibole and plagioclase fractionation is apparent from the mineral vectors plotted on Fig. 5.32 (d-f). Hornblende, plagioclase, and minor biotite appear to be the main phases controlling the compositional trend of the rocks of the Meenalargan complex.

(c) RE elements

From the evidence of Harker plots (Fig. 5.33 a) it is apparent that there is an increase in Ce with SiO₂ while Y remains relatively constant (Fig. 5.32 c) suggesting that Ce is incompatible and therefore allanite, which is the only granitoid mineral to fractionate Ce has not been fractionated.

(d) Compatible elements

Harker plots (Fig. 5.34 a-c) show Cr, Ni and V to fall as SiO₂ increases suggesting significant fractionation of mafic phases. Ni vs Cr shows best the effect of biotite and hornblende extraction on the geochemical trend of the fractionated rocks. Mineral vectors indicate that biotite and hornblende dominate the fractionation path from hornblende to associated granite (Fig. 5.34 d-f).

(ii) Mass balance modelling

(a) Generation of diorite by fractionation of a meladiorite

It is possible to derive a daughter composition similar in composition to that of the diorite by 13% fractionation of a mix comprising 65% hornblende, 17% biotite, 15% plagioclase (An₅₀) and 3% titanite, however the model fit ($R^2 = 2.07$) is not very good (Table 5.2 d).

(b) Generation of granodiorite by fractionation of diorite

Using two different granodiorite daughter compositions it was not found possible to model such compositions from a representative dioritic parent composition by removal of various phases (Table 5.2 d).

Trace and major element modelling of the Meenalargan complex suggest that the granites of the complex are quite separate from the more dioritic rocks. Hornblende, biotite and plagioclase are the main phases controlling the compositional trends of the Meenalargan complex. Major element modelling indicates that it may be possible to derive diorite from a meladioritic parent by Rayleigh fractionation.

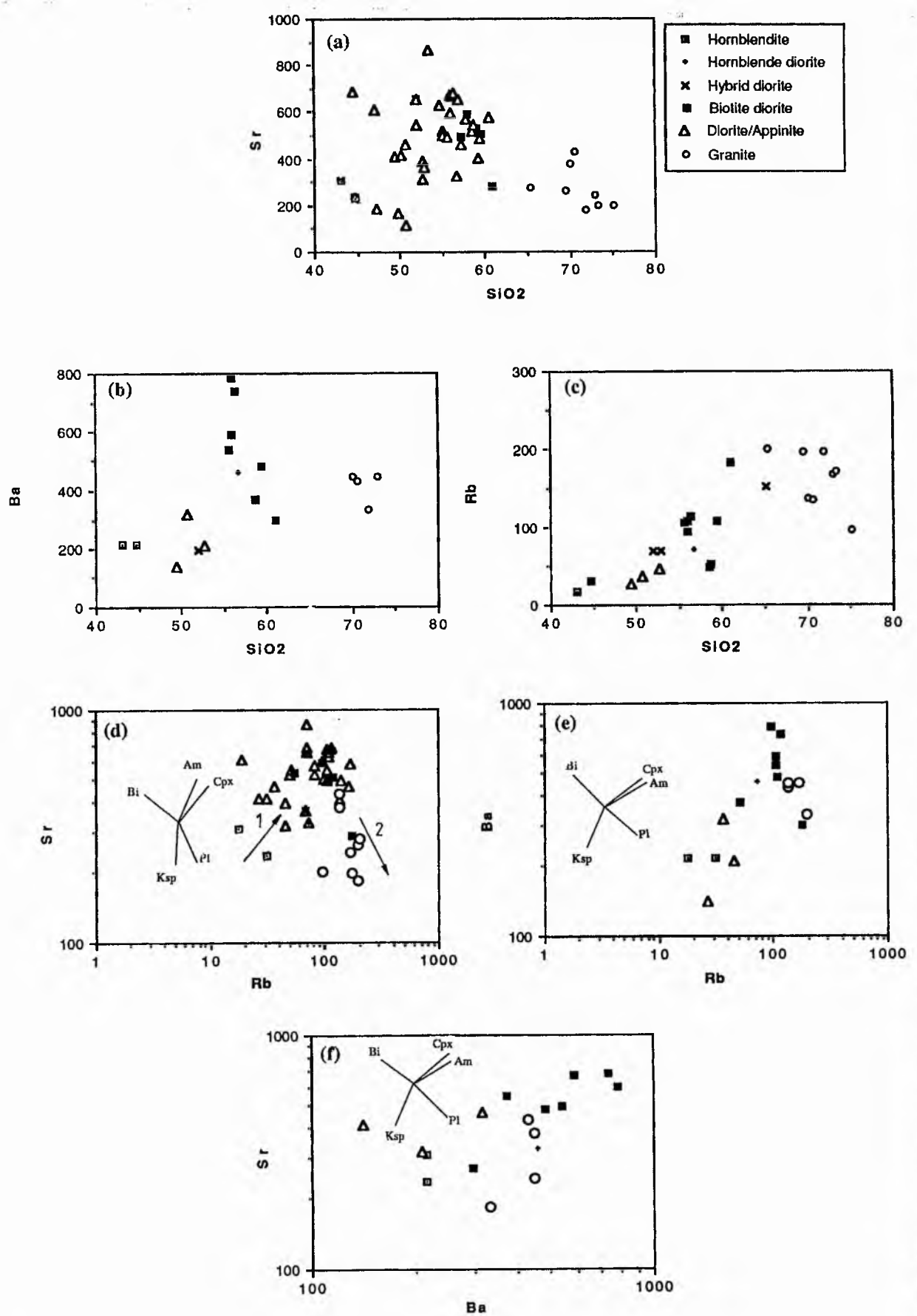


Fig. 5.28 (a-c) Variation plots of LIL elements Rb, Sr and Ba plotted against SiO₂ (d-f) Variation plots of LIL elements Rb, Sr and Ba with superimposed mineral vectors from the units of the Narin-Portnoo appinites. See Fig. 5.26 for key to mineral symbols.

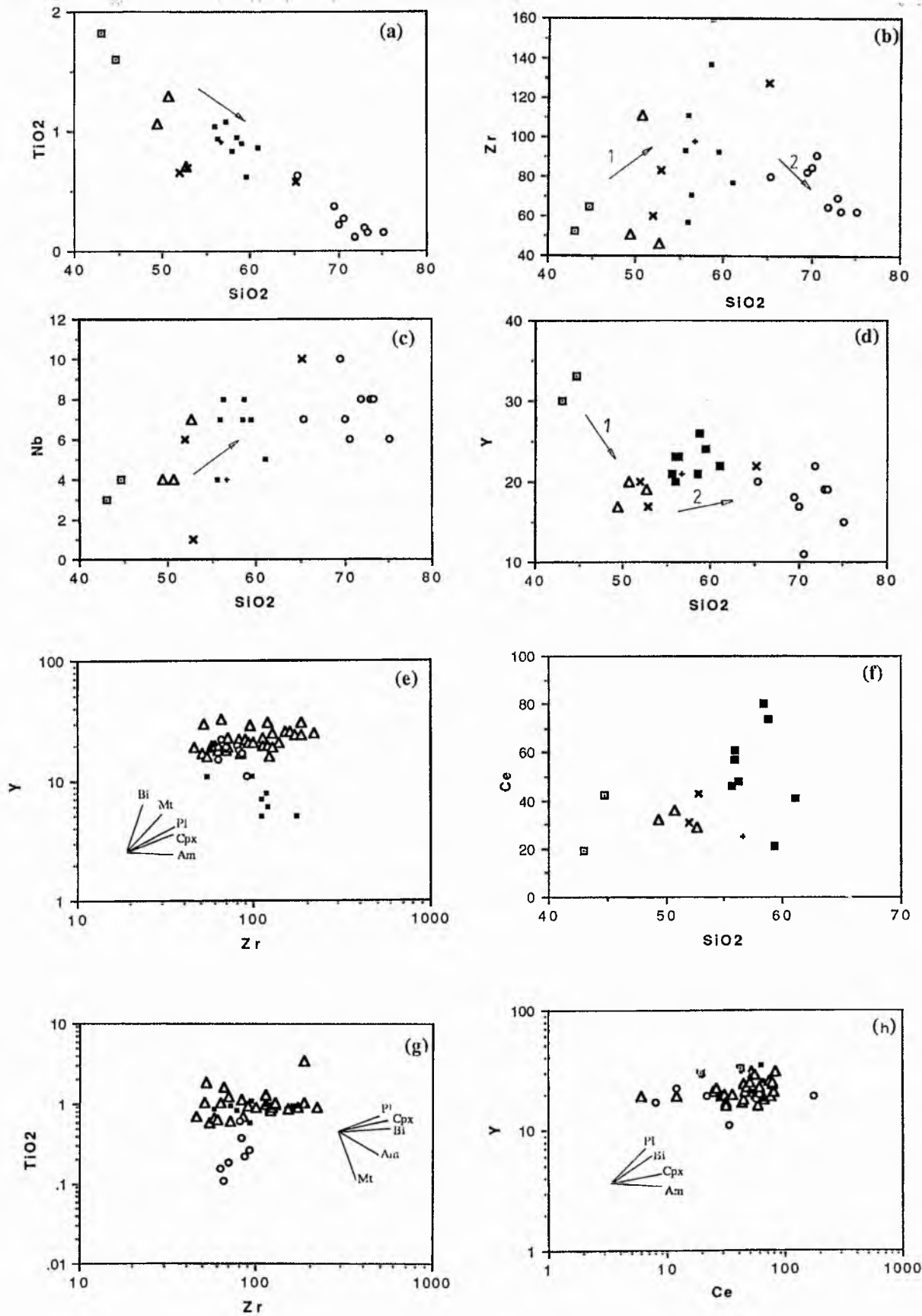


Fig. 5.29 (a-c) . Variation plots of HFS elements Zr, Ti, and Nb from the Narin-Portnoo appinites. (d-h) Variation plots of Y, Zr, Ce, and TiO₂ from the Narin-Portnoo appinites. Mineral vectors and apparent fractionation directions are superimposed. See Fig. 5.26 for key to mineral symbols.

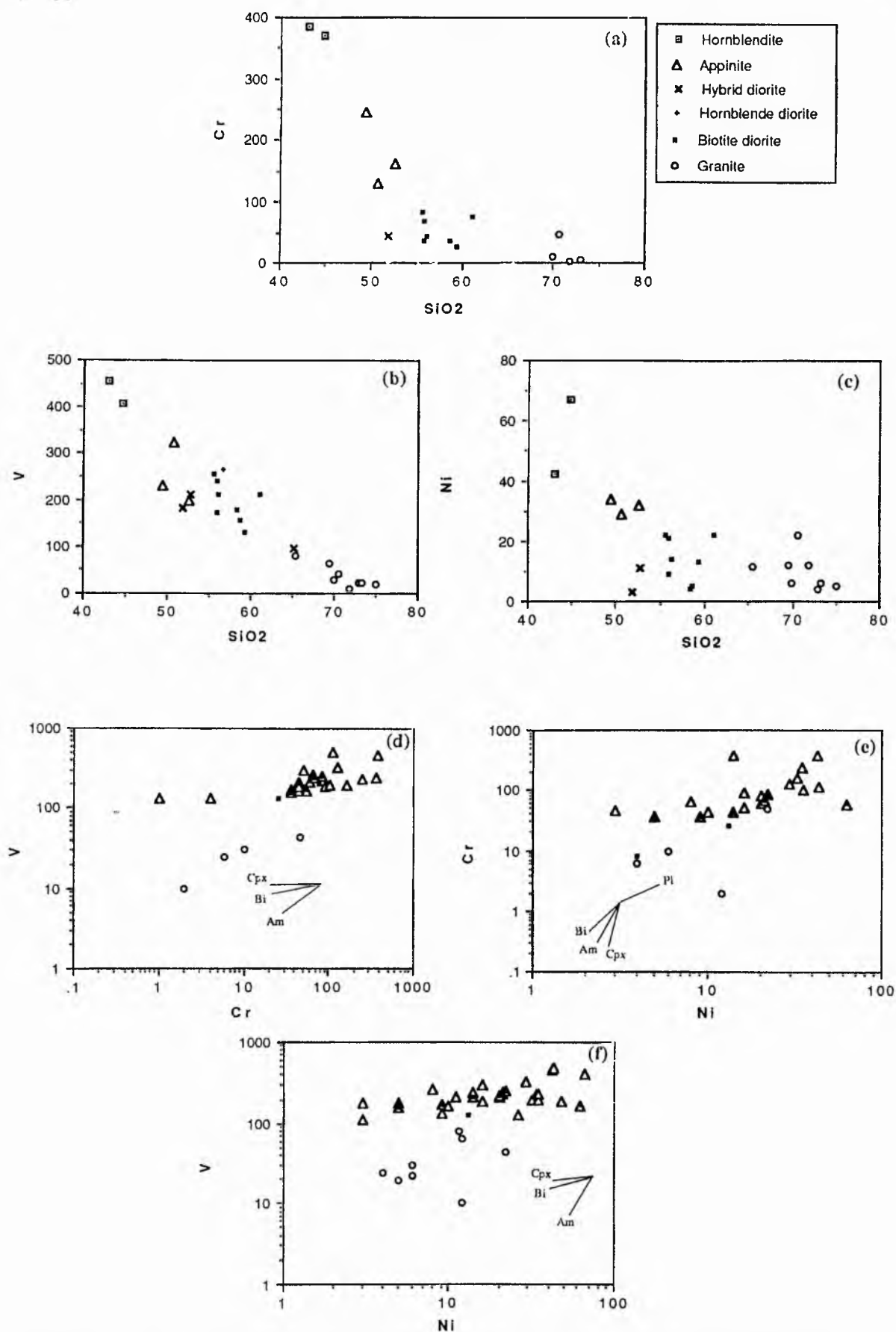


Fig. 5.30 (a-c) . Variation plots of compatible elements Cr, V and Ni from the Narin-Portnoo appinites plotted against SiO₂. (d-f) Variation plots of compatible elements Cr, V and Ni from the Narin-Portnoo appinites. Mineral vectors are superimposed, (see Fig. 5.26 for key to mineral symbols).

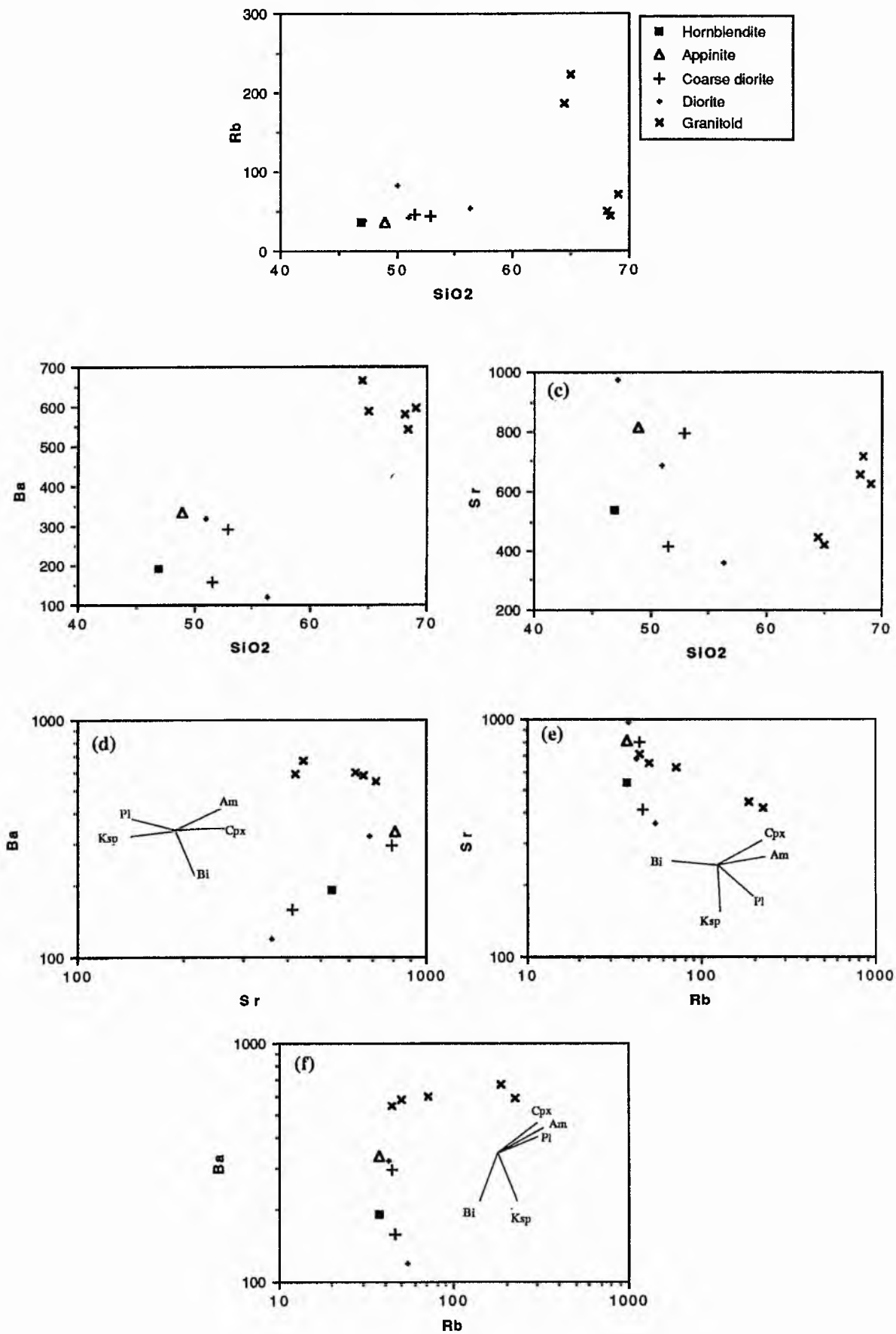


Fig. 5.31 (a-c) Variation plots of LIL elements Rb, Sr and Ba plotted against SiO₂ (d-f) Variation plots of LIL elements Rb, Sr and Ba with superimposed mineral vectors from the units of the Meenalargan dioritic complex. See Fig. 5.26 for key to mineral symbols.

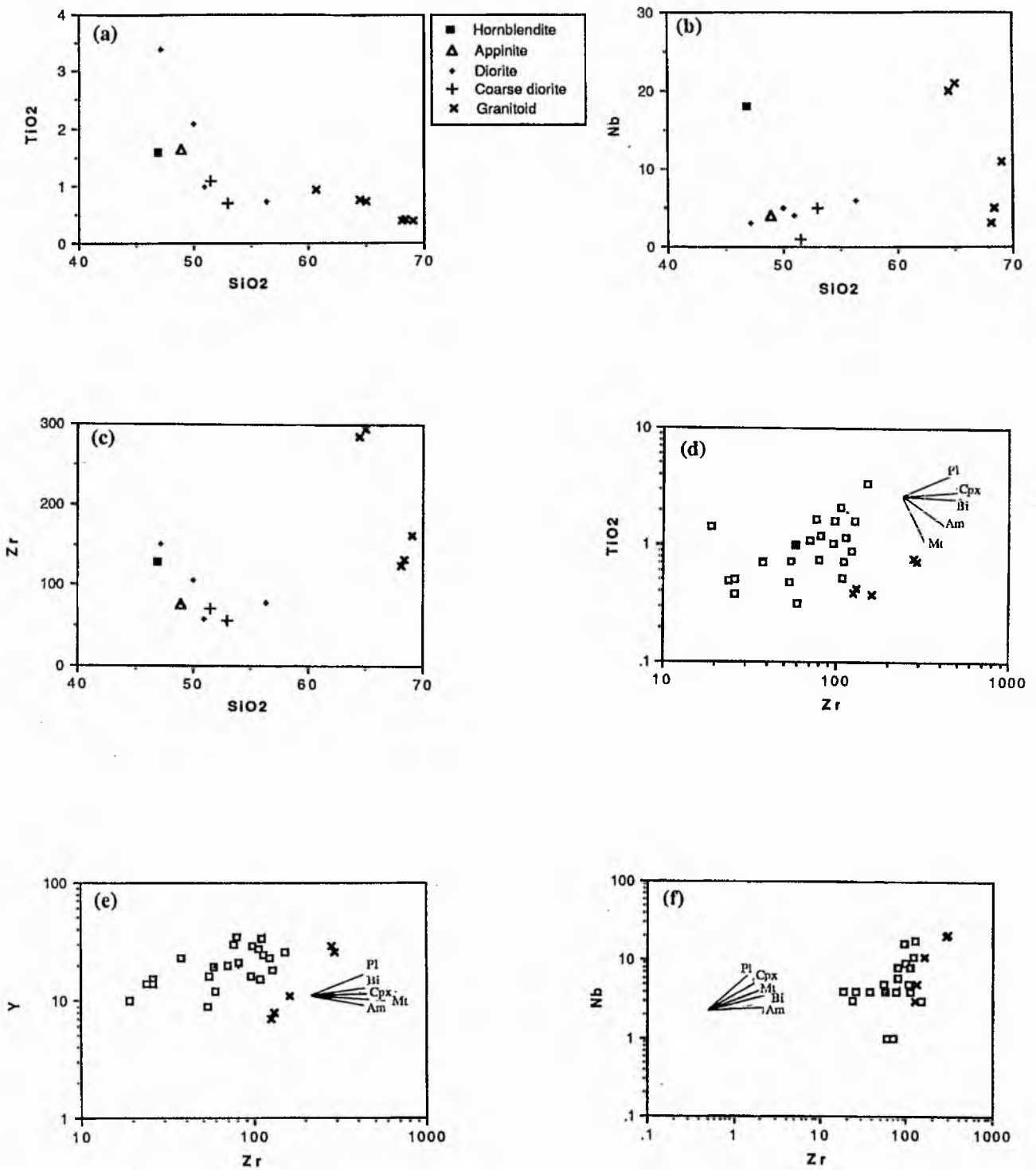


Fig. 5.32 (a-c) . Variation plots of HFS elements Zr, Ti, and Nb from the Meenalargan dioritic complex. (d-f) Variation plots of HFS elements Zr, Ti, and Nb from the Meenalargan dioritic complex. Mineral vectors and apparent fractionation directions are superimposed. See Fig. 5.26 for key to mineral symbols.

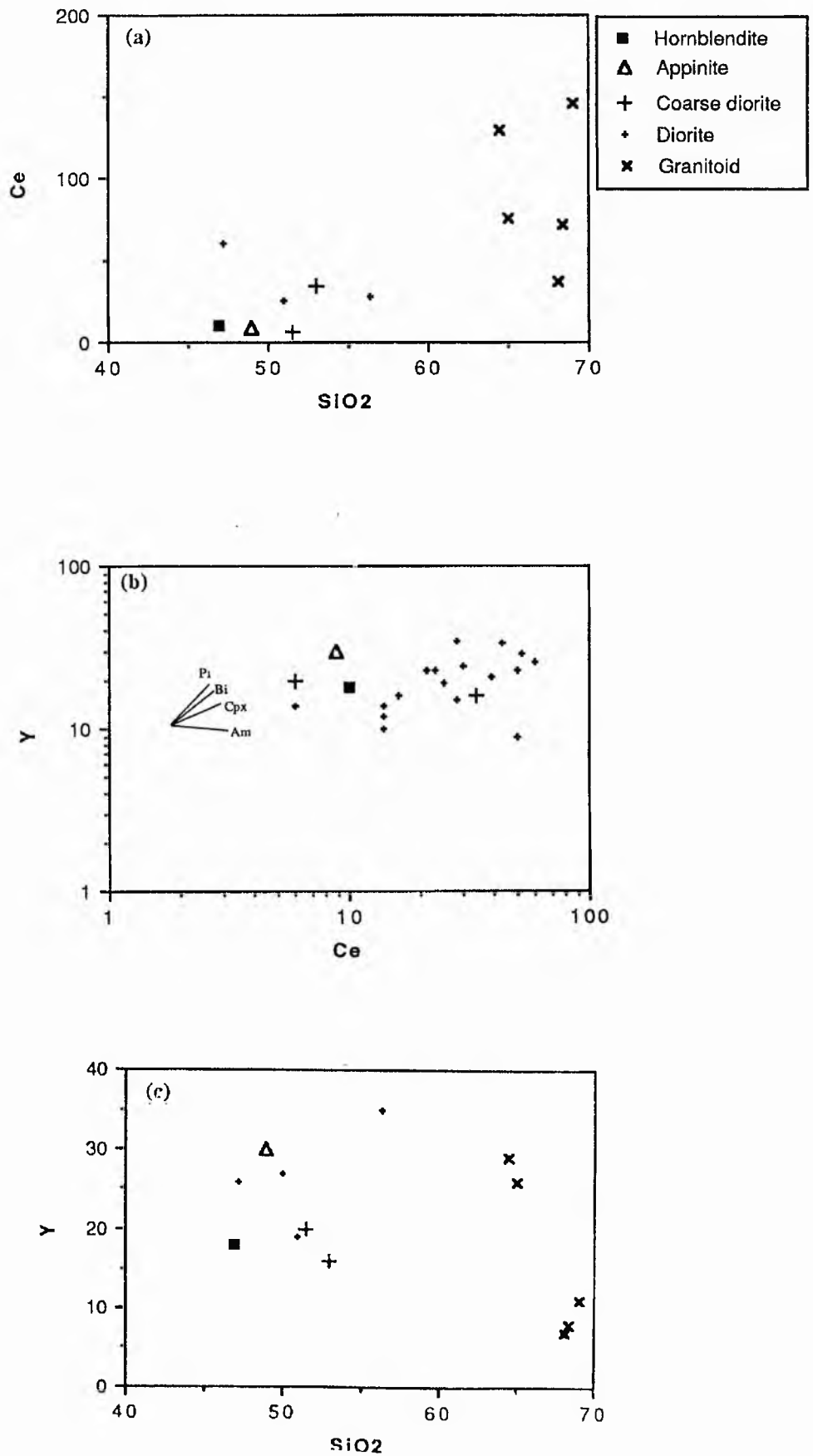


Fig. 5.33 (a-c) . Variation plots of Ce and Y from the Meenalargan dioritic complex. Mineral vectors are superimposed, (see Fig. 5.26 for key to mineral symbols).

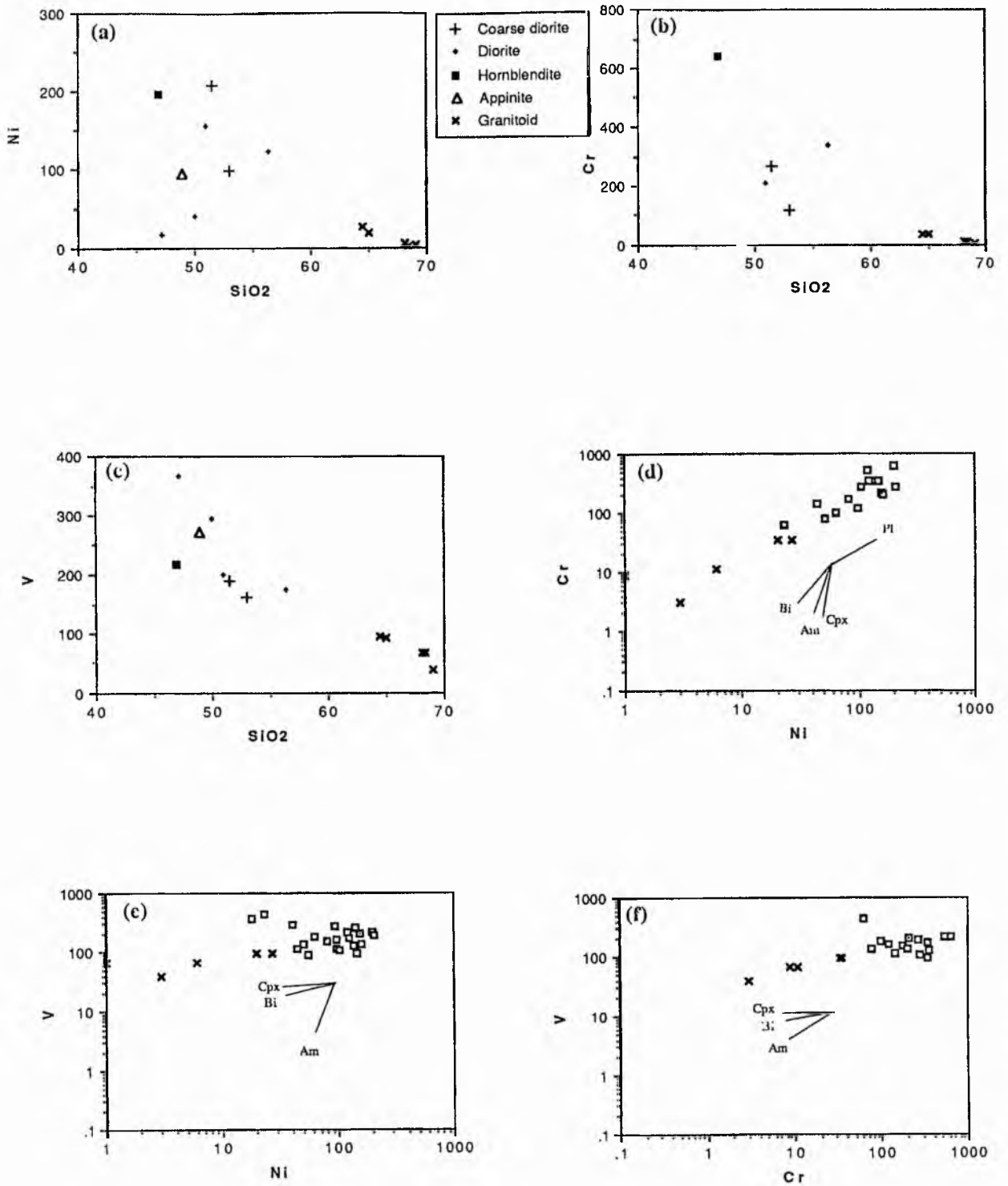


Fig. 5.34 (a-c) . Variation plots of compatible elements Ni, Cr and V plotted against SiO₂ from the Meenalargan dioritic complex. (d-f) Variation plots of compatible elements Ni, Cr and V from the Meenalargan dioritic complex. Mineral vectors and apparent fractionation directions are superimposed. See Fig. 5.26 for key to mineral symbols.

5.6.4 Summy Lough

(i) Trace element vector modelling

(a) LIL elements (Rb, Sr, Ba)

The diorite of Summy Lough shows some compositional variation from hornblendite to diorite mainly in terms of SiO_2 content (Fig. 5.35 a and b). The crystallisation trend seems to be largely controlled by augite, plagioclase and amphibole extraction (Fig. 5.35 d-f).

(b) HFS elements

Zr, Y, Nb, TiO_2 all increase with SiO_2 (Fig 5.36 a-d) and all plots indicate the strong control of hornblende, plagioclase, augite and to a lesser degree biotite, on the compositional trend (Fig. 5.36 e-g).

(c) RE elements

From the scatter in the variation plots of SiO_2 v Y, SiO_2 v Ce and Ce v Y (Fig 5.37) it is difficult to establish any major control in the trends.

(d) Compatible elements

Hornblende and augite appear to exert a strong control on the variation trend (Fig. 5.38).

(ii) Mass balance modelling

The limited compositional variation does not permit extensive mass balance modelling, however the presence of a small hornblendite body may be modelled as a cumulate of the diorite of Summy Lough (Table 5.2 e).

Results from modelling of hornblendite by accumulation from a dioritic magma indicate that the hornblendite may not easily be derived by simple crystal accumulation from a magma of dioritic composition. By 95% mass removal of a mix comprising 95% of An55 and 5% magnetite from diorite a cumulate hornblendite may be derived, but the fit is unacceptably poor.

5.6.5 Mulnamin

The limited samples available support a strong probable control on evolution by hornblende, augite, plagioclase and biotite fractionation (Fig. 5.39). No quantitative modelling was attempted.

5.7 APPINITE COMPOSITIONS AT A LIMESTONE-APPINITE CONTACT

Whole rock major and trace element geochemistry of the relationships at a limestone-appinite contact (where stable isotopic variation has also been studied) have been studied. The objective was to determine whether any changes in the whole rock geochemistry of the appinite occurred in proximity of with the contact with the limestone.

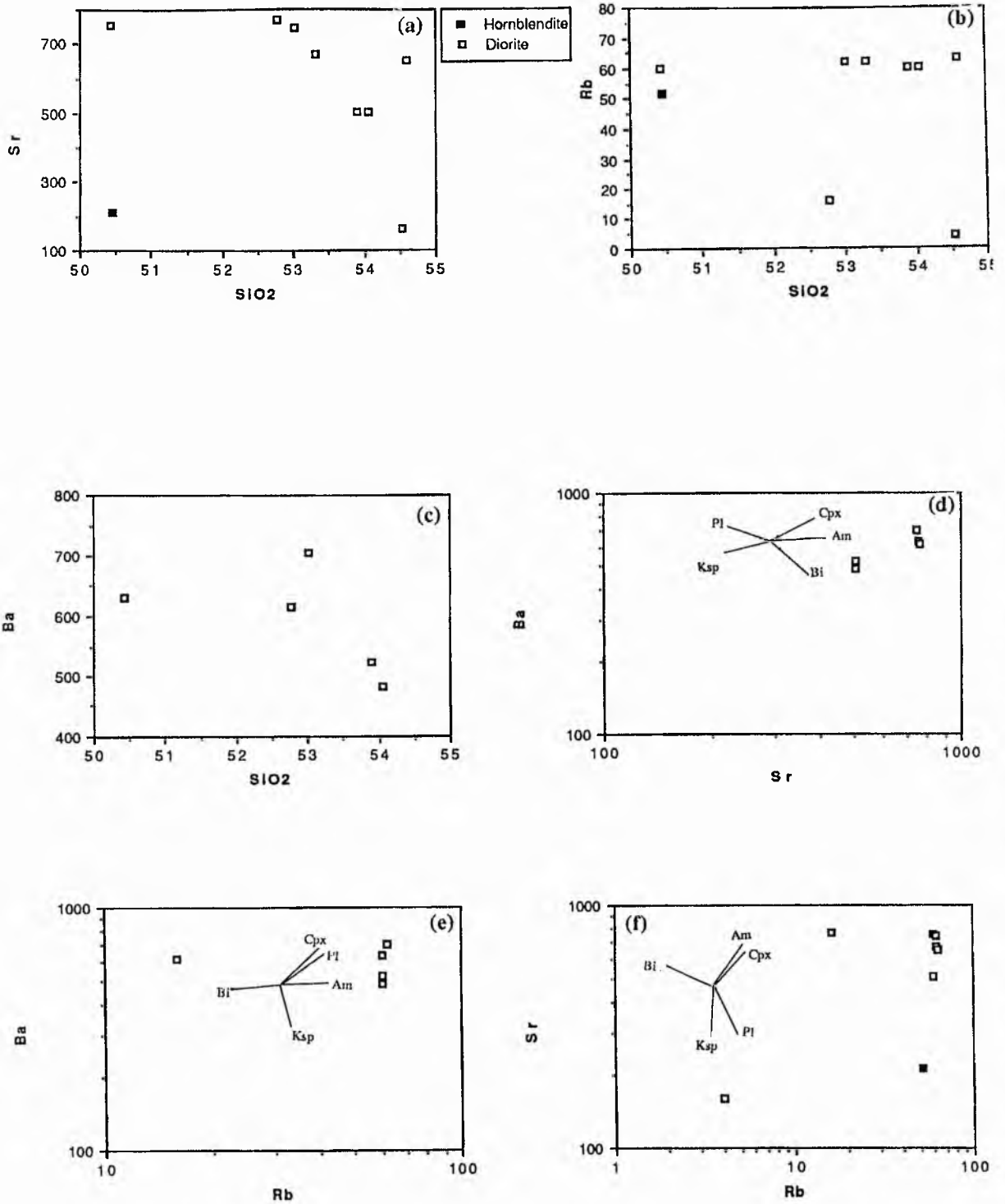


Fig. 5.35 (a-c) Variation plots of LIL elements Rb, Sr and Ba plotted against SiO₂ (d-f) Variation plots of LIL elements Rb, Sr and Ba with superimposed mineral vectors from the units of the Summy Lough diorite. See Fig. 5.26 for key to mineral symbols.

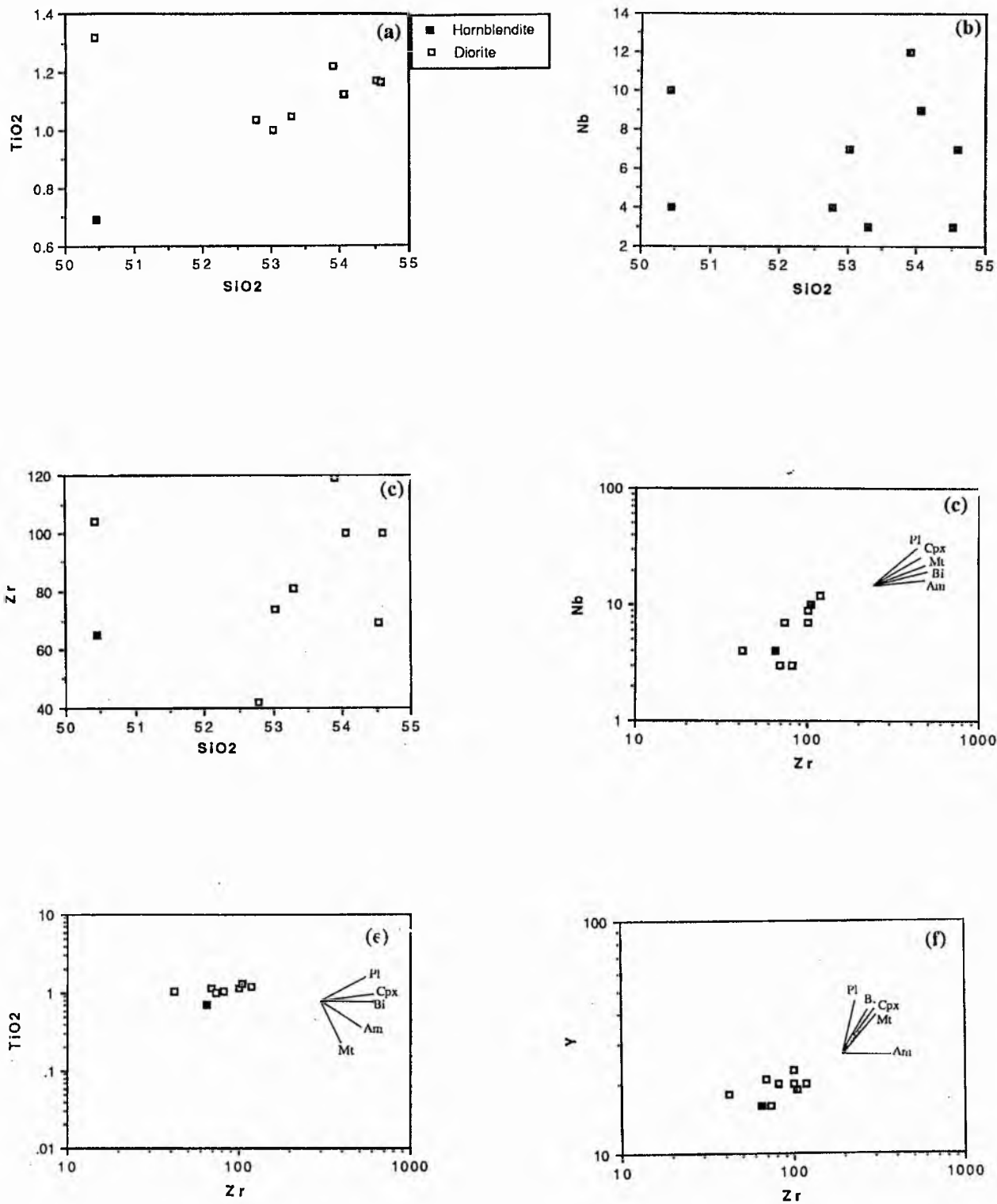
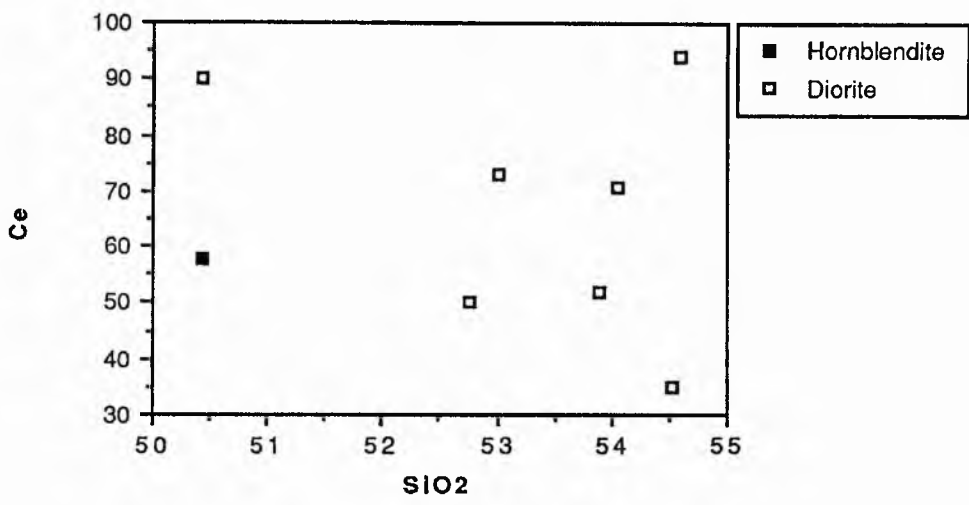
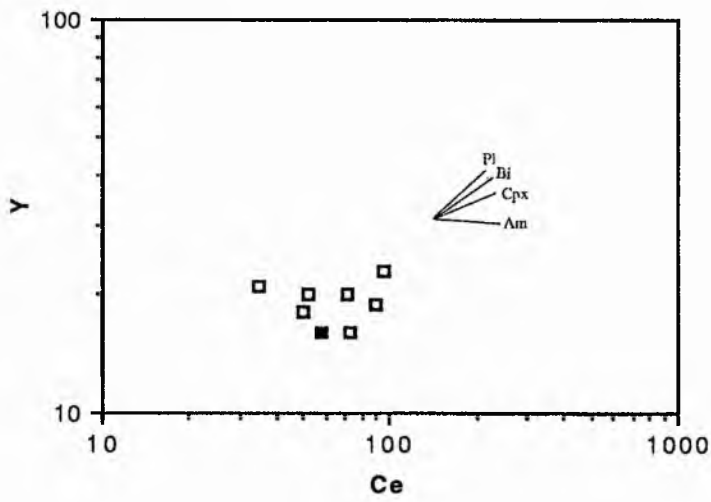


Fig. 5.36 (a-c) . Variation plots of HFS elements, Ti, Nb and Zr from the Meenalargan dioritic complex. (d-f) Variation plots of HFS elements Zr, Ti, and Nb from the Meenalargan dioritic complex. Mineral vectors and apparent fractionation directions are superimposed. See Fig. 5.26 for key to mineral symbols.



(a)



(b)

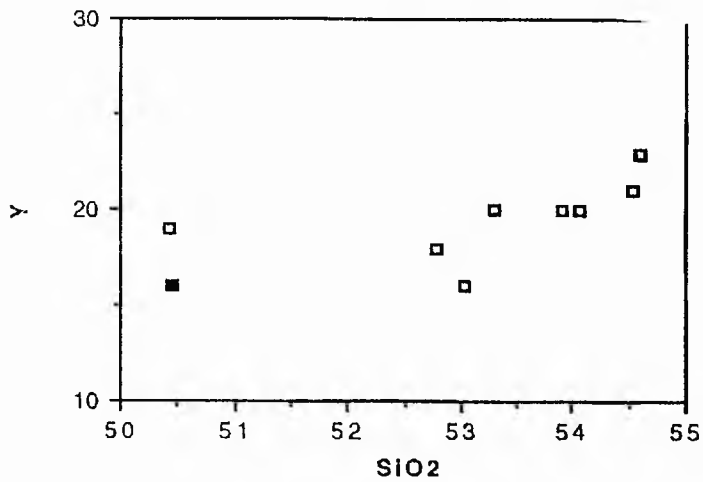


Fig. 5.37 (a-c) Variation plots of Ce and Y from the Summy Lough diorite. Mineral vectors are superimposed, (see Fig. 5.26 for key to mineral symbols).

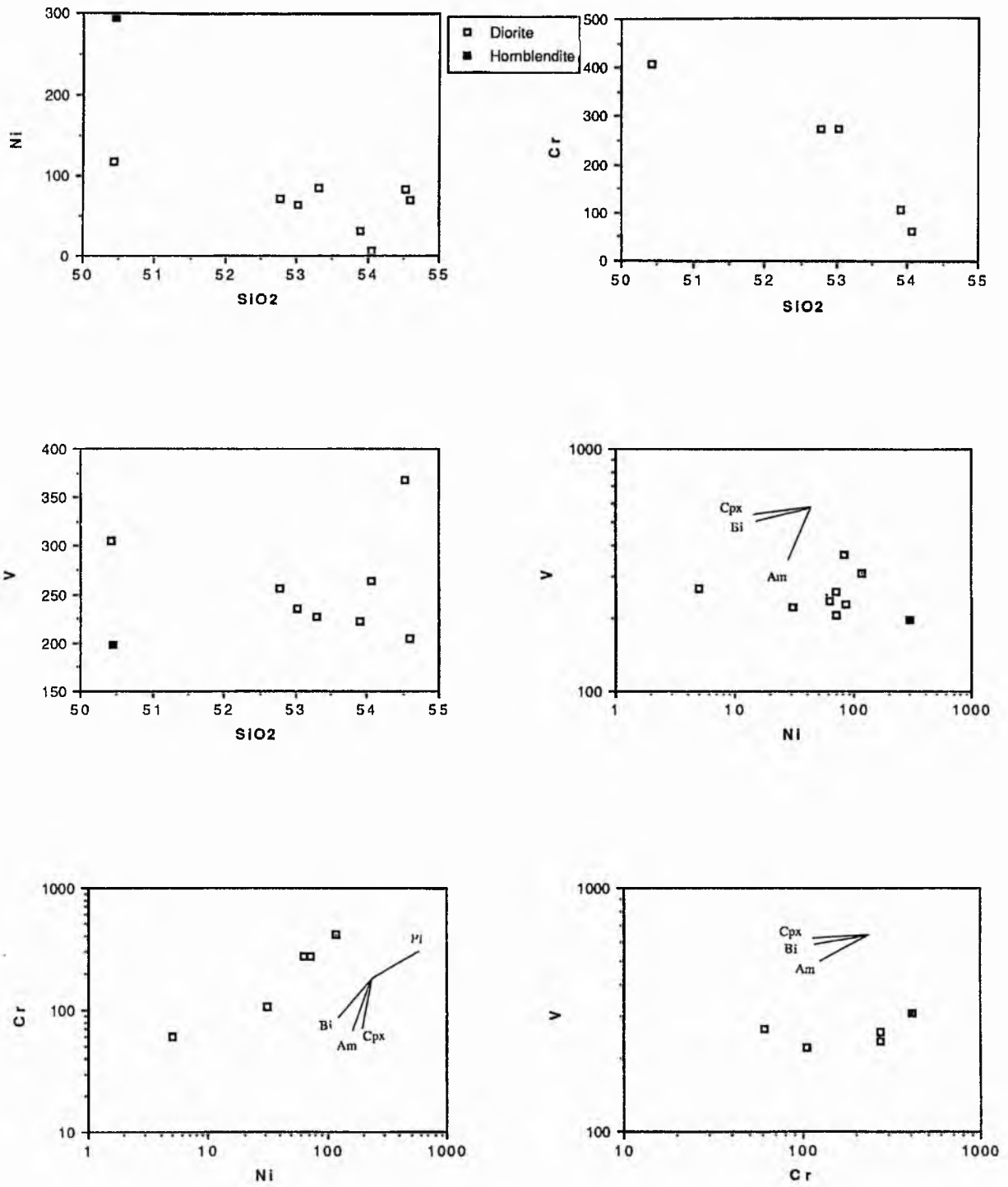


Fig. 5.38 (a-c) . Variation plots of compatible elements Ni, Cr and V plotted against SiO₂ from the Summy Lough diorite. (d-f) Variation plots of compatible elements Ni, Cr and V from the Summy Lough diorite. Mineral vectors and apparent fractionation directions are superimposed. See Fig. 5.26 for key to mineral symbols.

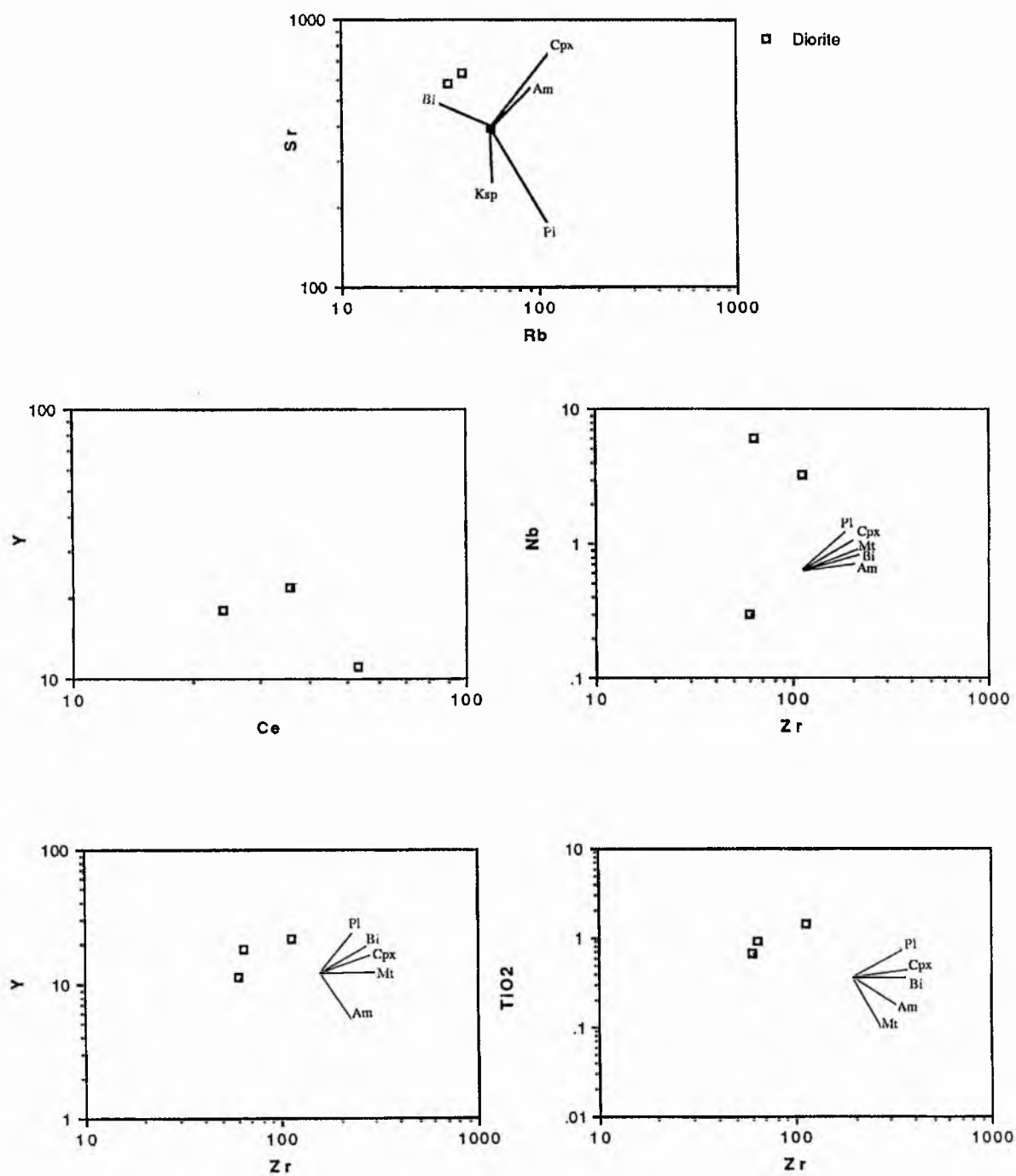


Fig. 5.39 (a-e) . Variation plots for the Mulnamin appinitic intrusion. Mineral vectors are superimposed. See Fig. 5.26 for key to mineral symbols.

Fig. 5.40 (a & b) displays the variation in $\delta^{18}\text{O}$ silicate and $\delta^{13}\text{C}$ along a traverse through the appinite at Portnoo (see Chapter 6). Total Fe_2O_3 , Sr and Ce increase as the contact is approached (Fig. 5.40 c-e) while MnO shows slight overall decrease towards the contact (Fig. 5.40 f).

Two samples (31515 and 3153) have higher values of $\delta^{13}\text{C}$ and $\delta^{18}\text{O}$ silicate respectively than the other rocks of the traverse. Both samples were collected in close proximity to limestone enclaves and may have suffered contamination with calcareous material. Sample 31515, which has a slightly higher $\delta^{13}\text{C}$ value than the other samples in this traverse, has a high content of Sr, Ce and Y, with low MnO, Total Fe_2O_3 , CaO and MgO. Sample 3153 which has a higher $\delta^{18}\text{O}$ silicate value than the other rocks of the traverse has a low Sr content and high MnO (Fig. 5.40 d & f). In sample 3153 high $\delta^{18}\text{O}$ silicate correlates positively with high values of CaO and MnO. In sample 31515 $\delta^{13}\text{C}$ is high, correlating negatively with high values of CaO and MnO and positively with Sr. The data suggest that if the value of $\delta^{18}\text{O}$ silicate is relatively high then the values of MgO and Sr remain relatively low (Fig. 5.40 d & i). The higher MgO, Total Fe_2O_3 and Sr close to the contact suggests that these may have been in part derived from the Portnoo Limestone although CaO does not increase as might be expected.

5.8 CONCLUSIONS

(a) The granites of the main Ardara pluton are calc alkaline to high-K calc alkaline in composition and possess geochemical characteristics typical of I-type magmas in a syn to post-collision setting.

(b) It is possible to discriminate differences between the outer (G1 and G2) and central (G3) units of the Ardara pluton with lower SiO_2 and higher TiO_2 , Al_2O_3 , Fe_2O_3 total, MnO, MgO, CaO and P_2O_5 in the outer G1 and G2 units. It is difficult to confidently discriminate between G1 and G2 of the Ardara pluton on the basis of major geochemistry but G2 is more primitive in terms of compatible trace elements.

(c) Granites associated with appinitic intrusions are generally similar in composition to the equivalent members of the main Ardara pluton though variations between individual bodies exist; Meenalargan granites are the least evolved, the Narin-Portnoo granites are the most highly evolved.

(d) Appinites of the Ardara igneous complex have compositions similar to orogenic subduction-related magmas, some are mildly alkaline while most are calc alkali to high-K calc alkali. Harker diagrams indicate that the appinites have a basaltic affinity, in terms of similar bulk chemistry and compatible element (Ni and Cr) characteristics, but are also geochemically similar to lamprophyric magmas in terms of bulk chemistry.

(e) The Meenalargan appinite has the most primitive characteristics of all the main appinites being enriched in Ni and Cr and depleted in Pb, V, Ce and Rb and Sr. The Narin-Portnoo is the most evolved of all the main appinites while Summy Lough and Mulnamin

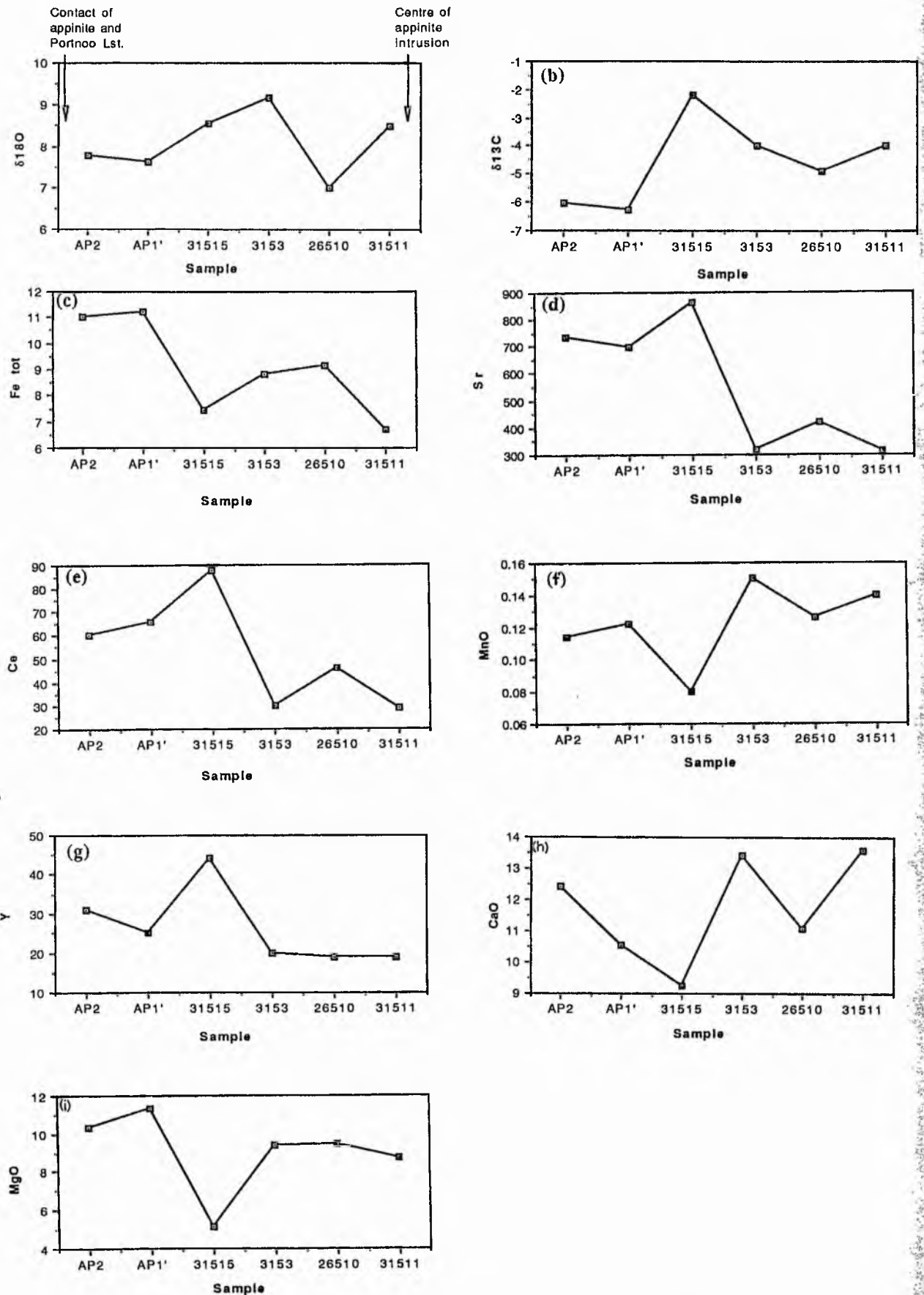


Fig. 5.40 Plots of sample vs major and trace elements, O and C isotopes highlighting the variation in major trace and stable isotope geochemistry along a traverse across part of the Narin-Portnoo appinite intrusion.

have similar compositions with minor variation in K_2O and V. Kilrean is the most primitive rock of the Ardara igneous complex with strong enrichment in MgO and Ni and depletion in K_2O , Nb, Zr and Rb.

(f) All appinitic intrusions display some geochemical variation, normally between hornblendite, enriched in MgO, Ni and Cr, and appinitic-dioritic rocks which are not.

(g) Trace element vector modelling indicates that plagioclase, hornblende and biotite exert the strongest control on the evolving compositional paths of the appinitic-dioritic series. Different blends of minerals are required to explain the variation between appinites and the fractionating minerals can change during a sequence. The granitic magmas of the appinite suite often fall on trends not explicable by the modelling.

(h) Mass balance modelling of the appinites indicates that it is possible to generate magmas of dioritic composition from a meladioritic parent especially in the Narin-Portnoo and Meenalargan intrusions.

(i) Trace element vector modelling indicates that plagioclase, hornblende, and augite exert the strongest control on the evolving compositional paths of the granitic units of G1 and G2 while hornblende and biotite seem to have controlled the composition variation of G3.

(j) Mass balance modelling indicates that G1, G2 and G3 magmas may be separate magmatic pulses. G1 and G2 seem closely related and the evidence of the modelling indicates that it is possible to generate a G2 composition from a G1-type parent. G3 is not related to G1 and G2 by simple fractional crystallisation.

The modelling illustrates the difficulty in accounting for rocks such as appinites with wide geochemical scatter and high volatile content. The results of modelling are often difficult to reconcile with simple fractionation processes. Other factors such as magma mingling, wall-rock contamination, assimilation and fractional crystallisation (AFC) and the influence of fluids may also be important. Such wide geochemical variation may indicate that the appinitic magmas were multiple pulses and rich in volatiles and thus prone to mingling and contamination prior to, and even during, emplacement. Isotopic determinations could improve the constraints on these models.

FRACTIONATION MODEL Parent ----- Daughter		% Extracted	CUMULATE (Composition)		R ²
G1	G2	33%	Augite	7.8	0.44
			Biotite	26.1	
			An30	64.9	
			Titanite	2.2	
G1	G2	41%	Homblende	9.2	0.59
			Biotite	23.5	
			An30	64.5	
			Titanite	2.2	
G1	G2	32%	Homblende	9.2	0.56
			Biotite	23.0	
			An30	64.6	
			Magnetite	0.5	
			Titanite	2.8	
G1	G2	31%	Homblende	12.4	1.10
			Biotite	21.6	
			An30	65.5	
			Magnetite	0.5	
G1	G2	19%	Homblende	2.8	1.4
			Biotite	30.1	
			An50	65.4	
			Magnetite	1.3	
			Titanite	0.4	
G2	G1	19%	Homblende	2.8	1.43
			Biotite	30.1	
			An50	65.4	
			Magnetite	1.3	
			Titanite	0.4	
G2	G3	17%	Homblende	46.2	2.78
			Biotite	10.7	
			An20	25.8	
			Magnetite	8.8	
			Titanite	8.5	
G2	G3	16%	Biotite	54.3	2.85
			An20	25.4	
			Magnetite	9.7	
			Titanite	10.7	
G2	G3	16%	Biotite	66.7	3.94
			An20	20.9	
			Magnetite	12.4	
G2	G3	16%	Homblende	25.3	3.23
			Biotite	41.7	
			An20	23.9	
			Magnetite	9.14	
G1	G3	36%	Homblende	8.9	4.29
			Biotite	28.6	
			An30	53.5	
			Magnetite	5.4	
			Titanite	3.5	

TABLE 5.2 (a)

cont/

FRACTIONATION MODEL Parent ----- Daughter		% Extracted	CUMULATE (Composition)		R ²	TABLE 5.2 (a)
G1	G3	36%	Augite	8.9	4.37	
			Biotite	28.6		
			An30	53.5		
			Magnetite	5.4		
			Titanite	3.5		
Diorite 2 (Narin- Portnoo)	Hornblendite (Narin- Portnoo)	55%	Biotite	16.2	23.85	TABLE 5.2 (b)
			An60	82.6		
			Magnetite	0.8		
			Titanite	0.3		
Diorite 2 (Narin- Portnoo)	Hornblendite (Narin- Portnoo)	57%	Biotite	19.0	22.96	
			An60	81.0		
Diorite 1 (Narin- Portnoo)	Biotite diorite (Narin- Portnoo)	54%	Augite	64.8	15.00	
			Hornblende	34.8		
			Magnetite	0.4		
Diorite 1 (Narin- Portnoo)	Biotite diorite (Narin- Portnoo)	53%	Augite	61.9	17.40	
			Hornblende	32.9		
			Magnetite	0.7		
			Epidote	4.5		
Diorite 2 (Narin- Portnoo)	Biotite diorite (Narin- Portnoo)	35%	Biotite	29.2	22.50	
			Epidote	66.6		
			Magnetite	4.2		
Diorite 2 (Narin- Portnoo)	Biotite diorite (Narin- Portnoo)	35%	Epidote	64.0	28.20	
			Biotite	36.0		
Other models tested yielded unrealistic results						
Biotite diorite (Narin- Portnoo)	Gr (Narin- Portnoo)	55%	Hornblende	36.4	7.25	
			Biotite	21.5		
			An60	37.0		
			Magnetite	3.4		
			Titanite	2.0		
Other models tested yielded unrealistic results						
G2	Gr (Narin-Portnoo)	20%	Hornblende	20.6	2.63	TABLE 5.2 (c)
			Biotite	39.2		
			An20	27.0		
			Magnetite	4.3		
			Titanite	9.0		
G2	Gr (Narin-Portnoo)	24%	Augite	13.4	1.89	
			Biotite	43.3		
			An30	37.2		
			Magnetite	1.1		
			Titanite	4.9		
G2	Gr (Narin-Portnoo)	22%	Hornblende	9.8	2.71	
			Biotite	47.2		
			An30	33.1		
			Magnetite	1.5		
			Titanite	8.4		

cont/

FRACTIONATION MODEL Parent ----- Daughter		% Extracted	CUMULATE (Composition)		R ²		
G3	Gr (Narin-Portnoo)	4%	Hornblende An30	64.0 36.0	1.16	TABLE 5.2 (c)	
G3	Gr (Narin-Portnoo)	3%	Biotite An20	17.2 82.8	2.25		
Meladiorite (Meenalargan)	Diorite (Meenalargan)	13%	Hornblende Biotite An37 Titanite	66.6 17.4 12.7 3.5	2.07	TABLE 5.2 (d)	
Meladiorite (Meenalargan)	Diorite (Meenalargan)	12%	Hornblende Biotite An37	72.5 15.7 11.7	2.32		
Diorite (Meenalargan)	Meladiorite (Meenalargan)	yielded unrealistic results					
Diorite (Meenalargan)	Granodiorite (Meenalargan)	yielded unrealistic results					
Diorite (Summy Lough)	Hornblendite (Summy Lough)	91%	An55 Magnetite	95.1 4.9	91.20	TABLE 5.2 (e)	

CHAPTER SIX

A STABLE ISOTOPE STUDY OF THE PORTNOO APPINITE AND ITS AUREOLE

6.1 INTRODUCTION

This chapter is a study of fluid/magma rock interaction using field, petrographic geochemical and isotopic methods, with particular reference to relationships at an appinite-impure limestone contact. Models are proposed for such fluid/magma-rock interaction and their practical validity tested, using carbon, oxygen and hydrogen isotopic data from samples taken along a traverse across the contact zone.

The effect which an appinitic intrusion has on its contact rocks has important implications for the role of fluids in hydrous magmas as similar rock types elsewhere may show similar relationships. Contact relationships of appinites and relatively inert rocks such as pelite, semi-pelite and quartzite are often sharp without any obvious reaction with the country rock (Hammidullah & Bowes 1987). However when the rock type is calcareous in nature the reactions can be intense and in some cases explosive due in part to the release of CO₂, causing brecciation of the contact rocks. The abundance of the fluid phase in appinites is thought to exert an important control on the emplacement mechanism of breccia pipes, their heterogeneous textures, and the reaction relationships between appinite and calcareous rocks, both at the margins of appinites and as xenoliths within the intrusions (Bowes & Wright 1961, Wright & Bowes 1979; French 1977; Pitcher & Berger 1972). The Portnoo shore section (Fig 6.1) allows detailed study of the relationships between the Portnoo Limestone of Dalradian age and numerous appinitic intrusions (Map 6, Appendix 6).

Along one such contact a meladiorite is in contact with a calc-silicate member of the Portnoo Limestone. The meladiorite has been emplaced as a dome-like body that was intruded both parallel to and across the bedding by a process of stoping. It is locally heterogeneous in composition and texture, and contains xenoliths of the Portnoo Limestone

The contact with the Portnoo Limestone is diffuse over a zone of 10 cm and involves the growth of diopside, hornblende, epidote and feldspar along bedding laminae in the calc-silicate, most intensely in a 1 cm wide zone adjacent to the contact (Fig 6.2). Away from the contact the calc-silicate has a more metasedimentary aspect and is composed of varying proportions of quartz, calcite, feldspar, epidote and biotite. It thus appears in the field that the calc-silicate has been metasomatised by the action of the appinitic magma and associated fluids. The field evidence, here and elsewhere in the area, suggests that this relationship is common but the lateral extent of the processes involved

in the reaction is unclear. Although there is an obvious mineralogical change at the contact with the appinite thought to have occurred during the recrystallisation of the limestone upon appinite intrusion, the extent of fluid-rock reaction is undetermined.

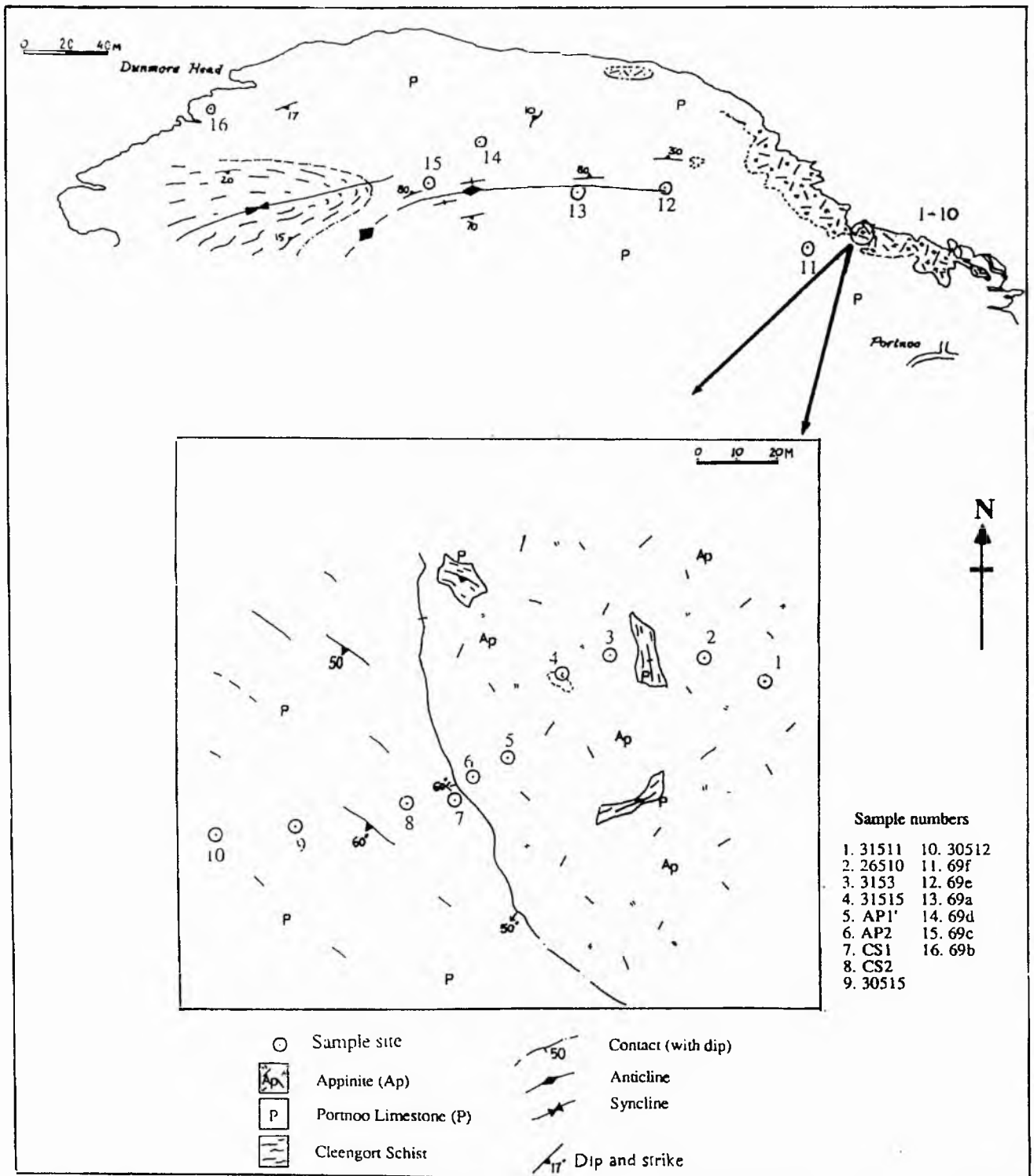


Fig 6.1 Location map of appinite/limestone isotope traverse, Portnoo.

In order to test the idea that the mineralogical growth occurred during the intrusion of the appinite, and in particular to discover the extent of the zone of fluid movement associated with this particular intrusion, a detailed sample traverse of the contact zone was made.

6.1.1 Aims and objectives of the stable isotope study

The objectives of the isotope studies were:

- (i) To sample and analyse the rocks across an appinite/limestone contact zone and to integrate field, petrographic, major and trace element and isotope geochemical techniques in a study of fluid behaviour in this contact zone.
- (ii) To model expected patterns of magma-fluid-rock interaction and to compare these models with the observations made under (i).
- (iii) To understand the processes and extent of fluid movement and isotopic exchange.

6.1.2 Sampling

Samples were collected, as far as possible, on a logarithmic scale of approximately 0.01m, 0.1m, 1m, 10m and so on, either side of the contact, in order to constrain the scales of processes operating. However, due to problems of outcrop beyond the 10m point, samples were collected in more regularly spaced intervals, up to 40m from the contact on the appinite side and up to 800m away on the limestone side. A sample of unaltered limestone (Limey 1) from the same Falcarragh Limestone succession, 2.5 km east of the village of Falcarragh in north Donegal (B9052 3015) and distant from any appinite and granite intrusion, was collected to act as control. Likewise for the appinite (31511) a control sample without any macroscopic calcareous contamination was analysed from as near the centre of the intrusion as possible. All samples analysed were fresh and relatively unweathered or unaltered hydrothermally so far as this is possible in such rocks.

6.1.3 Importance of volatiles in magmas

The presence of H₂O in a magma is important and, for instance, may control the magma fractionation path by determining the liquidus phases present (Yoder & Tilley, 1962). It also governs how rapidly a magma may rise through the crust; if an acid magma is relatively 'dry' it may rise quite far into the crust without crossing its solidus and starting to crystallise. A hydrous acid magma however, close to the minimum melt composition, will not rise as far into the crust before it crosses its solidus and begins to crystallise due to the negative dP/dT slopes of hydrous systems. The presence of H₂O may help determine the amount of melt generated in a particular magmatic setting, e.g.

whilst the maximum H₂O content of appinitic rocks in the Caledonian of the British Isles is 3.6% (Hall 1967), while basaltic magma can contain up to 9% H₂O (Burnham 1979).

In the tectonic setting of appinite petrogenesis, fluids and volatiles may be important in the emplacement of the magmas in the form of breccia pipes, by explosive release of gas (Pitcher & Read, 1952; Bowes & Wright, 1961). Two important lines of evidence support the idea that appinites originate from volatile-rich magmas:

(a) Mineralogy: the occurrence of hornblende as the dominant ferromagnesian phase, as well as the common presence of biotite, primary calcite, apatite and pyrites suggest that the magma source was hydrous and also rich in C, P and S.

(b) Textures: the acicular habit of hornblende (often up to 10cm in length) and megacrystic texture of "appinite", the great heterogeneity of composition and grain size within a single hand specimen, the intense and complex zonation of hornblende and mica, and the wide variation of pegmatitic, porphyritic, and xenocrystic textures in individual intrusions, all suggest an important volatile component.

6.1.4 Stable isotope analyses

a) Isotopic notation:

(i) The δ Value: variations in the ratio of the heavy to light isotopes of O, C, and H are measured relative to internationally accepted standards. The ratios are reported in parts per thousand or permil (‰), according to the equation:

$$\delta_{\text{SAMP}} = \frac{R_{\text{SAMP}} - R_{\text{STD}}}{R_{\text{STD}}} \times 1000 \text{‰}$$

where R is the atomic ratio of the heavy isotope to the light isotope (¹⁸O/¹⁶O, ¹³C/¹²C, D/H) and SAMP is the unknown and STD is the reference standard, (SMOW for O, H and PDB for C). O and H isotope ratios are measured relative to the standard V-SMOW (Vienna-Standard Mean Ocean Water). C isotope ratios are measured relative to the standard V-PDB (Vienna-Peedee Belemnite), defined by:

$$\delta^{13}\text{C}_{\text{NBS-19/V-PDB}} = 1.95, \text{ after O'Neil (1986).}$$

Usually the δ symbol is suffixed by the heavy isotope of the element in question, thus a sample with a $\delta^{13}\text{C}$ value of +20 ‰ is enriched in ¹³C by 20 ‰ or 2% relative to the standard. Similarly a negative δ value indicates depletion in the heavy isotope relative to the standard.

(ii) The α value: the isotopic fractionation factor (α) relates to a process of fractionation that may occur between two mineral species or a mineral and fluid (e.g. H₂O). The isotopic fractionation factor is defined by the following equation:

$$\alpha_{AB} = R_A / R_B$$

where R_A is the absolute isotopic ratio in phase A and R_B the ratio in B.

Often, instead of using the α value, authors may use the term $10^3 \ln \alpha$, the 'permil fractionation' (O'Neil, 1986). Faure (1977) derives the approximation,

$$\Delta_{A-B} = \delta_A - \delta_B \sim 10^3 \ln \alpha_{A-B}$$

This equation means that the difference in δ values between two phases is approximately equal to the per mil fractionation. The use of this approximation may not always be valid, especially for hydrogen isotope fractionations.

(b) Analytical techniques

Silicate oxygen determination is based on the extraction of O₂ and conversion of this O₂ to CO₂. Carbon is determined in carbonates by the extraction of CO₂, and hydrogen is extracted from hydrous phases as H₂O and is converted to H₂. The techniques used in the extraction of the various isotopes are summarised in Appendix 2 and will not be discussed further here.

6.1.5 Fluid movement associated with magmatic intrusions

Study of the stable isotope systematics of a magmatic intrusion and its aureole rocks can provide important constraints on the shape, extent and temperature of any circulatory/fluid system associated with the intrusion. One of the best examples of such a study is that of the hydrothermal system associated with the Tertiary Igneous complexes of Skye, Mull and Ardnamurchan (Taylor & Forrester 1971, Forester & Taylor 1977). Forester & Taylor determined the C, O and H signatures of representative samples of igneous and country rocks on the Central Ring Complex of Skye and found that there was a crudely circular zone of depletion in $\delta^{18}\text{O}$ of 6-7‰ for all the rocks within 4 km of the central igneous complex. Similarly on Mull a 3-4 km wide zone of depletion exists around the central ring complexes (Taylor & Forester 1971, 1977). The existence of very large hydrothermal convection systems involving heated low-¹⁸O groundwater at the time of igneous intrusion was clearly demonstrated by a combination of isotopic and petrologic study.

The importance of a fluid phase has been stressed by Sheppard & Gustrafson (1976) who demonstrated the existence of circulatory systems in porphyry copper deposits using stable isotopes. Burnham (1979) also studied the hydrothermal system associated with porphyry copper deposits and proposed a H₂O-rich 'carapace' around the granodiorite magma chamber. This carapace varied in width in his model from 1km at 2 km depth to 0.25km at 5 km depth and the fluid phase was dominated by Na-Ca-Cl brines which were responsible for wall rock alteration at the margin of the stock (Taylor, 1974).

6.1.6 Source of magmatic and meteoric fluids

It has recently become apparent through the use of oxygen and hydrogen isotopes that many high level igneous intrusions have interacted with meteoric ground waters. The process of hydrothermal interaction causes depletion in ¹⁸O of the igneous rocks involved. Such patterns are seen at Skaergaard, Stony Mountain ring complex and the San Juan volcanic field amongst others. Taylor (1974) suggested that the meteoric ground water becomes heated by magma at the margins of the intrusion and because of its lowered density, the hot water starts to rise. A hydrothermal convection system may then be set up, and after the outer part of the intrusion solidifies and fractures, the hot H₂O may penetrate into, and exchange with, the intrusion. The circulation is driven by buoyancy. A magmatic-hydrothermal fluid may retain its H and O isotope signature only as long as its composition is buffered by exchange with the magma or with silicate minerals at magmatic temperatures. However, upon cooling during a later stage in the magma's crystallisation history, magmatic fluid may become diluted by meteoric fluid and exchange and mixing during post-magmatic processes can modify both the δD and $\delta^{18}O$ values of magmatic water and minerals; hence the relative depletion seen, for example, on Skye.

It is likely that some form of 'fluid hydrothermal cell' is associated with most magmatic intrusions emplaced into water-rich country rocks in the upper crust and appinites may be amongst such intrusions. The fluid involved with the appinitic magmas of Ardara may be of a magmatic origin, considering the generally hydrous nature of appinite, however the process of fluid circulation is controversial as it is dependent on the enthalpy and pressure regime of the system. Several authors (Etheridge et al. 1984, Ferry 1985) have proposed that metamorphic fluids can circulate by convection in the deep crust but they also note the importance of factors such as convective permeability and density of the fluid. One way of constraining the influence of a magmatic fluid is to analyse the appinite and altered calcareous country rocks in the appinite contact zone to determine whether a zone of magmatic fluid circulation, interaction or expulsion existed around the appinite. The extent of such a zone of interaction and the effect it may have had on its country rock envelope will be discussed later in this chapter.

6.1.7 Application of stable isotopes to studies of fluid interaction

The $\delta^{18}\text{O}$ and $\delta^{13}\text{C}$ estimated for the appinite, Portnoo Limestone and potential fluid all have very distinct isotopic signatures, while the δD values for the appinite and limestone are broadly similar (Table 6.1). In the case of carbon isotopes, the contact rocks of the Portnoo area are calcareous and as such may be expected to show a heavier, ^{13}C -enriched isotopic signature, and than the fluids that may flow through them, similar to those of the Dalradian limestones of the Tayvallich peninsula (Graham, pers. comm.).

The stable isotopes of O, C and H are well suited to the study of fluid-rock interaction in the Portnoo area. In particular, oxygen is a structurally essential component of the lithosphere, lithospheric fluids and the hydrosphere. Perhaps the most sensitive isotope system to fluid-rock interaction is that of hydrogen, which is particularly sensitive to change because the amount of hydrogen in rocks is so low, whereas water is 66% hydrogen, on an atomic basis. Variations in these ratios result from the complex interplay of geological and chemical processes.

The isotopic compositions of the different lithological and fluid phases are dependent on the parameters of time, temperature, mineral/rock-fluid fractionation relationships, and although the natural abundances of O, C and H and their isotopes are restricted to relatively narrow limits and their isotope fractionation factors are relatively well known (Friedman & O'Neil 1977, O'Neil 1986, Graham et al. 1988) the complications of the above parameters can give rise to variations in the observed values.

6.1.8 Context of this research

The appinite suite often has complex contact relationships with its country rocks (Anderson, 1937; Iyengar et al., 1954; Deer, 1953; Haslam, 1970) as discussed in chapter 3. For instance Iyengar et al. (1954) described calc-silicate flags of the Mulnamin group striking into contact with rocks of the Meenalargan amphibolitic complex, and he observed how the calc-silicate layers became converted into appinitic amphibolite without disruption of the calc-silicate bedding. The importance of the volatile fluids involved in this process of contamination and in the formation of breccia pipes (Pitcher & Read 1952, Bowes & Wright 1961, Bowes & McArthur 1976) is well known; however, no detailed study exists of the isotopic implications of such processes. Similar studies such as those in the Inner Hebrides and the USA have documented the contact relationships of argillaceous and calcareous rocks with granitic plutons (Taylor & Forester 1971, Taylor & O'Neil 1977, Labotka et al. 1988, Nabelek et al. 1984). These studies used O, C and H isotopes to monitor the processes of decarbonation, devolatilisation and changes in composition either side of the contacts, with the aim of defining in detail the sources of the fluids and the temperatures of reactions involved in skarn formation and the exchange processes. Nabelek et al. (1984) noted that one of the important aspects of contact metamorphism is the potential for mass exchange between

an intrusion and its country rocks. The driving forces are dependent on the pressure, temperature and chemical gradients which in turn are dependent on transport by magmatic and meteoric fluids or those derived by devolatilisation reactions in the country rocks. Such processes of fluid-rock interaction will be used in the modelling of reaction relationships of the limestone/appinite contact seen on the Narin-Portnoo coast.

6.2 MODELS OF APPINITE-COUNTRY ROCK-FLUID INTERACTION

Before definition of a number of models it is important to consider the role of the fluid in the appinite magma, and by implication the country rocks it intruded. Average Caledonian appinite rock has a H₂O content of 3.6% (Hall, 1967). Such a fluid may have been present in the melt and in hydrous minerals and will influence the isotopic composition of the appinite as a result of varying degrees of equilibrium with minerals within the magma and with the country rock through which it may infiltrate or circulate. Magmatic fluid composition may be determined by applying the mineral-H₂O isotopic fractionation factors at igneous temperatures (700°C-1200°C) because no water of indisputable magmatic origin has yet been directly analysed isotopically (Sheppard 1986). Sheppard et al. (1969) defined waters in equilibrium with I-type magmas in the plutonic setting as having $\delta D = -40$ to -50‰ and $\delta^{18}O = +5.5$ to $+9.0\text{‰}$. In the case of appinites, this magmatic water may indeed have been primary magmatic water transported with the magma from its deep-seated source, or circulating at a higher level in a hydrothermal system.

6.2.1 Isotopic composition of model end-members

On the basis of existing isotopic analyses of basalts and impure calcareous rocks, a number of models have been erected to account for the isotopic effects as well as the macro- and microscopic textures seen on either side of the contact between the Portnoo limestone and appinite. The relative shape of the reaction path proposed is based on isotope results for O, C and H published in the literature (Table 6.1) and local field and petrographic constraints.

(i) Silicate oxygen

(a) Appinite: in view of the bulk similarities between appinites and basalts (Hall 1967, Pitcher & Berger 1972) and the likely mantle-derived origin of appinites

ISOTOPE	MARBLE (‰)	APPINITE (‰)	REFERENCE SOURCE
Silicate Oxygen $\delta^{18}\text{O}_{\text{SIL}}$	+18.5 to +21.1	+5 to +7	Marble: Nabelek et al. 1984 Appinite: Kyser et al. 1986
Carbonate Oxygen $\delta^{18}\text{O}_{\text{SMOW}}$	+20 to +24	+8 to +13	Portnoo Marble: Deines & Gold 1969 Appinite: Deines & Gold 1969
Carbon $\delta^{13}\text{C}_{\text{PDB}}$	+6	-5	Portnoo Marble: Graham. 1990 Appinite: Kyser et al. 1986
Hydrogen δD	-70 to -80	-60 to -80	Portnoo Marble: Taylor, 1974 Nabelek et al. 1984 Appinite: Taylor, 1974 Kyser & O'Neill, 1984

Table 6.1 showing approximate ranges in values estimated for Portnoo Marble and appinite based on the data for similar rock types. (Authors are listed in the table)

(Bowes & Wright 1979) it seems reasonable to estimate a whole rock (WR) $\delta^{18}\text{O}$ value as being similar to those of continental basalts with WR $\delta^{18}\text{O} = +5$ to $+7$ ‰ (Taylor et al. 1986, Sheppard 1986), which overlap MORB values of 5.7 ‰ (Kyser 1986).

(b) Portnoo Limestone: The Portnoo Limestone comprises on average 70% calcite, 10% mica, 5-10% feldspar, 5-10% epidote and 5% quartz. The limestone is considered to have been deposited in a shallow Dalradian shelf environment, (Pitcher & Berger 1972) and has subsequently suffered regional metamorphism up to greenschist facies. Dunn & Valley (1985) quoted values of $\delta^{18}\text{O} = +18.1$ to 28.1 ‰ for calcites from the greenschist facies limestones from the Grenvillian of Ontario. These values compare favourably with those of the Cambrian limestone from around the Notch Peak stock, Utah (Nabelek et al. 1984) which average $\delta^{18}\text{O} = 20$ ‰. If, as Rye et al. (1976) proposed, limestones are relatively impermeable units in metamorphic terranes, exchange with a metamorphic fluid may have been negligible and the overall effect on the oxygen isotope systematics would be small, and thus a value of WR $\delta^{18}\text{O} = +20$ ‰ may be reasonable for the Portnoo Limestone.

(ii) Carbon

(a) Appinite: using the same reasoning as for oxygen, estimates of WR $\delta^{13}\text{C}$ for the appinites are based on values gathered for basalts. Release of high temperature carbon (HTC) at $> 600^\circ\text{C}$ from vesicles within unaltered submarine basalts has yielded values of WR $\delta^{13}\text{C} = -5\text{‰}$ (Pineau & Javoy, 1983). As the calcite in appinites is largely a primary phase (Chapter 4.2.1) it probably crystallised at over 600°C , and so appinitic carbon is taken as WR $\delta^{13}\text{C} = -5\text{‰}$.

(b) Portnoo Limestone: the WR $\delta^{13}\text{C}$ value for the limestone could only be estimated on the basis of sedimentary carbon signatures which range from 0 to -5‰ for the late Precambrian (Schidlowski, 1988). This value is similar to those of modern marine carbonates of 0 to $+2\text{‰}$. However recent studies by Graham (pers. comm.) have yielded values of $+6$ to $+7.5\text{‰}$ for the Precambrian limestone of the Tayvallich Peninsula which is taken to be of sedimentary origin. Heavy carbon values such as this are not extraordinary for the Precambrian. Baker and Fallick (1989) analysed amphibolite facies Lewisian limestone from Loch Maree, in Scotland which they found to have $\delta^{13}\text{C}$ approximately $+12\text{‰}$ PDB. They attributed this to a worldwide excursion in the C isotope composition of sea-water at this time. In terms of the WR $\delta^{13}\text{C}$ value of the Portnoo Limestone, which is compositionally similar to the Tayvallich limestone and which is thought to have been deposited in a shallow tidal shelf region (Pitcher & Berger, 1972), it may also have a relatively 'heavy' carbon signature. This will be discussed later in this chapter.

(iii) Hydrogen

There is a considerable overlap in the δD signature of marine sediments, metamorphic rocks and unaltered basalts and gabbros, with values ranging from -180 to -40‰ , (Taylor, 1974) as shown in Fig 6.2. The similarity of δD for basalts, gabbros, sediments and metamorphic rocks in subduction zones suggests that the mantle associated with the development of basalts and gabbros (and perhaps even appinites) may be substantially enriched in δD as a result of the subduction of oceanic crust and sediments but that with the exception of these areas the average δD composition of the mantle must be $\sim -80\text{‰}$ (Kyser, 1986). Only a minimal number of δD analyses were performed to constrain the appinites of the traverse and to compare these results with the results for the country rocks in order to test whether there had been any meteoric water alteration.

6.2.2 Model variants

Fig 6.3 shows four possible reaction patterns for the contact zone, the shape of these curves is hypothetical and the only quantitative basis for their shape is the relative differences between the isotopic values of the end-members of the two rock types. All

subsequent figures show the observed results for O and C analyses from the traverse plotted against log distance, in metres (figures are not to scale).

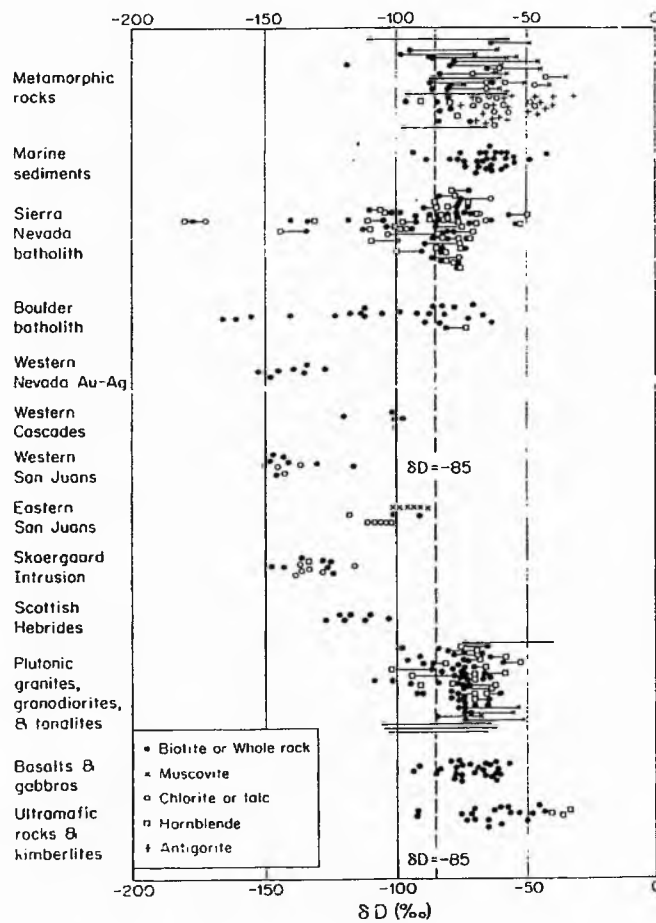


Fig 6.2 Compilation of available δD analyses of minerals from igneous, metamorphic and hydrothermally altered rocks from a variety of localities (from Taylor 1974).

The fluid exchange model (Fig 6.3 a) shows the expected pattern of isotopic variation in the case of circulation and exchange of fluids across the contact. Fluid of a magmatic origin, associated with the appinitic intrusion, together with the heat of the intrusion, may circulate within the aureole rocks (given appropriate permeability) and give rise to recrystallisation and new growth of minerals within the country rocks. This isotopically 'light' fluid circulating in the aureole rocks and appinite may equilibrate with the metamorphic fluid of the country rock and lower the isotopic ratio of minerals within the aureole of the intrusion whilst at the same time increasing the isotopic ratio in the magmatic fluid. This may circulate back into the magma giving rise to an increase of the isotopic ratio of the appinite. The process may continue until all the rocks in the aureole of the appinite and the appinite itself are in isotopic equilibrium.

The fluid expulsion model (Fig 6.3 b) requires the expulsion of fluid from the magmatic intrusion into the country rocks. This fluid will be hot and enriched in magmatic carbon and oxygen and may subsequently circulate within the aureole rocks. The resultant effect may be to decrease the WR $\delta^{18}\text{O}$ and WR $\delta^{13}\text{C}$ values of the country rocks up to a certain distance from the intrusion, beyond which the effects of the fluid will markedly decrease. The direction of movement of the fluid is assumed to be dominantly into the country rocks, as indicated by the arrow.

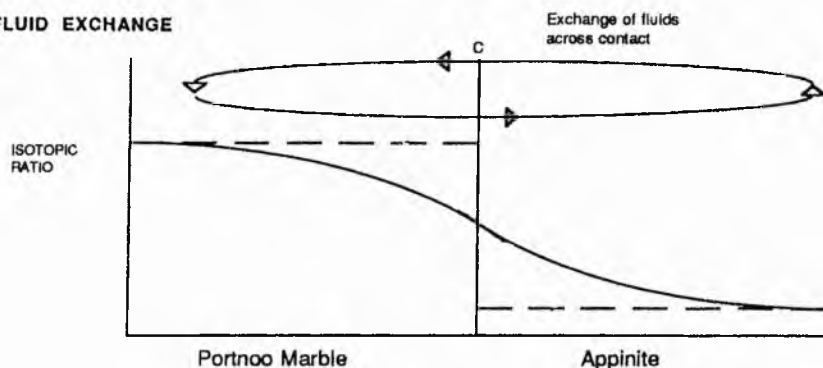
The assimilation model (Fig 6.3 c) requires assimilation of country rock into the appinitic magma. Assimilation is assumed to take place at a high crustal level, with mass flux from the country rock into the appinite. This has the effect of giving the contact zone appinite a heavier isotopic signature which then decreases to normal values with distance into the appinite as assimilation occurs.

The devolatilisation of limestone model (Fig 6.3 d) requires the loss of CO_2 which as a process is thought to mirror closely the effects of decarbonation reactions (Shieh & Taylor 1969a, Taylor & O'Neil 1984) that lead to a decrease in the $\delta^{13}\text{C}$ and $\delta^{18}\text{O}$ values of calcite in the country rocks (Nabelek 1984). The effects of this would be greatest close to the appinite where the limestone is heated most, and will decrease after a certain limit within the limestone.

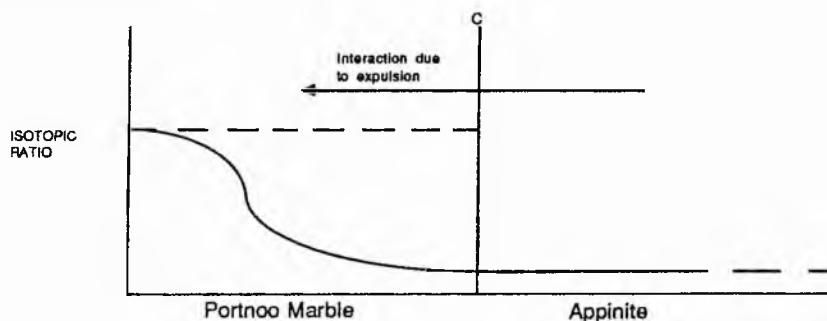
All four models offer possible isotopic profiles at the appinite/Portnoo Limestone contact. Both the fluid exchange and fluid expulsion models involve interaction of magmatic fluid within the aureole of the intrusion. The fluid exchange model involves a gradual change in isotopic ratio as fluid from the appinite exchanges with Portnoo Limestone across a common contact. The fluid expulsion model similarly implies a process of fluid expulsion from appinite into Portnoo Limestone, with circulation wholly within the Portnoo limestone or around the contact. The model involving assimilation of the country rock proposes high level incorporation of limestone into the appinite and mixing of it with the limestone, thus increasing the isotopic ratio of the appinite up to a certain distance within it. The devolatilisation model envisages the effects of thermal metamorphism on the Portnoo Limestone causing a decrease in the isotopic ratio of the Portnoo Limestone. Unlike the other models the contact will represent a sharp break across which there has been no exchange with the appinite. In the last three models the inflection of the curves is relatively steep implying a rapid change in the isotopic ratios in this area. It may also be possible that there is a combination of the processes expressed by the models. For instance there may be early fluid expulsion followed by circulation or devolatilisation of the Portnoo Limestone with passage of the evolved fluids into the appinite. The results obtained will be examined in terms of these simple end-member models.

FLUID-ROCK RELATIONSHIPS AT THE MARGIN OF AN APPINITIC INTRUSION - HYPOTHETICAL PROFILES

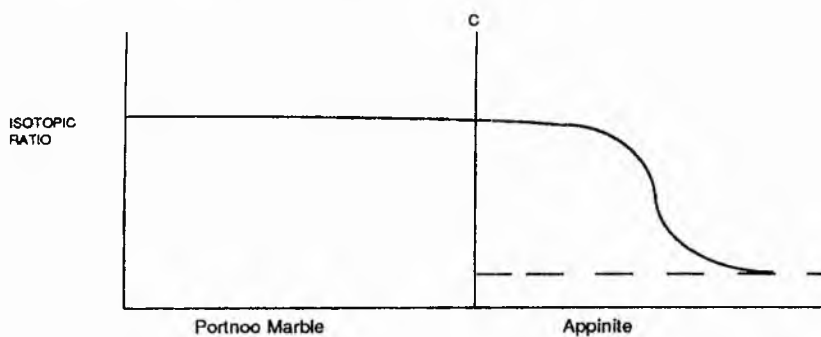
(a) FLUID EXCHANGE



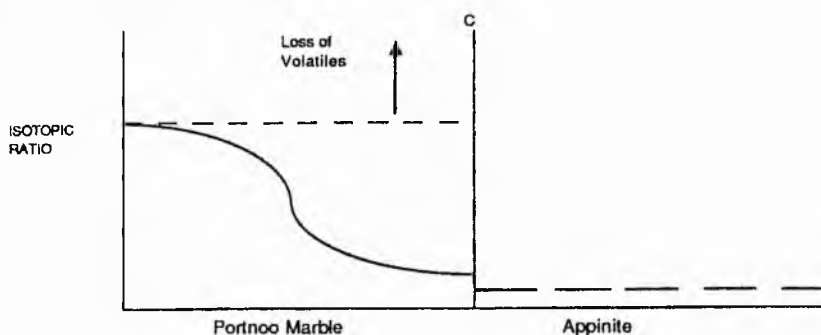
(b) FLUID EXPULSION



(c) ASSIMILATION



(d) DEVOLATILISATION OF MARBLE



Isotopic ratio = $\delta^{13}\text{C}$ and $\delta^{18}\text{O}$ are whole rock values
 Absolute $\delta^{13}\text{C}$ † $\delta^{18}\text{O}$ † % CaCO_3 . Assume Frac Marble = Frac Appinite

Fig 6.3 Hypothetical profiles of the fluid rock relationships at the margin of an appinitic intrusion. The vertical line marked C being the line of contact between the appinite and limestone. The horizontal axis is the distance (not to scale) either side of the contact over which the samples were collected. The vertical axis is the isotopic ratio, not constructed to scale.

6.2.3 The limestone-appinite contact at Portnoo

The constraints on the processes at the limestone-appinite contact gained from studies of the field relationships and petrography were examined prior to isotopic and geochemical study (chapters 3 and 4), these are summarised below:

(a) Field Studies: the contact between the appinitic intrusion and the Portnoo Limestone is sinuous and often lobate (see Map 6, appendix 6) suggesting that the country rock in the area of the isotope traverse behaved in a ductile rather than a brittle manner. On the centimetre scale the contact appears sharp and sinuous, however on the millimetre scale the contact is diffuse and transitional, often with growth of hornblende across the contact, from the appinite into the Portnoo Limestone. In all places Portnoo limestone at the contact is recrystallised, with a characteristic saccharoidal limestone texture developed up to 10 cm away from the contact. In this contact zone the grain size of the limestone is coarser (1 mm) than immediately at the contact where the grain size is typically 0.05 mm. Fine grained actinolitic hornblende is developed in this contact zone, often lying parallel to the relict bedding planes, which is partially lost due to the recrystallisation process (Fig 6.4). On the appinitic side there is no obvious incorporation of fragments or of minerals from the limestone. The texture is typically appinitic; coarse grained, euhedral to subhedral crystals of calcic hornblende are set in a matrix of altered plagioclase feldspar. Close to the contact the appinite is a relatively homogeneous meladiorite, mineral and textural variations being relatively minor in the other traverse samples, mainly involving an increase or decrease in the relative amounts of plagioclase. Elsewhere within the main part of the appinite there are xenoliths apparently of Portnoo Limestone, some of which show similar reaction features to those seen at the margin described for the contact zone, while elsewhere there is no reaction. This difference may relate to the timing of incorporation of limestone in the appinite.

(b) Petrography

(i) Meladiorite: this has the texture of typical meladiorite (see section 4.2. 1). It is rich in hornblende (70%), with less plagioclase (10-12%), quartz (5%), biotite (4.75%), epidote (5%). The remainder (approximately 3%) of the rock comprises accessories which include calcite (0.25%), magnetite, pyrite, titanite, sericite and apatite. The hornblende is brown and calcic, falling in the edenite-tremolite field (section 4.1.1). It is a primary phase, but is replaced by biotite, while at a later stage epidote appears in association with the hornblende and biotite. Most of the epidote replaces plagioclase along with sericite. Calcite everywhere appears to be a late interstitial phase, commonly found in the interstices between plagioclase and hornblende crystals, but of magmatic origin.

(ii) Altered Portnoo Limestone: two zones of variable width are recognised; the first, 1 - 10 cm wide is most strikingly seen adjacent to the contact. This area has within it four diffuse and highly variable subzones (Fig 6.4). A brief account is given here, a fuller

description is given in a later discussion of results.

The rock type in outer subzone 1, which is 1 cm from the contact and is 4 mm wide, consists of coarse actinolitic hornblende crystals (40%) intergrown with fine grained plagioclase, (5%) and a quartz (2-10%) matrix. This assemblage is heavily overprinted with epidote (40%) and sericitic mica (5%). Subzone 2 (Fig 6.4) is 2 mm wide and is dominated by an increase in hornblende grain size. This increase in grain size is gradational over 2 mm and relates to an increase in the amount of hornblende (86%); the matrix consists largely of quartz (8%), whilst calcite remains low (0.4%) and occurs along with rare epidote (5%) as inclusions within the hornblende.

Subzone 2 passes diffusely into subzone 3 which closely resembles subzone 1 except for the concentration of actinolitic hornblende in discrete laminae, which define relict bedding of the original metasediment. This zone then passes sharply into zone 4, which is adjacent to the contact, is 1 mm wide, and comprises a pyroxene and hornblende-rich facies. The notable feature of this subzone is the granularity of growth of the hornblende adjacent to the contact zone (Fig 6.4) and the highly diffuse contact this subzone makes with the appinite where hornblende and plagioclase from the appinite grow across the contact. These features suggest that the appinite/limestone contact involved a period of prolonged heating which involved recrystallisation of the mineral phases, particularly hornblende, on either side of the contact.

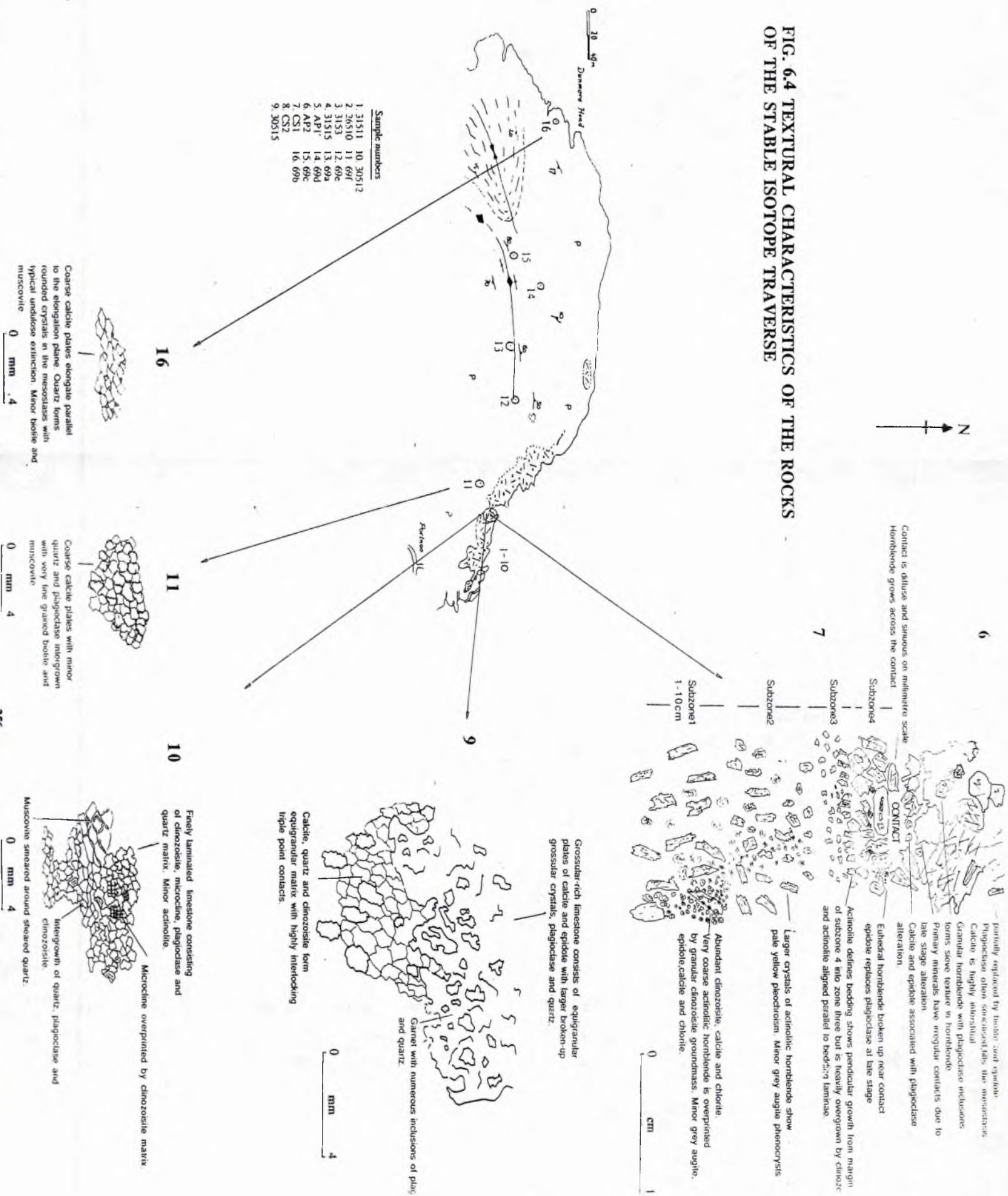
The second major zone forms an area 1 - 50 m wide, where, depending on the composition of the impure limestone it may contain grossular as a thermal metamorphic mineral (French 1966). This is commonly partly replaced by calcite, which usually forms the matrix of the rock and the whole is overprinted by late epidote and clinozoisite, minor staurolite is also present.

(iii) Unaltered Portnoo Limestone: this is best seen at least 40 m away from the contact (c-axis of Fig. 6.3) with the appinite. It consists of coarse calcite rhombs (88%) with preferred orientation, parallel to cleavage (S4). The rest of the rock consists of a matrix of rounded to angular quartz and feldspar (2%) grains, often surrounded by calcite plates. Also present in small amounts are biotite (5%) and muscovite (2-5%).

In summary, a detailed petrographic zonation away from the appinite contact is observed with altered limestone displaying hornblende growth in discrete bands, particularly in a 1 cm wide band adjacent to the contact. This then passes into a zone of limestone which still possesses some actinolitic hornblende but which given suitable composition may show the presence of grossular garnet and staurolite up to 50 m away from the contact. Finally this zone passes into the impure limestone typical of the rest of the Portnoo succession.

FOLD OUT

FIG. 6.4 TEXTURAL CHARACTERISTICS OF THE ROCKS OF THE STABLE ISOTOPE TRAVERSE



6.3 GEOCHEMISTRY

The field and petrographic evidence suggests a degree of interaction between appinite and host limestone but does not indicate the extent of material exchange that might have taken place. A promising approach to this problem is analytical, in particular isotopic.

6.3.1 Sampling

In order to collect samples representative of the contact zone a number of factors were taken into account.

(i) Heterogeneity of sample: because of the highly heterogeneous nature of the appinite in this area there are problems of representative sampling, particularly with regard to ferromagnesian content, grain size and degree of alteration. As most of the appinite is meladioritic, samples were taken of the most basic fraction with similar coarse grain sizes and least alteration. A similar situation pertains with the Portnoo Limestone, the main problem being the rapid change in texture and mineralogy seen directly adjacent to the contact (Section 6.2.3). Thus to avoid sampling across a zone boundary the sample directly closest to the contact was taken from zone 1, the outermost zone. Elsewhere in the limestone, traverse samples were taken at regular intervals of distance.

(ii) Alteration: weathered samples as well as those associated with vein systems or shear zones, or with obvious mineral pseudomorphs, were avoided.

(iii) Outcrop: problems of outcrop only arose in the sampling of the Portnoo Limestone where, because of lack of outcrop, the line of sampling had to be staggered (Fig 6.1).

6.3.2 Stable isotope analysis

All isotopic analytical methods and procedures are summarised in Appendix 2. All samples of the traverse were analysed for $\delta^{13}\text{C}_{\text{PDB}}$ and $\delta^{18}\text{O}_{\text{Carb}}$, all appinitic samples were analysed for $\delta^{18}\text{O}_{\text{silicate}}$ but only those Portnoo Limestone samples with sufficient silicate mineralogy were analysed for $\delta^{18}\text{O}_{\text{silicate}}$. Similarly for δD samples with hydrous mineralogy were analysed, this includes most of the appinitic rocks of the traverse and some of the Portnoo Limestone samples.

6.3.3 Description of results

The results obtained in the isotopic study of appinites are tabulated in Table 6.2 and those for $\delta^{18}\text{O}$ silicate, $\delta^{13}\text{C}$ PDB and $\delta^{18}\text{O}$ Carb across the traverse are plotted on Fig. 6.5. The following sections outline the specific results of the various isotopes.

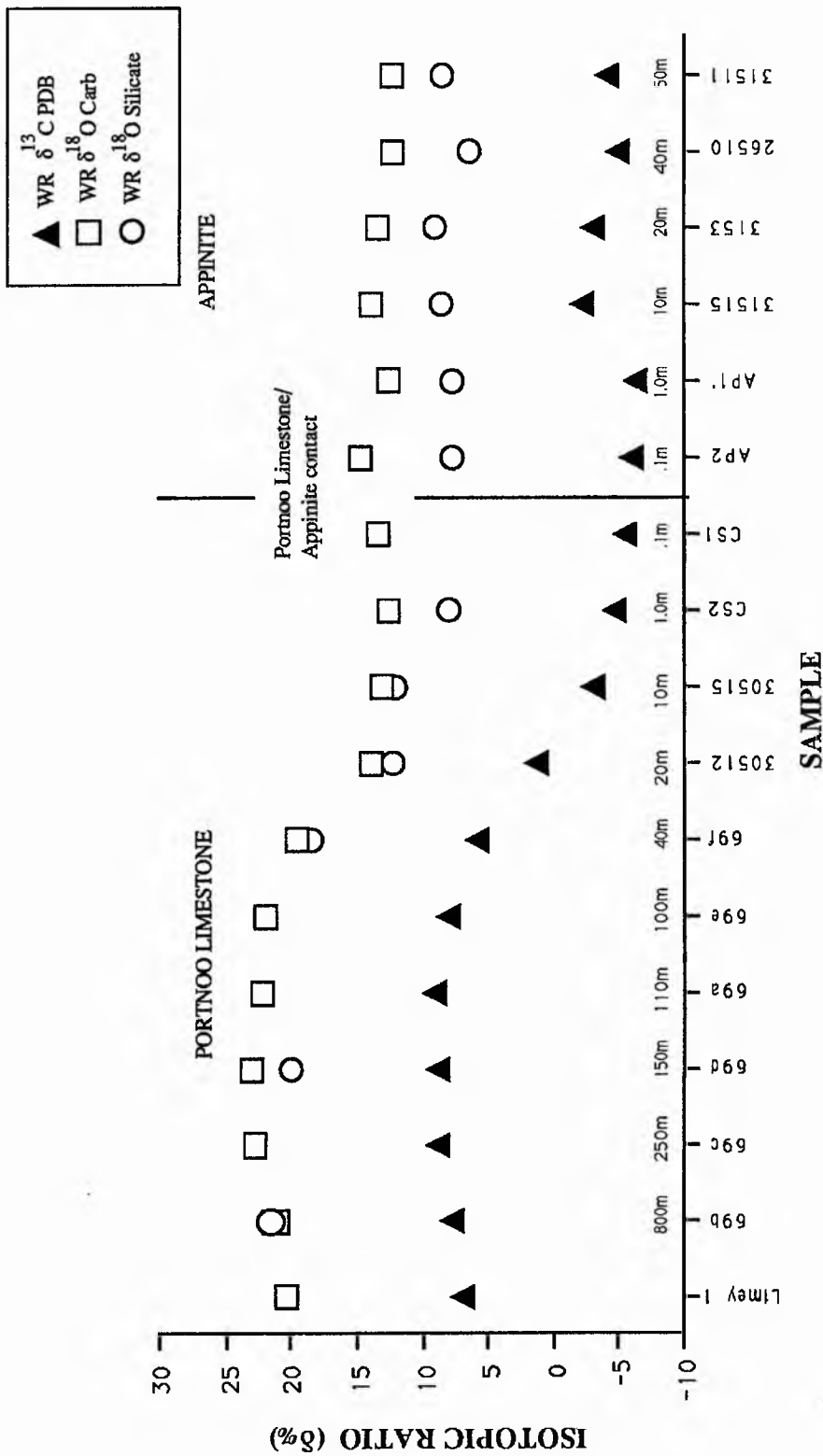


Fig. 6.5 Measured O and C isotope results for samples from isotope traverse across the Portnoo Limestone-appinite contact near Portnoo, Co. Donegal. Sample numbers are plotted on semi-log scale either side of the contact over which the samples were collected. The vertical scale is the whole rock (WR) isotopic ratio of O and C. 'Limey 1' is a sample of the same Falcarragh Limestone member in north Donegal collected as a 'control sample' away from the influence of igneous intrusions.

Sample	WR $\delta^{18}\text{O}_{\text{silicate}}$ ‰SMOW	WR $\delta^{13}\text{C}_{\text{PDB}}$ ‰PDB	WR $\delta^{18}\text{O}_{\text{Carb}}$ ‰SMOW	$\delta\text{D}_{\text{(Mineral)}}$ ‰SMOW	%CaCO ₃ Wt %	δWR^* ‰SMOW	$\Delta^{18}\text{O}^*$ ‰SMOW	$\delta^{18}\text{O}_{\text{Hornblende}}$ ‰SMOW	$\delta^{18}\text{O}_{\text{Quartz}}$ ‰SMOW
Limey 1		6.89	20.23		71.20				
69b	21.10	7.85	21.14	-58.70 (B)	71.70	21.19	0.05		22.36
69c		8.74	22.72		76.00				
69d	19.34	8.73	22.98		73.40	22.22	2.85		21.30
69a		9.00	22.11		83.10		0.00		
69e		7.90	21.92		75.00		0.00		
69f	18.54	5.95	19.56	-48.95 (M)	75.00	19.30	-0.19		19.72
30512	12.20	1.21	14.58		7.80	12.33	1.70		13.20
30515	11.99	-3.01	12.97		28.00	12.26	0.98		12.87
CS2	7.97	-4.54	12.44	-72.76 (A)	3.30	8.11	4.62		10.43
CS1	8.58	-5.44	13.39	-72.68 (A)	0.40	8.51	4.89		10.96
AP2	7.76	-6.04	14.80	-65.60 (H)	0.02	7.76	7.04	6.47/8.06	10.66
AP1'	7.60	-6.27	12.43	-65.63 (H)	1.24	7.65	4.83		10.55
31515	8.66	-2.19	13.89	-58.72 (C)	1.97	8.65	5.40		10.65
3153	9.17	-3.15	13.22		4.80	9.25	4.05		11.10
26510	6.46	-4.90	12.16	-62.68 (H)	7.87	6.90	5.70	7.00/7.34	8.60
31511	8.48	-3.97	12.35		1.61	8.54	3.87		10.44

$$\Delta^{18}\text{O} = \text{WR } \delta^{18}\text{O}_{\text{carb}} - \text{WR } \delta^{18}\text{O}_{\text{silicate}}$$

$$\delta\text{WR} = \frac{\delta_{\text{Calcite}} \times \text{wt \% CaCO}_3 + \delta_{\text{Silicate}} \times \text{wt \% silicate}}{100}$$

Table 6.2 Stable isotope data for all samples collected across Portnoo Limestone/appinite contact

i) Silicate oxygen: ($\delta^{18}\text{O}_{\text{silicate}}$)

(a) Appinites: the $\delta^{18}\text{O}$ values of the appinites range from 6.46 to 8.55‰ (Table 6.3), and although most strongly reflect mantle values, some variation away from typical mantle signatures is apparent.

(b) Portnoo Limestone: these have a high $\delta^{18}\text{O}$ (> +20‰) signature away from the appinite contact. This value (+20‰) may be typical of the Dalradian or it may be related to regional greenschist facies metamorphism. Closer to the appinite contact there is a considerable decrease in the $\delta^{18}\text{O}$ value of limestone with values of about 12‰ within 40m of the contact, decreasing to 8 - 9‰ at the contact.

SAMPLE	¹⁸ O _{silicate} WR δ [*]
Limey 1	---
69b	21.33
69c	---
69d	20.13
69a	---
69e	---
69f	18.54
30512-	12.20
30515	11.99
CS2	7.97
CS1	8.58
AP2	7.76 (8.06)
AP1'	7.60
31515	8.55
3153	9.17
26510	6.46 (7.00)
31511	8.48

Table 6.3 Silicate oxygen data for traverse samples

$\delta^{18}\text{O}$ WR and mineral values are quoted in ‰ relative to SMOW for silicate oxygen.

* Values in brackets are $\delta^{18}\text{O}$ hornblende results.

(ii) Carbon ($\delta^{13}\text{C}_{\text{PDB}}$)

(a) Appinite: The $\delta^{13}\text{C}$ values of the appinites range from -6.27 to -2.19‰ (Table 6.4). The lower values fall within the magmatic range described by Taylor (1986) which overlap with that of mean crustal carbon. Two samples (31515 and 3153) have slightly higher $\delta^{13}\text{C}$ values (-2.19‰ and -3.15‰ respectively), these rocks also have abundant brittle veins with late calcite and epidote infill.

(b) Portnoo Limestone: The pattern for $\delta^{18}\text{O}_{\text{silicate}}$ along the traverse is similar to that of $\delta^{13}\text{C}$ (Fig 6.5), with a decrease in $\delta^{13}\text{C}$ from high values away from the contact to lower values close to the contact with the appinitic intrusion. Away from the contact, apparently more typical values of $\delta^{13}\text{C}$ for the country rock may be found. These values (up to +9.0‰ for $\delta^{13}\text{C}$) are highly enriched relative to typical marine limestone values (Hudson, 1977). The abundance of CaCO_3 across the traverse also mirrors the trace of the $\delta^{13}\text{C}$ values (see Fig 6.6), except for sample 30512 which contains grossular garnet and is more quartz-rich than the other samples. It may have lost CaCO_3 as an effect of Ca redistribution into garnet during contact metamorphism.

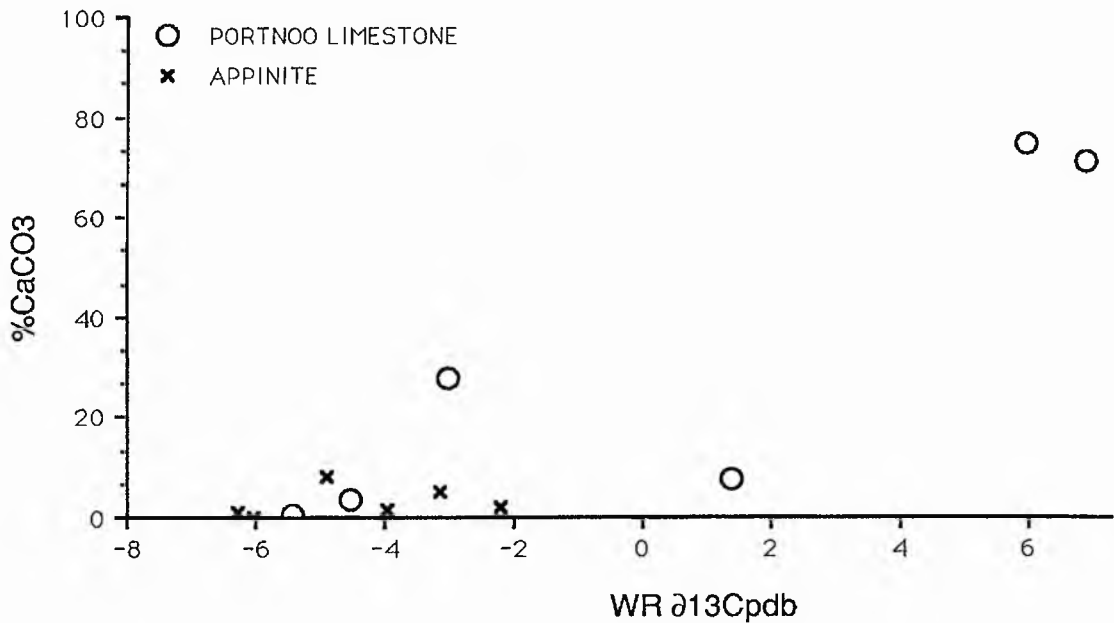


Fig 6.6 WR $\delta^{13}\text{C}$ versus %CaCO₃ showing the reduction of % Ca with $\delta^{13}\text{C}$.

The effect of CaCO₃ loss on the $\delta^{13}\text{C}$ value of this sample (30515) is unknown but if it had little effect it may suggest either attainment of equilibrium between the metamorphic fluid and the magmatic fluid, or that the limestone is relatively impermeable (O'Neil, 1986), impeding fluid movement and thus the magmatic signature strongly overprints that of the metamorphic fluid.

(iii) $\delta^{18}\text{O}_{\text{carbonate}}$

The most striking aspect of the $\delta^{18}\text{O}_{\text{carbonate}}$ of the appinite is the fact that the $\delta^{18}\text{O}_{\text{silicate}}$ and $\delta^{18}\text{O}_{\text{carbonate}}$ values mimic each other across the contact and both fall and rise sympathetically (Fig 6.5) as indeed does $\delta^{13}\text{C}$.

ROCK TYPE	SAMPLE	WR $\delta^{13}\text{C}_{\text{PDB}}$	WR $\delta^{18}\text{O}_{\text{Carb}}$	%CaCO ₃
PORTNOO LIMESTONE	Lim	6.89	20.23	71.20
	69b	7.85	21.14	71.70
	69c	8.74	22.72	76.00
	69d	8.73	22.98	73.40
	69a	9.00	22.11	83.10
	69e	7.90	21.92	75.00
	69f	5.95	19.56	75.00
	30512	1.21	13.90	7.80
	30515	-3.01	12.98	28.00
	CS2	-4.54	12.44	3.30
	CS1	-5.44	13.39	0.40
	APPINITE SUITE	AP 2	-6.04	14.88
AP 1		-6.27	12.43	1.24
31515		-2.19	13.89	1.97
3153		-3.15	13.24	4.80
26510		-4.90	12.16	7.87
31511		-3.97	12.35	1.61

Table 6.4 Carbon data for samples measured in stable isotope traverse at Portnoo
Carbonate oxygen isotope values are quoted in (‰) relative to SMOW
Carbon isotope values are quoted in (‰) relative to PDB
All values shown are for Whole Rock samples

That the isotope trends are linked may be shown by plotting the δ values against one another (Fig 6.7). The good positive correlation of all three possible pairs of isotopic systems is powerful evidence for their combined behaviour and modification through a single common process.

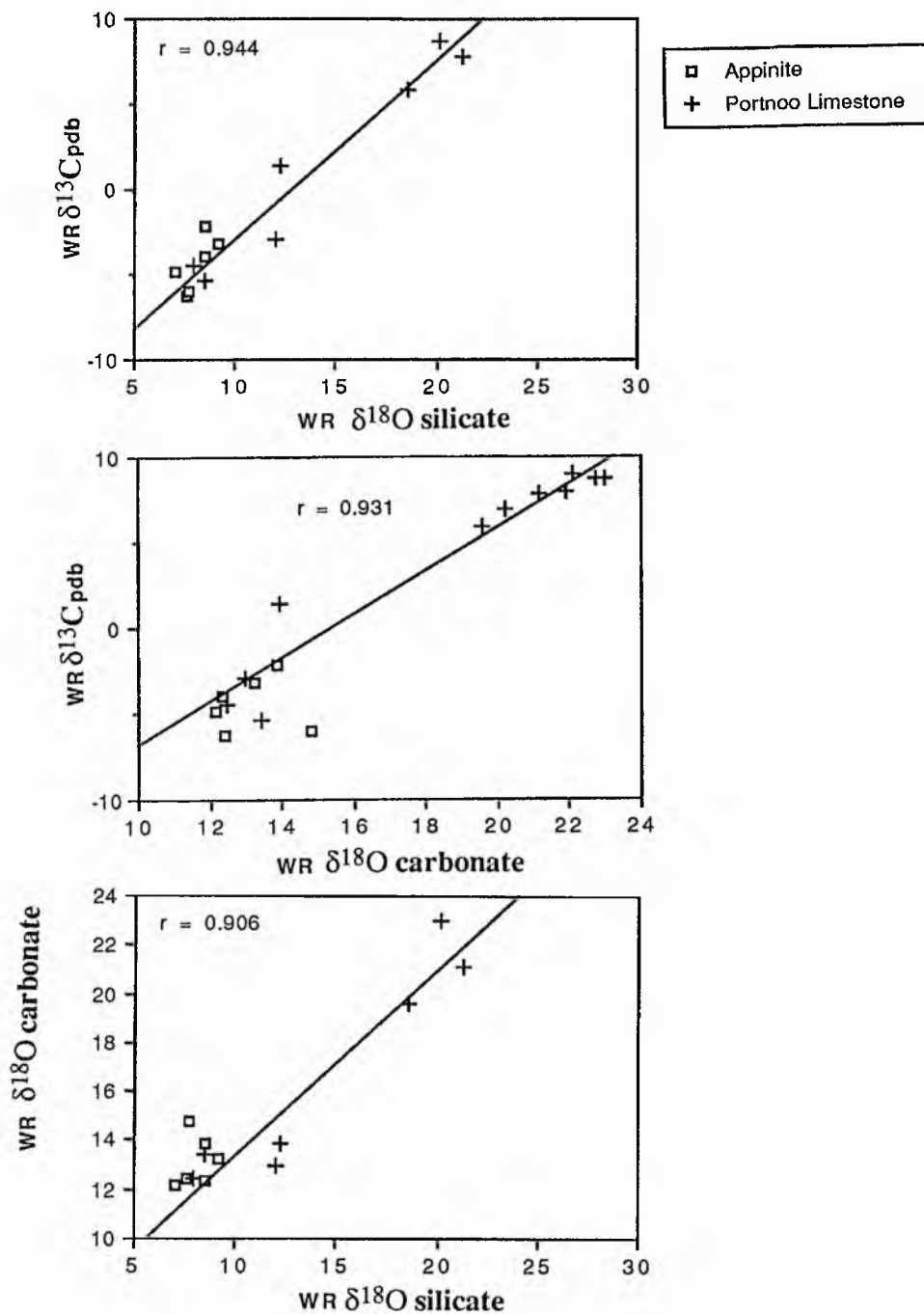


Fig 6.7 Variation plots showing the good correlation between the isotopic ratios for limestone and appinite samples.

(iii) Hydrogen, δD

Mineral δD analyses (Table 6.5) show an overlap in values (Fig 6.8). Appinites show a range from -57.0 to -65.6 ‰, while those in the Portnoo limestone samples range from -48.9 to -72.7‰.

ROCK TYPE	SAMPLE	MINERALOGY	δD (‰)
PORTNOO MARBLE	CS2	Actinolite	-72.76
	CS1	Actinolite	-72.68
	69f	Muscovite	-48.95
	69b	Biotite	-58.70
APPINITE SUITE	AP2	Hornblende	-65.60
	AP1'	Hornblende	-65.63
	26510	Hornblende	-62.68
	31515	Chlorite	-58.72
	31515med	Epidote	-57.01
	Kilr hb rim	Hornblende	-65.00
	1856	Hornblende	-58.47

δD values are quoted in ‰ relative to SMOW

Table 6.5. δD results for samples analysed long the isotope traverse. Samples 'Kilr hb rim' from the hornblendite of the Kilrean intrusion and '1856' from diorite of the Meenalargan intrusion are included for comparison with the data from Narin-Portnoo.

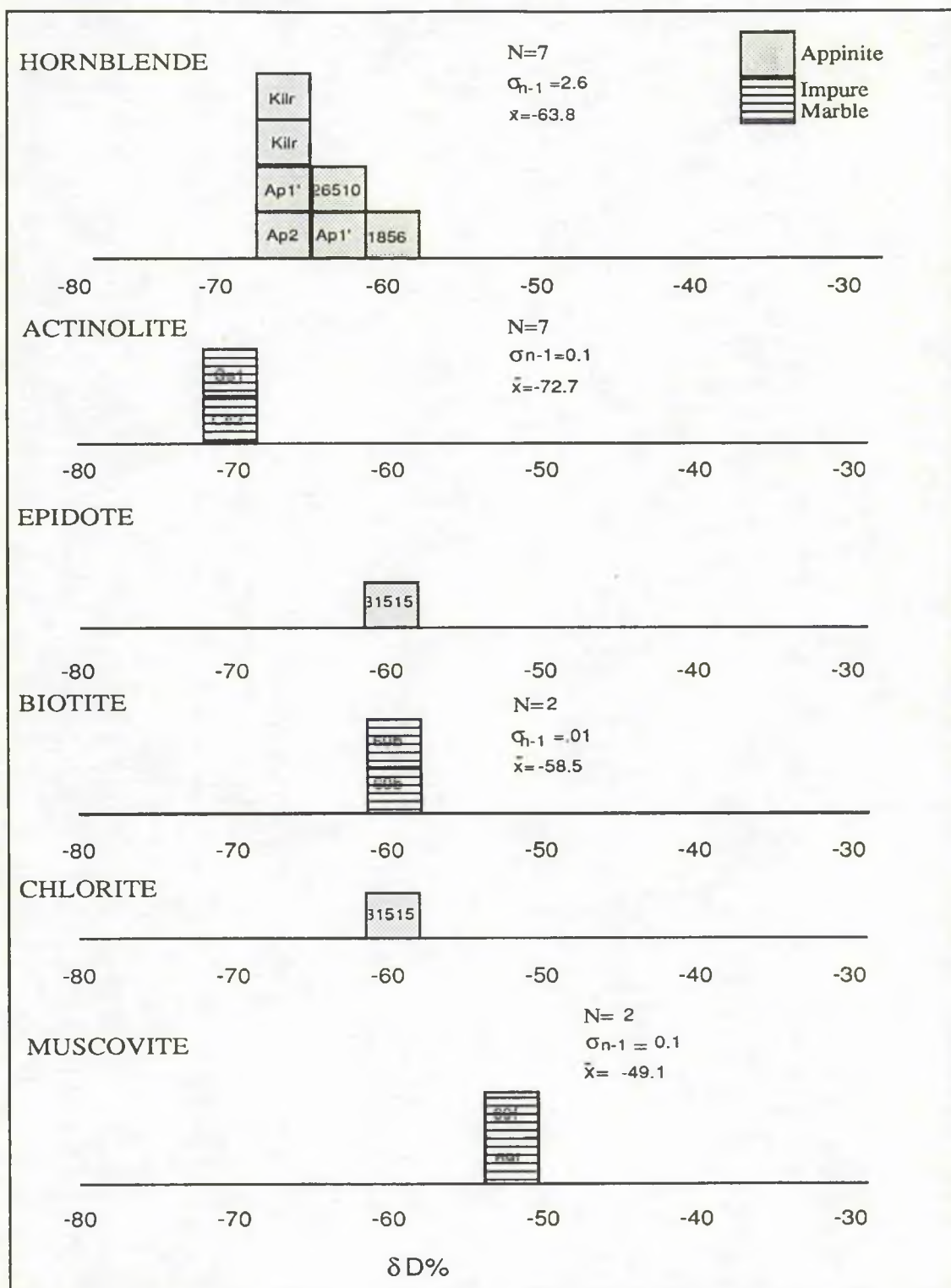


Fig 6.8 Histogram plot of δD data for minerals in appinites and limestones.

6.4 INTERPRETATION OF RESULTS

(i) $\delta^{18}\text{O}_{\text{silicate}}$

(a) Appinite.

Although the majority of results are similar to mantle values, the higher $\delta^{18}\text{O}$ values in some samples may have been caused by assimilation of high $\delta^{18}\text{O}$ oxygen prior to hornblende crystallisation. Mineral separates of hornblende (7.17, 8.06‰), give values consistent with having formed in a mantle-derived magmatic environment that has suffered some assimilation of high $\delta^{18}\text{O}$ crust prior to hornblende crystallisation, either at the present level or a deeper level.

(b) Portnoo Limestone.

The Portnoo Limestone has a heavy, crustal $\delta^{18}\text{O}$ silicate oxygen signature away from the appinite contact. This value is progressively lowered from up to 50m from the contact (Fig 6.5) suggesting exchange with a lower ^{18}O fluid expelled into the Portnoo Limestone.

(ii) $\delta^{13}\text{C}_{\text{PDB}}$

(a) Appinite.

Most samples have mantle-type signatures. However the slightly higher $\delta^{13}\text{C}$ values obtained in samples 3153 and 31515 may reflect the brittle-veined nature of these samples which have abundant calcite and epidote infill, which may have imparted a crustal source signature to the rocks, i.e. the fluid in the veins must have passed through the Portnoo Limestone.

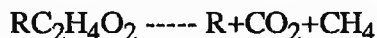
(b) Portnoo Limestone.

The magmatic values, within the Portnoo Limestone close to the contact may imply infiltration of a magmatic fluid into the country rock and subsequent isotopic exchange due to recrystallisation of the minerals of the impure limestone and calc-silicate to form actinolite and epidote with magmatic signatures (see Chapter 4.7). Away from the influence of the appinite, $\delta^{13}\text{C}$ values increase to a level greater than the modern-day marine limestone value. Such values have not so far been reported from the Lower Dalradian of Ireland, but Graham (pers. comm.) has obtained heavy carbon isotope values from Middle Dalradian limestone of the Tayvallich Peninsula, in Scotland. He found that the Tayvallich Limestone has values of between +6.0 to +7.5 for $\delta^{13}\text{C}$, which he believes are original sedimentary values.

(c) Heavy carbon in the Portnoo Limestone.

As discussed above the presence of heavy carbon has not before been reported in the Dalradian of Ireland. The range in $\delta^{13}\text{C}$ from -5.44 to +9.0‰ supports the idea that carbonate sediments during the Dalradian had a carbon isotope signature that was enriched in ^{13}C which, in samples close to the appinite contact were lowered to magmatic values during the appinite intrusion due to the action of a magmatic fluid from

the intrusion. The normal metasedimentary $\delta^{18}\text{O}$ carbonate results suggest that such rocks may contain $\delta^{13}\text{C}$ which represents original sedimentary values. A possible mechanism of heavy carbon formation may be by a process of fermentation in an enclosed basin. Fermentation of:



where R is any organic molecule, leads to high $\delta^{13}\text{C}_{\text{CO}_2}$ and low $\delta^{13}\text{C}_{\text{CH}_4}$. If the methane is lost, then the residual, high $\delta^{13}\text{C}$ -bearing CO_2 can be the only source of carbon available. Alternatively it is possible that high $\delta^{13}\text{C}$ in the Dalradian may have been caused by the environment of deposition of the sediments; because, a closed/semi-closed basin where extensive burial of organic carbon ($\delta^{13}\text{C} \sim -25\text{‰}$) resulted (by mass balance) in $\delta^{13}\text{C}$ -enriched inorganic carbon, recorded as high $\delta^{13}\text{C}$ carbonate. Some evidence for such basin restriction comes from the higher than usual sulphur $\delta^{34}\text{S}$ seen by Willan & Coleman (1983) in the Dalradian (barite) from Aberfeldy. Baker & Fallick (1989) have analysed Lewisian limestone where high $\delta^{13}\text{C}$ (up to $+12\text{‰}$) and normal or relatively low $\delta^{18}\text{O}$ limestones are attributed to a major global excursion in seawater composition. Whether an excursion was present during the Dalradian sedimentation of Scotland and Ireland must be tested by further analysis of stratigraphic variation in $\delta^{13}\text{C}$ in samples unaffected by appinitic magma. More data would thus be required and the effects of fluid-rock interaction would have to be unravelled before these data can be uniquely interpreted.

(iii) $\delta^{18}\text{O}$ carbonate.

The relative 'gap' between the $\delta^{18}\text{O}_{\text{carbonate}}$ and $\delta^{18}\text{O}_{\text{silicate}}$ values seen on the isotope traverse plot (Fig 6.5) may be due to differences in the fractionation factors for calcite and the silicate minerals namely plagioclase, hornblende, quartz and epidote, either side of the contact. In order to quantify the importance of silicate mineralogy to the WR $\delta^{18}\text{O}$ value, the $\delta^{18}\text{O}$ of quartz was calculated using the actual WR $\delta^{18}\text{O}$ silicate values and the mineral-water fractionation factors of Bottinga & Javoy (1973), Wenner & Taylor (1971), Matsuhisa et. al. (1979), and Clayton et al. (1972) as well as the modal percentages of each mineral phase in the rock, using the equation:

$$\delta^{18}\text{O}_{\text{Quartz}} = \delta^{18}\text{O}_{\text{WR silicate}} + \sum_{i=1}^{n-1} \Delta_{\text{quartz} - i} \cdot X$$

so for 4 phases of hornblende, epidote, plagioclase and quartz.....

$$\begin{aligned} \delta^{18}\text{O} = \delta^{18}\text{O}_{\text{silicate}} &+ \Delta_{\text{quartz} - \text{hornblende}} \cdot X_{\text{hornblende}} \\ &+ \Delta_{\text{quartz} - \text{epidote}} \cdot X_{\text{epidote}} \\ &+ \Delta_{\text{quartz} - \text{plagioclase}} \cdot X_{\text{plagioclase}} \end{aligned}$$

$$\Delta = \delta_{\text{quartz}} - \delta_i \approx 10^3 \ln \alpha_{q-i} \text{ at } T(^{\circ}\text{K})$$

X = mole fraction of oxygen in that phase
which approximates to the modal percentage

where $\delta^{18}\text{O}_Q$ is the calculated value for $\delta^{18}\text{O}$ of quartz, $\delta^{18}\text{O}_{\text{WR silicate}}$ is the measured value of $\delta^{18}\text{O}$ of the whole rock silicate samples from the traverse.

The parameter $\Delta_{\text{quartz} - i}$ is a function of temperature and from the results of geothermometry (Blundy 1989) of the mineral assemblages (Chapter 4.12.4 b) at calculated pressures, the fractionation temperature range of 500°C - 800°C was used. Results for calculations are given in Table 6.6 which shows the calculated $\delta^{18}\text{O}$ quartz values and also shows the calculated $\delta^{18}\text{O}$ epidote at 800°C and 500°C.

Tentative apparent temperatures were also calculated using the WR $\delta^{18}\text{O}$ silicate and $\delta^{18}\text{O}$ carbonate values of coexisting mineral phases along the traverse. These were derived from the calculated fractionation equations of O'Neil, Clayton et al. (1972), Wenner & Taylor (1971), Bottinga & Javoy (1973), assuming that :

$$10^3 \ln \alpha = A \left(\frac{10^6}{T^2} \right) + B$$

The results are represented on Fig 6.9, which shows that for $\delta^{18}\text{O}$ quartz and $\delta^{18}\text{O}$ WR silicate in the region of the appinite/limestone contact, the curve is very smooth and both $\delta^{18}\text{O}$ WR silicate and $\delta^{18}\text{O}$ quartz have a flat curve-trace, however at >20m from the contact the $\delta^{18}\text{O}$ quartz curve rises in parallel with the $\delta^{18}\text{O}$ silicate. This is suggestive of the activity of a magmatic fluid which has exchanged isotopically with country rock at least 40m into the country rocks. Most interestingly, the calculation of the $\delta^{18}\text{O}$ quartz for each of the rocks along the traverse cancels out any isotopic variation caused by differences in mode and mineralogy.

Sample	$\delta^{18}\text{O}$ WRsili	$\delta^{18}\text{O}_{\text{quartz}}$ (800°C)	$\delta^{18}\text{O}_{\text{epidote}}$ (800°C)	$\delta^{18}\text{O}_{\text{epidote}}$ (500°C)
69f	18.54	19.72	20.17	18.60
69b	21.33	22.36	22.90	21.04
69d	20.13	21.30	21.72	20.19
30512	12.20	13.20	12.42	11.84
30515	11.99	12.87	14.26	12.25
CS2	7.97	10.43	9.30	7.17
CS1	8.58	10.96	9.89	6.90
AP2	7.76	10.66	10.54	8.19
AP1'	7.60	10.55	10.38	7.99
31515	8.55	10.65	10.30	8.88
3153	9.17	11.10	10.96	8.93
26510	6.46	8.60	8.68	6.08
31511	8.48	10.44	10.19	7.97

Table 6.6 Estimated $\delta^{18}\text{O}$ values for quartz and epidote at varying temperatures.

In conclusion, the variation in WR $\delta^{18}\text{O}_{\text{silicate}}$ is due, not significantly to mineralogy and mode, but to the effect of fluids. Calculations of $\delta^{18}\text{O}_{\text{quartz}}$ using actual $\delta^{18}\text{O}_{\text{silicate}}$ values and known fractionation factors (Fig 6.9) show a strong similarity with the $\delta^{18}\text{O}_{\text{silicate}}$ values (Fig. 6.5) and strongly suggest that there is no significant mineralogical control on the isotopic trace. The similar shape of the profiles might suggest oxygen isotopic equilibrium between the silicates and carbonates (Fig 6.9 and Table 6.6.). To investigate this, temperatures assuming equilibrium were calculated for different phases. Table 6.7 shows the results calculated at different temperatures for different phases. The fact that apparent temperatures differ and do not correspond to formation temperature (500-800°C) indicates within-rock isotope disequilibrium. None of the results obtained has a consistent relationship across the aureole and are thus not considered further in this chapter.

(iii) Hydrogen.

Taylor and Sheppard (1986) noted that most igneous rocks had δD values ranging from -50 to -95 ‰. Any rocks which plot outside this range may have been affected by a weathering or hydrothermal/meteoric process during their diagenetic history; such processes may have been active in the rocks of this isotopic traverse.

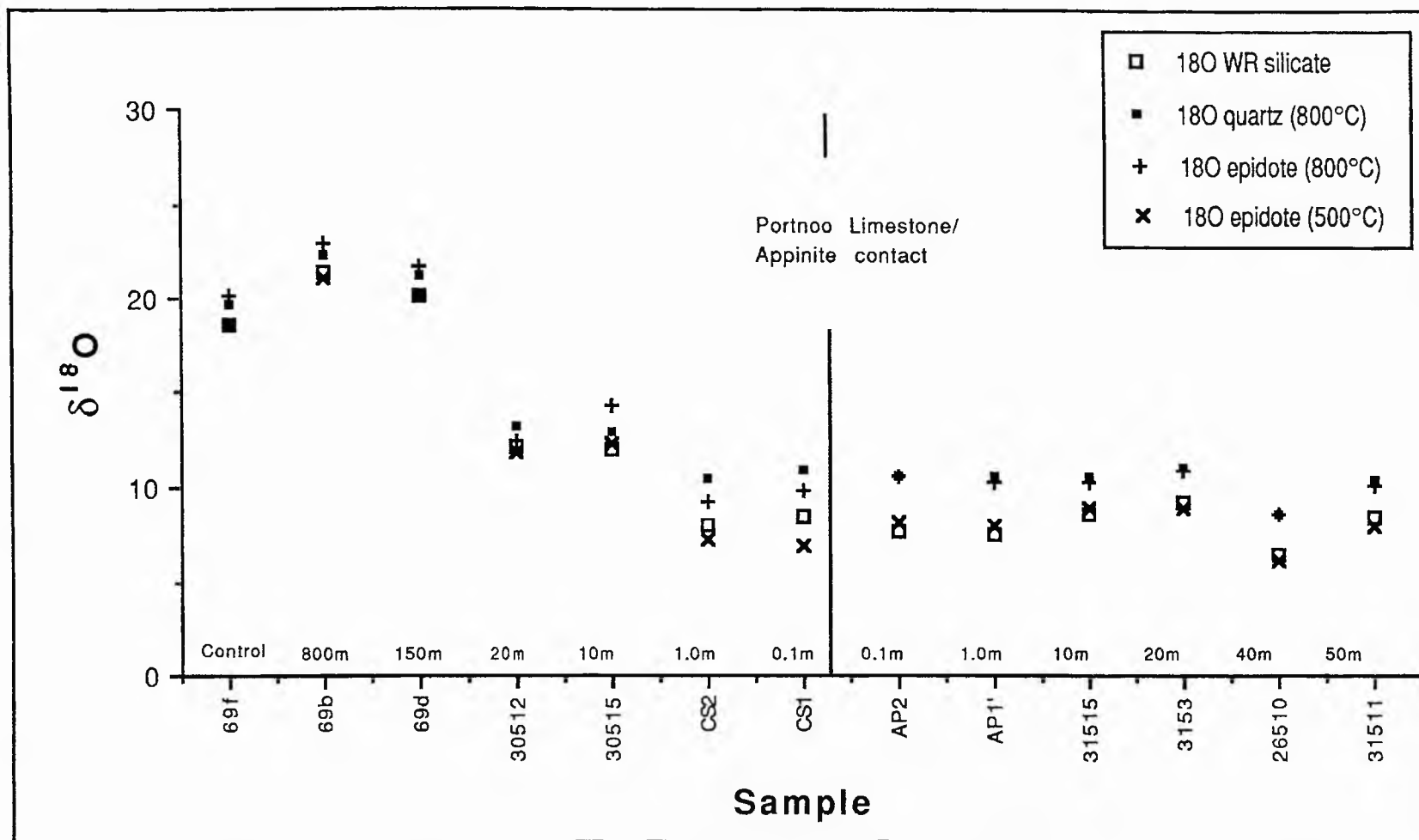


Fig. 6.9 Calculated values for $\delta^{18}\text{O}$ of quartz and epidote at 500°C and 800°C based on measured values of $\delta^{18}\text{O}$ silicate and the fractionation factors of O'Neil, Clayton and Mayeda (1969), Wenner & Taylor (1971), Bottinga & Javoy (1973)

Sample	Temp °C Calcite-h'blende 500-800°C	Temp °C Calcite-plag 500-800°C	Temp °C Calcite-epidote 800°C	Temp °C Calcite-epidote 500°C	Temp °C Calcite-tremolite 800°C
69b					
69d		149	870	475	
69f		521			
30512		296	790	642	
30515		544		817	
CS2	435		381	304	435
CS1	417		436	235	417
AP2	293		372	247	
AP1'	408		641	359	
31515	382		441	323	
3153	471		598	335	
26510	355		438	240	
31511	488		619	330	
\bar{x}	406		559		426
σ_{n-1}	63		174		

Table 6.7 Estimated temperatures of co-existing mineral pairs, using the fractionation factors of Bottinga & Javoy (1973) Matsuhisa et al. (1979), O.Neil, Clayton & Mayeda (1969) and Wenner & Taylor (1971).

The hydrogen isotope composition of Mid Ocean Ridge Basalt has been measured at $\delta D = -71$ to -84 ‰ (at 0.2 wt % H_2O) by Craig & Lupton (1976) while Kyser (1986) noted local variability in the mantle from -70 ‰ to -60 ‰. Rocks that have low δD values of -100 ‰ such as those of the Tertiary Inner Hebrides may have undergone subsolidus interaction with very low δD meteoric fluids (Taylor 1977). Those rocks that have high δD values may have been affected by fluids with high δD values, such as seawater or high latitude meteoric fluids. Such fluids may have been present in the Dalradian of Donegal and may thus have imparted a high δD value on the limestone.

Taylor (1977) noted that the δD signature of most sedimentary rocks falls in the restricted range of -40 to -85 ‰ due to equilibration of clay minerals with low temperature surface waters, and it is possible that the δD value of metamorphic rocks will reflect that of the sedimentary precursor. The calcic hornblende separates analysed from the appinites adjacent to the Portnoo Limestone contact give consistent mantle-type values of $\delta D = -63$ to -66 ‰. The actinolitic hornblende analysed from the Portnoo Limestone adjacent to the contact with the appinite has a value of $\delta D = -73$ ‰, which is also a mantle-type value.

The difference between these two results may be due to differences in H isotope fractionation factors between calcic hornblende in the appinite and actinolitic hornblende in the Portnoo Limestone. Graham et al. (1984) measured the experimental hydrogen isotope fractionation factors of hornblende, actinolite and epidote (Fig 6.10). From this graph the difference in δD between actinolite and hornblende at a realistic magmatic

temperature of 750°C is about 5-7 ‰ heavier than hornblende, not lighter, as has been observed, which may suggest the presence of a different fluid phase. Thus δD of magmatic fluid, which was present during the crystallisation of the hornblende in the appinite, may be slightly different from that responsible for the formation of actinolite in the Portnoo Limestone at the contact with the appinite.

It is apparent from Table 6.5 and Fig 6.11 that the two samples of biotite and muscovite from the Portnoo Limestone possess high $\delta^{18}O$ silicate and high δD values. The biotite sample was separated from limestone outside the area of magmatic fluid reaction. The muscovite was analysed from limestone from the margin of the aureole of magmatic fluid reaction. Both minerals are believed to have formed during greenschist facies metamorphism, before the intrusion of appinite. Two samples of chlorite and epidote were analysed from appinite 10m from the appinite/limestone contact, these have a secondary texture associated with biotite replacement. Both these minerals, like those from the Portnoo Limestone, have high δD values. Determination of the fluids in equilibrium with these respective minerals shows both waters to have significantly higher δD values (-11 to -21‰) than those of the H_2O in equilibrium with the hornblende analysed (-39.5 to -44‰). This may reflect the greater isotopic fractionation of epidote and chlorite at lower temperatures. Both the chlorite and the epidote phases taken from the appinite samples have similar δD values of -58.7 and -57.0, respectively. Both are texturally late stage minerals, formed as secondary alteration products of the appinite. Jenkin (1988) in calculating the hydrogen isotope compositions of the fluids in equilibrium with hornblende, epidote and chlorite from the Metagabbro Suite of Connemara noted a strong fractionation in epidote and to a lesser degree, chlorite at lower temperatures (300°C). Considering the late-stage textures of the epidote and chlorite, these high δD values in Ardara may reflect a regional circulation of a meteoric fluid enriched in deuterium, which may be related to the intrusion of the Ardara pluton. Alternatively this may correspond to a ?Devonian phase of regional fluid circulation identified in agates in Lower Devonian lavas from Scotland, (Fallick et al. 1985). The δD value of such a fluid may only be determined if data relating to fluid and mineral chemistry as well as equilibrium temperature are known.

6.5 SYNTHESIS OF RESULTS AND INTERPRETATION

The data obtained for silicate, carbonate oxygen and carbon isotopes must be considered in the context of the four models proposed in section 6.2.1. Examination of the data in Fig 6.5 indicates:

(i) The system most closely approximates to a model of fluid expulsion with primary expulsion of a magmatic fluid up to a point 40-50m within the Portnoo Limestone.

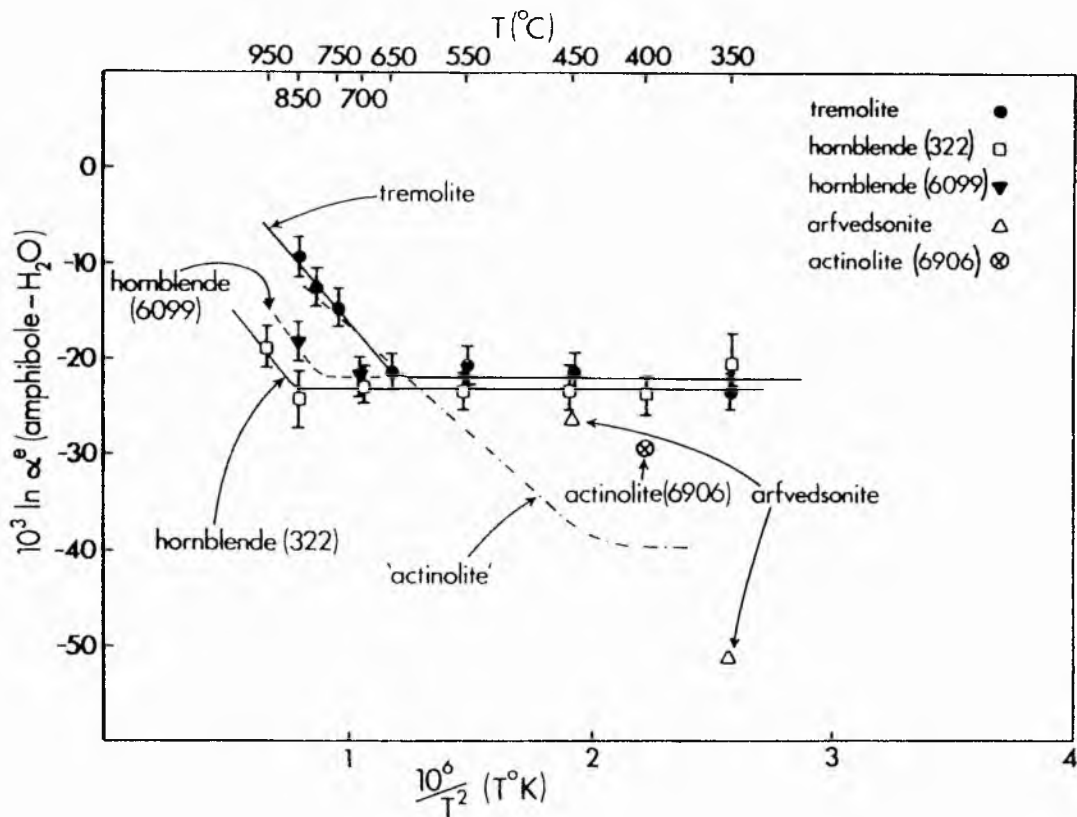


Fig. 6.10 Experimentally determined relationships between hydrogen isotope fractionation factor ($10^3 \ln \alpha^e$ amphibole- H_2O) and temperature (plotted as $10^6/T^2$) for the system amphibole- H_2O . Data for "actinolite"- H_2O after Suzuoki and Epstein (1976). Error bars indicate analytical precision. From Graham et al. (1984).

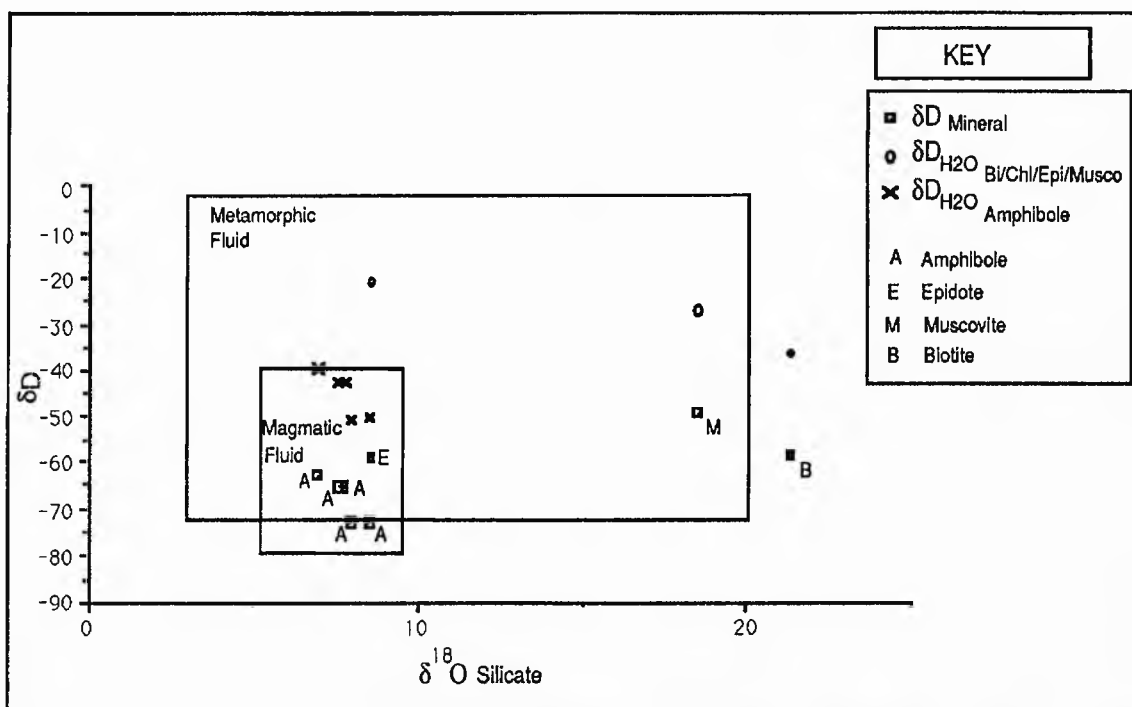


Fig 6.11 Plot of $\delta D - \delta^{18}O$, showing the measured compositions of δD and $\delta^{18}O$ for the hydrous minerals of the traverse in relation to known compositions of magmatic water and the δD_{H_2O} in equilibrium with the hornblende. Fractionation factors used are those for; biotite, muscovite and actinolite (Suzuoki & Epstein 1976), hornblende (Graham et al. 1984), epidote (Graham et al. 1980).

(ii) There is total overprinting of Portnoo Limestone metasedimentary isotopic values 1m from the appinite contact

(iii) There is a gradual decline in the degree of fluid-rock interaction with distance away from the appinite contact.

(iv) A process of devolatilisation at the contact causes shifts in the isotopic values but these are expected to be much less than those actually observed and this process is rejected as a major contributor of the results (Valley, 1986).

(v) The existence of two different sets of isotopic results is suggested by the two "plateaux" of results (Fig 6.5), that is, carbon and oxygen of typical mantle isotopic composition within the appinites continue into the Portnoo Limestone for at least 10m before the isotopic compositions start to rise sympathetically and at 100m reach the second plateau. The relationship between these two different isotopic ratios cannot be a fractionation effect.

The carbonate oxygen and the silicate oxygen of the appinites and 10 m into the Portnoo Limestone shows a larger difference than the difference in the area more than 10 m from the appinite contact (Fig. 6.5). This suggests that $\delta^{18}O$ silicate and $\delta^{18}O$ carbonate are less in equilibrium in the appinite and 10m into the Portnoo limestone

perhaps because the respective isotopic species have had a shorter time to achieve equilibrium, during the crystallisation period of the magma. The $\delta^{18}\text{O}$ silicate and $\delta^{18}\text{O}$ carbonate values of the Portnoo limestone more than 10 m from the appinite contact are closer to one another and so may have had a longer period over which to achieve equilibrium. Alternatively less equilibrium between the $\delta^{18}\text{O}$ silicate and $\delta^{18}\text{O}$ carbonate in the Portnoo Limestone may be due to the limestone having been subject to crystallisation at a lower temperature than the appinite and so the small fractionation seen in the marble may be due to coincidence.

A magmatic fluid appears to have exerted an influence as far as 40m into the country rocks. Isotopic evidence for the presence of another fluid apart from the magmatic appinite fluid comes from the patterns of isotope values in the silicate minerals. From the pattern of $\delta^{18}\text{O}$ silicate it is apparent that the silicate mineralogy plays no important part in determining the values of the appinite and limestone (Fig 6.9). The isotopic variation is thus thought to be a direct result of the action of fluids.

6.6 THE SHAPE OF GEOCHEMICAL FRONTS

The shape of geochemical fronts has been modelled by authors such as Lassey & Blattner (1988, 1989), Bickle & Baker (1989) and McKibbin & Absar (1989). These authors mathematically modelled the shape of geochemical fronts (GF) by considering a fluid of known isotopic composition against parameters of porosity, spatial variation, time dependent rock/water interaction and temperature, using equations of mass balance and exchange kinetics. Lassey & Blattner (1989) concluded that isotopes of different elements mapped over a one dimensional trajectory will give rise to GF at different distances according to the effective porosity of that element. As an example they cite $\delta^{18}\text{O}$ as moving twenty times faster than an $\epsilon^{87}\text{Sr}$ front related to the same infiltration event. They noted that a decoupling of a GF can occur in isotopes of a single element in mineral phases that differ in their kinetic properties with respect to that element.

The results obtained for $\delta^{13}\text{C}$ and $\delta^{18}\text{O}$ silicate and $\delta^{18}\text{O}$ carbonate across the appinite/limestone contact essentially represent a geochemical front for that particular fluid. At the scale studied here, the close spatial relationship between the different isotopic species across the traverse corresponds to the movement of a magmatic fluid through the different rock types. It seems from these data that the shape of the isotopic fronts represents a simultaneous movement front of $\delta^{13}\text{C}$ and $\delta^{18}\text{O}$ silicate and $\delta^{18}\text{O}$ carbonate.

6.7 DYNAMIC MODEL OF FLUID-ROCK INTERACTION AT A LIMESTONE/APPINITE CONTACT

From the evidence of this contact and others in the area, the mineralogical features of hornblende growth adjacent to the contact suggest that the process of fluid expulsion

may be common. Fig 6.12 is a hypothetical model representing the major fluid/rock processes at the margin of an appinite intruding impure limestone. The stable isotope results strongly support the existence of a magmatic fluid which interacts with the Portnoo Limestone, the intensity of interaction falls off 40-50m away from the contact. The intrusion is at least 50m wide where exposed and may be up to 100m wide, which suggests that the appinite body had a expulsion zone approximately equal to its radius. Such a fluid aureole may exist around other intrusions and may have variable influence depending on factors such as lithology, permeability, depth, form, shape and depth of the magmatic intrusion.

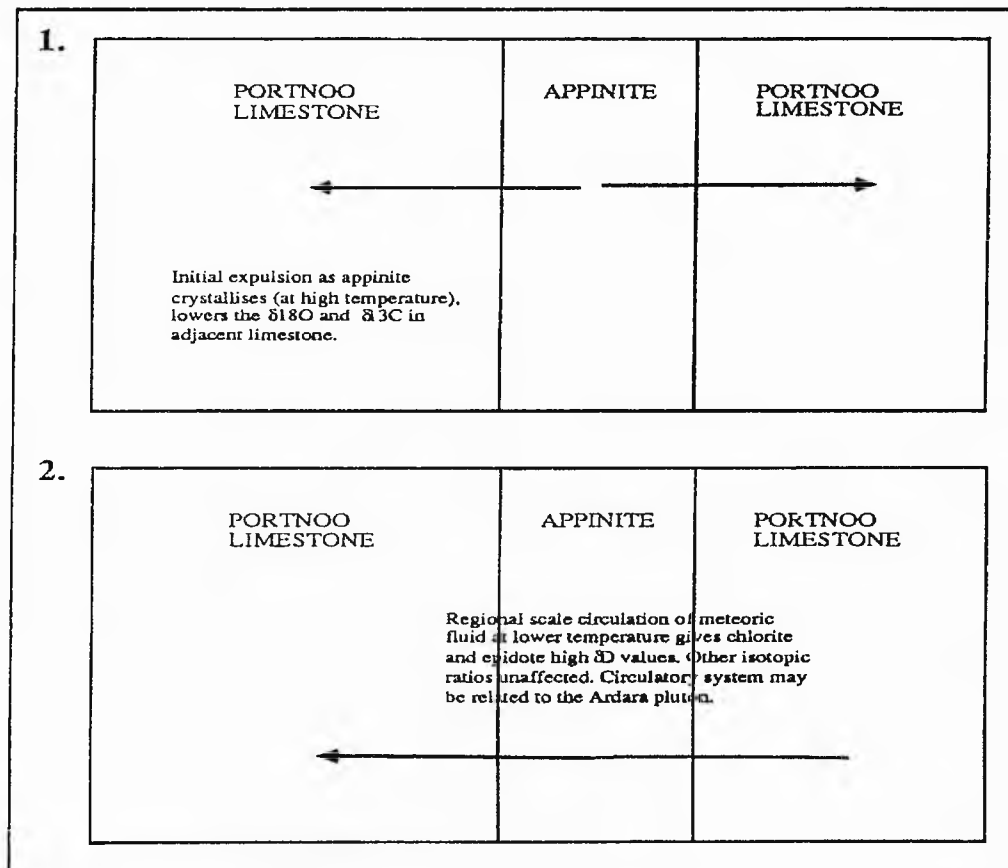


Fig 6.12 Hypothetical model representing the major fluid/rock processes at the margin of an appinite intrusion intruding impure limestone.

It is proposed that the process of interaction between magma and country rock may occur by intrusion of a dome to sheet-like body in a process of stopping into reactive impure limestone/ pure limestone lithologies. The form of the intrusions may be associated with abundant shearing and folding of the metasediment which may deform in a plastic manner. Magmatic fluid may have enhanced this plasticity by heating the country rock, and assisted exchange of material at the immediate contact. The magmatic fluid may cause the growth of new minerals such as actinolitic amphibole, plagioclase and epidote at the contact. This process may be relatively rapid before crystallisation

below the blocking temperature of hornblende for $\delta^{18}\text{O}$ (? at 500°C) thus explaining the large gap between $\delta^{18}\text{O}$ silicate and $\delta^{18}\text{O}$ carbonate values in the appinite. Ten metres from the appinite/limestone contact isotopic exchange was still active. The expulsion system may decline in intensity more than 40-50m from the contact, where it gave way to the influence of the metamorphic/meteoric system associated with the intrusion of the Ardara granitic pluton. Judging from the hydrous nature of appinite mineralogy, the composition of the expelled fluid may be dominantly aqueous. δD data on chlorite and epidote indicate the existence of a late stage high δD meteoric fluid. This may have been part of an end-stage process with circulation of meteoric groundwater in brittle, late-stage veins and veinlets which may locally raise the $\delta^{13}\text{C}$ and $\delta^{18}\text{O}$ silicate values of appinite which are cut by these calcite-rich veins. Thus samples 3153 and 31515 may have been affected by this process. In considering a process of devolatilisation at the contact, one might expect to see shifts in the isotopic values which may be much less than those actually observed.

Similar processes of fluid expulsion may occur in other intrusions in the Ardara and Appin areas of Scotland which show reaction with calcareous country rocks. Any basic intrusion with a strong associated hydrous and volatile-rich mineralogy intruding reactive metasediment, particularly limestone, may bring about the alteration of the metasediment.

CHAPTER SEVEN

PETROGENESIS OF THE APPINITES AND GRANITES: DISCUSSION AND CONCLUSIONS

7.1 INTRODUCTION

This study has primarily been concerned with the petrology of the appinitic intrusions clustered around the main Ardara pluton, focusing on the mechanisms of emplacement, the petrography and mineral chemistry, whole rock major, trace and isotopic geochemistry, and the P-T relationships of these volatile-rich magmas. The appinites of the Ardara pluton are very similar to those elsewhere in the Caledonides and in other orogens and a particular study has been made of the role of fluid interaction between magmas and their aureoles. The high volatile content of appinites is an important factor in their emplacement, particularly in the case of breccia pipes, which are analagous to the high level diatremes associated with Kimberlite emplacement. The appinites of the Ardara complex may be important in understanding relationships of acid-basic magma associations in orogenic granite belts. The main Ardara pluton has intimate contact relationships with some of the main basic to intermediate appinite intrusions. The emplacement of the main pluton by diapiric processes as described by Holder (1979) and associated explosive appinites underlines the importance of a structural control on the emplacement of granitic and appinitic magmas in this region of classic variation in plutonic emplacement mechanism (Pitcher & Berger 1972).

This chapter combines the evidence from field and laboratory studies with data and conclusions presented by other workers in presenting a petrogenetic model. The discussion outlines the various factors which affect the petrogenesis of appinites, the controls on emplacement, and the evolution of appinite. A model is proposed in the light of existing knowledge and evidence obtained during this research study. The classification of appinites is incidentally reviewed and a revised classification scheme proposed. The conclusions of the present study are presented along with suggestions for further research.

7.2 PETROGENESIS OF THE ARDARA APPINITES

7.2.1 Parental magmas

(i) Basalt

The close geochemical similarity of appinites and calc alkali basaltic rocks (section 5.2 iii), particularly in terms of incompatible trace element abundances (Table 7.1) suggests that the appinites may be genetically related to a basaltic parental magma, although the appinites are generally richer in Ti and Th and depleted in Zr compared with basalts. Moreover both appinites and basalts show Nb depletion indicative of the calc alkaline series. Isotopically the stable isotope results of three different appinite intrusions (Narin-

Portnoo, Meenalargan and Kilrean) indicate a mantle-type signature typical of mantle-derived basaltic magmas (see Chapter 6.3.3 i and iii). The high volatile content of the magmas (CO₂ & H₂O) may be attributed to the melting of a primitive hydrous mantle, and the magmatic origin of these volatiles is supported by the stable isotope data of this study. The range in Ni (5 - 294 ppm) and Cr (18 - 642 ppm) values in the appinites can be accounted for by cumulates and fractional crystallisation involving hornblende, pyroxene and olivine from basaltic-parental magmas. The source of the appinite magma may therefore be of a amphibole-peridotite (eclogite/lherzolite may be potential sources) composition.

Basaltic/andesitic magmas may be found in the Lorne lavas of the SW Highlands of Scotland, which are Old Red Sandstone in age (Thirlwall, 1982) and have high incompatible element contents and low Fe/Mg ratios (Table 7.1), and might represent parental magmas for the appinite suite. It is noteworthy that the Lorne lavas are regionally associated with the appinites of Appin, but there is no evidence of the development of appinitic compositions within the Lorne lava pile.

Element	L56	L23	Balla Ap (3)	Isl Arc Thol	Isl Arc Bas	Y1856	Y1999
SiO ₂	52.53	48.90	48.31	50.49	49.40	50.94	50.42
Al ₂ O ₃	16.19	17.47	12.71	19.44	13.29	13.36	14.70
Fe ₂ O ₃	7.91	9.87	9.23	9.83	10.15	7.89	9.82
MgO	7.60	7.19	11.60	4.26	10.44	10.26	8.55
CaO	7.44	10.57	8.40	11.66	12.22	10.20	8.17
Na ₂ O	3.54	2.70	2.44	2.53	2.16	2.34	3.42
K ₂ O	2.69	1.10	2.13	0.14	1.06	1.28	2.08
TiO ₂	1.17	1.54	0.97	0.70	0.70	1.00	1.32
MnO	0.13	0.14	0.13	0.17	0.20	0.15	0.15
P ₂ O ₅	0.55	0.40	0.25	0.11	0.20	0.16	0.32
Total	99.75	99.88	100.15	99.33	99.82	99.57	100.23
Nb	10	5.4	8	n.d.	14	4	10
Zr	192	160	87	21	43	58	104
Y	17	26.5	16	14	17	19	19
Sr	n.d.	n.d.	833	121	601	686	753
Rb	n.d.	n.d.	44	2	17	42	60
Th	3	n.d.	5	n.d.	1.16	0	6
Pb	7	4	15	n.d.	n.d.	9	18
Zn	82	70	93	n.d.	n.d.	64	103
Cu	38	46	107	n.d.	n.d.	44	122
Ni	216	92	160	5	150	155	118
Cr	413	149	453	55	490	211	408
V	160	205	223	n.d.	350	201	306
Ba	1259	695	899	36	310	321	631
Hf	n.d.	n.d.	n.d.	n.d.	1.37	2	3
Ce	87	57	37	n.d.	24	25	90
La	40	38	43	n.d.	10	12	n.d.

Table 7.1 Typical compositions of Lorne lavas (L56 and L23 after Thirlwall 1982) compared with appinite from Ballachulish (Balla Ap. (3) after Wright & Bowes 1979), typical island arc tholeiite (Isl Arc Thol after Luff, 1982), island arc basalt (Isl Arc Bas after Perfit et al. 1980) and diorites from the Ardara area (Y1856 and Y1999).

(ii) Lamprophyre

The close spatial association of appinites and lamprophyres may be important when considering the parental magma of appinites. The fact that the lamprophyres, like appinites, apparently evolve into intermediate and felsic compositions implies that they may represent the parental melts of high-K calc-alkaline-(peridotite-pyroxenite)-diorite-granodiorite-granite plutons (Rock 1991). Rock cited as evidence for this genetic relationship (a) the identical initial Sr isotopic ratios of lamprophyres and granitoids, (b) the close correspondence of lamprophyres with parental melts inferred by some granite specialists for the plutons and (c) the similarity in chemical composition between dyke porphyries, which may be the products of lamprophyre differentiation and plutonic granitoids.

Rock (1991) outlined the indications of the primary nature of lamprophyre magma as: high Mg# (65.8%), Sc (15 ppm), Cr (200-500 ppm), Co (25-80 ppm) and Ni (90-700 ppm) and represent 1-20% primary melts of a mantle lherzolite source. Similar levels of Mg#, Cr and Ni are seen in typical appinite compositions from the Ardara igneous complex (Sc has not been determined) (Table 7.2). Rock (1991) also noted the high LIL and HFS abundances in lamprophyres and noted that such enrichments present problems in that they cannot be generated from mantle materials using known partition coefficients and melting models; he offers three possible explanations. Firstly, extreme fractionation of a garnet-bearing assemblage, such as eclogite, which can account for steep REE profiles (but leads to melt extraction problems due to the extremely low degrees (<1%) of melting implied. Secondly, disequilibrium melting involving a phase rich in REE, and thirdly a metasomatised mantle source previously enriched in LILE and HFSE.

Any attempted petrogenetic model for the petrogenesis of (CAL) magmas must take into account the wide range of composition, association and setting of lamprophyres (Rock 1991). Rock (1984) argued on the basis of the comparative distributions, xenolith contents and petrography that calc alkaline lamprophyres are genetically connected with post-orogenic granites and their origin involves lower crustal processes and materials like the granites themselves. Rock (1984) proposed that these lamprophyres are the products of crustal modification of a basaltic magma but found difficulty in explaining the high F, Ba, Th, P and LREE abundances in lamprophyres. He suggested that the lamprophyres may be the product of crustal modification of a K-rich lamproite or leucititic magma (assumed to be primary). Rock (1984) described the wide variations in $^{87}\text{Sr}/^{86}\text{Sr}$ (seen in samples from America, Australia and the Massif Central of France) and varying degrees of crustal modification of the parental magmas and concluded that calc alkaline lamprophyres are normal expression of deep-seated K-rich magmatism in mobile areas.

Bulk chemistry indicates that the magma from which the appinitic rocks of the Ardara igneous complex crystallised was of a calc-alkaline to high-K calc-alkaline character. Such magmas are typical of modern-day calc-alkaline volcanic suites associated

with a subduction tectonic setting. The melt from which the appinitic magmas crystallised from had high levels of Mg, Ni and Cr and was slightly depleted in Ce and Zr relative to CAL (section 5.2 iv)). The appinites have similar contents of K, Ti and Y and are enriched in LIL elements as is CAL. If as is often quoted, the appinites are the plutonic equivalent of lamprophyres (Rock 1991), then the appinites should have mantle-type isotopic signatures. This is the case for Ardara where $\delta^{18}\text{O}$ ranges from +6.46 to +9.17‰, the lower values being typically mantle in origin. No Sr, Nd or Pb ratios are available for the appinites.

In summary, the close relationships between appinites and lamprophyres seen in the field, the similarity of bulk chemistry (including the volatile-rich character of appinites and lamprophyres) are all strong evidence for a link between the two rock types. Rock's model of lamprophyre petrogenesis involving crustal contamination of a basaltic (mantle-derived) magma might be applicable to the appinite suite.

Element	Average CAL	Average Ap	Y1856	Y1999	Balla Lamp (6)
SiO ₂	51.00	48.30	50.94	50.42	49.00
Al ₂ O ₃	14.00	13.80	13.36	14.70	13.82
Fe ₂ O ₃	8.20	9.20	7.89	9.82	8.39
MgO	7.00	8.00	10.26	8.55	8.62
CaO	7.00	9.80	10.20	8.17	7.73
Na ₂ O	2.70	2.80	2.34	3.42	2.79
K ₂ O	3.10	1.80	1.28	2.08	2.14
H ₂ O	2.40	2.20	1.00	n.d.	3.11
TiO ₂	1.10	1.10	1.00	1.32	0.76
P ₂ O ₅	0.60	0.45	0.15	0.15	0.28
MnO	0.13	0.16	0.16	0.32	0.13
CO ₂	2.00	2.40	n.d.	n.d.	3.29
S	0.12	0.12	n.d.	n.d.	0.19
Total	99.40	100.10	100.57	100.23	100.07
Nb	13	2	4	10	5
Zr	190	10	58	104	102
Y	23	20	19	19	15
Sr	715	730	686	753	942
Rb	70	45	42	60	57
Th	9	7	0	6	6
Pb	13	10	9	18	24
Zn	88	90	64	103	89
Cu	43	54	44	122	121
Ni	150	85	155	118	126
Cr	370	290	211	408	316
V	170	250	201	306	222
Ba	1050	640	321	631	825
Hf	5.2	2.1	2	3	n.d.
Ce	110	83	25	90	48
La	53	42	12	n.d.	34

Table 7.2. The compositions of average calc alkaline lamprophyre (CAL, after Rock 1991) and average appinite (Average AP, after Rock 1991) compared with two typical diorites from the Ardara igneous complex and average lamprophyre from Ballachulish (Balla Lamp, after Wright & Bowes 1979).

7.2.2 Source of volatiles

Volatile-rich magmas (other than appinites) include, carbonatites, kimberlites, many alkaline types (including syenite) and lamprophyres. The source of the volatiles such as

CO₂ in carbonatites and kimberlites is identified as primary based on the evidence of high temperature calcite with magmatic-type isotopic signature. The source of the volatiles in other volatile-rich magmas is attributed to input from other coeval magmas by a process of hybridisation (Rock 1979) or autoenrichment in volatiles through crystallisation in basaltic magma, may lead to the formation of a volatile rich lamprophyre (Ohashi 1980). Volatiles may also be generated from breakdown of hydrous phases at source, magma differentiation and contamination. The stable isotope signature of the Ardara appinites supports a primary mantle origin of the volatile phase of these appinites.

The enrichment of H₂O, CO₂ and sulphur in the appinite magmas is evidenced by their mineralogy and their explosive emplacement mechanisms in the form of pipes. Such volatile rich magmas offer the opportunity to determine the extent of the aureole of exchange. By analysis of the country rocks in the contact aureole, as in the case of Narin-Portnoo, it is possible to determine that a magmatic volatile circulatory system existed at the margin of the appinite of similar dimensions (~ 40 m) to the appinitic intrusion.

7.2.3 Magma mingling and mixing

Field evidence indicates that magma mingling and mixing may also be an important aspect of differentiation of the appinite suite, in particular at Meenalargan and Narin-Portnoo. There is evidence for magma mingling of biotite diorite and granodiorite at Burnfoot (the western end of the Narin-Portnoo intrusion). The biotite diorite, which is often meladioritic, has mingled with granodiorite and in places it becomes difficult to distinguish the rock types, suggesting mingling is approaching complete mixing. The apparently coeval nature of granitoid and dioritic rocks in the form of granodiorite with mingled textures are evidence of these intimate mixing and mingling processes.

7.2.4 Crustal contamination

Evidence for contamination of appinitic magma comes from field, petrological and textural characteristics of the appinite suite. At Meenalargan partially resorbed pelitic schlieren in the diorite and relict bedding are visible within calc-silicate horizons to the north and south west of Crocknadreeavarh which indicate significant contamination and at least partial assimilation of the Mulnamin Calc Silicate Flags by the appinitic magma. At Narin-Portnoo, where appinites are intruded into calcareous country rocks, evidence for the incorporation of xenoliths of Portnoo limestone is abundant. It is clear however from the evidence of stable isotopes that the oxygen is largely mantle-derived, and as oxygen is typically more than half the mass of the rock it is unlikely that the magmas have suffered very substantial crustal contamination as this would show up in the stable isotope signature. The effects of assimilation described here are thus very local in extent. Fluid from the appinite is expelled into the country rock and has the effect of changing the isotopic signature of the country rock towards a magmatic level but not vice versa to any

extent. Evidence from a δD isotopic study of an appinite/limestone contact also indicates the presence of a high level meteoric fluid circulation system possibly related to a regional fluid circulation system associated with the large granite body of the Ardara pluton.

Pitcher & Berger (1972), in considering the origin of breccia pipes, noted different compositional characteristics of the enclosing magma related to the composition of the incorporated xenolith suite. At Kilkenny, Pitcher & Read (1952) described the occurrence of quartzite and calc silicate xenoliths in granophyric and appinitic matrices respectively. The calc silicate xenoliths resemble the local country rock and are not thought to have been removed far from the present level of exposure, whilst the quartzite xenoliths are thought to have originated from a quartzite horizon 300m to ~1000m below the present level of exposure. The quartzite fragments are highly rounded due to attrition during transport in the igneous medium which is granophyric, becoming more siliceous apparently due to contamination by the quartzite xenoliths. The calc silicate xenoliths are exclusively found within an appinitic matrix suggesting that they also may have reacted with the magmatic host. Similar contamination by calcareous country rocks is apparent from the Biroke breccia pipe where calc silicate 'pebbles' (inclusions) now have an actinolite, hornblende, clinozoisite assemblage in place of the original clinozoisite, feldspar, calcite, quartz mineralogy due to recrystallisation in the presence of an appinitic host.

The effect of country rock contamination on the geochemistry of the appinites is difficult to quantitatively determine, isotopically it is apparent in the pipe studied in detail that there is only minor alteration of the isotopic signature of the appinite. The magmatic fluids of the intrusion appear to be expelled into the intrusion so lowering the country rock isotopic signature to a more magmatic value. In conclusion, while there is abundant evidence for local-scale contamination of appinite magmas with solid fragments of country rock evidence for large scale modification of the appinites by contamination is lacking.

7.2.5 *In-situ* differentiation

Zonation of the appinitic intrusions is apparent in almost all the appinitic intrusions examined in the Ardara area, but the degree and regularity of this zoning is, however highly variable. Commonly this zonation takes the form of an irregular compositional variation between hornblendite, enriched in Mg, K, Ca, total Fe, Ni and Cr, and the more evolved diorites and coarse diorite, as in the case of the Meenalargan intrusion. The crude zonation seen in the Meenalargan intrusion (Map 3 in Appendix 6) which has a coarse diorite core and dioritic rim with sporadic occurrences of hornblendite, is difficult to account for by *in-situ* processes although the transitional and diffuse contact between the two suggests the possibility of magma mingling. Geochemically the coarse diorite and diorite show little difference although the inner coarse diorite is slightly more primitive (higher Mg, Ni, lower Rb/Sr) than the outer diorite. This reverse zonation may be the result of crystallisation of

the magma in a roof zone with marginal mingling with hybridisation and envelopment by a slightly more evolved magma.

In the Narin-Portnoo intrusion zonation exists between the hornblendites, diorites and biotite diorites (enriched in K, Rb/Sr compared with the diorites and hornblendites), however in this intrusion such zonation is poorly defined as transitions between the rock units are highly variable (including sharp, diffuse, gradational and sinuous contacts which may be the result of both in-situ differentiation and the intrusion of a number of separate pulses.

The Mulnamin intrusion, like the Narin-Portnoo mass exhibits a wide range of compositional variation from hornblende diorite through biotite diorite and dioritic hornblendite to dioritic appinite and quartz appinite. French (1966) envisaged a process of *in-situ* differentiation to explain this trend, however Pitcher & Berger (1972) suggested that because the internal contacts were both gradational and sharp they may be represent different pulses possibly related to a single magma at depth. Only the granitic dykes and sheets are radically different in composition, like those of the Narin-Portnoo intrusion. Pitcher & Berger (1972) believed that their highly contaminated character indicated that they were emplaced prior to the end of crystallisation of the dioritic and hornblendic magmas. The Summy Lough Diorite also displays internal zonation between hornblendite and the diorite of the main intrusion.

The most regularly zoned intrusion of the Ardara igneous complex is the Kilrean body. This has a cortlanditic core immediately surrounded by a hornblendite rim with a strong steep foliation parallel to the margins of the intrusion, passing gradationally into appinitic hornblendite and appinite. The cortlandite is enriched in MgO (20.0 wt%), Ni and Cr, depleted in Al₂O₃ (5.0 wt%) and has a CaO content of 10.0 wt% and probably represents a cumulate. The hornblendite of the same intrusion has a lower MgO (10.0 wt%) and high Al₂O₃ (14 wt%) with 9.0 wt% CaO which suggests that the zonation may be the result of hornblende fractionation from a pyroxene olivine hornblende gabbro magma. The zoning has the most mafic cumulate in the core and is difficult to account for by in-situ processes.

The granodiorites and granites of the main Ardara pluton are also zoned and may form two separate pulses, that which formed the magma of G1 and G2 and the more evolved central unit of G3. The granites from the Narin-Portnoo appinite intrusion are the most evolved of all the granites in the Ardara igneous complex. The granites of the Glenard, Meenalargan, Mulnamin and Crockard intrusions most closely resemble the compositions of the G1 and G2 units of the Ardara pluton and it is likely that they were derived from the same magma chamber.

Despite the petrological diversity in the appinites and the apparent zonation in some bodies there is little consuming evidence that these features are due to in-situ processes,

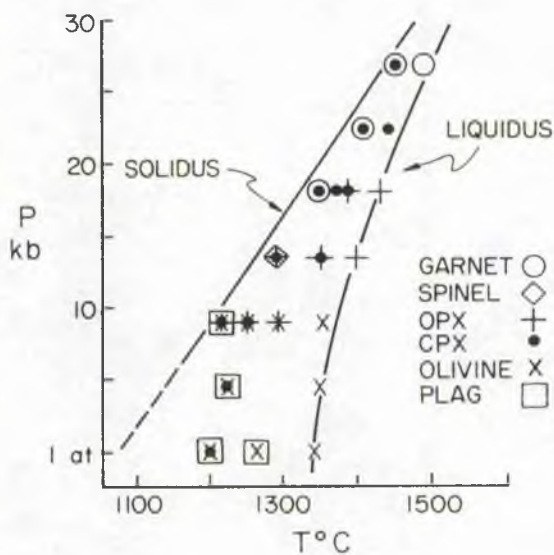
except perhaps where local fluid concentrations promote crystal growth producing new textures and possibly contributing to differentiation.

7.2.6 Petrogenetic model

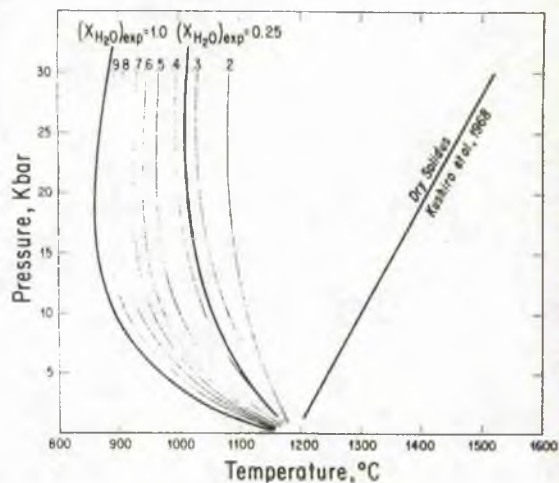
Bulk chemistry of the appinites indicates that they are calc alkaline to high-K calc alkaline rocks which are enriched in Mg, Ti, Ni and Cr, they also show enrichment in LIL elements and to a certain degree HFS elements. The range in Ni and Cr values can be accounted for by cumulates and fractional crystallisation involving hornblende, pyroxene and olivine from basaltic-type magma. However, the close genetic association of appinites to lamprophyres, in the field, petrographically and in terms of trace element geochemistry with references to the compilations of Rock (1991) suggests that they may be related to a lamprophyre-type magma which Rock (1991) regards as crustal modified primary lamproite/leucitic magma. The source of the appinite is clearly in the mantle. The high volatile content of the appinitic magmas may be attributed to the melting of a primitive hydrous mantle, possibly of amphibole-peridotite composition.

The confirmation of the magmatic nature of the volatiles is provided by the evidence of stable isotopes. From $\delta^{18}\text{O}$ values of +6.46 to +9.17‰, $\delta^{13}\text{C}$ values of -6.27 to -2.19‰ and δD values ranging from -66 to -59‰ support the contention that the magmas of the appinite suite have mantle sources. Other isotopic data for the appinites in the Caledonides do not exist. It is also apparent from the evidence of stable isotopes that certain values of $\delta^{18}\text{O}$ (+9.17‰), $\delta^{13}\text{C}$ (-2.19‰) indicate a degree of crustal contamination, probably at a high level.

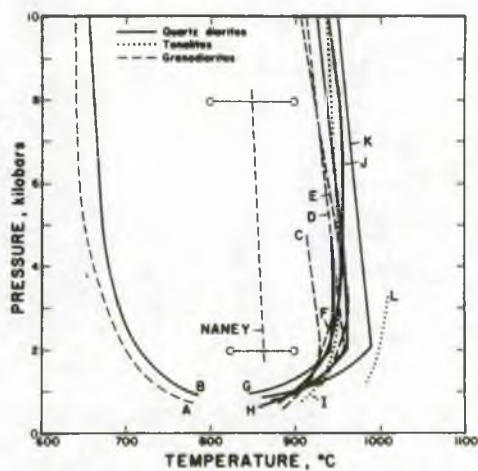
In considering the emplacement of the magma which formed the appinites, results of hornblende-plagioclase geobarometry and geothermometry indicate that most appinites crystallised in the range of 500-800°C at a pressure of ~5 kb. Pyroxene geothermometry of the most primitive rock of the appinite suite, the Kilrean cortlandtite, indicates that it crystallised at 976°C at ~5 kb. Such P-T estimates are in agreement with experimental results of the melting of wet basalt systems of, for example Yoder & Tilley (1962), indicating a wide stability field of hornblende at increased water vapour pressure. The characteristics of basaltic phase relations in the presence of H_2O are, as mentioned above, a wide stability field over a limited pressure range (Helz 1986) and depression of both solidus and liquidus temperatures relative to dry systems (Ragland 1989). Another important effect of H_2O concerns the shape of the liquidus and solidus, Ragland (1989) noted that in dry systems such as olivine tholeiite and peridotite, liquidus and solidus temperatures increase as confining pressure (P_T) increases (Fig. 7.1 a). By contrast in a water-saturated system where $P_{\text{H}_2\text{O}} = P_T$ liquidus and solidus temperatures are generally concave-up and decrease with increasing fluid pressure until high H_2O pressures are reached (Fig. 7.1 b). This has important implications for the depth and temperature of a crystallising appinitic magma, for instance experimental data compiled by Helz (1986) for



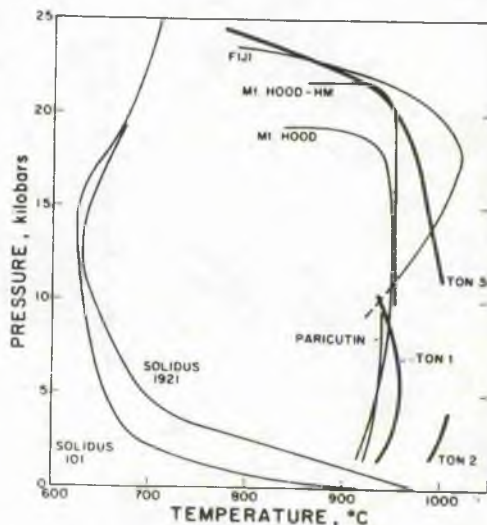
(a)



(b)



(c)



(d)

Fig. 7.1. P - T plots showing the experimental determinations of the effect of melting under water saturated and dry conditions. (a) Results of melting experiments on olivine tholeiite (Ragland 1979). (b) Peridotite solidi with theoretical X_{H_2O} (Mysen & Boettcher 1975). (c) Amphibole-in and selected solidus curves for intermediate granitoid rocks, at $P_{H_2O} = P_{Total}$ (Helz 1986). (d) Amphibole-in curves for andesites and tonalite at $P_{H_2O} = P_{Total}$ (Helz 1986).

water saturated andesites, quartz diorite, diorites and tonalites it is clear that at the temperatures and pressures estimated for the appinites of the Ardara complex the magma will not have crossed the solidus and may not do so until $\sim 650^{\circ}\text{C}$ at 5 kb or $\sim 800^{\circ}\text{C}$ at 1kb (Fig. 7.1 c & d).

In summary then, a petrogenetic model for the appinites must take into account the high compatible trace element abundances, low $\delta^{18}\text{O}$ and a generally basaltic-andesitic bulk composition, all of which suggest a source in typically upper mantle rocks. Hydrous magma compositions and trace element abundances suggest that amphibole breakdown in the source was possibly important, thus the source was probably an amphibole-bearing peridotite yielding a hydrous basaltic magma which evolved through appinites and diorites. The hydrous compositions seem to favour low temperature crystallisation and estimated conditions of crystallisation range from 980°C to 650°C at $\sim 5\text{kb}$. Emplacement conditions are not clear, geobarometry favours $\sim 5\text{ kb}$ while field evidence suggests much shallower emplacement. Fig. 7.2 is a cartoon illustrating the development of appinite from its origin as a mantle-derived hydrous melt, ascent through the lower crust to emplacement controlled by tectonic fractures.

The petrogenetic model of Hammidullah & Bowes (1987) stressed crystal differentiation of a calc alkaline to high-K calc alkaline magma of variable type under variable gas pressure with successive fractionation of the major mineral phases leading to the progressive development of the rocks of the appinite suite. Such a model is broadly in line with the evidence outlined in this study although this study has demonstrated the volatiles to be truly magmatic and that there is some local crustal contamination. The presence of some magmatic hybridisation, particularly amongst the more acidic magmas lends support to the Pitcher & Berger model (1972).

7.3 TECTONIC CONTROLS ON EMPLACEMENT

7.3.1 Structural controls

The appinites of the Ardara igneous complex display a wide range of form and emplacement style, from deep level stock (e.g. Meenalargan) to high level explosive breccia (e.g. Kilkenny). All the intrusions are closely related to the structures of the surrounding country rocks and thus to the regional Caledonian tectonic regime. The regional geology of the Ardara area is dominated by east-west striking upright (F4) folds and steeply dipping transcurrent shear zones. Similarly Bowes & Wright (1967) noted that the shape and distribution of appinitic breccia pipes and breccia pipes from Kentallen, Argyll were strongly controlled by a steeply-dipping regional cleavage and fold phase associated with the Cuil Bay synform. The pipes are steep-sided and emplaced parallel to the regional cleavage and upright fold hinges. Bowes & Wright (1967) also noted how competent and unfoliated quartzite horizons control the occurrences of breccia pipes which they postulated was due to the trapping of gas preventing further ascent.

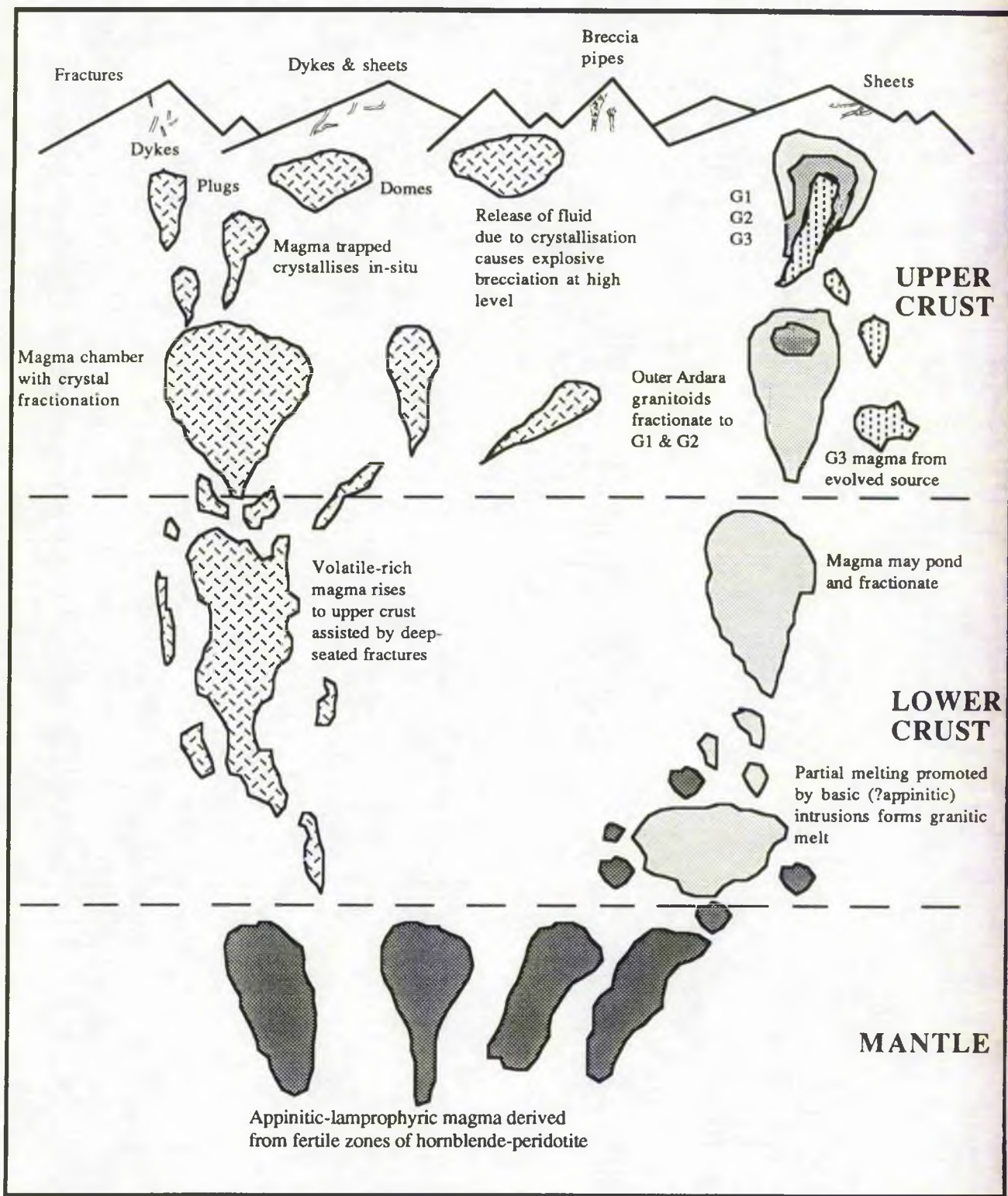


Fig. 7.2 Cartoon illustrating the development of appinite from its origin as a mantle-derived hydrous melt, and ascent through the lower crust to emplacement controlled by tectonic fractures. Also shown is the generation of the granitic units of the main Ardara pluton.

The diapiric Ardara pluton exerts an important control on the structure of the Ardara area. It is responsible for the development of an upright cleavage, steepening-up of bedding and local areas of intense shear band development. The Summy Lough diorite on the western flank of the Ardara pluton shows evidence of intrusion coeval with the granite pluton. It has an outcrop pattern which suggests that the diapirism associated with the Ardara pluton may have assisted diorite intrusion by opening up a gap for the diorite by a process of compression perpendicular to the margin and extension parallel to the margin of the granite intrusion.

7.3.2 Emplacement mechanisms

A wide range of emplacement mechanisms are apparent for the Ardara appinites including (a) plutonic intrusions such as the concentrically zoned Kilrean intrusion, (b) the elongate sheet-like pluton of Meenalargan emplaced by a process of stoping, (c) the elongate pluton of Mulnamin intruded by a process of internal dilation similar in form to the diapiric Ardara pluton, and (d) the dome-like body of Summy Lough on the western flank of the Ardara pluton, again emplaced parallel to the strike of bedding. The Narin-Portnoo intrusion exhibits a range of intrusion mechanisms including, dykes, sills, sheets, stocks and plugs which utilise bedding and local fractures and may represent the sub-volcanic expression of appinitic activity. The most dramatic mechanism of emplacement of the appinite suite is in the form of explosive breccia pipes and intrusion breccias (Kilkenny, Bioge, Dunmore) which commonly consist of a chaotic array of rounded to angular country rock and igneous fragments in an igneous matrix of both mafic and felsic type. These may be the near surface expression of appinitic activity and indicate the high volatile content of the magma, similar in form to diatremes.

7.3.3 Regional tectonic controls

Hutton (1987) noted that many of the major strike-slip faults (e.g. the Great Glen Fault) in the British and Irish Caledonides were active as sinistral strike-slip zones, related to movements of terranes lying between the Laurentian and Gondwanaland miogeoclines. From this interpretation certain strike-slip faults of Caledonian age in Donegal may be splays of larger faults such as the Great Glen fault, which passes to the north of Donegal. A good example of how a plutonic mass may be intruded in association with a major shear zone is present to the east and north east of the Ardara igneous complex. The Main Donegal Granite (MDG) shear zone is one of the best examples of a dated transcurrent shear zone in the British Isles, lying in a major bifurcation of the Great Glen fault. Halliday et al. (1980) obtained a minimum age of 388 ± 3 Ma by whole-rock Rb-Sr for the Main Donegal Granite. It is associated with an 80-km-long sinistral shear zone (Hutton 1982) which also transects part of the Meenalargan and Ardara plutonic complexes in its south eastern region. Further work by White & Hutton (1985) identified the northerly continuation of this shear

zone in north east Donegal, at Fanad and beyond where it is thought to terminate in a large scale compressional tip structure (Hutton 1987).

Other large faults associated with dioritic complexes in the Caledonides of the British Isles include the Garabal and the closely related Tyndrum transcurrent faults which are associated with the Garabal Hill dioritic complex, dated at 429 ± 2 Ma (Rogers & Dunning 1990). The Ratagain dioritic and monzonitic intrusion has a crystallisation age of 425 Ma (Rogers & Dunning 1990) and is associated with the sinistral transcurrent Strathconnan fault. Hutton & McErlean (1991) noted that the Ratagain intrusion was deformed by sinistral shear associated with the Strathconnan fault during the crystallisation interval of the main magmatic phases (425 Ma) and that the Ratagain intrusion was later deformed by a more minor phase of sinistral deformation at 410 - 395 Ma by Rb/Sr dating of the offset of a swarm of Caledonian lamprophyre minettes.

Appinitic and dioritic intrusions associated with the Strontian granodiorite are also related to a major sinistral transcurrent fault, the Great Glen fault, as are the appinites of the Ardsheal peninsula and Kentallen, whilst the small dioritic complex at Glen Tilt is deformed by the transcurrent Loch Tay fault.

The Leinster granitic and appinitic complex comprises 44 appinitic and lamprophyric intrusions of the Mount Leinster swarm and the Blackstairs granite pluton. These are intimately associated with a major dip-slip ductile shear zone with a NE-SW strike parallel to the pluton (McArdle & O'Connor 1987). The intrusions follow the trend of the shear zone and are also emplaced within early (F1) fold phases. O'Connor (1974) and McArdle & O'Connor (1987) suggested that the scarcity of explosive breccias amongst the appinites of the Mount Leinster swarm may be due to ease of movement of the magma within the F1 fold phase so not allowing any build up of volatiles, however this too may depend on the P-T environment of the appinite magma, its volatile content and the nature of the country rocks.

P-T results in chapter 4.11.3 indicate a relatively high pressure of crystallisation of some of the appinites from about 4 - 8 kb. Emplacement of magmas from such pressures requires a route to the level of emplacement. This may be provided by large-scale transcurrent faults (Fig. 7.3.) which descend as deep as the upper mantle and which were active during the crystallisation period of the appinitic and granitic magmas 429 - 400 Ma (Hutton, 1988; Hutton & McErlean, 1991). Reconciliation of the high appinite pressures of crystallisation and the high levels of emplacement might be possible if the magmas were emplaced as crystal mushes which had formed at deep levels subsequently to be emplaced at higher levels along structures. However the geobarometry techniques of Zen & Hammarstrom and Hollister et al. are meant to record the emplacement pressure as it measures the last crystallising amphiboles, not their cores.

Alkaline Syenites of the
NW Highlands



Fig. 7.3 Map showing the location of the major transcurrent faults in the Caledonides of the British Isles, after Hutton (1987) and the location of intrusive granitoid and appinite complexes and major faults in N. Britain and Ireland. Key of intrusion names is as for Fig. 2.3. Faults additional to those of Fig. 2.3 are included in order to highlight their close relationship to the granitoid-appinite complexes. EL = Erich-Laidon Fault, LT = Loch Tay Fault, SB = Sgurr Beag Slide, G = Garabal Hill Fault, K = Killin Fault, S = Strathconnan Fault.

7.4 ARDARA APPINITES: SOME IMPLICATIONS

7.4.1 Appinite nomenclature

The classification scheme of the appinites is sometimes confusing, as discussed in section 2.4.3. The term "appinite" describes a rock with a distinctive texture and form, principally acicular hornblende in a plagioclase matrix. The term appinite has been used in this thesis to describe a rock which occurs in the appinite suite, is very rich in hornblende (often stumpy or acicular), is related to a granitic intrusion both temporally and spatially, and with a high volatile content. The appinite suite refers to any rock type with these "appinite" associations including the rock types around the Ardara igneous complex.

The first person to classify the rocks of the appinite suite of Donegal was French (1966), who proposed the following classification scheme (Fig. 7.4).

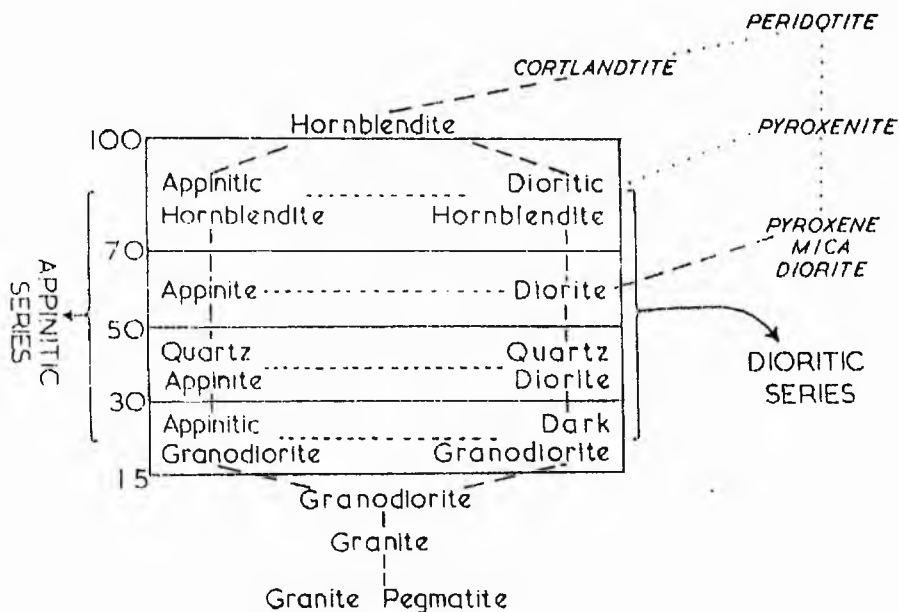


Fig. 7.4 The classification scheme of French (1966) for the appinitic and dioritic rocks of Co. Donegal and their associated rocks.

French (1966) divided the rock types according to colour index which defined a dioritic series and an appinitic series. Only the dioritic series of French's classification is consistent with the IUGS classification scheme of Streckeisen (1970). Using the modal

percentages of the major rock-forming minerals present in the rock the following subset of the Streckeisen nomenclature is appropriate to the appinite suite (Fig. 7.5).

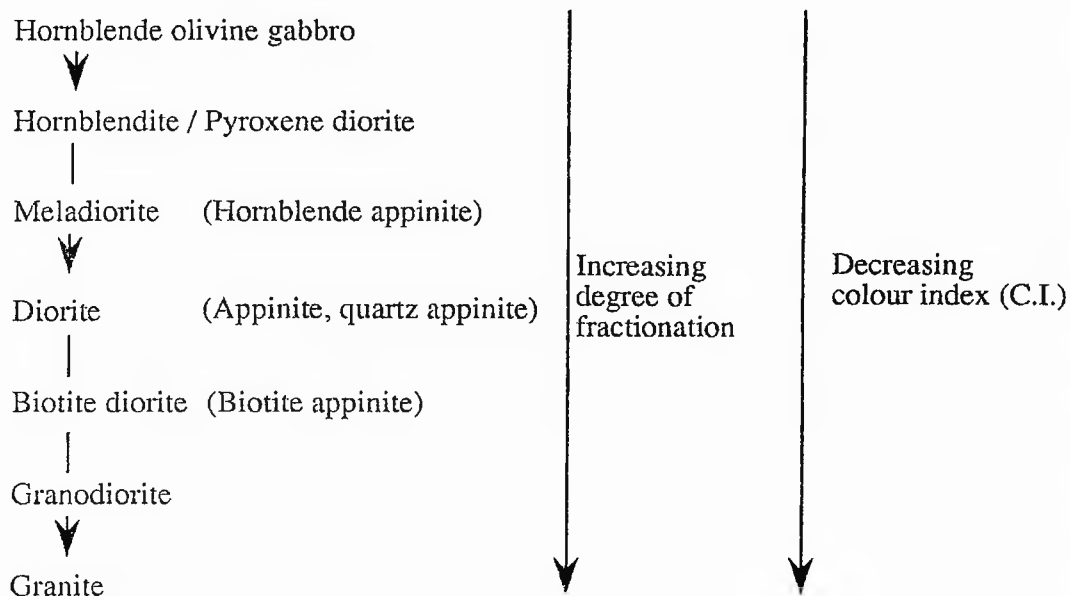


Fig. 7.5 Classification scheme for the rocks of the Ardara igneous complex using the classification method of Streckeisen (1970), names not available in the IUGS scheme but widely used, especially in the field, are given in parentheses.

This IUGS classification does not recognise the term appinite and the term appinite has textural connotations and so only the equivalent rock type within the Streckeisen scheme should be used by prefixing it with hornblende, biotite, quartz, etc. The geological literature on the occurrence of appinites is handicapped by the nomenclature of these rocks. This problem also applies to the term 'lamprophyre' which is intimately related to the appinitic and granitic rocks of the Caledonides. Like "appinite" the term "lamprophyre" is ambiguous and complex as the number of compositional varieties and nomenclature is so

great. There is a need for an agreed, workable classification of the appinites analogous to that for lamprophyres, as proposed by Rock (1991).

7.4.2 Fluid circulation systems

Stable isotope observations at a limestone-appinite contact indicate the presence of a fluid infiltration system. This magmatic fluid system had the effect of lowering the $\delta^{18}\text{O}$ and $\delta^{13}\text{C}$ signatures of the limestone up to 40 m away from the appinite contact. There is mineralogical growth of hornblende and epidote within the limestone in a narrow zone at the margin of the appinite contact. The presence of a meteoric circulatory system is proven by the existence of meteoric δD values measured from the same set of samples used in the limestone-appinite traverse. Such fluid circulation systems may exist at the margins of many, if not all, hydrous magmatic intrusions which intrude fractured country rock, including other appinites in the Ardara area and within the Caledonides as a whole and even the main granitic intrusions.

This particular example of limestone-appinite fluid circulation was amenable to study because the stable isotopic constraints were sufficiently large as to be detectable. The scale of the circulation system in the aureole (~40 m) is on a scale similar to the appinite body giving rise to the system. Whether this is due to the nature of the host limestone or whether this is typical is not known, but if it is the general case then we might expect fluid circulation in high level aureoles to be a very important feature, especially adjacent to larger igneous bodies.

7.4.3 Composition-emplacement mechanism relationships

High level breccia pipes indicating explosive emplacement mechanisms have a dominantly felsic to dioritic composition with only minor associated mafic rocks. More passively emplaced plutonic intrusions such as Kilrean, Meenalargan, Mulnamin and Summy Lough have ranges of composition which include an ultramafic component usually in the form of hornblendite or meladiorite and hornblende pyroxene olivine gabbro, with only minor granitoids. There seem to be no significant differences between the appinites showing a plutonic style of emplacement compared with those with sub-volcanic dyke, sill and sheet-type emplacement mechanisms as exhibited by the rocks of the Narin-Portnoo intrusion.

7.5 PETROGENESIS OF THE MAIN PLUTON

7.5.1 Parental magmas of G1 and G2

The parental magma to the main pluton may only be accurately defined with the help of radiogenic isotopes. Rb/Sr and Sm/Nd data on the Ardara pluton and other Donegal granites have been described in Halliday et al., (1980), O'Connor et al., (1982, 1987) and Dempsey et al. (1990). Geochronological data indicate that the granites were all emplaced

within a narrow range at around 400 Ma into a thick sequence of Dalradian metasediments, highly deformed by greenschist-amphibolite facies metamorphism. Concerning the source of the magma, initial Sr ratios indicate that the granites of the Donegal batholith all have a relatively narrow Sr_i range from 0.7050 to 0.7068 (O'Connor et al., 1987, Dempsey et al. 1990), however Dempsey et al. using ϵ_{Nd} pointed out that there is considerable spread in ϵ_{Ndi} (-1.2 for unit G2a of the Ardara pluton to -8.3 in the Main Donegal Granite), which they could not link to any systematic variation in emplacement style or age. The ϵ_{Ndi} value of -1.2 obtained by Dempsey et al. (1990) from the inner unit (G2a of Akaad 1956) of Ardara is consistent with a mafic source such as a slightly contaminated mantle-derived magma or young basic lower crust. Such a primitive source for the G1 & G2 units of the Ardara pluton is supported by the intimate association between the magmas of the Ardara pluton and the mantle-derived magmas of the surrounding appinite intrusions. Such evidence for a mantle-type source for the Ardara pluton must be balanced by the observation of inherited zircon in the Ardara G2a granodiorite by Halliday et al. (1980) which indicates a significant crustal component in this pluton. It thus seems likely that the granitoids of the outer Ardara pluton were derived from a young mafic lower crustal material.

7.5.2 Parental magma of G3 (central granodiorite)

G3 is more evolved than G1 and G2 and is depleted in many major elements, notably Fe_{tot} , Mg and Ca. Trace element compositions indicate that it is also depleted in Rb, Nb, Zr, Y, P_2O_5 and MnO compared with G1 & G2. As discussed in Chapter 5 there are distinct differences in composition between G1 & G2 on the one hand and G3 on the other which make it impossible to model derivation of G3 from G1 & G2 by simple crystal-liquid processes. Thus it seems likely that G3 represents a separate, discrete pulse of more felsic magma quite probably from a different and more evolved source than G1 & G2. The lack of any isotopic data for this unit make it difficult to be confident about its source, but again it is likely to be of crustal origin.

7.5.3 Characterisation of the granite of the main Ardara pluton

The granites of the Ardara pluton have been characterised as calc alkaline to high-K calc alkaline composition of I-type affinity with similarities to syn- and post-collision-type granites. They possess many major and trace element values similar to those of the Scottish Caledonides (Halliday & Stephens 1984). Elsewhere in Donegal the Ardara pluton is similar to the Fanad pluton in terms of having a low initial Sr isotope ratio and may have an origin similar to that of the Fanad pluton involving fractionation at depth of a dioritic magma with a high Sr content (O'Connor et al. 1987). Other I-type granites in Donegal are the Barnesmore and Main Donegal granites while parts of the Rosses, Trawenagh Bay and Thorr granites exhibit some mild S-type or transitional I-S-type characteristics. Elsewhere

in Ireland the Ardara pluton bears geochemical similarities to the Newry granodiorite, and on a larger scale the granites of Ireland as a whole show uniformity in age (405 ± 15 Ma), however south of the Iapetus suture line late magmatism has significantly high initial Sr isotope ratios, suggesting derivation from a different crustal source (Stephens 1988).

7.5.4 Differentiation of the complex

The complex is differentiated into G1, G2 and G3. The G1-G2 differentiation is real in terms of several major and trace element characteristics and the question is whether this was due to open or closed system processes. Attempts to model the variation by major and trace element techniques were reasonably successful and it is likely that the bulk of the compositional variation can be attributed to fractional removal of hornblende-plagioclase dominated assemblages. This probably occurred in situ mainly from the margins inwards, and G2 magma probably "surged" upwards into its carapace of G1 due to its slightly greater buoyancy. Such a mechanism would be necessary to reconcile in-situ differentiation with the pulsing required by Holder (1979) on structural grounds. Alternatively the differentiation may have occurred in a chamber below the present level of emplacement and intruded as a series of pulses.

Derivation of G3 from the G1-G2 pulse is less easy to achieve by in situ processes (see Chapter 5.6.1 d) and G3 almost certainly represents a separate pulse as indicated by Holder (1979). Whether this pulse was derived from the same magma source or parental magma is difficult to determine without isotopic evidence but the geochemistry suggests that G3 has a distinct petrogenesis from G1 and G2.

The plutonism of the Ardara complex as a whole is dominated by two end-member types, appinite and granitoid. Their intimate relationships in the field and geochemically suggest while apparently a bi-modal suite, they are quite closely associated and linked in petrogenesis. The coeval relationships between the Summy Lough diorite and the outer unit of the Ardara pluton (G1) indicate a close spatial and temporal relationship between the early units of the main Ardara pluton and appinitic magma and the high levels of Ni and Cr in G1 and G2 while the presence of enclaves of dioritic composition may suggest the involvement of appinite-type material in the development of the granitoids.

7.5.5 Model for the development of the plutonic complex

Tectonic controls are of considerable importance in the Ardara plutonic complex. The importance of large-scale tectonic structures to pluton emplacement in the Caledonides is well documented (Bowes & Wright, 1967, Hutton, 1988, Hutton & McErlean, 1991). The Ardara pluton is widely accepted in the literature as the classic example of a distensional diapir and this view dominates consideration of the emplacement of the plutonic complex. The emplacement of the appinites clustered around the Ardara pluton is intimately associated with local and regional structures, possibly including the distension

associated with the emplacement of the Ardara pluton. The appinites are commonly emplaced as large bodies parallel to strike, e.g. Mulnamin, Meenalargan, Summy Lough, and also on a smaller scale as sheets, dykes and plugs which utilise bedding fractures and pre-existing shear zones, such as those of the Narin-Portnoo intrusion. The appinites are commonly transected by shear zones which may have existed prior to the emplacement of the appinites, indeed emplacement may have been controlled by those shear zones, which on a regional scale may be related to larger dislocations on the scale of the Great Glen fault. The Ardara diapir itself shows evidence of shear fabric (C/S) prior to full crystallisation. The coeval nature and intimate relationships between the Ardara pluton and the appinite suite suggests that the emplacement of the appinites may be controlled by structural traps, and that the appinites rose along fractures driven by their high volatile content, reacting with the wall rocks. This ascent took place parallel to the local strike and bedding at the margin of the main Ardara pluton which at the same time was slowly dilating the country rock by distension.

The Ardara pluton may have fractionated internally at depth and may have been contaminated by mafic (appinitic) magmas now seen as enclaves which contributed to the G1 and G2 variation. G3 may represent a separate pulse. A geochemical relationship between the appinite suite and the granite of the main Ardara pluton is possible on the basis of geochemistry (section 5.2 vi) by a process of fractionation although it is suggested on the basis of geochemical modelling that simple fractionation cannot always explain the wide compositional variations in the rocks of the complex. It is possible that processes of magma mixing, contamination and hybridisation in the presence of volatiles may have important effects on the geochemical signature of the appinite-granite complex.

7.6 THE ARDARA PLUTONIC-APPINITIC COMPLEX AND THE CALEDONIAN OROGENY

7.6.1 Tectonic setting

The timing of appinite emplacement in the Caledonian orogeny of the Western Highlands has been dated by Rogers & Dunning (1990) to between 429 and 423 ± 3 Ma. Only one absolute date exists for appinites of the Ardara complex and that is from the Kilrean hornblendite which was dated to 410 ± 6 Ma by O'Connor et al. (1982) using the $^{40}\text{Ar}/^{39}\text{Ar}$ technique. O'Connor et al. (1982) argued that this date was the minimum age for the intrusion of the hornblendite. This date is within error of the Rb-Sr whole rock age for the Ardara pluton of 405 ± 5 Ma (Halliday et al., 1980) and is consistent with field evidence for contemporaneous intrusion. Such relationships thus support a partly coeval plutonism of the appinites and main granite of the Ardara plutonic complex with the likelihood that the appinites were emplaced early and continued to overlap with the earliest stages of plutonism. There is no evidence for appinite activity during the emplacement of G3 or afterwards.

7.6.2 Emplacement level

Field relations highlight variation in the emplacement mode of the appinites from plutonic masses such as Summy Lough, Kilrean, Meenalargan and Mulnamin, the sub-volcanic dykes and sheets of the Narin-Portnoo complex, to the sub-volcanic and breccia pipes of Biroge, Dunmore and Kilkenny. The diatreme-like nature of these pipes suggests a volcanic aspect to the magmatism, record of which is not preserved in the Ardara area.

(i) Results of geobarometry and geothermometry.

Amphibole-plagioclase geobarometry and geothermometry studies of the main Ardara pluton and appinites in this study suggest that the outer units of the main Ardara pluton (G1 & G2) crystallised at pressures of $4.0\text{-}6.0 \pm 1\text{ kb}$ at a temperature interval of 800°C . The appinites show a range of crystallisation pressures from 3.5 to 8.0 kb with an average of $5.0 \pm 1\text{ kb}$ and yield crystallisation temperatures of 800°C . The appinite with the lowest estimated crystallisation pressure (3.5 kb) is the Summy Lough diorite. This appinite is thought to be coeval with the outer unit of the Ardara pluton (G1) estimated to have been emplaced at 4.0-6.0 kb.

Previous work by Naggar & Atherton (1970) in a study of the metamorphic reactions of the thermal aureoles of the Donegal batholith determined that the aureoles formed over a relatively narrow pressure band and wide temperature range. They proposed a pressure of 3.5-5.0 kb and a temperature range of $500\text{-}700^\circ\text{C}$ based on experimental equilibria for the Al silicates, garnet, staurolite, cordierite and other contact metamorphic aureoles.

In a more recent study of the fibrolite of thermal contact aureoles of Donegal, Kerrick (1987) obtained a pressure estimate of the emplacement regime using the garnet-plagioclase- Al_2SiO_5 -quartz geobarometer in sillimanite-zone rocks of the Ardara granite. Rim compositions of zoned plagioclases, representing the final crystallisation conditions yielded pressures of 4.0-5.0 kb (beyond the stability limit of andalusite) while core compositions yielded pressures of 2.0-3.0 kb. Kerrick argued that the core and rim compositions of the plagioclases were sharp and distinct, influenced on the rim by later alkali-rich fluids emanating from the Ardara pluton. Consequently Kerrick used a pressure of $2.5 \pm 0.5\text{ kb}$ for temperature estimates of the contact metamorphism of the Ardara aureole. Kerrick determined that the temperature at the sillimanite isograd was between $550\text{ and }600^\circ\text{C}$ which is in good agreement with Holdaway's (1971) determination of the andalusite = sillimanite equilibrium at 2.5 kb, thus providing independent support for the pressure estimate obtained from using core compositions of plagioclase.

(ii) Field evidence

Field evidence shows that the outer units of the Ardara pluton crystallised in a regime of high strain. The samples analysed in this study come from the outermost margin of the outer unit (G1) and from the margin of the inner unit (G2), both of which are in

zones of high strain. Some of the appinites have been emplaced in the form of breccia pipes analagous to diatremes which are thought to be high level features (Dawson 1975). Those appinites analysed in this study commonly have associated breccia complexes (Narin-Portnoo, Meenalargan, Mulnamin). The problems of reconciling the field evidence with the barometric estimates remains.

(iii) Hydrogen isotopes

Analyses of mineral separates from three different appinite intrusions indicate that while there is a strong mantle-type signature of the appinites, there is also evidence to suggest the presence of a meteoric circulation system, possibly related to the Ardara pluton (6.4 iii). The high pressure estimates obtained for the granites and appinites may indicate that meteoric circulation may by inference extend to great depths.

(iv) Discussion

The studies of Kerrick (1987) and Naggar & Atherton (1970) indicate the possibility of a pressure of ~5.0 kb at 500-700°C for the crystallisation of the Ardara pluton which is consistent with the geobarometry and geothermometry of this study confirming their findings. Kerrick (1987) adopted a working pressure of 2-3 kb despite having to use core as opposed to rim compositions which yielded higher pressure estimates. The hornblende-plagioclase geobarometer of Hollister et al. (1987) employed in this study requires the use of rim compositions of coexisting phases in order to obtain a realistic estimate of conditions at the time of final crystallisation of the minerals of the rock. The results of this study contradict the field evidence of a shallow emplacement regime of the appinites but may support the findings of earlier workers of a deeper emplacement environment for the Ardara pluton and intimately associated appinites such as the Summy Lough diorite.

The application of the amphibole-plagioclase geobarometer may be inappropriate to apply to the granites and appinites of the Ardara igneous complex for a number of reasons. Firstly, in the case of the appinites, resetting may be a problem due to the re-equilibration of amphibole under sub-solidus conditions (analyses of rim compositions of amphibole was also a problem as these are often actinolitic). Secondly, in the case of the Ardara pluton, areas of high strain, based on the evidence of xenolith ratios (Holder 1979) may provide high pressure estimates on a local scale and so unrealistic pressures may be obtained. If the geobarometer is reliable in this case then appinites may be deep-level intrusions whose great volatile content allowed them to reach high levels in the form of fluidised crystal mushes intruding as breccia pipes. Finally, in considering hydrogen isotope results, the presence of a meteoric circulatory system, possibly related to the Ardara pluton and the possibility of high pressure values for the pluton and associated appinites might infer that the meteoric system may reach great depths in the upper crust.

7.6.3 Regional correlations

The Main Donegal granite was emplaced in a syntectonic sinistral shear zone, believed to be a splay of the Great Glen fault. If this fracture was an active shear zone over a large period then this may provide an explanation of the concentration of both the Ardara pluton and the appinites in this same region, which is also located at the bend of regional Caledonian strike from NE-SW to W-E in the south of Donegal (Fig. 3.1). Such a correlation between regional tectonics, in particular large shear zones and granitic/appinitic magmas, is analogous to many other parts of the Scottish and Irish Caledonides. At Strontian Hutton (1988) assigns the emplacement of the granite (with associated appinites) to a termination of a dextral shear zone. Similarly at Ratagain which has associated diorite and appinite, Hutton & McErlean (1991) interpreted its emplacement to the sinistral shear zone associated with the Strathconnan fault. The classic area of Ardsheal and Kentallen in Argyll is thought to be related to the major Cuil Bay synform (Bowes & Wright, 1967) and very close to the Great Glen fault. The appinitic intrusions of Garabal Hill and Glen Tilt are also related to nearby transcurrent faults.

In SE Ireland the 44 appinitic intrusions associated with the Tullow Lowlands and the Blackstairs pluton, forming part of the Leinster Granite, are spatially related to the East Carlow Deformation Zone, a major dip-slip ductile shear zone (McArdle & O'Connor, 1987).

An Italian example from the Serie dei Laghi also indicates a close association of appinites with calc-alkaline granites along a major transcurrent fault (Borioni 1984). This association with large scale tectonic lineaments is also common in the calc-alkaline granites and associated mafic rock types of all orogenic regions. In the Cordillera of North and South America, there is a close association between the plutonic granitic and basic components in that there are voluminous granite/tonalites associated with gabbros, diorites and hybrid basic rocks in which there is considerable development of hornblende. These are also occasionally associated with explosive breccias. The magmas are entirely I-type and plutonism is related to large-scale vertical movements with lateral shortening, in a destructive margin setting (Pitcher et al. 1985).

The implication of these global comparisons relate to the common genetic, temporal and spatial link between hydrous mafic magmas which are normally hornblende-rich, and large volumes of granitic magma of high-K calc-alkaline, I-type affinity. The mafic magmas appear to have a deep-seated origin and be emplaced at high levels as explosive breccia and have significant volatile content. These hornblendic magmas appear to be closely linked to major tectonic lineaments, usually of a transcurrent nature, which may be extend deep into the lower crust and might have acted as magma pathways to the emplacement level.

7.7 SUGGESTIONS FOR FURTHER STUDY

The precise nature of the protolith which yielded appinitic magmas, particularly concentrated in areas such as Ardara and Appin has yet to be determined. The source of the magmatic volatiles is an important aspect of this question and may be addressed by further stable (O, C, H and S) isotope study.

Many of the unanswered questions arising from this study could be answered by further study involving radiogenic isotopes, especially Sr, Nd and Pb. The problem of the G1 & G2 relationship with G3, the relationships between the appinites and G1 & G2, and the within- and between-appinite variations could all be better constrained with such data. This leads to the need for a closer examination of the relationships between the appinites and the plutonic enclaves, and between the appinites and the lamprophyre suite.

Another major problem lies in reconciling the apparent deep level of plutonic emplacement (3-8 kb) with the apparently shallow diatreme emplacement of some of the appinites.

The relationship between appinites and the major late regional structures presents a tantalising problem in which igneous studies could contribute to the understanding of the effect of the penetration of these major faults into deep magma source regions.

7.8 CONCLUSIONS

1. The Ardara igneous complex consists of over 30 appinitic intrusions clustered around a diapiric granitoid pluton. The appinites comprise a suite of coarse grained, melanocratic to leucocratic rocks rich in hornblende, plagioclase, calcite and sulphides, ranging from hornblende pyroxene olivine gabbro to hornblendite, meladiorite, diorite granodiorite and granite which are texturally and compositionally complex. Fractional crystallisation processes cannot easily explain the whole compositional variation found in the suite of rocks. "Appinite" itself forms a minor fraction of this suite and occurs sporadically in the form of lenses, pockets and veins within the other rock types suggesting its formation as late stage, product of a volatile-rich magma.

2. The intrusions vary in size from 2m² breccia pipes to large igneous complexes several kilometres in length and width. The appinites display a range of form and emplacement mechanism including deep-seated plutonic intrusions such as Meenalargan, Summy Lough, Kilrean and Mulnamín as well as the subvolcanic dykes, sills, sheets and domes of the Narin-Portnoo intrusion, and high level explosion and intrusion breccias of Dunmore, Kilkenny and Biroge, which may represent a volcanic expression of basic magmatism in the Caledonian of Donegal. The complexity of texture and composition provide evidence of magma mingling and magma mixing, assimilation and contamination by country rock. Many of these appinitic intrusions were emplaced into brittle-ductile country rocks after the peak of regional metamorphism prior to, and coeval with, the diapiric granitoid pluton of Ardara.

3. There is a strong tectonic control on the emplacement of the appinite suite and the main Ardara pluton. This takes the form of local structure, dip and strike of bedding, strike-slip faulting and regional structure in the form of large-scale, deep-seated shear zones which may have acted as pathways for the intrusion and emplacement of appinitic and granitic magma.

4. Hornblende geobarometry and hornblende-plagioclase geothermometry indicates that the most primitive rocks of the appinite suite crystallised at ~8kb, at a temperature of 976°C (two-pyroxene geothermometry) whilst the majority of the appinite suite crystallised at 5-8kb near 800°C. Evidence of sub-solidus re-equilibration of the appinites means these results must be viewed with caution. The granites of the Ardara pluton crystallised at ~5kb over a temperature interval including 800°C for amphibole-plagioclase crystallisation.

5. The appinites crystallised from calc-alkaline to high-K calc-alkaline and mildly alkaline melts rich in volatiles (H₂O and CO₂). The granitic members crystallised from metaluminous melts; they are medium to coarse-grained granodiorites and biotite granites with steep sharp outer contacts.

6. Stable isotope studies ($\delta^{18}\text{O}$ and $\delta^{13}\text{C}$) indicate that the appinites have isotopic values consistent with magmatic values ($\delta^{18}\text{O} = +6.46$ to $+8.55\text{‰}$, $\delta^{13}\text{C} = -6.27$ to -2.19‰). Some appinites show evidence of an increase in $\delta^{18}\text{O}$ and $\delta^{13}\text{C}$ as a result of exchange with country rock.

7. Stable isotope studies ($\delta^{18}\text{O}$, $\delta^{13}\text{C}$ and δD) indicate the presence of an aureole of magmatic fluid around an intrusion from the Narin-Portnoo shore section. The contact of the appinite and the Portnoo Limestone shows evidence of the growth of hornblende across the contact boundary over a few centimetres. The intrusion of appinite into Portnoo Limestone has the effect of lowering the $\delta^{18}\text{O}$ SMOW and $\delta^{13}\text{C}$ PDB signature of the Portnoo Limestone from a metasedimentary value to a magmatic value. This magmatic fluid aureole extends up to 40 m from the contact with the appinite into the Portnoo Limestone.

8. δD values indicate the presence of a meteoric-type fluid which has circulated through the rocks of the area. This may be related to a fluid circulation system associated with the Ardara pluton.

9. Stable isotope studies of $\delta^{13}\text{C}$ PDB indicate the presence of heavy carbon in the Portnoo Limestone ($\delta^{13}\text{C}$ PDB = -5.44 to $+9.00\text{‰}$) indicating that the sediments during the Lower Dalradian were enriched in $\delta^{13}\text{C}$. This finding has two implications; the first is that the sediments were deposited in a closed/semi-closed basin; the second is that there was a major excursion in the C isotope seawater composition during the time of deposition of the Portnoo Limestone, similar to that which is thought to have occurred during the deposition of the Lewisian limestone ($\delta^{13}\text{C}$ PDB = $+12.00\text{‰}$) from Loch Maree, in Scotland (Baker & Fallick 1989). The Tayvallich Limestone of the Middle

Dalradian has been reported to have a $\delta^{13}\text{C}$ PDB of +6.00 to +7.5 ‰ (Graham pers. comm)

10. The Ardara pluton consists of three units, an outer quartz monzodiorite (G1), an inner quartz monzodiorite/granodiorite (G2) and a central granodiorite (G3). G1 and G2 are believed to be related by a process of fractionation from a dioriticgranodioritic magma derived from a mantle or young rather primitive crustal source. G1 and G2 may have undergone some contamination by entrainment of some dioritic enclaves.

11. The G3 unit of the Ardara complex may have a separate petrogenesis from the G1 & G2 units, and may be derived from a more evolved source.

12. Mineral vectors indicate that there is a strong control exerted by the crystallisation of hornblende, pyroxene and plagioclase on the petrogenetic evolution of the appinites and granites of the Ardara igneous complex

13. The rocks of the Ardara igneous complex have similar field, petrographic and geochemical characteristics to other granite-dioritic associations in the Irish and Scottish Caledonides. The appinites also bear strong similarity to other dioritic rock types from other parts of the world (Spain, U.S.A, Italy, Australia) but may differ in their age, tectonic setting and isotopic characteristics. The Ardara igneous complex offers a unique view of the close affinity between regional structure and the satellitic nature of the appinites clustered around the Ardara diapiric pluton.

BIBLIOGRAPHY

- ADAMS, C.J.D. (1976). Geochronology of the Channel Islands and the adjacent French mainland. *Quart. Jl Geol. Soc. London* **132**, 233-250.
- AGATA, T. (1981). Hornblende-rich gabbro-diorite sequence in the Oura igneous complex, Maizuru city, Japan; Part 1, A generation of late differentiates midway in the layered sequence: *Japan Assoc. Mineral. Petrol. Econ. Geol. J.* **75** No. 12, 396-410.
- AKAAD, M. K. (1956). The Ardara granitic diapir of Co. Donegal, Ireland. *Quart. Jl geol. Soc London.* **112**, 263-88.
- AKAAD, M. K. (1956). The northern aureole of the Ardara pluton of Co. Donegal. *Geol Mag.* **93**, 377-92.
- ANDERSON, J.G.C. (1935) The Arrochar intrusive complex. *Geol. Mag.* **72**, 263-283.
- ANDERSON, J.G.C., (1937) Intrusions of the Glen Falloch Area. *Geol. Mag.* **74**, 458-468.
- ARTH, J.G. (1976). Behaviour of trace elements during magmatic processes - a summary of theoretical models and their applications. *J. Res. U.S. Geol. Surv.* **4**, 41-47.
- BAILEY, E.B. and MAUFE, H.B. (1916). The geology of Ben Nevis and Glencoe and the surrounding country (Expl. Sheet 53). *Mem. Geol. Surv. Scotland; Edinburgh.*
- BAILEY, E.B. and MAUFE, H.B. (1960). The geology of Ben Nevis and Glencoe and the surrounding country (Expl. Sheet 53; 2nd edn.). *Mem Geol Surv Scotland, Edinburgh.*
- BAKER, A.J. and FALLICK, A.E (1989). Evidence from Lewisian limestones for isotopically heavy carbon in two thousand-million-year-old sea water. *Nature.* **337**, No.6205 , 352-354.
- BENDER, J.F., HANSON, G.N. and BENCE, A.E. (1982). The Cortlandt complex: evidence for large-scale liquid immiscibility involving granodiorite and diorite magmas. *Earth Planet. Sci. Lett.* **58**, 330-344.
- BICKLE, M.J. and BAKER, J. (1989). Infiltration driven reaction front velocities and fractionation of oxygen and carbon isotopes by fluid flow in metamorphic rocks. *Isotope Geology* , **1**. p. 329.
- BLUNDY, J.D. (1989). The geology of the southern Adamello Massif. Unpublished Ph.D thesis, University of Cambridge.
- BLUNDY, J.D. and HOLLAND, T.J.B. (1990). Calcic amphibole equilibria and a new amphibole-plagioclase geothermometer. *Contrib. Mineral. Petrol.* **104**, 208-224.
- BOHLEN, S.R. and ESSENE, E.J. (1978). Igneous pyroxenes from metamorphosed anorthosite massifs, *Contr. Mineral. Petrol.* **65**, 433-442.
- BORIANI, A., BURLINI, L., CAIRONI, V., ORIGONI, E.G., SASSI, A. and SESENA, E. (1988). Geological and petrological studies on the Hercynian plutonism of Serie dei Laghi- geological map of its occurrence between Valsesia and Lago Maggiore (N-Italy). *Societa Italiana di Mineralogia e Petrologica.* **43** (2), 367-383.
- BOTTINGA, Y. and JAVOY, M. (1973). Comments on isotope geothermometry. *Earth Planet. Sci. Lett.* **20**, 250-265.
- BOWES, D.R. and WRIGHT, A.E. (1961). An explosion-breccia complex at Back Settlement near Kentallen, Argyll. *Trans. Edinb. Geol. Soc.* **18**, 293-314.
- BOWES, D. R., KINLOCH, D.E. and WRIGHT, A.E. (1964). Rhythmic amphibole overgrowths in apinites associated with explosion breccias in Argyll, *Min. Mag.* **33**, 963-973.
- BOWES, D.R. and WRIGHT, A.E. (1967). The explosion breccia pipes near Kentallen, Scotland and their geological setting. *Trans Royal Soc. Edin.* **67** 109-142.

- BOWES, D.R. and McARTHUR, A.C. (1976). Nature and genesis of the Appinite suite. *Krystalanikum* 12, 31-46.
- BREWER, J., MATTHEWS, D., WARNER, M., HALL, J., SMYTHE, D. and WHITTINGTON, R. (1983). BIRPS deep seismic reflection studies of the British Caledonides, *Nature*. 305, 206-210.
- BRINDLEY, J.C. (1957). The aureole rocks of the Leinster Granite in south Dublin, Ireland. *Proc. R. Ir. Acad.* 59B, 1-18.
- BRINDLEY, J.C. (1970). Appinitic intrusions associated with the Leinster granite, Ireland. *Proc R.Ir. Acad.* 70 Sect. B., 93-105.
- BROWN, G.C. (1979). Geochemical and geophysical constraints on the origin and evolution of Caledonian granites. In, HARRIS, A.L., HOLLAND, C.H. and LEAKE, B.E. (eds). *The Caledonides of the British Isles- Reviewed.*, Geological Society of London 645-651.
- BROWN, P.E., MILLER, J.A. and GRASTY, R.L. (1964). Isotopic ages of late Caledonian granitic intrusions in the British Isles. *Proc. Yorks. Geol. Soc.* 36, 251-271.
- BRUCK, P.M. and O'CONNOR, P.J. (1977). The Leinster Batholith: Geology and Geochemistry of the Northern units. *Geol. Surv. Ireland. Bull.* 2, 107-141.
- BURNHAM, C.W. (1979). Magmas and hydrothermal fluids. In BARNES, H.L. (ed): *Geochemistry of Hydrothermal Ore deposits*, Wiley.
- BUSECK, P.R., NORD, G.C. Jr. and VEBLEN, D.R. (1982). Subsolidus phenomena in pyroxenes, In, PREWITT, C.T. (ed), *Reviews in Mineralogy, Pyroxenes* 7, 117-212.
- CHANDLER, F.W., SULLIVAN, R.W. and CURRIE, K.L. (1987). The age of the Springdale group West Newfoundland, and correlative rocks-evidence for a Llandoverly overlap assemblage in the Canadian Appalachians. *Trans. Roy Soc Ed Earth Sci.* 78, 41-49.
- CHAPPELL, B.W. and STEPHENS, W.E. (1988). Origin of infracrustal [I-Type] granite magmas. *Trans. Royal Soc. Edinburgh Earth Sciences* 79, 71-86.
- CHAPPELL, B.A. and WHITE, A.J.R. (1974). Two contrasting granite types. *Pacific Geology* 8, 173-174.
- CHAPPELL, B.W., WHITE, A.J.R., WYBORN, D. (1987). The importance of residual source material [restite] in granite petrogenesis. *Jl Petrol.* 28. 1111-1138.
- CLAYBURN, J.A.P., HARMON, R.S., PANKHURST, R.J. and BROWN, J.F. (1983). Sr, O and Pb isotope evidence for origin and evolution of the Etive igneous complex, Scotland. *Nature* 303, 492-497.
- CLAYTON, R.N., O'NEILL, J.R. and MAYEDA, T.K. (1972). Oxygen isotope fractionation between quartz and water. *Jl Geophys. Res.* 77, 3057-3067.
- CLEMENS, J.D. and WALL, V.J. (1981). Origin and crystallisation of some peraluminous (S-type) granitic magmas. *Can. Mineral.* 19, 111-131.
- COBBING, E.J. (1985). The tectonic setting of the Peruvian Andes. In PITCHER, W.S., ATHERTON, M.P., COBBING, E.J. and BECKINSALE, R.D. (eds), *Magmatism at a Plate Edge*, Blackie, 3-12.
- CONNOR, B. (1974). An igneous breccia in the Clara area, Co. Wicklow. *Sci. Proc. R. Dubl. Soc.* 5A, 113-115.
- COX, K.G., BELL, J.D. and PANKHURST, R.J. (1979). *The Interpretation of Igneous Rocks*. Allen and Unwin 450 pp.
- CRAIG, H and LUPTON, J.E. (1976). Primordial neon, helium and hydrogen in oceanic basalts. *Earth Planet. Sci. Lett.* 31, 369-385.
- DE LA ROSA, J. and CASTRO, A. (1990). The ultrabasic rocks of the Castillo de las Guardas massif (Seville). *Geocaceta.* 7, 47-49.

- DEER, W.A. (1950). The diorites and associated rocks of the Glen Tilt complex, Perthshire:II. Diorites and appinites. *Geol. Mag.* **87**, 181-195.
- DEER, W.A. (1953). The diorites and associated rocks of the Glen Tilt complex. *Geol.Mag.* **90**, 27-35.
- DEER, W.A., HOWIE, R.A. and ZUSSMAN, J. (1966). *An Introduction to the Rock Forming Minerals*, Longman 528 pp.
- DEMPSEY, C.S., HALLIDAY, A.N. and MEIGHAN, I.G. (1989). Combined Sm-Nd and Rb-Sr isotope systematics in the Donegal granitoids and their petrogenetic implications. *Geol. Mag.* **127**, 75-80.
- DEWEY, J.F. (1982). Plate tectonics and the evolution of the British Isles. *Quart.Jl geol. Soc. London* **139**, 371-412.
- DUNN, S.R. and VALLEY, J.W. (1985). Fluid infiltration of the Tudor gabbro during regional metamorphism. *Geol. Soc. Am. Abstr. Prog.* **17**, 570.
- ETHERIDGE, M.A., WALL, V.J., COX, S.F. and VERNON, R.H. (1984). In, KIRBY, S.H. (ed), Chemical effects of water on the strength and deformation of crustal rocks. *Jl Geophys. Res.* **89**, 4344-4358.
- FALLICK, A.E., JOCELYN, J., DONNELLY, T. GUY, M. and BEHAN, C. (1985). Origin of agates in volcanic rocks from Scotland. *Nature* **313**, 672-674.
- FAURE, G. (1977). *Principles of isotope geology*, Wiley 464 pp.
- FERRIER, G (1986). The Geology of the Glen Doll Complex. Unpublished B. Sc. thesis, St. Andrews University.
- FERRY, J.M. (1985). Hydrothermal alteration of Tertiary igneous rocks from the isle of Skye, northwest Scotland. *Contrib. Mineral. Petrol.* **95**, 264-282.
- FIGUEROLA, L.C. GARCIA DE, UGIDOS, J.M., BEA, F., CARNICERO, A., FRANCO, P., RODRIGUEZ, D. and LOPEZ-PLAZA, M. (1980). Plutonism of Central Western Spain. A preliminary note. *Estudios Geol.* **36**, 339-348.
- FORESTER, R.W. and TAYLOR, H.P. (1977). $^{18}\text{O}/^{16}\text{O}$, D/H and $^{13}\text{C}/^{12}\text{C}$ studies of the Tertiary igneous complex of Skye, Scotland., *Am. Jl Sci.* **277**, 136-177.
- FOWLER, M.B. (1988). Ach'uaire hybrid appinite pipes: Evidence for mantle-derived shoshonitic parent magmas in Caledonian granite genesis. *Geology* **16**, 1026-1030.
- FRANCHI, I.A. (1983). The Geology of the Arrochar complex, Argyll, Scotland. Unpublished B.Sc. thesis, University of St. Andrews, St. Andrews.
- FRENCH, W.J. (1966). Appinitic intrusions clustered around the Ardara pluton, Co. Donegal. *Proc. R. Irish Acad.* **64B**, 303-322.
- FRENCH, W.J. (1976). The origin of leucodiorites associated with the appinitic intrusion of Co. Donegal. *Proc. Yorks. Geol. Soc.* **41**, 107-126.
- FRENCH, W.J. (1977). Lamprophyric dykes associated with the appinitic intrusions of Co. Donegal. *Sci. Proc. R. Dublin Soc. Series A.* **6**, 97-107.
- FRENCH, W.J. and PITCHER, W.S. (1959). The intrusion-breccia of Dunmore, Co. Donegal. *Geol. Mag.* **96**, 69-74.
- FRIEDMAN, I. and O'NEIL, J.R. (1977). Compilation of stable isotope fractionation factors of geochemical interest. In: *Data of Geochemistry U.S.G.S. Prof. Papers.* 440 KK
- GALAN, G. (1984). Las rocas graníticas del macizo de Vivero: une association de roches ultramafiques et de granites- Comparison avec d'autres exemples des orogenes hercyniens et caledonien. Unpublished thesis, Pierre and Marie Curie University, Paris, 404 pp.

- GALAN, G. and SUAREZ, O. (1989). Cortlanditic enclaves associated with calc-alkaline granites from Tapia-Asturias (Hercynian Belt, northwestern Spain). *Lithos* **23**, 233-245.
- GAPAIS, D. and BALE, P. (1990). Shear zone pattern and granite emplacement within a Cadomian sinistral wrench zone at St. Cast, N. Brittany. D'LEMOS, R.S., STRACHAN, R.A. and TOPLEY, C.G. (eds). In, *The Cadomian Orogeny, Geol. Soc. Sp. Pub. No. 51*, 169-179.
- GAPAIS, D. and BARBARIN, B. (1986). Quartz fabric transition in a cooling syntectonic granite, (Hermitage massif, France). *Tectonophysics* **125**, 357-370.
- GEIST, D.J., McBIRNEY, A.R. and BAKER, B.H. (1989). MacGPP: A program for creating and using geochemical data files. Unpublished report, University of Oregon.
- GHOSE, S. (1981). Subsolidus reactions and microstructures in amphiboles: In VEBLEN, D.R. (ed), *Amphiboles and other hydrous pyriboles-mineralogy, Min. Soc. Amer. Rev. in Mineralogy* **9A**, 325-372.
- GINDY, A.R. (1951). The production of amphibolitic and other skarn rocks from limestone at Cor, Co. Donegal. *Geol. Mag.* **88**, 103-112.
- GRAHAM, C.M., SHEPPARD, S.M.F., HEATON, T.H.E. (1980). Experimental hydrogen isotope studies-1. Systematics of hydrogen isotope fractionation in the systems epidote-H₂O and AlO (OH)-H₂O. *Geoch. Cosmoch. Acta.* **44**, 353-364.
- GRAHAM, C.M., HARMON, R.S., SHEPPARD, S.M.F. (1984). Experimental hydrogen isotope studies: hydrogen isotope exchange between amphibole and water. *Amer Mineral.* **69**, 128-138.
- HALL, A. (1965). The occurrence of prehnite in appinitic rocks from Donegal, Ireland. *Min Mag.* **35**, 234-236.
- HALL, A. (1966). The Ardara pluton: A study of the chemistry and crystallization of a contaminated granite intrusion. *Proc. Royal Irish Acad.* **65B**, 203-235.
- HALL, A. (1967). The distribution of some major and trace elements in Feldspars from the Rosses and Ardara granite complexes, Donegal, Ireland. *Geochim. Geocosm. Acta.* **31**, 835-848.
- HALLIDAY, A.N., AFTALION, M., and LEAKE, B.E. (1980). A Revised age for the Donegal granites. *Nature.* **284** 542-543.
- HALLIDAY, A.N., FALLICK, A.E., HUTCHINSON, J., and HILDRETH, W. (1984). A Nd-Sr and O isotopic investigation into the causes of chemical and isotopic zonation in the Bishop Tuff, California. *Earth Planet Sci Lett.* **68**, 379-391.
- HAMIDULLAH, S. (1983). Petrogenetic studies of the appinite suite, northwestern Scotland. Unpublished Ph.D thesis, Glasgow University.
- HAMIDULLAH, S. and BOWES, D.R. (1987). Petrogenesis of the appinite suite, Appin district, W.Scotland. *Acta Universitatis Carolinae-Geologica* **4**, 295-396.
- HAMMARSTROM, M.J. and ZEN, E.-AN. (1983). Possible use of Al content in hornblende as a geobarometer for plutonic rocks. *Geol.Soc. Amer. Abs. with Progs.* **15**, 590.
- HAMMARSTROM, M.J. and ZEN, E.-AN. (1985). An empirical equation for igneous calcic amphibole geobarometry. *Geol.Soc. Amer. Abs. with Progs.* **17**, 602
- HAMMARSTROM, M.J. and ZEN, E.-AN. (1986). Aluminium in hornblende: an empirical igneous geobarometer. *Am. Mineral.* **71**, 1057.
- HARKER, A. (1908). The geology of the small isles of Invernesshire. *Mem. Geol. Surv. Scot.* 210p.
- HASLAM, H.W. (1970). Appinite xenoliths and associated rocks from the Ben Nevis igneous complex. *Geol. Mag.* **10**, 341-356.
- HELZ, R.T. (1982). Phase relations and compositions of amphiboles produced in studies of the melting behaviour of rocks. *Min. Soc. Amer. Rev. in Mineralogy* **9B**, 279-346.

- HENDERSON, P. (1982). *Inorganic Geochemistry*, Pergamon 353 pp.
- HENNEY, P.J., GASKARTH, J.W., SHAND, P. and HOLDEN, P. (1989). Geochemistry and petrogenesis of Late Caledonian lamprophyres from S.W. Scotland. *Min. Soc. meeting abstracts*, Leicester Univ.
- HILL, J.B. and KYNASTON, H. (1900). On Kenatallinite and its relations to other igneous rocks in Argyllshire. *Quart. Jl geol. Soc. London* 68, 531.
- HOLDEN, P. (1987). Source and equilibration studies of Scottish Caledonian xenolith suites. Unpublished Ph. D thesis, University of St. Andrews, 293pp.
- HOLDER, M.T. (1979). An emplacement mechanism for post-tectonic granites and its implications for their geochemical features. In, ATHERTON, M. P. and TARNEY, J. (eds). *Origin of granite batholiths*, 116-128.
- HOLGATE, N. (1950). The Glen Banvie igneous complex of Perthshire. *Quart. Jl geol. Soc. London* 106, 433-460.
- HOLLISTER, L.S., GRISSOM, G.C., PETERS, E.K., STOWELL, H.H., and SISSON, V.B. (1987). Confirmation of the empirical correlation of Al in hornblende with pressure of solidification of calc-alkaline plutons. *Am. Mineral.* 72, 231-239.
- HOLLOWAY, J.R. and BURNHAM, C.W. (1972). Melting relations of basalt with equilibrium water pressures less than total pressure. *Jl Petrol.* 13, 1-29.
- HUDSON, J.D.(1977). Stable isotopes in limestone lithification. *Jl geol. Soc. London*, 133, 637-660.
- HUTTON, D.H.W. (1982). A tectonic model for the emplacement of the Main Donegal Granite. NW Ireland. *Jl geol. Soc. London* 139. 516-631.
- HUTTON, D.H.W. (1987). Strike-slip terranes and a model for the evolution of the British and Irish Caledonides. *Geol. Mag.* 5, 405-425.
- HUTTON, D.H.W. (1988). Granite emplacement mechanisms and tectonic controls: inferences from deformation studies. In, *The origin of granites* (Brown, P.E., ed), Trans R. Soc. Edinb, Earth Sciences, 79, 245-255.
- HUTTON, D.H.W. and McERLEAN, M. (1991). Silurian and Early Devonian sinistral deformation of the Ratagain granite, Scotland: constraints on the age of Caledonian movements on the Great Glen fault system. *Jl geol. Soc. London* 148, 1-4.
- I.U.G.S. (1973). Plutonic Rocks: classification and nomenclature recommended by the I.U.G.S. subcommission on the systematic classification of igneous rocks. *Geotimes* 18. 26-30,
- IYENGAR, S.V.P., PITCHER, W.S. and READ, H.H. (1954). The plutonic history of the Maas area, Co. Donegal, *Quart. Jl geol. Soc. London* 110, 203-228.
- JENKIN, G.R.T. (1988). Stable isotope studies in the Caledonides of S.W. Connemara, Ireland. Unpub. Ph.D thesis, University of Glasgow.
- JENKIN, G.R.T. and FALLICK, A.E. (1989). Hydrogen isotope kinematics during hydrothermal alteration in S.W. Connemara, Ireland. *Proc. of Water-rock Interactions* 6, 331-335.
- JOHANNSEN, A. (1938). *A Descriptive Petrography of the Igneous Rocks*. Chicago, Univ. of Chicago Press.
- JOHNSON, M.C. and RUTHERFORD M.J. (1988). Experimental calibration of an Aluminium-in-Hornblende geobarometer applicable to calc-alkaline rocks. *EOS* 69, 1511.
- JOPLIN, G.A. (1957). Basic and ultrabasic rocks near Happy Jacks and Tumut Pond in the Snowy Mountains of New South Wales. *Jl Proc. Royal Soc New South Wales* 91, 120-141.

- JOPLIN, G.A. (1959). On the origin and occurrence of basic bodies associated with discordant batholiths. *Geol. Mag.* **46**, 361-373.
- KENNAN, P.S., PHILLIPS, W.E.A. and STROGEN, P. (1979). Pre-Caledonian basement to the paratectonic Caledonides in Ireland. In HARRIS, A.L., HOLLAND, C.H. and LEAKE, B.E. (Eds.). In *The Caledonides of the British Isles- Reviewed.*, Spec Publ. geol. Soc. London 157-161.
- KERRICK, D.M. (1987). Fibrolite in contact aureoles of Donegal, Ireland. *Am Mineral.* **72** 240-254.
- KING, B.C. (1982). The Caledonide intrusives in their structural environment. In *Igneous rocks of the British Isles*, Wiley Interscience, 129-134.
- KOEPPEL, V. and GRUENENFELDER, M. (1979). Monazite and zircon U/Pb ages from the Ivrea and Ceneri zones. *Mem. Sci. Geol.* **33**, 257.
- KYSER, T.K. (1986). Stable isotope variations in the mantle. In VALLEY, J.W., TAYLOR, H.P. and O'NEIL, J.R. (1986). Stable Isotopes in high temperature geological processes, *Min. Soc. Amer. Rev. in Mineral* **16**, 141-162.
- LABOTKA, T.C., NABELEK, P.I., PAPIKE, J.J., HOVER-GRANATH, V.C. and LAUL, J.C. (1988). Effects of contact metamorphism on the chemistry of calcareous rocks in the Big Horse Limestone member, Notch Peak, Utah. *Amer Mineral* **73**, 1095-1110.
- LASSEY, K.R. and BLATTNER, P. (1988). Kinetically controlled oxygen isotope exchange between fluid and rock in one-dimensional advective flow. *Geochim Cosmochim Acta* **52**. 2169-2175.
- LASSEY, K.R. and BLATTNER, P. (1989). Unidimensional transport of stable isotopes: The shapes of geochemical fronts. *Water rock resources* **25**, 2357-2366.
- LEAKE, B.E. (1978). Nomenclature of amphiboles. *Can. Mineral.* **16**, 501-520.
- LE FORT, P. (1986). Metamorphism and magmatism during the Himalayan collision. In, (Eds: Coward M.P. and Reis A.C) *Collision Tectonics, Geol Soc Spec Publ.* **19**. 159-172.
- LEES, G.J. (1990). The geochemical character of late Cadomian extensional magmatism in Jersey, Channel Islands. From D'LEMOIS, R.S., STRACHAN, R.A. and TOPLEY, C.G. (eds), 1990, *The Cadomian Orogeny Geol. Soc. Spec. Public.* **51**, 273-291.
- LEGGET, J.K., MCKERROW, W.S., OLIVER, G.J.H. and PHILLIPS, W.E.A. (1979). The north-western margin of the Iapetus ocean. From HARRIS, A.L., HOLLAND, C.H. and LEAKE, B.E (eds). *The Caledonides of the British Isles- reviewed.* Spec Publ. geol. Soc. London.
- LETTERIER, J. (1972). Etude petrographique et geochemique du massif granitique de Queriget (Ariege). Unpublished thesis, University of Nancy, Nancy, 292pp.
- LINDBERG, B. and EKLUND, O. (1988). Interactions between basaltic and granitic magmas in a Svecofennian post-orogenic granitic intrusion, Aland, S.W. Finland. *Lithos*, **22**. 13-23.
- LINDSLEY, D.N. (1981). The formation of pigeonite on the join hedenbergite-ferrosillite at 11.5 and 15 kbar: Experiments and a solution model, *Am. Mineral.* **66**, 1175-1182.
- LINDSLEY, D.N. (1983). A two-pyroxene thermometer (abstract). *Lunar and Planetary Science* **13**, 435-436.
- LINDSLEY, D.N., and ANDERSON, D.J. (1983). A two-pyroxene geothermometer. *Jl Geophys. Res.* **88** (Suppl. A), 887-906.
- LUFF, I.W. (1982). Petrogenesis of the island arc tholeiite series of the South Sandwich Islands. Unpubl. Ph.D thesis, Univ. Leeds, U.K.
- McARDLE, P. and O'CONNOR, P.J. (1987). The distribution, geochemistry and origin of appinites and lamprophyres associated with the east Carlow deformation zone of SE Ireland. *Bull Geol Survey Ireland* **4**, 77-88.

- McCALL, J. (1953). The Dalradian geology of the Creeslough area, Co. Donegal. *Quart. Jl geol. Soc. London* **110**, 153-173.
- McKIBBEN, R. and ABSAR, A. (1989). A model for oxygen isotope transport in hydrothermal systems. *Jl Geophys. Res.* **94**, 7065-7070.
- MARSH, B.D. (1982). On the mechanics of igneous diapirism, stoping, and zone melting. *Amer. J. Sci.* **282**, 808-855.
- MATSUHISA, Y., GOLDSMITH, J.R. and CLAYTON, R.N. (1979). Oxygen isotope fractionation in the system quartz-albite-anorthite-water. *Geochim. Cosmochim. Acta.* **43**, 1131-1140.
- MEIGHAN, I.G. and NEESON, J.C. (1979). The Newry igneous complex, County Down. In, HARRIS, A.L., HOLLAND, C.H. and LEAKE, B.E. (eds). *The Caledonides of the British Isles- Reviewed.*, Spec Publ. geol. Soc. London.
- MENEILLY, A.W. (1982). Regional structure and syntectonic granite intrusion in the Dalradian of the Gweebarra Bay area, Donegal. *Jl. geol. Soc. London* **139**, 633-646.
- MENEILLY, A.W. (1983) Development of early composite cleavage in pelites from W. Donegal. *Jl Structural Geology* **5**, 83-97.
- MILLER, C.F., WATSON, E.B. and HARRISON, T.M. (1987). Perspectives on the source, segregation and transport of granitoid magmas. In *The Origin of Granites*, (Brown, P.E. ed), *Trans. Roy. Soc. Edin. Earth Sciences* **79** (2-3), 245-255.
- MULLAN, H.S. and BUSSEL, M.A. (1977). The basic rock series in batholithic association. *Geol. Mag.* **114**, 265-280.
- MYSEN, B.O. and BOETTCHER, A.L. (1975) Melting of a hydrous mantle: I. Phase relations of natural peridotite at high pressures and temperatures with controlled activities of water, carbon dioxide, and hydrogen. *Jl. Petrol.* **16**, 520-548.
- NABELEK, C.R., LINDSLEY, D.H. (1983). Tetrahedral aluminium in amphibole: A potential geobarometer. *Geol. Soc. America. Abs. with Progs.* **17**, p 673.
- NABELEK, P.I., LABOTKA, T.C., O'NEILL, J.R., PAPIKE, J.J. (1984). Contrasting fluid/rock interaction between the Notch Peak granitic intrusion and argillites and limestones in W. Utah: evidence from stable isotopes and phase assemblages. *Contrib. Mineral. Petrol.* **86**, 25-34.
- NAGGAR, M.H. and ATHERTON, M.P. (1970). The composition and metamorphic history of some aluminium silicate-bearing rocks from the aureoles of the Donegal Granites. *Jl Petrol.* **11**, 549-589.
- NANEY, M.T. (1983). Phase equilibria of rock-forming ferromagnesian silicates in granitic systems. *Am. Jl Sci.* **283**, 993-1033.
- NEESON, J.C. and MEIGHAN, I.G. (1977). The geochemistry of the Newry igneous complex, Co. Down. In STILLMAN, C.J. Conference report: Palaeozoic volcanism in Great Britain and Ireland. *Jl geol. Soc. London* **133**, 401-411.
- NICHOLLS, G.D. (1951). The geology of the Glenelg-Ratagain igneous complex. *Quart Jl geol. Soc. London* **55**, 309-344.
- NOCKOLDS, S.R. (1934). The contaminated tonalites of Loch Awe, Argyll, *Quart Jl geol. Soc. London* **90**, 302-321.
- NOCKOLDS, S.R. (1941). The Garabal Hill-Glen Fyne igneous complex. *Quart Jl geol. Soc. London* **96**, 451-511.
- O'CONNOR, P. J. (1974). Some Caledonian intrusives in East Carlow, Ireland. *Ir. Nat. Jl* **18**, 103-108.
- O'CONNOR, P. J. and BRUCK, P.M. (1976). Strontium isotope ratios for some Caledonian igneous rocks from central Leinster, Ireland. *Geol. Surv. Ire. Bull.* **2**, 69-77.

- O'CONNOR, P. J. and BRUCK, P.M. (1978). Age and origin of the Leinster granite. *Jl Earth Sci. R. Dubl. Soc.* **1**, 105-113.
- O'CONNOR, P. J., LONG, C.B. and EVANS, J.A. (1987). Rb-Sr whole rock isochron studies of the Barnesmore and Fanad plutons, Donegal, Ireland. *Geological Jl*, **22**, 11-23.
- O'HARA, M.J. (1968). The bearing of phase equilibria studies and natural systems on the origin and evolution of basic and very basic rocks. *Earth Sci. Reviews* **4**, 69-133.
- O'NEIL, J.R. (1986). Theoretical and experimental aspects of isotopic fractionation, and Appendix: terminology and standards; In, VALLEY, J.W., TAYLOR, H.P. and O'NEIL, J.R. Stable Isotopes in high temperature geological processes, *Min. Soc. Amer. Rev. in Mineralogy* **16**, 1-40.
- O'NEIL, J.R., CLAYTON, R.N. and MAYEDA, T.K. (1969) Oxygen isotopic fractionation in divalent metal carbonates. *J. Chem. Phys.*, **51**, 5547-5558.
- OBA, T. (1980). Phase relations in the tremolite-pargasite join. *Contrib. Mineral. Petrol.* **71**, 247-256.
- OHASHI, F. (1980). An alkali olivine basalt and its related rocks from the Setogawa Group, Shizuoki Prefecture. *Geol. Soc. Jap. Jl.* **86**, 799-814.
- OLLILA, P.W., JAFFE, H.W. and JAFFE, E.B. (1988). Pyroxene exsolution: An indicator of high pressure igneous crystallisation of pyroxene-bearing quartz syenite gneiss from the High peaks region of the Adirondack mountains. *Am. Mineral.* **73**, 261-273.
- PANKHURST, R.J. (1970). The geochronology of the basic igneous complexes. *Scott. Jl Geol.* **6**, 83-107.
- PANKHURST, R.J. (1974). Rb-Sr whole rock chronology of Caledonian events in Northeast Scotland. *Bull. Geol. Soc. Am.* **85**, 345-350.
- PANKHURST, R.J. and SUTHERLAND, D.S. (1982). Caledonian granites and diorites of Scotland and Ireland. In SUTHERLAND, D.S. (Ed), *Igneous rocks of the British Isles*, Wiley Interscience.
- PEARCE, J.A. (1983). The role of sub-continental lithosphere in magma genesis at destructive plate margins. In *Continental basalts and their mantle xenoliths*. HAWKESWORTH, C.J. AND NORRY, M.J. (eds), 230-249. Nantwich: Shiva.
- PEARCE, J.A. and NORRY, M.J. (1979). Petrogenetic implications of Ti, Zr, Y and Nb Variations in Volcanic Rocks. *Contrib. Mineral. Petrol.* **69**, 33-47.
- PEARCE, J.A., HARRIS, N.B.W. and TINDLE, A.G. (1984). Trace element discrimination diagrams for the tectonic interpretation of granitic rocks. *Jl Petrol.* **25**, 956-983.
- PE PIPER, G. (1988). Calcic amphiboles of mafic rocks of the Jeffers Brook plutonic complex, Nova Scotia, Canada. *Am. Mineral.* **73**, 993-1006.
- PECCERILLO, A. and TAYLOR, S.R., (1976). Geochemistry of Eocene calc alkaline volcanic rocks from the Kastasmona area, northern Turkey. *Contr. Mineral Petrol.* **58**, 63-81.
- PERFIT, M.R., GUST, D. BENCE, A.E., ARCULUS, R.J. and TAYLOR, S.R. (1980). Chemical characteristics of island arc basalts: implications for mantle sources. *Chem. Geol.* **30**, 217-56.
- PIDGEON, R.T. and AFTALION, M., (1978) Cogenetic and inherited zircon U-Pb systems in granites: Palaeozoic granites of Scotland and England. In, BOWES, D.R. and LEAKE, B.E. (eds) *Crustal evolution in northwestern Britain and adjacent regions*. *Geol. J. Spec. Issue* **10**, 183-248.
- PINEAU, F. and JAVOY, M. (1983). Carbon isotopes and concentration in mid-ocean ridge basalts. *Earth Planet. Sci. Lett.* **62**, 239-257.
- PITCHER, W.S. and READ H.H. (1952). An appinitic intrusion-breccia at Kilkenny, Maas, Co. Donegal. *Geol. Mag.* **89**, 328-336.
- PITCHER, W.S. and FRENCH, W.J. (1959). The intrusion breccia of Dunmore, Co. Donegal. *Geol. Mag.* **96**, 69-74.

- PITCHER W.S. and SHACKLETON R.M. (1966). On the correlation of certain Lower Dalradian successions in Northwest Donegal. *Geol. Jl*, 5, 149-156.
- PITCHER, W.S. and BERGER, A. R. (1972). *The Geology of Donegal: A study of Granite Emplacement and Unroofing*. Wiley-interscience 435 pp.
- PITCHER, W.S., ATHERTON, M.P., COBBING, E.J. and BECKINSALE, R.D. (1985). *Magmatism at a plate edge: The Peruvian Andes*. Blackie 328 pp.
- PIWINSKI, A.J. and WYLLIE, P.J. (1968). Experimental studies of igneous rock series: A zoned pluton in the Wallowa Batholith, Oregon. *Jl Geology* 76, 205-234.
- PIWINSKI, A.J. (1975). Experimental studies of granitoid rocks near the San Andreas fault zone in the Coast and Transverse Ranges and Mojave Desert, California. *Tectonophysics* 25, 217-231.
- PLANT, J.A., BROWN, G.C., SIMPSON, P.R. and SMITH, R.T. (1980). Signatures of metalliferous granites in the Scottish Caledonides. *Trans. Instn. Min. Metall.* (Sect B.) 89, 198-210.
- PLANT, J.A., SIMPSON, P.R., GREEN, P.M., WATSON, J.V. and FOWLER, M.B. (1983). Metalliferous and mineralised Caledonian granites in relation to regional metamorphism and fracture systems in northern Scotland. *Trans. Instn. Min. Metall.* (Sect. B.), 92, 33-41
- PLANT, J.A. (1986). Models for granites and their mineralizing systems in the British and Irish Caledonides. In, ANDREW, C.J. et al. (eds) *Geology and genesis of mineral deposits in Ireland*, Irish Association for Economic Geology (Dublin), 121-156.
- RAASE, P. (1974). Aluminium and Titanium contents of hornblende, indicators of pressure and temperature of metamorphism. *Contrib. Mineral. Petrol.* 45, 231-236.
- RAGLAND, P.C. (1989). *Basic analytical petrology*. Oxford Uni. Press, 369 pp.
- RAMSAY, J.G. (1980). Shear zone geometry: a review. *Journal of Structural Geology*. 2, 83-99.
- READ, H.H. (1961). Aspects of Caledonian magmatism in Britain. *Liverpool and Manchester Geological Journal* 2, 653-683.
- REGAN, P.F. (1985). The early basic intrusions. In PITCHER, W.S., ATHERTON, M.P., COBBING, E.J. and BECKINSALE, R.D. (eds), In *Magmatism at a Plate Edge*, Blackie, 72-89.
- REYNOLDS, D.L. (1936). Demonstration in petrogenesis from Kiloran Bay, Colonsay. *Min. Mag.* 24, 237-407.
- REYNOLDS, D.L. (1954). Fluidisation as a geological process and its bearing on the problem of intrusive granites. *Am. J. Sci.* 252, 577-614.
- ROBIN, P.Y.F. and BALL, D.G.A. (1988). Coherent lamellar exsolution in ternary pyroxenes: A pseudobinary approximation. *Am Mineral.* 73, 253-260.
- ROBINSON, P., SPEAR, F.S., SCHUMAKER, J.C., LAIRD, J., KLEIN, C, EVANS, B.W. and DOOLAN, B.L. (1982) Phase relations of metamorphic amphiboles: Natural occurrences and theory. *Min. Soc. Amer. Rev. in Mineralogy*, 9B, 381-387.
- ROCK, N.M.S. (1984). Nature and origin of calc alkaline lamprophyres: minettes, vogesites, kersantites and spessartites. *Trans. Royal Soc. Edinburgh. Earth Sciences* 74 193-227.
- ROCK, N.M.S. (1991). *Lamprophyres*, Blackie 285 pp.
- ROCK, N.M.S., DULLER, P., HAZELDINE, R.S. and GROVES, D.I. (1985). Lamprophyres as potential Gold exploration targets: some preliminary observations and speculations. *University of Western Australia* 11, 271-286.
- ROGERS, G., and DUNNING, G.R. (1990). Geochronology of appinitic and related granitic magmatism in the W Highlands of Scotland: constraints on the timing of transcurrent fault movement. *Jl geol. Soc. London* 147, 1-11.

RYE, R.O., SCHUILING, R.D., RYE, D.M. and JANSEN, J.B.H. (1976). Carbon, hydrogen and oxygen isotope studies of the regional metamorphic complex at Naxos, Greece. *Geochim Cosmochim Acta*, **40**, 1031-1049.

SABINE, P.A. (1963). The Strontian granite complex, Argyllshire: *Bulletin of the Geological Survey of Great Britain* **20**, 6-42.

SANDERSON, D.J. and MENEILLY, A.W. (1981). Analyses of 3D. strain modified uniform distributions: Andalusite fabrics from a granite aureole. *Journal of Structural Geology*, **3**, 109-116.

SCHLIDOWSKI, M. (1988). A 3,800-million-year isotopic record of life from carbon in sedimentary rocks. *Nature*, **333**, 313-318.

SHEPPARD, S.M.F., NIELSEN, R.L. and TAYLOR, H.P. Jr. (1969). Oxygen and hydrogen isotope ratios of clay minerals from porphyry copper deposits. *Econ. Geol.* **64**, 755-777.

SHEPPARD, S.M.F. (1986). Characterisation and isotopic variations in natural waters. In, VALLEY, J.W., TAYLOR, H.P. and O'NEIL, J.R. (1986). Stable isotopes in high temperature geological processes, *Min. Soc. Amer. Rev. in Mineralogy* **16**, 165-181.

SHEPPARD, S.M.F. and GUSTAFSON, L.B. (1976). Oxygen and hydrogen isotopes in the porphyry copper deposit at El Salvador, Chile. *Econ. Geol.* **71**, 1549-1559.

SHERATON, J. W. and BLACK, L.P. (1981) *Contrib. Mineral. Petrol.* **78**, 305-317.

SHIEH, Y.N. and TAYLOR, H.P. (1969a). O and C isotope studies of contact metamorphism of carbonate rocks. *Jl Petrol.* **10**, 307-331.

SIMPSON, P.R., BROWN, G.C., PLANT, J. and OSTLE, D. (1979). Uranium mineralisation and granite magmatism in Britain. *Phil. Trans. R. Soc. Lond.* **291**, 385-412..

SPEAR, F.S. (1988). Depth and mineralogy of the magma source or pause region for the Carboniferous Liberty Hill pluton, South Carolina, *Geology* **16**, 521-524.

STEPHENS, W.E. (1988). Granitoid plutonism in the Caledonian orogen of Europe. From: Harris, A.L. and Fettes, D.J. [eds.] *The Caledonian-Appalachian orogen*. Geological Soc. Spec Pub. **38**, 389-403.

STEPHENS, W.E. and HALLIDAY, A.N. (1984). Geochemical contrasts between late Caledonian granitoid plutons of northern, central and southern Scotland. *Trans. Royal Society of Edinburgh. Earth Sciences*, **75**, 259-273, Special Publication.

STORMER, J.C. Jr and NICHOLLS, J. (1978). XLFRAC: A program for the interactive testing of magmatic differentiation models. *Computers and Geosciences*, **4**, pp 143-159. Pergamon.

STRECKEISEN, A. (1976). To each rock its proper name. *Earth Sci. Rev.* **12**, 1-33.

SUN, S - S. (1980). Lead isotopic study of young volcanic rocks from mid-ocean ridges, ocean islands and island arcs. *Phil. Trans. R. soc. Lond.* **A297**, 409-445.

SUTHERLAND, D.S. (1982). Igneous Rocks of the British Isles, Wiley Interscience. In, SUTHERLAND, D.S. (Ed), *Igneous rocks of the British Isles*, Wiley Interscience.

SUZUOKI, T. and EPSTEIN, S. (1976). Hydrogen isotope fractionation between OH-bearing minerals and water. *Geochim. Cosmochim Acta.* **40**, 1229-1240.

TAGIRI, M. (1977). Fe-Mg partition and miscibility gap between co-existing calcic amphiboles from the Southern Abakuma plateau, Japan. *Contrib. Mineral. and Petrol.* **62**.

TARNEY, J., SAUNDERS, A.D., MATLEY, D.P., WOOD, D.A. and MARSH, N.G. (1981). Geochemical aspects of back arc spreading in the Scotia sea and western Pacific: In Extensional tectonics associated with convergent plate boundaries. *Phil. Trans. R. Soc. Lond.* **300**, 263-285.

THOMPSON, R.N., MORRISON, M.A., HENDRY, G.L. AND PARRY, S.J. (1984). *An assessment of the relative roles of crust and mantle in magma genesis: an elemental approach.*

- TAYLOR, H.P. Jr. (1974). The application of oxygen and hydrogen isotope studies to problems of hydrothermal alteration and ore deposition: *Econ. Geol.* **69**, 843-883.
- TAYLOR, H.P. Jr. (1977). Water/rock interactions and the origin of H₂O in granitic batholiths. *Jl geol. Soc. London.*, **133**, 509-558.
- TAYLOR, H.P. Jr. (1986). Igneous rocks II. Isotopic case studies of circumPacific magmatism. In, VALLEY, J.W., TAYLOR, H.P. and O'NEIL, J.R. (1986) Stable isotopes in high temperature geological processes. *Min. Soc. Amer. Rev. in Mineralogy* **16**, 165-181.
- TAYLOR, H.P. Jr. and SHEPPARD, S.M.F. (1986). Igneous rocks I. Processes of isotopic fractionation and isotope systematics. In VALLEY, J.W., TAYLOR, H.P. and O'NEIL, J.R. (1986) Stable isotopes in high temperature geological processes. *Min. Soc. Amer. Rev. in Mineralogy* **16**, 227-271.
- TAYLOR, H.P. Jr. and FORESTER, R.W. (1971). Low-¹⁸O Igneous rocks from the intrusive complexes of Skye, Mull, and Ardnamurchan, Western Scotland. *Jl Petrol.* **12**, 465-497.
- TAYLOR, B.E. and O'NEIL, J.R. (1977). Stable isotope studies of metasomatic Ca,Fe,Al, Si skarns and associated metamorphic and igneous rocks, Osgood mountains, Nevada. *Contrib Mineral Petrol.* **63**, 1-49.
- THIRLWALL, M.F. (1981). Implications for Caledonian plate tectonic model of chemical data from volcanic rocks of the British Old Red Sandstone. *Jl geol. Soc. London* **138**, 123-138.
- THIRLWALL, M.F. (1982). Systematic variation in chemistry and Nd-Sr isotopes across a Caledonian calc-alkaline volcanic arc: implications for source materials. *Earth Planet. Sci. Lett.* **58**, 27-50.
- THOMPSON, R.N., MORRISON, M.A., HENDRY, G.L. and PARRY, S.J. (1984). An assessment of the relative roles of crust and mantle in magma genesis: an elemental approach. In MOORBATH, S., THOMPSON, R.N. and OXBURGH, E.R. (eds) *The relative contributions of mantle, oceanic crust and continental crust to magma genesis*. Phil. Trans. R. Soc. Lond. **310**, 437-480.
- THORPE, R.S. (1982). Precambrian igneous rocks of England, Wales and south-eastern Ireland. In, SUTHERLAND, D.S. (ed) *Igneous rocks of the British Isles*, 19-35.
- TINDLE, A.G., MCGARVIE, D.W. and WEBB, P.C. (1988). The role of hybridization and crystal fractionation in the evolution of the Cairnsmore of Carsphairn Intrusion, Southern Uplands of Scotland. *J. Geol. Soc. Lond.* **145**, 11-21.
- TOMKIEFF, S.I. (1983) *Dictionary of petrology*, Wiley 680 pp.
- TYRELL, G.W. (1928). The Geology of Arran, *Mem. Geol. Surv. Scotland*, 168 pp.
- VALLEY, J.W. (1986). Stable isotope geochemistry of metamorphic rocks. In VALLEY, J.W., TAYLOR, H.P. and O'NEIL, J.R. (1986) Stable isotopes in high temperature geological processes. *Min. Soc. Amer. Rev. in Mineralogy* **16**, 445-486.
- VYHNAL, C.R., McSWEEN, H.Y Jr. and SPEER, J.A. (1991). Hornblende chemistry in southern Appalachian granitoids: Implications for aluminium hornblende thermobarometry and magmatic epidote stability. *Am. Mineral.* **76**, 176-188.
- WADSWORTH, W.J. (1982). The basic plutons. In, *Igneous rocks of the British Isles*. Eds: Sutherland D.S. (ed) 135-148.
- WALKER, F. (1927). The igneous geology of the Ardsheal Hill, Argyllshire. *Trans Royal Soc. Edin.* **4**, 147-157.
- WALKER, G.P.L. (1975). Evolution of the British Tertiary centres. *Jl geol Soc London.* **131**, 121-141.
- WALKER, G.P.L. and LEEDAL, G.P. (1954). The Barnesmore granite complex, Co. Donegal, *Sci. Proc. R. Dubl. Soc.* **26**, 207-243.

- WATSON, J. (1984) The ending of the Caledonian orogeny in Scotland. *Jl geol. Soc. London* **141**, 193-214.
- WEAVER, B.L. and TARNEY, J. (1981). *Contrib. Mineral. Petrol.* **78**, 175-188.
- WEISS, S. and TROLL, G. (1989). The Ballachullish igneous complex, Scotland: Petrography, mineral chemistry, and order of crystallisation in the monzodiorite-quartz diorite suite and in the granite. *Jl Petrol.* **30**, 1069-1115.
- WELLS, A.K. and BISHOP, A.C. (1955). An appinitic facies associated with certain granites in Jersey, Channel islands. *Quart. Jl geol. Soc. London* **111**, 143-163.
- WENNER, D.B. and TAYLOR, H.P. (1971). Temperatures of serpentinisation of ultramafic rocks based on $^{18}\text{O}/^{16}\text{O}$ fractionation between co-existing serpentine and magnetite. *Contrib. Mineral. Petrol.* **32**, 165-185.
- WHALEN, J.B., CURRIE, K.L. and VAN BREEMEN, D. (1987). Episodic Ordovician - Silurian plutonism in the Topsails Igneous Terrane, W Newfoundland. *Trans R Soc Edinburgh, Earth Sci.* **78**, 17-28.
- WHITE, S. (1976) Inter-relationship between chemistry and deformation in tectonically deformed minerals (abstr) *Int. Congr. Electron Microscop.* (Proc.) **8**, 482-483.
- WHITE A.J.R. and CHAPPELL B.W. (1983). Granitoid types and their distribution in the Lachlan fold belt, southern Australia. *Mem. Geol. Soc. Am.* **159**, 21-34.
- WHITE, N.J. and HUTTON, D.H.W. (1985) The structure of the Dalradian rocks in West Fanad, Co. Donegal. *Ir. Jl Earth Sci.* **7**, 79-92.
- WHITFORD, D.J., NICHOLLS, I.A. and TAYLOR, S.R. (1979). Spatial Variations in the Geochemistry of Quaternary lavas across the Sunda Arc in Java and Bali. *Contrib. Mineral. Petrol.* **70**, 341-356.
- WILLAN, R.C. and COLEMAN, M.L. (1983). Sulfur isotope study of the Aberfeldy barite, zinc, lead and minor sulfide mineralisation in the Dalradian metamorphic terrane, Scotland. *Econ. Geol.* **78**, 1169-1650.
- WRIGHT A.E. and BOWES D.R. (1968). Formation of explosion breccias. *Bull Volcanologique.* **32**, 15-32
- WRIGHT A.E. and BOWES D.R. (1979). Geochemistry of the Appinite suite. In *The Caledonides of the British Isles- Reviewed.*, Spec Publ. geol. Soc. London.
- YARDLEY, B.W.D., VINE, F.J. and BALDWIN, C.T. (1982). The plate tectonic setting of N.W. Britain and Ireland in Late Cambrian and Early Ordovician times. *Jl geol. Soc. London* **139**, 455-463.
- YODER, H.S. and TILLEY, C.E. (1962). Origin of basalt magmas: an experimental study of natural and synthetic rock systems. *Jl Petrol.* **3**, 342-532.
- ZALESKI, E. (1982). The Geology of Speyside and Lower Findhorn Granitoids. Unpublished M. Sc. thesis, University of St. Andrews.
- ZEN, E.-AN. and HAMMARSTROM, M.J. (1984). Magmatic epidote and its petrological significance. *Geology*, **12**, 515-518.

APPENDICES

APPENDIX 1

Sample Location

Grid references quoted correspond to the 1/4" survey maps of Ireland

SAMPLE	GRID REF.	ROCK UNIT/TYPE	INTRUSION
Y2559	G 8110 9735	Hornblendite	Meenalargan
M5	G 7910 9660	Coarse diorite	Meenalargan
Y13	G 7970 9703	Coarse diorite	Meenalargan
Y1859	G 7920 9660	Coarse diorite	Meenalargan
Y1858	G 7935 9661	Coarse diorite	Meenalargan
Y25519	G 8155 9773	Coarse diorite	Meenalargan
Y1751	G 8220 9807	Diorite	Meenalargan
Y1751/	G 8220 9807	Diorite	Meenalargan
Y2554/	G 8057 9728	Diorite	Meenalargan
Y2554	G 8057 9728	Diorite	Meenalargan
Y1854	G 7951 9697	Diorite	Meenalargan
Y2552	G 8051 9735	Diorite	Meenalargan
Y458	G 7951 9701	Diorite	Meenalargan
Y2556	G 8060 9715	Diorite	Meenalargan
Y1856	G 7952 9678	Diorite	Meenalargan
Y2159	G 7913 9624	Diorite	Meenalargan
M14	G 7895 9674	Diorite	Meenalargan
M11	G 7896 9663	Diorite	Meenalargan
M10	G 9703 9659	Diorite	Meenalargan
Y25518	G 8159 9763	Diorite	Meenalargan
Y25511	G 8114 9772	Diorite	Meenalargan
Y453	G 7951 9666	Migmatitic diorite	Meenalargan
Y1851	G 7957 9677	Hybrid diorite	Meenalargan
Y1	G 7910 9682	"Appinite"	Meenalargan
Y1452	G 7969 9710	Tonalite	Meenalargan
Y4	G 7952 9687	Melagabbro	Meenalargan
Y2557	G 8055 9688	Metadolerite	Meenalargan
76c	G 7070 9925	Hornblendite	Narin-Portnoo
Y2657	G 7069 9925	Hornblendite	Narin-Portnoo
Ap2	G 6950 9972	Meladiorite	Narin-Portnoo
AP1'	G 6950 9973	Meladiorite	Narin-Portnoo
HB	G 7068 9923	Hornblendite	Narin-Portnoo
Y2652	G 7069 9924	Meladiorite	Narin-Portnoo
Y27517	G 7063 9930	Hornblende diorite	Narin-Portnoo
Y30517	G 7052 9937	Hornblende diorite	Narin-Portnoo
Y77	G 7035 9940	Diorite	Narin-Portnoo
Y55	G 7040 9940	Diorite	Narin-Portnoo
Y80	G 6990 9971	Diorite	Narin-Portnoo
Y71	G 7036 9940	Diorite	Narin-Portnoo
31515	G 6950 9973	Diorite	Narin-Portnoo
3153	G 6950 9974	Diorite	Narin-Portnoo
Y26523	G 7060 9938	Diorite	Narin-Portnoo
Y31512	G 7030 9941	"Appinite"	Narin-Portnoo
31511	G 7030 9941	"Appinite"	Narin-Portnoo
Y168	G 7010 9967	"Appinite"	Narin-Portnoo
26510	G 7078 9931	"Appinite"	Narin-Portnoo
Y167	G 7009 9967	Biotite meladiorite	Narin-Portnoo
Y30513'	G 7052 9937	Contaminated diorite	Narin-Portnoo
Y2655	G 7062 9938	Contaminated diorite	Narin-Portnoo
Y27512	G 7061 9939	Contaminated diorite	Narin-Portnoo
Y3059	G 7051 9937	Hybrid diorite	Narin-Portnoo
Y1951	G 6993 9965	Dioritic xenolith	Narin-Portnoo
Y663	G 6972 9965	Dioritic xenolith	Narin-Portnoo

SAMPLE	GRID REF.	ROCK UNIT/TYPE	INTRUSION
Y27511	G 7062 9939	Biotite diorite	Narin-Portnoo
Y6614	G 6972 9971	Biotite diorite	Narin-Portnoo
Y3612	G 6980 9971	Biotite diorite	Narin-Portnoo
Y667	G 6971 9971	Biotite diorite	Narin-Portnoo
Y6612	G 6972 9971	Biotite diorite	Narin-Portnoo
Y268	G 6980 9972	Biotite diorite	Narin-Portnoo
Y269	G 6980 9972	Biotite diorite	Narin-Portnoo
Y6611	G 6981 9971	Biotite diorite	Narin-Portnoo
Y668	G 6980 9971	Biotite diorite	Narin-Portnoo
Y6613	G 6979 9971	Biotite diorite	Narin-Portnoo
Y3613	G 6979 9972	Biotite diorite	Narin-Portnoo
Y761	G 6949 9960	Biotite diorite	Narin-Portnoo
CS1	G 6970 9970	Portnoo Limestone	Narin-Portnoo
CS2	G 6970 9970	Portnoo Limestone	Narin-Portnoo
30515	G 6967 9968	Portnoo Limestone	Narin-Portnoo
30512	G 6965 9965	Portnoo Limestone	Narin-Portnoo
69f	G 6960 9965	Portnoo Limestone	Narin-Portnoo
69e	G 6915 9990	Portnoo Limestone	Narin-Portnoo
69a	G 6899 9982	Portnoo Limestone	Narin-Portnoo
69d	B 6880 0000	Portnoo Limestone	Narin-Portnoo
69c	G 6875 9985	Portnoo Limestone	Narin-Portnoo
69b	G 6805 0010	Portnoo Limestone	Narin-Portnoo
Limey 1	B 9052 3015	Falcarragh Limestone	E. of Falcarragh
S5	G 7002 9645	Meladiorite	Summy Lough
Y21	G 7050 9647	Meladiorite/hornblendite	Summy Lough
Y17	G 7070 9730	Coarse appinite dyke/H'ite	Summy Lough
Y1796	G 7026 9865	Diorite	Summy Lough
Y19911	G 7050 9648	Diorite	Summy Lough
Y1991/	G 7085 9732	Diorite	Summy Lough
Y1691	G 7030 9632	Diorite	Summy Lough
Y1996	G 7049 9647	Diorite	Summy Lough
Y1995	G 7049 9647	Diorite	Summy Lough
Y1999	G 7049 9647	Diorite	Summy Lough
Y1694	G 7042 9635	Diorite	Summy Lough
Y1992	G 7048 9646	Diorite	Summy Lough
Y1997	G 7048 9648	Diorite	Summy Lough
Y2093	G 7850 9905	Diorite	Mulnamin
Y2098	G 7849 9905	Meladiorite/Hornblendite	Mulnamin
Y20911	G 7851 9904	Hornblende diorite	Mulnamin
GLAP	G 7797 9735	"Appinite"	Glenard
Kilr	G 7970 9222	Cortlandtite	Kilrean
Kilr Hb Rim	G 7990 9217	Hornblendite	Kilrean
Bir Dio	G 6898 9872	Diorite	Biroge Pipe
Y65	G 7075 9920	Lamprophyre	Narin-Portnoo
Y68	G 7070 9921	Lamprophyre	Narin-Portnoo
Y164	G 6995 9970	Lamprophyre	Narin-Portnoo
Y168	G 6996 9971	Lamprophyre	Narin-Portnoo
Y27516	G 7062 9934	Lamprophyre	Narin-Portnoo
Y163	G 6994 9970	Lamprophyre	Narin-Portnoo
Y43	G 7330 9901	Quartz Monzodiorite	Ardara pluton
Y861	G 7207 9861	Quartz Monzodiorite	Ardara pluton
Y862	G 7220 9848	Quartz Monzodiorite	Ardara pluton
Y863	G 7225 9840	Quartz Monzodiorite	Ardara pluton
Y864	G 7227 9824	Quartz Monzodiorite	Ardara pluton
Y866	G 7225 9820	Quartz Monzodiorite	Ardara pluton
Y1262	G 7320 9863	Quartz Monzodiorite	Ardara pluton
Y1265	G 7365 9858	Quartz Monzodiorite	Ardara pluton
Y1266	G 7370 9850	Quartz Monzodiorite	Ardara pluton
Y8610	G 7261 9825	Qtz M'diorite/granodiorite	Ardara pluton
Y49	G 7252 9754	Qtz M'diorite/granodiorite	Ardara pluton
Y8611/	G 7261 9791	Qtz M'diorite/granodiorite	Ardara pluton

SAMPLE	GRID REF.	ROCK UNIT/TYPE	INTRUSION
Y8612	G 7259 9773	Qtz M'diorite/granodiorite	Ardara pluton
Y8613	G 7292 9773	Qtz M'diorite/granodiorite	Ardara pluton
Y1264	G 7362 9838	Qtz M'diorite/granodiorite	Ardara pluton
Y1268	G 7390 9830	Qtz M'diorite/granodiorite	Ardara pluton
Y1362	G 7395 9848	Qtz M'diorite/granodiorite	Ardara pluton
Y1364	G 7395 9842	Qtz M'diorite/granodiorite	Ardara pluton
Y1365	G 7390 98254	Qtz M'diorite/granodiorite	Ardara pluton
Y1367	G 7402 9822	Qtz M'diorite/granodiorite	Ardara pluton
Y965	G 7458 9760	Qtz M'diorite/granodiorite	Ardara pluton
Y2153	G 7810 9680	Qtz M'diorite/granodiorite	Ardara pluton
Y451	G 7910 9650	Qtz M'diorite/granodiorite	Ardara pluton
Y63e	G 8072 9640	Qtz M'diorite/granodiorite	Ardara pluton
Y34	G 7580 9540	Granodiorite	Ardara pluton
Y37	G 7420 9375	Granodiorite	Ardara pluton
Y868	G 7240 9819	Granodiorite	Ardara pluton
Y37/	G 7420 9375	Granodiorite	Ardara pluton
Y90	G 7040 9555	Granodiorite	Ardara pluton
Y94	G 7250 9500	Granodiorite	Ardara pluton
Y961	G 7470 9730	Granodiorite	Ardara pluton
Y962	G 7470 9731	Granodiorite	Ardara pluton
Y963	G 7471 9740	Granodiorite	Ardara pluton
Y8615	G 7315 9720	Granodiorite	Ardara pluton
Y8616	G 7316 9728	Granodiorite	Ardara pluton
Y8616/	G 7316 9728	Granodiorite	Ardara pluton
Y1368	G 7420 9750	Granodiorite	Ardara pluton
Y1267	G 7370 9839	Granodiorite	Ardara pluton
Y7612	G 6950 9961	Granitoid	Narin-Portnoo
Y763	G 6950 9960	Granitoid	Narin-Portnoo
Y3610	G 6985 9973	Granitoid	Narin-Portnoo
Y2611	G6986 9972	Granitoid	Narin-Portnoo
Y466	G 6977 9978	Granitoid	Narin-Portnoo
Y665	G 6971 9974	Granitoid	Narin-Portnoo
Y661	G 6872 9973	Granitoid	Narin-Portnoo
Y169	G 7010 9964	Granitoid	Narin-Portnoo
Y261	G 7000 9966	Granitoid	Narin-Portnoo
Y1952	G 6994 9966	Granitoid	Narin-Portnoo
Y1451	G 7930 9720	Granitoid	Narin-Portnoo
GL1	G 7778 9734	Granodiorite	Glenard
Y9	G 7797 9728	Granitoid	Glenard
GLGR1	G 7796 9730	Hornblende granodiorite	Glenard
Y556	G 8020 9615	Granite	Meenalargan
Y2057	G 8210 9728	Granite	Meenalargan
Y555	G 8025 9620	Granite	Meenalargan
Y2455	G 7840 9665	Granite	Meenalargan
Y658	G 8075 9698	Granite	Meenalargan
Y359	G 7950 9682	Granite	Meenalargan
Y1656	G 8130 9755	Granite	Meenalargan
Y6204	G 8320 9825	Granite	Meenalargan
Y16511	G 8320 9810	Granite	Meenalargan
Y25514	G 8125 9757	Granite	Meenalargan
MDG	G 8425 9850	Granite	Main Donegal Gr
Y2096	G 7900 9910	Granite	Mulnamin
Y31	G 7600	Xenolith	Ardara pluton
YSH1	G 7020 9680	Xenolith	Ardara pluton
YSH5	G 7065 9560	Xenolith	Ardara pluton

APPENDIX 2

Sample Preparation and Analytical Techniques

A 2.1 STABLE ISOTOPIC ANALYSIS-PREPARATION

A 2.1.1. PREPARATION

(i) **Crushing:** Samples were analysed in two forms, as whole rock powders for both oxygen and carbon and some as mineral separates for oxygen and hydrogen. All samples were jaw crushed to small chips and then powdered in a Tema tungsten carbide swing mill and sieved to less than 240 mesh for whole rock.

(ii) **Acid Leaching:** the samples of Portnoo marble and the appinites required removal of the carbonate component before analysing for $\delta^{18}\text{O}$ silicate. The marble was acid leached in 10% HCl for 3 days and then analysed for purity using XRD methods (see section A 1.3). For hydrogen analysis it was also necessary to remove the carbonate component but in the case of marble away from the contact leaching in a strong acid would have affected the muscovite and chlorite component. Thus the samples were leached in 17% acetic acid over several days. In the case of the appinite only hornblende was to be preserved so a solution of 50% acetic acid was used. Those samples which were analysed for δD were not acid leached.

(iii) **Mineral Separation:** several samples of hornblende, biotite, muscovite and epidote were separated using the techniques of Hutchison, (1974), namely heavy liquid and electromagnetic separation and hand-picking. A sample size fraction of 120μ was firstly thoroughly washed in distilled water to remove rock flour and to clean the sample and then mineral species were hand-picked with the assistance of a binocular microscope, then 'purified' by separation in solutions of tetrabromoethane, ($\text{SG}=2.967$ at 20°C) and di-iodomethane, ($\text{SG}=3.325$ at 20°C), and diluted by Analar grade acetone if required. Finally, in order to concentrate hornblende and biotite the samples were passed through a Franz electromagnetic resonator and the purity of the separates was estimated with the aid of a binocular microscope, and as a final check of purity they were analysed using XRD. Purity of separates is thought to be better than 98%. Samples separated in heavy liquid were thoroughly rinsed in Analar grade acetone after separation, filtered through fine filter paper and rinsed in distilled water to remove any further dust particles. Godfrey (1962) states that the use of heavy liquids does not affect the deuterium content of hydrous minerals.

(iv) Accuracy and Precision.

The yield of oxygen and hydrogen from whole rock appinite samples was compared with the calculated yields of mineral separates of hornblende and was found to be within 5-10% of the calculated yield for hornblende (AP2 and 26510). The yield was then used as a measure of the accuracy of the measured result from each sample together with those yields calculated by Jenkin (pers comm.) for calcite and biotite.

A2.1.2. ISOTOPIC RATIO DETERMINATION

(i) Silicate oxygen ($\delta^{18}\text{O}$)

Whole rock samples were acid-leached to remove the calcareous fraction and mineral separates were analysed using the fluorination technique of Borthwick and Harmon (1982), by reaction with ClF_3 in nickel furnaces at 600°C for 12 hours, using 10-20 mg of powdered sample and mineral separate. CO_2 was produced from the liberated oxygen by combustion with a resistance-heated carbon rod, using the method of Taylor & Epstein (1962). Analysis of the gas was made on a M^cKinney-Nier type mass spectrometer 'VG Sira 10', with total analytical precision of $\pm 0.2\text{‰}$ for $\delta^{18}\text{O}$ ratios. This error value includes combined sampling, analytical and instrumental errors. The laboratory standard run in repeat analyses was NBS#28 which gives an average delta value of $+9.6\text{‰}$. Where possible samples were duplicated and replicated until acceptable precision was attained.

(ii) Carbon ($\delta^{13}\text{C}_{\text{PDB}}$) and carbonate oxygen ($\delta^{18}\text{O}_{\text{carbonate}}$)

Carbon and oxygen isotope compositions of the carbonate fractions in the form of fine (60μ) whole rock powder were determined on CO_2 that was liberated by reaction with 100% orthophosphoric acid (McCrea, 1950). The whole rock samples were reacted with the acid at 25°C for 15 hours. Again CO_2 released was measured on a M^cKinney-Nier type mass spectrometer 'VG Sira 10', with total analytical precision of $\pm 0.02\text{‰}$ for $\delta^{13}\text{C}$ and $\delta^{18}\text{O}$. The laboratory standard used for the carbonates was NBS#19 which gives an average $\delta^{13}\text{C}$ value of $+1.92$ (PDB) ‰ and a $\delta^{18}\text{O}$ value of -2.19 (SMOW) ‰ . Another laboratory standard used was the SURRC MBL1 standard which gives an average $\delta^{13}\text{C}$ value of $+2.0$ (PDB) ‰ and a $\delta^{18}\text{O}$ value of -1.8 (SMOW) ‰ .

(iii) Hydrogen

H_2O was liberated from whole rock and mineral separate samples of the hydrous minerals by induction heating, subsequent reaction with a hot uranium furnace allowed conversion to hydrogen following the technique of Friedman (1953). Hydrogen released was measured on a M^cKinney-Nier type mass spectrometer 'VG Micromass 602B', with analytical precision of $\pm 1-2\text{‰}$ for δD ratios. This value includes analytical and instrumental error. The standard used for repeat analyses was NBS #30 which gives repeat analyses of -64‰ .

A 2.2 X-RAY FLUORESENCE ANALYSIS.

Samples for XRF analysis were prepared initially by crushing cleaned whole rock samples in a Tema tungsten carbide swing mill to a powder of less than 240 mesh. X-ray analysis was performed on a Philips PW 1212 using a Rh tube for primary excitation. Major elements were determined from fused glass beads of the powder essentially following the method of Norrish & Hutton (1969), fusing with Spectroflux 105. Weight loss was determined by weighing before and after fusing the glass bead. Trace elements were analysed on pressed powder discs prepared by pressing to 12 tons a 6g powder mixed with Moviol as a binder. The elements were excited with a Rh tube and analysed with either Li F200 or Li F220 crystals. All elements were determined by ratio to a minitor for which the composition is accurately known. For major elements For trace elements a mass absorption correction based on major oxide composition was applied.

The precision estimates are based on six replicate analyses on six separate beads or pressed powder pellets (trace elements and MnO) of a granodiorite and the standard deviation values are derived in the manner of Harvey et al. (1973). Precision estimates are expressed as wt% for major elements and ppm for trace elements.

Element	Standard Deviation	Element	Standard Deviation
SiO ₂	0.177	Sr	1.8
TiO ₂	0.006	Rb	1.4
Al ₂ O ₃	0.042	Th	4.2
Fe ₂ O ₃	0.114	Pb	0.8
MnO	0.0003	Zn	0.7
MgO	0.035	Cu	0.8
CaO	0.010	Ni	1.2
Na ₂ O	0.099	Cr	1.4
K ₂ O	0.013	V	0.9
P ₂ O ₅	0.011	Ba	8.0
Nb	2.0	Hf	0.41
Zr	6.9	Ce	2.0
Y	1.5	La	1.3

A 2.3 X-RAY DIFFRACTION ANALYSIS

X-ray diffraction techniques were used to determine unknown minerals and to test for the presence of CaCO₃ in whole rock powders which had been previously acid leached using a Philips PW 1049 diffractometer with Hilton Brooks DG2 generator and Cu anode. The operating conditions were set at 40 Kv and 25mA through a 1° division slit and 0.2mm receiving slit with graphite monochromator. Samples were step-scanned at 0.2° per second.

APPENDIX 3

Whole rock analysis by X-Ray fluorescence.

Sample	M10	Y25518	Y25511	Y453	Y1851	Y1	Y1452	Y4	Y2557
SiO ₂	52.8	56.1	56.3	54.9	52.0	48.9	56.9	48.1	46.0
TiO ₂	0.48	0.38	0.74	0.32	0.50	1.65	0.88	2.41	3.85
Al ₂ O ₃	19.73	12.79	11.30	13.60	15.17	15.51	18.91	13.35	12.37
Fe ₂ O ₃ *	4.78	5.48	8.64	6.51	4.60	9.18	8.00	13.83	17.50
MnO	0.07	0.12	0.15	0.14	0.09	0.13	0.09	0.24	0.28
MgO	5.91	8.51	8.77	9.90	7.63	9.10	2.78	7.22	5.36
CaO	8.04	8.38	8.82	9.31	15.38	9.96	5.45	11.86	9.69
Na ₂ O	4.8	2.8	2.1	3.1	2.6	2.6	3.6	2.1	2.1
K ₂ O	1.59	1.83	1.40	1.25	0.62	1.20	3.09	0.23	0.64
P ₂ O ₅	0.15	0.07	0.12	0.04	0.13	0.37	0.25	0.27	0.47
Loss	1.80	3.80	1.00	1.20	1.20	2.20	0.60	0.00	1.00
Total	100.16	100.35	99.52	100.39	100.08	100.80	100.79	99.69	99.44

Sample	Y2554	Y2554	Y1854	Y458	Y2552	Y458	Y2556	Y1856	Y2159	M14	M11
SiO ₂	52.7	53.0	52.2	52.8	52.3	52.8	47.1	50.9	53.7	50.0	53.4
TiO ₂	0.71	0.73	0.49	1.19	1.44	1.19	3.40	1.00	1.16	2.10	0.53
Al ₂ O ₃	13.24	12.89	12.33	16.34	16.34	16.34	17.39	13.36	15.38	17.37	16.20
Fe ₂ O ₃	1.90	4.21	2.49	2.20	2.20	2.20	5.36	5.34	4.41	1.60	0.50
MnO	5.80	3.73	4.52	5.73	6.00	6.00	2.55	5.00	6.98	5.04	5.04
FeO	0.15	0.14	0.14	0.15	0.15	0.15	0.13	0.09	0.11	0.09	0.11
MgO	10.16	9.62	11.99	6.77	11.74	11.74	4.69	10.26	7.54	8.21	7.54
CaO	10.60	10.31	9.95	9.04	13.97	13.97	8.87	10.20	6.78	8.87	9.13
Na ₂ O	2.1	2.2	2.2	3.0	2.3	2.3	4.0	2.3	3.4	3.4	3.1
K ₂ O	1.01	1.00	1.16	1.35	1.27	1.27	1.28	1.28	2.31	1.92	1.93
P ₂ O ₅	0.11	0.09	0.12	0.15	0.15	0.20	0.44	0.16	0.14	0.14	0.26
Loss	1.40	1.40	1.60	2.00	2.00	2.00	1.60	1.80	1.20	0.00	2.20
Total	100.00	99.30	99.42	99.14	101.18	101.18	99.58	99.57	100.17	99.99	100.57

Fe₂O₃* : refers to wt % of total iron

Sample	76C	Y2657	AP2	API'	Y2652	Y27517	Y30517	Y77	Y55
SiO ₂	44.7	43.0	42.6	41.5	48.7	56.6	47.0	50.7	62.6
TiO ₂	1.61	1.82	1.36	1.96	0.85	0.91	0.58	0.67	0.70
Al ₂ O ₃	10.87	12.30	16.60	12.43	8.69	16.27	15.52	7.37	17.68
Fe ₂ O ₃ *	11.32	12.01	11.01	11.23	8.27	9.09	5.38	10.77	6.12
MnO	0.15	0.15	0.11	0.12	0.15	0.09	0.08	0.18	0.07
MgO	12.58	11.30	10.34	11.31	9.68	4.20	4.52	13.82	4.52
CaO	11.49	11.41	12.41	10.43	15.77	6.51	15.50	11.88	0.63
Na ₂ O	2.2	2.5	1.7	2.0	1.7	3.5	1.8	1.3	1.2
K ₂ O	1.21	1.04	0.97	1.20	0.39	2.51	0.79	0.56	3.2
P ₂ O ₅	0.06	0.10	0.02	0.05	0.08	0.29	0.11	0.05	0.13
Loss	3.80	3.60	2.40	2.40	4.60	1.40	8.00	2.00	3.40
Total	100.03	99.37	99.72	94.71	98.90	101.45	99.39	99.32	100.49

Sample	Y2559	M5	Y13	Y1859	Y1858	Y25519	Y1751	Y1751/
SiO ₂	46.95	48.65	53.46	52.92	51.48	48.95	50.54	49.34
TiO ₂	1.60	1.58	0.73	0.72	1.10	1.04	1.50	1.49
Al ₂ O ₃	13.79	14.66	14.10	14.57	16.81	14.01	18.26	17.47
Fe ₂ O ₃	0.47	2.06	1.40	0.01	2.90	2.87	3.08	7.76
FeO	9.79	7.00	5.30	7.34	4.95	6.14	4.70	n.d.
MnO	0.15	0.13	0.14	0.13	0.14	0.15	0.11	0.10
MgO	11.36	9.50	9.25	9.30	7.69	7.80	6.56	6.21
CaO	9.51	9.67	8.98	9.38	9.84	12.26	10.10	10.17
Na ₂ O	2.56	3.04	2.86	2.57	3.27	2.83	3.07	3.49
K ₂ O	1.77	1.37	1.47	1.25	1.28	0.96	1.42	1.36
P ₂ O ₅	0.32	0.11	0.12	0.15	0.23	0.33	0.23	0.22
Loss	0.80	3.00	1.60	1.60	0.40	1.80	1.60	2.20
Total	99.28	100.78	99.59	99.93	100.24	99.31	101.93	99.81

Sample	Y80	Y71	Y31515	Y3153	Y26523	Y31512	Y31511	Y168	Y26510
SiO ₂	53.4	55.1	48.8	53.2	55.1	50.2	52.6	50.7	45.2
TiO ₂	1.14	1.03	0.90	0.51	1.02	1.00	0.71	1.29	1.53
Al ₂ O ₃	16.98	17.05	19.43	10.62	17.41	14.30	10.63	16.35	12.25
Fe ₂ O ₃ *	7.05	7.78	7.42	8.78	7.51	7.70	6.78	8.72	9.15
MnO	0.10	0.10	0.08	0.15	0.14	0.10	0.14	0.16	0.13
MgO	5.79	3.90	5.14	9.37	4.64	7.90	8.72	7.20	9.46
CaO	8.01	6.78	9.23	13.43	6.12	11.80	13.59	8.13	11.09
Na ₂ O	3.1	3.5	3.1	1.0	3.7	2.8	2.2	3.7	3.1
K ₂ O	1.80	3.04	2.42	0.74	2.00	1.00	1.33	1.15	1.26
P ₂ O ₅	0.22	0.00	0.54	0.06	0.19	0.30	0.11	0.21	0.05
Loss	1.80	0.60	1.80	2.80	1.60	2.40	3.60	2.00	6.00
Total	99.43	99.10	98.84	100.66	99.56	100.50	100.56	99.30	99.16
Nb	5	11	2	8	8	4	7	4	n.d.
Zr	82	186	144	47	126	62	46	111	n.d.
Y	22	31	44	20	25	18	19	20	n.d.
Sr	864	497	861	317	521	415	316	462	n.d.
Rb	70	100	130	47	83	31	46	36	n.d.
Th	3	16	7	9	6	4	8	9	n.d.
Pb	9	20	16	13	14	11	12	17	n.d.
Zn	62	136	54	65	78	75	64	89	n.d.
Cu	n.d.	62	n.d.	27	17	n.d.	26	14	n.d.
Ni	48	62	10	33	20	35	32	29	n.d.
Cr	n.d.	56	n.d.	164	83	n.d.	163	130	n.d.
V	191	162	192	199	223	230	198	323	n.d.
Ba	n.d.	606	n.d.	210	577	n.d.	209	316	n.d.
Hf	n.d.	5	n.d.	2	3	n.d.	1	3	n.d.
Ce	60	84	88	30	50	45	29	36	n.d.
La	140	27	n.d.	12	20	94	11	16	n.d.

Fe₂O₃* : refers to wt % of total iron

Sample	Y167	Y30513/Y2655	Y27512	Y3059	Y1951	Y663	Y2751	Y27511/
SiO ₂	47.2	52.8	49.8	43.9	51.9	57.3	59.3	56.8
TiO ₂	3.43	0.70	0.62	1.27	0.65	0.90	0.80	0.87
Al ₂ O ₃	12.54	11.22	6.14	23.84	14.18	16.68	15.49	18.02
Fe ₂ O ₃ *	16.80	6.90	9.07	7.53	5.37	7.01	6.29	7.01
MnO	0.24	0.11	0.19	0.05	0.10	0.1	0.10	0.08
MgO	5.68	8.36	11.81	1.99	5.33	4.97	3.65	2.50
CaO	9.82	15.41	18.72	10.89	16.18	6.23	5.37	5.30
Na ₂ O	2.12	1.92	0.98	3.28	2.31	3.40	3.46	3.01
K ₂ O	0.52	1.59	0.83	2.15	1.89	2.50	2.90	3.93
P ₂ O ₅	0.37	0.08	0.09	0.61	0.17	0.22	0.20	0.28
Loss	2.00	1.00	2.40	1.00	1.20	2.00	2.80	0.00
Total	100.83	100.75	100.76	96.68	99.45	101.48	100.57	97.98
Nb	13	1	1	4	6	13	11	11
Zr	186	83	71	69	60	121	94	151
Y	24	17	19	18	20	16	29	26
Sr	185	364	166	685	652	462	489	653
Rb	8	69	17	71	70	161	139	110
Th	0	4	1	5	6	10	5	12
Pb	4	7	7	14	9	23	29	12
Zn	136	57	62	24	56	64	67	90
Cu	262	0	46	n.d.	3	37	29	16
Ni	43	11	16	3	3	35	10	n.d.
Cr	112	n.d.	51	n.d.	45	103	44	1
V	492	211	302	112	182	192	164	133
Ba	102	n.d.	61	n.d.	197	365	498	704
Hf	3	n.d.	2	n.d.	2	3	3	4
Ce	44	43	60	67	31	59	56	74
La	5	n.d.	13	91	26	21	24	24

Fe₂O₃* : refers to wt % of total iron

Sample	Y6614	Y3612	Y667	Y6612	Y268	Y269	Y6611	Y668	Y6613
SiO ₂	56.2	55.9	55.9	58.4	54.7	59.2	61.0	55.6	58.7
TiO ₂	0.96	1.01	0.86	0.95	1.06	0.84	0.85	1.08	0.94
Al ₂ O ₃	16.80	15.85	16.11	17.23	16.50	15.76	13.84	15.40	17.45
Fe ₂ O ₃ *	6.77	7.15	6.32	6.80	7.49	6.11	6.32	7.82	6.62
MnO	0.12	0.12	0.10	0.10	0.13	0.11	0.09	0.12	0.11
MgO	4.10	4.72	3.66	3.66	4.79	4.23	4.72	5.47	3.47
CaO	5.87	6.53	5.38	6.41	6.60	5.68	4.52	6.30	6.71
Na ₂ O	3.6	3.4	3.8	4.6	2.8	3.4	3.2	3.0	3.8
K ₂ O	2.80	2.35	2.56	1.46	2.53	2.43	2.86	2.23	1.42
P ₂ O ₅	0.28	0.21	0.23	0.25	0.21	0.17	0.29	0.20	0.20
Loss	1.80	2.80	4.60	0.00	2.80	1.80	2.60	1.80	0.20
Total	99.51	100.22	99.76	99.96	99.83	99.81	100.45	99.16	99.78
Nb	8	7	7	7	9	7	5	4	8
Zr	71	111	57	137	128	119	77	93	159
Y	23	23	20	21	19	31	22	21	26
Sr	678	674	597	521	627	405	270	492	546
Rb	114	107	95	49	108	135	182	105	51
Th	12	13	9	8	9	10	8	7	10
Pb	25	22	21	8	24	34	51	18	15
Zn	70	81	70	78	89	62	78	86	75
Cu	49	35	38	n.d.	37	36	19	9	124
Ni	14	21	9	5	20	16	22	22	5
Cr	44	69	36	n.d.	60	92	77	84	36
V	212	239	173	179	210	189	212	256	157
Ba	736	589	787	n.d.	636	373	297	539	371
Hf	3	3	2	n.d.	4	3	2	2	4
Ce	48	61	57	80	75	52	41	46	74
La	19	25	27	101	31	20	16	17	27

Fe₂O₃* : refers to wt % of total iron

Sample	Y3613	Y21
SiO ₂	59.6	50.5
TiO ₂	0.62	0.70
Al ₂ O ₃	15.38	8.57
Fe ₂ O ₃ *	5.54	9.34
MnO	0.08	0.14
MgO	4.45	14.89
CaO	6.42	10.50
Na ₂ O	3.5	2.20
K ₂ O	2.51	1.17
P ₂ O ₅	0.28	0.12
Loss	1.40	2.0
Total	100.31	100.13
Nb	8	4
Zr	103	66
Y	28	17
Sr	509	212
Rb	119	52
Th	6	6
Pb	14	10
Zn	70	64
Cu	n.d.	n.d.
Ni	11	290
Cr	n.d.	n.d.
V	126	201
Ba	n.d.	n.d.
Hf	n.d.	n.d.
Ce	51	54
La	n.d.	n.d.

Fe₂O₃* : refers to wt % of total iron

Sample	Y65	Y68	Y164	Y168	Y27516	Y163
SiO ₂	49.37	52.30	57.66	50.67	56.16	57.89
TiO ₂	3.15	1.39	0.92	1.29	0.92	0.95
Al ₂ O ₃	13.42	16.86	17.99	16.35	17.18	18.38
Fe ₂ O ₃ *	14.29	6.16	5.60	8.72	7.24	6.97
MnO	0.23	0.14	1.10	0.16	0.12	0.13
MgO	5.64	6.30	2.06	7.20	3.61	2.18
CaO	9.90	8.17	5.61	8.13	6.59	6.09
Na ₂ O	2.57	3.48	3.65	3.26	3.16	3.55
K ₂ O	0.51	1.19	2.32	1.15	1.92	2.08
P ₂ O ₅	0.36	1.60	2.20	2.00	2.40	1.40
Total	99.63	100.77	99.56	99.30	99.57	99.89

Sample	Y43	Y861	Y862	Y863	Y864	Y866	Y1262	Y1265	Y1266
SiO ₂	63.5	64.0	63.3	64.1	62.1	63.7	61.8	61.4	63.4
TiO ₂	0.79	0.80	0.78	0.82	0.79	0.80	0.80	0.90	0.84
Al ₂ O ₃	16.59	17.00	16.69	16.56	16.48	16.70	17.33	17.51	17.31
Fe ₂ O ₃ *	4.46*	0.50	1.89	3.85	3.10	3.93	4.96	5.16	4.91*
FeO	0.06	0.10	0.07	0.07	0.07	0.06	0.08	0.09	0.07
MnO	1.88	1.60	1.63	1.83	2.12	1.83	2.20	2.59	2.27
MgO	3.44	3.40	3.45	3.03	3.26	3.38	4.09	4.16	3.84
CaO	4.3	4.1	4.1	4.1	4.2	4.1	4.8	4.5	4.4
Na ₂ O	3.93	4.00	4.28	4.54	4.17	4.04	3.50	3.55	3.69
K ₂ O	0.29	0.30	0.30	0.31	0.31	0.28	0.30	0.29	0.30
P ₂ O ₅	0.80	0.20	1.40	1.00	2.20	0.80	0.80	0.60	0.00
Total	100.04	99.60	100.44	100.87	100.46	100.14	100.93	101.18	101.02

Fe₂O₃* : refers to wt % of total iron

Sample	Y43	Y861	Y862	Y863	Y864	Y866	Y1262	Y1265	Y1266
SiO ₂	63.5	64.0	63.3	64.1	62.1	63.7	61.8	61.4	63.4
TiO ₂	0.79	0.80	0.78	0.82	0.79	0.80	0.80	0.90	0.84
Al ₂ O ₃	16.59	17.00	16.69	16.56	16.48	16.70	17.33	17.51	17.31
Fe ₂ O ₃ *	4.46*	0.50	1.89	3.85	3.10	3.93	4.96	5.16	4.91*
FeO	0.06	0.10	0.07	0.07	0.07	0.06	0.08	0.09	0.07
MnO	1.88	1.60	1.63	1.83	2.12	1.83	2.20	2.59	2.27
MgO	3.44	3.40	3.45	3.03	3.26	3.38	4.09	4.16	3.84
CaO	4.3	4.1	4.1	4.1	4.2	4.1	4.8	4.5	4.4
Na ₂ O	3.93	4.00	4.28	4.54	4.17	4.04	3.50	3.55	3.69
K ₂ O	0.29	0.30	0.30	0.31	0.31	0.28	0.30	0.29	0.30
P ₂ O ₅	0.80	0.20	1.40	1.00	2.20	0.80	0.80	0.60	0.00
Total	100.04	99.60	100.44	100.87	100.46	100.14	100.93	101.18	101.02

Sample	Y43	Y861	Y862	Y863	Y864	Y866	Y1262	Y1265	Y1266
Nb	17	22	24	21	18	21	13	15	15
Zr	287	408	360	360	313	304	188	200	221
Y	24	27	28	31	29	26	22	24	23
Sr	441	423	428	420	498	446	582	600	556
Rb	204	202	211	227	193	208	142	129	156
Th	23	31	35	34	31	27	21	20	21
Pb	35	30	40	39	36	36	38	27	35
Zn	62	52	55	58	59	61	63	69	66
Cu	<2	24	34	46	25	39	24	52	41
Ni	24	19	22	20	22	24	28	30	29
Cr	<2	22	29	25	34	27	41	43	40
V	106	103	98	97	105	102	109	112	110
Ba	<5	724	659	667	696	642	728	819	680
Hf	<5	9	8	9	8	5	5	5	6
Ce	112	70	113	137	122	100	55	88	94
La	<5	15	44	64	55	39	30	36	43

Fe₂O₃* : refers to wt % of total iron

Sample	S5	17/89	Y1796	Y1991/	Y1991	Y1691	Y1996	Y1995
SiO ₂	50.5	50.4	53.90	57.1	49.1	54.1	53.0	52.8
TiO ₂	0.89	0.69	1.22	1.02	1.33	1.12	1.00	1.03
Al ₂ O ₃	10.63	8.58	16.50	16.62	15.30	17.08	14.98	14.37
Fe ₂ O ₃ *	9.04	9.33	8.28	7.45	9.80	9.34	8.77	9.23
MnO	0.12	0.16	0.14	0.12	0.16	0.14	0.22	0.13
MgO	12.86	14.87	5.50	4.45	8.78	5.52	7.80	7.95
CaO	10.25	10.54	7.18	6.05	8.24	7.66	6.64	8.71
Na ₂ O	2.5	2.1	3.3	3.6	3.1	3.4	3.1	3.2
K ₂ O	1.45	1.19	2.05	2.75	2.09	1.71	2.37	1.30
P ₂ O ₅	0.19	0.14	0.28	0.25	0.35	0.20	0.33	0.21
Loss	1.80	2.20	2.20	0.80	2.00	0.20	1.40	0.80
Total	100.24	100.20	100.73	100.25	100.26	100.34	100.85	99.75

Sample	Y1999	Y1694	Y1992	Y2093	Y2098	20911	KILR	BIRDIO
SiO ₂	50.42	54.60	54.52	53.31	52.81	48.53	50.52	47.16
TiO ₂	1.32	1.16	1.17	1.04	0.68	1.44	0.92	0.55
Al ₂ O ₃	14.70	15.19	15.23	14.59	17.06	12.93	17.04	3.87
Fe ₂ O ₃ *	9.82	8.24	8.30	9.42	8.24	9.74	8.80	11.37
MnO	0.15	0.13	0.13	0.15	0.13	0.12	0.15	0.17
MgO	8.55	6.52	6.56	7.99	7.09	11.27	7.82	22.76
CaO	8.17	7.25	7.32	8.72	8.53	10.47	9.06	10.26
Na ₂ O	3.42	3.52	3.54	3.24	3.08	2.81	3.30	4.48
K ₂ O	2.08	2.26	2.27	1.32	1.42	1.62	1.33	0.22
P ₂ O ₅	0.32	0.40	0.40	0.22	0.08	0.05	0.16	0.00
Loss	1.00	0.60	1.00	0.60	1.40	1.00	1.00	4.60
Total	100.23	99.97	100.46	100.62	100.53	100.27	100.03	99.27

Fe₂O₃* : refers to wt % of total iron

Sample	Y1999	Y1694	Y1992	Y2093	Y2098	20911	KILR	BIRDIO
Nb	10	7	3	3	0.3	3	6	0
Zr	104	100	69	81	61	113	64	14
Y	19	23	21	20	11	22	18	7
Sr	753	653	161	668	629	393	576	67
Rb	60	63	4	62	41	58	35	4
Th	6	4	2	3	4	5	5	4
Pb	18	19	3	17	10	5	12	n.d.
Zn	103	80	72	84	69	68	72	66
Cu	122	n.d.	n.d.	n.d.	n.d.	n.d.	20	n.d.
Ni	118	70	82	85	33	42	40	268
Cr	408	0	0	0	0	0	199	n.d.
V	306	205	368	227	225	388	275	187
Ba	631	n.d.	n.d.	n.d.	n.d.	n.d.	297	n.d.
Hf	3	n.d.	n.d.	n.d.	n.d.	n.d.	2	n.d.
Ce	90	94	35	53	36	24	25	41
La	n.d.	n.d.	n.d.	n.d.	n.d.	12	n.d.	n.d.

Sample	Y1999	Y1694	Y1992	Y2093	Y2098	20911	KILR	BIRDIO
SiO ₂	50.42	54.60	54.52	53.31	52.81	48.53	50.52	47.16
TiO ₂	1.32	1.16	1.17	1.04	0.68	1.44	0.92	0.55
Al ₂ O ₃	14.70	15.19	15.23	14.59	17.06	12.93	17.04	3.87
Fe ₂ O ₃ *	9.82	8.24	8.30	9.42	8.24	9.74	8.80	11.37
MnO	0.15	0.13	0.13	0.15	0.13	0.12	0.15	0.17
MgO	8.55	6.52	6.56	7.99	7.09	11.27	7.82	22.76
CaO	8.17	7.25	7.32	8.72	8.53	10.47	9.06	10.26
Na ₂ O	3.42	3.52	3.54	3.24	3.08	2.81	3.30	4.48
K ₂ O	2.08	2.26	2.27	1.32	1.42	1.62	1.33	0.22
P ₂ O ₅	0.32	0.40	0.40	0.22	0.08	0.05	0.16	0.00
Loss	1.00	0.60	1.00	0.60	1.40	1.00	1.00	4.60
Total	100.23	99.97	100.46	100.62	100.53	100.27	100.03	99.27

Fe₂O₃* : refers to wt % of total iron

Sample	Y8610	Y49	Y8611/	Y8612	Y8613	Y1264	Y1268	Y1362	Y1364
SiO ₂	64.23	63.91	61.68	61.79	61.72	64.05	63.58	64.04	64.72
TiO ₂	0.66	0.61	0.65	0.71	0.71	0.75	0.63	0.74	0.86
Al ₂ O ₃	15.87	16.28	17.07	17.04	16.35	16.97	16.76	17.00	13.63
Fe ₂ O ₃	1.04	1.55	4.77	4.75	0.14	4.59	1.91	0.70	2.36
FeO	3.10	2.65	0.00	0.00	5.00	0.00	2.21	4.01	1.54
MnO	0.06	0.08	0.08	0.82	0.09	0.07	0.08	0.07	0.06
MgO	1.80	2.54	3.26	2.57	3.37	2.30	2.01	2.10	2.16
CaO	3.37	3.45	3.27	3.81	4.17	3.68	3.27	3.60	3.20
Na ₂ O	4.21	4.67	4.03	4.27	4.26	4.37	4.82	4.50	4.42
K ₂ O	3.93	3.39	3.60	3.17	3.04	3.46	3.57	3.30	3.66
P ₂ O ₅	0.24	0.24	0.23	0.24	0.22	0.26	0.23	0.25	0.20
Loss	1.60	0.60	1.00	1.60	1.00	0.80	1.40	0.20	0.80

Total	100.22	100.18	99.85	100.96	100.27	101.50	100.65	100.74	99.93
-------	--------	--------	-------	--------	--------	--------	--------	--------	-------

Nb	15	10	0	14	14	14	10	12	9
Zr	205	170	157	144	125	171	158	210	150
Y	19	22	17	13	13	20	19	22	18
Sr	520	611	593	615	632	594	567	579	579
Rb	132	118	134	104	109	148	125	143	120
Th	30	22	5	18	11	16	9	12	9
Pb	36	41	25	35	23	33	24	27	31
Zn	53	62	61	59	67	65	50	61	50
Cu	19	33	29	27	35	23	36	147	35
Ni	24	35	39	18	45	29	23	27	30
Cr	30	70	89	42	102	44	34	36	59
V	n.d.	96	101	109	121	104	92	127	88
Ba	n.d.	761	732	601	651	633	624	723	736
Hf	n.d.	6	4	5	5	5	5	5	5
Ce	n.d.	53	64	68	62	72	42	88	76
La	n.d.	33	31	31	30	29	20	37	33

Sample	Y1365	Y1367	Y965	Y2153	Y451	Y63e	Y34	Y37	Y868
SiO ₂	67.67	64.31	68.55	66.91	63.34	63.63	70.29	71.06	71.39
TiO ₂	0.45	0.56	0.38	0.53	0.46	0.75	0.25	0.26	0.14
Al ₂ O ₃	16.45	16.16	15.58	15.91	18.00	17.49	15.67	15.09	14.86
Fe ₂ O ₃	2.02	1.83	1.51	0.24	1.62	1.30	0.64	0.20	0.26
FeO	1.07	2.32	1.10	3.40	1.26	3.37	1.20	1.45	0.90
MnO	0.05	0.07	0.05	0.08	0.04	0.05	0.05	0.04	0.02
MgO	1.69	2.31	1.85	2.22	1.52	1.41	0.99	1.22	0.51
CaO	2.74	2.79	2.09	3.04	3.30	3.20	1.64	1.20	1.45
Na ₂ O	4.35	4.31	4.51	4.99	4.84	6.34	5.32	5.66	4.15
K ₂ O	3.95	4.05	3.75	2.44	3.65	1.61	3.13	2.81	4.77
P ₂ O ₅	0.16	0.20	0.13	0.17	0.34	0.48	0.12	0.06	0.09
Loss	0.20	1.60	0.60	0.20	1.60	0.60	1.00	1.20	0.80

Total	100.78	100.50	100.29	100.31	100.16	100.24	100.47	100.38	99.52
-------	--------	--------	--------	--------	--------	--------	--------	--------	-------

Nb	7	10	12	6	12	n.d.	7	6	10
Zr	124	158	104	120	191	n.d.	101	91	121
Y	16	20	17	19	19	n.d.	13	6	15
Sr	562	515	571	726	619	n.d.	592	407	478
Rb	136	141	113	106	171	n.d.	86	58	116
Th	10	15	14	7	5	n.d.	6	13	10
Pb	31	30	27	24	31	n.d.	23	6	29
Zn	41	48	38	73	53	n.d.	49	41	42
Cu	10	52	10	53	10	n.d.	20	20	187
Ni	26	29	25	31	25	n.d.	17	12	19
Cr	48	63	56	74	44	n.d.	25	27	31
V	63	97	49	87	<5	n.d.	36	36	75
Ba	760	800	761	409	50	n.d.	635	514	550
Hf	5	5	4	4	641	n.d.	5	5	5
Ce	30	57	45	48	6	n.d.	39	35	54
La	18	29	27	25	41	n.d.	19	16	21

Fe2O3* : refers to wt % of total iron

Sample	Y37/	Y90	Y94	Y961	Y962	Y963	Y8615	Y8616	Y8616/
SiO ₂	71.88	69.37	70.66	75.86	67.37	68.43	69.25	66.89	67.02
TiO ₂	0.26	0.33	0.23	0.05	0.26	0.34	0.26	0.35	0.38
Al ₂ O ₃	15.62	15.23	15.40	13.43	15.19	15.59	16.14	15.56	15.44
Fe ₂ O ₃	0.27	0.90	0.38	0.20	0.00	1.27	0.08	0.07	0.84
FeO	1.35	1.65	1.38	0.50	2.09	0.20	2.00	2.50	2.05
MnO	0.04	0.06	0.06	0.02	0.05	0.05	0.05	0.05	0.04
MgO	1.07	1.48	0.94	0.25	1.57	1.57	1.14	1.80	1.04
CaO	1.20	1.67	1.22	0.66	1.60	2.45	1.79	2.10	3.65
Na ₂ O	5.41	5.08	4.91	4.01	4.87	4.61	4.45	4.78	5.03
K ₂ O	3.08	3.04	3.57	4.53	3.00	3.59	3.00	3.00	2.74
P ₂ O ₅	0.06	0.10	0.09	0.00	0.10	0.13	0.10	0.11	0.15
Loss	1.40	1.00	0.80	0.20	3.60	0.80	1.00	2.80	0.80

Total	101.77	99.90	99.81	99.82	99.85	99.21	99.40	100.18	99.19
-------	--------	-------	-------	-------	-------	-------	-------	--------	-------

Nb	7	7	7	4	5	9	10	11	n.d.
Zr	90	91	79	57	87	120	108	101	n.d.
Y	6	10	8	9	10	15	6	7	n.d.
Sr	431	527	499	206	536	548	505	554	n.d.
Rb	68	95	103	125	94	123	92	98	n.d.
Th	13	15	13	7	9	15	14	6	n.d.
Pb	17	32	32	42	23	33	38	38	n.d.
Zn	41	54	39	5	45	45	39	40	n.d.
Cu	12	42	16	20	19	14	21	46	n.d.
Ni	20	19	16	5	18	25	17	23	n.d.
Cr	27	40	19	<2	32	55	30	47	n.d.
V	36	57	30	11	36	53	34	44	n.d.
Ba	514	567	830	594	536	623	449	616	n.d.
Hf	5	4	4	2	4	4	4	4	n.d.
Ce	35	32	30	0	40	47	43	40	n.d.
La	16	14	24	6	21	32	22	20	n.d.

Fe2O3* : refers to wt % of total iron

Sample	Y1368	Y1267	Y7612	Y763	Y3610	Y2611	Y466	Y665	Y661
SiO ₂	70.38	69.90	73.27	75.05	71.89	72.97	70.58	69.98	65.42
TiO ₂	0.21	0.24	0.15	0.16	0.11	0.19	0.27	0.22	0.62
Al ₂ O ₃	15.90	15.06	14.35	14.83	14.10	14.30	15.40	16.08	16.73
Fe ₂ O ₃ *	1.49	2.42	1.22	1.1	1.1	1.9	2.15	1.91	4.67
MnO	0.03	0.05	0.03	0.02	0.03	0.04	0.05	0.03	0.05
MgO	0.76	1.30	0.48	0.54	0.52	0.61	1.20	1.05	1.71
CaO	1.37	1.29	1.34	1.01	1.18	1.14	1.98	1.99	3.08
Na ₂ O	5.18	5.60	3.89	5.12	3.68	4.05	4.44	4.27	4.46
K ₂ O	3.22	3.40	4.27	2.84	4.40	4.08	3.89	3.28	3.35
P ₂ O ₅	0.07	0.09	0.08	0.08	0.09	0.11	0.10	0.11	0.21
Loss	2.40	0.20	1.40	0.00	3.20	1.40	0.00	1.00	1.00

Total	101.01	99.69	100.48	100.76	100.40	100.90	100.20	100.04	100.31
-------	--------	-------	--------	--------	--------	--------	--------	--------	--------

Nb	5	4	8	6	8	8	6	7	7
Zr	63	83	62	62	65	69	91	85	80
Y	11	12	19	15	22	19	11	17	20
Sr	511	455	198	200	182	241	432	378	277
Rb	101	90	172	96	196	168	135	137	200
Th	10	9	7	6	5	10	27	4	8
Pb	38	25	39	36	51	42	37	32	52
Zn	35	32	19	16	25	29	32	29	20
Cu	12	15	<2	<2	12	12	16	11	<2
Ni	13	12	6	5	12	4	22	6	11
Cr	19	22	<2	<2	2	6	47	10	<2
V	26	28	22	19	10	24	43	30	80
Ba	509	581	250	n.d.	332	448	429	448	<5
Hf	3	4	<5	n.d.	2	3	3	3	<5
Ce	40	31	173	n.d.	12	22	34	8.00	60
La	10	21	n.d.	n.d.	13	15	26	10	92

Fe2O3* : refers to wt % of total iron

Sample	Y169	Y261	Y1451	GL1	Y9/89	GLGR1	Y556	Y2057
SiO ₂	61.893	69.54	68.16	59.18	57.09	69.22	64.46	69.00
TiO ₂	0.465	0.38	0.40	0.81	0.84	0.31	0.77	0.38
Al ₂ O ₃	18.304	15.76	16.03	17.50	17.52	15.63	16.41	15.76
Fe ₂ O ₃ *	4.554	3.09	2.78	6.30	7.73	2.12	4.27	2.36
MnO	0.046	0.06	0.06	0.12	0.11	0.04	0.06	0.06
MgO	1.318	1.96	1.56	2.89	2.84	1.12	1.77	0.76
CaO	3.593	2.11	2.25	5.48	6.24	1.97	3.23	2.84
Na ₂ O	4.726	4.12	5.27	3.58	4.53	5.10	4.03	4.11
K ₂ O	1.996	2.80	2.80	2.35	1.77	3.00	4.07	3.06
P ₂ O ₅	0.259	0.14	0.11	0.22	0.21	0.10	0.27	0.16
Loss	0.800	1.00	0.40	1.00	1.00	0.00	1.40	0.20
Total	97.96	100.95	99.80	99.44	99.89	98.65	100.73	98.88
Nb	n.d.	10	5	11	7	3	20	11
Zr	n.d.	82	90	156	168	93	285	162
Y	n.d.	18	12	24	22	9	29	11
Sr	n.d.	262	638	602	615	598	445	626
Rb	n.d.	196	81	79	66	82	186	71
Th	n.d.	9	8	3	7	6	30	13
Pb	n.d.	17	27	8	13	33	37	13
Zn	n.d.	53	49	81	77	49	61	78
Cu	n.d.	<2	10	17	<2	<2	31	15
Ni	n.d.	12	23	10	12	17	27	3
Cr	n.d.	<2	43	24	<2	0	35	3
V	n.d.	64	52	144	148	45	95	39
Ba	n.d.	<5	526	573	<5	<5	667	595
Hf	n.d.	<5	4	4	<5	<5	7	6
Ce	n.d.	58	26	55	77	58	129	146
La	n.d.	<5	26	26	<5	<5	83	95

Sample	Y2455	Y658	Y359	Y1656	Y6204	Y16511	Y25514	MDG
SiO ₂	60.67	68.15	61.27	68.32	71.41	67.84	68.09	71.39
TiO ₂	0.94	0.39	0.43	0.42	0.21	0.49	0.46	0.27
Al ₂ O ₃	17.78	16.19	22.03	16.80	15.11	16.04	16.84	14.71
Fe ₂ O ₃ *	6.64	2.48	0.65	2.70	1.95	3.06	2.64	2.30
MnO	0.08	0.04	0.02	0.04	0.03	0.05	0.04	0.03
MgO	1.72	0.88	0.82	1.21	0.91	0.85	1.15	0.68
CaO	4.13	3.64	6.27	4.04	1.63	3.16	3.50	1.90
Na ₂ O	4.81	4.42	7.64	4.35	5.13	4.03	4.54	4.19
K ₂ O	2.49	2.02	0.35	2.19	3.35	2.91	2.00	3.38
P ₂ O ₅	0.43	0.13	0.22	0.17	0.10	0.20	0.16	0.08
Loss	0.80	1.80	0.20	0.20	1.00	0.40	1.20	1.00
Total	100.49	100.31	99.91	100.60	100.83	99.22	100.80	99.91
Nb	14	3	2	5	n.d.	8	4	n.d.
Zr	202	125	137	132	n.d.	168	129	n.d.
Y	24	7	5	8	n.d.	11	9	n.d.
Sr	573	656	685	716	n.d.	717	760	n.d.
Rb	168	50	51	44	n.d.	78	53	n.d.
Th	5	8	6	7	n.d.	16	7	n.d.
Pb	22	12	9	9	n.d.	17	13	n.d.
Zn	74	58	60	65	n.d.	78	67	n.d.
Cu	<2	16	<2	22	n.d.	11	28	n.d.
Ni	22	6	5	1	n.d.	3	3	n.d.
Cr	<2	11	<2	9	n.d.	7	9	n.d.
V	132	66	66	66	n.d.	61	73	n.d.
Ba	<5	579	<5	542	n.d.	627	553	n.d.
Hf	<2	5	<5	5	n.d.	6	5	n.d.
Ce	<5	37	92	72	n.d.	92	70	n.d.
La	<2	29	168	35	n.d.	<2	<2	<2

Y555	Sample	Y31	YSH1	YSH5
64.99	SiO ₂	55.80	45.78	53.42
0.73	TiO ₂	1.02	1.66	1.16
16.26	Al ₂ O ₃	16.08	15.85	14.68
4.20	Fe ₂ O ₃ *	7.63	12.54	7.67
0.07	MnO	0.16	0.20	0.13
1.69	MgO	5.89	6.36	7.61
3.17	CaO	5.68	8.74	6.22
4.23	Na ₂ O	4.58	3.30	4.09
4.41	K ₂ O	2.24	2.29	3.43
0.26	P ₂ O ₅	0.36	0.67	0.33
0.00	Loss	0.80	1.60	1.80
100.21	Total	100.46	98.96	100.54
21	Nb	20	10	13
295	Zr	70	174	182
26	Y	30	37	25
420	Sr	566	628	523
224	Rb	117	163	176
34	Th	16	5	2
40	Pb	20	13	14
54	Zn	115	122	87
23	Cu	74.00	<2	<2
20	Ni	90	17	174
34	Cr	265	<2	<2
92	V	180	326	184
589	Ba	393	<5	<5
7	Hf	3	<5	<5
76	Ce	116	97	76
19	La	84		

Y2096

66.62
0.35
16.94
3.21
0.04
1.05
3.65
5.03
2.74
0.15
0.80

100.58

4
141
8
552
114
9
19
48
<2
6
<2
44
<5
<5
75
92

APPENDIX 4

Stable Isotope Analyses

1. $\delta^{18}\text{O}$ silicate

<u>Sample name</u>	<u>Sample Type (WR/Min separate)</u>	<u>Rock Type</u>	<u>Intrusion</u>
AP1'	WR	Meladiorite	Narin-Portnoo
AP2	WR	Meladiorite	Narin-Portnoo
31515	WR	Diorite	Narin-Portnoo
3153	WR	Diorite	Narin-Portnoo
26510	WR	"Appinite"	Narin-Portnoo
31511	WR	Hornblende diorite	Narin-Portnoo
AP2 (Hb)	Hornblende	Meladiorite	Narin-Portnoo
26510 (Hb)	Hornblende	"Appinite"	Narin-Portnoo
CS1-69b	WR	Portnoo Limestone	Narin-Portnoo

2. $\delta^{13}\text{C}$ PDB

<u>Sample</u>	<u>Sample Type (WR/Min separate)</u>	<u>Rock Type</u>	<u>Intrusion</u>
AP1'	WR	Meladiorite	Narin-Portnoo
AP2	WR	Meladiorite	Narin-Portnoo
31515	WR	Diorite	Narin-Portnoo
3153	WR	Diorite	Narin-Portnoo
26510	WR	"Appinite"	Narin-Portnoo
31511	WR	Hornblende diorite	Narin-Portnoo
CS1-69b	WR	Portnoo Limestone	Narin-Portnoo
Limey 1	WR	Falcarragh Limestone	'Control'*

* Control sample of Falcarragh Limestone, a lateral equivalent to the Portnoo limestone collected away from the influence of any igneous intrusion, 2.5 km east of the village of Falcarragh, Co., Donegal.

3. δD

<u>Sample</u>	<u>Sample Type (WR/Min separate)</u>	<u>Rock Type</u>	<u>Intrusion</u>
CS2	Actinolite	Portnoo Limestone	Narin-Portnoo
CS1	Actinolite	Portnoo Limestone	Narin-Portnoo
69f	Muscovite	Portnoo Limestone	Narin-Portnoo
69b	Biotite	Portnoo Limestone	Narin-Portnoo
Kilr Hb rim	Hornblende	Hornblendite	Kilrean
1856	Hornblende	Diorite	Meenalargan
AP2	Hornblende	Meladiorite	Narin-Portnoo
AP1'	Hornblende	Meladiorite	Narin-Portnoo
26510	Hornblende	"Appinite"	Narin-Portnoo
31515	Hornblende	Diorite	Narin-Portnoo
31515	Epidote	Diorite	Narin-Portnoo

A.4.1. OXYGEN

SAMPLE	Wt(mg)	YIELD	WR δ RAW	WR δ ^{18}O Silicate ‰SMOW
Ap1'	14.20	12.51	-23.11	7.72
Ap1'	17.10	11.85	-23.74	7.48
average	15.70	12.18	-23.63	7.60
Ap 2	10.50	12.70	-23.55	7.68
Ap 2	15.40	13.04	-23.41	7.83
average	12.95	12.87	-23.48	7.76
31515	19.40	10.31	-22.38	8.77
31515	20.60	9.01	-22.59	8.55
average	20.00	9.65	-22.48	8.66
3153 Ap	14.00	13.03	-22.13	9.15
3153 Ap	14.00	11.26	-22.12	9.16
3153 Ap	13.70	12.73	-22.08	9.20
average	13.85	12.34	-22.11	9.17
26510 bas	12.10	12.32	-24.63	6.57
26510 bas	11.80	12.02	-24.84	6.35
average	12.00	12.17	-24.74	6.46
31511 Ap	13.00	13.78	-22.78	8.48
AP1	11.80	11.70	-23.67	7.56
Ap1	12.10	10.68	-23.11	8.14
average	11.90	11.19	-23.39	7.85
Ap 2 Hb	10.50	12.54	-26.89	6.47
Ap 2 Hb	11.00	12.75	-26.65	8.06
26510 Hb	10.50	12.68	-26.60	7.00
26510 Hb	10.00	12.11	-26.84	7.34
CS1	13.00	13.56	-22.57	8.70
CS1	11.70	11.74	-22.67	8.46
average	12.40	12.65	-22.62	8.58
CS2	11.20	14.50	-23.18	8.06
CS2	14.60	5.40	-23.24	7.87
average	12.90	9.95	-23.21	7.97
30515	12.30	6.24	-19.38	11.99
30512	13.40	9.55	-18.97	12.41
30512	15.40	7.07	-19.38	12.00
average	14.40	8.31	-19.02	12.20
69f	12.40	9.97	-19.99	18.17
69f	12.30	8.78	-19.27	18.92
average	12.35	9.38	-19.58	18.54
69d	12.74	8.92	-19.62	18.55
69d	13.01	14.66	-18.11	20.13
average	12.88	11.79	18.87	19.34
69b	12.38	9.99	-17.41	20.86
69b	13.05	14.78	-16.95	21.33
average	12.72	12.39	-17.18	21.10

A4.2. CARBON

SAMPLE	Wt (mg)	YIELD	WR $\delta^{13}\text{C}$ ‰PDB	WR $\delta^{18}\text{O}$ ‰PDB	WR $\delta^{18}\text{O}$ ‰SMOW	% CaCO_3
Ap1'	208.60	0.131	-6.16	-17.78	12.58	1.31
Ap1'	204.20	0.117	-6.38	-18.07	12.28	1.17
average	206.40	0.124	-6.27	-17.93	12.43	1.24
Ap2	240.60	0.006	-7.86	-13.80	16.70	0.06
Ap2	307.30	0.015	-6.04	-15.62	14.80	0.02
31515	271.20	0.217	-2.15	-16.47	13.93	2.17
31515	64.80	0.176	-2.22	-16.55	13.85	1.76
average	-----	0.197	-2.19	-16.51	13.89	1.97
3153 Ap	223.60	0.484	-3.13	-17.18	13.20	4.84
3153 Ap	238.80	0.477	-3.16	-17.16	13.23	4.77
average		0.481	-3.15	-17.17	13.22	4.80
26510 bas	282.30	0.740	-4.90	-18.10	12.15	7.40
26510 bas	298.50	0.830	-4.90	-18.20	12.17	8.34
average	290.40	0.790	-4.90	-18.20	12.16	7.87
31511 Ap	265.20	0.158	-3.95	-17.96	12.40	1.58
31511 Ap	257.00	0.164	-3.98	-18.07	12.30	1.64
average	261.10	0.164	-3.97	-18.02	12.35	1.61
CS1	256.10	0.040	-5.27	-16.81	13.58	0.40
CS1	256.40	0.040	-5.61	-17.17	13.20	0.40
average	256.30	0.040	-5.44	-16.95	13.39	0.40
CS2	200.90	0.316	-4.48	-17.99	12.36	3.16
CS2	199.80	0.345	-4.60	-17.84	12.52	3.45
average	200.40	0.040	-4.54	-17.92	12.44	3.30
30515	21.50	2.860	-3.09	-17.53	12.83	28.50
30515	25.10	2.780	-2.93	-17.27	13.10	27.50
average	23.30	2.820	-3.01	-17.40	12.97	28.00
30512	113.10	0.808	1.01	-15.20	15.25	7.80
30512	113.20	0.790	1.40	-16.50	13.90	7.80
average	113.15	0.759	1.21	-15.90	14.58	7.80
69f	26.10	7.130	5.86	-11.08	19.49	75.00
69f	26.50	7.120	6.04	-10.96	19.62	75.00
average	26.30	7.130	5.95	-11.02	19.56	75.00
69e	26.50	7.950	7.84	-8.66	21.98	75.00
69e	23.20	7.150	7.95	-8.80	21.85	75.00
average	24.80	7.550	7.90	-8.73	21.92	75.00
69a	20.10	8.460	8.94	-8.57	22.07	83.10
69a	20.20	8.270	9.06	-8.50	22.15	83.10
average	20.20	8.340	9.00	-8.54	22.11	83.10
69d	23.70	7.770	8.76	-7.75	22.92	73.40
69d	25.50	7.080	8.70	-7.63	23.04	73.40
average	24.60	7.430	8.73	-7.69	22.98	73.40
69c	20.90	8.050	8.75	-7.93	22.75	76.00
69c	20.50	7.220	8.73	-7.98	22.69	76.00
average	20.70	7.640	8.74	-7.96	22.72	76.00
69b	20.60	7.190	7.84	-9.47	21.15	71.70
69b	21.21	7.170	7.85	-9.48	21.13	71.70
average	20.91	7.180	7.85	-9.48	21.14	71.70
limey1	35.00	7.110	6.90	-10.34	20.25	71.20
limey1	34.50	7.220	6.87	-10.40	20.20	71.20
average	34.75	7.170	6.89	-10.37	20.23	71.20

A.4.3. HYDROGEN

Sample	Wt (mg)	Yield	δ Raw ‰SMOW	δ D ‰SMOW	Mineral
CS2	128.8	1.38	-26.10	-72.8	Actinolite
CS1	181.4	0.70	-26.00	-72.7	Actinolite
69f	162.6	1.16	-3.55	-49.0	Muscovite
69b	156.6	0.57	-12.61	-58.7	Biotite
Kilr Hb Rim	90.1	1.16	-18.72	-65.0	Hornblende
1856	91.9	1.26	-12.56	-58.5	Hornblende
AP2	90.7	1.13	-19.30	-65.6	Hornblende
AP1'	88.6	1.16	-19.34	-65.6	Hornblende
26510	76.7	1.56	-16.55	-62.7	Hornblende
31515	19.9	7.01	-12.80	-58.7	Chlorite
31515	193.5	0.86	-11.18	-57.0	Epidote

APPENDIX 5

Mineral Chemistry

i. Pyroxene analyses

<u>Sample</u>	<u>Mineral Type</u>	<u>Rock Type</u>	<u>Intrusion</u>
Y30513.4-Y30513.8	Augite	Diorite	Narin-Portnoo
Y861.3	Augite	Quartz monzodiorite	G1 (Ardara)
Cort 3-Cort 26	Augite	Cortlandtite	Kilrean
Cort 6-Cort 12	Orthopyroxene	Cortlandtite	Kilrean
RY4.1	Orthopyroxene	Melagabbro	Meenalargan
RY4.4	Subcalcic augite exsolution lamella	Melagabbro	Meenalargan
RY4.5	Subcalcic augite exsolution lamella	Melagabbro	Meenalargan
RY 4.10	Augite host	Melagabbro	Meenalargan

Sample	30513.4	30513.5	30513.8	861.3	Cort 3	Cort 26	Cort 6	Cort 9
SiO ₂	53.54	53.64	53.31	52.14	52.44	52.67	54.45	54.73
TiO ₂	0.02	0.13	0.09	0.26	0.38	0.28	0.18	0.09
Al ₂ O ₃	0.36	0.80	0.58	1.69	2.03	1.83	1.38	0.99
Cr ₂ O ₃	0.01	0.03	0.02	0.05	0.29	0.49	0.02	0.04
FeO	7.79	8.18	8.05	9.19	4.73	5.38	13.43	12.95
NiO	0.00	0.00	0.01	0.00	0.00	0.00	0.00	0.03
MnO	0.21	0.22	0.22	0.36	0.07	0.13	0.22	0.26
MgO	13.36	13.40	13.25	13.30	17.09	16.97	28.96	29.47
CaO	24.54	23.80	24.07	22.03	21.94	21.90	1.11	1.23
Na ₂ O	0.25	0.33	0.26	0.47	0.28	0.31	0.07	0.02
K ₂ O	0.03	0.00	0.00	0.05	0.03	0.00	0.00	0.03
Total	100.11	100.53	99.86	99.54	99.29	99.96	99.81	99.84

Number of ions on the basis of 6 oxygens

Si	2.00	1.99	1.99	1.96	1.93	1.93	1.95	1.95
Al IV	0.00	0.01	0.01	0.04	0.07	0.07	0.05	0.05
Al VI	0.02	0.04	0.03	0.07	0.09	0.08	0.06	0.04
Ti	0.00	0.00	0.00	0.01	0.01	0.01	0.01	0.00
Fe ³⁺	0.01	0.00	0.00	0.04	0.05	0.06	0.05	0.05
Fe ²⁺	0.23	0.25	0.25	0.25	0.09	0.10	0.35	0.33
Cr	0.00	0.00	0.00	0.00	0.01	0.01	0.00	0.00
Ni	0.00	0.00	0.00	0.00	0.00	0.00	0.00	0.00
Mn	0.01	0.01	0.01	0.01	0.00	0.00	0.01	0.01
Mg	0.74	0.74	0.74	0.74	0.94	0.93	1.54	1.57
Ca	0.98	0.95	0.96	0.89	0.86	0.86	0.04	0.05
Na	0.02	0.02	0.02	0.03	0.02	0.02	0.01	0.00
K	0.00	0.00	0.00	0.00	0.00	0.00	0.00	0.00
Total	4.02	4.01	4.01	4.04	4.07	4.07	4.08	4.05

Sample	Cort 11	Cort 12	RY4.1	RY4.2	RY4.4	RY4.5	RY4.10
SiO ₂	54.46	55.70	50.60	50.22	50.83	50.62	50.90
TiO ₂	0.17	0.09	0.21	0.35	0.20	0.23	0.50
Al ₂ O ₃	1.71	0.14	1.35	2.17	1.60	1.83	2.84
Cr ₂ O ₃	0.00	0.08	0.00	0.00	0.00	0.03	0.03
FeO	13.21	13.51	28.08	11.87	25.96	27.43	11.58
NiO	0.06	0.00	0.00	0.00	0.00	0.01	0.03
MnO	0.30	0.34	0.53	0.25	0.54	0.63	0.29
MgO	28.95	29.99	17.27	11.59	13.90	14.02	11.39
CaO	0.98	0.13	1.06	21.77	8.31	6.72	22.13
Na ₂ O	0.00	0.00	0.00	0.44	0.11	0.11	0.49
K ₂ O	0.00	0.00	0.00	0.02	0.00	0.01	0.01
Total	99.84	99.99	99.71	98.68	101.45	101.54	100.19

Number of ions on the basis of 6 oxygens

Si	1.94	1.98	1.95	1.92	1.94	1.94	1.92
Al IV	0.06	0.02	0.05	0.08	0.06	0.06	0.08
Al VI	0.07	0.01	0.06	0.10	0.07	0.08	0.13
Ti	0.01	0.00	0.01	0.01	0.01	0.01	0.01
Fe ³⁺	0.03	0.02	0.02	0.07	0.04	0.04	0.04
Fe ²⁺	0.36	0.38	0.91	0.30	0.79	0.83	0.32
Cr	0.00	0.00	0.00	0.00	0.00	0.00	0.00
Ni	0.00	0.00	0.00	0.00	0.00	0.00	0.00
Mn	0.01	0.01	0.02	0.01	0.02	0.02	0.01
Mg	1.54	1.59	0.99	0.66	0.79	0.80	0.64
Ca	0.04	0.01	0.04	0.89	0.34	0.28	0.89
Na	0.00	0.00	0.00	0.03	0.01	0.01	0.04
K	0.00	0.00	0.00	0.00	0.00	0.00	0.00
Total	4.06	4.02	4.05	4.07	4.07	4.07	4.08

ii. Amphibole analyses

<u>Sample</u>	<u>Rock Type</u>	<u>Intrusion</u>
Kilr 10-16	Cortlandtite	Kilrean
Hb rim 4-Hb rim 11	Hornblendite	Kilrean
Bir Br.2-.1	Breccia	Biroge breccia pipe
Bir Di.5-Bir Di.6	Diorite	Biroge diorite
1856.4-1856.7	Diorite	Meenalargan
M10.3	Quartz diorite	Meenalargan
M14.2	Diorite	Meenalargan
25515.8-25515.10	Diorite	Meenalargan
25512.12-25512.13	Coarse diorite	Meenalargan
17.1-17.10	Coarse meladiorite dyke	Summy Lough
21.1-21.11	Hornblendite	Summy Lough
s5.2-s5.21	Diorite	Summy Lough
1797.1-1797.5	Diorite	Summy Lough
Mulna di.9-Mulna di.7	Diorite	Mulnamin
Mul di ap.1-Mul di ap.7	Diorite	Mulnamin
2093.1-2093.4	Diorite	Mulnamin
Isl Mul.1-.6	Breccia	Mulnamin
27520.1-27520.10	Diorite	Narin-Portnoo
2658.82-2658.90	Meladiorite	Narin-Portnoo
3153.1-3153.27	Diorite	Narin-Portnoo
2651.1-2651.10	Hornblendite	Narin-Portnoo
76c.1-76c.2	Hornblendite	Narin-Portnoo
26510.8-26510.7	"Appinite"	Narin-Portnoo
RY 4.15	Melagabbro	Meenalargan
Ry 4.16	Melagabbro	Meenalargan
RY 4.1	Melagabbro	Meenalargan
861.16-861.23	Quartz monzodiorite	G1 (Ardara)
862.1-862.36	Quartz monzodiorite	G2 (Ardara)
8613.1-8613.5	Granodiorite	G2 (Ardara)
31.7-31.12	Dioritic xenolith	G1 (Ardara)
Glen 9.1-9.2	Granite	Glenard
Glen 13.1-13.6	Granodiorite	Glenard
GLAP 1-28	"Appinite"	Glenard
RY 4.2'	Melagabbro	Meenalargan

Sample	Kilr 10	Kilr 25	Kilr 4	Kilr 1	Kilr 16	Hb Rim 4	Hb Rim 5	HbRim
SiO ₂	46.37	43.55	43.37	46.37	48.47	41.84	41.93	42.34
TiO ₂	1.18	2.28	1.55	1.18	0.85	1.74	1.37	1.53
Al ₂ O ₃	9.69	11.39	11.78	9.69	7.54	13.51	13.84	12.63
Cr ₂ O ₃	0.41	0.26	0.12	0.41	0.17	0.03	0.00	0.09
FeO	6.80	7.15	8.57	6.80	7.40	10.99	11.16	11.01
MnO	0.06	0.05	0.00	0.06	0.08	0.09	0.09	0.13
NiO	0.05	0.03	0.05	0.05	0.03	0.01	0.00	0.00
MgO	17.42	16.94	16.28	17.42	18.68	13.11	12.73	13.42
CaO	12.06	11.78	11.37	12.06	10.67	11.65	11.64	11.92
Na ₂ O	1.68	2.32	2.12	1.68	1.57	1.86	2.18	2.12
K ₂ O	0.59	0.74	0.90	0.59	0.39	0.75	0.70	0.84
Total	96.31	96.49	96.09	96.30	96.35	95.58	95.66	96.04

Number of ions on the basis of 23 oxygens

Si	6.65	6.28	6.27	6.65	6.83	6.19	6.22	6.27
Al(IV)	1.35	1.72	1.73	1.35	1.17	1.81	1.78	1.73
Al(VI)	0.28	0.21	0.28	0.28	0.09	0.54	0.64	0.48
Ti	0.13	0.25	0.17	0.13	0.09	0.19	0.15	0.17
Cr ³⁺	0.05	0.03	0.01	0.05	0.02	0.00	0.00	0.01
Fe ³⁺	0.48	0.55	0.81	0.48	1.16	0.51	0.38	0.35
Fe ²⁺	0.34	0.32	0.24	0.34	0.25	0.85	1.01	1.02
Mn	0.01	0.01	0.00	0.01	0.01	0.01	0.01	0.02
Ni	0.01	0.00	0.01	0.01	0.00	0.00	0.00	0.00
Mg	3.72	3.64	3.51	3.72	3.92	2.89	2.81	2.96
Ca	1.85	1.82	1.76	1.85	1.61	1.84	1.85	1.89
Na(M4)	0.14	0.17	0.22	0.14	0.36	0.15	0.15	0.10
Na(A)	0.33	0.48	0.38	0.33	0.07	0.39	0.48	0.50
K	0.11	0.14	0.17	0.11	0.07	0.14	0.13	0.16
Total	15.44	15.61	15.54	15.44	15.14	15.53	15.61	15.66

Sample	Hb Rim11	Bir Br.2	Bir br.3	Bir br.5	Bir di.5	Bir di.6	Bir br.1	1856.4
SiO ₂	41.34	55.67	54.31	56.52	53.38	52.58	47.07	54.71
TiO ₂	2.48	0.07	0.10	0.06	0.23	0.17	1.50	0.16
Al ₂ O ₃	13.02	2.17	3.21	2.21	2.65	4.27	8.35	2.62
Cr ₂ O ₃	0.00	0.04	0.07	0.00	0.13	0.21	0.09	0.04
FeO	11.11	7.06	5.39	3.35	9.42	9.73	10.46	7.13
MnO	0.21	0.19	0.10	0.14	0.31	0.19	0.19	0.17
NiO	0.00	0.00	0.05	0.00	0.00	0.00	0.00	0.04
MgO	12.67	19.39	19.84	22.03	16.80	16.56	15.04	18.80
CaO	11.56	12.47	12.94	13.48	12.04	12.17	11.81	12.83
Na ₂ O	2.17	0.26	0.38	0.21	0.30	0.58	1.46	0.31
K ₂ O	0.90	0.06	0.06	0.03	0.07	0.11	0.91	0.08
Total	95.44	97.40	96.45	98.02	95.33	96.54	96.90	96.90

Number of ions on the basis of 23 oxygens

Si	6.18	7.76	7.64	7.74	7.71	7.52	6.84	7.72
Al(IV)	1.81	0.24	0.36	0.26	0.28	0.48	1.16	0.28
Al(VI)	0.48	0.12	0.17	0.10	0.17	0.24	0.27	0.16
Ti	0.28	0.01	0.01	0.01	0.02	0.02	0.16	0.02
Cr ³⁺	0.00	0.01	0.01	0.00	0.01	0.02	0.01	0.01
Fe ³⁺	0.27	0.30	0.13	0.13	0.23	0.27	0.29	0.09
Fe ²⁺	1.12	0.53	0.51	0.25	0.91	0.90	0.99	0.76
Mn	0.03	0.02	0.01	0.02	0.04	0.02	0.02	0.02
Ni	0.00	0.00	0.01	0.00	0.00	0.00	0.00	0.01
Mg	2.82	4.03	4.16	4.50	3.62	3.53	3.26	3.96
Ca	1.85	1.86	1.95	1.98	1.86	1.86	1.84	1.94
Na(M4)	0.14	0.14	0.04	0.02	0.13	0.13	0.16	0.05
Na(A)	0.48	0.00	0.06	0.04	0.00	0.03	0.25	0.03
K	0.17	0.01	0.01	0.01	0.01	0.02	0.17	0.01
Total	15.65	15.03	15.07	15.04	15.01	15.05	15.42	15.05

Sample	1856.6	1856.11	1856.12	1856.14	1856.15	1856.16	1856.17	1856.18
SiO ₂	53.92	49.92	43.06	53.79	54.87	49.38	54.50	49.19
TiO ₂	0.07	0.24	2.29	0.08	0.03	0.33	0.07	0.24
Al ₂ O ₃	2.73	6.38	11.38	1.82	1.29	7.14	2.75	7.40
Cr ₂ O ₃	0.03	0.06	0.05	0.01	0.09	0.01	0.02	0.01
FeO	7.50	10.18	12.88	14.41	11.68	9.32	7.70	10.17
MnO	0.22	0.28	0.30	0.29	0.16	0.19	0.23	0.23
NiO	0.03	0.06	0.03	0.00	0.06	0.00	0.02	0.01
MgO	18.88	16.08	12.35	14.10	16.44	15.48	18.57	15.59
CaO	13.21	12.90	12.17	12.30	12.84	12.76	13.10	12.51
Na ₂ O	0.30	0.70	1.31	0.30	0.24	0.78	0.30	0.87
K ₂ O	0.09	0.33	0.82	0.10	0.05	0.42	0.05	0.38
Total	97.98	97.12	96.63	97.19	97.74	97.81	97.30	96.61

Number of ions on the basis of 23 oxygens

Si	7.63	7.18	6.38	7.83	7.85	7.21	7.69	7.10
Al(IV)	0.37	0.82	1.61	0.17	0.15	0.79	0.31	0.90
Al(VI)	0.09	0.26	0.38	0.14	0.07	0.43	0.15	0.36
Ti	0.01	0.03	0.26	0.01	0.00	0.04	0.01	0.03
Cr ³⁺	0.00	0.01	0.01	0.00	0.01	0.00	0.00	0.00
Fe ³⁺	0.14	0.26	0.32	0.07	0.04	-0.00	0.09	0.29
Fe ²⁺	0.74	0.97	1.28	1.69	1.35	1.14	0.82	0.94
Mn	0.03	0.03	0.04	0.04	0.02	0.02	0.03	0.03
Ni	0.00	0.01	0.00	0.00	0.01	0.00	0.00	0.00
Mg	3.98	3.45	2.73	3.06	3.50	3.37	3.91	3.35
Ca	2.00	1.99	1.93	1.92	1.97	2.00	1.98	1.94
Na(M4)	0.01	0.00	0.06	0.08	0.03	0.01	0.02	0.06
Na(A)	0.09	0.19	0.32	0.00	0.04	0.22	0.06	0.18
K	0.02	0.06	0.15	0.02	0.01	0.08	0.01	0.07
Total	15.11	15.25	15.47	15.02	15.05	15.29	15.07	15.25

Sample	1856.20	1856.22	1856.23	1856.24	1856.25	1856.26	1856.27	1856.28
SiO ₂	44.45	54.76	54.64	53.05	54.22	54.70	51.13	50.89
TiO ₂	0.61	0.09	0.04	0.13	0.07	0.11	0.24	0.24
Al ₂ O ₃	11.21	2.19	1.80	3.39	2.52	2.21	5.23	5.32
Cr ₂ O ₃	0.05	0.04	0.02	0.00	0.02	0.01	0.04	0.05
FeO	12.73	8.40	8.62	9.19	9.19	8.58	10.19	10.57
MnO	0.24	0.23	0.18	0.19	0.16	0.21	0.24	0.24
NiO	0.02	0.06	0.08	0.00	0.02	0.06	0.02	0.00
MgO	12.57	18.50	18.50	17.74	18.13	18.61	16.01	16.02
CaO	12.36	12.80	12.90	12.58	12.72	13.05	12.62	12.59
Na ₂ O	1.11	0.20	0.24	0.42	0.28	0.29	0.66	0.75
K ₂ O	0.82	0.06	0.07	0.18	0.10	0.10	0.32	0.35
Total	96.16	97.32	97.09	96.86	97.45	97.91	96.70	97.01

Number of ions on the basis of 23 oxygens

Si	6.59	7.72	7.74	7.54	7.65	7.69	7.38	7.33
Al(IV)	1.41	0.28	0.26	0.46	0.35	0.31	0.62	0.67
Al(VI)	0.54	0.08	0.04	0.11	0.07	0.06	0.27	0.23
Ti	0.07	0.01	0.00	0.01	0.01	0.01	0.03	0.03
Cr ³⁺	0.01	0.01	0.00	0.00	0.00	0.00	0.00	0.01
Fe ³⁺	0.33	0.23	0.19	0.33	0.31	0.19	0.15	0.23
Fe ²⁺	1.25	0.76	0.83	0.76	0.78	0.82	1.08	1.05
Mn	0.03	0.03	0.02	0.02	0.02	0.03	0.03	0.03
Ni	0.00	0.01	0.01	0.00	0.00	0.01	0.00	0.00
Mg	2.78	3.88	3.91	3.76	3.81	3.90	3.44	3.44
Ca	1.96	1.93	1.96	1.92	1.92	1.97	1.95	1.94
Na(M4)	0.03	0.06	0.03	0.08	0.07	0.03	0.05	0.06
Na(A)	0.29	0.00	0.03	0.04	0.00	0.05	0.14	0.15
K	0.15	0.01	0.01	0.03	0.02	0.02	0.06	0.07
Total	15.44	15.01	15.05	15.07	15.02	15.07	15.20	15.22

Sample	1856.3	1856.7	M10.3	M14.7	M14.2	25515.8	25515.925515.10	
SiO ₂	42.80	42.87	47.92	42.62	42.78	42.36	41.85	53.44
TiO ₂	2.21	0.49	0.26	1.24	0.82	0.63	0.70	0.07
Al ₂ O ₃	11.52	12.69	7.52	12.28	12.23	13.11	13.18	3.14
Cr ₂ O ₃	0.10	0.10	0.02	0.00	0.03	0.00	0.03	0.00
FeO	11.30	13.49	10.31	13.05	11.68	15.21	16.21	9.26
MnO	0.18	0.23	0.20	0.14	0.26	0.14	0.11	0.18
NiO	0.00	0.10	0.00	0.01	0.00	0.07	0.00	0.00
MgO	12.56	11.91	15.31	12.11	12.27	10.40	10.17	16.87
CaO	12.13	12.39	11.75	12.06	12.13	11.88	11.79	12.35
Na ₂ O	1.29	1.49	0.93	1.70	1.56	1.59	1.65	0.43
K ₂ O	0.96	1.08	0.45	1.18	1.06	0.59	0.65	0.04
Total	95.25	96.83	94.67	96.39	94.81	95.99	96.33	95.79

Number of ions on the basis of 23 oxygens								
Si	6.45	6.37	7.03	6.36	6.46	6.36	6.27	7.70
Al(IV)	1.55	1.63	0.97	1.64	1.54	1.64	1.73	0.30
Al(VI)	0.49	0.59	0.33	0.52	0.64	0.68	0.60	0.23
Ti	0.25	0.06	0.03	0.14	0.09	0.07	0.08	0.01
Cr ³⁺	0.01	0.01	0.00	0.00	0.00	0.00	0.00	0.00
Fe ³⁺	0.09	0.31	0.54	0.27	0.14	0.41	0.58	0.12
Fe ²⁺	1.33	1.36	0.73	1.36	1.34	1.50	1.46	1.00
Mn	0.02	0.03	0.03	0.02	0.03	0.02	0.01	0.02
Ni	0.00	0.01	0.00	0.00	0.00	0.01	0.00	0.00
Mg	2.81	2.64	3.35	2.69	2.76	2.33	2.27	3.62
Ca	1.95	1.97	1.85	1.93	1.96	1.91	1.89	1.91
Na(M4)	0.05	0.01	0.15	0.07	0.04	0.08	0.10	0.09
Na(A)	0.33	0.41	0.12	0.42	0.42	0.39	0.38	0.03
K	0.18	0.20	0.08	0.22	0.20	0.11	0.12	0.01
Total	15.51	15.62	15.20	15.65	15.62	15.50	15.50	15.03

Sample	25512.12	25512.13	17.1	17.2	17.3	17.5	17.8	17.10
SiO ₂	42.14	42.09	56.14	44.49	56.31	52.64	49.62	52.53
TiO ₂	0.78	0.56	0.05	1.29	0.08	0.15	0.69	0.35
Al ₂ O ₃	13.09	12.81	1.18	9.42	0.44	4.01	5.87	3.35
Cr ₂ O ₃	0.03	0.05	0.00	0.15	0.14	0.22	0.13	0.06
FeO	15.84	14.57	4.89	9.27	3.39	5.73	6.50	7.83
MnO	0.13	0.12	0.06	0.31	0.17	0.19	0.11	0.18
NiO	0.00	0.02	0.03	0.02	0.00	0.00	0.00	0.04
MgO	10.03	10.23	21.10	15.26	22.24	18.61	17.99	18.01
CaO	11.99	11.82	13.19	11.86	12.75	12.45	12.30	11.85
Na ₂ O	1.65	1.70	0.31	2.01	0.28	0.77	1.23	0.71
K ₂ O	0.60	0.39	0.10	0.74	0.11	0.10	0.52	0.27
Total	96.27	94.37	97.04	94.83	95.90	94.90	94.95	95.20

Number of ions on the basis of 23 oxygens								
Si	6.33	6.42	7.83	6.62	7.86	7.58	7.21	7.56
Al(IV)	1.67	1.58	0.17	1.39	0.14	0.42	0.79	0.44
Al(VI)	0.66	0.73	0.03	0.27	0.00	0.26	0.21	0.13
Ti	0.09	0.07	0.01	0.14	0.01	0.02	0.08	0.04
Cr ³⁺	0.00	0.01	0.00	0.02	0.01	0.03	0.01	0.01
Fe ³⁺	0.37	0.26	0.08	0.31	0.26	0.04	0.14	0.32
Fe ²⁺	1.62	1.60	0.49	0.85	0.13	0.65	0.65	0.63
Mn	0.02	0.02	0.01	0.04	0.02	0.02	0.01	0.02
Ni	0.00	0.00	0.00	0.00	0.00	0.00	0.00	0.01
Mg	2.25	2.33	4.39	3.38	4.63	3.99	3.90	3.86
Ca	1.93	1.93	1.97	1.89	1.91	1.92	1.91	1.83
Na(M4)	0.07	0.06	0.03	0.10	0.09	0.08	0.09	0.17
Na(A)	0.41	0.44	0.06	0.47	0.02	0.14	0.26	0.03
K	0.12	0.08	0.02	0.14	0.02	0.02	0.10	0.05
Total	15.53	15.52	15.07	15.61	15.10	15.15	15.36	15.08

Sample	21.1	21.2	21.11	s5.2	s5.5	s5.7	s5.10	s5.10'
SiO ₂	49.50	49.47	44.95	45.56	51.33	49.37	50.80	45.62
TiO ₂	0.76	0.83	1.47	0.82	0.48	0.59	0.43	0.93
Al ₂ O ₃	5.93	5.98	9.85	9.72	3.92	5.11	4.17	8.19
Cr ₂ O ₃	0.15	0.14	0.15	0.17	0.07	0.14	0.09	0.08
FeO	10.30	10.31	11.80	10.96	11.06	10.15	8.85	10.99
MnO	0.23	0.14	0.14	0.14	0.16	0.18	0.15	0.15
NiO	0.02	0.12	0.01	0.00	0.02	0.02	0.00	0.01
MgO	15.39	15.87	12.78	15.06	16.31	16.60	16.94	14.42
CaO	12.13	12.07	12.00	11.80	11.69	11.81	11.98	11.42
Na ₂ O	1.04	1.11	1.48	2.12	1.02	0.77	1.19	1.92
K ₂ O	0.45	0.47	0.94	0.74	0.32	0.36	0.30	0.65
Total	95.92	96.50	95.56	97.09	96.38	95.10	94.90	94.38

Number of ions on the basis of 23 oxygens

Si	7.24	7.17	6.73	6.62	7.41	7.18	7.43	6.83
Al (IV)	0.76	0.83	1.27	1.38	0.59	0.81	0.57	1.17
Al (VI)	0.26	0.20	0.47	0.28	0.08	0.06	0.15	0.27
Ti	0.08	0.09	0.17	0.09	0.05	0.06	0.05	0.10
Cr ³⁺	0.02	0.02	0.02	0.02	0.01	0.02	0.01	0.01
Fe ³⁺	0.13	0.26	0.00	0.50	0.44	0.64	0.17	0.33
Fe ²⁺	1.13	0.99	1.49	0.84	0.90	0.61	0.92	1.05
Mn	0.03	0.02	0.02	0.02	0.02	0.02	0.02	0.02
Ni	0.00	0.01	0.00	0.00	0.00	0.00	0.00	0.00
Mg	3.35	3.43	2.85	3.26	3.51	3.60	3.69	3.22
Ca	1.90	1.88	1.93	1.84	1.81	1.84	1.88	1.83
Na (M4)	0.10	0.11	0.07	0.16	0.19	0.15	0.12	0.17
Na (A)	0.20	0.20	0.35	0.44	0.10	0.07	0.21	0.39
K	0.09	0.09	0.18	0.14	0.06	0.07	0.06	0.12
Total	15.28	15.29	15.54	15.57	15.16	15.14	15.27	15.52

Sample	s5.11	s5.12	s5.13	s5.14	s5.15	s5.20	s5.21	1797.100
SiO ₂	45.18	52.58	46.58	53.75	45.96	51.80	54.05	42.93
TiO ₂	0.74	0.15	0.55	0.04	0.98	0.54	0.01	2.37
Al ₂ O ₃	9.69	2.92	8.35	2.06	8.45	5.23	3.25	10.65
Cr ₂ O ₃	0.12	0.05	0.17	0.13	0.08	0.08	0.07	0.09
FeO	9.82	8.01	9.16	7.34	9.86	9.75	8.71	15.05
MnO	0.11	0.16	0.18	0.24	0.10	0.15	0.13	0.26
NiO	0.03	0.05	0.03	0.04	0.04	0.00	0.00	0.07
MgO	15.06	18.37	16.00	18.90	15.23	17.38	18.91	10.77
CaO	11.66	12.11	11.44	11.98	11.86	12.23	12.99	11.36
Na ₂ O	2.19	0.79	2.11	0.76	1.86	1.16	0.63	1.55
K ₂ O	0.78	0.20	0.65	0.06	0.58	0.37	0.14	0.64
Total	95.37	95.39	95.21	95.30	95.01	98.68	98.89	95.80

Number of ions on the basis of 23 oxygens

Si	6.67	7.56	6.83	7.69	6.81	7.27	7.51	6.47
Al(IV)	1.33	0.44	1.17	0.31	1.19	0.73	0.49	1.53
Al(VI)	0.36	0.06	0.28	0.04	0.29	0.14	0.05	0.37
Ti	0.08	0.02	0.06	0.00	0.11	0.06	0.00	0.27
Cr ³⁺	0.01	0.01	0.02	0.01	0.01	0.01	0.01	0.01
Fe ³⁺	0.32	0.34	0.43	0.34	0.26	0.41	0.37	0.35
Fe ²⁺	0.90	0.62	0.70	0.55	0.96	0.74	0.65	1.55
Mn	0.01	0.02	0.02	0.03	0.01	0.02	0.02	0.03
Ni	0.00	0.01	0.00	0.00	0.01	0.00	0.00	0.01
Mg	3.32	3.94	3.50	4.03	3.36	3.64	3.92	2.42
Ca	1.85	1.87	1.80	1.84	1.88	1.84	1.93	1.83
Na(M4)	0.15	0.12	0.20	0.16	0.11	0.16	0.06	0.15
Na(A)	0.48	0.09	0.41	0.06	0.42	0.16	0.11	0.30
K	0.15	0.04	0.12	0.01	0.11	0.07	0.03	0.12
Total	15.62	15.13	15.53	15.07	15.53	15.23	15.13	15.42

Sample	1797.2	1797.5	Mulna di.6	Mulna di.9	Mulna di.15	Mul di ap.1	Mul di ap.5	Mul diap.
SiO ₂	43.37	43.80	44.35	43.53	44.23	49.07	45.26	46.22
TiO ₂	1.96	2.14	1.01	0.98	0.94	0.62	0.92	0.59
Al ₂ O ₃	10.69	9.83	11.66	12.13	12.20	5.88	10.48	9.06
Cr ₂ O ₃	0.04	0.10	0.00	0.04	0.00	0.07	0.00	0.00
FeO	15.82	15.83	12.81	13.02	12.46	11.80	13.79	14.01
MnO	0.30	0.20	0.14	0.14	0.27	0.30	0.28	0.22
NiO	0.06	0.03	0.00	0.00	0.00	0.05	0.01	0.01
MgO	9.93	10.40	12.50	12.23	12.23	14.98	12.20	12.71
CaO	11.79	12.11	11.93	11.85	11.71	11.86	11.78	12.04
Na ₂ O	1.46	1.41	1.51	1.56	1.60	0.81	1.35	1.28
K ₂ O	0.76	0.79	0.60	0.58	0.63	0.28	0.61	0.47
Total	96.17	96.62	96.50	96.05	96.26	95.71	96.67	96.60

Number of ions on the basis of 23 oxygens

Si	6.57	6.62	6.53	6.44	6.52	7.17	6.67	6.81
Al(IV)	1.43	1.38	1.47	1.56	1.48	0.83	1.33	1.19
Al(VI)	0.48	0.37	0.55	0.56	0.64	0.18	0.49	0.39
Ti	0.22	0.24	0.11	0.11	0.10	0.07	0.10	0.07
Cr ³⁺	0.00	0.01	0.00	0.01	0.00	0.01	0.00	0.00
Fe ³⁺	0.07	0.01	0.39	0.46	0.36	0.49	0.42	0.41
Fe ²⁺	1.94	1.99	1.19	1.16	1.18	0.95	1.28	1.32
Mn	0.04	0.03	0.02	0.02	0.03	0.04	0.04	0.03
Ni	0.01	0.00	0.00	0.00	0.00	0.01	0.00	0.00
Mg	2.24	2.34	2.74	2.70	2.69	3.26	2.68	2.79
Ca	1.92	1.96	1.88	1.88	1.85	1.86	1.86	1.90
Na(M4)	0.08	0.04	0.12	0.12	0.15	0.13	0.14	0.09
Na(A)	0.35	0.38	0.32	0.33	0.31	0.10	0.25	0.27
K	0.15	0.15	0.11	0.11	0.12	0.05	0.12	0.09
Total	15.53	15.43	15.44	15.43	15.15	15.36	15.36	15.33

Sample	2093.1	2093.3	2093.4	Y20.1	Y20.3	Isl mul.1	Isl mul.3	Isl mul.
SiO ₂	46.53	45.90	47.35	44.84	43.63	53.05	55.14	48.70
TiO ₂	0.74	0.60	0.42	0.51	0.64	0.05	0.04	0.34
Al ₂ O ₃	9.97	9.91	9.07	12.41	12.22	3.43	2.00	7.54
Cr ₂ O ₃	0.00	0.12	0.00	0.01	0.00	0.01	0.02	0.06
FeO	12.47	12.77	12.45	11.38	11.36	8.81	8.13	11.82
MnO	0.18	0.23	0.22	0.14	0.16	0.18	0.17	0.19
NiO	0.00	0.03	0.00	0.03	0.05	0.01	0.09	0.02
MgO	12.98	13.00	13.78	13.45	12.99	17.44	18.70	14.80
CaO	12.37	12.03	12.03	11.95	11.81	12.78	12.73	12.40
Na ₂ O	1.06	1.09	1.04	1.85	1.82	0.48	0.24	1.05
K ₂ O	0.46	0.37	0.40	0.61	0.58	0.14	0.04	0.43
Total	96.75	96.04	96.77	97.16	95.25	96.37	97.31	97.33

Number of ions on the basis of 23 oxygens

Si	6.81	6.75	6.88	6.51	6.48	7.61	7.76	7.04
Al(IV)	1.19	1.25	1.12	1.49	1.52	0.39	0.24	0.96
Al(VI)	0.54	0.47	0.43	0.64	0.62	0.19	0.09	0.32
Ti	0.08	0.07	0.05	0.06	0.07	0.01	0.00	0.04
Cr ³⁺	0.00	0.01	0.00	0.00	0.00	0.00	0.00	0.01
Fe ³⁺	0.22	0.45	0.48	0.38	0.35	0.10	0.20	0.35
Fe ²⁺	1.31	1.12	1.03	1.00	1.07	0.95	0.76	1.08
Mn	0.02	0.03	0.03	0.02	0.02	0.02	0.02	0.02
Ni	0.00	0.00	0.00	0.00	0.01	0.00	0.01	0.00
Mg	2.83	2.85	2.98	2.91	2.88	3.73	3.92	3.19
Ca	1.94	1.90	1.87	1.86	1.88	1.96	1.92	1.92
Na(M4)	0.06	0.10	0.12	0.13	0.11	0.04	0.07	0.08
Na(A)	0.24	0.21	0.17	0.39	0.41	0.10	0.00	0.22
K	0.09	0.07	0.07	0.11	0.11	0.03	0.01	0.08
Total	15.33	15.28	15.24	15.50	15.52	15.12	15.00	15.29

Sample	Isl mul.6	27520.1	27520.01	27520.2	27520.4	27520.5	27520.7	27520.10
SiO ₂	46.94	48.38	42.52	44.23	45.01	48.89	49.13	43.23
TiO ₂	0.77	1.15	1.56	1.48	1.41	1.02	0.69	2.16
Al ₂ O ₃	8.96	7.52	13.22	11.48	10.88	6.75	6.86	11.78
Cr ₂ O ₃	0.09	0.03	0.26	0.05	0.02	0.07	0.12	0.27
FeO	11.87	10.83	12.00	9.95	11.68	10.77	10.32	9.00
MnO	0.13	0.19	0.23	0.19	0.15	0.18	0.17	0.15
NiO	0.05	0.00	0.01	0.01	0.03	0.03	0.00	0.02
MgO	14.04	14.62	11.88	14.01	13.51	15.17	15.05	15.01
CaO	12.37	11.51	11.52	11.22	11.38	11.03	11.60	11.51
Na ₂ O	1.38	1.20	1.31	1.96	1.63	1.12	0.98	1.65
K ₂ O	0.61	0.47	0.75	0.66	0.65	0.39	0.45	0.84
Total	97.21	95.91	95.26	95.22	96.34	95.44	95.36	95.61

Number of ions on the basis of 23 oxygens

Si	6.85	7.05	6.32	6.51	6.58	7.11	7.17	6.32
Al(IV)	1.15	0.94	1.68	1.49	1.42	0.89	0.83	1.68
Al(VI)	0.39	0.35	0.64	0.51	0.45	0.26	0.35	0.34
Ti	0.08	0.13	0.17	0.16	0.15	0.11	0.08	0.24
Cr ³⁺	0.01	0.00	0.03	0.01	0.00	0.01	0.01	0.03
Fe ³⁺	0.20	0.32	0.47	0.42	0.50	0.57	0.32	0.60
Fe ²⁺	1.25	1.00	1.03	0.81	0.94	0.75	0.94	0.51
Mn	0.02	0.02	0.03	0.02	0.02	0.02	0.02	0.02
Ni	0.01	0.00	0.00	0.00	0.00	0.00	0.00	0.00
Mg	3.05	3.18	2.63	3.08	2.94	3.29	3.27	3.27
Ca	1.93	1.80	1.83	1.77	1.78	1.72	1.81	1.80
Na(M4)	0.06	0.20	0.16	0.23	0.21	0.27	0.18	0.19
Na(A)	0.33	0.14	0.22	0.33	0.25	0.04	0.09	0.28
K	0.11	0.09	0.14	0.12	0.12	0.07	0.09	0.16
Total	15.44	15.23	15.36	15.46	15.37	15.12	15.18	15.44

Sample	2658.82	2658.83	2658.84	2658.85	2658.86	2658.87	2658.88	2658.89	2658.9
SiO ₂	46.12	42.90	41.88	42.34	41.86	40.16	40.52	42.80	43.0
TiO ₂	1.36	2.13	2.32	2.24	2.21	2.23	2.57	2.12	1.0
Al ₂ O ₃	10.21	12.39	12.83	12.50	13.12	14.55	14.11	12.18	11.0
Cr ₂ O ₃	0.13	0.14	0.00	0.03	0.00	0.01	0.05	0.02	0.0
FeO	9.53	11.69	11.47	11.35	11.27	11.04	12.20	12.18	12.0
MnO	0.12	0.18	0.22	0.12	0.18	0.13	0.16	0.14	0.0
NiO	0.01	0.00	0.05	0.01	0.01	0.05	0.00	0.00	0.0
MgO	15.40	13.84	13.27	13.56	12.81	12.57	12.17	12.57	13.0
CaO	11.65	11.54	11.70	11.62	11.35	12.20	12.27	12.11	12.0
Na ₂ O	2.20	2.36	2.48	2.50	2.29	2.07	2.15	2.01	1.0
K ₂ O	0.56	0.95	0.90	0.96	1.10	1.74	1.39	1.48	1.0
Total	97.30	98.12	97.11	97.24	96.19	96.80	97.60	97.61	97.0

Number of ions on the basis of 23 oxygens

Si	6.64	6.21	6.17	6.21	6.21	6.00	6.01	6.34	6.0
Al(IV)	1.36	1.79	1.83	1.79	1.79	2.00	1.99	1.66	1.0
Al(VI)	0.37	0.33	0.39	0.38	0.50	0.56	0.48	0.46	0.0
Ti	0.15	0.23	0.26	0.25	0.25	0.25	0.29	0.24	0.0
Cr ³⁺	0.01	0.02	0.00	0.00	0.00	0.00	0.01	0.00	0.0
Fe ³⁺	0.37	0.56	0.35	0.37	0.32	0.10	0.14	0.02	0.0
Fe ²⁺	0.78	0.87	1.07	1.03	1.08	1.28	1.38	1.48	1.0
Mn	0.01	0.02	0.03	0.01	0.02	0.02	0.02	0.02	0.0
Ni	0.00	0.00	0.01	0.00	0.00	0.01	0.00	0.00	0.0
Mg	3.30	2.99	2.91	2.97	2.83	2.80	2.69	2.77	2.0
Ca	1.80	1.79	1.84	1.83	1.80	1.95	1.95	1.92	1.0
Na(M4)	0.20	0.20	0.15	0.17	0.19	0.04	0.05	0.08	0.0
Na(A)	0.41	0.46	0.56	0.54	0.46	0.56	0.57	0.50	0.0
K	0.10	0.18	0.17	0.18	0.21	0.33	0.26	0.28	0.0
Total	15.52	15.64	15.73	15.72	15.67	15.89	15.84	15.78	15.0

Sample	3153.1	3153.2	3153.4	3153.5	3153.7	3153.8	3153.9	3153.14
SiO ₂	47.04	48.86	48.81	46.69	44.73	54.39	53.58	48.16
TiO ₂	0.91	0.33	0.72	1.05	1.57	0.02	0.08	0.93
Al ₂ O ₃	7.53	6.78	6.16	7.98	10.06	1.43	2.34	6.56
Cr ₂ O ₃	0.05	0.01	0.00	0.04	0.02	0.03	0.00	0.10
FeO _t	11.75	11.44	11.33	12.04	12.24	9.04	9.14	11.52
MnO	0.19	0.20	0.24	0.23	0.20	0.33	0.21	0.26
NiO	0.00	0.00	0.04	0.05	0.02	0.03	0.00	0.00
MgO	14.11	14.65	15.17	14.12	12.99	17.67	17.38	14.71
CaO	11.66	11.74	11.60	11.77	11.56	12.42	12.39	12.00
Na ₂ O	0.98	0.95	1.00	1.22	1.54	0.15	0.28	0.91
K ₂ O	0.58	0.18	0.42	0.62	0.73	0.00	0.09	0.51
Total	94.78	95.15	95.47	95.81	95.70	95.50	95.50	95.65

Number of ions on the basis of 23 oxygens

Si	6.98	7.16	7.14	6.88	6.64	7.83	7.73	7.08
Al(IV)	1.02	0.84	0.86	1.12	1.36	0.17	0.27	0.92
Al(VI)	0.29	0.33	0.20	0.27	0.40	0.07	0.13	0.21
Ti	0.10	0.04	0.08	0.12	0.17	0.00	0.01	0.10
Cr ³⁺	0.01	0.00	0.00	0.01	0.00	0.00	0.00	0.01
Fe ³⁺	0.43	0.44	0.50	0.42	0.34	0.21	0.20	0.36
Fe ²⁺	1.04	0.97	0.89	1.06	1.18	0.88	0.90	1.06
Mn	0.02	0.03	0.03	0.03	0.03	0.04	0.03	0.03
Ni	0.00	0.00	0.00	0.01	0.00	0.00	0.00	0.00
Mg	3.12	3.20	3.31	3.10	2.88	3.79	3.74	3.22
Ca	1.85	1.84	1.82	1.86	1.84	1.92	1.92	1.89
Na(M4)	0.14	0.15	0.17	0.13	0.16	0.08	0.08	0.11
Na(A)	0.14	0.12	0.11	0.22	0.29	0.04	0.01	0.15
K	0.11	0.03	0.08	0.12	0.14	0.00	0.02	0.10
Total	15.25	15.15	15.19	15.33	15.43	14.96	15.01	15.25

Sample	3153.15	3153.22	3153.23	3153.24	3153.25	3153.27	2651.1	2651.3
SiO ₂	43.80	47.04	48.94	50.38	49.43	48.79	44.92	42.62
TiO ₂	1.75	1.12	1.02	0.34	0.27	0.27	1.54	2.13
Al ₂ O ₃	11.03	7.87	6.48	5.25	6.31	5.94	9.45	12.12
Cr ₂ O ₃	0.07	0.00	0.01	0.02	0.00	0.05	0.03	0.08
FeO _t	12.35	12.25	11.06	10.85	11.64	12.65	11.85	10.16
MnO	0.21	0.22	0.27	0.16	0.14	0.21	0.17	0.09
NiO	0.00	0.02	0.05	0.02	0.00	0.00	0.02	0.00
MgO	12.83	13.61	14.66	15.28	14.40	12.95	13.29	14.68
CaO	11.42	11.61	11.62	12.01	11.65	11.73	11.55	11.18
Na ₂ O	1.79	1.05	0.98	0.52	0.86	0.80	1.91	2.24
K ₂ O	0.83	0.60	0.43	0.28	0.21	0.18	0.84	0.89
Total	96.06	95.38	95.51	95.10	94.91	93.56	95.60	96.20

Number of ions on the basis of 23 oxygens

Si	6.49	6.96	7.17	7.37	7.27	7.37	6.70	6.22
Al(IV)	1.51	1.04	0.82	0.63	0.73	0.63	1.30	1.78
Al(VI)	0.41	0.33	0.29	0.28	0.36	0.43	0.37	0.31
Ti	0.19	0.12	0.11	0.04	0.03	0.03	0.17	0.23
Cr ³⁺	0.01	0.00	0.00	0.00	0.00	0.01	0.00	0.01
Fe ³⁺	0.41	0.36	0.28	0.30	0.35	0.07	0.17	0.69
Fe ²⁺	1.12	1.16	1.07	1.03	1.08	1.52	1.31	0.56
Mn	0.03	0.03	0.03	0.02	0.02	0.03	0.02	0.01
Ni	0.00	0.00	0.01	0.00	0.00	0.00	0.00	0.00
Mg	2.83	3.00	3.20	3.33	3.16	2.91	2.96	3.19
Ca	1.81	1.84	1.83	1.88	1.83	1.90	1.85	1.75
Na(M4)	0.18	0.15	0.17	0.11	0.16	0.10	0.15	0.24
Na(A)	0.33	0.15	0.11	0.04	0.08	0.13	0.40	0.40
K	0.16	0.11	0.08	0.05	0.04	0.03	0.16	0.17
Total	15.48	15.26	15.19	15.09	15.12	15.17	15.56	15.56

Sample	2651.5	2651.6	2651.7	2651.8	2651.10	76c.1	76c.2	26510.8
SiO ₂	40.73	52.97	51.90	47.02	42.20	42.69	42.22	41.43
TiO ₂	2.37	0.12	0.13	2.38	2.26	2.44	2.15	2.20
Al ₂ O ₃	12.80	3.22	3.62	13.26	12.46	11.78	11.80	12.63
Cr ₂ O ₃	0.05	0.09	0.14	0.13	0.02	0.11	0.10	0.04
FeO _t	12.09	9.92	10.31	11.29	11.25	9.76	10.09	12.34
MnO	0.14	0.12	0.18	0.13	0.11	0.12	0.15	0.16
NiO	0.00	0.04	0.05	0.03	0.09	0.07	0.01	0.06
MgO	12.14	17.11	16.51	15.87	13.41	14.12	14.23	13.13
CaO	11.65	12.47	12.35	12.64	11.35	11.14	11.25	11.39
Na ₂ O	1.95	0.48	0.49	2.28	2.06	2.36	2.10	2.09
K ₂ O	1.15	0.16	0.12	0.90	0.87	0.80	0.79	0.81
Total	95.06	96.69	95.80	105.94	96.07	95.38	94.89	96.28

Number of ions on the basis of 23 oxygens

Si	6.16	7.58	7.52	6.25	6.23	6.32	6.27	6.12
Al(IV)	1.84	0.42	0.48	1.75	1.77	1.68	1.73	1.88
Al(VI)	0.44	0.13	0.14	0.33	0.40	0.38	0.33	0.32
Ti	0.27	0.01	0.01	0.24	0.25	0.27	0.24	0.24
Cr ³⁺	0.01	0.01	0.02	0.01	0.00	0.01	0.01	0.00
Fe ³⁺	0.29	0.26	0.30	0.57	0.51	0.37	0.58	0.70
Fe ²⁺	1.25	0.93	0.95	0.69	0.88	0.85	0.68	0.83
Mn	0.02	0.01	0.02	0.01	0.01	0.01	0.02	0.02
Ni	0.00	0.01	0.01	0.00	0.01	0.01	0.00	0.01
Mg	2.73	3.65	3.56	3.15	2.95	3.12	3.15	2.89
Ca	1.89	1.91	1.92	1.80	1.79	1.77	1.79	1.80
Na(M4)	0.11	0.08	0.08	0.19	0.19	0.22	0.20	0.18
Na(A)	0.46	0.05	0.06	0.40	0.40	0.46	0.40	0.42
K	0.22	0.03	0.02	0.15	0.16	0.15	0.15	0.15
Total	15.68	15.08	15.08	15.55	15.56	15.61	15.55	15.57

Sample	26510.9	26510.4	26510.10	26510.5	26510.7	Ry4.15	Ry4.16	Ry 4.1
SiO ₂	41.60	42.29	42.19	54.16	54.03	45.98	45.81	45.42
TiO ₂	2.32	2.17	2.26	0.07	0.06	0.03	0.05	1.04
Al ₂ O ₃	12.72	12.25	12.99	2.21	0.18	9.15	8.92	9.20
Cr ₂ O ₃	0.00	0.00	0.02	0.00	0.00	0.00	0.00	0.00
FeO _t	11.71	11.58	12.15	10.54	14.76	18.04	20.14	19.28
MnO	0.11	0.20	0.13	0.17	1.23	0.16	0.30	0.27
NiO	0.01	0.00	0.00	0.00	0.00	0.00	0.00	0.00
MgO	13.17	13.33	12.81	17.23	13.54	10.67	10.82	11.00
CaO	11.39	11.40	11.26	12.51	12.34	11.55	9.57	10.31
Na ₂ O	1.94	1.87	1.89	0.41	0.10	0.85	0.81	1.18
K ₂ O	0.91	0.90	0.91	0.06	0.06	0.50	0.51	0.79
Total	95.87	96.56	96.56	97.35	96.30	96.93	96.93	98.51

Number of ions on the basis of 23 oxygens

Si	6.16	6.24	6.19	7.70	8.00	6.80	6.65	6.58
Al(IV)	1.84	1.76	1.81	0.30	0.00	1.20	1.35	1.43
Al(VI)	0.37	0.37	0.44	0.07	0.03	0.39	0.17	0.15
Ti	0.26	0.24	0.25	0.01	0.01	0.00	0.01	0.11
Cr ³⁺	0.00	0.00	0.00	0.00	0.00	0.00	0.00	0.00
Fe ³⁺	0.61	0.59	0.62	0.28	0.01	0.81	1.87	1.38
Fe ²⁺	0.85	0.84	0.88	0.97	1.82	1.44	0.65	1.00
Mn	0.01	0.03	0.02	0.02	0.15	0.02	0.04	0.03
Ni	0.00	0.00	0.00	0.00	0.00	0.00	0.00	0.00
Mg	2.90	2.93	2.80	3.65	2.99	2.35	2.34	2.37
Ca	1.81	1.80	1.77	1.91	1.96	1.83	1.49	1.60
Na(M4)	0.18	0.19	0.22	0.09	0.04	0.16	0.44	0.36
Na(A)	0.37	0.34	0.32	0.02	-0.01	0.09	0.21	0.03
K	0.17	0.17	0.17	0.01	0.01	0.10	0.10	0.15
Total	15.54	15.52	15.48	15.03	15.00	15.18	14.89	15.12

Sample	861.16	861.19	861.20	861.21	861.22	861.23	862.1	862.4
SiO ₂	43.45	42.84	42.68	42.97	42.86	42.67	44.37	43.60
TiO ₂	1.55	0.87	0.86	0.85	0.96	0.69	1.34	0.69
Al ₂ O ₃	8.76	9.84	9.71	9.50	9.15	9.91	8.46	9.16
Cr ₂ O ₃	0.00	0.00	0.03	0.04	0.00	0.06	0.01	0.01
FeO _t	17.51	18.29	18.18	18.72	18.75	18.65	17.67	19.29
MnO	0.46	0.36	0.42	0.43	0.39	0.34	0.39	0.40
NiO	0.02	0.09	0.04	0.08	0.00	0.05	0.00	0.08
MgO	9.68	9.23	9.16	9.27	9.60	9.61	9.88	9.30
CaO	11.21	11.26	11.14	11.12	10.58	10.89	10.96	11.43
Na ₂ O	1.46	1.36	1.27	1.49	1.49	1.29	1.79	1.74
K ₂ O	1.10	1.15	1.14	1.09	1.10	1.12	0.82	0.94
Total	95.19	95.30	94.62	95.56	94.88	95.28	95.70	96.63

Number of ions on the basis of 23 oxygens

Si	6.69	6.59	6.60	6.60	6.58	6.52	6.77	6.65
Al(IV)	1.31	1.41	1.40	1.40	1.42	1.48	1.23	1.35
Al(VI)	0.28	0.38	0.38	0.32	0.24	0.30	0.29	0.29
Ti	0.18	0.10	0.10	0.10	0.11	0.08	0.15	0.08
Cr ³⁺	0.00	0.00	0.00	0.01	0.00	0.01	0.00	0.00
Fe ³⁺	0.31	0.46	0.51	0.55	0.82	0.84	0.35	0.45
Fe ²⁺	1.95	1.90	1.85	1.86	1.60	1.56	1.90	2.02
Mn	0.06	0.05	0.06	0.06	0.05	0.04	0.05	0.05
Ni	0.00	0.01	0.01	0.01	0.00	0.01	0.00	0.01
Mg	2.22	2.12	2.11	2.12	2.20	2.19	2.25	2.11
Ca	1.85	1.86	1.85	1.83	1.74	1.78	1.79	1.87
Na(M4)	0.15	0.13	0.14	0.15	0.24	0.20	0.20	0.12
Na(A)	0.29	0.28	0.24	0.29	0.20	0.18	0.32	0.40
K	0.22	0.23	0.23	0.21	0.21	0.22	0.16	0.18
Total	15.51	15.50	15.46	15.50	15.41	15.40	15.48	15.58

Sample	862.6	862.8	862.9	862.10	862.13	862.14	862.15	862.16
SiO ₂	44.14	43.75	44.35	44.37	43.79	44.05	44.25	44.23
TiO ₂	0.68	0.99	1.52	1.55	0.94	1.08	1.19	1.37
Al ₂ O ₃	9.04	9.25	8.51	8.61	9.15	8.86	8.64	8.64
Cr ₂ O ₃	0.02	0.01	0.01	0.04	0.03	0.03	0.03	0.00
FeO _t	19.46	19.66	17.71	17.89	18.80	18.97	18.96	18.66
MnO	0.44	0.37	0.50	0.48	0.49	0.47	0.41	0.37
NiO	0.00	0.00	0.00	0.04	0.00	0.00	0.00	0.05
MgO	9.31	8.91	9.81	9.78	9.32	9.43	9.67	9.90
CaO	11.13	10.61	11.01	11.09	11.45	11.20	11.14	11.21
Na ₂ O	1.54	1.90	1.82	1.89	1.74	1.82	1.81	1.84
K ₂ O	0.91	1.03	1.04	0.94	1.15	1.02	0.99	1.03
Total	96.67	96.49	96.27	96.66	96.84	96.92	97.09	97.29

Number of ions on the basis of 23 oxygens

Si	6.68	6.66	6.75	6.74	6.67	6.69	6.69	6.68
Al(IV)	1.31	1.34	1.25	1.26	1.33	1.31	1.31	1.32
Al(VI)	0.30	0.32	0.28	0.28	0.32	0.27	0.23	0.21
Ti	0.08	0.11	0.17	0.18	0.11	0.12	0.14	0.15
Cr ³⁺	0.00	0.00	0.00	0.01	0.00	0.00	0.00	0.00
Fe ³⁺	0.62	0.58	0.29	0.28	0.32	0.42	0.47	0.42
Fe ²⁺	1.85	1.93	1.97	2.00	2.08	2.00	1.93	1.94
Mn	0.06	0.05	0.06	0.06	0.06	0.06	0.05	0.05
Ni	0.00	0.00	0.00	0.01	0.00	0.00	0.00	0.01
Mg	2.10	2.02	2.23	2.21	2.12	2.13	2.18	2.23
Ca	1.81	1.73	1.79	1.80	1.87	1.82	1.80	1.81
Na(M4)	0.19	0.26	0.20	0.19	0.13	0.17	0.19	0.18
Na(A)	0.27	0.30	0.33	0.37	0.39	0.36	0.34	0.36
K	0.18	0.20	0.20	0.18	0.22	0.20	0.19	0.20
Total	15.44	15.50	15.54	15.55	15.61	15.56	15.53	15.56

Sample	862.17	862.18	862.19	862.20	862.21	862.22	862.24	862.35
SiO ₂	44.35	44.14	44.20	44.25	44.27	44.16	43.89	43.19
TiO ₂	1.34	1.45	1.52	1.37	1.45	1.41	0.83	0.81
Al ₂ O ₃	8.77	8.57	8.66	8.68	8.81	8.66	8.95	9.34
Cr ₂ O ₃	0.00	0.03	0.02	0.05	0.01	0.04	0.09	0.01
FeO _t	18.33	18.20	18.44	18.96	18.35	18.68	20.10	18.75
MnO	0.42	0.45	0.45	0.48	0.48	0.46	0.50	0.48
NiO	0.04	0.06	0.07	0.10	0.06	0.00	0.01	0.10
MgO	9.77	9.69	9.61	9.67	9.72	9.81	9.22	8.01
CaO	11.07	11.19	11.12	11.20	11.16	11.16	11.57	9.41
Na ₂ O	1.84	1.75	1.83	1.81	1.80	1.74	1.40	1.80
K ₂ O	0.96	0.98	1.01	1.00	0.99	0.95	0.91	0.88
Total	96.88	96.51	96.93	97.55	97.10	97.05	97.47	92.75

Number of ions on the basis of 23 oxygens

Si	6.71	6.72	6.71	6.67	6.69	6.67	6.63	6.78
Al(IV)	1.29	1.28	1.29	1.33	1.31	1.33	1.37	1.22
Al(VI)	0.27	0.26	0.25	0.21	0.26	0.21	0.22	0.51
Ti	0.15	0.17	0.17	0.16	0.17	0.16	0.09	0.10
Cr ³⁺	0.00	0.00	0.00	0.01	0.00	0.01	0.01	0.00
Fe ³⁺	0.39	0.32	0.33	0.43	0.37	0.49	0.63	0.61
Fe ²⁺	1.93	2.00	2.02	1.96	1.96	1.87	1.92	1.86
Mn	0.05	0.06	0.06	0.06	0.06	0.06	0.06	0.06
Ni	0.01	0.01	0.01	0.01	0.01	0.00	0.00	0.01
Mg	2.20	2.20	2.17	2.17	2.19	2.21	2.07	1.87
Ca	1.79	1.82	1.81	1.81	1.81	1.80	1.87	1.58
Na(M4)	0.20	0.17	0.18	0.17	0.18	0.19	0.12	0.40
Na(A)	0.34	0.35	0.36	0.35	0.34	0.32	0.29	0.15
K	0.18	0.19	0.20	0.19	0.19	0.18	0.17	0.17
Total	15.53	15.54	15.55	15.55	15.54	15.50	15.47	15.32

Sample	862.36	8613.1	8613.2	8613.6	8613.7	8613.8	8613.9	8613.4
SiO ₂	43.56	51.47	48.27	50.88	46.25	50.69	50.82	45.00
TiO ₂	0.67	0.33	0.56	0.34	0.49	0.40	0.40	0.65
Al ₂ O ₃	8.65	5.02	7.84	5.53	9.03	5.44	4.90	10.82
Cr ₂ O ₃	0.00	0.29	0.18	0.16	0.23	0.11	0.32	0.22
FeO _t	18.67	7.80	8.41	8.38	8.06	8.27	8.25	11.39
MnO	0.39	0.12	0.22	0.26	0.23	0.13	0.13	0.31
NiO	0.05	0.00	0.05	0.00	0.00	0.04	0.02	0.00
MgO	9.45	17.45	16.41	17.38	16.04	16.90	17.10	13.33
CaO	11.30	12.38	11.80	12.05	11.42	12.09	12.24	11.78
Na ₂ O	1.63	0.99	1.46	1.00	1.82	1.01	1.07	1.99
K ₂ O	0.79	0.39	0.75	0.42	0.78	0.43	0.41	0.94
Total	95.16	96.25	95.93	96.42	94.34	95.51	95.63	96.42

Number of ions on the basis of 23 oxygens

Si	6.72	7.39	6.99	7.28	6.81	7.35	7.37	6.64
Al(IV)	1.28	0.61	1.01	0.72	1.19	0.65	0.63	1.36
Al(VI)	0.29	0.24	0.33	0.21	0.38	0.28	0.21	0.53
Ti	0.08	0.04	0.06	0.04	0.05	0.04	0.04	0.07
Cr ³⁺	0.00	0.03	0.02	0.02	0.03	0.01	0.04	0.03
Fe ³⁺	0.44	0.10	0.31	0.38	0.41	0.15	0.12	0.19
Fe ²⁺	1.97	0.84	0.71	0.63	0.58	0.85	0.88	1.22
Mn	0.05	0.01	0.03	0.03	0.03	0.02	0.01	0.04
Ni	0.01	0.00	0.01	0.00	0.00	0.01	0.00	0.00
Mg	2.17	3.74	3.54	3.70	3.52	3.65	3.70	2.93
Ca	1.87	1.91	1.83	1.85	1.80	1.88	1.90	1.86
Na(M4)	0.12	0.10	0.16	0.15	0.20	0.12	0.10	0.14
Na(A)	0.37	0.18	0.25	0.13	0.32	0.17	0.20	0.43
K	0.16	0.07	0.14	0.08	0.15	0.08	0.08	0.18
Total	15.52	15.25	15.39	15.20	15.47	15.25	15.28	15.61

Sample	8613.5	31.7	31.11	31.12	Glen 9.1	Glen 9.2	Glen 13.1	Glen 13.2
SiO ₂	43.99	43.12	43.63	43.93	43.49	42.87	51.85	47.02
TiO ₂	0.71	0.78	0.91	0.94	0.60	0.74	0.11	1.25
Al ₂ O ₃	11.44	9.42	9.43	9.03	11.39	11.81	5.07	9.16
Cr ₂ O ₃	0.26	0.04	0.03	0.04	0.00	0.00	0.00	0.06
FeO _t	10.04	18.87	18.54	18.32	17.81	15.67	7.37	9.99
MnO	0.21	0.41	0.49	0.36	0.44	0.45	0.13	0.18
NiO	0.04	0.00	0.03	0.00	0.00	0.01	0.00	0.05
MgO	14.49	9.37	9.24	9.42	9.91	10.88	17.75	14.97
CaO	11.87	10.87	11.38	11.30	11.52	11.58	12.19	12.13
Na ₂ O	1.97	1.33	1.51	1.38	1.22	1.46	0.90	1.38
K ₂ O	1.10	1.09	0.99	1.01	0.78	0.84	0.17	0.46
Total	96.12	95.29	96.18	95.70	97.20	96.30	95.54	96.64

Number of ions on the basis of 23 oxygens

Si	6.47	6.60	6.66	6.72	6.47	6.40	7.44	6.82
Al(IV)	1.53	1.40	1.34	1.28	1.53	1.60	0.56	1.18
Al(VI)	0.45	0.30	0.36	0.35	0.47	0.48	0.29	0.39
Ti	0.08	0.09	0.10	0.11	0.07	0.08	0.01	0.14
Cr ³⁺	0.03	0.01	0.00	0.01	0.00	0.00	0.00	0.01
Fe ³⁺	0.37	0.74	0.40	0.40	0.76	0.66	0.22	0.26
Fe ²⁺	0.87	1.68	1.97	1.95	1.47	1.30	0.67	0.96
Mn	0.03	0.05	0.06	0.05	0.06	0.06	0.01	0.02
Ni	0.01	0.00	0.00	0.00	0.00	0.00	0.00	0.01
Mg	3.17	2.14	2.10	2.15	2.20	2.42	3.79	3.24
Ca	1.87	1.78	1.86	1.85	1.83	1.85	1.87	1.89
Na(M4)	0.12	0.21	0.13	0.14	0.15	0.14	0.13	0.11
Na(A)	0.44	0.19	0.31	0.26	0.20	0.29	0.12	0.28
K	0.21	0.21	0.19	0.20	0.15	0.16	0.03	0.09
Total	15.64	15.40	15.51	15.46	15.35	15.45	15.16	15.37

Sample	Glen 13.5	Glen 13.6	Glen 13.7	GLAP1	GLAP3	GLAP11	GLAP12	GLAP13
SiO ₂	51.17	53.49	50.34	42.06	43.48	45.80	48.61	41.77
TiO ₂	0.25	0.28	0.44	1.19	0.85	0.98	0.64	1.42
Al ₂ O ₃	5.67	3.24	6.27	13.74	11.98	9.57	7.25	13.81
Cr ₂ O ₃	0.00	0.08	0.00	0.04	0.05	0.00	0.03	0.04
FeO _t	7.68	7.40	8.03	12.85	12.66	12.02	10.76	13.65
MnO	0.22	0.11	0.13	0.27	0.27	0.19	0.14	0.21
NiO	0.04	0.00	0.00	0.02	0.04	0.00	0.00	0.20
MgO	17.84	18.72	17.28	12.01	12.36	13.85	15.57	11.43
CaO	12.57	12.24	12.60	12.10	12.16	12.16	12.39	12.13
Na ₂ O	0.89	0.69	0.84	1.98	1.52	1.19	1.01	1.84
K ₂ O	0.18	0.09	0.37	0.82	0.93	0.90	0.65	0.88
Total	96.51	96.35	96.29	97.09	96.28	96.65	97.06	97.25

Number of ions on the basis of 23 oxygens

Si	7.29	7.58	7.22	6.21	6.46	6.71	7.02	6.19
Al(IV)	0.71	0.42	0.78	1.79	1.54	1.28	0.98	1.81
Al(VI)	0.24	0.12	0.28	0.60	0.56	0.37	0.26	0.60
Ti	0.03	0.03	0.05	0.13	0.10	0.11	0.07	0.16
Cr ³⁺	0.00	0.01	0.00	0.01	0.01	0.00	0.00	0.00
Fe ³⁺	0.29	0.31	0.23	0.37	0.29	0.37	0.34	0.30
Fe ²⁺	0.63	0.57	0.73	1.22	1.28	1.10	0.96	1.39
Mn	0.03	0.01	0.02	0.03	0.03	0.02	0.02	0.03
Ni	0.01	0.00	0.00	0.00	0.00	0.00	0.00	0.02
Mg	3.79	3.95	3.69	2.64	2.74	3.03	3.35	2.52
Ca	1.92	1.86	1.94	1.91	1.94	1.91	1.92	1.92
Na(M4)	0.07	0.14	0.06	0.08	0.06	0.09	0.08	0.05
Na(A)	0.17	0.05	0.17	0.49	0.38	0.25	0.20	0.48
K	0.03	0.02	0.07	0.15	0.18	0.17	0.12	0.17
Total	15.20	15.07	15.24	15.64	15.56	15.42	15.32	15.64

Sample	GLAP14	GLAP15	GLAP25	GLAP26	GLAP27	GLAP28	RY 4.2'
SiO ₂	48.97	51.76	42.30	53.49	45.09	47.36	54.30
TiO ₂	0.33	0.19	1.18	0.15	0.41	0.32	0.11
Al ₂ O ₃	7.55	4.74	13.28	3.46	11.02	8.26	5.12
Cr ₂ O ₃	0.00	0.01	0.02	0.01	0.05	0.04	0.00
FeO _t	10.02	8.99	13.26	7.74	12.20	10.68	13.89
MnO	0.27	0.22	0.18	0.20	0.22	0.28	0.13
NiO	0.03	0.00	0.02	0.05	0.00	0.00	0.00
MgO	15.69	17.26	11.94	18.47	13.58	14.89	15.83
CaO	12.20	12.42	12.11	12.69	12.42	12.55	12.12
Na ₂ O	0.98	0.62	1.71	0.47	1.51	1.20	0.12
K ₂ O	0.32	0.19	1.06	0.13	0.75	0.50	0.04
Total	96.36	96.38	97.05	96.86	97.25	96.08	97.69
Number of ions on the basis of 23 oxygens							
Si	7.07	7.40	6.26	7.57	6.58	6.94	7.49
Al(IV)	0.93	0.60	1.74	0.43	1.42	1.06	0.51
Al(VI)	0.35	0.20	0.57	0.15	0.48	0.36	0.32
Ti	0.04	0.02	0.13	0.02	0.04	0.04	0.01
Cr ³⁺	0.00	0.00	0.00	0.00	0.01	0.00	0.00
Fe ³⁺	0.40	0.35	0.38	0.24	0.39	0.24	0.76
Fe ²⁺	0.81	0.73	1.27	0.68	1.10	1.06	0.90
Mn	0.03	0.03	0.02	0.02	0.03	0.03	0.01
Ni	0.00	0.00	0.00	0.01	0.00	0.00	0.00
Mg	3.37	3.68	2.63	3.90	2.96	3.25	3.25
Ca	1.89	1.90	1.92	1.92	1.94	1.97	1.79
Na(M4)	0.11	0.09	0.08	0.07	0.05	0.03	0.00
Na(A)	0.17	0.08	0.41	0.06	0.38	0.31	0.03
K	0.06	0.04	0.20	0.02	0.14	0.09	0.01
Total	15.23	15.11	15.61	15.08	15.52	15.41	15.08

iii. Biotite Analyses

Sample	Rock Type	Intrusion
861.10-861.15	Quartz monzodiorite	G1 (Ardara)
8613.10	Granodiorite	G2 (Ardara)
963.3-963.4	Granodiorite	G3 (Ardara)
Glen 9.3-9.4	Granite	Glenard
Glen ap.21-30	"Appinite"	Glenard
Bir Br.1	Breccia	Biroge breccia pipe
17.4-17.7	Hornblendite dyke	Summy Lough
SLD.9	Diorite	Summy Lough
85.1-85.10	Diorite	Summy Lough
M14.4-M14.5	Diorite	Meenalargan
M10.7	Quartz diorite	Meenalargan
64a.1-64a.3	Tonalite	Meenalargan
76c.3-7	Hornblendite	Narin-Portnoo
2651.9	Hornblendite	Narin-Portnoo
2658.51-2658.18	Meladiorite	Narin-Portnoo
27520.10	Diorite	Narin-Portnoo
3158.3-3158.5	Diorite	Narin-Portnoo
Bio Di	Biotite diorite	Narin-Portnoo
Bio Gr.2-Bio Gr.10	Biotite granite	Narin-Portnoo
Mulna di.4	Diorite	Mulnamin
Mul di ap.2-Mul di ap.8	Diorite	Mulnamin
2093.6	Diorite	Mulnamin
MDG.2-MDG.5	Granite	Main Donegal Granite

Sample	861.10	861.13	861.15	8613.10	963.30	963.40	Glen 9.3	Glen 9.4
SiO ₂	36.79	36.28	36.95	36.99	37.07	37.61	36.36	36.26
TiO ₂	1.87	2.39	1.81	2.66	2.97	2.89	2.02	2.16
Al ₂ O ₃	16.09	15.39	16.28	15.28	15.22	15.37	16.63	16.36
FeO	20.40	18.29	18.93	16.57	17.83	18.12	18.48	18.72
MnO	0.32	0.22	0.33	0.29	0.25	0.34	0.20	0.17
MgO	9.54	10.54	10.65	12.81	11.16	10.91	11.26	10.98
CaO	0.02	0.04	0.00	0.03	0.03	0.06	0.05	0.00
Na ₂ O	0.03	0.03	0.03	0.05	0.08	0.01	0.13	0.08
K ₂ O	9.02	9.12	9.62	9.37	9.37	9.16	9.86	10.50
Total	94.08	92.30	94.58	94.05	93.94	94.48	94.97	95.22
Number of ions on the basis of 22 oxygens								
Si	5.70	5.68	5.66	5.64	5.68	5.74	5.56	5.56
Ti	0.22	0.28	0.20	0.30	0.34	0.34	0.24	0.24
Al	2.94	2.84	2.94	2.74	2.76	2.76	3.00	2.96
Fe	2.64	2.40	2.42	2.12	2.28	2.30	2.36	2.40
Mn	0.04	0.02	0.04	0.04	0.04	0.04	0.02	0.02
Mg	2.20	2.46	2.44	2.92	2.56	2.48	2.56	2.50
Ca	0.00	0.00	0.00	0.00	0.00	0.02	0.00	0.00
Na	0.00	0.00	0.00	0.02	0.02	0.00	0.04	0.02
K	1.78	1.82	1.88	1.82	1.84	1.78	1.92	2.04
Total	15.52	15.50	15.58	15.60	15.52	15.46	15.70	15.74

cont/

Sample	Glen ap 21	Glen ap 22	Glen ap 29	Glen ap 30	Bir br.1	17.40	17.60	17.70
SiO ₂	36.44	36.57	38.85	37.45	39.29	38.57	37.91	39.22
TiO ₂	0.92	1.22	1.23	1.16	1.33	2.37	2.20	2.39
Al ₂ O ₃	17.07	16.99	17.22	17.42	15.14	15.71	15.46	15.72
FeO	13.44	14.11	12.70	12.10	11.98	10.34	11.08	11.83
MnO	0.09	0.17	0.13	0.16	0.10	0.09	0.10	0.07
MgO	15.94	15.19	16.15	16.05	16.72	16.60	17.04	15.75
CaO	0.02	0.00	0.05	0.07	0.06	0.05	0.00	0.01
Na ₂ O	0.08	0.14	0.11	0.14	0.03	0.13	0.05	0.10
K ₂ O	9.25	10.41	6.29	9.66	9.19	9.44	9.95	7.88
Total	93.19	94.79	92.73	94.20	93.85	93.29	93.79	92.96

Number of ions on the basis of 22 oxygens

Si	5.50	5.50	5.74	5.56	5.82	5.72	5.64	5.80
Ti	0.10	0.14	0.14	0.14	0.14	0.26	0.24	0.26
Al	3.04	3.00	3.00	3.06	2.64	2.74	2.70	2.74
Fe	1.70	1.78	1.56	1.50	1.48	1.28	1.38	1.46
Mn	0.02	0.02	0.02	0.02	0.02	0.02	0.02	0.00
Mg	3.58	3.40	3.56	3.56	3.70	3.66	3.78	3.48
Ca	0.00	0.00	0.00	0.02	0.02	0.00	0.00	0.00
Na	0.02	0.04	0.04	0.04	0.02	0.04	0.02	0.02
K	1.78	2.00	1.18	1.84	1.74	1.78	1.88	1.48
Total	15.74	15.88	15.24	15.74	15.58	15.50	15.66	15.24

Sample	SLD.9	85.10	85/10	M14.4	M14.5	M10.7	64a.1	64a.3
SiO ₂	37.90	36.65	37.51	37.70	38.39	37.60	37.76	37.72
TiO ₂	1.41	2.39	2.25	1.22	1.17	1.72	1.62	1.90
Al ₂ O ₃	16.99	16.05	16.04	16.55	16.95	16.94	15.64	15.71
FeO	16.05	16.31	16.58	12.52	11.52	12.97	19.66	19.81
MnO	0.04	0.12	0.16	0.11	0.11	0.21	0.33	0.38
MgO	12.98	12.22	12.80	16.33	16.31	15.76	11.01	10.58
CaO	0.01	0.10	0.13	0.00	0.06	0.08	0.06	0.01
Na ₂ O	0.04	0.00	0.12	0.07	0.08	0.08	0.01	0.18
K ₂ O	9.69	9.52	9.59	10.22	9.74	8.58	8.91	8.59
Total	95.12	93.35	95.17	94.71	94.32	93.92	94.99	94.89

Number of ions on the basis of 22 oxygens

Si	5.66	5.62	5.64	5.60	5.66	5.60	5.74	5.74
Ti	0.16	0.28	0.26	0.14	0.14	0.20	0.18	0.22
Al	3.00	2.90	2.84	2.90	2.96	2.98	2.80	2.82
Fe	2.00	2.08	2.08	1.56	1.42	1.62	2.50	2.52
Mn	0.00	0.02	0.02	0.02	0.02	0.02	0.04	0.04
Mg	2.90	2.80	2.86	3.62	3.58	3.50	2.50	2.40
Ca	0.00	0.02	0.02	0.00	0.00	0.02	0.02	0.00
Na	0.02	0.00	0.04	0.02	0.02	0.02	0.00	0.06
K	1.84	1.86	1.84	1.94	1.84	1.62	1.72	1.66
Total	15.58	15.58	15.60	15.80	15.64	15.58	15.50	15.46

Sample	76c.3	76c.7	2651.9	2658.51	2658.56	2658.81	2658.18	27520.10
SiO ₂	38.22	37.85	37.12	38.62	38.99	39.91	38.41	37.02
TiO ₂	1.32	1.14	1.11	0.75	0.81	1.02	0.85	2.13
Al ₂ O ₃	16.12	16.15	16.92	18.21	16.67	16.54	16.65	16.86
FeO	15.26	14.72	14.79	13.70	12.30	11.85	11.97	14.88
MnO	0.12	0.09	0.07	0.15	0.08	0.09	0.13	0.16
MgO	14.56	14.70	14.89	18.68	16.75	17.19	17.09	13.67
CaO	0.00	0.00	0.01	0.07	0.06	0.01	0.08	0.03
Na ₂ O	0.07	0.12	0.01	0.10	0.15	0.02	0.15	0.10
K ₂ O	8.24	9.21	8.49	10.42	10.19	9.73	9.57	10.41
Total	93.90	93.96	93.40	100.70	95.99	96.36	94.89	95.26

Number of ions on the basis of 22 oxygens

Si	5.72	5.70	5.60	5.42	5.70	5.76	5.66	5.54
Ti	0.14	0.12	0.12	0.08	0.08	0.12	0.10	0.24
Al	2.84	2.86	3.00	3.00	2.86	2.82	2.90	2.98
Fe	1.90	1.86	1.86	1.60	1.50	1.42	1.48	1.86
Mn	0.02	0.02	0.00	0.02	0.02	0.02	0.02	0.02
Mg	3.24	3.30	3.34	3.90	3.64	3.70	3.76	3.06
Ca	0.00	0.00	0.00	0.02	0.00	0.00	0.02	0.00
Na	0.02	0.04	0.00	0.02	0.04	0.00	0.04	0.02
K	1.58	1.76	1.64	1.86	1.90	1.80	1.80	1.98
Total	15.46	15.66	15.56	15.92	15.74	15.64	15.78	15.70

Sample	3158.3	3158.5	Bio Di	Bio Gr 2	Bio Gr 4	Bio Gr 7	Bio Gr 9	Bio Gr 10
SiO ₂	37.58	38.27	36.80	36.88	36.71	35.62	36.96	35.48
TiO ₂	1.50	2.23	3.17	1.75	2.61	2.95	1.23	3.30
Al ₂ O ₃	16.61	17.32	15.10	16.66	15.97	16.25	16.45	16.42
FeO	14.97	15.35	20.55	18.41	18.97	18.70	17.92	18.79
MnO	0.17	0.03	0.23	0.15	0.17	0.25	0.12	0.18
MgO	14.29	13.72	9.84	11.06	10.98	10.54	11.39	10.18
CaO	0.22	0.06	0.01	0.16	0.11	0.07	0.19	0.06
Na ₂ O	0.07	0.04	0.00	0.13	0.14	0.04	0.04	0.11
K ₂ O	7.96	9.68	9.63	9.68	9.71	10.11	9.29	9.58
Total	93.37	96.70	95.34	94.87	95.37	94.52	93.59	94.11

Number of ions on the basis of 22 oxygens

Si	5.66	5.60	5.64	5.62	5.58	5.50	5.68	5.48
Ti	0.18	0.24	0.36	0.20	0.30	0.34	0.14	0.38
Al	2.94	3.00	2.74	3.00	2.86	2.96	2.98	3.00
Fe	1.88	1.88	2.64	2.34	2.42	2.42	2.30	2.42
Mn	0.02	0.00	0.02	0.02	0.02	0.04	0.02	0.02
Mg	3.20	3.00	2.24	2.52	2.50	2.42	2.60	2.34
Ca	0.04	0.00	0.00	0.02	0.02	0.02	0.04	0.02
Na	0.02	0.02	0.00	0.04	0.04	0.02	0.02	0.04
K	1.52	1.82	1.88	1.88	1.88	1.98	1.82	1.88
Total	15.46	15.56	15.52	15.64	15.62	15.70	15.60	15.58

Sample	Mulna di.4	Mul di ap.2	Mul di ap.8	2093.6	MDG.2	MDG.5
SiO ₂	35.86	36.94	37.00	38.30	35.04	34.24
TiO ₂	1.77	1.42	1.51	2.51	3.06	3.26
Al ₂ O ₃	16.89	16.82	17.13	16.90	16.80	16.47
FeO	14.08	15.38	15.75	14.42	21.05	20.92
MnO	0.04	0.17	0.19	0.20	0.35	0.34
MgO	16.17	14.07	14.34	14.01	7.51	7.79
CaO	0.09	0.01	0.03	0.02	0.00	0.05
Na ₂ O	0.12	0.12	0.13	0.06	0.08	0.04
K ₂ O	7.88	9.61	8.82	8.02	10.39	10.23
Total	92.90	94.52	94.90	94.44	94.27	93.34
Number of ions on the basis of 22 oxygens						
Si	5.42	5.56	5.54	5.66	5.50	5.44
Ti	0.20	0.16	0.18	0.28	0.36	0.40
Al	3.00	2.98	3.02	2.94	3.10	3.08
Fe	1.78	1.94	1.96	1.78	2.76	2.78
Mn	0.00	0.02	0.02	0.02	0.04	0.04
Mg	3.64	3.16	3.20	3.08	1.76	1.84
Ca	0.02	0.00	0.00	0.00	0.00	0.02
Na	0.04	0.04	0.04	0.02	0.02	0.02
K	1.52	1.84	1.68	1.52	2.08	2.08
Total	15.62	15.70	15.64	15.30	15.62	15.70

iv. Plagioclase analyses

Sample	Zone position	Rock Type	Intrusion
1797.3,4	Core-margin pair	Diorite	Summy Lough
s5.16,17	Core-margin pair	Diorite	Summy Lough
85.16	Core (light)	Diorite	Summy Lough
sld.2	Core	Diorite	Summy Lough
3,4,7	Core-dark margin-light margin	Diorite	Summy Lough
21.6	Margin	Hornblendite	Summy Lough
21.8	Margin	Hornblendite	Summy Lough
17.9	Margin	Hornblendite dyke	Summy Lough
2093.2	Margin	Diorite	Mulnamin
Mulna di.7	Core	Diorite	Mulnamin
Mulna di.14	Core	Diorite	Mulnamin
Mul di.3,4	Core-Margin pair	Diorite	Mulnamin
20.2	Core	Hornblende diorite	Mulnamin
23.5,4	Core-margin pair	Granite dyke	Mulnamin
861.2	Core	Quartz monzodiorite	G1 (Ardara)
861.17	Margin	Quartz monzodiorite	G1 (Ardara)
862.3	Margin	Quartz monzodiorite	G1 (Ardara)
862.25	Core	Quartz monzodiorite	G1 (Ardara)
863.5	Margin	Quartz monzodiorite	G1 (Ardara)
8610.7	Core	Granodiorite	G2 (Ardara)
963.2	Margin	Granodiorite	G3 (Ardara)
963.5	Core	Granodiorite	G3 (Ardara)
3153.3	Core	Diorite	Narin-Portnoo
27515.11	Core	Diorite	Narin-Portnoo
27520.3	Margin	Diorite	Narin-Portnoo

<u>Sample</u>	<u>Zone position</u>	<u>Rock Type</u>	<u>Intrusion</u>
2658.28	Margin	Meladiorite	Narin-Portnoo
31511.10	Core	Diorite	Narin-Portnoo
31511.9	Margin	Diorite	Narin-Portnoo
667.1	Margin	Biotite diorite	Narin-Portnoo
667.2	Margin	Biotite diorite	Narin-Portnoo
Bio gr.5,6	Core-margin pair	Biotite granite	Narin-Portnoo
Glenap.4	Margin	"Appinite"	Glenard
Glenap.5	Margin	"Appinite"	Glenard
Glenap.17	Margin	"Appinite"	Glenard
Glenap.18	Margin	"Appinite"	Glenard
9.6,7	Core-margin pair	Granite	Glenard
25510.8	Core	Diorite	Meenalargan
1856.33, 34	Margin	Diorite	Meenalargan
25514.6,7,8,9	Core-margin traverse	Felsite	Meenalargan
M11.1	Core	Diorite	Meenalargan
M14.1	Margin	Diorite	Meenalargan
M14.3	Margin	Diorite	Meenalargan
M12.5,6	Core-margin pair	Diorite	Meenalargan
64b.2	Core	Coarse diorite	Meenalargan
M10.5,6	Core-margin pair	Diorite	Meenalargan
64a.2	Core	Granitoid	Meenalargan

Sample	1797.30	1797.40	s5.16	s5.17	85.16	sld.2	sld.3	sld.4
SiO2	53.77	52.05	57.22	59.00	59.92	59.79	62.47	59.99
TiO2	0.03	0.01	0.00	0.04	0.07	0.01	0.01	0.02
Al2O3	29.10	30.03	25.92	26.75	25.22	25.53	23.92	25.69
FeO	0.24	0.14	0.11	0.05	0.24	0.00	0.14	0.05
MnO	0.02	0.01	0.01	0.00	0.01	0.03	0.00	0.00
MgO	0.00	0.00	0.05	0.00	0.00	0.03	0.06	0.00
CaO	11.49	12.47	7.72	7.69	6.46	6.85	4.78	6.79
Na2O	5.05	4.19	8.00	7.99	8.49	8.23	9.60	8.46
K2O	0.07	0.05	0.07	0.06	0.12	0.06	0.12	0.07
Total	99.78	98.95	99.11	101.58	100.42	100.59	101.1	101.01

Sample	sld.7	21.60	21.80	17.90	2093.20	mulnadi.7	mulnadi.14	muldi.:
SiO2	59.31	58.76	61.54	63.38	55.10	58.08	54.67	58.32
TiO2	0.18	0.00	0.00	0.01	0.04	0.00	0.00	0.04
Al2O3	25.47	26.20	24.67	22.48	28.00	26.45	28.35	26.28
FeO	0.15	0.04	0.06	0.06	0.08	0.24	0.15	0.13
MnO	0.00	0.00	0.01	0.00	0.00	0.05	0.00	0.04
MgO	0.00	0.00	0.00	0.00	0.00	0.02	0.00	0.00
CaO	6.58	7.94	5.94	3.32	9.93	7.80	10.54	7.42
Na2O	8.07	6.76	6.98	9.63	5.98	7.02	5.68	7.29
K2O	0.08	0.06	0.09	0.07	0.06	0.08	0.01	0.07
Total	99.82	99.76	99.28	99.02	99.19	99.74	99.40	99.62

Sample	muldi.4	20.2	23.5	23.4	861.2	861.17	862.3	862.25
SiO2	58.36	60.74	56.98	60.16	58.22	62.25	63.23	63.97
TiO2	0.00	0.01	0.02	0.00	0.00	0.00	0.00	0.00
Al2O3	26.54	24.73	26.92	24.70	26.01	23.10	23.14	23.04
FeO	0.06	0.00	0.03	0.04	0.03	0.04	0.09	0.38
MnO	0.00	0.06	0.00	0.03	0.00	0.04	0.00	0.03
MgO	0.00	0.03	0.00	0.00	0.26	0.01	0.00	0.00
CaO	7.83	5.97	8.36	6.34	7.69	4.10	3.91	3.11
Na2O	6.63	7.80	6.70	7.91	6.88	9.37	9.34	9.66
K2O	0.04	0.07	0.13	0.12	0.10	0.08	0.10	0.23
Total	99.47	99.42	99.39	99.33	99.17	99.00	100.36	99.13

Sample	863.50	8610.70	8613.10	963.20	963.50	3153.30	27515.11	27520.3
SiO2	63.03	61.91	61.34	62.71	61.71	57.92	58.96	61.67
TiO2	0.00	0.00	.05	0.04	0.00	0.01	0.00	0.00
Al2O3	22.95	22.93	23.96	23.74	23.27	25.90	25.69	23.53
FeO	0.01	.04	.05	0.22	0.06	0.09	0.15	0.20
MnO	0.00	0.00	0.00	0.00	0.00	0.00	0.00	0.09
MgO	0.00	.03	0.00	0.00	0.03	0.04	0.02	0.00
CaO	3.71	4.29	5.35	4.83	4.47	7.44	7.18	4.73
Na2O	9.69	9.36	8.58	8.60	8.83	7.06	7.45	9.06
K2O	0.17	0.14	0.08	0.15	0.14	0.14	0.10	0.09
Total	99.57	98.71	99.45	100.27	98.49	98.65	99.65	99.39

Sample	2658.28	31511.1	31511.9	667.1	667.2	biogr.5	biogr.6	glenap.4
SiO2	66.39	54.83	61.70	52.19	53.10	60.74	61.28	59.36
TiO2	0.11	0.02	0.00	0.00	0.00	0.04	0.02	0.04
Al2O3	20.21	27.74	23.34	29.85	29.12	24.72	24.36	26.07
FeO	0.21	0.22	0.03	0.14	0.23	0.14	0.12	0.10
MnO	0.02	0.00	0.02	0.01	0.03	0.00	0.01	0.02
MgO	0.00	0.03	0.00	0.05	0.00	0.01	0.03	0.02
CaO	5.01	10.46	4.59	12.15	11.74	5.84	5.46	7.57
Na2O	7.87	5.52	8.96	4.70	5.17	8.23	8.65	7.01
K2O	0.06	0.25	0.17	0.26	0.14	0.10	0.08	0.06
Total	99.98	99.06	98.85	99.34	99.55	99.82	100.03	100.25

Sample	glenap.5	glenap.17	glenap.18	9.60	9.70	25510.80	1856.33	1856.34
SiO2	59.09	61.12	57.14	54.30	59.68	60.57	61.27	61.07
TiO2	0.00	0.00	0.00	0.06	0.03	0.00	0.00	0.00
Al2O3	25.28	24.30	26.43	28.81	24.61	25.10	24.60	24.61
FeO	0.02	0.01	0.07	0.11	0.23	0.00	0.06	0.11
MnO	0.02	0.00	0.00	0.00	0.00	0.00	0.01	0.00
MgO	0.00	0.01	0.00	0.00	0.00	0.01	0.00	0.00
CaO	6.82	5.48	8.49	10.87	6.45	6.59	5.58	5.90
Na2O	7.74	8.55	7.04	5.61	8.08	8.23	9.11	8.99
K2O	0.09	0.05	0.03	0.06	0.09	0.06	0.07	0.06
Total	99.07	99.53	99.20	99.82	99.17	100.56	100.73	100.74

Sample	25514.4	25514.5	25514.6	25514.7	25514.8	25514.9	m11.1	m14.1
SiO2	55.34	54.08	54.71	60.18	58.67	54.60	57.07	54.56
TiO2	0.06	0.00	0.00	0.01	0.00	0.00	0.00	0.00
Al2O3	29.28	27.84	28.59	24.59	25.82	28.73	27.75	28.86
FeO	0.69	0.05	0.09	0.18	0.00	0.02	0.03	0.10
MnO	0.02	0.02	0.00	0.03	0.02	0.00	0.00	0.05
MgO	0.43	0.01	0.02	0.03	0.01	0.02	0.00	0.04
CaO	9.53	10.80	10.79	6.00	7.57	11.00	9.06	11.16
Na2O	6.28	5.43	5.44	8.16	7.27	5.18	6.40	5.24
K2O	0.61	0.09	0.07	0.25	0.14	0.07	0.05	0.03
Total	102.24	98.32	99.73	99.43	99.50	99.63	100.39	100.03

Sample	m14.3	m12.5	M12.6	64b.2	m10.5	m10.6	64a.2
SiO2	60.05	58.95	58.52	59.47	56.36	58.56	60.52
TiO2	0.00	0.05	0.01	0.00	0.00	0.01	0.00
Al2O3	24.52	25.03	25.49	24.81	26.46	25.16	24.01
FeO	0.08	0.20	0.18	0.03	0.02	0.09	0.03
MnO	0.02	0.00	0.000	0.00	0.03	0.00	0.01
MgO	0.00	0.03	0.01	0.00	0.00	0.05	0.02
CaO	5.88	6.49	7.05	5.78	7.86	6.37	5.11
Na2O	8.33	7.40	7.72	9.02	7.65	8.23	9.54
K2O	0.11	0.13	0.02	0.06	0.06	0.06	0.13
Total	99.02	98.33	99.00	99.15	98.44	98.54	99.37

v. Epidote Analyses

Index of Epidote Analysis

2658.9
2658.7

Meladiorite
Meladiorite

Narin-Portnoo
Narin-Portnoo

Sample	2658.9	2658.7
SiO2	37.31	37.83
TiO2	0.11	0.07
Al2O3	22.73	23.62
FeO	11.84	10.85
MnO	0.00	0.08
MgO	0.03	0.00
CaO	23.01	22.90
Na2O	0.00	0.00
K2O	0.00	0.02
Total	95.03	95.37

Number of ions on
the basis of 13 oxygens

Si	3.17	3.22
Al	---	---
Al	2.25	2.33
Fe+3	0.75	0.61
Ti	0.01	0.01
Mg	0.01	0.00
Ca	2.10	2.09
K	0.00	1.02
Pistacite	25%	21%
Fe+3/(Fe+3+Al)		

APPENDIX 6

GEOLOGICAL MAPS OF THE ARDARA IGNEOUS COMPLEX.

(all maps are in seperate folder attached to back cover).

MAP 1 GENERAL LOCATION MAP OF THE ARDARA AREA

MAP 2 THE GEOLOGY OF THE NORTHERN PART OF THE ARDARA PLUTON.

MAP 3 THE GEOLOGY OF THE MEENALARGAN INTRUSION

MAP 3' THE GEOLOGY OF THE AREA S.E. OF LOUGH LARAGH, MEENALARGAN

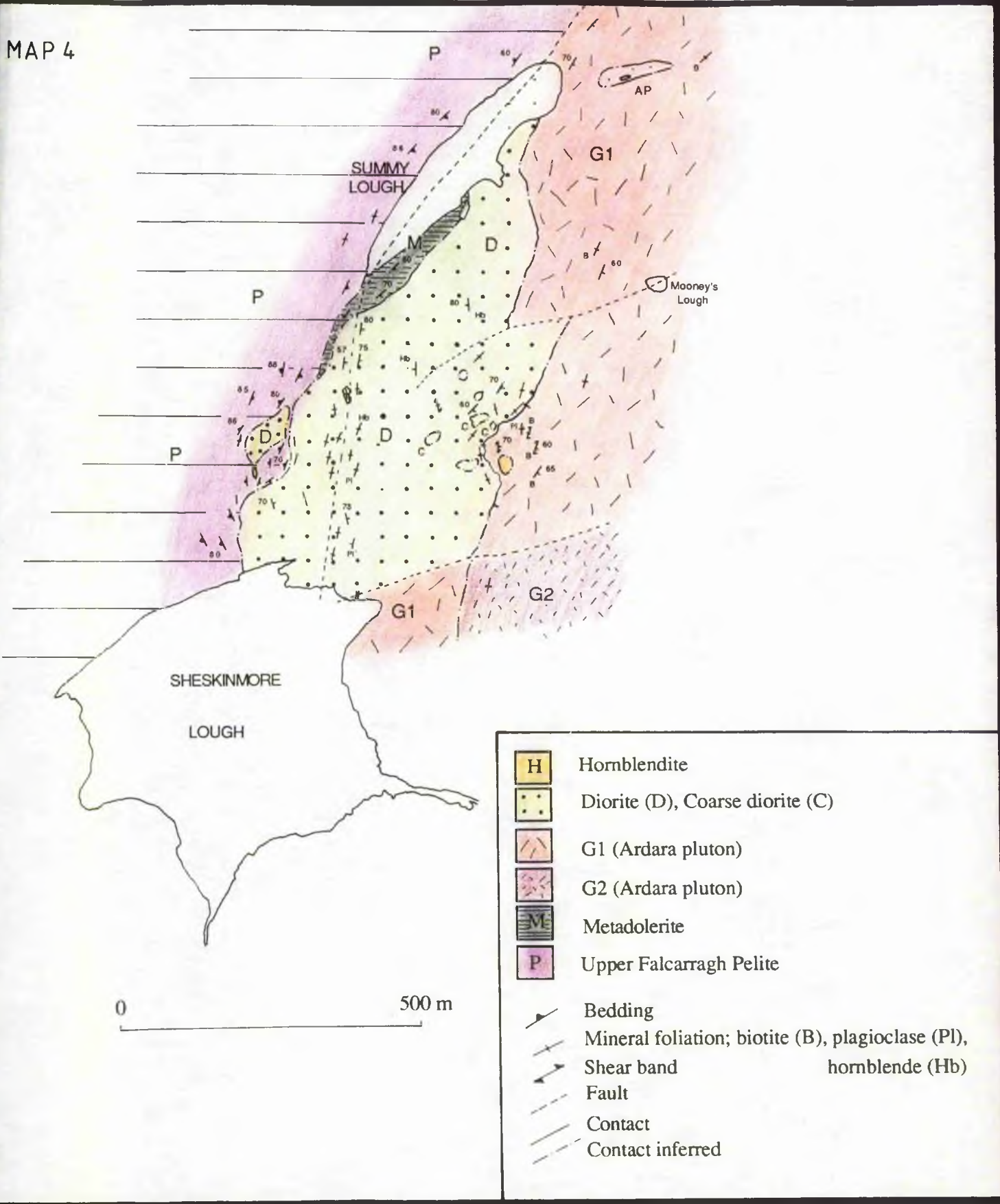
MAP 4 THE GEOLOGY OF THE SUMMY LOUGH DIORITE

MAP 5 THE GEOLOGY OF THE MULNAMIN INTRUSION

MAP 6 THE GEOLOGY OF THE NARIN-PORTNOO COMPLEX

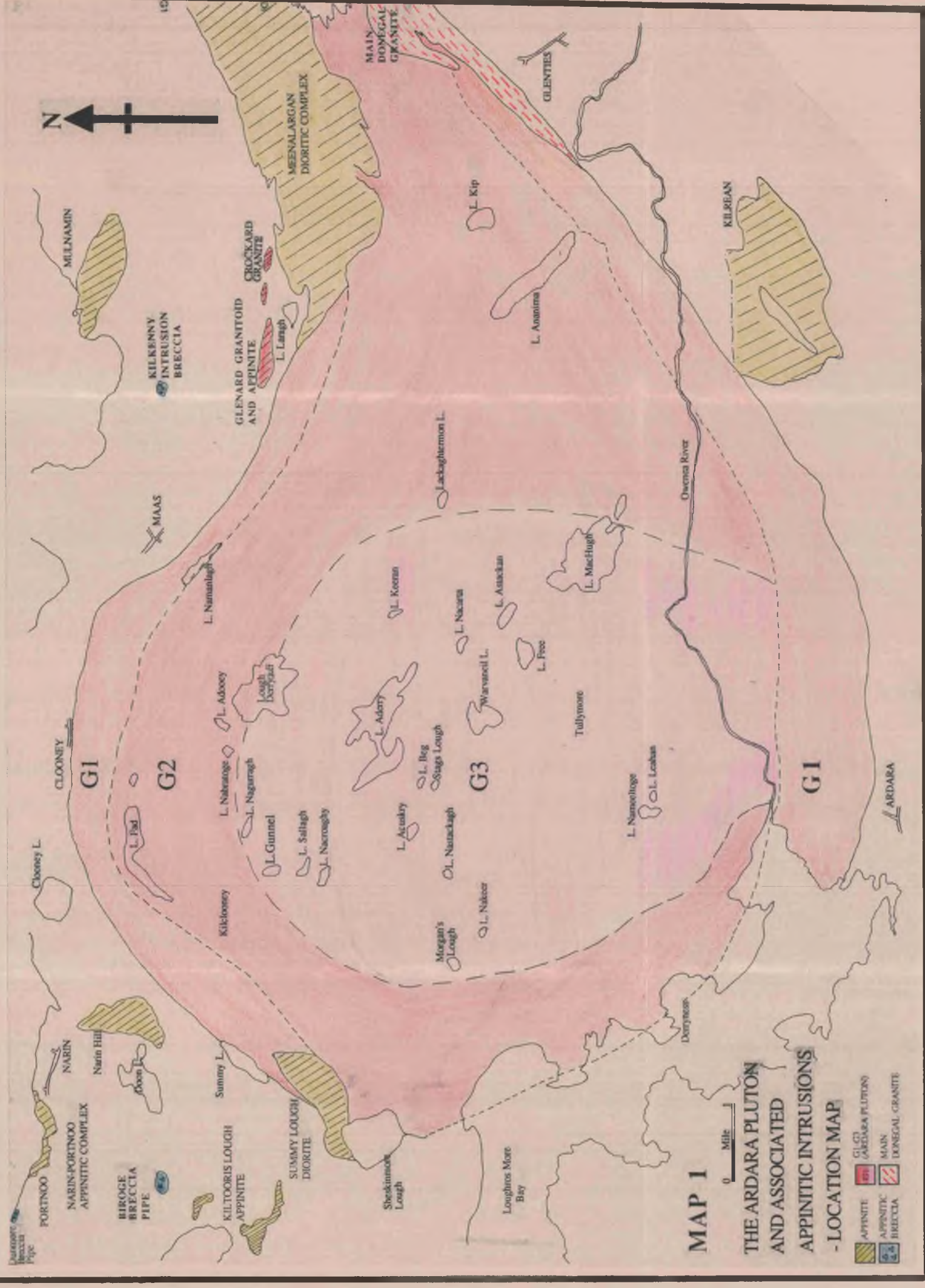
SOLID GEOLOGY OF THE SUMMY LOUGH AREA, CO. DONEGAL, EIRE.

MAP 4



- | | |
|---|---|
|  | Hornblendite |
|  | Diorite (D), Coarse diorite (C) |
|  | G1 (Ardara pluton) |
|  | G2 (Ardara pluton) |
|  | Metadolerite |
|  | Upper Falcarragh Pelite |
|  | Bedding |
|  | Mineral foliation; biotite (B), plagioclase (Pl), hornblende (Hb) |
|  | Shear band |
|  | Fault |
|  | Contact |
|  | Contact inferred |

0 500 m



MAP 1

THE ARDARA PLUTON AND ASSOCIATED APPINITIC INTRUSIONS - LOCATION MAP

- APPINITIC
- APPINITIC BRECCIA
- G1, G2 (ARDARA PLUTON)
- MAIN
- DONEGAL GRANITE

0 Mile 1



Donegal
Breccia
Pipe



MAP 2 THE SOLID GEOLOGY OF THE NORTHERN PART OF THE ARDARA PLUTON, CO. DONEGAL, EIRE

LITHOLOGICAL KEY

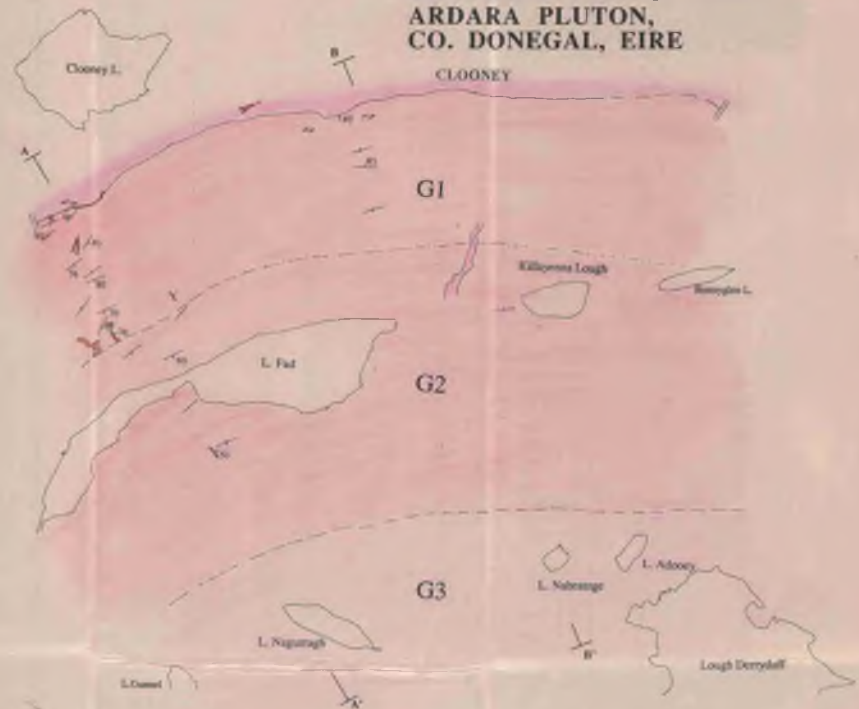
	Dionite (Di)	Aplite/Pegmatite
	Ardara Pluton (Outer unit, G1)	Dyke/Vein
	Ardara Pluton (Inner unit, G2)	Xenolith (Metasedimentary)
	Ardara Pluton (Central unit, G3)	Xenolith (Basic igneous)
	Metakolite (M)	
	Cleengon Pelite (P)	

STRUCTURAL KEY

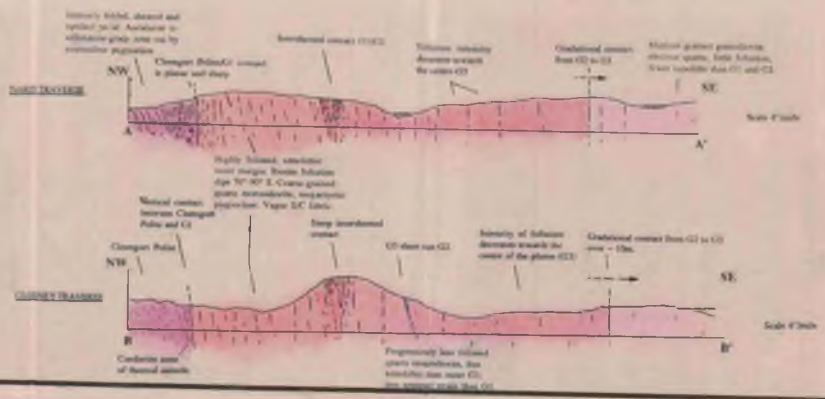
	Contact: definite
	Contact: inferred
	Contact: transitional
	Bedding
	Foliation
	Foliation: vertical
	Lamination
	Fracture (if sense shown)
	Shear band



Sarn Hill



MAAS

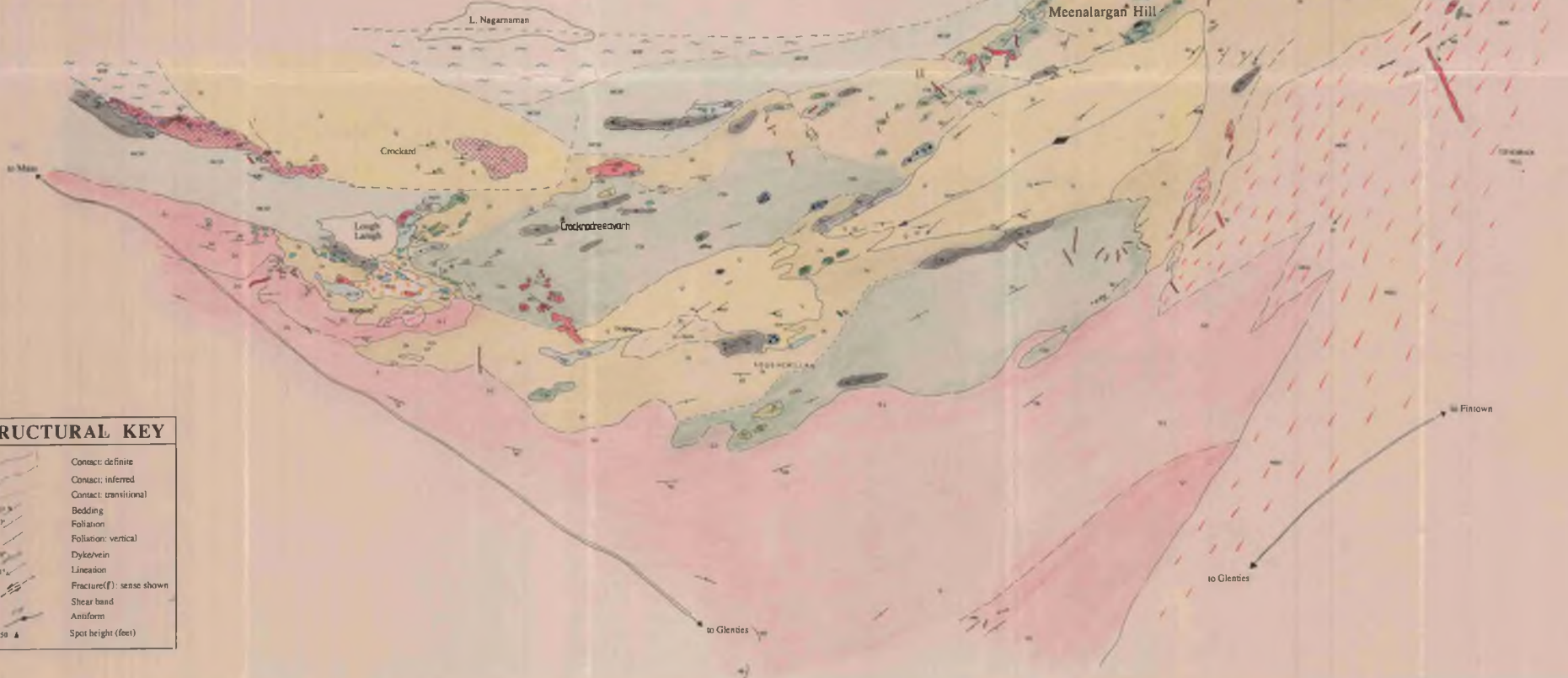


LITHOLOGICAL KEY

IGNEOUS (Major)	IGNEOUS (Minor)
Hornblende (H)	Felsic
Meladiorite (M)	Basalt
Coarse Diorite (CD)	Granite/Granodiorite
Diorite (D)	Apophanite
Comminuted Diorite (Com D)	Agnatite/Basalts
Appinitic (Ap)	DALRADIAN
Ardara Pluton (Outer unit, G1)	Mulnamin Calc-silicate Flags (MCSF)
Ardara Pluton (Inner unit, G2)	Mulnamin Silicate Flags (MSF)
Main Donegal Granite (MDG)	Cir Quartzite (Q)
Glenard Granite	Micaschist (M)
Crockard Granite	

MAP 3

THE SOLID GEOLOGY OF THE MEENALARGAN DIORITIC COMPLEX, CO. DONEGAL, EIRE.



STRUCTURAL KEY

	Contact: definite
	Contact: inferred
	Contact: transitional
	Bedding
	Foliation
	Foliation: vertical
	Dyke/vein
	Lineation
	Fracture(F): sense shown
	Shear band
	Antiform
	Spot height (feet)

THE SOLID GEOLOGY OF THE AREA EAST OF LOUGH LARAGH, MEENALARGAN, CO. DONEGAL.

MAP 3'

STRUCTURAL KEY

- Contact: definite (dip shown)
- Contact: inferred (dip shown)
- Contact: transitional
- Bedding
- Foliation
- Foliation: vertical
- Dyke/vein
- Lineation
- Fracture (f): sense shown
- Thrust fault
- Shear band
- Antiform
- Synform

LOUGH LARAGH

Contact visible to within two metres. Gradational over seven metres.

Highly sheared porphyroblastic granitoid shows evidence of contamination by pelitic country rock

Coarse diorite remains undeformed in those islands away from the main deformation zones

Mingled material, diorite to granodiorite in composition, in 4m wide outcrop. Granodiorite has veined diorite when diorite was plastic, resulting in a mingled texture. Late sulphides.

Gradational contact of diorite and coarse diorite. Diorite occurs in discrete patches

Sporadic outcrops of dioritic-type rock. Increase in plagioclase and hornblende grain size as pelite is approached

Gradational contact related to increase in biotite

Hornblende diorite rim but no metasomatism of pelite

Sharp contact between coarse diorite and pelite

Pelitic matrix is recrystallised to granite-like rock due to peritectic reaction

Banded zone

Meladiorite is highly altered. CI = 80%. Few felsics

Microbreccia of diorite and calc silicate. Diorite has intruded calc silicate in brittle fashion.

Much mineralogical exchange across the boundary. Bedding is preserved within the altered calc silicate. Replacement and recrystallisation apparent

Tremolitic bands growing parallel to the shear zone

Mel dyke with pegmatitic and granitic fractions cross-cut all fabrics

LITHOLOGICAL KEY

IGNEOUS (Major)

- Hornblende (H)
- Meladiorite (Mja)
- Coarse Diorite (CDi)
- Diorite (Di)
- Contaminated Diorite (Cont Di)
- Appinite (TAp)
- Ardara Pluton (Outer unit, G1)
- Ardara Pluton (Inner unit, G2)
- Main Donegal Granite (MDG)

IGNEOUS (Minor)

- Felsite
- Basalt
- Granite/Granodiorite
- Aplite/Pegmatite
- Agmatite/Breccia

DALRADIAN

- Mulnamin Calc-silicate Flags (MCSF)
- Mulnamin Silicate Flags (MSF)
- Cor Quartzite (Q)
- Metadolerite (M)

